PHYSIOLOGY OF MYELIN FORMING CELLS, FROM MYELINATION TO NEURAL MODULATORS

EDITED BY: Mauricio Antonio Retamal, Fernando C. Ortiz and Marion Baraban

PUBLISHED IN: Frontiers in Cellular Neuroscience

frontiers Research Topics

frontiers

ISSN 1664-8714
ISBN 978-2-88963-274-9
DOI 10.3389/978-2-88963-274-9

About Frontiers

Frontiers is more than just an open-access publisher of scholarly articles: it is a pioneering approach to the world of academia, radically improving the way scholarly research is managed. The grand vision of Frontiers is a world where all people have an equal opportunity to seek, share and generate knowledge. Frontiers provides immediate and permanent online open access to all its publications, but this alone is not enough to realize our grand goals.

Frontiers Journal Series

The Frontiers Journal Series is a multi-tier and interdisciplinary set of open-access, online journals, promising a paradigm shift from the current review, selection and dissemination processes in academic publishing. All Frontiers journals are driven by researchers for researchers; therefore, they constitute a service to the scholarly community. At the same time, the Frontiers Journal Series operates on a revolutionary invention, the tiered publishing system, initially addressing specific communities of scholars, and gradually climbing up to broader public understanding, thus serving the interests of the lay society, too.

Dedication to Quality

Each Frontiers article is a landmark of the highest quality, thanks to genuinely collaborative interactions between authors and review editors, who include some of the world's best academicians. Research must be certified by peers before entering a stream of knowledge that may eventually reach the public - and shape society; therefore, Frontiers only applies the most rigorous and unbiased reviews.
Frontiers revolutionizes research publishing by freely delivering the most outstanding research, evaluated with no bias from both the academic and social point of view. By applying the most advanced information technologies, Frontiers is catapulting scholarly publishing into a new generation.

What are Frontiers Research Topics?

Frontiers Research Topics are very popular trademarks of the Frontiers Journals Series: they are collections of at least ten articles, all centered on a particular subject. With their unique mix of varied contributions from Original Research to Review Articles, Frontiers Research Topics unify the most influential researchers, the latest key findings and historical advances in a hot research area! Find out more on how to host your own Frontiers Research Topic or contribute to one as an author by contacting the Frontiers Editorial Office: researchtopics@frontiersin.org

PHYSIOLOGY OF MYELIN FORMING CELLS, FROM MYELINATION TO NEURAL MODULATORS

Topic Editors:
Mauricio Antonio Retamal, Universidad del Desarrollo, Chile
Fernando C. Ortiz, Universidad Autónoma de Chile, Chile
Marion Baraban, University of Edinburgh, United Kingdom

Citation: Retamal, M. A., Ortiz, F. C., Baraban, M., eds. (2019). Physiology of Myelin Forming Cells, from Myelination to Neural Modulators. Lausanne: Frontiers Media SA. doi: 10.3389/978-2-88963-274-9

Table of Contents

frontiers in Cellular Neuroscience

EDITORIAL
published: 22 October 2019
doi: 10.3389/fncel.2019.00475

Editorial: Physiology of Myelin Forming Cells, From Myelination to Neural Modulators

Marion Baraban[1], *Mauricio A. Retamal*[2,3] *and Fernando C. Ortiz*[4]*

[1] *Mechanics of Neuronal Development Laboratory, Institut de Biologie Paris-Seine—Developmental Biology Laboratory, CNRS UMR7622, Sorbonne Université, UPMC Univ Paris 06, Paris, France,* [2] *Universidad del Desarrollo, Centro de Fisiologia Celular e Integrativa, Facultad de Medicina Clinica Alemana, Santiago, Chile,* [3] *Department of Cell Physiology and Molecular Biophysics, Center for Membrane Protein Research, Texas Tech University Health Sciences Center, Lubbock, TX, United States,* [4] *Mechanisms of Myelin Formation and Repair Laboratory, Instituto de Ciencias Biomédicas, Facultad de Ciencias de la Salud, Universidad Autónoma de Chile, Santiago, Chile*

Keywords: oligodendrocyte, Schwann cell, oligodendrocyte precursor cell, myelin, myelin repair, axon physiology

Editorial on the Research Topic

Physiology of Myelin Forming Cells, From Myelination to Neural Modulators

Myelin is a specialized glial-derived membrane that enwraps axons enabling them for saltatory conduction of action potentials. It is organized in sheaths along the axonal compartment, separated by regions enriched in voltage-gated sodium channels—called *nodes of Ranvier*—where the action potential is regenerated. For many years myelin was considered a static structure, however, the idea of myelin coating as a rigid insulator of axons has been challenged in the last decades. Indeed, both central and peripheral myelin forming cells, namely oligodendrocytes and Schwann cells, interact actively with the surrounding neuronal and non-neuronal cells supporting many processes such as neuronal activity and metabolic supply. In addition, evidences provided by several research groups indicate that myelin synthesis is not only restricted to development, but it is also contributing to the remodeling in adulthood and the repair under pathological conditions. The aim of the present Research Topic is to group articles, reviews and technical reports exploring different aspects of the myelinating cells function in health and disease.

Intercellular communication between myelinating glial cells and the rest of the cellular components of the nervous tissue is essential to maintain CNS homeostasis. This function is mainly based on the ability of glial cells to be metabolic and electrically coupled between themselves and neurons, participating in trophic support and synchronization of the glial network. This communication is established by devoted channels constituted by connexins or pannexins which are permeables to ions and small molecules. In this regard, Cisterna et al. summarize the organization and the functional role of gap junction channels constituted by connexins in Schwann cells. They further report the consequences of the mutation of genes encoding connexin 32, leading to Charcot Marie Tooth X-linked form 1 disease (Cisterna et al.). Vejar et al. review the functional evidence of electrical and metabolic coupling through connexin- and pannexin-based channels within and between oligodendrocytes in the central nervous system. Afterward, the authors focus on the interaction and function of oligodendrocytes/astrocytes coupling, a well-known process that provides metabolic support to axons.

Subsequently, two technical reports illustrate the use of advanced techniques based on optogenetics and optical sensors, applied to the study of oligodendroglia physiology (Looser et al.; Ortolani et al.). Looser et al. optimize the combination of electrophysiological recordings and imaging of an ATP biosensor in the fully myelinated optic nerve. The ATP sensor was delivered

Edited and reviewed by:
Arianna Maffei,
Stony Brook University, United States

***Correspondence:**
Fernando C. Ortiz
fernando.ortiz@uautonoma.cl

Specialty section:
This article was submitted to Cellular Neurophysiology, a section of the journal Frontiers in Cellular Neuroscience

Received: *30 July 2019*
Accepted: *08 October 2019*
Published: *22 October 2019*

Citation:
Baraban M, Retamal MA and Ortiz FC (2019) Editorial: Physiology of Myelin Forming Cells, From Myelination to Neural Modulators. Front. Cell. Neurosci. 13:475. doi: 10.3389/fncel.2019.00475

by reliable intravitreal injections of adeno-associated virus vectors which make this protocol adaptable to any genetically encoded sensor in any mutated mice. This method will permit to gain knowledge on the metabolism and homeostasis of this myelinated nerve in both physiological and pathological conditions. Moreover, Ortolani et al. established a protocol to perform photo-stimulation of GABAergic neurons *in vivo,* in the awake mouse pups. The authors confirmed that GABAergic synaptic inputs have no effect on OPC proliferation of the somatosensory cortex during development. Remarkably, this framework was optimized at an early post-natal stage, during the critical period of intense myelination. This might be readily adapted to investigate activity-dependent myelination occurring in other brain areas of the mouse.

The next section recapitulates some of the key aspects of myelination in the central nervous system. While it is known that oligodendrocytes myelinate specific axons, the complex rules governing the correct targeting of CNS myelination only begin to be understood. Almeida highlights the molecular and cellular codes that possibly target the myelination of the appropriate axon. After the initial step of targeted myelination, one can ask how the CNS myelination pattern changes during adulthood. Williamson and Lyons provide an overview of the recent findings on myelination dynamics and remodeling, specially they discuss the interesting results obtained by recent longitudinal imaging studies, concerning the apparent stability of the myelination patterns along the axon over lifetime.

Many human neurologic conditions have been associated with glial cells dysfunction or destruction in the CNS. Among them multiple sclerosis (MS) represents the archetypical example of a demyelinating disease, being the second cause of disabilities for the young adult population and more than 2 million people having the condition worldwide. By using the experimental autoimmune encephalomyelitis (EAE) MS model, Osorio-Barrios et al. examine the contribution of dopamine receptor D5 pathway on T-Cells, knowing to play a key role on the early stages of the demyelination insult in MS. It is known that after this initial demyelinated stage there is a spontaneous remyelination process that normally remains incomplete. This has led to the develop of many studies trying to shed light on the remyelination mechanisms, aiming to improve this spontaneous repair process. One strategy to increase the efficiency of remyelination might be to produce additional myelinating cells with the help of neighboring cells. In this regard, Silva et al. demonstrate that pericytes, central components of the vascular niche, influence neural stem cells toward the generation of oligodendrocytes. In this same line, to identify molecular factors involved in adult oligodendrogenesis is central in the search of myelin regeneration strategies. Laouarem and Traiffort highlight the importance of the neural morphogen hedgehog and its pathway during myelin repair, as well as providing an overview on the role of this signaling molecule during oligodendrogenesis at early developmental stages. Recent studies have pointed out oligodendroglia abnormalities as a contributing factor on complex pathologies such as the autistic spectrum disorder (ASD). To investigate in further details those abnormalities, Graciarena et al. characterize myelination and oligodendroglia population of different brain areas in a murine ASD model induced by prenatal exposition to valproic acid. In addition, Shen et al. summarize the contribution of adenosine signaling to both oligodendrocyte homeostasis and myelination in the context of the ASD.

Finally, a collection of reviews and articles concentrates on summarizing the miscellaneous functions of myelinating glial cells. Couve and Schmachtenberg describe the dental pulp system in human, focused on its innervation, the myelinating and the non-myelinating Schwann cells. Interestingly, they review the striking plasticity of those two types of Schwann cells preserving the dental pulp innervation, after an acute nerve injury caused by caries as well as the long-term changes related to aging. Fontenas and Kucenas introduce and depict an exceptional novel population of glial cells called motor exit point (MEP) glia. MEP glial cells are located at the transition zone in the interface between the peripheral and the central nervous systems, being able to myelinate motor neurons at that particular axonal region. The authors report the main characteristics of this recently described glia population based on their *in vivo* studies in zebrafish, emphasizing the importance of *in vivo* experimental models to study cellular dynamics (Fontenas and Kucenas). The next article examines one particular aspect of the microglia/oligodendroglia interaction: Thomas and Pasquini concentrate on the role of microglia derived-galectin-3 in oligodendrocyte differentiation and how this signaling molecule can foster remyelination. Finally, Nayak et al. bring our attention to the intracellular domain (ICD) of the NG2 proteoglycan, a molecular hallmark of oligodendrocyte progenitors, by showing that this domain induce mRNA translation mainly through the mTOR pathway. They suggest that the intracellular domain of NG2 could accelerate cell cycle kinetic in OPC and hypothesize that NG2 ICD might play a role also in tumor progression.

Summarizing, this Research Topic present original articles and updating reviews on the cellular and molecular mechanisms of the classical function associated with myelin forming cells, namely myelin formation and repair processes. But more interestingly, the topic also recapitulates evidence on, possibly unexpected, new functions (i.e., preserving dental pulp cytoarchitecture); new cellular interactions, such as the role of pericytes on remyelination; and even a new population of myelinating glia (i.e., MEP glia). By organizing this topic, we expect to provide a unique and broad overview on myelinating cells function in health and disease, encouraging to the community to develop more investigation on this very active field.

AUTHOR CONTRIBUTIONS

MB and FO conceived the major ideas developed in the manuscript. MB wrote the original manuscript which was edited and corrected by all the authors. MB, MR, and FO approved the final manuscript.

ACKNOWLEDGMENTS

The editors are grateful to all the authors for their contributions to this topic. We also thank the reviewers of all the articles

who kindly helped us to improve the content of this compelling Research Topic. We thank Rodrigo Varas for his helpful comments on the manuscript.

Conflict of Interest: The authors declare that the research was conducted in the absence of any commercial or financial relationships that could be construed as a potential conflict of interest.

frontiers in Cellular Neuroscience

ORIGINAL RESEARCH
published: 10 July 2018
doi: 10.3389/fncel.2018.00192

Dopamine Receptor D5 Signaling Plays a Dual Role in Experimental Autoimmune Encephalomyelitis Potentiating Th17-Mediated Immunity and Favoring Suppressive Activity of Regulatory T-Cells

Francisco Osorio-Barrios[1], *Carolina Prado*[1], *Francisco Contreras*[1] *and Rodrigo Pacheco*[1,2]*

[1]*Laboratorio de Neuroinmunología, Fundación Ciencia & Vida, Santiago, Chile,* [2]*Departamento de Ciencias Biológicas, Facultad de Ciencias de la Vida, Universidad Andres Bello, Santiago, Chile*

A number of studies have shown pharmacologic evidence indicating that stimulation of type I dopamine receptor (DR), favors T-helper-17 (Th17)-mediated immunity involved in experimental autoimmune encephalomyelitis (EAE) and in some other inflammatory disorders. Nevertheless, the lack of drugs that might discriminate between DRD1 and DRD5 has made the pharmacological distinction between the two receptors difficult. We have previously shown genetic evidence demonstrating a relevant role of DRD5-signaling in dendritic cells (DCs) favoring the $CD4^+$ T-cell-driven inflammation in EAE. However, the role of DRD5-signaling confined to $CD4^+$ T-cells in the development of EAE is still unknown. Here, we analyzed the functional role of DRD5-signaling in $CD4^+$ T-cell-mediated responses and its relevance in EAE by using a genetic approach. Our results show that DRD5-signaling confined to naive $CD4^+$ T-cells exerts a pro-inflammatory effect promoting the development of EAE with a stronger disease severity. This pro-inflammatory effect observed for DRD5-signaling in naive $CD4^+$ T-cells was related with an exacerbated proliferation in response to T-cell activation and to an increased ability to differentiate toward the Th17 inflammatory phenotype. On the other hand, quite unexpected, our results show that DRD5-signaling confined to Tregs strengthens their suppressive activity, thereby dampening the development of EAE manifestation. This anti-inflammatory effect of DRD5-signaling in Tregs was associated with a selective increase in the expression of glucocorticoid-induced tumor necrosis factor receptor-related protein (GITR), which has been described to play a critical role in the expansion

OPEN ACCESS

Edited by:
Mauricio Antonio Retamal, Universidad del Desarrollo, Chile

Reviewed by:
Robert Weissert, University of Regensburg, Germany
Marcella Reale, Università degli Studi G. d'Annunzio Chieti e Pescara, Italy

***Correspondence:**
Rodrigo Pacheco
rpacheco@cienciavida.org;
rodrigo.pacheco@unab.cl

Received: *22 February 2018*
Accepted: *14 June 2018*
Published: *10 July 2018*

Citation:
Osorio-Barrios F, Prado C, Contreras F and Pacheco R (2018) Dopamine Receptor D5 Signaling Plays a Dual Role in Experimental Autoimmune Encephalomyelitis Potentiating Th17-Mediated Immunity and Favoring Suppressive Activity of Regulatory T-Cells. Front. Cell. Neurosci. 12:192. doi: 10.3389/fncel.2018.00192

Abbreviations: Ab, antibody; CFSE, carboxyfluorescein succinimidyl ester; CNS, central nervous system; CD*n*, cluster of differentiation *n*; CFA, complete Freund's adjuvant; CTLA4, cytotoxic T-lymphocyte antigen 4; DCs, dendritic cells; DR, Dopamine Receptor; DRD*n*, DR D*n*; DRD*n*KO, DRD*n* Knockout; EAE, Experimental Autoimmune Encephalomyelitis; IFN-*n*, interferon *n*; IL-*n*, interleukin *n*; mAb, monoclonal antibody; MFI, mean fluorescence intensity; MOG, myelin oligodendrocyte glicoprotein; OVA, ovalbumin; pOT-II, peptide $OVA_{323–339}$; pMOG, peptide $MOG_{35–55}$; PE, phycoerythrin; PMA, phorbol 12-myristate 13-acetate; RORγt, RAR-related orphan receptor gamma; STAT3, signal transducer and activator of transcription 3; TGF-β, transforming growth factor β; Tregs, regulatory T-cells; Tbet, T-box transcrption factor encoded by TBX21; Th*n*, T helper *n*; WT, wild-type.

of Tregs. Our findings here indicate a complex role for DRD5-signaling in $CD4^+$ T-cells-driven responses potentiating early inflammation mediated by effector T-cells in EAE, but exacerbating suppressive activity in Tregs and thereby dampening disease manifestation in late EAE stages.

Keywords: Th17 response, T-cell activation, regulatory T-cells, dopamine, knockout mice, experimental autoimmune encephalomyelitis, neuroimmunology

INTRODUCTION

During last 15 years dopamine has emerged as a major regulator of inflammation. All five dopamine receptors (DRs, DRD1-DRD5) have been found to be expressed in immune cells, including dendritic cells (DCs) and T-cells among others, where they exert a complex regulation of immunity (Pacheco et al., 2014). The outcome of the dopamine effects in the immune response depends in many factors, including differential expression of DRs in the immune cells present in the inflamed tissue, the local levels of dopamine and the signaling coupled to and the affinity of the different DRs involved. Current evidence has indicated that stimulation of low-affinity DRs, for instance DRD1 and DRD2, are coupled to anti-inflammatory mechanisms, thereby dampening inflammation (Shao et al., 2013; Yan et al., 2015). Conversely, signaling triggered by high-affinity DRs, including DRD3 and DRD5, has been found consistently to promote inflammation (Prado et al., 2012, 2018; Contreras et al., 2016).

Multiple sclerosis (MS) is an inflammatory disorder involving a $CD4^+$ T-cells driven response against the myelin sheath in the central nervous system (CNS). Previous evidence suggested that T-helper-1 (Th1) as well as T-helper-17 (Th17) cells are the phenotypes of autoreactive T-cells involved in MS and its mouse model, the experimental autoimmune encephalomyelitis (EAE; Dardalhon et al., 2008; Oukka, 2008). Importantly, DCs by producing interleukin 12 (IL-12) and IL-23, might induce the differentiation of naive $CD4^+$ T-cells into Th1 and Th17 cells respectively (Haines et al., 2013; O'Connor et al., 2013). Consistent with the prominent role of dopamine in regulating adaptive immunity, relevant effects for dopaminergic-signaling have been found in MS (Prado et al., 2012, 2018). In this regard, $CD4^+$ T-cells infiltrate the CNS where they can be exposed to dopamine and other neurotransmitters. In fact, striatal dopamine levels are significantly altered in mouse models of MS (Balkowiec-Iskra et al., 2007). Accordingly, emerging evidence has shown a relevant role of type I DRs (including DRD1 and DRD5) in the regulation of $CD4^+$ T-cell-mediated autoimmune response involved in human individuals undergoing MS and in EAE (Prado et al., 2013). In this regard, type I DRs have been described to be expressed in DCs (Nakano et al., 2008; Prado et al., 2012) and $CD4^+$ T-cells from human and mouse origin (Kipnis et al., 2004; Cosentino et al., 2007; Kim et al., 2013; Franz et al., 2015).

The first work addressing the role of DRs in T-cell mediated immunity, showed that antagonizing type I DRs expressed on human DCs altered acquisition of functional phenotype by naive $CD4^+$ T-cells increasing the Th1-to-Th17 ratio in co-cultures of DCs and T-cells *in vitro* (Nakano et al., 2008). Moreover, the same authors reported later that human DCs contain intracellular vesicles loaded with dopamine, which are released during Ag-presentation to naive $CD4^+$ T-cells *in vitro* (Nakano et al., 2009). The *in vivo* relevance of these observations was evaluated by using a pharmacological approach in EAE (Nakano et al., 2008). In that study, the treatment of mice with the systemic administration of a type I DRs antagonist, (*R*)-(+)-7-Chloro-8-hydroxy-3-methyl-1-phenyl-2,3,4,5-tetrahydro-1*H*-3-benzazepine hydrochloride (SCH23390), reduced disease severity by impairing the Th17 response. However, this pharmacologic approach does not allow the discrimination between the effects mediated by DRD5 or DRD1 since the drug inhibits both type I DRs with similar affinities (Bourne, 2001). Furthermore, this study could not identify the cell-type responsible for the anti-inflammatory effect of type I DRs antagonism. Importantly, we have contributed to elucidate this mechanism using a genetic approach that allows us to determine the contribution of DRD5-signaling in DCs and its consequences in EAE development. In agreement with previous studies (Nakano et al., 2008), we demonstrate that DRD5-deficient mice exhibited delayed EAE progression with reduced severity compared with normal mice (Prado et al., 2012). In addition, we demonstrated that DRD5-deficiency confined to DCs resulted in exacerbated activation of signal transducer and activator of transcription 3 (STAT3), triggering impaired production of IL-12 and IL-23 with a consequent attenuation in Th1 and Th17 responses and reduced EAE manifestation (Prado et al., 2018). Nevertheless, the extent of attenuation of disease severity was stronger when EAE manifestation was compared between wild-type (WT) and general DRD5 knockout (DRD5KO) mice than when comparing WT animals with mice harboring DRD5-deficiency confined to DCs, suggesting that DRD5 expressed in other cell types different of DCs were also relevant in the regulation of EAE development (Prado et al., 2012).

Addressing the dopaminergic regulation of $CD4^+$ T-cells mediated by type I DRs, pharmacological evidence has suggested that signaling triggered by these receptors in human T-cells *in vitro* favors the differentiation toward the Th2 phenotype (Nakano et al., 2009). Another study performed in a mouse model of ovalbumin (OVA)-induced acute asthma shows that pharmacologic antagonism of type I DRs impaired Th17 function and thereby ameliorated the allergic response (Gong et al., 2013). In addition, our previous results using a genetic approach have shown that DRD5-stimulation in mouse $CD4^+$ T-cells favors T-cell activation and without detectable effects in Th1 differentiation when activated with Abs to CD3 and

CD28 and a Th1-biased mixture of blocking Abs and cytokine milieu *in vitro* (Franz et al., 2015). Regarding the role of type I DRs on Tregs physiology, two independent groups have shown pharmacological evidence indicating that, by stimulating DRD1/DRD5, dopamine reduces the suppressive function of Tregs (Kipnis et al., 2004; Cosentino et al., 2007). This dopamine-mediated inhibitory mechanism involves a reduction in IL-10 and transforming growth factor β (TGF-β) production and diminished expression of cytotoxic T-lymphocyte antigen 4 (CTLA4), which participate in the cytokine-mediated and contact-mediated suppression exerted by Tregs, respectively. Together, these findings support an important role for type I DRs in the regulation of $CD4^+$ T-cells physiology and reveal a relevant involvement of these receptors in autoimmunity. Nonetheless, the precise contribution of DRD1- and DRD5-signaling in the regulation of the $CD4^+$ T-cell mediated autoimmune response associated to EAE remains unknown.

In this study, we analyzed the precise role of DRD5-signaling in the $CD4^+$ T-cell response *in vivo* using a genetic approach. For this purpose, we dissected the role of DRD5 expressed in naive $CD4^+$ T-cells and Tregs from that of DRD5 expressed in other hematopoietic cells in EAE. Afterward, the role of DRD5 expressed in $CD4^+$ T-cells in inflammation was validated in other *in vivo* paradigms. Our results indicate that DRD5-signaling in $CD4^+$ T-cells favors T-cell activation and contributes significantly to the differentiation toward the Th17-inflammatory phenotype *in vivo*. Furthermore, our data show unexpectedly that DRD5-signaling potentiates the suppressive activity of Tregs *in vivo* and *in vitro*. Thus, our findings indicate that DRD5-signaling in $CD4^+$ T-cells plays a dual role in EAE development favoring early to the Th17-mediated inflammation and later contributing to the suppressive activity of Tregs.

MATERIALS AND METHODS

Animals

C57BL/6 WT (*cd45.2*$^{+/+}$) mice and B6.SJL-*Ptprc*^{a} (*cd45.1*$^{+/+}$) mice in the C57BL/6 background were purchased from The Jackson Laboratory (Bar Harbor, ME, USA). DRD5KO mice were kindly donated by Dr. David Sibley (Hollon et al., 2002), which were back-crossed for at least ten-generations in the C57BL/6 (*cd45.2*$^{+/+}$) genetic background. OVA-specific OT-II transgenic mice expressing specific T-cell receptors (TCRs) for I-A^b/$OVA_{323–339}$ in the C57BL/6 (*cd45.2*$^{+/+}$) genetic background were gently donated by Dr. María Rosa Bono (Ureta et al., 2007). DRD5KO/OT-II mice were generated by crossing parental DRD5KO and OT-II mice. Six-to-10 weeks old mice were used in all experiments. All mice were maintained and manipulated according to institutional guidelines at the pathogen-free facility of the Fundación Ciencia and Vida.

Reagents

Monoclonal antibodies (mAbs) for flow cytometry: anti-FoxP3 (clone FJK-16S) conjugated to Phycoerythrin (PE)-Cyanine 7 (Cy7) and Allophycocyanin (APC), and anti-IFN-γ (clone XMG1.2) conjugated to PE-Cy7 were obtained from eBioscience (San Diego, CA, USA). Anti-CD4 (clone GK1.5) conjugated to APC and APC-Cy7; anti-CD25 (clone PC61) conjugated to Fluorescein isothiocyanate (FITC); anti-CD44 (clone IM7) conjugated to PE; anti-CD62L (clone MEL14) conjugated to APC-Cy7; anti-IL-17A (clone TC11-181710.1) conjugated to APC; anti-CD45.2 (clone 104) conjugated to PE-Cy7; anti-CD45.1 (clone A20) conjugated to Brilliant Violet (Bv)421; anti-CTLA4 (clone UC10-4139) conjugated to Bv421; anti-ICOS (clone C398.4A) conjugated to PE-Cy7; anti-CD39 (clone Duha59) conjugated to PE; anti-CD73 (clone Ty/11.8) conjugated to Peridin-Chlorophyll (PerCP); anti-CCR6 (clone 29-2L17) conjugated to APC; anti-glucocorticoid-induced tumor necrosis factor receptor-related protein (GITR; clone YGITR756) conjugated to PE-Cy7; anti-CD104 (clone 2E7) conjugated to Pacific Blue; anti-B220 (clone RA3-6B2) conjugated to PerCP; anti-TCRVα2 (clone B20.1) conjugated to PE and TCRVβ5 (clone MR9-4) conjugated to APC were purchased from Biolegend (San Diego, CA, USA). mAbs for Cell Culture: the followings mAbs low in endotoxins and azida free (LEAF) were purchased from Biolegend: anti-IL-4 (clone 11B11), anti-CD28 (clone 37.51), anti-CD3ε (clone 145-2C11), anti-IFN-γ (clone AN-18) and anti-IL-2 (clone JES6-1A12). Carrier-Free cytokines TGF-β3, TGF-β1, IL-6, IL-12, IL-23, IL-1β and IL-2 were purchased from Biolegend. Zombie Aqua™ Fixable Viability dye detectable by flow cytometry was purchased from Biolegend. Phorbol 12-myristate 13-acetate (PMA) and ionomycin were purchased from Sigma-Aldrich (St. Louis, MO, USA). Cell Trace Carboxyfluorescein succinimidyl ester (CFSE), Brefeldin A and Fetal Bovine Serum (FBS) were obtained from Life Technologies (Carlsbad, CA, USA). The peptide derived from myelin oligodendrocyte glycoprotein ($pMOG_{35–55}$) was purchased from GeneTel Laboratories (Madison, WI, USA). The peptide derived from the chicken ovalbumin ($OVA_{323–339}$; OT-II peptide or pOT-II) was purchased from Genescript (Piscataway, NJ, USA). Freund's Complete Adjuvant (CFA) was purchased from Thermo Scientific. Bovine Serum Albumin (BSA) was purchased to Rockland (Limerick, PA, USA).

Generation of Bone Marrow Chimeras

Five-to-six weeks old B6.SJL-*Ptprc*^{a} (*cd45.1*$^{+/+}$) mice were lethally irradiated with two doses of 550 rad each (source of Co^{60}) separated for 3 h. One-day later, irradiated mice received the i.v. transference of bone marrow precursors (10^7 cells per mouse) obtained from WT (*cd45.2*$^{+/+}$) or DRD5KO (*cd45.2*$^{+/+}$) donor mice and maintained for 8 weeks with antibiotics (Trimethroprim and Sulfadoxine; Gorban 0.1% purchased from Merck Animal Health, Madison, NJ, USA) in the drinking water. The percentage of chimerism was determined as the percentage of $CD45.2^+$ cells from the $CD45^+$ leukocytes in peripheral blood, typically fluctuating between 80% and 85% (see Supplementary Figure S1). Bone marrow precursors were obtained from femurs and tibias as described before (Inaba et al., 1992).

EAE Induction and Evaluation

Mice were injected s.c. with 50 μg pMOG (Genetel Laboratories, Madison, WI, USA) emulsified in complete Freund's adjuvant (CFA; Invitrogen) supplemented with heat-inactivated

Mycobacterium tuberculosis H37 RA (Difco Laboratories, Detroit, MI, USA). In addition, mice received 500 ng pertussis toxin (Calbiochem, La Jolla, CA, USA) i.p. on days 0 and 2. Clinical signs were assessed daily according to the following scoring criteria: 0, no detectable signs; 1, flaccid tail; 2, hind limb weakness or abnormal gait; 3, complete hind limb paralysis; 4, paralysis of fore and hind limbs; and 5, moribund or death. In some EAE experiments, total splenic $CD4^+$ T-cells were purified by negative selection using magnetic beads-based kit (MACS®, Miltenyi Biotec, Bergisch Gladbach, Germany) and i.v. injected (5×10^6 cells per mouse) 24 h before EAE induction. In other EAE experiments, splenic naive ($CD25^-CD62L^+CD44^-$) $CD4^+$ T-cells were purified by cell-sorting and i.v. injected (3×10^6 cells per mouse) 24 h before EAE induction. In other experiments splenic Tregs ($CD4^+$ $CD25^{high}$ T-cells) were purified by cell-sorting and i.v. injected (7×10^5 cells per mouse) 24 h before EAE induction.

$CD4^+$ T-Cell Isolation and Activation *in Vitro*

Total $CD4^+$ T-cells were obtained by negative selection of splenocytes (MACS®). Naive ($CD4^+$ $CD25^-$) T-cell isolation was achieved by cell sorting using a FACS Aria II (BD, Franklin Lakes, NJ, USA), obtaining purities over 98%. Splenic DCs were purified using a CD11c+ magnetic selection kit (MACS®). All *in vitro* experiments were performed using complete IMDM medium (Life Technologies) 10% FBS. To assess proliferation, naive T-cells from OT-II mice were stained with CFSE (10 μM as indicated in figure legends) and cultured on a 5:1 (T-cells:DCs) ratio on U-bottom 96-well plates in the presence of OT-II peptide ($OVA_{323-339}$, pOT-II; 200 ng/ml) for 2 or 3 days. T-cell activation was determined as IL-2 secretion in the co-culture supernatant by ELISA as previously described (González et al., 2013). The extent of T-cell proliferation was determined as the percentage of dilution of CFSE-associated fluorescence by flow cytometry.

$CD4^+$ T-Cell Differentiation *in Vitro*

Naive ($CD4^+CD62L^+CD44^-CD25^-$) T-cell were isolated by cell-sorting and stimulated with 50 ng/well of plate-bound anti-CD3 and 2 μg/mL soluble anti-CD28 Abs on flat-bottom 96-well plates (Thermo Scientific) for 5 days. To force the differentiation of the different Th phenotypes, naïve $CD4^+$ T-cells were incubated in the conditions indicated above, in addition to a mixture of cytokines and blocking antibodies: Th1: 20 ng/mL IL-12, 10 ng/mL IL-2 and 5 μg/mL anti-IL-4; non-pathogenic Th17 (Th17np): during the first 2 days with 25 ng/mL IL-6, 5 ng/mL TGF-β1, 20 ng/mL IL-1β, 5 μg/mL anti-IL-4, 5 μg/mL anti-IL-2 and 5 μg/mL anti-IFN-γ and during the last 3 days with 25 ng/mL IL-6, 5 ng/mL TGF-β1; pathogenic Th17 (Th17p): during the first 2 days with 25 ng/mL IL-6, 5 ng/mL TGF-β3, 20 ng/mL IL-1β, 5 μg/mL anti-IL-4, 5 μg/mL anti-IL-2 and 5 μg/mL anti-IFN-γ and during the last 3 days with 25 ng/mL IL-6, 20 ng/mL IL-1β and 20 ng/mL IL-23. At different incubation times, cells were assessed for gene expression real time RT-PCR.

Quantitative RT-PCR

Total RNA extracted from cells using the Total RNA EZNA kit (Omega Bio-Tek, Norcross, GA, USA), was DNase-digested using the TURBO DNA-free kit (Ambion, Thermo Fisher Scientific) and 1 μg of RNA was used to synthesize cDNA utilizing M-MLV reverse transcriptase, according to manufacturer's instructions (Life Technologies). Quantitative gene expression analysis was performed using Brilliant II SYBR Green QPCR Master Mix (Agilent Technologies, Santa Clara, CA, USA), according to manufacturer's recommendations. Primers were used at a concentration of 0.5 μM. We used 40 PCR cycles as follows: denaturation 10 s at 95°C, annealing 20 s at 60°C and extension 20 s at 72°C. Expression of target genes was normalized to *Gapdh*. The sequences of the primers used are indicated in **Table 1**.

$CD4^+$ T-Cell Proliferation and Differentiation *in Vitro*

To analyze T-cell proliferation *in vivo*, splenic $CD4^+$ T-cells were isolated from OT-II mice, stained with 10 μM CFSE and then i.v. transferred (12.5×10^6 cells/mouse) into WT recipient mice. One-day later mice were i.p. immunized with

TABLE 1 | Primers sequences used for quantitative RT-PCR analyses.

Gene	Forward (5' → 3')	Reverse (5' → 3')	Reference
rorc	CAGAGGAAGTCAATGTGGGA	GTGGTTGTTGGCATTGTAGG	Fernández et al. (2016)
runx1	TGGCACTCTGGTCACCGTCAT	GAAGCTCTTGCCTCTACCGC	Logan et al. (2013)
runX3	CGACCGTTTGGAGACCTGC	GCGTAGGGAAGGAGCGGTCA	Wang et al. (2014)
tbx21	CCTGTTGTGGTCCAAGTTCAAC	CACAAACATCCTGTAATGGCTTGT	Smeltz et al. (1999)
il9	CTGATGATTGTACCACACCGTGC	GCCTTTGCATCTCTGTCTTCTGG	Li et al. (2014)
il10	GAAGACAATAACTGCACCCA	CAACCCAAGTAACCCTTAAAGTC	Fernández et al. (2016)
il17a	TTCATCTGTGTCTCTGATGCT	AACGGTTGAGGTAGTCTGAG	Fernández et al. (2016)
Il22	GACAGGTTCCAGCCCTA CAT	ATCGCCTTGATCTCTCCACT	Peng et al. (2014)
csf2	ACCACCTATGCGGATTTCAT	TCATTACGCAGGCACAAAAG	Kim et al. (2008)
grzb	ATCAAGGATCAGCAGCCTGA	TGATGTCATTGGAGAATGTCT	Fernández et al. (2016)
ifng	GAGCCAGATTATCTCTTTCTACC	GTTGTTGACCTCAAACTTGG	Fernández et al. (2016)
tgfb1	GCAACAACGCCATCTATGAG	TATTCCGTCTCCTTGGTTCAG	Fernández et al. (2016)
tgfb3	AGCGCACAGAGCAGAGAAT	GTCAGTGACATCGAAAGACAG	Yin et al. (2013)
drd5	CCCTAACATAACTCATCTTCTCC	TAACCCTGCAAGTTCATCCA	Franz et al. (2015)
gapdh	TCCGTGTTCCTACCCCCAATG	GAGTGGGAGTTGCTGTTGAAG	Prado et al. (2012)

25 μg OVA or just injected with vehicle (PBS). Three-days after immunization mice were sacrificed and spleen cells were isolated, immunostained with fluorochrome-conjugated antibodies for B220, CD4, TCR-Vα2 and TCR-Vβ5 and then CFSE-associated fluorescence was analyzed in the $B220^{-}$ $CD4^{+}$ TCR-$V\alpha2^{+}$ TCR-$V\beta5^{+}$ gate. The extent of T-cell proliferation was determined as the percentage of cells displaying dilution of CFSE-associated fluorescence or by the decrease of MFI in CFSE associated fluorescence in the CD4+ T-cell population expressing the transgenic OT-II TCR (TCR composed by Vα2 and Vβ5 chains) by flow cytometry. To determine the acquisition of inflammatory phenotypes by CD4+ T-cells *in vivo*, naive $CD4^{+}$ $CD25^{-}$ $CD44^{-}$ $CD62L^{+}$ T-cells were isolated from OT-II/*cd45.2*$^{+/+}$ mice by cell-sorting and then i.v. transferred (10^5 cells/mice) into WT/*cd45.1*$^{+/+}$ recipient mice. One-day later, mice were s.c. immunized with 100 μg of pOT-II in CFA and the inflammatory phenotype of $CD4^{+}$ T-cells in the draining lymph nodes (inguinal lymph nodes) was analyzed 7 and 14 days after immunization by intracellular cytokine staining of IL-17 and IFN-γ .

Tregs Suppression Assay

Splenic naive $CD4^{+}$ $CD25^{-}$ T-cells were isolated from OT-II mice by cell-sorting, stained with 5 μM CFSE and then co-cultured with splenic DCs on a 5:1 (T-cells:DCs) ratio on U-bottom 96-well plates in the presence of OVA (5 μM) for 5 days. Splenic $CD4^{+}$ $CD25^{high}$ T-cells (nTregs) were isolated from OT-II mice by cell-sorting and added to the co-cultures at indicated ratios. The extent of proliferation of naive T-cells (effector T cells; Teffs) was determined as the percentage of cells displaying dilution of the CFSE-associated fluorescence. One-hundred percent proliferation corresponded to the extent of proliferation of Teffs in the absence of nTregs (positive control). % Suppression was calculated as 100% proliferation (from positive control) minus % proliferation observed for each sample.

Flow Cytometry

For analysis of cytokine production, cells were restimulated with 1 μg/mL ionomycin and 50 ng/mL PMA in the presence of 5 μg/mL brefeldin A for 4 h. Cell surface staining was carried out in PBS with 2% FBS. For intracellular staining, cells were first stained with Zombie Aqua Fixable Viability kit (Biolegend), followed by staining for cell-surface markers and then resuspended in fixation/permeabilization solution (3% BSA and 0.5% saponin in PBS). Samples including the analysis of Foxp3 transcription factor were resuspended in fixation/permeabilization solution (Foxp3 Fixation/Permeabilization; eBioscience) according to the manufacturer instructions. To determine absolute number of cells, samples were analyzed in the presence of 123count eBeads (eBioscience) according to manufacturer's guidelines. Data were collected with a Canto II (BD) and results were analyzed with FACSDiva (BD) and FlowJo software (Tree Star, Ashlan, OR, USA).

Statistical Analysis

Differences in means between two groups (different genotype or different conditions) were analyzed by unpaired 2-tailed Student's *t*-test. Progression of EAE severity curves were compared with a non-parametric Mann–Whitney rank sums two-tailed *U* test. *P* value ≤ 0.05 was considered significant. Analyses were performed with GraphPad Prism 6 software.

Ethics Statement

This study was carried out in accordance with the recommendations of the institutional guidelines of Fundación Ciencia & Vida. The protocol was approved by the Bioethics and Biosecurity committee of the Fundación Ciencia & Vida.

RESULTS

DRD5-Signaling in Naive $CD4^{+}$ T-Cells Favors the Development of the Inflammatory Response Associated to EAE

Since we previously appreciated a difference in the severity of EAE manifestation between animals deficient in DRD5 confined to DCs and animals displaying a global deficiency of DRD5 (Prado et al., 2012), we wondered whether DRD5-signaling in other immune cells was relevant in the regulation of the inflammatory response involved in EAE. To address this question, we first compared how was the development of EAE in animals displaying a global deficiency of DRD5 with animals bearing DRD5-deficiency confined to the hematopoietic compartment. For this purpose, we generated chimeric animals by killing bone marrow of WT recipient animals with a myeloablative dose of γ-irradiation and then transferring WT or DRD5-deficient bone marrow. Eight weeks after bone marrow transplantation, we obtained chimeric animals bearing WT or DRD5-deficient blood cells and WT genetic background outside the hematopoietic compartment (Supplementary Figure S1). When EAE was induced in these chimeric animals we observed that DRD5-deficiency confined to bone marrow resulted in attenuated EAE manifestation (**Figure 1A**), although the reduction in EAE severity was less marked than attenuation observed between WT and DRD5KO mice (**Figure 1B**). Of note, this lower difference in EAE manifestation observed between chimeric animals bearing WT or DRD5-deficient bone marrow may be due to the fact that the percentage of chimerism was around 80%–85% but not complete (Supplementary Figure S1). For this reason and also considering that autoimmune response in EAE is driven by $CD4^{+}$ T-cells, which have been described to express DRD5 (Franz et al., 2015), we next carried out gaining of function experiments by performing adoptive transfer of $CD4^{+}$ T-cells. In this regard, we hypothesized that if DRD5-signaling in $CD4^{+}$ T-cells is relevant in contributing to the inflammation associated to EAE, we should rescue the phenotype of DRD5KO mice in EAE upon transfer of WT $CD4^{+}$ T-cells. Accordingly, our results show that when DRD5KO mice received the transference of WT $CD4^{+}$ T-cells, EAE severity was significantly stronger than DRD5KO mice, although still in a lesser extent than EAE severity observed in WT mice (**Figure 1C**). Since

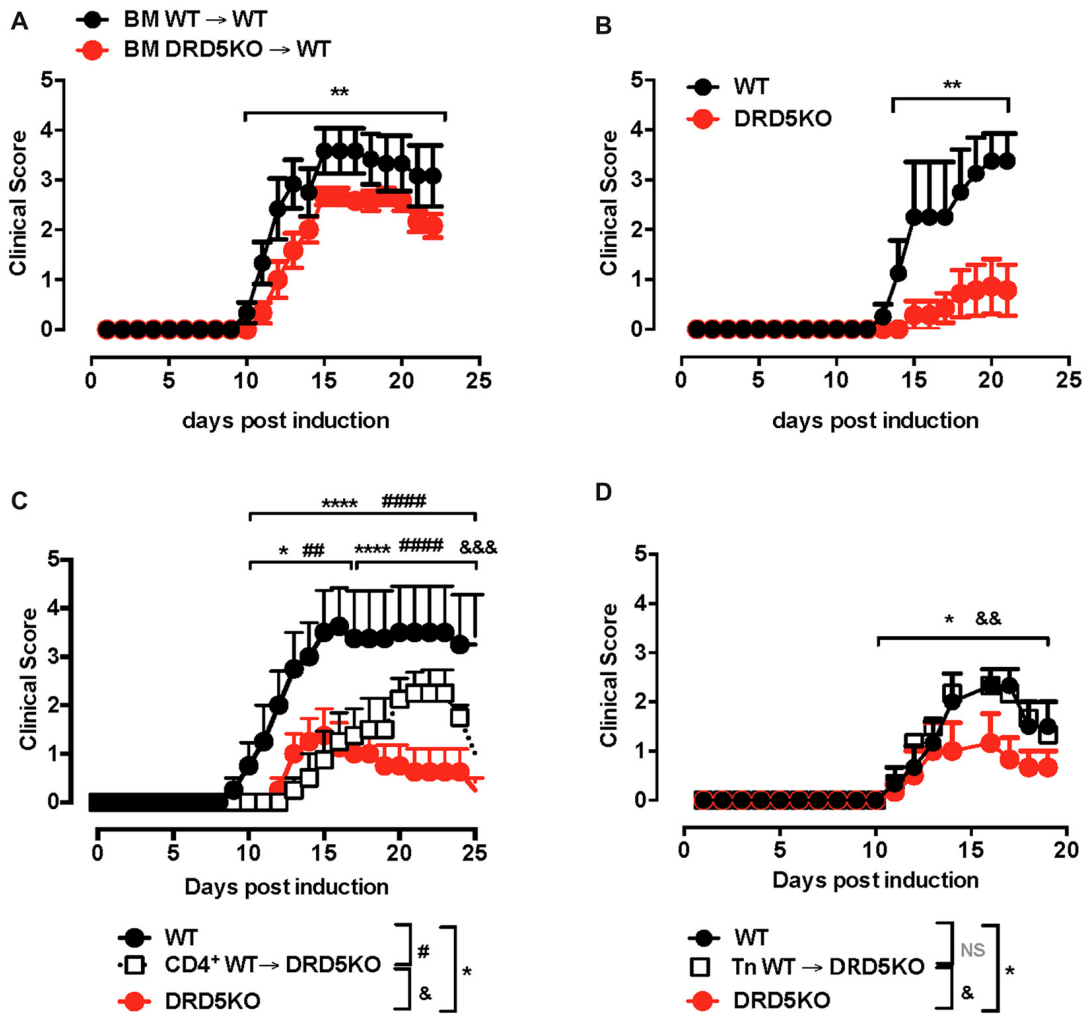

FIGURE 1 | DRD5-signaling in naive $CD4^+$ T-cells favors the development of the inflammatory response associated to experimental autoimmune encephalomyelitis (EAE). **(A)** Wild-type (WT) *cd45.1*$^{+/+}$ mice were lethally irradiated and then bone marrow (10^7 cells/per mouse) from WT *cd45.2*$^{+/+}$ (black symbols) or DRD5KO *cd45.2* $^{+/+}$ (red symbols) mice were i.v. transferred to reconstitute the hematopoietic compartment. Eight-week later, EAE was induced by immunization with pMOG in freund's complete adjuvant (CFA) followed by *Pertussis* Toxin injection and disease severity was daily determined throughout the time-course of disease development. Values represent mean ± SEM with n = 5–6 mice per group. $^{**}p < 0.01$ by Mann-Whitney U-test. **(B)** EAE was induced in WT (black symbols) and DRD5KO (red symbols) mice by immunization with pMOG in CFA followed by *Pertussis* Toxin injection and disease severity was daily determined throughout the time-course of disease development. Values represent mean ± SEM with n = 4–7 mice per group. $^{**}p < 0.01$ by Mann-Whitney U-test. **(C)** Total splenic $CD4^+$ T-cells were isolated from WT mice by negative selection using magnetic beads-based kit (from Miltenyi) and then they were i.v. injected into DRD5KO mice (5×10^6 cells/per mouse; white symbols). One-day later, EAE was induced by immunization with pMOG in CFA followed by *Pertussis* Toxin injection and disease severity was daily determined throughout the time-course of disease development. EAE was also induced in WT (black symbols) and untransferred DRD5KO (red symbols) mice as control groups. Values represent mean ± SEM with n = 4 mice per group. $^{*}p < 0.05$ and $^{****}p < 0.0001$ WT vs. untransferred DRD5KO mice; $^{\#\#}p < 0.01$ and $^{\#\#\#\#}p < 0.0001$ WT vs. transferred DRD5KO; $^{\&\&\&}p < 0.001$ transferred vs. untransferred DRD5KO mice by Mann-Whitney U-test. **(D)** Naive $CD4^+$ T-cells ($CD4^+$ $CD25^-$ $CD62L^+$ $CD44^-$) were isolated from WT mice by cell-sorting and then they were i.v. injected into DRD5KO mice (3×10^6 cells/per mouse; white symbols). One-day later, EAE was induced by immunization with pMOG in CFA followed by *Pertussis* Toxin injection and disease severity was daily determined throughout the time-course of disease development. EAE was also induced in WT (black symbols) and untransferred DRD5KO (red symbols) mice as control groups. Values represent mean ± SEM with n = 3–4 mice per group. $^{*}p < 0.05$ WT vs. untransferred DRD5KO mice; $^{\&\&}p < 0.01$ transferred vs. untransferred DRD5KO mice by Mann-Whitney U-test.

Tregs, a subpopulation of $CD4^+$ T-cells, play a relevant role attenuating EAE development in late stages of the disease manifestation (Petermann et al., 2010) and they also express DRD5 (Kipnis et al., 2004; Cosentino et al., 2007), we next wanted to evaluate the effect of DRD5-signaling confined to $CD4^+$ T-cells without the potential contribution of DRD5-signaling from Tregs. For this purpose, we next performed a set of experiments in which we isolate naive $CD25^-$ $CD4^+$ $CD44^-$ $CD62L^+$ T-cells from WT mice, a subset devoid of Tregs cells ($CD25^{high}$ $CD4^+$), and then these cells were transferred

into DRD5KO recipient mice just before EAE induction. The results show that the transfer of DRD5-sufficient naive $CD4^+$ T-cells, in the absence of Tregs, into DRD5-defficient animals results in a complete rescue in EAE manifestation, displaying similar EAE severity than observed for WT mice (**Figure 1D**). Thereby, these results indicate that DRD5-signaling in naive $CD4^+$ T-cells exerts a pro-inflammatory role favoring EAE development.

DRD5-Signaling in $CD4^+$ T-Cells Potentiates T-Cell Activation

To address the question of how DRD5-signaling favors the inflammatory potential of $CD4^+$ T-cells we next evaluated the role of this receptor in T-cells activation. Accordingly, we first determined the role of DRD5-signaling in the proliferation of $CD4^+$ T-cells *in vivo*, which is directly related with the potency of T-cell activation. For this purpose, we performed adoptive transfer experiments using $CD4^+$ T-cells from OT-II transgenic mice, which express a transgenic T-cell receptor (TCR) specific for the recognition of a peptide derived from the chicken ovalbumin ($OVA_{323–339}$; pOT-II). To determine T-cell activation *in vivo*, we isolate $CD4^+$ T-cells from WT/OT-II or from DRD5KO/OT-II mice, which were loaded with the fluorescent probe CFSE and then transferred into WT recipient mice. Subsequently, transferred mice were immunized with pOT-II in CFA and the potency of proliferation induced in pOT-II-specific T-cells was determined 3 days later in the spleen as the extent of the dilution of CFSE-associated fluorescence as previously described

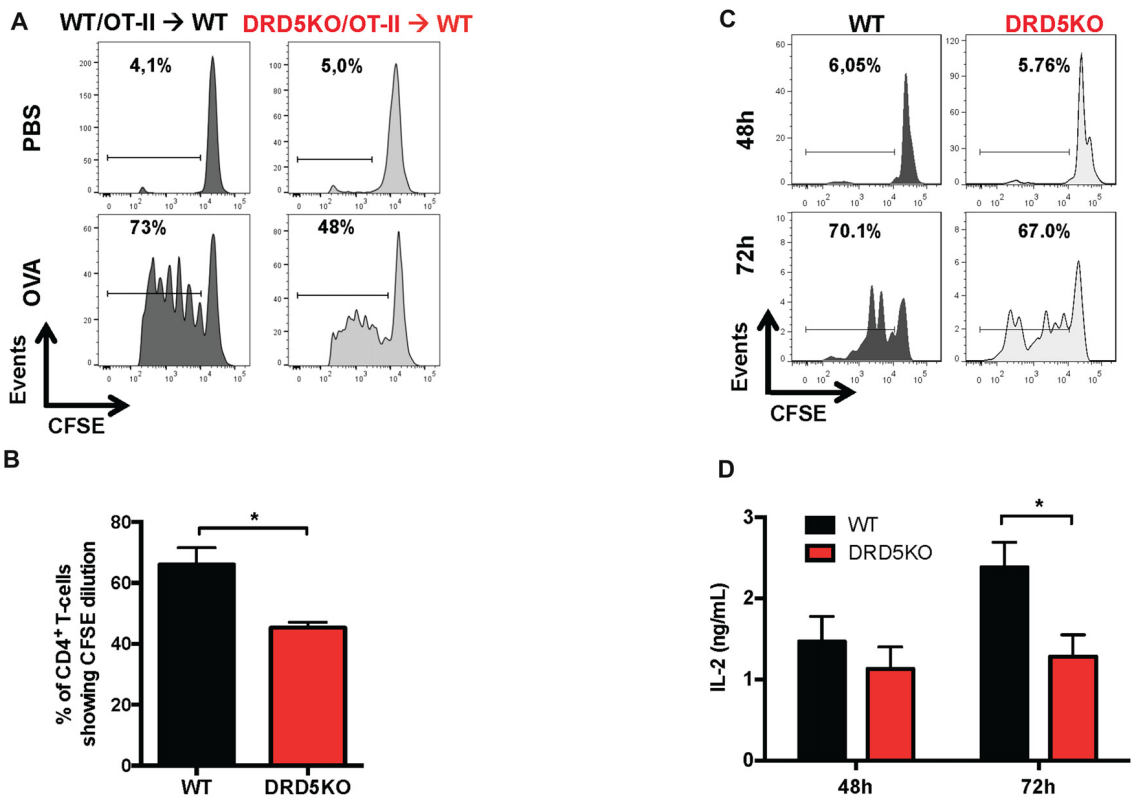

FIGURE 2 | DRD5-signaling in $CD4^+$ T-cells potentiates T-cell activation. **(A,B)** $CD4^+$ T-cells were isolated from WT/OT-II or DRD5KO/OT-II mice by negative selection using magnetic beads-based kit (from Miltenyi), stained with 10 μM carboxyfluorescein succinimidyl ester (CFSE) and then i.v. transferred (12.5×10^6 cells/mice) into WT recipient mice. One-day later mice were i.p. immunized with 25 μg ovalbumin (OVA) or just injected with vehicle (PBS). Three-day after immunization mice were sacrificed and spleen cells were isolated, immunostained with fluorochrome-conjugated antibodies for B220, CD4, TCR-Va2 and TCR-Vβ5 and then CFSE-associated fluorescence was analyzed in the $B220^-$ $CD4^+$ TCR-$Va2^+$ TCR-$Vβ5^+$ gate. **(A)** Representative histograms of CFSE-associated fluorescence vs. number of cells (events) are shown. Markers delimiting proliferating cells are shown. Percentages of $CD4^+$ T-cells in the region of proliferating cells are indicated. **(B)** Percentages of $CD4^+$ T-cells in the proliferating area from three independent experiments are represented in the bars graphs. Values represent mean ± SEM. *$p < 0.05$ by unpaired Student's *t*-test. **(C,D)** Naive $CD4^+$ $CD25^-$ $CD62L^+$ $CD44^-$ T-cells were isolated from WT/OT-II or DRD5KO/OT-II mice by cell-sorting, stained with 10 μM CFSE and then co-cultured with splenic Dendritic cells (DCs) isolated by positive $CD11c^+$ selection using magnetic beads based kit (from Miltenyi) at a ratio of CD4+ T-cells:DCs = 5:1, in the presence of pOT-II (200 ng/ml) for 48 h or 72 h. **(C)** Cells were immunostained with fluorochrome-conjugated antibodies for CD4, TCR-Va2 and TCR-Vβ5 and then CFSE-associated fluorescence was analyzed in the $CD4^+$ TCR$Va2^+$ TCR$Vβ5^+$ gate. Representative histograms of CFSE-associated fluorescence vs. number of cells (events) are shown. Markers delimiting proliferating cells are shown. Percentages of $CD4^+$ T-cells in the region of proliferating cells are indicated. **(D)** IL-2 production was determined in the culture supernatant by ELISA. Data from three independent experiments is shown. Values represent mean ± SEM. *$p < 0.05$ by unpaired Student's *t*-test.

(Contreras et al., 2016). The results show that DRD5-deficiency resulted in attenuated CD4$^+$ T-cell proliferation as indicated by a lower percentage of OT-II cells displaying dilution of CFSE-associated fluorescence (**Figures 2A,B**). To obtain further evidence in the role of DRD5-signaling in CD4$^+$ T-cell activation, we next performed *in vitro* experiments in which antigen-specific T-cell activation was induced by incubating naive CD4$^+$ T-cells isolated from WT/OT-II or DRD5KO/OT-II in the presence or WT DCs loaded with OVA. To evaluate the potency of T-cell activation, we determined the extent of proliferation as the level of CFSE dilution and the secretion of IL-2 into the culture supernatant, which corresponds to the main T-cell growth factor. The results show that DRD5-deficiency in CD4$^+$ T-cells not only resulted in decreased proliferation (**Figure 2C**) but also in reduced IL-2 production (**Figure 2D**). Thus, these results indicate that DRD5-signaling potentiates CD4$^+$ T-cell activation *in vitro* and *in vivo*.

DRD5-Signaling in CD4$^+$ T-Cells Favors the Acquisition of Th17 Phenotype

To gain deeper insight in the role of DRD5-signaling in the CD4$^+$ T-cell response, we next determined how this receptor affects the differentiation of naive CD4$^+$ T-cells into effector phenotypes. Because the Th1 and Th17 are the main subsets of effector T-cells (Teffs) driving the inflammatory response involved in EAE (Prado et al., 2013) and both of them express DRD5 transcripts (Supplementary Figure S2), we next evaluated the potential role of DRD5-signaling in the acquisition of these functional phenotypes. For this purpose, we performed experiments in which naive CD4$^+$ T-cells were isolated from WT/OT-II or from DRD5KO/OT-II mice and transferred into WT recipients. Afterward, these recipient mice were subcutaneously immunized with pOT-II and then the extent of acquisition of Th1 and Th17 functional phenotypes by the transferred CD4$^+$ T-cells was analyzed in the draining lymph nodes at different time points. The results show that despite there were no significant differences in the absolute number and frequency of Th1 cells (see IFN-γ^+ IL-17$^-$ T-cells in **Figure 3A** and in **Figure 3B** middle panels), DRD5-deficiency in CD4$^+$ T-cells resulted in a strong reduction in the absolute number of Th17 cells in the draining lymph nodes 1 week after immunization (see IFN-γ^- IL-17$^+$ T-cells in **Figures 3A** and in **Figure 3B** right-bottom panel). DRD5-deficiency in CD4$^+$ T-cells resulted also in a trend of decreased Th17 frequency in the draining lymph nodes 1 week after immunization, although this difference was not statistically significant (**Figure 3B** right-top panel). To evaluate whether difference in the acquisition of functional phenotypes observed between DRD5-deficient and DRD5-suficient CD4$^+$ T-cells was due to altered viability of these cells, we determined the percentage of living cells among transferred CD4$^+$ T-cells. The analyses show that frequencies of viable cells were similar in both genotypes, ruling out this possibility (Supplementary Figure S3A). Interestingly, irrespective of the genotype of CD4$^+$ T-cells, the absolute number of Th1 OT-II CD4$^+$ T-cells in the draining lymph nodes was increased after 2 weeks (**Figure 3B** middle-bottom panel), whilst the number of Th17 OT-II CD4$^+$ T-cells was strongly reduced (**Figure 3B** right-bottom panel), which is probably explained by the faster exit of Th17 cells

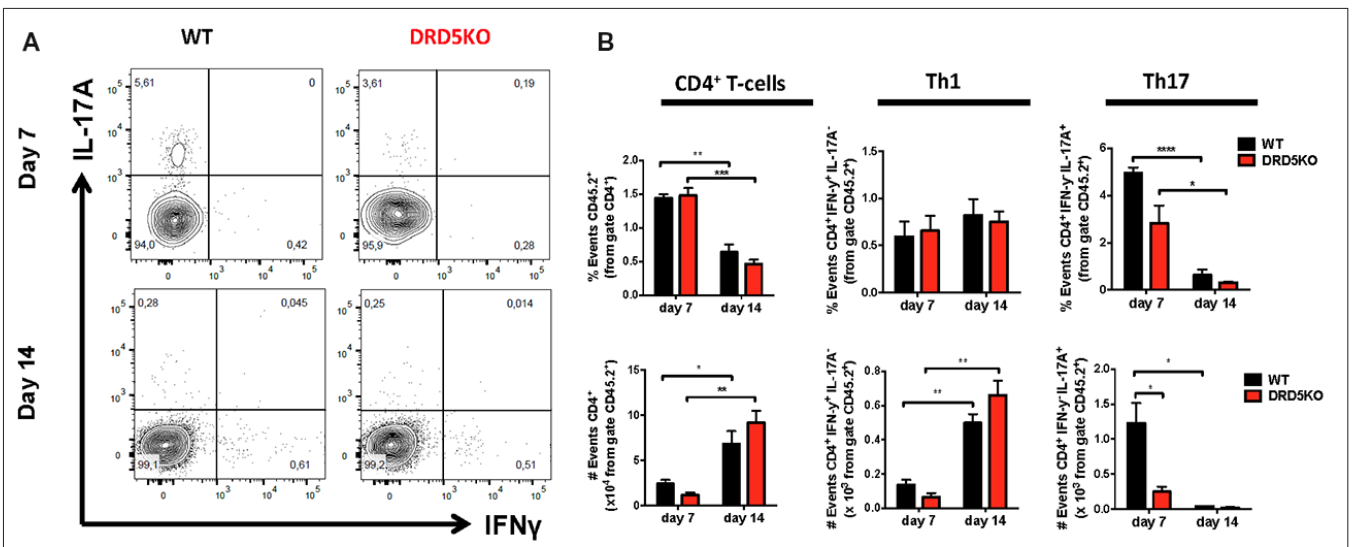

FIGURE 3 | DRD5-signaling in CD4$^+$ T-cells favors the acquisition of Th17 phenotype. **(A,B)** Naive CD4$^+$ CD25$^-$ T-cells were isolated from WT/OT-II/*cd45.2*$^{+/+}$ or DRD5KO/OT-II/*cd45.2*$^{+/+}$ mice by cell-sorting and then i.v. transferred (10^5 cells/mouse) into WT/*cd45.1*$^{+/+}$ recipient mice. One-day later, mice were s.c. immunized with 100 μg of pOT-II in CFA and CD4$^+$ T-cells were analyzed by flow cytometry in the draining lymph nodes (inguinal lymph nodes) 7 and 14 days after immunization. **(A)** Representative contour-plots analyzing IFN-γ vs. IL-17 in the CD45.2$^+$ CD4$^+$ gated population. Numbers in each quadrant represent the percentage of cells in the corresponding quadrant. **(B)** Quantification of the percentage (top panels) and absolute number (bottom panels) of total CD4$^+$ T-cells (left panels), Th1 cells (central panels) and Th17 cells (right panels) contained in the CD45.2$^+$ population. Values represent mean ± SEM with $n = 4$ mice per group. $^*p < 0.05$; $^{**}p < 0.01$; $^{***}p < 0.001$; $^{****}p < 0.0001$ by unpaired Student's *t*-test.

from the draining lymph nodes after activation (Dardalhon et al., 2008; Reboldi et al., 2009). It is also noteworthy that, irrespective of their phenotype and genotype, the frequency of total OT-II CD4$^+$ T-cells transferred is reduced in the draining lymph nodes 2 weeks after immunization (**Figure 3B** left-top panel) even when the absolute number is increased (**Figure 3B** left-bottom panel). This fact is likely to be due to the activation of endogenous CD4$^+$ T-cells (CD45.1$^+$) with specificity for pOT-II or for different antigens from mycobacterium tuberculosis contained in the CFA used as adjuvant in these experiments. To further explore the role of DRD5-signaling in Teffs, we quantified the transcriptional levels of a panel of different cytokines and transcription factors involved in the effector function of Th1 and Th17 cells. For this purpose, we performed a quantitative RT-PCR array of a set of relevant functional molecules in naive CD4$^+$ T-cells, Th1 and Th17 cells obtained from WT or DRD5KO mice. To gain a deeper insight in the role of DRD5-signaling in Th17 function, we evaluated the transcriptional panel of these molecules in Th17 cells differentiated in pathogenic (Th17p) or non-pathogenic (Th17np) conditions (Lee et al., 2012). The results show that DRD5-deficiency results in decreased IFN-γ transcription by naive CD4$^+$ T-cells or Th17np (**Figure 4A** left and right panels, and **Figure 4B**), increased transcription of IL-10 and IL-22 by Th17p (**Figure 4A** middle-right panel, and **Figure 4B**), exacerbated transcription of IL-17 and IL-22 by Th1 (**Figure 4A** middle-left panel, and **Figure 4B**) and increased transcription of granzyme B and IL-22 by naive CD4$^+$ T-cells (**Figure 4A** left panel, and **Figure 4B**). Of note, we observed similar frequency of viable cells after CD4$^+$ T-cell differentiation (Supplementary Figure S3B), ruling out the possibility that differential expression of cytokines and transcription factors was due to altered cell viability. Taken together, these results suggest that DRD5-defficiency in CD4$^+$ T-cells results in impaired acquisition of the inflammatory Teff phenotypes and reduced expansion of Th17 cells.

DRD5-Signaling in Tregs Favors Their Suppressive Activity

Since we observed that the transference of DRD5-sufficient total CD4$^+$ T-cells into DRD5KO mice just partially rescues the phenotype on EAE manifestation (**Figure 1C**), whilst the transference of DRD5-sufficient naive CD25$^-$ CD4$^+$ CD44$^-$

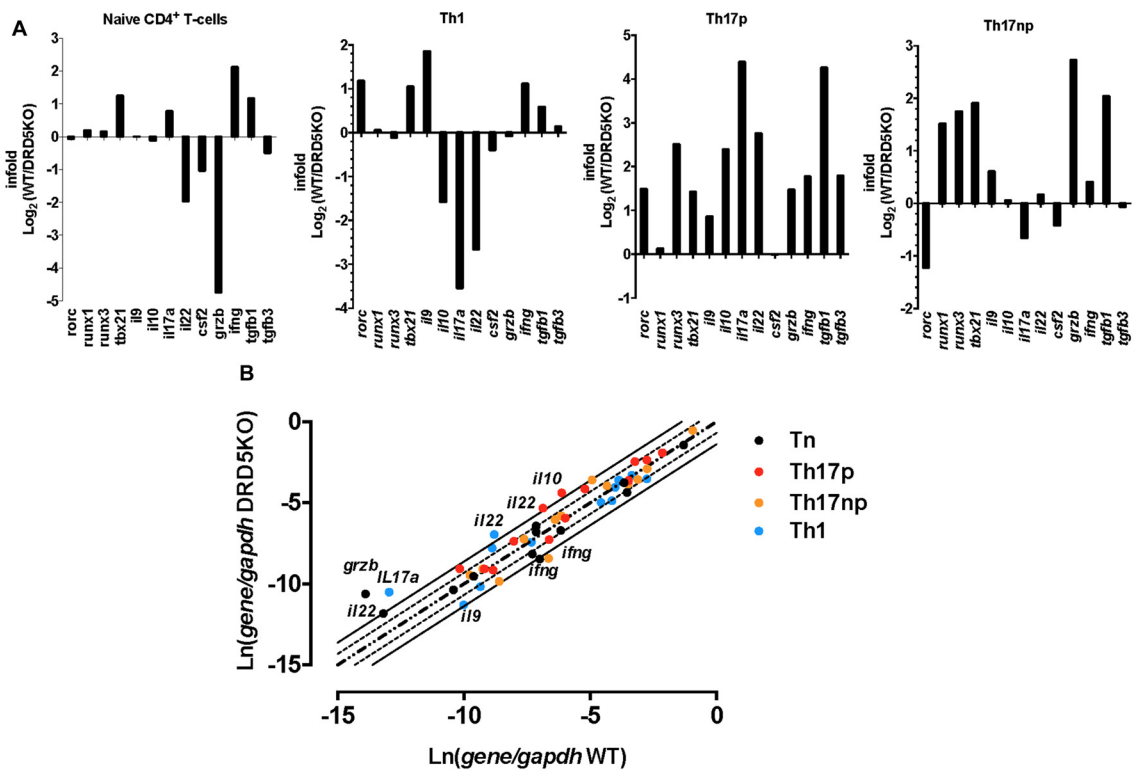

FIGURE 4 | DRD5-deficiency alters the transcriptional pattern of different effector phenotypes of CD4$^+$ T-cells. Splenic naive (CD4$^+$ CD62L$^+$ CD44$^-$CD25$^-$) T-cell were isolated from WT or DRD5KO mice by cell-sorting and immediately analyzed (Tn) or stimulated with anti-CD3 and anti-CD28 Abs in the presence of biased conditions to differentiate to Th1, Th17p or Th17np for 5 days and then analyzed. Afterward, total RNA was extracted and the transcription of a panel of relevant genes was analyzed by qRT-PCR. *Gapdh* transcription was used as house keeping. **(A)** Data represented as infold (WT relative to DRD5KO) indicating how many times the levels of mRNA obtained in WT duplicates those obtained in DRD5KO. **(B)** Data represented as Ln of mRNA levels/house keeping (WT vs. DRD5KO). Central diagonal dotted line indicates same mRNA levels. External dotted lines indicate 2-fold mRNA levels and external solid lines indicate 4-fold mRNA levels. **(A,B)** Values are the mean from three independent experiments.

$CD62L^+$ T-cells into DRD5KO mice completely rescues the phenotype on EAE manifestation (**Figure 1D**), we next wondered whether DRD5-signaling plays a relevant role in the Tregs ($CD25^{high}$ $CD4^+$) response. To address this question, we first determined the effect of DRD5-signaling in the suppressive activity of Tregs. For this purpose, we performed *in vitro* assays in which WT naive OT-II $CD4^+$ T-cells (Teff) were loaded with CFSE, activated with OVA-loaded DCs and co-incubated with increasing concentrations of DRD5-defficient or DRD5-sufficient OT-II Tregs and the extent of inhibition of Teff proliferation was quantified. The results show that DRD5-sufficient Tregs exert a stronger inhibition of Teff proliferation than that exerted by DRD5-defficient Tregs (**Figures 5A,B**), thus indicating that DRD5-signaling favors a stronger suppressive activity by Tregs. To evaluate whether DRD5-signaling in Tregs plays a relevant role in the suppressive activity *in vivo*, we next performed experiments in which DRD5-sufficient or DRD5-defficient Tregs were transferred into WT recipient mice just before EAE induction. In the same direction of conclusions obtained from *in vitro* experiments (**Figures 5A,B**), these results show that EAE severity was reduced by DRD5-sufficient Tregs in a higher extent than that exerted by DRD5-defficient Tregs (**Figure 5C**), thus indicating that DRD5-signaling in Tregs favors a more potent suppressive activity *in vivo*. It is noteworthy that there was not differences in the extent of attenuation of EAE manifestation exerted by DRD5-sufficient and DRD5-defficient Tregs until late stages (after day 15 post-induction) in the time-course of EAE development, indicating that DRD5-signaling in Tregs was relevant only in late stages of EAE manifestation. To gain insight in the mechanism of how DRD5-signaling favors the suppressive activity of Tregs, we next evaluated the transcriptional level of the main cytokines associated to Tregs function, IL-10 and TGF-β, however we did not find any difference between DRD5-sufficient and DRD5-defficient Tregs (**Figure 5D**). To confirm whether IL-10 production was not affected by DRD5-signaling in Tregs we also analyzed the extent of IL-10 production at the level of protein and we found no differences between WT and knockout cells (Supplementary Figure S4). To further explore how DRD5-signaling potentiates the suppressive activity of Tregs, we next evaluated the level of protein expression of a panel of surface molecules and

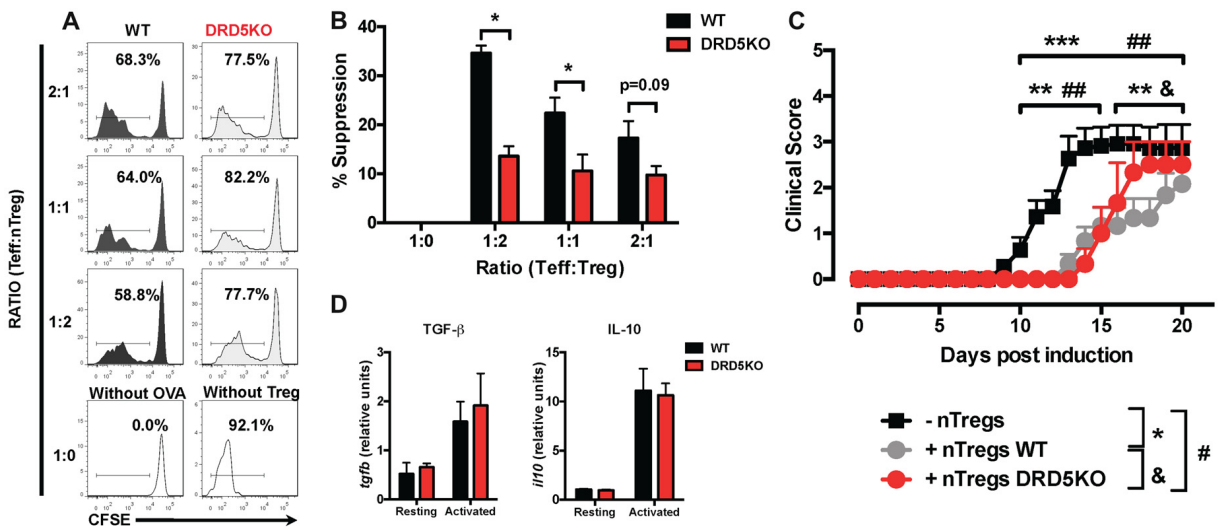

FIGURE 5 | DRD5-signaling in Tregs favors their suppressive activity *in vitro* and *in vivo*. **(A,B)** Splenic $CD4^+$ $CD25^-$ T-cells (Teff) were isolated from WT/OT-II mice by cell-sorting, stained with 5 μM CFSE and then co-cultured with splenic DCs isolated from WT mice by positive $CD11c^+$ selection using magnetic beads based kit (MACS) at a ratio of CD4+ T-cells:DCs = 5:1, in the presence of OVA (5 μM) for 5 days. Splenic $CD4^+$ $CD25^{high}$ T-cells (nTregs) were isolated from WT/OT-II or DRD5KO/OT-II mice by cell-sorting and added to the co-cultures at indicated ratios. **(A)** Representative histograms of CFSE-associated fluorescence vs. number of cells (events) in the $CD4^+$ TCR-Va2$^+$ TCR-Vβ5$^+$ gate are shown. Markers delimiting proliferating cells are indicated. Percentage of $CD4^+$ T-cells in the region of proliferating cells are indicated. **(B)** Percentages of suppression of Teff proliferation from three independent experiments are represented in the bars graphs. One-hundred percent proliferation corresponds to the extent of proliferation of Teffs in the absence of nTregs (positive control). % Suppression is calculated as 100% proliferation (from positive control) minus % proliferation observed for each sample. Values represent mean ± SEM. *$p < 0.05$ by unpaired Student's *t*-test. **(C)** Splenic $CD4^+$ $CD25^{high}$ T-cells (nTregs) were isolated from WT (gray symbols) or DRD5KO (red symbols) mice by cell-sorting and i.v. transferred into WT recipient mice (7×10^5 cells per mouse). One-day later, EAE was induced by immunization with pMOG in CFA followed by *Pertussis* Toxin injection and disease severity was daily determined throughout the time-course of disease development. EAE was also induced in untransferred WT (black symbols) as a control group. Values represent mean ± SEM with n = 3–12 mice per group. $^{\#\#}p < 0.01$ untransferred WT vs. DRD5KO nTregs transferred into WT mice; $^{**}p < 0.01$ and $^{***}p < 0.001$ untransferred WT vs. WT nTregs transferred into WT mice; $^{\&}p < 0.05$ WT nTregs transferred into WT mice vs. DRD5KO nTregs transferred into WT mice by Mann-Whitney *U*-test. **(D)** Splenic $CD4^+$ $CD25^{high}$ T-cells (nTregs) were isolated from WT or DRD5KO mice by cell-sorting and immediately analyzed (resting) or activated with anti-CD3 and anti-CD28 antibodies in the presence of IL-2 for 36 h (activated). Afterward, total RNA was extracted and the levels of transcripts for TGF-β and IL-10 were quantified by real time RT-PCR. Data is represented as the levels of transcripts relative to the house-keeping *gapdh*. Values represent mean ± SD from at least three independent experiments. No significant differences were found between different genotypes.

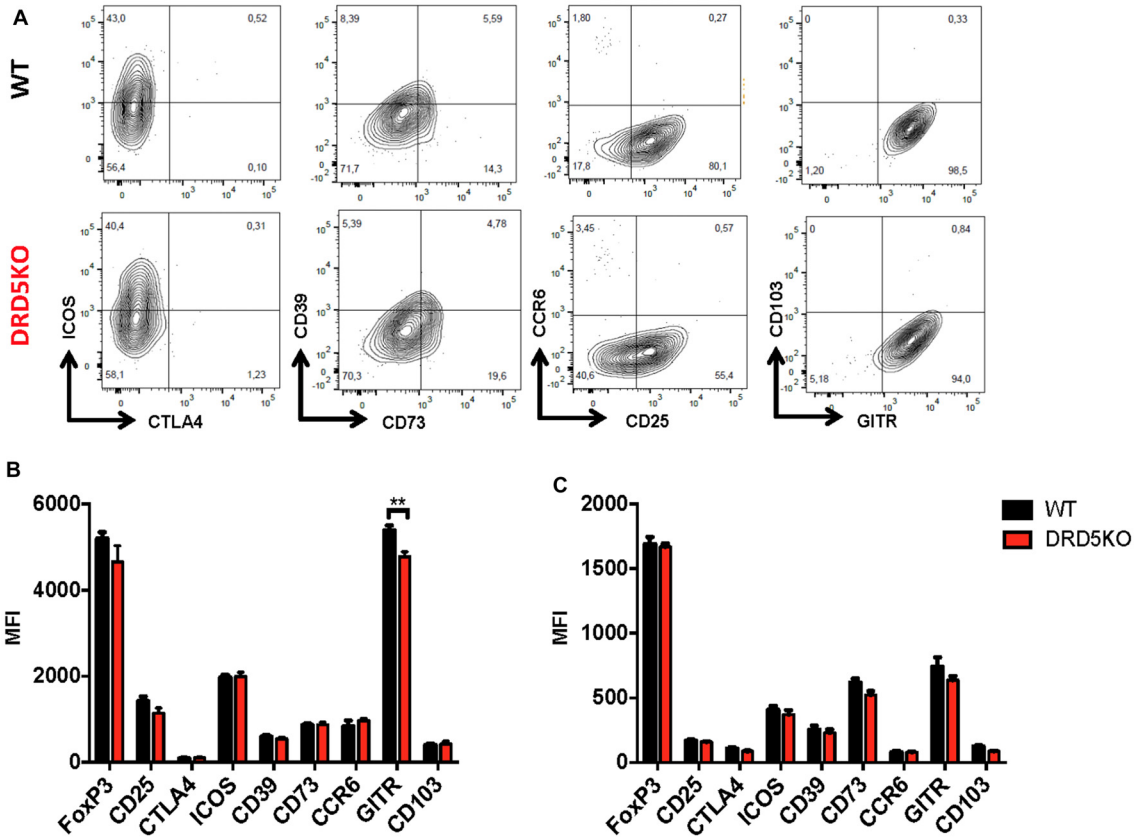

FIGURE 6 | DRD5-signaling favors glucocorticoid-induced tumor necrosis factor receptor-related protein (GITR) expression in Tregs. Splenic $CD4^+$ $CD25^{high}$ T-cells (nTregs) were isolated from WT or DRD5KO mice by cell-sorting and immediately analyzed (resting) or activated with anti-CD3 and anti-CD28 antibodies in the presence of IL-2 for 36 h (activated). Cells were immunostained for a panel of surface markers associated to Tregs function, then permeabilized and immunostained for Foxp3 and analyzed by flow cytometry. **(A)** Representative dot plots are shown. Percentage of cells in each quadrant associated to immunostaining of each molecule is indicated. Data from activated **(B)** and resting **(C)** Tregs are represented as MFI. Values represent mean ± SD from at least four independent experiments. $^{**}p < 0.01$ by unpaired Student's *t*-test.

transcription factor associated with the suppressive activity of Tregs. The results show that the only difference detected between DRD5-sufficient and DRD5-defficient Tregs was that DRD5-deficiency results in a significant reduction in the expression of GITR (**Figures 6A,B**), a molecule that has been related with the expansion of Tregs (Ronchetti et al., 2015). Of note, this difference in GITR expression was observed only in activated Tregs (**Figure 6B**), but not in resting conditions (**Figure 6C**). Thus, these results together indicate that DRD5-signaling in Tregs plays a relevant role favoring Tregs-mediated suppressive response, an effect that would be exerted at least in part by increasing the expression of GITR.

DISCUSSION

Our findings here described represent the first genetic evidence indicating a relevant role of DRD5-signaling in the $CD4^+$ T-cell response involved in EAE. Interestingly these findings suggest a dual role of DRD5-signaling, which are manifested at different stages during the time-course of EAE development and trigger opposite outcomes. Whereas the stimulation of DRD5 in naive $CD4^+$ T-cells potentiates the inflammatory Th17-driven response early after the onset of the disease, DRD5-signaling in Tregs favors the suppressive activity of these cells dampening inflammation just once the peak of disease manifestation has been reached. Thus, these findings contribute to a better understanding of the complex regulation of the $CD4^+$ T-cell driven autoimmune response involved in EAE and also illustrate how depending on the timing and on the precise T-cell subset, neuroimmune communications may exert different outcomes.

In a previous study, we showed genetic and pharmacologic evidence indicating that DRD5-signaling in $CD4^+$ T-cells favored T-cell activation *in vitro*, a process that was mediated by ERK1/2 phosphorylation (Franz et al., 2015). In the same study we appreciated that DRD5-signaling in $CD4^+$ T-cells had no effect in the process of Th1 differentiation *in vitro*. According with this previous study, our present results indicate that DRD5-signaling is relevant *in vivo* favoring T-cell activation (**Figure 2**) and without effect in the acquisition

of the Th1 phenotype (**Figure 3**). Moreover, in agreement with our results about the role of DRD5-signaling in the effector $CD4^+$ T-cell response *in vivo*, previous studies have shown pharmacologic evidence suggesting that the systemic antagonism of type I DRs attenuates the potency of Th17-driven responses (Nakano et al., 2008, 2011; Hashimoto et al., 2009; Okada et al., 2009; Nakagome et al., 2011; Nakashioya et al., 2011). In this regard, the systemic administration of the type I DRs antagonist SCH23390 reduces the clinical manifestation of EAE in mice immunized with a peptide derived from myelin proteolipid protein (Nakano et al., 2008). Similarly, subsequent studies showed that the same drug attenuates the inflammatory response in collagen-induced arthritis (Nakano et al., 2011; Nakashioya et al., 2011), allergic asthma (Nakagome et al., 2011; Gong et al., 2013), diabetes (Hashimoto et al., 2009) and nephrotoxic serum nephritis (Okada et al., 2009). Mechanistic analyses suggested that the therapeutic effect exerted by SCH23390 in these inflammatory disorders is due to the type I DRs antagonism in both $CD4^+$ T-cells and DCs. Addressing the molecular mechanism involved in type I DRs signaling in $CD4^+$ T-cells, the evidence suggests that type I DRs stimulation promotes B-cell activating transcription factor activity, favoring RORγt up-regulation and consequently Th17-mediated responses, which is inhibited by SCH23390 (Gong et al., 2013). Nevertheless, the pharmacologic approach used in all those studies does not allow the discrimination between the effects mediated by DRD5 or DRD1 since the drug inhibits both type I DRs with similar affinities (Bourne, 2001). Here we present genetic evidence indicating an important role of DRD5-signaling in promoting the acquisition of Th17 inflammatory phenotype *in vivo* (**Figure 3**).

Two previous studies have addressed the role of dopaminergic regulation of Tregs function (Kipnis et al., 2004; Cosentino et al., 2007). In apparent controversy with the present work, the studies carried out by Kipnis et al. (2004) and Cosentino et al. (2007) indicated that type I DRs stimulation attenuates Tregs suppressive activity by using a pharmacologic approach. Nonetheless, these studies were performed with drugs that cannot discriminate between their effects mediated by DRD1 or DRD5, as those drugs display very similar affinities for both receptors (Kipnis et al., 2004; Cosentino et al., 2007). Thus, it is likely that the inhibitory effect of dopamine or dopaminergic analogs on Tregs activity appreciated in those studies was mediated by DRD1 rather than DRD5. Here, we show genetic evidence indicating unequivocally that DRD5-deficiency in Tregs results in impaired suppressive activity of these cells *in vitro* and *in vivo* (**Figure 5**).

With these results in mind arise the question of where and when dopamine is relevant as a source available for $CD4^+$ T-cells. In this regard, relevant sources of dopamine have been described in secondary lymphoid organs, the organs where T-cell responses are initiated, as well as in some target organs, where effector $CD4^+$ T-cells promote inflammation. For instance, secondary lymphoid organs such as lymph nodes and the spleen are highly innervated by sympathetic fibers immunoreactive for dopamine (Weihe et al., 1991; Haskó and Szabó, 1998). In this way, the peripheral nervous system might exert regulation of the initiation of T-cell responses (Ben-Shaanan et al., 2016). According to this possibility, the present results (**Figures 2**, **3**) and previous studies (Pacheco et al., 2014) suggest that dopamine produced in draining lymph nodes shapes the expansion and differentiation of naive $CD4^+$ T-cells toward the different functional T-cell phenotypes. In addition to the sympathetic fibers, DCs and follicular helper T-cells (T_{FH}) may also represent important sources of dopamine in secondary lymphoid organs. Indeed, we have recently described how dopamine contained in DCs plays an important role potentiating Th1 and Th17 responses involved in EAE (Prado et al., 2012, 2018). Furthermore, Papa et al. (2017) recently described how T_{FH} produce high amounts of dopamine and release it upon cognate interaction with B-cells in the germinal center, thus accelerating the production of high-affinity antibodies by plasma-cells. Thereby, dopamine produced in different specific locations inside secondary lymphoid organs might strengthen the initiation and development of adaptive immunity. With regard to the organs target of inflammation as potential relevant sources of dopamine for regulation of effector $CD4^+$ T-cell response, altered levels of dopamine in different structures of the brain have been associated with neuroinflammation involved in some neurodegenerative disorders. For instance, dopamine levels have been found to be dramatically reduced in the nigrostriatal pathway of Parkinson's disease patients as well as in animal models of this disorder (Ehringer and Hornykiewicz, 1960; Brochard et al., 2009). We have previously suggested that this pathologic reduction in dopamine levels results in the selective stimulation of the DR displaying the highest affinity for dopamine, the DRD3 (Pacheco, 2017). In this regard, we have previously found that DRD3-signaling triggers a strong inflammatory behavior of $CD4^+$ T-cells that infiltrate the brain in an animal model of Parkinson's diseases favoring the neurodegenerative process in the nigrostriatal pathway (González et al., 2013). On the other hand, EAE, the animal model used here to study MS and the autoimmune response associated, involves an increase of dopamine levels in the striatum during the peak of the disease (Balkowiec-Iskra et al., 2007). Since we observed a role of DRD5 in Tregs only once the peak of EAE manifestation has been reached, our results here suggest that the increase of striatal dopamine would be relevant stimulating DRD5 in Tregs, thus favoring their suppressive activity and dampening disease manifestation (**Figure 5**). Another potential source of dopamine present in the tissues target of inflammation may be Tregs. According to this idea, Tregs represent an important $CD4^+$ T-cell subset infiltrating the brain and spinal cord during late stages of EAE manifestation, which is associated with the recovery phase of the disease (Petermann et al., 2010). Moreover, these cells have been described to synthesize and store important amounts of dopamine, which can be released upon treatment with reserpine (Cosentino et al., 2007). Despite the endogenous stimulus triggering dopamine release from Tregs has not been found yet, IFN-β has been proposed as a plausible candidate (Cosentino et al., 2012). Taken together these studies suggest

that dopamine produced in the secondary lymphoid organs may strengthen the initial development of adaptive immune responses, whilst dopamine present in the inflamed target tissue may shape the effector and suppressive T-cell response depending in the timing and in the precise levels of available dopamine.

Interestingly, not only the CNS may represent a target tissue of inflammation with relevant sources of dopamine, but also the gut mucosa. In this regard, the gut mucosa has been found to be a major source of dopamine in healthy conditions, a source that is strongly reduced upon inflammation (Magro et al., 2002, 2004; Asano et al., 2012). Previous evidence has suggested that in healthy conditions high dopamine levels in the gut promote the stimulation of the low affinity DRs, specially the DRD2, whilst under inflammatory conditions low dopamine levels favors the selective stimulation of DRD3 (Pacheco, 2017). Furthermore, whereas DRD3-stimulation has been shown to promote pro-inflammatory $CD4^+$ T-cell responses in the gut mucosa, including Th1 and Th17-driven immunity (Contreras et al., 2016), DRD2-signaling has been associated with anti-inflammatory effects (Pacheco et al., 2014). Indeed, a genetic polymorphism of DRD2 gene, which results in decreased receptor expression, has been reported as a risk factor for inflammatory bowel diseases (Magro et al., 2006). Accordingly, although the frequency of Tregs was not changed in the gut, suppressive activity of intestinal Tregs was compromised in inflammatory colitis (Wu et al., 2014), a condition associated to decreased dopamine levels (Magro et al., 2004). Interestingly, the impairment of suppressive Tregs function was abolished by the administration of cabergoline, a DRD2 agonist (Wu et al., 2014). Thus, these results together suggest that, whereas DRD2-signaling in Tregs promotes suppressive function in a healthy gut mucosa containing high dopamine levels, the selective DRD3-signaling in the inflamed gut mucosa containing low dopamine levels favors the inflammatory potential of effector $CD4^+$ T-cells promoting further inflammation.

It is noteworthy that one of the main sources of dopamine present in the gut mucosa is given by the commensal gut microbiota. In this regard, it has been described that most dopamine arrives to the gut mucosa as glucuronide conjugated, which is biologically inactive. Nevertheless, *Clostridium* species present in the gut microbiota express β-glucuronidase activity, which catalyzes the production of free dopamine in the gut mucosa (Asano et al., 2012). In addition, recent studies have shown *in vitro* evidence indicating that some components of gut microbiota, including *Bacillus cereaus, Bacillus mycoides, Bacillus subtilis, Proteus vulgaris, Serratia marcescens, S. aureus, E. coli K-12, Morganella morganii, Klebisella pneumoniae and Hafnia alvei*, can also produce dopamine (Clark and Mach, 2016). Of note, a recent study performed with 34 monozygotic twin pairs discordant for MS has shown that when microbiota from the MS twin is transplanted into a transgenic mouse model of spontaneous brain autoimmunity, mice developed autoimmunity with higher incidence than when transplanted with microbiota coming from the healthy twin (Berer et al., 2017). Importantly, when mice were transplanted with microbiota obtained from MS twins, immune cells present in the gut mucosa produced significantly lower levels of the anti-inflammatory cytokine IL-10 than those immune cells of animals receiving microbiota coming from healthy twins. In addition, the analysis in the composition of gut microbiota shows clear differences between healthy and MS twins (Berer et al., 2017). Taken together, these findings indicate that gut microbiota, which can strongly regulate dopamine levels present in the gut mucosa, constitutes a pivotal factor in the control of gut inflammation and in the triggering of MS.

AUTHOR CONTRIBUTIONS

RP designed the study and wrote the manuscript. FO-B, CP and FC conducted experiments and acquired data. FO-B, CP, FC and RP analyzed data.

FUNDING

This work was supported by grants FONDECYT-1170093 (to RP) and FONDECYT-3160383 (to CP) from "Fondo Nacional de Desarrollo Científico y Tecnológico de Chile", AFB170004 (to RP) from "Comisión Nacional de Investigación Científica y Tecnológica de Chile (CONICYT)" and DI-1224-16/R (to RP) from Universidad Andres Bello.

ACKNOWLEDGMENTS

We thank Dr. David Sibley for donation of DRD5KO mice and Dr. María Rosa Bono for providing OT-II and B6.SJL-*Ptprc*^{a} (*cd45.1*$^{+/+}$) mice. We also thank Dr. Sebastián Valenzuela for his valuable veterinary assistance in our animal facility and María José Fuenzalida for her technical assistance in cell-sorting.

SUPPLEMENTARY MATERIAL

The Supplementary Material for this article can be found online at: https://www.frontiersin.org/articles/10.3389/fncel.2018.00192/full#supplementary-material

REFERENCES

Asano, Y., Hiramoto, T., Nishino, R., Aiba, Y., Kimura, T., Yoshihara, K., et al. (2012). Critical role of gut microbiota in the production of biologically active, free catecholamines in the gut lumen of mice. *Am. J. Physiol. Gastrointest Liver Physiol.* 303, G1288–G1295. doi: 10.1152/ajpgi.00341.2012

Balkowiec-Iskra, E., Kurkowska-Jastrzebska, I., Joniec, I., Ciesielska, A., Czlonkowska, A., and Czlonkowski, A. (2007). Dopamine, serotonin and noradrenaline changes in the striatum of C57BL mice following myelin oligodendrocyte glycoprotein (MOG) 35–55 and complete Freund adjuvant (CFA) administration. *Acta Neurobiol. Exp.* 67, 379–388.

Ben-Shaanan, T. L., Azulay-Debby, H., Dubovik, T., Starosvetsky, E., Korin, B., Schiller, M., et al. (2016). Activation of the reward system boosts innate and adaptive immunity. *Nat. Med.* 22, 940–944. doi: 10.1038/nm.4133

Berer, K., Gerdes, L. A., Cekanaviciute, E., Jia, X., Xiao, L., Xia, Z., et al. (2017). Gut microbiota from multiple sclerosis patients enables spontaneous autoimmune

encephalomyelitis in mice. *Proc. Natl. Acad. Sci. U S A* 114, 10719–10724. doi: 10.1073/pnas.1711233114

Bourne, J. A. (2001). SCH 23390: the first selective dopamine D1-like receptor antagonist. *CNS Drug Rev.* 7, 399–414. doi: 10.1111/j.1527-3458.2001.tb00207.x

Brochard, V., Combadiere, B., Prigent, A., Laouar, Y., Perrin, A., Beray-Berthat, V., et al. (2009). Infiltration of $CD4^+$ lymphocytes into the brain contributes to neurodegeneration in a mouse model of Parkinson disease. *J. Clin. Invest.* 119, 182–192. doi: 10.1172/JCI36470

Clark, A., and Mach, N. (2016). Exercise-induced stress behavior, gut-microbiota-brain axis and diet: a systematic review for athletes. *J. Int. Soc. Sports Nutr.* 13:43. doi: 10.1186/s12970-016-0155-6

Contreras, F., Prado, C., González, H., Franz, D., Osorio-Barrios, F., Osorio, F., et al. (2016). Dopamine receptor D3 signaling on $CD4^+$ T cells favors Th1- and Th17-mediated immunity. *J. Immunol.* 196, 4143–4149. doi: 10.4049/jimmunol.1502420

Cosentino, M., Fietta, A. M., Ferrari, M., Rasini, E., Bombelli, R., Carcano, E., et al. (2007). Human $CD4^+CD25^+$ regulatory T cells selectively express tyrosine hydroxylase and contain endogenous catecholamines subserving an autocrine/paracrine inhibitory functional loop. *Blood* 109, 632–642. doi: 10.1182/blood-2006-01-028423

Cosentino, M., Zaffaroni, M., Trojano, M., Giorelli, M., Pica, C., Rasini, E., et al. (2012). Dopaminergic modulation of CD4+CD25 regulatory T lymphocytes in multiple sclerosis patients during interferon-β therapy. *Neuroimmunomodulation* 19, 283–292. doi: 10.1159/000336981

Dardalhon, V., Korn, T., Kuchroo, V. K., and Anderson, A. C. (2008). Role of Th1 and Th17 cells in organ-specific autoimmunity. *J. Autoimmun.* 31, 252–256. doi: 10.1016/j.jaut.2008.04.017

Ehringer, H., and Hornykiewicz, O. (1960). Distribution of noradrenaline and dopamine (3-hydroxytyramine) in the human brain and their behavior in diseases of the extrapyramidal system. *Klin. Wochenschr.* 38, 1236–1239. doi: 10.1007/BF01485901

Fernández, D., Flores-Santibáñez, F., Neira, J., Osorio-Barrios, F., Tejón, G., Nunez, S., et al. (2016). Purinergic signaling as a regulator of Th17 cell plasticity. *PLoS One* 11:e0157889. doi: 10.1371/journal.pone.0157889

Franz, D., Contreras, F., González, H., Prado, C., Elgueta, D., Figueroa, C., et al. (2015). Dopamine receptors D3 and D5 regulate $CD4^+$T-cell activation and differentiation by modulating ERK activation and cAMP production. *J. Neuroimmunol.* 284, 18–29. doi: 10.1016/j.jneuroim.2015.05.003

Gong, S., Li, J., Ma, L., Li, K., Zhang, L., Wang, G., et al. (2013). Blockade of dopamine D1-like receptor signaling protects mice against OVA-induced acute asthma by inhibiting B-cell activating transcription factor signaling and Th17 function. *FEBS J.* 280, 6262–6273. doi: 10.1111/febs.12549

González, H., Contreras, F., Prado, C., Elgueta, D., Franz, D., Bernales, S., et al. (2013). Dopamine receptor D3 expressed on $CD4^+$ T cells favors neurodegeneration of dopaminergic neurons during Parkinson's disease. *J. Immunol.* 190, 5048–5056. doi: 10.4049/jimmunol.1203121

Haines, C. J., Chen, Y., Blumenschein, W. M., Jain, R., Chang, C., Joyce-Shaikh, B., et al. (2013). Autoimmune memory T helper 17 cell function and expansion are dependent on interleukin-23. *Cell Rep.* 3, 1378–1388. doi: 10.1016/j.celrep.2013.03.035

Hashimoto, K., Inoue, T., Higashi, T., Takei, S., Awata, T., Katayama, S., et al. (2009). Dopamine D1-like receptor antagonist, SCH23390, exhibits a preventive effect on diabetes mellitus that occurs naturally in NOD mice. *Biochem. Biophys. Res. Commun.* 383, 460–463. doi: 10.1016/j.bbrc.2009.04.034

Haskó, G., and Szabó, C. (1998). Regulation of cytokine and chemokine production by transmitters and co-transmitters of the autonomic nervous system. *Biochem. Pharmacol.* 56, 1079–1087. doi: 10.1016/s0006-2952(98)00153-1

Hollon, T. R., Bek, M. J., Lachowicz, J. E., Ariano, M. A., Mezey, E., Ramachandran, R., et al. (2002). Mice lacking D5 dopamine receptors have increased sympathetic tone and are hypertensive. *J. Neurosci.* 22, 10801–10810. doi: 10.1523/JNEUROSCI.22-24-10801.2002

Inaba, K., Inaba, M., Romani, N., Aya, H., Deguchi, M., Ikehara, S., et al. (1992). Generation of large numbers of dendritic cells from mouse bone marrow cultures supplemented with granulocyte/macrophage colony-stimulating factor. *J. Exp. Med.* 176, 1693–1702. doi: 10.1084/jem.176.6.1693

Kim, C., Ho, D. H., Suk, J. E., You, S., Michael, S., Kang, J., et al. (2013). Neuron-released oligomeric α-synuclein is an endogenous agonist of TLR2 for paracrine activation of microglia. *Nat. Commun.* 4:1562. doi: 10.1038/ncomms2534

Kim, D. H., Sandoval, D., Reed, J. A., Matter, E. K., Tolod, E. G., Woods, S. C., et al. (2008). The role of GM-CSF in adipose tissue inflammation. *Am. J. Physiol. Endocrinol. Metab.* 295, E1038–E1046. doi: 10.1152/ajpendo.00061.2008

Kipnis, J., Cardon, M., Avidan, H., Lewitus, G. M., Mordechay, S., Rolls, A., et al. (2004). Dopamine, through the extracellular signal-regulated kinase pathway, downregulates $CD4^+CD25^+$ regulatory T-cell activity: implications for neurodegeneration. *J. Neurosci.* 24, 6133–6143. doi: 10.1523/JNEUROSCI.0600-04.2004

Lee, Y., Awasthi, A., Yosef, N., Quintana, F. J., Xiao, S., Peters, A., et al. (2012). Induction and molecular signature of pathogenic TH17 cells. *Nat. Immunol.* 13, 991–999. doi: 10.1038/ni.2416

Li, P., Zheng, S. J., Jiang, C. H., Zhou, S. M., Tian, H. J., Zhang, G., et al. (2014). Th2 lymphocytes migrating to the bone marrow under high-altitude hypoxia promote erythropoiesis via activin A and interleukin-9. *Exp. Hematol.* 42, 804–815. doi: 10.1016/j.exphem.2014.04.007

Logan, T. T., Villapol, S., and Symes, A. J. (2013). TGF-β superfamily gene expression and induction of the Runx1 transcription factor in adult neurogenic regions after brain injury. *PLoS One* 8:e59250. doi: 10.1371/journal.pone.0059250

Magro, F., Cunha, E., Araujo, F., Meireles, E., Pereira, P., Dinis-Ribeiro, M., et al. (2006). Dopamine D2 receptor polymorphisms in inflammatory bowel disease and the refractory response to treatment. *Dig. Dis. Sci.* 51, 2039–2044. doi: 10.1007/s10620-006-9168-3

Magro, F., Fraga, S., Ribeiro, T., and Soares-da-Silva, P. (2004). Decreased availability of intestinal dopamine in transmural colitis may relate to inhibitory effects of interferon-γ upon L-DOPA uptake. *Acta Physiol. Scand.* 180, 379–386. doi: 10.1111/j.1365-201x.2004.01260.x

Magro, F., Vieira-Coelho, M. A., Fraga, S., Serrão, M. P., Veloso, F. T., Ribeiro, T., et al. (2002). Impaired synthesis or cellular storage of norepinephrine, dopamine, and 5-hydroxytryptamine in human inflammatory bowel disease. *Dig. Dis. Sci.* 47, 216–224. doi: 10.1023/A:1013256629600

Nakagome, K., Imamura, M., Okada, H., Kawahata, K., Inoue, T., Hashimoto, K., et al. (2011). Dopamine D1-like receptor antagonist attenuates Th17-mediated immune response and ovalbumin antigen-induced neutrophilic airway inflammation. *J. Immunol.* 186, 5975–5982. doi: 10.4049/jimmunol.1001274

Nakano, K., Higashi, T., Hashimoto, K., Takagi, R., Tanaka, Y., and Matsushita, S. (2008). Antagonizing dopamine D1-like receptor inhibits Th17 cell differentiation: preventive and therapeutic effects on experimental autoimmune encephalomyelitis. *Biochem. Biophys. Res. Commun.* 373, 286–291. doi: 10.1016/j.bbrc.2008.06.012

Nakano, K., Higashi, T., Takagi, R., Hashimoto, K., Tanaka, Y., and Matsushita, S. (2009). Dopamine released by dendritic cells polarizes Th2 differentiation. *Int. Immunol.* 21, 645–654. doi: 10.1093/intimm/dxp033

Nakano, K., Yamaoka, K., Hanami, K., Saito, K., Sasaguri, Y., Yanagihara, N., et al. (2011). Dopamine induces IL-6-dependent IL-17 production via D1-like receptor on CD4 naive T cells and D1-like receptor antagonist SCH-23390 inhibits cartilage destruction in a human rheumatoid arthritis/SCID mouse chimera model. *J. Immunol.* 186, 3745–3752. doi: 10.4049/jimmunol.1002475

Nakashioya, H., Nakano, K., Watanabe, N., Miyasaka, N., Matsushita, S., and Kohsaka, H. (2011). Therapeutic effect of D1-like dopamine receptor antagonist on collagen-induced arthritis of mice. *Mod. Rheumatol.* 21, 260–266. doi: 10.1007/s10165-010-0387-2

O'Connor, R. A., Cambrook, H., Huettner, K., and Anderton, S. M. (2013). T-bet is essential for Th1-mediated, but not Th17-mediated, CNS autoimmune disease. *Eur. J. Immunol.* 43, 2818–2823. doi: 10.1002/eji.201343689

Okada, H., Inoue, T., Hashimoto, K., Suzuki, H., and Matsushita, S. (2009). D1-like receptor antagonist inhibits IL-17 expression and attenuates crescent formation in nephrotoxic serum nephritis. *Am. J. Nephrol.* 30, 274–279. doi: 10.1159/000225902

Oukka, M. (2008). Th17 cells in immunity and autoimmunity. *Ann. Rheum. Dis.* 67, iii26–iii29. doi: 10.1136/ard.2008.098004

Pacheco, R. (2017). Targeting dopamine receptor D3 signaling in inflammation. *Oncotarget* 8, 7224–7225. doi: 10.18632/oncotarget.14601

Pacheco, R., Contreras, F., and Zouali, M. (2014). The dopaminergic system in autoimmune diseases. *Front. Immunol.* 5:117. doi: 10.3389/fimmu.2014.00117

Papa, I., Saliba, D., Ponzoni, M., Bustamante, S., Canete, P. F., Gonzalez-Figueroa, P., et al. (2017). TFH-derived dopamine accelerates productive synapses in germinal centres. *Nature* 547, 318–323. doi: 10.1038/nature23013

Peng, Y., Gao, X., Yang, J., Shekhar, S., Wang, S., Fan, Y., et al. (2014). Interleukin-22 promotes T helper 1 (Th1)/Th17 immunity in chlamydial lung infection. *Mol. Med.* 20, 109–119. doi: 10.2119/molmed.2013.00115

Petermann, F., Rothhammer, V., Claussen, M. C., Haas, J. D., Blanco, L. R., Heink, S., et al. (2010). γδ T cells enhance autoimmunity by restraining regulatory T cell responses via an interleukin-23-dependent mechanism. *Immunity* 33, 351–363. doi: 10.1016/j.immuni.2010.08.013

Prado, C., Bernales, S., and Pacheco, R. (2013). Modulation of T-cell mediated immunity by dopamine receptor d5. *Endocr. Metab. Immune Disord Drug Targets* 13, 184–194. doi: 10.2174/1871530311313020007

Prado, C., Contreras, F., González, H., Díaz, P., Elgueta, D., Barrientos, M., et al. (2012). Stimulation of dopamine receptor D5 expressed on dendritic cells potentiates Th17-mediated immunity. *J. Immunol.* 188, 3062–3070. doi: 10.4049/jimmunol.1103096

Prado, C., Gaiazzi, M., Gonzalez, H., Ugalde, V., Figueroa, A., Osorio-Barrios, F. J., et al. (2018). Dopaminergic stimulation of myeloid antigen-presenting cells attenuates signal transducer and activator of transcription 3-activation favoring the development of experimental autoimmune encephalomyelitis. *Front. Immunol.* 9:571. doi: 10.3389/fimmu.2018.00571

Reboldi, A., Coisne, C., Baumjohann, D., Benvenuto, F., Bottinelli, D., Lira, S., et al. (2009). C-C chemokine receptor 6-regulated entry of TH-17 cells into the CNS through the choroid plexus is required for the initiation of EAE. *Nat. Immunol.* 10, 514–523. doi: 10.1038/ni.1716

Ronchetti, S., Ricci, E., Petrillo, M. G., Cari, L., Migliorati, G., Nocentini, G., et al. (2015). Glucocorticoid-induced tumour necrosis factor receptor-related protein: a key marker of functional regulatory T cells. *J. Immunol. Res.* 2015:171520. doi: 10.1155/2015/171520

Shao, W., Zhang, S. Z., Tang, M., Zhang, X. H., Zhou, Z., Yin, Y. Q., et al. (2013). Suppression of neuroinflammation by astrocytic dopamine D2 receptors via αB-crystallin. *Nature* 494, 90–94. doi: 10.1038/nature11748

Smeltz, R. B., Wolf, N. A., and Swanborg, R. H. (1999). Inhibition of autoimmune T cell responses in the DA rat by bone marrow-derived NK cells *in vitro*: implications for autoimmunity. *J. Immunol.* 163, 1390–1397.

Ureta, G., Osorio, F., Morales, J., Rosemblatt, M., Bono, M. R., and Fierro, J. A. (2007). Generation of dendritic cells with regulatory properties. *Transplant. Proc.* 39, 633–637. doi: 10.1016/j.transproceed.2006.12.032

Wang, Y., Godec, J., Ben-Aissa, K., Cui, K., Zhao, K., Pucsek, A. B., et al. (2014). The transcription factors T-bet and Runx are required for the ontogeny of pathogenic interferon-γ-producing T helper 17 cells. *Immunity* 40, 355–366. doi: 10.1016/j.immuni.2014.01.002

Weihe, E., Nohr, D., Michel, S., Müller, S., Zentel, H. J., Fink, T., et al. (1991). Molecular anatomy of the neuro-immune connection. *Int. J. Neurosci.* 59, 1–23. doi: 10.3109/00207459108985446

Wu, W., Sun, M., Zhang, H. P., Chen, T., Wu, R., Liu, C., et al. (2014). Prolactin mediates psychological stress-induced dysfunction of regulatory T cells to facilitate intestinal inflammation. *Gut* 63, 1883–1892. doi: 10.1136/gutjnl-2013-306083

Yan, Y., Jiang, W., Liu, L., Wang, X., Ding, C., Tian, Z., et al. (2015). Dopamine controls systemic inflammation through inhibition of NLRP3 inflammasome. *Cell* 160, 62–73. doi: 10.1016/j.cell.2014.11.047

Yin, Y., Wang, G., Liang, N., Zhang, H., Liu, Z., Li, W., et al. (2013). Nuclear export factor 3 is involved in regulating the expression of TGF-β3 in an mRNA export activity-independent manner in mouse Sertoli cells. *Biochem. J.* 452, 67–78. doi: 10.1042/BJ20121006

Conflict of Interest Statement: The authors declare that the research was conducted in the absence of any commercial or financial relationships that could be construed as a potential conflict of interest.

frontiers in Cellular Neuroscience

ORIGINAL RESEARCH
published: 07 August 2018
doi: 10.3389/fncel.2018.00231

The Intracellular Cleavage Product of the NG2 Proteoglycan Modulates Translation and Cell-Cycle Kinetics via Effects on mTORC1/FMRP Signaling

Tanmoyita Nayak[1], *Jacqueline Trotter*[1] *and Dominik Sakry*[1,2]*

[1] *Department of Biology, Molecular Cell Biology, Institute of Developmental Biology and Neurobiology, Johannes Gutenberg University Mainz, Mainz, Germany,* [2] *Department of Molecular Neurobiology, Max Planck Institute for Experimental Medicine, Göttingen, Germany*

The NG2 proteoglycan is expressed by oligodendrocyte precursor cells (OPCs) and is abundantly expressed by tumors such as melanoma and glioblastoma. Functions of NG2 include an influence on proliferation, migration and neuromodulation. Similar to other type-1 membrane proteins, NG2 undergoes proteolysis, generating a large ectodomain, a C-terminal fragment (CTF) and an intracellular domain (ICD) via sequential action of α- and γ-secretases which is enhanced by neuronal activity. Functional roles of NG2 have so far been shown for the full-length protein, the released ectodomain and CTF, but not for the ICD. In this study, we characterized the role of the NG2 ICD in OPC and Human Embryonic Kidney (HEK) cells. Overexpressed ICD is predominantly localized in the cell cytosol, including the distal processes of OPCs. Nuclear localisation of a fraction of the ICD is dependent on Nuclear Localisation Signals. Immunoprecipitation and Mass Spectrometry followed by functional analysis indicated that the NG2 ICD modulates mRNA translation and cell-cycle kinetics. In OPCs and HEK cells, ICD overexpression results in an mTORC1-dependent upregulation of translation, as well as a shift of the cell population toward S-phase. NG2 ICD increases the active (phosphorylated) form of mTOR and modulates downstream signaling cascades, including increased phosphorylation of p70S6K1 and increased expression of eEF2. Strikingly, levels of FMRP, an RNA-binding protein that is regulated by mTOR/p70S6K1/eEF2 were decreased. In neurons, FMRP acts as a translational repressor under activity-dependent control and is mutated in Fragile X Syndrome (FXS). Knock-down of endogenous NG2 in primary OPC reduced translation and mTOR/p70S6K1 phosphorylation in Oli-*neu*. Here, we identify the NG2 ICD as a regulator of translation in OPCs via modulation of the well-established mTORC1 pathway. We show that FXS-related FMRP signaling is not exclusive to neurons but plays a role in OPCs. This provides a signal cascade in OPC

OPEN ACCESS

Edited by:
Marion Baraban,
University of Edinburgh,
United Kingdom

Reviewed by:
Akiko Nishiyama,
University of Connecticut,
United States
Marta Fumagalli,
Università degli Studi di Milano, Italy
Arthur Butt,
University of Portsmouth,
United Kingdom

***Correspondence:**
Dominik Sakry
sakry@em.mpg.de

Received: *15 March 2018*
Accepted: *16 July 2018*
Published: *07 August 2018*

Citation:
Nayak T, Trotter J and Sakry D (2018) The Intracellular Cleavage Product of the NG2 Proteoglycan Modulates Translation and Cell-Cycle Kinetics via Effects on mTORC1/FMRP Signaling. Front. Cell. Neurosci. 12:231. doi: 10.3389/fncel.2018.00231

which can be influenced by the neuronal network, since the NG2 ICD has been shown to be generated by constitutive as well as activity-dependent cleavage. Our results also elucidate a possible role of NG2 in tumors exhibiting enhanced rates of translation and rapid cell cycle kinetics.

Keywords: NG2, ICD, γ-secretase, OPC, FMRP, mTOR, S6K1, eEF2

INTRODUCTION

NG2 (*CSPG4*) is a type-1 membrane protein (300 kD MW), belonging to the chondroitin sulfate proteoglycan protein family with a large extracellular region (290 kD) and a very short intracellular domain (8.5 kD). It was first discovered in the rat nervous system (Stallcup, 1977) and has reported homologs in mouse (Niehaus et al., 1999; Schneider et al., 2001; Stegmüller et al., 2002), human (Pluschke et al., 1996), and Drosophila (Estrada et al., 2007; Schnorrer et al., 2007).

In the nervous system, oligodendrocyte precursor cells (OPC) express the NG2 protein, while neurons (Karram et al., 2008; Clarke et al., 2012), astrocytes (Zhu et al., 2008; Huang et al., 2014) and resident microglia (Moransard et al., 2011) do not. Additionally, a subpopulation of pericytes, cells from the vascular system, also express the NG2 protein (Ozerdem et al., 2002; You et al., 2014; Attwell et al., 2016). NG2 is expressed by many tumor types, including glioblastoma multiform (GBM) and melanoma (Chekenya et al., 2008; Prestegarden et al., 2010; Al-Mayhani et al., 2011), and is thus considered a potential therapeutic target in cancer.

OPCs are a self-renewing, and proliferating cell population found at all stages of development in gray and white matter. In the adult mammalian brain, around 5% of total neural cells comprise the OPC cell population (Dawson et al., 2003). During differentiation of OPCs into myelinating mature oligodendrocytes, NG2 expression is down-regulated (Nishiyama et al., 2009; De Biase et al., 2010; Kukley et al., 2010). NG2+ OPCs are unique as they are the only glial cell population receiving direct synaptic input from neurons (Bergles et al., 2000; Jabs et al., 2005; Kukley et al., 2008; Mangin and Gallo, 2011; Sakry et al., 2011).

Regulated intramembrane proteolysis (RIP) of type-1 membrane proteins involves sequential cleavage by α- and γ-secretases. The action of endogenous α-secretase on the full-length (FL) protein leads to release of the ectodomain into the extracellular matrix, termed as shedding. Subsequent cleavage of the remaining C- terminal fragment (CTF) by the γ-secretase releases the intracellular region into the cytoplasm, the released peptide is a functional unit and therefore termed intracellular domain (ICD), also referred to as the released ICD in the following text (Brown et al., 2000; Lal and Caplan, 2011; Saftig and Lichtenthaler, 2015). Notch was the first-reported, well-characterized membrane-protein undergoing RIP (Levitan and Greenwald, 1995; Blaumueller et al., 1997; De Strooper et al., 1999) and the released Notch ICD exhibits defined cellular functions, acting as a transcription factor (Bailey and Posakony, 1995; Baker and Zitron, 1995). Although release of the NG2 ectodomain had been previously documented (Nishiyama et al., 1995; Deepa et al., 2006), our published work demonstrated that NG2 undergoes RIP, generating a CTF and ICD in OPCs (Sakry et al., 2014, 2015; Sakry and Trotter, 2016). Recently, RIP has been shown for the neuronal CNS proteins neuroligin-1 and N-cadherin (Malinverno et al., 2010; Suzuki et al., 2012). Interestingly, this process is enhanced by neuronal activity, and similarly, we demonstrated that RIP of NG2 was also enhanced by activity (Sakry et al., 2014; **Figure 1A**). Thus, the cleavage and signaling pathways of these membrane proteins can be potentially modulated by the neuronal network.

The intracellular region of NG2 is known to bind to scaffold proteins such as Mupp1, Syntenin and GRIP1(Barritt et al., 2000; Stegmuller et al., 2003; Chatterjee et al., 2008), and protects cell from oxidative stress by binding to OMI/HtrA2 (Maus et al., 2015). It has also been associated with directed migration of OPCs (Binamé et al., 2013) and has a regulatory influence on the expression of the neuromodulator enzyme PTGDS in OPCs (Sakry et al., 2015).

In this study, we focused on basic cellular functions and signaling pathways which are specifically altered by the released NG2 ICD in OPCs. This is especially important because it would directly demonstrate the NG2 ICD is a functional domain. Additionally, NG2 cleavage-dependent pathways in OPCs are potentially regulated by the neuronal network. The NG2 ICD signaling cascade that we describe may be pertinent for other NG2 expressing cell-types, especially tumors.

MATERIALS AND METHODS

Cell Culture

The OPC cell-line, Oli-*neu*, was used as described in Jung et al. (1995). Cells were cultured at 37°C, with 5% CO_2 and expanded in Sato medium containing 1% horse serum [DMEM, with 0.2% (w/v) sodium bicarbonate, 0.01 mg/ml insulin, 0.01 mg/ml transferrin, 220 nm sodium selenite, 100 μm putrescine, 500 nm triiodothyronine, 520 nm thyroxine, and 200 nm progesterone]. HEK 293 (HEK, Invitrogen) cells were cultivated at 37°C in DMEM (Sigma) with 1% pyruvate and 10% FCS with 8% CO_2. For primary OPC (pOPC), single cell suspensions were obtained from total brains of the Postnatal day (P) P6-9 of C57Bl/6N mice using the NTDK-P Kit (Miltenyi Biotec). Magnetic isolation (MACS) was performed as described previously (Diers-Fenger et al., 2001). 300,000 cells were plated in each well of a PLL-coated dish (6-well format) and cultured in OPC proliferation medium. OPC proliferation medium consists of NeuroMACS medium (Miltenyi) supplemented with 1:50 of NeuroBrew Miltenyi, 1:100 of L-Glutamine, 1:100 Pen-strep and 1:1,000 of stock conc.

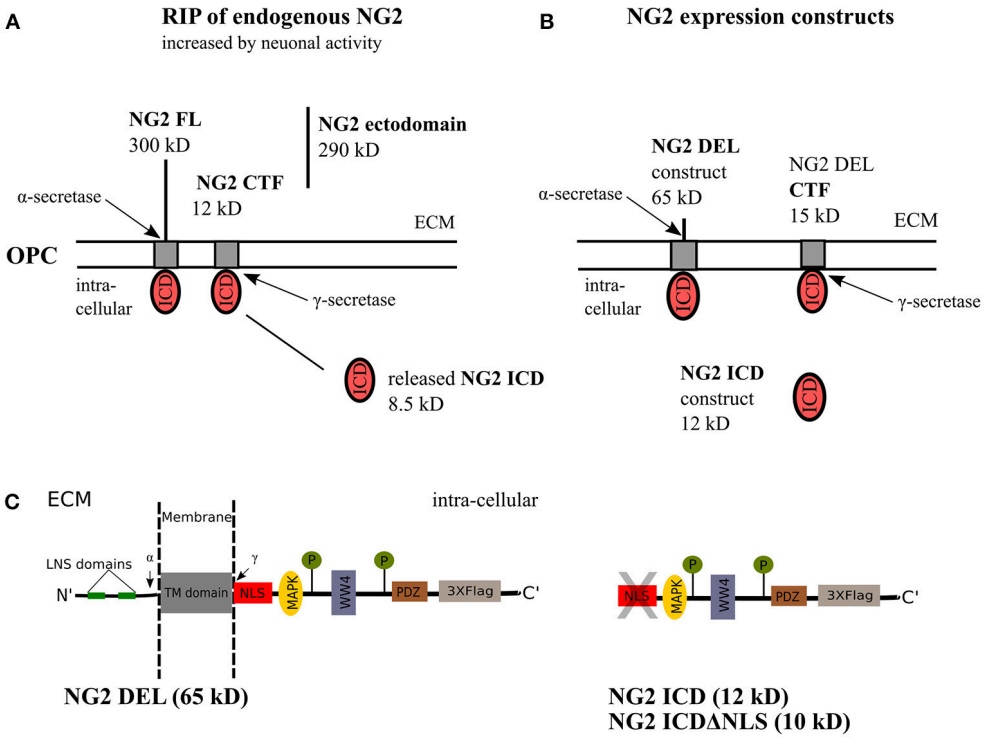

FIGURE 1 | NG2 cleavage and expression constructs. **(A)** In OPCs, NG2 full-length (FL) protein undergoes regulated intramembrane proteolysis (RIP) leading to the release of an ectodomain into the extracellular matrix (ECM) and generation of a c-terminal fragment (CTF) by α-secretase activity. γ-secretase activity on the NG2 CTF releases the NG2 intracellular domain (ICD) into the cytoplasm. This NG2 cleavage happens constitutively in OPCs and can be increased by neuronal activity over Neuron-OPC synaptic innervations (Sakry et al., 2014). **(B)** The NG2 DEL and NG2 ICD expression construct used in this study. NG2 DEL (65 kD) mimics full-length NG2 (300 kD) but comprises one large deletion within the ectodomain, it can be processed by α- and γ-secretases like the FL protein as outlined in **(A)**. The NG2 ICD expression construct mimics released NG2 ICD by γ-secretase. **(C)** Sequence overview of the NG2 DEL, ICD and ICDΔNLS expression construct. The NLS, WW4 and MAPK binding motif have been predicted by an ELM database (elm.eu.org) analysis. The highlighted LNS domains, the two phosphorylation sites, and the PDZ binding motif have distinct cellular functions as described in the introduction.

of each of Forskolin (4.2 mg/ml), CNTF (10 µg/ml), PDGF (10 µg/ml) and NT-3 (1 µg/ml). pOPCs were maintained at 37°C with 8%CO_2. All animal experiments were carried out in strict accordance with protocols approved by local Animal Care and Use Committee of Johannes Gutenberg University of Mainz. Mice were sacrificed by decapitation to remove the brain.

Expression Vectors and Transfection

NG2 expression vectors were derived from pRK5 constructs used in Sakry et al. (2015) by PCR amplification. NG2 DEL expresses a short recombinant version of full-length NG2 (consisting the signal sequence, one-fourth of the extracellular portion including two laminin G-type motifs, a transmembrane domain, and intracellular domain). Two other constructs are expressing only the intracellular domain (NG2 ICD, AA 2251-2327, UniProt: Q8VHY0) and without the predicted Nuclear Localization Signal (NLS) of ICD (NG2 ICDΔNLS, AA 2259–2327). All cDNAs were cloned into the p3X-Flag CMV14 expression vector (c-terminal 3X flag-tag) and used for transfection. Additionally, the H2B-GFP plasmid (gift of Dr. Vijay Tiwari) was co-transfected along with NG2 ICD-Flag expression vector for immunocytochemistry study.

HEK and Oli-*neu* cells were plated 1 day before transfection and transfected using either PEI or Fugene HD reagent (Promega) at a ratio of 1:3 (2 µg DNA: 6 µl Fugene for the 3 cm dish). 48 h after transfection, cells were harvested and processed for analysis.

Primary OPCs were transfected after 1 day *in vitro* (DIV 1) using Lipofectamine RNAiMAX reagent (Thermo Fisher) according to the protocol. 120 pmol siRNA (final concentration) was used per well (6-well format), and the medium was changed 5–6 h after transfection. Cells were processed for analysis at DIV 2.

Cell Lysates, SDS PAGE, and Western Blotting

Cells were washed with PBS and scraped with a rubber policeman into lysis buffer (PBS, 1% TX-100, 1X protease inhibitor (PI) cocktail from Roche) from the culture plate on ice. After incubation for 20 min on the rotor at 4°C, cells were spun down by centrifugation at 1,000 g, 10 min, 4°C. Supernatants were defined as postnuclear (PN) cell-lysates (lysates). The same volume of lysis buffer was used per sample, and all samples were diluted with 4x SDS or LDS (Invitrogen) sample buffer, heated

to 80°C for 10 min and resolved on 4–12% NuPage Bis-Tris gradient gel in combination with MES or MOPS running buffer (Invitrogen). Western blotting (WB) was done with NuPage Blot system utilizing a PVDF membrane (Millipore). The latter was blocked for 30 min in PBS containing 0.1% Tween 20 (PBST) and 4% nonfat milk or 4% BSA.

Blocked membranes were incubated with primary antibodies (AB) overnight at 4°C in blocking solution, followed by three washes (PBST). Subsequently, they were incubated with 1:10,000 HRP-conjugated secondary AB (Dianova) in blocking solution for 1 h and washed for three times again. Signal detection was carried out using enhanced chemiluminescence (ECL) assay solution (Millipore) and hyperfilms (GE). ImageJ 1.46 (NIH) was used for signal quantification, and all protein levels were normalized against GAPDH from the same sample. In some experiments, for checking total loaded protein level, membranes were stained with Ponceau S solution for 5 min on a shaker and later rinsed with deionized water three times for 5 min each.

Sub-cellular Fractionation Assay

For subcellular fractionation, cells were plated 1 day before transfection and transfected with NG2 ICD or ICDΔNLS-Flag plasmids. After 48 h, cells were lysed with cytosolic lysis buffer (1X PBS+ 1% NP-40, 1X PI) on ice for 30 min and centrifuged at 2,000 g for 10 min. Supernatants which were enriched with cytosolic fraction were collected. The pelleted nuclei were further digested with nuclear lysis buffer [20 mM Tris-HCl (pH 7.4), 150 mM NaCl, 10 mM MgCl2, 1% TX-100, 2.5 mM Beta-glycerophosphate, 1 mM NaF, 1 mM DTT, 2 mM EDTA, 10% glycerol 10U of Benzonase, 1X Protease inhibitor cocktail]. for 1 h on a rotor at 4°C. Samples were centrifuged at 7,000 g for 10 min, and the supernatant was collected which comprises nuclear proteins.

Immunoprecipitation (IP) and Mass Spectrometry (MS)

Cells were plated in 100 mm dishes, and at ∼80% confluency were transiently transfected with 8 μg plasmid DNA of ICD and BAP-flag tagged constructs. After 48 h, cells were washed, lysed (1x PBS+ 0.5% TX-100+ 1x protease inhibitor), scraped off and centrifuged (3000 g). Prior to IP, the supernatant was precleared at 12,000 g for 10 min and incubated with anti-flag M2 magnetic beads (Sigma) for 2 h on a rotor at 4°C. The beads were collected and washed three times (with PBS+0.3% TX-100) and heated at 85°C for 10 min with 2X LDL sample buffer. Later, the IPed samples were used for various functional assays (coomassie staining, Mass Spec, CoIP). Mass-spectrometry based analysis of the IPed samples was done by chemical labeling method (DML labeling) in both forward and reverse way (IMB, Mainz). Data was analyzed by Maxquant software where the potential contaminants were removed, and the threshold was set to a minimum of 2X enrichment.

Primary Antibodies

The following antibodies are used for WB, ICC or FC: 1:200 (WB) of rabbit anti-NG2 cyto (Stegmüller et al., 2002), 1:1,000 (WB) of mouse anti-Flag (Sigma, F1804); 1: 200 (FC) of anti-Flag-FITC (Sigma, F4049); 1:1,000 (WB) of rabbit anti-FMRP (Sigma, F4055); 1:1,000 (WB) of rabbit anti-eEF2 antibody (Abcam, ab40812); 1:1,000 (WB) of rabbit anti-eIF4B (CST, 3592T); 1:1,000 (WB) of rabbit anti-phospho (Ser422) eIF4B (CST, 3591S); 1:200 (ICC) of rabbit anti-PCNA (NEB, 13110); 1:1,000 (WB) of mouse anti-Puromycin (Millipore, MABBE343); 1:5,000 (WB) of rabbit anti-GAPDH (Biomol, A-300-641A); 1:400 (WB) of mouse anti-Cyclin E (SCBT, E-4), 1:1,000 (WB) of rabbit anti-p70S6K1 (CST, 9202). For studying mTOR and p70S6K1 phosphorylation, substrate sampler kit (CST, 9862T) was used and the antibody dilutions were made for WB according to kit suggestions.

Immunocytochemistry

Oli-*neu* cells were cultured on poly-L-Lysine coated coverslips, washed with PBS and fixed with 4% PFA for 15 min at RT, washed and permeabilized for 5 min with PBS containing 0.3% TX-100. Blocking was with PBS+10%HS for 30 min at RT. Primary AB incubation was done overnight at 4°C, and secondary antibodies were applied for 30 min at RT. Coverslips were mounted in Moviol. For PCNA staining, cells were washed (1X PBS) and incubated with PBS+ 0.3% Triton-X on ice for 5 min and immediately fixed with acetone: methanol (1:1) solution for 10 min at −20°C. Later, cells were blocked with PBS containing 3% goat serum for 1 h at RT. Primary and secondary AB incubation was done as described above. DAPI (0.1 μg/ml) was added along with secondary antibodies. The following secondary AB were used: goat or donkey anti mouse and anti-rabbit coupled with Alexa488, 546 or 647 (Invitrogen).

Images were taken with a Leica DM6000 fluorescent microscope or an SP5 laser scanning confocal microscope (IMB, Mainz). Image processing was done with Leica LAS AF and ImageJ (NIH), specifically the ImageJ3DViewer. Nuclear morphology of immunostained cells were also analyzed for two indices; area and roundness with ImageJ.

SUnSET Assay

HEK293 and Oli-*neu* cells were transiently transfected with either NG2 ICD or empty flag control vector. After 48 h, cells were incubated with puromycin (10 μg/mL) for 15 min in the culture medium and lysed afterwards for WB as described above. Anisomycin, a translation blocker, was used as a negative control (40 μM final concentration) to confer puromycin incorporation only in active ongoing nascent polypeptide chains. The same protocol was repeated with siCNT, and siNG2 transfected primary OPCs and puromycin incubation was carried out 24 h post-transfection.

In an additional and independent experiment, Oli-*neu* cells were treated with a mTORC1 inhibitor, Temsirolimus (ab141999). Cells, overexpressing control or ICD, were treated with Temsirolimus (TM) at a final concentration of 12 μM for 24 h and then treated with Puromycin as previously described. Cells were subsequently lysed (PBS + 0.5% TX-100 + 1X PI), and lysates were used for WB and signals developed after incubation with the anti-puromycin antibody. Before Western-Blotting, total loading of puromycin-treated protein samples was checked by Ponceau S staining.

FACS

HEK293 cells were transfected with NG2 ICD or BAP-flag (as a positive control) and pelleted in a falcon after 48 h by centrifugation (800 rpm, 10 min, 4°C). Cells were fixed with pre-chilled 80% ethanol in a dropwise manner and incubated for 10 min on ice. After permeabilization (PBS, 0.3% TX-100, 1X PI) and blocking with PBS+10% HS for 1 h, cells were incubated with the primary anti-Flag-FITC conjugated antibody (in permeabilization buffer) for 2 h at 4°C. For DNA content analysis, cells were treated with RNase (10 μg/mL) and stained with propidium iodide (50 μg/mL) for 30 min at dark. Cell cycle distribution was checked only for Flag+ cell population, and data were analyzed by FlowJo software (IMB, Mainz).

Statistics

Each experiment was repeated independently at least three or more times. The numerical data of multiple experiments is expressed as mean ± standard error of the mean (SEM). Statistical analysis was done using Excel and Graph Pad Prism. For significance analysis, normal distribution was tested by the Shapiro-Wilk Normality test. For parametric distributed datasets two tailed *t*-test was applied: In the case of non-parametric distribution, Mann-Whitney or Wilcoxon Signed rank test was used. Significance was classified as follows: $^{*}p \leq 0.05$; $^{**}p < 0.01$; $^{***}p < 0.001$; n.s. $p > 0.05$.

RESULTS

NG2 Expression Constructs

As a tool for analyzing the cellular localization and functions of NG2 ICD, the following expression constructs were used (for details see the Methods section). NG2 DEL (65 kD) mimics a shortened version of the full-length NG2 protein, NG2 ICD (12 kD) encodes the intracellular domain of NG2 and ICDΔNLS (10 kD) encodes the ICD lacking the first nine amino acids which consist the predicted Nuclear Localization Signal(s). All these constructs were c-terminally tagged with three flag epitopes (p3X-Flag-CMV-14, Sigma) and are shown in detail in **Figures 1B,C**.

NG2 ICD Localizes Predominantly to the Cytosol and Distal Processes With Limited Nuclear Expression

First, we checked the expression of the different NG2 constructs and their size-difference pattern in a gradient gel by western blot analysis (WB). The HEK 293 cell-line (HEK), as well as the OPC cell line, Oli-*neu* and primary OPCs (pOPC) from total brain (mouse), were routinely used for transfection. The small endogenous NG2 ICD has an MW of 8.5 KD and thus, like other gamma-secretase products, was unstable and hard to detect in WB with a specific antibody recognizing the intracellular part of NG2 (NG2-cyto). To initially validate the expression of ICD constructs, we used sodium butyrate to enhance the expression levels. However, sodium butyrate was not used in any other experiments. Expression of ICDΔNLS only lead to sufficient protein levels in WB if sodium butyrate was added, while NG2 ICD levels were high even in the absence of butyrate. NG2 CTF (15 kD) derived from NG2 Del expression construct was the predominant, membrane-bound cleavage product recognized by the NG2 cyto antibody (**Figure 2A**). The localization of NG2 ICD and function of the predicted NLS was analyzed by performing subcellular fractionation of ICD over-expressing Oli-*neu* cells. NG2 ICD was detected in the nuclear fraction (Nuclear) as well as in the cytosolic fraction (Cyto) while expression of ICDΔNLS was restricted to the cytosolic fraction (**Figure 2B**). These observations were confirmed when Oli-*neu* cells transiently expressing the NG2 ICD and ICDΔNLS were immunostained and analyzed by confocal microscopy (**Figures 2C,D**). However, the cytosolic levels of ICD were always higher than the levels in the nucleus.

Identification of the NG2 ICD Interactome

Since the major fraction of the ICD was present in the cell cytosol and the NG2 ICD has several predicted protein binding motifs, we characterized the interactome of the NG2 ICD. HEK cells were transiently transfected with NG2 ICD or BAP (Flag-tagged control protein) and immunoprecipitation was carried out using magnetic anti-Flag antibody conjugated beads (Scheme shown in **Figure 3A**). Proteins that co-precipitated with NG2 ICD were identified by mass spectrometry (MS) from total IP samples run on gradient SDS-PAGE. Red arrows in **Figure 3B** indicate heavy (55 kD) and light chain (25 kD) of the Flag IgG used for IP. The NG2 ICD (around 12 kD) is also shown on the gel image, while BAP (control) protein (around 51 kD) overlaps with the IgG heavy chain and is indistinguishable from the latter on the Coomassie gel. Additionally, in an independent experiment, observed unique bands in ICD IP lane from the Coomassie-stained gradient gel were excised between 70 and 100 kD and sent for mass spectrometry-based band identification analysis (indicated by black arrows in **Figure 3B**). Band identification revealed that peptides corresponding to *two* translation factors eEF2 (100 kD) and eIF4B (70 kD) were highly represented in these excised bands (**Table 1**). Strikingly, KEGG biological pathway analysis based on Gene ontology from whole NG2 ICD-IPs also suggested an enrichment of DNA replication, translation regulators, PI3K-Akt-mTOR signaling pathways and cell-cycle stages (**Figure 3C**). Additionally, a functional annotation clustering analysis of the putative interaction partners of NG2 ICD was performed with FUNRICH proteomic analysis tool. This analysis also confirmed that protein clusters involved in translation regulation, cell-cell adhesion RNA metabolism, and DNA replication were highly represented in the identified annotated peptide list (**Table 2**).

NG2 ICD Increases Translation Rate in Cultured OPCs in an mTORC1-Dependent Manner

The GO-based analysis strongly suggested an influence of the NG2 ICD on translation. To test this directly, we pulse-labeled Oli-*neu* and HEK cells with puromycin followed by immunoblotting with an anti-puromycin antibody, a technique known as SUnSET assay (Schmidt et al., 2009). Low concentrations of puromycin are incorporated into nascent

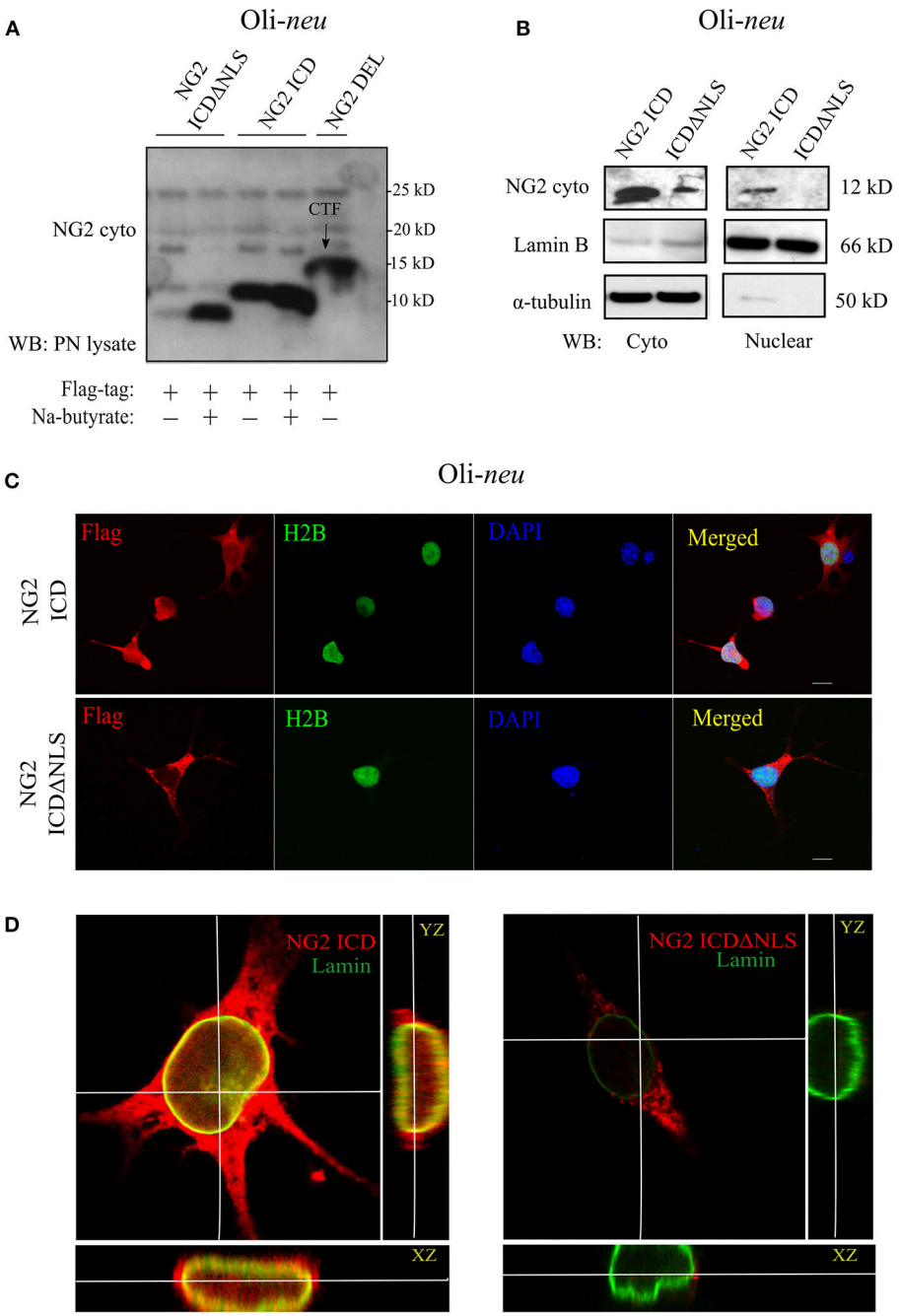

FIGURE 2 | Cellular localization of NG2 ICD in cultured OPCs. **(A)** Western blot analysis of post-nuclear (PN) cell-lysates of the OPC cell-line, Oli-*neu*. Different NG2 expression-constructs have been transiently transfected for 48 h before cell-lysis. Flag-tagged constructs show their size-based differences, NG2 ICD runs at 11 kD, and NG2 ICDΔNLS (NLS was deleted) runs just below ICD at 10 kD. NG2 DEL (65 kD) strongly shows processed membrane-bound CTF (15 kD) at the shown lower molecular masses. Na-butyrate was used only in this experiment to enhance the expression of ICD constructs. **(B)** Sub-cellular fractionation assay was done from Oli-*neu* after overexpressing ICD or ICDΔNLS for 48 h. Lamin B and α-tubulin were used as nuclear and cytosolic markers respectively. **(C)** Confocal laser scanning microscope images (z-stack, max. intensity projection) of Oli-*neu* expressing NG2 ICD or ICDΔNLS (flag; red) fixed after 48 h of transfection. Cells were immunostained with anti-flag antibody. NG2 ICD shows a distinguishable homogeneous staining pattern including nucleus where in case of ICDΔNLS, expression remained cytosolic. H2B (green) and DAPI (blue) were used as nuclear markers. **(D)** Three-dimensional orthogonal view of a z-stack of an Oli-*neu* showed the presence of NG2 ICD (red) within the nucleus, whereas ICDΔNLS expression was limited to the cytosol and peri-nuclear area. Lamin B (green) was used as a nuclear envelope marker. (Scale bar = 10 μm).

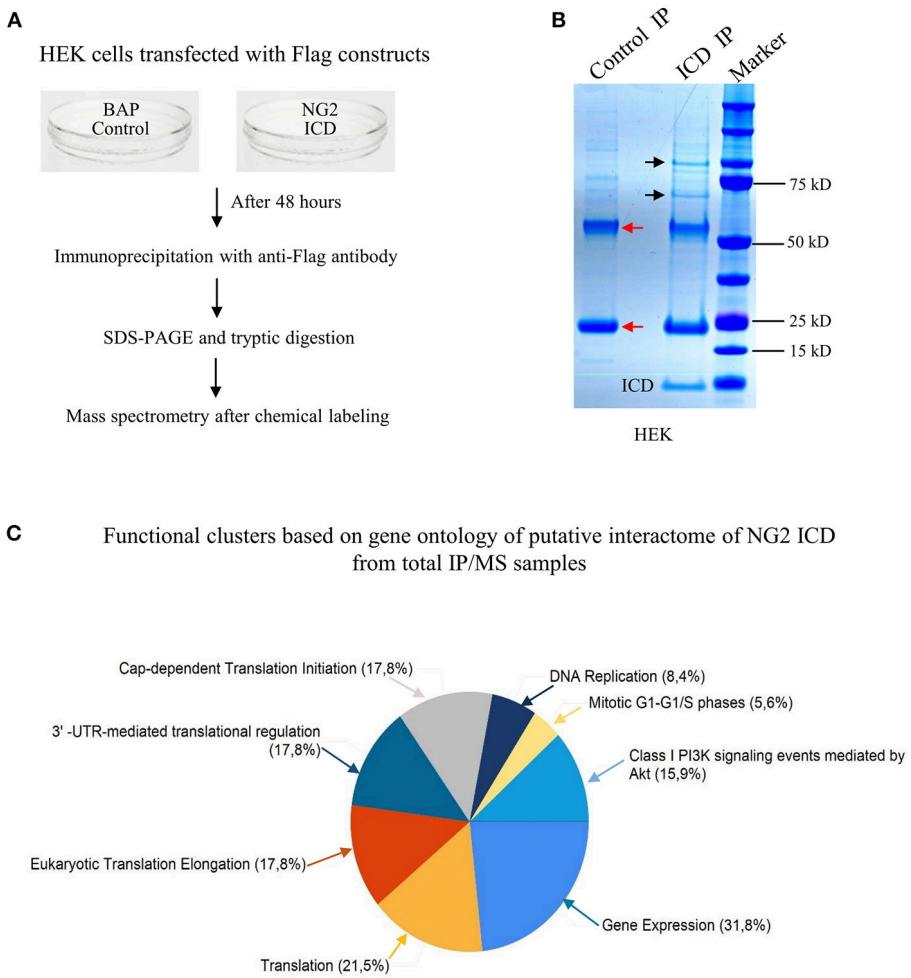

FIGURE 3 | Screening for the NG2 ICD interactome by IP-MS demonstrated enrichment of translation cluster. **(A)** Schematic of experimental conditions, immunoprecipitation and Mass spectrometry (MS) to isolate proteins that potentially interact with released NG2 ICD in HEK cells. Bacterial Alkaline Phosphatase (BAP) expression construct was used as control (control). **(B)** Representative Coomassie-stained gradient gel of NG2 ICD (ICD IP) and BAP-overexpressing samples (Control IP) after IP. Unique bands present in ICD-IP lane are indicated by black arrows, and red arrows indicate heavy and light chain (55 and 25 kD respectively) from anti-flag IgG used for IP. The unique bands were excised from gel between 70 and 100 kD and subjected to MS-based analysis. **(C)** MS analysis of whole IPed samples was carried out in two independent experiments, each time with additional reversed peptide-labeling. The putative IP-MS candidates were analyzed by using FUNRICH analysis tool. Altered biological functional annotation based on gene ontology represented translation, ribosomal biogenesis, and DNA replication to be significantly enriched.

polypeptide chains labeling the newly synthesized proteome. Increased puromycin incorporation reflects a higher translation rate (**Figure 4A**). The translation blocker Anisomycin was used as negative control. In cells overexpressing ICD, puromycin incorporation was increased by ∼90% in HEK and ∼70% in Oli-*neu* cells compared to controls, indicating an increased translation rate (**Figure 4B**). To validate that the observed increased translation rate is specific for cleaved NG2 ICD, NG2 DEL was used. NG2 DEL mimics membrane-bound NG2 and is cleaved in the cell yielding small amounts of ICD. Expression of NG2 DEL in Oli-*neu* yielded a smaller increase in the puromycin signal compared to control (∼22%). Specific inhibition of mTORC1 by temsirolimus (TM) completely blocked the NG2 ICD dependent increase of translation in Oli-*neu* (ICD + TM) compared to the control (TM) (**Figure 4B**) and reduced the translation rate to slightly below control levels. Knock-down of endogenous NG2 (siNG2) in primary OPC by siRNA reduced NG2 levels by 40% and total translation was also reduced by around 30% in pOPC transfected with siNG2 compared to control (**Figures 4C,D**).

NG2 ICD Increases Cell Population in S-Phase

The proteomics data showed that DNA replication was one of the top altered processes in cells overexpressing ICD. Furthermore, exaggerated protein synthesis often leads to cell proliferation (Bilanges and Stokoe, 2007). We thus investigated whether cleaved NG2 ICD plays a role in cell-cycle regulation.

TABLE 1 | Unique band identification of IPed samples by MS revealed enrichment of two translation factors in ICD IP lane.

Gene name	Protein name	UniProt ID	Molecular weight	Unique peptides	Sequence coverage
EEF2	Eukaryotic elongation factor 2	P13639	95.33	24	32.4
EIF4B	Eukaryotic initiation factor 4B	P23588	66.12	15	28.8

TABLE 2 | Functional annotation clusters of putative interactome of cleaved NG2 ICD by FUNRICH analysis software from whole IP/MS data.

	count(% total)	*p*-value
GO-MOLECULAR FUNCTION		
RNA binding	75 (58.1)	1.1E-41
Nucleotide binding	46 (35.7)	3.0E-11
Cadherin binding involved in cell-cell adhesion	14 (10.9)	7.0E-6
GO-BIOLOGICAL PATHWAY		
Ribosome	20 (15.05)	5.25E-15
Proteasome	5 (3.87)	0.002
PI3K-Akt Signaling pathway	4 (3.1)	0.807
GO-CELLULAR COMPARTMENT		
Ribosomal complex	22 (17.05)	3.04E-20
Spliceosomal complex	7 (5.42)	5.38E-5
ER-Chaperone complex	4 (3.1)	5.67E-5

HEK cells were transfected with NG2 ICD or BAP-Flag (Flag positive control). After 24 h, the cells were fixed and stained with anti-Flag-FITC conjugated antibody after permeabilization and analyzed by FACS after staining with PI.

Only FITC+ cells were gated for PI (DNA-binding dye) signal measurement. From the cell cycle distribution, in the ICD transfected population, 45.95 ± 6.53% of the cells were in S-phase compared to 35.41 ± 6.7% in S phase in the control population (**Figures 5A,B**). Due to low transfection efficiency and technical difficulties, FACS experiments could not be performed on Oli-*neu*. However, to address this issue in Oli-*neu*, cells were immunostained for PCNA (Proliferating cell nuclear antigen) which is an S-phase marker (**Figure 5C**). PCNA-staining revealed that 21.04 ± 1.26% Oli-*neu* cells were PCNA+ (out of total DAPI+ cells) in the ICD-transfected population. In the control population, 9.33 ± 2.01% Oli-*neu* were PCNA+ (**Figure 5D**), resulting in a 2-fold increase of Oli-*neu* cells in S-phase after ICD overexpression. 10% more Oli-*neu* were in S-phase after ICD expression, similar to increase in HEK cells. Levels of the G1 to S-phase regulator Cyclin E, increased around 2-fold on the protein level in Oli-*neu* total cell lysates, after NG2 ICD overexpression (**Figures 5E,F**).

Recent literature implies that nuclear morphology is correlated with distinct phases of cell-cycle and it is reported that most G1 phase cell nuclei appear round. As cells progress from late S-phase to mitosis, the nuclear shape also changes to a more elongated or dumbbell-shaped appearance (Wang et al., 2016). We examined the nuclear morphology by nuclear area and roundness of cells expressing the ICD. We found a significant difference between mean nuclear area and roundness of ICD transfected cell nuclei compared to controls (**Figures 6A,B**). While roundness was slightly reduced in ICD overexpressing Oli-*neu* cells, the nuclear area was increased around 1.6 fold in ICD overexpressing cells.

NG2 ICD Increases Translation by Modulating mTOR Signaling Components

We further investigated molecular mechanisms behind the translational and cell-cycle effects mediated by the NG2 ICD. To address this, we studied the expression of the global translation and proliferation regulator mTOR and components of the related signal-cascade. As described before, HEK and Oli-*neu* cells were transiently transfected with ICD or mock vector, and after 48 h, cell lysates were prepared and run on an SDS-PAGE gradient gel followed by WB analysis. In ICD-overexpressing cells, levels of phospho-mTOR (Ser2481) were increased and levels of the phosphorylated form (Thr 389) of the downstream target of mTOR, p70S6K1 were also increased, suggesting that this signaling pathway is a target of NG2 ICD (**Figures 7A,B**). Active (phosphorylated) S6K1 phosphorylates and inactivates eEF2K resulting in an upregulation of eEF2 protein, and it also phosphorylates and activates eIF4B. In support of this, we found an increase of phospho-eIF4B (Ser422) in ICD-transfected cells (**Figures 7A,B**). Knock-down of total NG2 protein in Oli-*neu* by siRNA (siNG2) resulted in a decrease of mTOR and p70S6K1 phosphorylation of around 20–25% compared to control (siCNT) (**Figures 7C,D**).

In the nervous system, S6K1 has been reported to phosphorylate FMRP, a protein acting as a general repressor of translation (Narayanan et al., 2008). Mutation of FMRP is the causal link to the intellectual disorder; Fragile-X Mental Syndrome (Santos et al., 2014). FMRP is an RNA binding protein with a wide range of substrates including dendritic mRNAs (Nalavadi et al., 2012) thus FMRP plays a key role in maintaining local translation and neuronal development (Zalfa et al., 2003; Nalavadi et al., 2012; Pasciuto and Bagni, 2014b). In recent studies, Eef2 mRNA has been recognized as an additional substrate of FMRP (Pasciuto and Bagni, 2014a; Richter et al., 2015) and FMRP/Eef2 signaling has been suggested to regulate translation of mRNAs involved in LTD in neurons (Park et al., 2008). Furthermore, FMRP-KO mice show exaggerated protein synthesis (Darnell et al., 2011) as a result of hyperactive S6K1 signaling (Bhattacharya et al., 2012). Intrigued by this reported molecular interplay, we checked the level of FMRP and found significant downregulation (∼70%) in ICD-overexpressing Oli-*neu* cells (**Figures 8A,B**). Downregulation of FMRP was much lower in HEK (∼30%) compared to Oli-*neu*. Moreover, the total cellular levels of eEF2 were increased in both NG2 ICD-transfected (**Figures 8A,B**) cell-types.

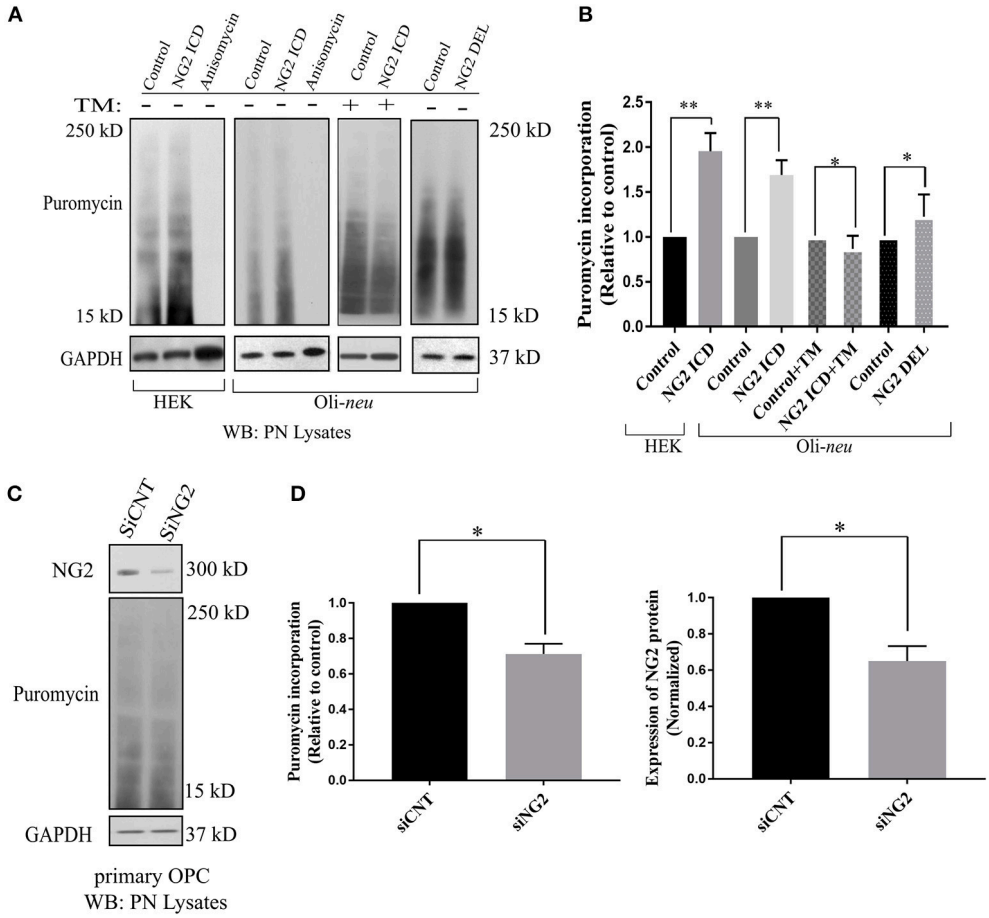

FIGURE 4 | Released NG2 ICD stimulates *in-vitro* translation in a mTORC1-dependent manner. **(A)** HEK ($n = 5$) and Oli-*neu* ($n = 4$) cells were treated with 10 μM puromycin after 48 h of transient transfection with different NG2 expression constructs (DEL and ICD) or empty expression vector (control). Puromycin incorporates into newly synthesized proteins during translation. Western blot analysis of post-nuclear (PN) cell-lysates after puromycin treatment was done with a specific antibody against puromycin, the translation blocker Anisomycin was used as a negative control. Additionally, a selective mTORC1 complex inhibitor, Temsirolimus (TM), was used (10 μM) to investigate mTORC1 specific contribution to total translation rate between control (+TM) and ICD (+TM) ($n = 3$). **(B)** Densitometric analysis was done for puromycin (from 15 to 250 kD) normalized to GAPDH. NG2 ICD showed an increase of puromycin incorporation (translation rate) by 70% in Oli-*neu* and by 90% in HEK cells compared to control. When treated with a mTORC1 inhibitor (TM), the ICD-mediated effect on translational is reduced slightly below control levels (control+TM vs. ICD+TM), indicating a mTORC1-dependent increase and a mTORC1-independent decrease of translation by NG2 ICD overexpression. NG2 DEL mimics full-length NG2, and it predominantly expresses membrane-bound NG2 CTF but not cleaved ICD (**Figures 1B**, **2A**). NG2 DEL was used as an additional control to confer cleaved ICD-specificity in stimulating translation, and it shows only ∼22% increase in translation rate compared to control ($n = 4$). **(C)** Full-length NG2 knockdown (siRNA transfection) was performed in cultured primary OPCs (pOPCs) to check the effect on translation. **(D)** NG2 knockdown (siNG2) in pOPCs revealed a knockdown efficiency of around 40% compared to control (siCNT), translation (puromycin level) was reduced by ∼30% by NG2 knock-down. [Data represents mean ±SEM. Statistical analysis was done by two-tailed paired *t*-test after checking the data is normally distributed by Shapiro-Wilk normality test by PRISM (GraphPad)]. Significance was classified as defined in the Materials and Methods part.

DISCUSSION

NLS-Dependent Localization of the NG2 ICD

An initial study by our group investigated the localization of the NG2 ICD. After transfection, most of the protein was localized in the cytoplasm, but lower nuclear levels were also reported (Sakry et al., 2015); in the present study, we confirm this localization pattern. However, immunofluorescent staining of cells expressing an NLS-truncated ICD construct showed only cytoplasmic and no nuclear localization, suggesting an NLS-dependent transport of the NG2 ICD into the cell nucleus. In contrast to the NOTCH ICD which contains a DNA binding domain, the much smaller NG2 ICD does not contain such conserved DNA/TF binding domains implying that a direct function of the NG2 ICD as a transcription factor is unlikely. According to ELM motif database, the NG2 intracellular sequence harbors a predicted site for MAPK interaction, suggesting additional involvement in cell signaling pathways. So far, no nuclear function or binding partner has been identified for the released NG2 ICD, but the predicted intracellular WW4 binding sequence of NG2 (**Figure 1C**) could be of interest, since WW4 domain-containing proteins have distinct roles, including nuclear functions (Sudol et al., 2001). In this study, we did not use the NLS deletion

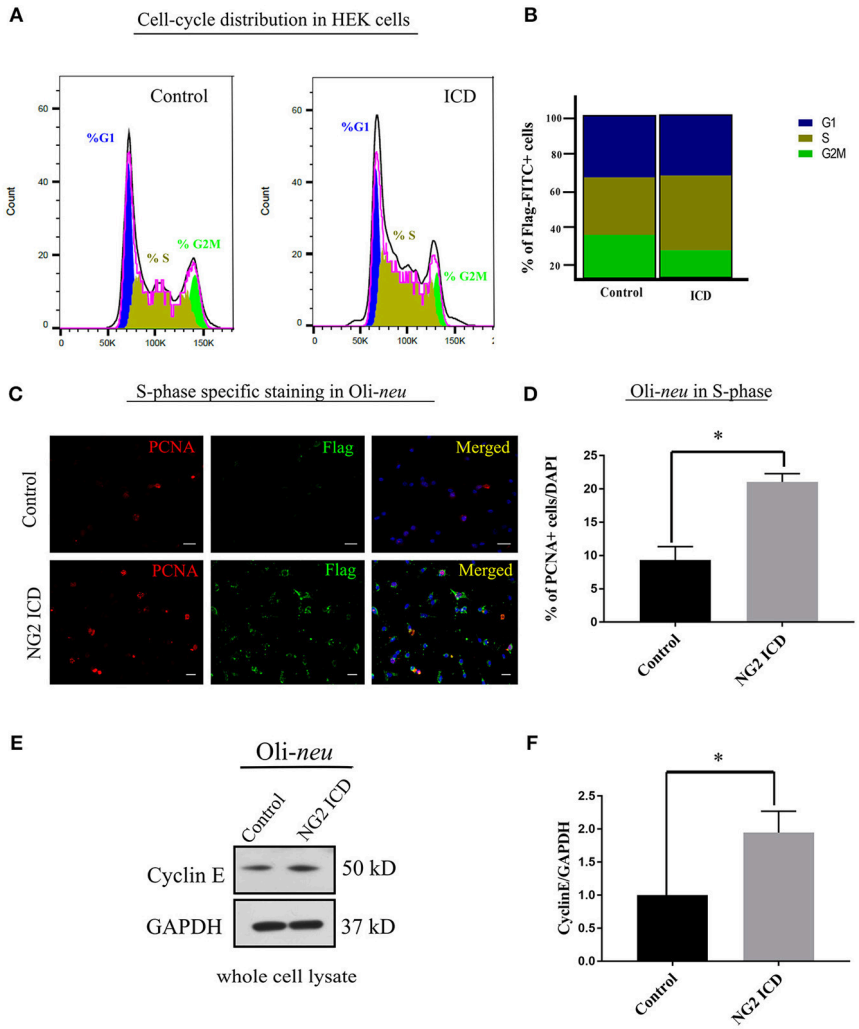

FIGURE 5 | NG2 ICD accumulates cells in S-phase. **(A)** Representative images of DNA histogram analysis for cell-cycle distribution in asynchronized HEK cells transfected with ICD-flag (ICD) or BAP-flag (control). Cells were harvested, fixed, immunostained with Flag-FITC antibody and subjected to FACS analysis. Propidium iodide (PI) was used for DNA staining. Only flag-FITC+ cells were analyzed for PI quantification. **(B)** Quantification of FACS data from HEK cells represented in a stacked bar column shows that ICD promotes the cell population in S-phase by ∼10%, while G2M phase fraction is reduced ($n = 3$). **(C)** Oli-*neu* cells immunostained with the anti-PCNA antibody (red) indicate increased PCNA-associated nuclear puncta when transfected with ICD (stained with anti-Flag antibody, green). PCNA is an S-phase specific marker and puncta in nucleus represent active replisomes. Cell nuclei were stained with DAPI (blue). **(D)** Quantification of PCNA staining in Oli-*neu* reveals that the proportion of PCNA+ cells out of total cells (total counted DAPI+) is significantly increased in case of ICD overexpression (21.04 ± 1.26%) compared to control (9.33 ± 2.03%). **(E)** Cyclin E is upregulated during G1 to S-phase progression, Cyclin E total protein levels were checked in Control, and NG2 ICD transfected Oli-*neu* cells. **(F)** Whole cell lysates were subjected to WB analysis, where Cyclin E was increased ∼2 fold in ICD compared to control. [Data represents mean ±SEM. Statistical analysis was done by two-tailed paired *t*-test after checking the data is normally distributed by Shapiro-Wilk normality test by PRISM (GraphPad). For **(C,D)** Experiments were done in three independent sets ($n = 3$) where 2,000 events counted for each condition in each experiment for **(B)** and a total of ∼250 cells were counted for **D**]. Significance was classified as defined in the Materials and Methods part.

construct for further experiments because of its low detectable protein levels, reflecting a much lower expression or a much higher degradation rate compared to the NG2 ICD expression construct.

NG2 ICD Increases Translation and DNA Replication

Based on the results from the ontology analysis of our proteomics data, we investigated the effect of the NG2 ICD on mRNA translation and cell-cycle kinetics.

Strikingly, total translation rate was increased by at least ∼70% after NG2 ICD overexpression in Oli-*neu* and HEK cells, but not increased in the presence of an inhibitor of mTORC1. These results demonstrate an essential role of mTORC1 signaling in the increase in translation due to overexpression of the NG2 ICD. Additionally, NG2 DEL expression only slightly increased translation (∼22%) in Oli-*neu*. In our present and previous studies (Sakry et al., 2014, 2015) we show that the NG2 CTF but not the ICD, is the major fragment generated after NG2 DEL expression, resulting in much lower levels of

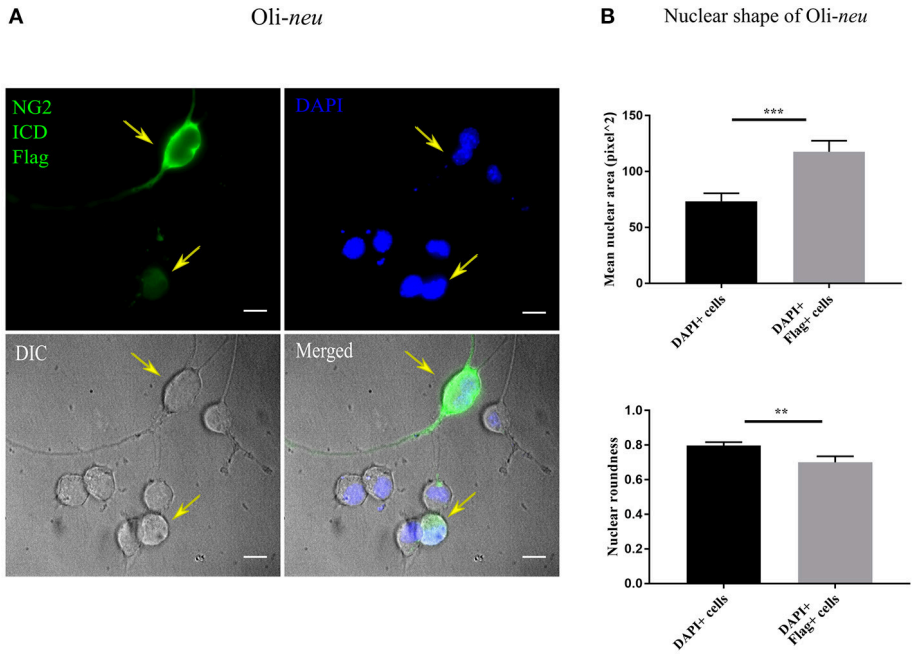

FIGURE 6 | Altered nuclear morphology in ICD-overexpressing cells. **(A)** Immunofluorescent images of Oli-*neu* cells expressing ICD-flag (green), the nucleus was stained with DAPI (blue). The arrows indicate ICD-transfected cells. **(B)** Quantification of nuclear shape based on two indices (ImageJ); nuclear area (unit for area) and roundness (0.0–1.0), revealed that nuclei of ICD-transfected Oli-*neu* were ∼1.6 times larger (area) and less round (roundness) than Oli-*neu* from control [Mean values ± SEM was shown in the data. Total 50 cells were counted from three independent experiments ($n = 3$) for each condition. Statistical test was carried out by Mann-Whitney-rank based test]. Significance was classified as defined in the Materials and Methods part.

overexpressed NG2 ICD protein after NG2 DEL transfection compared to expression of the NG2 ICD construct. The much lower translational increase observed with NG2 DEL compared to NG2 ICD (22 vs. 70%), suggests a protein-level dependent effect of the released NG2 ICD on mTORC1-dependent translational regulation. In support of this, we found that the reduction of total endogenous NG2 protein levels in primary OPCs by siRNA knock-down decreased total translation rate.

Cell cycle analysis demonstrated a shift toward S-phase of cells expressing the NG2 ICD, where the percentage of the cell-population in S-phase increased by about 10% both for Oli-*neu* and HEK cells, reflecting increased DNA replication after NG2 ICD overexpression. We also detected changes in nuclear morphology of ICD-transfected Oli-*neu* concomitant with the observed alterations in nuclear shape reported in S-phase cells (Wang et al., 2016). In the case of Oli-*neu*, the cell number in S-phase increased by 2-fold, interestingly we found that Cyclin E, the major Cyclin upregulated during G1 to S-phase shift (Sgambato et al., 2003; Loeb et al., 2005), is increased around 2-fold on the protein level in Oli-*neu* under the same experimental conditions.

To date, NG2 protein or cleavage fragments have not been reported to modulate translation. However, NG2 expression is characteristic for proliferating cells, both in normal tissue and tumors. OPCs are the only proliferating cell population in the adult unlesioned mammalian CNS, apart from stem cells (Simon et al., 2011; Dimou and Götz, 2014). The ICD-mediated drive toward S-phase progression in OPCs that we report is striking as it has been recently published that stimulation of neuronal circuits causes an increase in adjacent neuronal progenitor proliferation, including NG2+ OPCs (Gibson et al., 2014). Since neuronal activity stimulates NG2 cleavage leading to increased release of the NG2 ICD in the cell cytoplasm (Sakry et al., 2014), our observation of ICD stimulation of cell-cycle progression is of interest in this context.

NG2 ICD Regulates mTOR and FMRP Signaling

Since mRNA translation and cell-cycle kinetics were the major biological processes altered upon ICD overexpression, we investigated the potential underlying molecular mechanism behind these regulated biological processes. We started by analyzing the mTOR signaling cascade, as the mTOR pathway is a central regulator of cell growth, proliferation, and survival and growing evidence also supports its role in cell-cycle progression and tumorigenesis (Fingar et al., 2003; Ohanna et al., 2005; Laplante and Sabatini, 2012).

We found an increase of phosphorylated (p-ser2481, active) mTOR in ICD-overexpressing Oli-*neu* and HEK cells, indicating activation by PI3K, which is responsible for phosphorylation of this specific residue (Soliman et al., 2010). Active mTOR, part of the mTOR complex1 (mTORC1), is known to phosphorylate

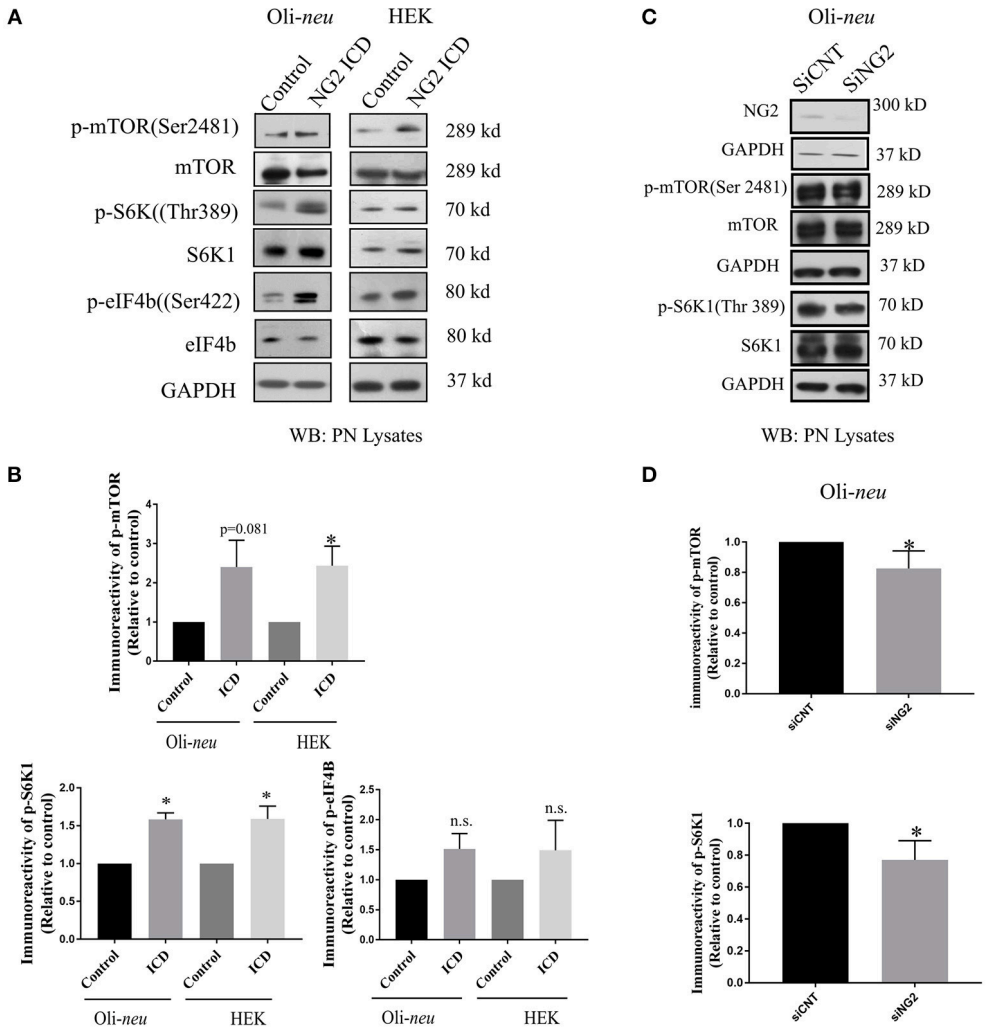

FIGURE 7 | NG2 ICD regulates mTORC1ignaling pathway. **(A,C)** Western blot analysis of post-nuclear (PN) lysate from NG2 ICD transfected HEK ($n = 3$) and Oli-*neu* ($n = 4$) cells compared to empty vector (control). PN lysates were prepared 48 h after transfection. NG2 knockdown was carried out by siRNA transfection in Oli-*neu* cells. **(B)** Quantification of western blot analysis was done by normalizing both phospho-protein and total individual protein against GAPDH (loading control), then individual ratios of phosphorylated over total proteins levels were calculated. Several components of mTOR signaling cascade were regulated by NG2 ICD overexpression. Phospho-specific expression of S6K1 (Thr389) is significantly upregulated in both cell lines and correlates with the increase of phospho-mTOR (Ser2481) levels. The downstream target of pS6K1, p-eIF4B was also increased in both cell lines. **(D)** In the NG2-knockdown experiment, the key components of mTORC1 signaling cascades were checked, and p-mTOR and p-S6K1 both were reduced (∼20–25%) in NG2 knockdown (efficacy 80%) samples compared to control. [Data represents mean ± SEM. Statistical analysis was done by two-tailed paired *t*-test after checking the data is normally distributed by Shapiro-Wilk normality test by PRISM (GraphPad)]. Significance was classified as defined in the Materials and Methods part.

the downstream target S6K1 at the Thr389 residue (Saitoh et al., 2002). Phosphorylated (active) S6K1 phosphorylates several downstream targets including the translation regulators eIF4B and eEF2K (Wang et al., 2001; Holz et al., 2005). Phosphorylated eIf4B promotes initiation of cap-dependent translation (Dennis et al., 2012), while phosphorylated eEF2K (the inactive form) leads to an increased level of the eEF2 protein resulting in elevated translation rates (Wang et al., 2001). Focusing on mTOR downstream targets, we found significantly increased levels of phosphorylated S6K1 in both cell lines after NG2 ICD overexpression. Additionally, total amounts of eEF2 protein and levels of p-eIF4B (the active form) were upregulated in both cell-lines, supporting the activation of the mTOR signaling cascade. Knock-down of endogenous NG2 in Oli-*neu* lead to decreased levels of phosphorylated mTOR/S6K1.

In addition to acting on the translation factors as described above, active S6K1 has been reported to phosphorylate FMRP, a protein highly expressed in the brain (Narayanan et al., 2008). Furthermore, eEF2 is a reported target of FMRP (Darnell and Klann, 2013). In FMRP knockout mice, total eEF2 protein and levels of p-eIF4B were higher than in wild-type mice (Bhattacharya et al., 2012). In line with this observation, we found significant downregulation of FMRP protein levels of

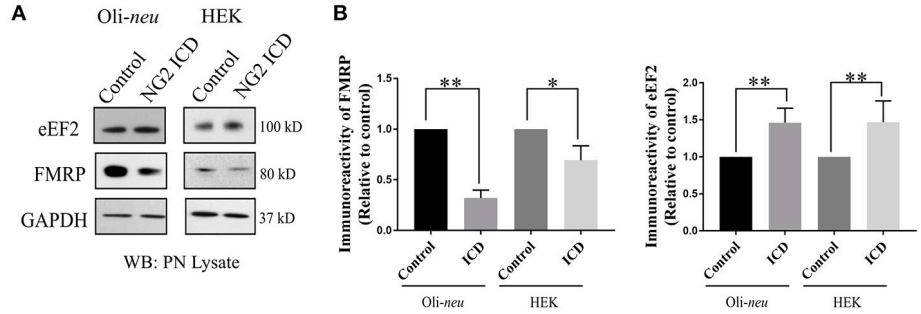

FIGURE 8 | NG2 ICD regulates expression of eEF2 and FMRP. **(A)** Western blot analysis of post-nuclear (PN) lysate from NG2 ICD transfected HEK ($n = 6$) and Oli-*neu* ($n = 7$) cells compared to empty vector (control). PN lysates were prepared 48 h after transfection. **(B)** Total protein levels (normalized against GAPDH) of eEF2 were increased in both cell-lines, while FMRP protein levels were significantly reduced after ICD-overexpression only in Oli-*neu*, both are key regulators of transcription. [Data represents mean ± SEM. Statistical analysis was done by two-tailed paired *t*-test after checking the data is normally distributed by Shapiro-Wilk normality test by PRISM (GraphPad)]. Significance was classified as defined in the Materials and Methods part.

70% compared to the normal protein levels in NG2 ICD-overexpressing Oli-*neu*, but in HEK cells overexpressing the NG2 ICD, FMRP protein levels were only 30% lower. These NG2 ICD-mediated effects on FMRP were thus much stronger in Oli-*neu*, in contrast to the ICD mediated effects on the mTOR and S6K1 pathway which were similar in both cell types.

Fragile X protein (FMRP) is an RNA binding protein with demonstrated roles in mRNA transport, localization, stability, and translation. Mutations in FMRP are a major cause of the human cognitive disorder Fragile-X syndrome. In FMRP knock-out mice, increased S6K1 signaling was reported (Bhattacharya et al., 2012) leading to exaggerated protein synthesis, similar to observations in FXS. Reduced expression of functional FMRP in both FXS patients (Qin et al., 2013) and animal models (Weiler et al., 2004; Gross et al., 2010) leads to excessive protein synthesis in neurons, suggesting that FMRP acts as a general repressor of translation. Since we found reduced FMRP levels and increased translation after NG2 ICD overexpression in Oli-*neu*, it is likely that FMRP also acts as a translational repressor in OPCs, as well as in neurons.

In our study of OPC, we identified two translation-related pathways affected by the NG2 ICD. One is responsible for general translation regulation in cells (mTORC1/S6K1 signaling cascade), and the other is important for regulating local translation and synaptic strength including LTD (FMRP-eEF2) in neurons (Park et al., 2008). Recent studies have shown that FMRP also activates the mTOR-signaling pathway in neurons (Sharma et al., 2010), combining these two signaling cascades. We thus suggest a new signaling paradigm for the NG2 protein in OPCs involving the neuronal network, as summarized in the graphical illustration in **Figure 9**.

NG2 ICD Signaling in OPCs

Our findings establish a model for NG2 ICD dependent modulation of FMRP/mTOR signaling cascades in OPCs with associated increased translation rate and an increased fraction of the cell population in the S-phase. OPCs are the only glial cell-type that receives direct synaptic input from neurons in all major brain areas (Bergles et al., 2000; Jabs et al., 2005; Mangin and Gallo, 2011; Sakry et al., 2011). Furthermore, cleavage of NG2 leading to the cytoplasmic release of NG2 ICD has been shown to be increased by neuronal activity (Sakry et al., 2014).

The mTOR pathway has been shown to be crucial for OPC differentiation to myelinating oligodendrocytes (Tyler et al., 2009; Zou et al., 2014). However, NG2 is downregulated during early OPC differentiation (Nishiyama et al., 2009; De Biase et al., 2010; Kukley et al., 2010) making it unlikely that regulation of mTOR by NG2 is contributing to OPC differentiation.

NG2 ICD Signaling in Tumors

Interestingly, dysregulation of the FMRP/Akt/mTOR pathway has been reported to promote tumorigenesis (Rajasekhar et al., 2003; Lucá et al., 2013) and impaired mTOR cascade has especially been linked to Glioblastoma, the most common form of primary brain tumor (Akhavan et al., 2010; Li et al., 2016). NG2 is abundantly expressed by highly proliferative tumor cells in melanomas and gliomas (Chekenya et al., 2008; Al-Mayhani et al., 2011). The migration-promoting function of NG2 (Binamé et al., 2013) as well as the binding to OMI/HtrA2 (Maus et al., 2015) are features favoring NG2 expression by tumor cells promoting invasion and increasing resistance to oxidative stress. NG2 is included in a pool of several antigens used in a vaccine therapy against glioblastoma multiform, which reduces tumor growth (Poli et al., 2013). Additionally, OPCs are discussed as the major cells of origin for gliomas (Liu and Zong, 2012). NG2 is also involved in regulating symmetric vs. asymmetric cell-division of OPCs, the mode of division influences the likelihood of an OPC to become a tumor cell (Sugiarto et al., 2011).

Our findings of increased translation and DNA-synthesis (S-phase) by NG2 ICD correlates with the high proliferation and expression rates of these NG2-expressing tumors and is therefore likely to be one contributing factor to increased translation and DNA-synthesis within these cancers. One could speculate, that targeting NG2 as an antigen in the vaccine therapy described

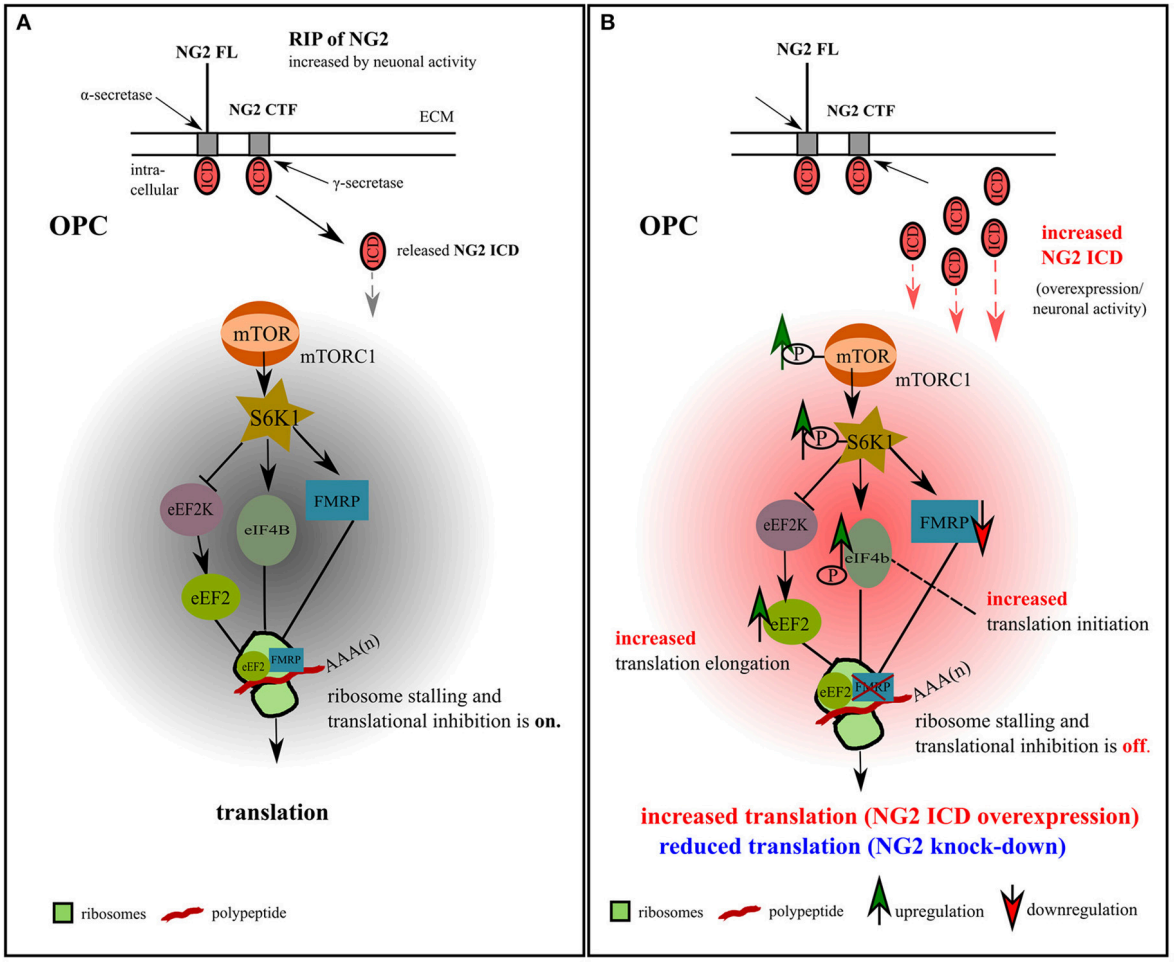

FIGURE 9 | Model for NG2 ICD-mediated intracellular signaling in OPCs. **(A)** We propose the signaling pathway shown for OPCs, based on our previous NG2 cleavage study (Sakry et al., 2014; Sakry and Trotter, 2016) and the present NG2 ICD overexpression and NG2 knock-down study (highlighted in part **B**). The mTOR pathway shown has been suggested by Bhattacharya et al. (2012) for neurons (without NG2 signaling). In OPCs, NG2 full-length (FL) protein undergoes regulated intramembrane proteolysis (RIP) leading to the release of an ectodomain into the extracellular matrix (ECM) and generation of a c-terminal fragment (CTF) by α-secretase activity. γ-secretase activity on the NG2 CTF releases the NG2 intracellular domain (ICD) into the cytoplasm. This NG2 cleavage occurs constitutively in OPCs and can be increased by neuronal activity (Sakry et al., 2014). Under normal conditions, FMRP, which is a translation repressor and target of the mTOR-S6K1 signaling cascade, binds to eEF2 on ribosomal subunits and stalls translation, as suggested for neurons (Bhattacharya et al., 2012). **(B)** Increased NG2 cleavage generates an increased amount of NG2 ICD by γ-secretase activity. NG2 ICD overexpression mimics an increase in products of intracellular NG2 cleavage, elevating levels of phosphorylated (active) p-mTOR/p-S6K1/p-eIF4B, all known downstream components of the mTORC1 signal cascade, and thus indicating an increase in p-eIF4B dependent translation initiation. P-S6K1 phosphorylates and inactivates eEF2K leading to increased levels of active eEF2 protein favoring translation elongation. Increasing levels of NG2 ICD resulted in a higher levels of eEF2 and a reduction of FMRP protein, leading to a reduction of stalled FMRP-eEF2 complexes and relieving translation inhibition. These combined effects on the signaling cascade favor the observed mTORC1-dependent increase of overall translation in OPCs (**Figures 4A,B**) after ICD overexpression. A reduction of NG2 protein level in primary OPCs leads to a reduction of the total translation rate (**Figures 4C,D**).

above may affect NG2 signaling and modulate the signaling-pathway presented here. It could further explain part of the reduction in tumor growth observed during such therapy by reduced translation and proliferation effected by NG2 signaling.

SUMMARY

In summary, our results add new insights to the role of NG2 cleavage in OPC and tumor signaling pathways. In addition to effects of the released NG2 ectodomain on the glutamatergic properties of neurons (Sakry et al., 2014), we show here that the released NG2 ICD can signal as a functional domain affecting translation and cell-cycle kinetics. These effects are important both for OPC under normal physiological conditions as well as NG2-expressing tumors. Our results imply translational regulation of localized (synaptic) mRNAs by FMRP in OPCs that can be influenced by the neuronal network.

AUTHOR CONTRIBUTIONS

TN and DS conceived and designed the experiments. TN performed the experiments and analyzed the data. DS and JT supervised the experiments. TN, DS, and JT wrote the manuscript.

FUNDING

This study was supported by the Deutsche Forschungsgemeinschaft (DFG TR 231/8-1 to JT; CRC TRR 128: TPB07 to JT) and a graduate stipendium to TN in the International PhD Programme on Gene Regulation, Epigenetics & Genome Stability, Mainz, Germany.

ACKNOWLEDGMENTS

We thank Dr. Eva-Maria Albers for her critical and valuable input and Dr. Vijay Tiwari for sharing a plasmid and thoughts on experiment design. We acknowledge the support and guidance provided by the Core facilities of Microscopy, Proteomics and Flow cytometry of the Institute of Molecular Biology, Mainz. We are grateful to Cornelia Braun for technical support.

REFERENCES

Akhavan, D., Cloughesy, T. F., and Mischel, P. S. (2010). mTOR signaling in glioblastoma: lessons learned from bench to bedside. *Neuro Oncol.* 12, 882–889. doi: 10.1093/neuonc/noq052

Al-Mayhani, M. T., Grenfell, R., Narita, M., Piccirillo, S., Kenney-Herbert, E., Fawcett, J. W., et al. (2011). NG2 expression in glioblastoma identifies an actively proliferating population with an aggressive molecular signature. *Neuro Oncol.* 13, 830–845. doi: 10.1093/neuonc/nor088

Attwell, D., Mishra, A., Hall, C. N., O'Farrell, F. M., and Dalkara, T. (2016). What is a pericyte? *J. Cereb. Blood Flow Metab.* 36, 451–455. doi: 10.1177/0271678X15610340

Bailey, A. M., and Posakony, J. W. (1995). Suppressor of hairless directly activates transcription of enhancer of split complex genes in response to Notch receptor activity. *Genes Dev.* 9, 2609–2622. doi: 10.1101/gad.9.21.2609

Baker, N. E., and Zitron, A. E. (1995). Drosophila eye development: notch and Delta amplify a neurogenic pattern conferred on the morphogenetic furrow by scabrous. *Mech. Dev.* 49, 173–189. doi: 10.1016/0925-4773(94)00314-D

Barritt, D. S., Pearn, M. T., Zisch, A. H., Lee, S. S., Javier, R. T., Pasquale, E. B., et al. (2000). The multi-PDZ domain protein MUPP1 is a cytoplasmic ligand for the membrane-spanning proteoglycan NG2. *J. Cell Biochem.* 79, 213–224. doi: 10.02/1097-4644(20001101)79

Bergles, D. E., Roberts, J. D., Somogyi, P., and Jahr, C. E. (2000). Glutamatergic synapses on oligodendrocyte precursor cells in the hippocampus. *Nature* 405, 187–191. doi: 10.1038/35012083

Bhattacharya, A., Kaphzan, H., Alvarez-Dieppa, A. C., Murphy, J. P., Pierre, P., and Klann, E. (2012). Genetic removal of p70 S6 kinase 1 corrects molecular, synaptic, and behavioral phenotypes in fragile X syndrome mice. *Neuron* 76, 325–337. doi: 10.1016/j.neuron.2012.07.022

Bilanges, B., and Stokoe, D. (2007). Mechanisms of translational deregulation in human tumors and therapeutic intervention strategies. *Oncogene* 26, 5973–5990. doi: 10.1038/sj.onc.1210431

Binamé, F., Sakry, D., Dimou, L., Jolivel, V., and Trotter, J. (2013). NG2 regulates directional migration of oligodendrocyte precursor cells via Rho GTPases and polarity complex proteins. *J. Neurosci.* 33, 10858–10874. doi: 10.1523/JNEUROSCI.5010-12.2013

Blaumueller, C. M., Qi, H., Zagouras, P., and Artavanis-Tsakonas, S. (1997). Intracellular cleavage of Notch leads to a heterodimeric receptor on the plasma membrane. *Cell* 90, 281–291. doi: 10.1016/S0092-8674(00)80336-0

Brown, M. S., Ye, J., Rawson, R. B., and Goldstein, J. L. (2000). Regulated intramembrane proteolysis: a control mechanism conserved from bacteria to humans. *Cell* 100, 391–398. doi: 10.1016/S0092-8674(00)80675-3

Chatterjee, N., Stegmuller, J., Schatzle, P., Karram, K., Koroll, M., Werner, H. B., et al. (2008). Interaction of syntenin-1 and the NG2 proteoglycan in migratory oligodendrocyte precursor cells. *J. Biol. Chem.* 283, 8310–8317. doi: 10.1074/jbc.M706074200

Chekenya, M., Krakstad, C., Svendsen, A., Netland, I. A., Staalesen, V., Tysnes, B. B., et al. (2008). The progenitor cell marker NG2/MPG promotes chemoresistance by activation of integrin-dependent PI3K/Akt signaling. *Oncogene* 27, 5182–5194. doi: 10.1038/onc.2008.157

Clarke, L. E., Young, K. M., Hamilton, N. B., Li, H., Richardson, W. D., and Attwell, D. (2012). Properties and fate of oligodendrocyte progenitor cells in the corpus callosum, motor cortex, and piriform cortex of the mouse. *J. Neurosci.* 32, 8173–8185. doi: 10.1523/JNEUROSCI.0928-12.2012

Darnell, J. C., and Klann, E. (2013). The translation of translational control by FMRP: therapeutic targets for FXS. *Nat. Neurosci.* 16, 1530–1536. doi: 10.1038/nn.3379

Darnell, J. C., Van Driesche, S. J., Zhang, C., Hung, K. Y., Mele, A., Fraser, C. E., et al. (2011). FMRP stalls ribosomal translocation on mRNAs linked to synaptic function and autism. *Cell* 146, 247–261. doi: 10.1016/j.cell.2011.06.013

Dawson, J., Hotchin, N., Lax, S., and Rumsby, M. (2003). Lysophosphatidic acid induces process retraction in CG-4 line oligodendrocytes and oligodendrocyte precursor cells but not in differentiated oligodendrocytes. *J. Neurochem.* 87, 947–957. doi: 10.1046/j.1471-4159.2003.02056.x

De Biase, L. M., Nishiyama, A., and Bergles, D. E. (2010). Excitability and synaptic communication within the oligodendrocyte lineage. *J. Neurosci.* 30, 3600–3611. doi: 10.1523/JNEUROSCI.6000-09.2010

Deepa, S. S., Carulli, D., Galtrey, C., Rhodes, K., Fukuda, J., Mikami, T., et al. (2006). Composition of perineuronal net extracellular matrix in rat brain: a different disaccharide composition for the net-associated proteoglycans. *J. Biol. Chem.* 281, 17789–17800. doi: 10.1074/jbc.M600544200

Dennis, M. D., Jefferson, L. S., and Kimball, S. R. (2012). Role of p70S6K1-mediated phosphorylation of eIF4B and PDCD4 proteins in the regulation of protein synthesis. *J. Biol. Chem.* 287, 42890–42899. doi: 10.1074/jbc.M112.404822

De Strooper, B., Annaert, W., Cupers, P., Saftig, P., Craessaerts, K., Mumm, J. S., et al. (1999). A presenilin-1-dependent gamma-secretase-like protease mediates release of Notch intracellular domain. *Nature* 398, 518–522.

Dimou, L., and Götz, M. (2014). Glial cells as progenitors and stem cells: new roles in the healthy and diseased brain. *Physiol. Rev.* 94, 709–737. doi: 10.1152/physrev.00036.2013

Diers-Fenger, M., Kirchhoff, F., Kettenmann, H., Levine, J. M., and Trotter, J. (2001). AN2/NG2 protein-expressing glial progenitor cells in the murine CNS: isolation, differentiation, and association with radial glia. *Glia* 34, 213–228.

Estrada, B., Gisselbrecht, S. S., and Michelson, A. M. (2007). The transmembrane protein Perdido interacts with Grip and integrins to mediate myotube projection and attachment in the Drosophila embryo. *Development* 134, 4469–4478. doi: 10.1242/dev.014027

Fingar, D. C., Richardson, C. J., Tee, A. R., Cheatham, L., Tsou, C., and Blenis, J. (2003). mTOR controls cell cycle progression through its cell growth effectors S6K1 and 4E-BP1/eukaryotic translation initiation factor 4E. *Mole. Cell. Biol.* 24, 200–216. doi: 10.1128/MCB.24.1.200-216.2004

Gibson, E. M., Purger, D., Mount, C. W., Goldstein, A. K., Lin, G. L., Wood, L. S., et al. (2014). Neuronal activity promotes oligodendrogenesis and adaptive myelination in the mammalian brain. *Science* 344:1252304. doi: 10.1126/science.1252304

Gross, C., Nakamoto, M., Yao, X., Chan, C. B., Yim, S. Y., Ye, K., et al. (2010). Excess phosphoinositide 3-kinase subunit synthesis and activity as a novel therapeutic target in fragile X syndrome. *J. Neurosci.* 30, 10624–10638. doi: 10.1523/JNEUROSCI.0402-10.2010

Holz, M. K., Ballif, B. A., Gygi, S. P., and Blenis, J. (2005). mTOR and S6K1 mediate assembly of the translation preinitiation complex through dynamic protein interchange and ordered phosphorylation events. *Cell* 123, 569–580. doi: 10.1016/j.cell.2005.10.024

Huang, W., Zhao, N., Bai, X., Karram, K., Trotter, J., Goebbels, S., et al. (2014). Novel NG2-CreERT2 knock-in mice demonstrate heterogeneous differentiation potential of NG2 glia during development. *Glia* 62, 896–913. doi: 10.1002/glia.22648

Jabs, R., Pivneva, T., Huttmann, K., Wyczynski, A., Nolte, C., Kettenmann, H., et al. (2005). Synaptic transmission onto hippocampal glial cells with hGFAP promoter activity. *J. Cell. Sci.* 118, 3791–3803. doi: 10.1242/jcs.02515

Jung, M., Kramer, E., Grzenkowski, M., Tang, K., Blakemore, W., Aguzzi, A., et al. (1995). Lines of murine oligodendroglial precursor cells immortalized by an activated neu tyrosine kinase show distinct degrees of interaction with axons *in vitro* and *in vivo*. *Eur. J. Neurosci.* 7, 1245–1265. doi: 10.1111/j.1460-9568.1995.tb01115.x

Karram, K., Goebbels, S., Schwab, M., Jennissen, K., Seifert, G., Steinhauser, C., et al. (2008). NG2-expressing cells in the nervous system revealed by the NG2-EYFP-knockin mouse. *Genesis* 46, 743–757. doi: 10.1002/dvg.20440

Kukley, M., Kiladze, M., Tognatta, R., Hans, M., Swandulla, D., Schramm, J., et al. (2008). Glial cells are born with synapses. *FASEB J* 22, 2957–2969. doi: 10.1096/fj.07-090985

Kukley, M., Nishiyama, A., and Dietrich, D. (2010). The fate of synaptic input to NG2 glial cells: neurons specifically downregulate transmitter release onto differentiating oligodendroglial cells. *J. Neurosci.* 30, 8320–8331. doi: 10.1523/JNEUROSCI.0854-10.2010

Lal, M., and Caplan, M. (2011). Regulated intramembrane proteolysis: signaling pathways and biological functions. *Physiology* 26, 34–44. doi: 10.1152/physiol.00028.2010

Laplante, M., and Sabatini, D. M. (2012). mTOR signaling in growth control and disease. *Cell* 149, 274–293. doi: 10.1016/j.cell.2012.03.017

Levitan, D., and Greenwald, I. (1995). Facilitation of lin-12-mediated signalling by sel-12, a Caenorhabditis elegans S182 Alzheimer's disease gene. *Nature* 377, 351–354.

Li, X., Wu, C., Chen, N., Gu, H., Yen, A., Cao, L., et al. (2016). PI3K/Akt/mTOR signaling pathway and targeted therapy for glioblastoma. *Oncotarget* 7, 33440–33450. doi: 10.18632/oncotarget.7961

Liu, C., and Zong, H. (2012). Developmental origins of brain tumors. *Curr. Opin. Neurobiol.* 22, 844–849. doi: 10.1016/j.conb.2012.04.012

Loeb, K. R., Kostner, H., Firpo, E., Norwood, T., Tsuchiya, K. D., Clurman, B. E., et al. (2005). A mouse model for cyclin E-dependent genetic instability and tumorigenesis. *Cancer Cell* 8, 35–47. doi: 10.1016/j.ccr.2005.06.010

Lucá, R., Averna, M., Zalfa, F., Vecchi, M., Bianchi, F., La Fata, G., et al. (2013). The fragile X protein binds mRNAs involved in cancer progression and modulates metastasis formation. *EMBO Mol. Med.* 5, 1523–1536. doi: 10.1002/emmm.201302847

Malinverno, M., Carta, M., Epis, R., Marcello, E., Verpelli, C., Cattabeni, F., et al. (2010). Synaptic localization and activity of ADAM10 regulate excitatory synapses through N-cadherin cleavage. *J. Neurosci.* 30, 16343–16355. doi: 10.1523/JNEUROSCI.1984-10.2010

Mangin, J. M., and Gallo, V. (2011). The curious case of NG2 cells: transient trend or game changer? *ASN Neuro* 3:e00052. doi: 10.1042/AN20110001

Maus, F., Sakry, D., Biname, F., Karram, K., Rajalingam, K., Watts, C., et al. (2015). The NG2 proteoglycan protects oligodendrocyte precursor cells against oxidative stress via interaction with omi/htra2. *PLoS ONE* 10:e0137311. doi: 10.1371/journal.pone.0137311

Moransard, M., Dann, A., Staszewski, O., Fontana, A., Prinz, M., and Suter, T. (2011). NG2 expressed by macrophages and oligodendrocyte precursor cells is dispensable in experimental autoimmune encephalomyelitis. *Brain 134*, 1315–1330. doi: 10.1093/brain/awr070

Nalavadi, V. C., Muddashetty, R. S., Gross, C., and Bassell, G. J. (2012). Dephosphorylation-induced ubiquitination and degradation of FMRP in dendrites: a role in immediate early mGluR-stimulated translation. *J. Neurosci.* 32, 2582–2587. doi: 10.1523/JNEUROSCI.5057-11.2012

Narayanan, U., Nalavadi, V., Nakamoto, M., Thomas, G., Ceman, S., Bassell, G. J., et al. (2008). S6K1 phosphorylates and regulates fragile X mental retardation protein (FMRP) with the neuronal protein synthesis-dependent mammalian target of rapamycin (mTOR) signaling cascade. *J. Biol. Chem.* 283, 18478–18482. doi: 10.1074/jbc.C800055200

Niehaus, A., Stegmuller, J., Diers-Fenger, M., and Trotter, J. (1999). Cell-surface glycoprotein of oligodendrocyte progenitors involved in migration. *J. Neurosci.* 19, 4948–4961. doi: 10.1523/JNEUROSCI.19-12-04948.1999

Nishiyama, A., Komitova, M., Suzuki, R., and Zhu, X. (2009). Polydendrocytes (NG2 cells): multifunctional cells with lineage plasticity. *Nat. Rev. Neurosci.* 10, 9–22. doi: 10.1038/nrn2495

Nishiyama, A., Lin, X. H., and Stallcup, W. B. (1995). Generation of truncated forms of the NG2 proteoglycan by cell surface proteolysis. *Mol. Biol. Cell.* 6, 1819–1832. doi: 10.1091/mbc.6.12.1819

Ohanna, M., Sobering, A. K., Lapointe, T., Lorenzo, L., Praud, C., Petroulakis, E., et al. (2005). Atrophy of S6K1(-/-) skeletal muscle cells reveals distinct mTOR effectors for cell cycle and size control. *Nat. Cell. Biol.* 7, 286–294. doi: 10.1038/ncb1231

Ozerdem, U., Monosov, E., and Stallcup, W. B. (2002). NG2 proteoglycan expression by pericytes in pathological microvasculature. *Microvasc. Res.* 63, 129–134. doi: 10.1006/mvre.2001.2376

Park, S., Park, J. M., Kim, S., Kim, J. A., Shepherd, J. D., Smith-Hicks, C. L., et al. (2008). Elongation factor 2 and fragile X mental retardation protein control the dynamic translation of Arc/Arg3.1 essential for mGluR-LTD. *Neuron* 59, 70–83. doi: 10.1016/j.neuron.2008.05.023

Pasciuto, E., and Bagni, C. (2014a). SnapShot: FMRP interacting proteins. *Cell* 159, 218–218.e1. doi: 10.1016/j.cell.2014.08.036

Pasciuto, E., and Bagni, C. (2014b). SnapShot: FMRP mRNA targets and diseases. *Cell* 158, 1446-1446.e1. doi: 10.1016/j.cell.2014.08.035

Pluschke, G., Vanek, M., Evans, A., Dittmar, T., Schmid, P., Itin, P., et al. (1996). Molecular cloning of a human melanoma-associated chondroitin sulfate proteoglycan. *Proc. Natl. Acad. Sci. U.S.A.* 93, 9710–9715. doi: 10.1073/pnas.93.18.9710

Poli, A., Wang, J., Domingues, O., Planaguma, J., Yan, T., Rygh, C. B., et al. (2013). Targeting glioblastoma with NK cells and mAb against NG2/CSPG4 prolongs animal survival. *Oncotarget* 4, 1527–1546. doi: 10.18632/oncotarget.1291

Prestegarden, L., Svendsen, A., Wang, J., Sleire, L., Skaftnesmo, K. O., Bjerkvig, R., et al. (2010). Glioma cell populations grouped by different cell type markers drive brain tumor growth. *Cancer Res.* 70, 4274–4279. doi: 10.1158/0008-5472.CAN-09-3904

Qin, M., Schmidt, K. C., Zametkin, A. J., Bishu, S., Horowitz, L. M., Burlin, T. V., et al. (2013). Altered cerebral protein synthesis in fragile X syndrome: studies in human subjects and knockout mice. *J. Cereb. Blood Flow Metab.* 33, 499–507. doi: 10.1038/jcbfm.2012.205

Rajasekhar, V. K., Viale, A., Socci, N. D., Wiedmann, M., Hu, X., and Holland, E. C. (2003). Oncogenic Ras and Akt signaling contribute to glioblastoma formation by differential recruitment of existing mRNAs to polysomes. *Mol. Cell.* 12, 889–901. doi: 10.1016/S1097-2765(03)00395-2

Richter, J. D., Bassell, G. J., and Klann, E. (2015). Dysregulation and restoration of translational homeostasis in fragile X syndrome. *Nat. Rev. Neurosci.* 16, 595–605. doi: 10.1038/nrn4001

Saftig, P., and Lichtenthaler, S. F. (2015). The alpha secretase ADAM10: a metalloprotease with multiple functions in the brain. *Prog. Neurobiol.* 135, 1–20. doi: 10.1016/j.pneurobio.2015.10.003

Saitoh, M., Pullen, N., Brennan, P., Cantrell, D., Dennis, P. B., and Thomas, G. (2002). Regulation of an activated S6 kinase 1 variant reveals a novel mammalian target of rapamycin phosphorylation site. *J. Biol. Chem.* 277, 20104–20112. doi: 10.1074/jbc.M201745200

Sakry, D., Karram, K., and Trotter, J. (2011). Synapses between NG2 glia and neurons. *J. Anat.* 219, 2–7. doi: 10.1111/j.1469-7580.2011.01359.x

Sakry, D., Neitz, A., Singh, J., Frischknecht, R., Marongiu, D., Biname, F., et al. (2014). Oligodendrocyte precursor cells modulate the neuronal network by activity-dependent ectodomain cleavage of glial NG2. *PLoS Biol.* 12:e1001993. doi: 10.1371/journal.pbio.1001993

Sakry, D., and Trotter, J. (2016). The role of the NG2 proteoglycan in OPC and CNS network function. *Brain Res.* 1638, 161–166. doi: 10.1016/j.brainres.2015.06.003

Sakry, D., Yigit, H., Dimou, L., and Trotter, J. (2015). Oligodendrocyte precursor cells synthesize neuromodulatory factors. *PLoS ONE* 10:e0127222. doi: 10.1371/journal.pone.0127222

Santos, A. R., Kanellopoulos, A. K., and Bagni, C. (2014). Learning and behavioral deficits associated with the absence of the fragile X mental retardation protein: what a fly and mouse model can teach us. *Learn Mem.* 21, 543–555. doi: 10.1101/lm.035956.114

Schmidt, E. K., Clavarino, G., Ceppi, M., and Pierre, P. (2009). SUnSET, a nonradioactive method to monitor protein synthesis. *Nat. Methods* 6, 275–277. doi: 10.1038/nmeth.1314

Schneider, S., Bosse, F., D'Urso, D., Muller, H., Sereda, M. W., Nave, K., et al. (2001). The AN2 protein is a novel marker for the Schwann cell lineage expressed by immature and nonmyelinating Schwann cells. *J. Neurosci.* 21, 920–933. doi: 10.1523/JNEUROSCI.21-03-00920.2001

Schnorrer, F., Kalchhauser, I., and Dickson, B. J. (2007). The transmembrane protein Kon-tiki couples to Dgrip to mediate myotube targeting in Drosophila. *Dev. Cell.* 12, 751–766. doi: 10.1016/j.devcel.2007.02.017

Sgambato, A., Camerini, A., Pani, G., Cangiano, R., Faraglia, B., Bianchino, G., et al. (2003). Increased expression of cyclin E is associated with an increased resistance to doxorubicin in rat fibroblasts. *Br. J. Cancer* 88, 1956–1962. doi: 10.1038/sj.bjc.6600970

Sharma, A., Hoeffer, C. A., Takayasu, Y., Miyawaki, T., McBride, S. M., Klann, E., et al. (2010). Dysregulation of mTOR signaling in fragile X syndrome. *J. Neurosci.* 30, 694–702. doi: 10.1523/JNEUROSCI.3696-09.2010

Simon, C., Gotz, M., and Dimou, L. (2011). Progenitors in the adult cerebral cortex: cell cycle properties and regulation by physiological stimuli and injury. *Glia* 59, 869–881. doi: 10.1002/glia.21156

Soliman, G. A., Acosta-Jaquez, H. A., Dunlop, E. A., Ekim, B., Maj, N. E., Tee, A. R., et al. (2010). mTOR Ser-2481 autophosphorylation monitors mTORC-specific catalytic activity and clarifies rapamycin mechanism of action. *J. Biol. Chem.* 285, 7866–7879. doi: 10.1074/jbc.M109.096222

Stallcup, W. B. (1977). Nerve and glial-specific antigens on cloned neural cell lines. *Prog. Clin. Biol. Res.* 15, 165–178.

Stegmüller, J., Schneider, S., Hellwig, A., Garwood, J., and Trotter, J. (2002). AN2, the mouse homologue of NG2, is a surface antigen on glial precursor cells implicated in control of cell migration. *J. Neurocytol.* 31, 497–505. doi: 10.1023/A:1025743731306

Stegmuller, J., Werner, H., Nave, K. A., and Trotter, J. (2003). The proteoglycan NG2 is complexed with alpha-amino-3-hydroxy-5-methyl-4-isoxazolepropionic acid (AMPA) receptors by the PDZ glutamate receptor interaction protein (GRIP) in glial progenitor cells. Implications for glial-neuronal signaling. *J. Biol. Chem.* 278, 3590–3598. doi: 10.1074/jbc.M210010200

Sudol, M., Sliwa, K., and Russo, T. (2001). Functions of WW domains in the nucleus. *FEBS Lett.* 490, 190–195. doi: 10.1016/S0014-5793(01)02122-6

Sugiarto, S., Persson, A. I., Munoz, E. G., Waldhuber, M., Lamagna, C., Andor, N., et al. (2011). Asymmetry-defective oligodendrocyte progenitors are glioma precursors. *Cancer Cell* 20, 328–340. doi: 10.1016/j.ccr.2011.08.011

Suzuki, K., Hayashi, Y., Nakahara, S., Kumazaki, H., Prox, J., Horiuchi, K., et al. (2012). Activity-dependent proteolytic cleavage of neuroligin-1. *Neuron* 76, 410–422. doi: 10.1016/j.neuron.2012.10.003

Tyler, W. A., Gangoli, N., Gokina, P., Kim, H. A., Covey, M., Levison, S. W., et al. (2009). Activation of the mammalian target of rapamycin (mTOR) is essential for oligodendrocyte differentiation. *J. Neurosci.* 29, 6367–6378. doi: 10.1523/JNEUROSCI.0234-09.2009

Wang, R., Kamgoue, A., Normand, C., Leger-Silvestre, I., Mangeat, T., and Gadal, O. (2016). High resolution microscopy reveals the nuclear shape of budding yeast during cell cycle and in various biological states. *J. Cell. Sci.* 129, 4480–4495. doi: 10.1242/jcs.188250

Wang, X., Li, W., Williams, M., Terada, N., Alessi, D. R., and Proud, C. G. (2001). Regulation of elongation factor 2 kinase by p90(RSK1) and p70 S6 kinase. *EMBO J.* 20, 4370–4379. doi: 10.1093/emboj/20.16.4370

Weiler, I. J., Spangler, C. C., Klintsova, A. Y., Grossman, A. W., Kim, S. H., Bertaina-Anglade, V., et al. (2004). Fragile X mental retardation protein is necessary for neurotransmitter-activated protein translation at synapses. *Proc. Natl. Acad. Sci. U.S.A.* 101, 17504–17509. doi: 10.1073/pnas.0407533101

You, W. K., Yotsumoto, F., Sakimura, K., Adams, R. H., and Stallcup, W. B. (2014). NG2 proteoglycan promotes tumor vascularization via integrin-dependent effects on pericyte function. *Angiogenesis* 17, 61–76. doi: 10.1007/s10456-013-9378-1

Zalfa, F., Giorgi, M., Primerano, B., Moro, A., Di Penta, A., Reis, S., et al. (2003). The fragile X syndrome protein FMRP associates with BC1 RNA and regulates the translation of specific mRNAs at synapses. *Cell* 112, 317–327. doi: 10.1016/S0092-8674(03)00079-5

Zhu, X., Bergles, D. E., and Nishiyama, A. (2008). NG2 cells generate both oligodendrocytes and gray matter astrocytes. *Development* 135, 145–157. doi: 10.1242/dev.004895

Zou, Y., Jiang, W., Wang, J., Li, Z., Zhang, J., Bu, J., et al. (2014). Oligodendrocyte precursor cell-intrinsic effect of Rheb1 controls differentiation and mediates mTORC1-dependent myelination in brain. *J. Neurosci.* 34, 15764–15778. doi: 10.1523/JNEUROSCI.2267-14.2014

Conflict of Interest Statement: The authors declare that the research was conducted in the absence of any commercial or financial relationships that could be construed as a potential conflict of interest.

frontiers in Cellular Neuroscience

MINI REVIEW
published: 05 September 2018
doi: 10.3389/fncel.2018.00299

Schwann Cell Responses and Plasticity in Different Dental Pulp Scenarios

Eduardo Couve[1]* *and Oliver Schmachtenberg*[2]

[1]*Laboratorio de Microscopía Electrónica, Instituto de Biología, Facultad de Ciencias, Universidad de Valparaíso, Valparaíso, Chile,* [2]*Centro Interdisciplinario de Neurociencias de Valparaíso (CINV), Facultad de Ciencias, Universidad de Valparaíso, Valparaíso, Chile*

Mammalian teeth have evolved as dentin units that enclose a complex system of sensory innervation to protect and preserve their structure and function. In human dental pulp (DP), mechanosensory and nociceptive fibers form a dense meshwork of nerve endings at the coronal dentin-pulp interface, which arise from myelinated and non-myelinated axons of the Raschkow plexus (RP). Schwann cells (SCs) play a crucial role in the support, maintenance and regeneration after injury of these fibers. We have recently characterized two SC phenotypes hierarchically organized within the coronal and radicular DP in human teeth. Myelinating and non-myelinating SCs (nmSCs) display a high degree of plasticity associated with nociceptive C-fiber sprouting and axonal degeneration in response to DP injuries from dentin caries or physiological root resorption (PRR). By comparative immunolabeling, confocal and electron microscopy, we have characterized short-term adaptive responses of SC phenotypes to nerve injuries, and long-term changes related to aging. An increase of SCs characterizes the early responses to caries progression in association with axonal sprouting in affected DP domains. Moreover, during PRR, the formation of bands of Büngner is observed as part of SC repair tracks functions. On the other hand, myelinated axon density is significantly reduced with tooth age, as part of a gradual decrease in DP defense and repair capacities. The remarkable plasticity and capacity of SCs to preserve DP innervation in different dental scenarios constitutes a fundamental aspect to improve clinical treatments. This review article discusses the central role of myelinating and non-mSCs in long-term tooth preservation and homeostasis.

Keywords: tooth, glia, myelin, aging, caries, dentin

OPEN ACCESS

Edited by:
Mauricio Antonio Retamal, Universidad del Desarrollo, Chile

Reviewed by:
Ivo Lambrichts, University of Hasselt, Belgium
Igor Adameyko, Karolinska Institutet (KI), Sweden

***Correspondence:**
Eduardo Couve
eduardo.couve@uv.cl

Received: *16 June 2018*
Accepted: *17 August 2018*
Published: *05 September 2018*

Citation:
Couve E and Schmachtenberg O (2018) Schwann Cell Responses and Plasticity in Different Dental Pulp Scenarios. Front. Cell. Neurosci. 12:299. doi: 10.3389/fncel.2018.00299

THE DENTIN-PULP INTERFACE IN MULTICUSP TEETH

From an evolutionary perspective, a single tooth is a dentin unit formed by odontoblasts, protected by enameloide or enamel and containing an innervated dental pulp (DP). During vertebrate evolution, the appearance of cone-shaped teeth in fish constitutes a crucial event within the adaptation of vertebrate feeding mechanisms, from sucking to predatory animals (Smith and Johanson, 2015). Moreover, the increase in tooth size and shape complexity is related with a gradual reduction of the robust mechanisms of continuous tooth replacement observed in polyphyodonts, to a non- or single-renewal mechanism in mammals (monophyodont or diphyodont dentition).

These phenomena became associated with an increase in DP complexity to ensure tooth preservation for a prolonged time. In fact, the mode of tooth replacement is critical for the maintenance of dentition (Jernvall and Thesleff, 2012). Different shedding mechanisms have been characterized for tooth replacement, as in chondrichthyans (e.g., sharks), where the whole tooth is shed, or in osteichthyes and tetrapods, where a progressive resorption of the attachment system occurs prior to exfoliation (Chen et al., 2016). Accordingly, increasing dental complexity in mammal's dentition is associated with a limited capacity for tooth replacement and increasingly sophisticated mechanisms to prolong the life of the tooth, like hypsodonty and continuously growing (hypselodont) teeth.

In mammals, the transition from predatory to masticator dentition has also been characterized by the innovative formation of multicusp teeth and the development of roots to provide strong attachment and to increase the maximum allowable biting force (Constantino et al., 2016). While the early emergence and evolution of dentin in primitive vertebrates has been related to a nascent sensory function of the DP (Smith and Sansom, 2000; Farahani et al., 2011), it is attractive to hypothesize that in mammalian teeth, the limited replacement and increased longevity of dentition required an enlargement and an increased complexity of the DP, in which odontoblasts, sensory nerve endings and Schwann cells (SCs), in association with immune and vascular components, create a multicellular interface, which fulfills critical functions in sensory protection, defense and repair of the tooth (**Figures 1A,B**). Thus, nerves, glial and immune components interact to sense and respond to external stimuli and changes at the dentin-pulp interface (Couve et al., 2014, 2018).

From a general perspective, different barrier surfaces of the body (i.e., skin, gut and respiratory tract) harbor numerous nerve endings, glial and immune cells to ensure permanent monitoring of pathogen infection and tissue damage. The development of physical barriers in multicellular organisms constitutes the first line of defense against environmental changes and threats. Moreover, there is evidence that functional integration of nerve endings, immune and glial cells at barrier surfaces is essential to guarantee tissue homeostasis, defense and repair (Ordovas-Montanes et al., 2015; Veiga-Fernandes and Mucida, 2016; Chavan et al., 2018). In other words, the neuronal, glial and immune cell triad orchestrates a complex scenario between the internal and external environment (Scholz and Woolf, 2007; Veiga-Fernandes and Artis, 2018).

Currently, three competing theories regarding sensory transduction in the DP are being considered (Chung et al., 2013). In the neural theory, transduction of thermal and mechanical stimuli occurs in nerve terminals within dentinal tubules. In the hydrodynamic theory, both mechanical and thermal stimuli are converted to fluid pressure changes within the dentinal tubules, which are sensed and transduced by odontoblast processes and/or sensory nerve terminals (Shibukawa et al., 2015). In the third theory, odontoblasts act as direct transducers of thermal and mechanical stimuli, which then transmit sensory information to afferent nerve endings, possibly involving the release of ATP through pannexin channels. Indeed, thermal and mechanosensitive TRPV1, TRPM7 and pannexin channel expression has been reported in odontoblasts (Shibukawa et al., 2015; Won et al., 2018). Whatever the precise contribution of odontoblasts to sensory transduction, they have been referred to as relevant players during dentin stimulation according to their strategic location at the dentin-pulp interface (Couve et al., 2013).

INNERVATION AND SCHWANN CELLS IN THE HUMAN DENTAL PULP

During tooth development in mammals, non-myelinated axons display continuous terminal sprouting as they approach the dentin-pulp interface in proximity to the pulp horns, a phenomenon that is mediated by diffusible neurotrophic factors which coordinate sensory nerve growth and tooth morphogenesis (Byers, 1984; Mitsiadis and Luukko, 1995; Luukko and Kettunen, 2014). Indeed, the role of innervation and expression of nerve growth factor (NGF) is considered crucial for the development of the tooth (Mitsiadis and Pagella, 2016). In mature rat molars, phenotypically different nerve endings innervate buccal or lingual pulp horns, suggesting a surprisingly complex somatosensory situation within the DP (Byers and Cornel, 2018).

The human DP is densely innervated by trigeminal sensory afferents consisting mainly of specialized polymodal nociceptors morphologically characterized as myelinated (Aδ) and non-myelinated axons (C-fibers), which are supported by two phenotypes of SCs, myelinating and non-myelinating, respectively (**Figure 1C**).

The function of both myelinated and non-myelinated nociceptors is crucial for the detection of noxious stimuli, like excessive pressures or lateral forces for example, and to protect the dental tissue from injuries through the activation of pain perception (Woolf and Ma, 2007; Smith and Lewin, 2009; Dubin and Patapoutian, 2010; Pinho-Ribeiro et al., 2017). Even though SCs are mainly associated with a myelinating function, they are also involved in the regulation of immune responses by secreting cytokines and chemokines (Ydens et al., 2013), and could amplify inflammation in association with nociceptors and dendritic cells (Ordovas-Montanes et al., 2015).

Morphological and quantitative studies in human DP have determined the number and size of myelinated and non-myelinated axons. The average number of myelinated axons at the juxta-apical region of root pulp is about 312 ± 149 axons (average diameter 3.5 μm), while the average of non-myelinated axons is about 2,000 ± 1,023 (average diameter 0.5 μm), suggesting that more than three quarters of axons within the pulp are non-myelinated nociceptors (Nair et al., 1992; Nair and Schroeder, 1995). At the radicular pulp, both types of axons form large nerve bundles that become highly arborized at the Raschkow plexus (RP) within the coronal pulp, from where the nerve endings traverse through the odontoblast layer to reach the adjacent predentin/dentin domain (Byers et al., 2003). Nociceptors are able to detect noxious stimuli to protect the organism from danger and also play a critical role in the modulation of immune responses,

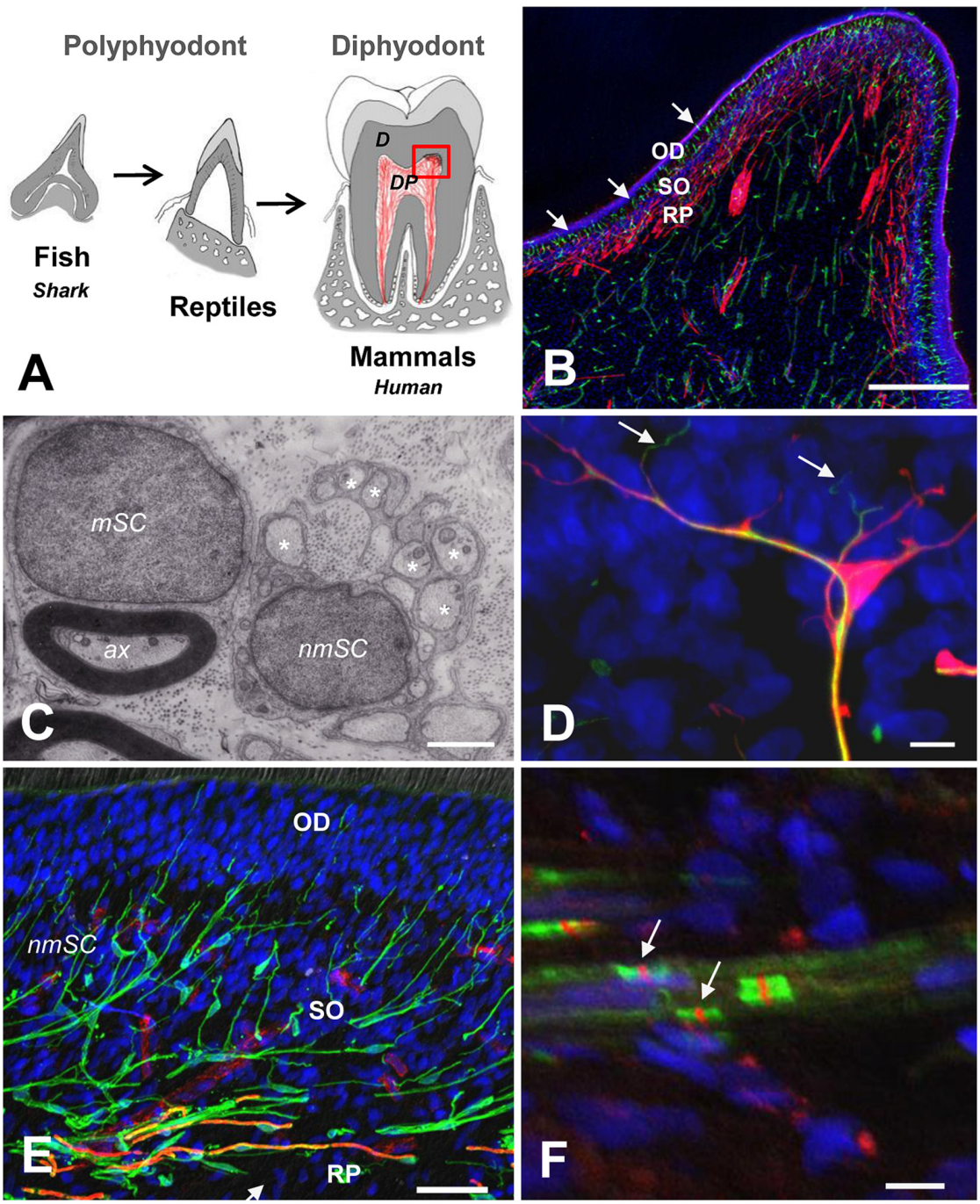

FIGURE 1 | (A) Schematic representation of vertebrate tooth evolution. In lower vertebrates like fishes (chondrichthyes and osteichthyes) and reptiles, dentition is characterized by cone-shaped teeth that are continuously replaced (polyphyodont). In mammals, teeth developed a complex attachment system associated with a root anchored to the jaw bone. Tooth replacement in most mammals is characterized by a diphyodont dentition. The dental pulp (DP) in mammals is enlarged and contains a complex multicellular system. **(B)** Magnification of the dentin-pulp interface from the coronal DP (red square on the left). Schwann cells (SCs; S100, red) are densely arranged at the Raschkow plexus (RP), while dendritic cells (HLA-DR, green, arrows) are radially projected from the sub-odontoblastic region (SO) into the odontoblastic layer (OD). Scale bar: 200 μm. **(C)** Electron microscopy of a myelinating SC (mSC) showing a 1:1 relationship with an axon (ax) and a non-mSC Schwann cell (nmSC) associated with several small-diameter axons (asterisks: remak bundles). Scale bar: 1 μm. **(D)** Terminal SC (S100, red) close to the odontoblast layer showing nerve endings (NF200, green, arrows) emerging from glial processes. Scale bar: 10 μm. **(E)** Triple immunolabeling showing the SC glial network at the dentin-pulp interface (S100, green). Myelinated fibers (MBP, orange, arrows) are located at the RP. Terminal capillary vessels (CD31, red) are evident at the base of the OD. Scale bar: 50 μm. **(F)** Nodes of Ranvier showing sodium channel clusters (Nav, red, arrows) between perinodal Caspr labeling (green). Scale bar: 10 μm. **(B,D,E)** Modified from Couve et al. (2018). **(F)** Modified from Sepulveda (2017).

producing among others neuropeptides like CGRP, which have potent effects on vascular and immune components, mediating neurogenic inflammation (Chiu et al., 2012, 2013). Thus, in the coronal mammalian DP, a profuse neurosensory system forms a complex nociceptive network to ensure defense and preservation of the tooth, for almost a whole life in humans.

Accordingly, in deciduous and permanent human teeth, SCs form a prominent glial network at the dentin-pulp interface consisting of myelinating and non-myelinating phenotypes (**Figure 1B**). Peripheral glial cells have emerged as crucial protective components to preserve nerve fibers and guide innervation (Kastriti and Adameyko, 2017). SCs are derived from multipotent migratory neural crest cells through an intermediate cell type, the SC precursor (SCP; Jessen and Mirsky, 2005). Moreover, SCPs represent the source of all subtypes of peripheral glial cells and other cell types; including myelinating and non-myelinating SC (nmSCs; Furlan and Adameyko, 2018). SCPs are able to proliferate and migrate in association with neuronal fibers, and transform into immature SCs in response to coordinated signaling events during the early development of peripheral nerves (Mirsky et al., 2002; Monk et al., 2015). The differentiation of immature SCs into mature myelinating and non-mSCs is a dynamic process (radial sorting) that restricts their functional fate and serves to separate those axons destined to be myelinated from those that remain unmyelinated and will reside as Remak bundles (Monk et al., 2015).

Moreover, during peripheral nerve development, SCs associate with blood vessels and influence arterial differentiation and angiogenic remodeling by local expression of VEGF, allowing vessels to follow nerve fiber outgrowth (Mukouyama et al., 2002; Jessen and Mirsky, 2005). SCs are also able to release a number of signaling molecules in response to nerve injuries. The expression of NGF receptors (NGFR), like the p75 neurotrophin receptor (p75NTR) is up-regulated by SCs in injured nerves. Non-mSCs classically referred to as Remak SCs play important roles in trophic support and plasticity of terminal axons through the expression of neurotrophin receptors, like p75NTR (Couve et al., 2018).

At the dentin-pulp interface of human teeth, SCs are integrated within a complex multicellular organization together with sensory nerve endings and immunocompetent cells (dendritic cells), suggesting a concerted function in the defense against pathogens, dentin repair and regeneration (Couve et al., 2018). At the main barrier surfaces of the body (i.e., skin, gut, airways), nerve fibers and immune cells form sensory interfaces able to detect pathogens and mediate responses to tissue-specific environmental changes (Veiga-Fernandes and Mucida, 2016).

Diverse molecular markers have been used to characterize different phenotypic profiles for SC stages (Jessen and Mirsky, 2005). In the DP of mature permanent human teeth, the classic SC markers S100 and GFAP are expressed by myelinating and non-mSCs, showing different locations at the dentin-pulp interface. Myelinating SCs also express myelin proteins (e.g., myelin basic protein, MBP), and are only present at the nerve bundles and the RP, while non-mSCs locate to nerve bundles as elongated cells, and to the dentin-pulp interface as highly branched (arborized) terminal SCs (**Figures 1D,E**). Terminal non-mSCs are located preferentially at barrier surfaces and have the capacity to response to an injury (Griffin and Thompson, 2008).

Myelinated axons are characterized by the nodes of Ranvier to allow saltatory conduction of action potentials and increase signal conduction speed. The accumulation of sodium channels at caspr perinodal sites identifies this property (**Figure 1F**). Changes in the expression of sodium channels have been observed in injured nerves associated to inflammatory conditions, suggesting that nodal modifications contribute to different pain states (Henry et al., 2007). Moreover, remodeling of the molecular organization of the nodes of Ranvier has been associated with painful DP conditions and spontaneous pulpal pain generation (Henry et al., 2009; Levinson et al., 2012).

Peripheral nerves also have a remarkable capacity to regenerate axons after injury, a process in which SCs play a central role (Jessen and Mirsky, 2016). The plasticity of SCs contributes to the regenerative capacity of damaged peripheral nerves (Gaudet et al., 2011). However, SCs require the other pulpal cellular players to promote axonal regeneration (Cattin and Lloyd, 2016). Injury of peripheral nerve fibers induces mature myelinating and non-mSCs to dedifferentiate into a repair phenotype, allowing axonal regeneration and re-innervation of sensory target areas (Jessen and Mirsky, 2008, 2016). The reprogramming of SCs constitutes an adaptive process in response to nerve fiber injury, and involves major changes in gene expression that promote SC repair phenotypes and the regeneration of damaged peripheral axons (Arthur-Farraj et al., 2012; Fontana et al., 2012; Jessen and Mirsky, 2016).

SCHWANN CELLS IN RESPONSE TO CARIES

Dental caries is a dynamic process initiated by a microbial biofilm that leads to demineralization of the hard dental tissues (Kidd and Fejerskov, 2004; Pitts et al., 2017). Dental pain prevalence is consistently associated with caries experience and socioeconomic status (Slade, 2001). Dental caries progress affects dentin and causes conspicuous changes within the DP. Moderate caries promotes the formation of reactionary dentin in association with local sprouting of nerve endings and a coordinated neuroimmune reaction (Couve et al., 2014). However, the response of the pulpal glial network to caries progression has been scarcely investigated. Changes in the expression of SC markers (S100 and GFAP) in response to caries pathogens are evident at initial caries stages (**Figures 2A,B**), while a major expansion of the reactive glial network occurs in response to advancing pathogen bacteria during severe dentin caries stages, indicating a dynamic pulpal reaction to control the caries advance (Houshmandi et al., 2014). If this response remains unsuccessful, DP inflammation mediated by caries pathogens can lead to pulpal tissue necrosis (Farges et al., 2015).

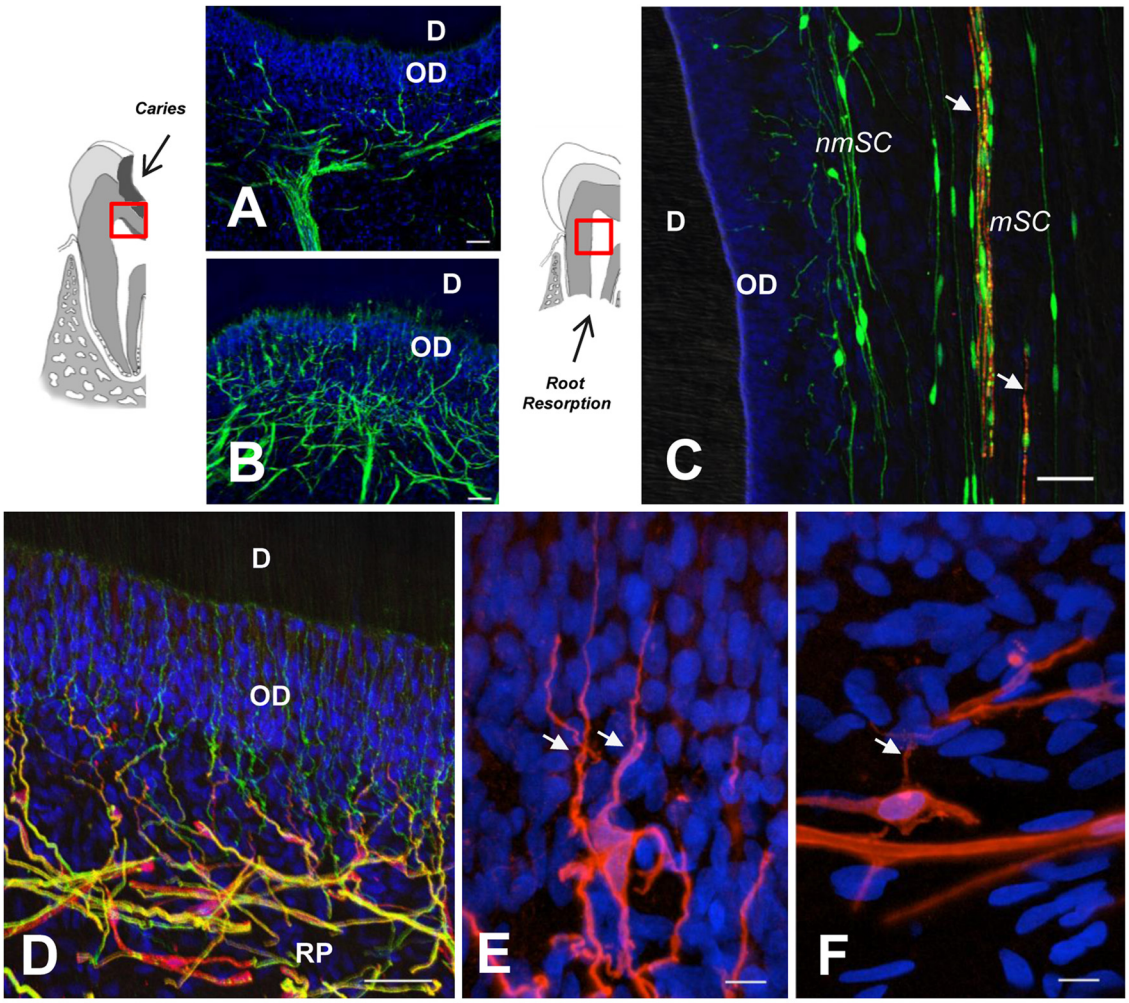

FIGURE 2 | (A,B) GFAP immunolabeling reveals SC network differences between a healthy dentin-pulp interface **(A)** and beneath a dentin caries lesion, as indicated in the sketch to the left **(B)**. Note SC profiles interspersed between OD. **(C)** Double immunolabeling of a deciduous tooth with physiological root resorption (PRR), showing highly fragmented myelin (MBP, red, arrows) and terminal SCs (S100, green) at the periphery. **(D)** Terminal nmSCs (S100, red) close to the OD supporting nerve endings (TUBB3, green). **(E,F)** High magnification showing the arborization of terminal SCs from a young individual compared with an aged sample, which displays comparatively fewer branches. RP, Raschkow plexus. Scale bars: **(A–D)**, 50 μm; **(E,F)**, 10 μm. **(C)**, modified from Suzuki et al. (2015); **(D)** modified from Couve et al. (2014); **(E,F)** modified from Couve et al. (2018).

It has been suggested that odontoblasts are the first barrier against invading caries pathogens and that they are also capable of orchestrating an inflammatory response that may lead to pulp necrosis (Cooper et al., 2010; Horst et al., 2011). At the dentin-pulp interface, the triad of nerve endings, glial and dendritic cells senses incipient damage, and is able to crank up defense, repair and regenerative processes. DP inflammation is a localized response defending the dental superstructure. Under affected dentin caries domains, noxious stimulation causes a local neurogenic inflammation during early stages of caries progression, modulating the expression of neuropeptides, growth factors, cytokines and chemokines (Cooper et al., 2014). In this process, the expression of NGF, p75NTR and TrkA has been detected in human carious teeth (Mitsiadis et al., 2017). SCs underneath carious lesions are activated by the expression of p75NTR, suggesting that the expression of NGF and neurogenic receptors participate in the nerve sprouting process. These data suggest that neurotrophic molecules activate SCs to regenerate affected nerve endings and avoid sensory loss and preserve the tooth (Mitsiadis et al., 2017). It is also possible that reprogrammed SCs acquire a SCP phenotype, as a multipotent cell that can become involved in the formation of odontoblast-like cells to promote the formation of reparative dentin in injured teeth (Kaukua et al., 2014). Indeed, the robust repair capacity of SCs is associated with their dedifferentiation capacity to coordinate repair in different tissues (Carr and Johnston, 2017).

Moreover, DP cells extracted from human third molars cultured under special conditions allow establishing

different human DP stem cell populations (hDPSCs) which can be induced to differentiate into SCs, expressing p75NTR, Sox10 and S100 (Al-Zer et al., 2015). hDPSCs also express neurotrophic factors like NGF, and are able to promote axonal outgrowth *in vitro* (Martens et al., 2014), suggesting the potential usefulness of hDPSCs for tissue engineering therapies of injured peripheral nerves (Luo et al., 2018).

THE SCHWANN CELL RESPONSE TO ROOT RESORPTION

Physiological root resorption (PRR) is an asymptomatic process which in humans forms part of the natural mechanism of tooth replacement. It is mediated by odontoclasts that progressively reduce the root and DP tissue prior to exfoliation (Moorrees et al., 1963). During the PRR process, a reduction of DP innervation has been characterized as a Wallerian-like axonal degeneration process (Monteiro et al., 2009), leading to a reduction of nerve fiber bundles and nerve endings. In parallel, myelin sheath degradation (**Figure 2C**) and a progressive reduction of myelinated axons is associated with an activation of autophagic activity by SCs (Suzuki et al., 2015). In fact, a chronic compression of peripheral nerves constitutes an injury that promotes demyelination and activation of repair SC phenotypes, suggesting that SCs are directly sensitive to mechanical stimuli (Belin et al., 2017). SCs display considerable phenotypic plasticity and facilitate the surprisingly fast recovery of peripheral nerves after PRR or other insults (Boerboom et al., 2017).

Demyelination of damaged axons implies the accumulation of myelin debris within the SC. Myelin debris acts as an obstacle for the regeneration of axons and is considered a major contributor to the inflammatory response after nerve injury (Gaudet et al., 2011). Indeed, there is an increase of immunocompetent cells during the PRR process, suggesting a progressive inflammatory condition (Angelova et al., 2004). However, SCs are able to activate an autophagic pathway to promote myelin clearance during Wallerian degradation (Gomez-Sanchez et al., 2015).

In injured peripheral nerves, adaptive SCs reprogram into immature phenotypes with proliferative capacity forming bands of Büngner to allow axonal regeneration (Suzuki et al., 2015). Moreover, a remarkable feature at advanced stages of root resorption in deciduous teeth is an increase of major histocompatibility complex (MHC) class II (HLA-DR) expression in SCs in association with immunocompetent cell recruitment (Suzuki et al., 2015). PRR is associated with a progressive asymptomatic chronic inflammatory process that comprises axonal degeneration of DP nerves, in which dedifferentiation of SCs, proliferation and expression of repair SC markers is observed. The immunocompetent function of SCs as antigen processing and presenting cells has been associated with immune responses and the recruitment of inflammatory cells to injured peripheral nerves; observations that remain an attractive topic for the understanding of the immunomodulatory functions of SCs (Meyer zu Hörste et al., 2008; Meyer Zu Horste et al., 2010).

AGING OF SCHWANN CELLS

A reduced expression in SC phenotype markers (S100 and MBP) has been determined at the dentin-pulp interface in aged permanent teeth, suggesting a reduction in the sensory and regenerative capacity of the DP with age (Couve et al., 2018). Furthermore, at the dentin-pulp interface of aged teeth, a smaller number of nerve endings projects through the odontoblast layer, and terminal SCs display a reduced degree of arborization (**Figures 2D–F**). Age-related changes within the glial network of the DP are related to the diminished regenerative capacity observed for peripheral sensory nerves with age (Verdú et al., 2000; Painter et al., 2014). It has been suggested that the impairment of regenerative capacity associated to the aging progress derives from reduced SC plasticity related to myelin debris clearance (Painter et al., 2014; Painter, 2017). Dedifferentiation of SCs following peripheral nerve injury tends to be delayed with age in correspondence with a delayed onset of key regulatory factor signaling, like c-jun expression (Chen et al., 2017). During the reprogramming process of SCs within injured peripheral nerves, a downregulation of myelin protein expression (e.g., MBP), is accompanied by an upregulation of the transcription factor c-jun, the low affinity neurotrophin receptor (p75NTR) and GFAP (Arthur-Farraj et al., 2012). However, in the DP of teeth from aged individuals, a reduced expression of p75NTR suggests a limited defense and regenerative capacity of SCs (Couve et al., 2018).

CONCLUSION

The evolution of vertebrate teeth produced an increasingly complex neuronal and glial network within the DP to protect the longer lasting teeth. Specifically, SCs form a prominent network at the coronal dentin-pulp interface in human teeth, playing a crucial role in the support and maintenance of DP nerves. SCs, nerve endings and immune cells create a multicellular barrier at the dentin-pulp interface sensing and responding to environmental changes and threats. The characterization of terminal SC plasticity contributes to our growing understanding of the central roles of these versatile cells within the DP scenario.

AUTHOR CONTRIBUTIONS

EC wrote the manuscript with OS.

ACKNOWLEDGMENTS

This study was supported by Fondecyt Grant nos. 1141281 (EC) and 1171228 (OS). The Centro Interdisciplinario de Neurociencias de Valparaíso (CINV) is a Millenium Institute (P09-022-F) supported by the Millennium Scientific Initiative of the Ministry of Economy, Development and Tourism (Chile).

REFERENCES

Al-Zer, H., Apel, C., Heiland, M., Friedrich, R. E., Jung, O., Kroeger, N., et al. (2015). Enrichment and Schwann cell differentiation of neural crest-derived dental pulp stem cells. *In Vivo* 29, 319–326.

Angelova, A., Takagi, Y., Okiji, T., Kaneko, T., and Yamashita, Y. (2004). Immunocompetent cells in the pulp of human deciduous teeth. *Arch. Oral Biol.* 49, 29–36. doi: 10.1016/s0003-9969(03)00173-0

Arthur-Farraj, P. J., Latouche, M., Wilton, D. K., Quintes, S., Chabrol, E., Banerjee, A., et al. (2012). c-Jun reprograms Schwann cells of injured nerves to generate a repair cell essential for regeneration. *Neuron* 75, 633–647. doi: 10.1016/j.neuron.2012.06.021

Belin, S., Zuloaga, K. L., and Poitelon, Y. (2017). Influence of mechanical stimuli on schwann cell biology. *Front. Cell. Neurosci.* 11:347. doi: 10.3389/fncel.2017.00347

Boerboom, A., Dion, V., Chariot, A., and Franzen, R. (2017). Molecular mechanisms involved in Schwann cell plasticity. *Front. Mol. Neurosci.* 10:38. doi: 10.3389/fnmol.2017.00038

Byers, M. R. (1984). Dental sensory receptors. *Int. Rev. Neurobiol.* 25, 39–94. doi: 10.1016/s0074-7742(08)60677-7

Byers, M. R., and Cornel, L. M. (2018). Multiple complex somatosensory systems in mature rat molars defined by immunohistochemistry. *Arch. Oral Biol.* 85, 84–97. doi: 10.1016/j.archoralbio.2017.09.007

Byers, M. R., Suzuki, H., and Maeda, T. (2003). Dental neuroplasticity, neuropulpal interactions and nerve regeneration. *Microsc. Res. Tech.* 60, 503–515. doi: 10.1002/jemt.10291

Carr, M. J., and Johnston, A. P. W. (2017). Schwann cells as drivers of tissue repair and regeneration. *Curr. Opin. Neurobiol.* 47, 52–57. doi: 10.1016/j.conb.2017.09.003

Cattin, A. L., and Lloyd, A. C. (2016). The multicellular complexity of peripheral nerve regeneration. *Curr. Opin. Neurobiol.* 39, 38–46. doi: 10.1016/j.conb.2016.04.005

Chavan, S. S., Ma, P., and Chiu, I. M. (2018). Neuro-immune interactions in inflammation and host defense: implications for transplantation. *Am. J. Transplant.* 18, 556–563. doi: 10.1111/ajt.14515

Chen, D., Blom, H., Sanchez, S., Tafforeau, P., and Ahlberg, P. E. (2016). The stem osteichthyan Andreolepis and the origin of tooth replacement. *Nature* 539, 237–241. doi: 10.1038/nature19812

Chen, W. A., Luo, T. D., Barnwell, J. C., Smith, T. L., and Li, Z. (2017). Age-dependent schwann cell phenotype regulation following peripheral nerve injury. *J. Hand Surg. Asian Pac. Vol.* 22, 464–471. doi: 10.1142/S0218810417500514

Chiu, I. M., Heesters, B. A., Ghasemlou, N., von Hehn, C. A., Zhao, F., Tran, J., et al. (2013). Bacteria activate sensory neurons that modulate pain and inflammation. *Nature* 501, 52–57. doi: 10.1038/nature12479

Chiu, I. M., von Hehn, C. A., and Woolf, C. J. (2012). Neurogenic inflammation and the peripheral nervous system in host defense and immunopathology. *Nat. Neurosci.* 15, 1063–1067. doi: 10.1038/nn.3144

Chung, G., Jung, S. J., and Oh, S. B. (2013). Cellular and molecular mechanisms of dental nociception. *J. Dent. Res.* 92, 948–955. doi: 10.1177/0022034513501877

Constantino, P. J., Bush, M. B., Barani, A., and Lawn, B. R. (2016). On the evolutionary advantage of multi-cusped teeth. *J. R. Soc. Interface* 13:20160374. doi: 10.1098/rsif.2016.0374

Cooper, P. R., Holder, M. J., and Smith, A. J. (2014). Inflammation and regeneration in the dentin-pulp complex: a double-edged sword. *J. Endod.* 40, S46–S51. doi: 10.1016/j.joen.2014.01.021

Cooper, P. R., Takahashi, Y., Graham, L. W., Simon, S., Imazato, S., and smith, A. J. (2010). Inflammation-regeneration interplay in the dentine-pulp complex. *J. Dent.* 38, 687–697. doi: 10.1016/j.jdent.2010.05.016

Couve, E., Lovera, M., Suzuki, K., and Schmachtenberg, O. (2018). Schwann cell phenotype changes in aging human dental pulp. *J. Dent. Res.* 97, 347–355. doi: 10.1177/0022034517733967

Couve, E., Osorio, R., and Schmachtenberg, O. (2013). The amazing odontoblast: activity, autophagy, and aging. *J. Dent. Res.* 92, 765–772. doi: 10.1177/0022034513495874

Couve, E., Osorio, R., and Schmachtenberg, O. (2014). Reactionary dentinogenesis and neuroimmune response in dental caries. *J. Dent. Res.* 93, 788–793. doi: 10.1177/0022034514539507

Dubin, A. E., and Patapoutian, A. (2010). Nociceptors: the sensors of the pain pathway. *J. Clin. Invest.* 120, 3760–3772. doi: 10.1172/jci42843

Farahani, R. M., Simonian, M., and Hunter, N. (2011). Blueprint of an ancestral neurosensory organ revealed in glial networks in human dental pulp. *J. Comp. Neurol.* 519, 3306–3326. doi: 10.1002/cne.22701

Farges, J-C., Alliot-Licht, B., Renard, E., Ducret, M., Gaudin, A., Smith, A. J., et al. (2015). Dental pulp defence and repair mechanisms in dental caries. *Mediators Inflamm.* 2015:230251. doi: 10.1155/2015/230251

Fontana, X., Hristova, M., Da Costa, C., Patodia, S., Thei, L., Makwana, M., et al. (2012). c-Jun in Schwann cells promotes axonal regeneration and motoneuron survival via paracrine signaling. *J. Cell Biol.* 198, 127–141. doi: 10.1083/jcb.201205025

Furlan, A., and Adameyko, I. (2018). Schwann cell precursor: a neural crest cell in disguise? *Dev. Biol.* 1606, 30852–30857. doi: 10.1016/j.ydbio.2018.02.008

Gaudet, A. D., Popovich, P. G., and Ramer, M. S. (2011). Wallerian degeneration: gaining perspective on inflammatory events after peripheral nerve injury. *J. Neuroinflammation* 8:110. doi: 10.1186/1742-2094-8-110

Gomez-Sanchez, J. A., Carty, L., Iruarrizaga-Lejarreta, M., Palomo-Irigoyen, M., Varela-Rey, M., Griffith, M., et al. (2015). Schwann cell autophagy, myelinophagy, initiates myelin clearance from injured nerves. *J. Cell Biol.* 210, 153–168. doi: 10.1083/jcb.201503019

Griffin, J. W., and Thompson, W. J. (2008). Biology and pathology of nonmyelinating Schwann cells. *Glia* 56, 1518–1531. doi: 10.1002/glia.20778

Henry, M., Freking, A. R., Johnson, L. R., and Levinson, S. R. (2007). Sodium channel $Na_V1.6$ accumulates at the site of infraorbital nerve injury. *BMC Neurosci.* 8:56. doi: 10.1186/1471-2202-8-56

Henry, M. A., Luo, S., Foley, B. D., Rzasa, R. S., Johnson, L. R., and Levison, S. R. (2009). Sodium channel expression and localization at demyelinated sites in painful human dental pulp. *J. Pain* 10, 750–758. doi: 10.1016/j.jpain.2009.01.264

Horst, O. V., Horst, J. A., Samudrala, R., and Dale, B. A. (2011). Caries induced cytokine network in the odontoblast layer of human teeth. *BMC Immunol.* 12:9. doi: 10.1186/1471-2172-12-9

Houshmandi, M., Ye, P., and Hunter, N. (2014). Glial network responses to polymicrobial invasion of dentin. *Caries Res.* 48, 534–548. doi: 10.1159/000360610

Jernvall, J., and Thesleff, I. (2012). Tooth shape formation and tooth renewal: evolving with the same signals. *Development* 139, 3487–3497. doi: 10.1242/dev.085084

Jessen, K. R., and Mirsky, R. (2005). The origin and development of glial cells in peripheral nerves. *Nat. Rev. Neurosci.* 6, 671–682. doi: 10.1038/nrn1746

Jessen, K. R., and Mirsky, R. (2008). Negative regulation of myelination: relevance for development, injury and demyelinating disease. *Glia* 56, 1552–1565. doi: 10.1002/glia.20761

Jessen, K. R., and Mirsky, R. (2016). The repair Schwann cell and its function in regenerating nerves. *J. Physiol.* 594, 3521–3531. doi: 10.1113/jp270874

Kastriti, M. E., and Adameyko, I. (2017). Specification, plasticity and evolutionary origin of peripheral glial cells. *Curr. Opin. Neurobiol.* 47, 196–202. doi: 10.1016/j.conb.2017.11.004

Kaukua, N., Shahidi, M. K., Konstantinidou, C., Dyachuk, V., Kaucka, M., Furlan, A., et al. (2014). Glial origin of mesenchymal stem cells in a tooth model system. *Nature* 513, 551–554. doi: 10.1038/nature13536

Kidd, E. A. M., and Fejerskov, O. (2004). What constitutes dental caries? Histopathology of carious enamel and dentin related to the action of cariogenic biofilms. *J. Dent. Res.* 83, C35–C38. doi: 10.1177/154405910408301s07

Levinson, S. R., Luo, S., and Henry, M. A. (2012). The role of sodium channels in chronic pain. *Muscle Nerve* 46, 155–165. doi: 10.1002/mus.23314

Luo, L., He, Y., Wang, X., Key, B., Lee, B. K., Li, H., et al. (2018). Potential roles of dental pulp stem cells in neural regeneration and repair. *Stem Cells Int.* 2018:1731289. doi: 10.1155/2018/1731289

Luukko, K., and Kettunen, P. (2014). Coordination of tooth morphogenesis and neuronal development through tissue interactions: lessons from mouse models. *Exp. Cell Res.* 325, 72–77. doi: 10.1016/j.yexcr.2014.02.029

Martens, W., Sanen, K., Georgiou, M., Struys, T., Bronckaers, A., Ameloot, M., et al. (2014). Human dental pulp stem cells can differentiate into Schwann cells and promote and guide neurite outgrowth in an aligned tissue-engineered collagen construct *in vitro*. *FASEB J.* 28, 1634–1643. doi: 10.1096/fj.13-243980

Meyer Zu Horste, G., Heidenreich, H., Lehmann, H. C., Ferrone, S., Hartung, H.-P., Wiendl, H., et al. (2010). Expression of antigen processing and presenting molecules by Schwann cells in inflammatory neuropathies. *Glia* 58, 80–92. doi: 10.1002/glia.20903

Meyer zu Hörste, G., Hu, W., Hartung, H. P., Lehmann, H. C., and Kieseier, B. C. (2008). The immunocompetence of Schwann cells. *Muscle Nerve* 37, 3–13. doi: 10.1002/mus.20893

Mirsky, R., Jessen, K. R., Brennan, A., Parkinson, D., Dong, Z., Meier, C., et al. (2002). Schwann cells as regulators of nerve development. *J. Physiol. Paris* 96, 17–24. doi: 10.1016/S0928-4257(01)00076-6

Mitsiadis, T. A., and Luukko, K. (1995). Neurotrophins in odontogenesis. *Int. J. Dev. Biol.* 39, 195–202.

Mitsiadis, T. A., Magloire, H., and Pagella, P. (2017). Nerve growth factor signalling in pathology and regeneration of human teeth. *Sci. Rep.* 7:1327. doi: 10.1038/s41598-017-01455-3

Mitsiadis, T. A., and Pagella, P. (2016). Expression of nerve growth factor (NGF), TrkA and $p75^{NTR}$ in developing human fetal teeth. *Front. Physiol.* 7:338. doi: 10.3389/fphys.2016.00338

Monk, K. R., Feltri, M. L., and Taveggia, C. (2015). New insights on schwann cell development. *Glia* 63, 1376–1393. doi: 10.1002/glia.22852

Monteiro, J., Day, P., Duggal, M., Morgan, C., and Rodd, H. (2009). Pulpal status of human primary teeth with physiological root resorption. *Int. J. Paediatr. Dent.* 19, 16–25. doi: 10.1111/j.1365-263X.2008.00963.x

Moorrees, C. F., Fanning, E. A., and Hunt, E. E. Jr. (1963). Formation and resorption of three deciduous teeth in children. *Am. J. Phys. Anthropol.* 21, 205–213. doi: 10.1002/ajpa.1330210212

Mukouyama, Y., Shin, D., Britsch, S., Taniguchi, M., and Anderson, D. J. (2002). Sensory nerves determine the pattern of arterial differentiation and blood vessel branching in the skin. *Cell* 109, 693–705. doi: 10.1016/s0092-8674(02)00757-2

Nair, P. N. R., Luder, H. U., and Schroeder, H. E. (1992). Number and size-spectra of myelinated nerve fibers of human premolars. *Anat. Embryol.* 186, 563–571. doi: 10.1007/bf00186979

Nair, P. N. R., and Schroeder, H. E. (1995). Number and size spectra of non-myelinated axons of human premolars. *Anat. Embryol.* 192, 35–41. doi: 10.1007/bf00186989

Ordovas-Montanes, J., Rakoff-Nahoum, S., Huang, S., Riol-Blanco, L., Barreiro, O., and von Andrian, U. H. (2015). The regulation of immunological processes by peripheral neurons in homeostasis and disease. *Trends Immunol.* 36, 578–604. doi: 10.1016/j.it.2015.08.007

Painter, M. W. (2017). Aging schwann cells: mechanisms, implications, future directions. *Curr. Opin. Neurobiol.* 47, 203–208. doi: 10.1016/j.conb.2017.10.022

Painter, M. W., Brosius Lutz, A., Cheng, Y. C., Latremoliere, A., Duong, K., Miller, C. M., et al. (2014). Diminished Schwann cell repair responses underlie age-associated impaired axonal regeneration. *Neuron* 83, 331–343. doi: 10.1016/j.neuron.2014.06.016

Pinho-Ribeiro, F. A., Verri, W. A. Jr., and Chiu, I. M. (2017). Nociceptor sensory neuron-immune interactions in pain and inflammation. *Trends Immunol.* 38, 5–19. doi: 10.1016/j.it.2016.10.001

Pitts, N. B., Zero, D. T., Marsh, P. D., Ekstrand, K., Weintraub, J. A., Ramos-Gomez, F., et al. (2017). Dental caries. *Nat. Rev. Dis. Primers* 3:17030. doi: 10.1038/nrdp.2017.30

Scholz, J., and Woolf, C. J. (2007). The neuropathic pain triad: neurons, immune cells and glia. *Nat. Neurosci.* 10, 1361–1368. doi: 10.1038/nn1992

Sepulveda, M. (2017). *Desorganización Molecular del Nodo de Ranvier en Periodontitis Crónica.* Master Thesis, Chile: Universidad de Valparaíso.

Shibukawa, Y., Sato, M., Kimura, M., Sobhan, U., Shimada, M., Nishiyama, A., et al. (2015). Odontoblasts as sensory receptors: transient receptor potential channels, pannexin-1 and ionotropic ATP receptors mediate intercellular odontoblast-neuron signal transduction. *Pflugers Arch.* 467, 843–863. doi: 10.1007/s00424-014-1551-x

Slade, G. D. (2001). Epidemiology of dental pain and dental caries among children and adolescents. *Community Dent. Health* 18, 219–227.

Smith, M. M., and Johanson, Z. (2015). "Origin of the vertebrate dentition: teeth transform jaws into a biting force," in *Great Transformations in Vertebrate Evolution*, eds K. P. Dial, N. Shubin and E. L. Brainerd (Chicago, IL: The University of Chicago Press), 9–29.

Smith, E. S., and Lewin, G. R. (2009). Nociceptors: a phylogenetic view. *J. Comp. Physiol. A Neuroethol. Sens. Neural Behav. Physiol.* 195, 1089–1106. doi: 10.1007/s00359-009-0482-z

Smith, M. M., and Sansom, I. J. (2000). "Evolutionary origins of dentine in the fossil record of early vertebrates: diversity, development and function," in *Development, Function and Evolution of Teeth*, eds M. F. Teaford, M. M. Smith, and M. W. Ferguson (Cambridge, UK: Cambridge University Press), 65–81.

Suzuki, K., Lovera, M., Schmachtenberg, O., and Couve, E. (2015). Axonal degeneration in dental pulp precedes human primary teeth exfoliation. *J. Dent. Res.* 94, 1446–1453. doi: 10.1177/0022034515593055

Veiga-Fernandes, H., and Artis, D. (2018). Neuronal-immune system cross-talk in homeostasis. *Science* 359, 1465–1466. doi: 10.1126/science.aap9598

Veiga-Fernandes, H., and Mucida, D. (2016). Neuro-immune interactions at barrier surfaces. *Cell* 165, 801–811. doi: 10.1016/j.cell.2016.04.041

Verdú, E., Ceballos, D., Vilches, J. J., and Navarro, X. (2000). Influence of aging on peripheral nerve function and regeneration. *J. Peripher. Nerv. Syst.* 5, 191–208. doi: 10.1111/j.1529-8027.2000.00026.x

Won, J., Vang, H., Kim, J. H., Lee, P. R., Kang, Y., and Oh, S. B. (2018). TRPM7 mediates mechanosensitivity in adult rat odontoblasts. *J. Dent. Res.* 97, 1039–1046. doi: 10.1177/0022034518759947

Woolf, C. J., and Ma, Q. (2007). Nociceptors—noxious stimulus detectors. *Neuron* 55, 353–364. doi: 10.1016/j.neuron.2007.07.016

Ydens, E., Lornet, G., Smits, V., Goethals, S., Timmerman, V., and Janssens, S. (2013). The neuroinflammatory role of Schwann cells in disease. *Neurobiol. Dis.* 55, 95–103. doi: 10.1016/j.nbd.2013.03.005

Conflict of Interest Statement: The authors declare that the research was conducted in the absence of any commercial or financial relationships that could be construed as a potential conflict of interest.

frontiers in Cellular Neuroscience

MINI REVIEW
published: 06 September 2018
doi: 10.3389/fncel.2018.00305

Developmental and Repairing Production of Myelin: The Role of Hedgehog Signaling

*Yousra Laouarem and Elisabeth Traiffort**

Small Molecules of Neuroprotection, Neuroregeneration and Remyelination – U1195, INSERM, University Paris-Sud/Paris-Saclay, Kremlin-Bicêtre, France

Since the discovery of its role as a morphogen directing ventral patterning of the spinal cord, the secreted protein Sonic Hedgehog (Shh) has been implicated in a wide array of events contributing to the development, maintenance and repair of the central nervous system (CNS). One of these events is the generation of oligodendrocytes, the glial cells of the CNS responsible for axon myelination. In embryo, the first oligodendroglial cells arise from the ventral ventricular zone in the developing brain and spinal cord where Shh induces the basic helix-loop-helix transcription factors Olig1 and Olig2 both necessary and sufficient for oligodendrocyte production. Later on, Shh signaling participates in the production of oligodendroglial cells in the dorsal ventricular-subventricular zone in the postnatal forebrain. Finally, the modulation of Hedgehog signaling activity promotes the repair of demyelinated lesions. This mini-review article focuses on the Shh-dependent molecular mechanisms involved in the spatial and temporal control of oligodendrocyte lineage appearance. The apparent intricacy of the roles of two essential components of Shh signaling, Smoothened and Gli1, in the postnatal production of myelin and its regeneration following a demyelinating event is also highlighted. A deeper understanding of the implication of each of the components that regulate oligodendrogenesis and myelination should beneficially influence the therapeutic strategies in the field of myelin diseases.

Keywords: oligodendrocyte, brain, spinal cord, smoothened, Gli

OPEN ACCESS

Edited by:
Fernando C. Ortiz, Universidad Autónoma de Chile, Chile

Reviewed by:
Michael P. Matise, Rutgers University – The State University of New Jersey, United States
Regina Armstrong, Uniformed Services University of the Health Sciences, United States

***Correspondence:**
Elisabeth Traiffort
elisabeth.traiffort@inserm.fr

Received: *15 June 2018*
Accepted: *22 August 2018*
Published: *06 September 2018*

Citation:
Laouarem Y and Traiffort E (2018) Developmental and Repairing Production of Myelin: The Role of Hedgehog Signaling. Front. Cell. Neurosci. 12:305. doi: 10.3389/fncel.2018.00305

INTRODUCTION

The generation of oligodendrocyte progenitor cells (OPCs) comprises several spatiotemporal waves localized firstly in ventral regions of the central nervous system (CNS) and slightly later in more dorsal domains. Although most generated OPCs differentiate into mature oligodendrocytes leading to CNS myelination, a small fraction remains in a slowly proliferative or quiescent state in the adult tissue (Dawson et al., 2003). After a demyelinating insult, these OPCs constitute one of the cell populations responsible for myelin repair (Franklin et al., 1997). Dorsal and ventral OPCs display intrinsic differences regarding migration and differentiation capacities when they are considered in a similar environment. These differences are more apparent in progenitors derived from the adult brain than from the neonatal brain (Crawford et al., 2016). Besides OPCs, neural stem cells

(NSCs) or neuroblasts located in the ventricular-subventricular zone (V-SVZ) can also generate oligodendroglial cells after demyelination (Picard-Riera et al., 2002; Cayre et al., 2006; Menn et al., 2006; Aguirre et al., 2007). However, OPCs and NSCs differently contribute to remyelination according to the demyelination model that is used or the brain region that is considered (Xing et al., 2014; Brousse et al., 2016; Kazanis et al., 2017).

The signaling pathway induced by the secreted proteins Hedgehog has been discovered three decades ago and is well-known as a regulator of oligodendrocyte and myelin production. The transduction of the Hedgehog signal classically involves a major receptor complex associating the 12-pass transmembrane protein Patched (Ptc) and one of its co-receptors including Cell adhesion molecule-related, down-regulated by oncogenes (Cdo), Brother of Cdo (Boc), or Growth-arrest-specific 1 (Gas1) (**Figure 1A**). Hedgehog binding to its receptors relieves the repression exerted by Ptc on the G protein-coupled receptor Smoothened (Smo), which triggers either a complex intracellular signaling cascade involving the transcription factors of the Glioma-associated oncogene (Gli) family or mechanisms independent of Gli-mediated transcription known as 'non-canonical' (Ferent and Traiffort, 2015).

The present mini-review reports Hedgehog protein involvement in the development of oligodendroglial cells in the vertebrate spinal cord and brain from embryonic until neonatal stages. Moreover, the contribution of Hedgehog signaling to myelin repair will be discussed in the light of recent data implicating the transcription factor Gli1 and the receptor Smo.

HEDGEHOG-DEPENDENT OPC PRODUCTION IN THE SPINAL CORD

The involvement of Hedgehog morphogens in the specification of OPCs was proposed in the mid-1990s, when Sonic Hedgehog (Shh) signaling derived from the notochord and/or floorplate cells was found to be required for the development of the oligodendroglial lineage (Marti et al., 1995; Poncet et al., 1996; Pringle et al., 1996). Shh appeared to be both necessary and sufficient for expression of the genes encoding the oligodendrocyte transcription factors 1 (Olig1) and 2 (Olig2), associated with the oligodendroglial lineage in the motoneuron progenitor (pMN) domain of the developing neural tube. In the mouse, both genes are highly upregulated in the dorsal neural tube of embryonic day (E) 14.5 pups ectopically expressing Shh, just before the appearance of oligodendroglial cells (Lu et al., 2000). Consistent with this, in the zebrafish, several Smo mutants where most Hedgehog signaling is absent, exhibit an almost complete absence of oligodendrocytes in the spinal cord (Park et al., 2002; Schebesta and Serluca, 2009).

Floorplate-Derived Hedgehog Proteins Contribute to OPC Specification

Although Shh is produced in both the notochord and floorplate, the rapid loss of contact between the notochord and the neural tube by E10.5–E11.5 led to analyze whether the floorplate could be the sole source of Hedgehog proteins during oligodendrogenesis. This single contribution was demonstrated by the selective inactivation of Shh in this area via mutagenesis approaches in the mouse. As soon as the E10.5 stage, the $Olig2^{+}$ progenitors are significantly decreased in the mutant in a consistent manner with the requirement of Shh-derived floorplate to maintain the formation of this progenitor domain during neurogenesis. On later stages, while oligodendrogenesis occurs, several genes linked to gliogenesis including the fibroblast growth factor binding protein 3 (Fgfbp3) are also decreased as well as the Olig2 labeling that reaches a quite undetectable level at E12.5. The expression of OPC markers such as Nk2 homeobox 2 (Nkx2.2), Olig2, Sex determining region Y-box 10 (Sox10) and platelet-derived growth factor receptor alpha (Pdgfrα) is similarly reduced in the E15.5 mutant spinal cord (Yu et al., 2013). Unexpectedly, in the zebrafish, the $syu^{-/-}$ mutant embryos, which are deficient for Shh, express Olig2 nevertheless more ventrally than normal and without giving rise to OPCs in the spinal cord. This species difference is related to the involvement of additional Hedgehog homologs (**Table 1**) including Indian Hedgehog b (Ihhb) and Tiggy winckle (Twhh) expressed in the notochord and/or floorplate during motoneuron and OPC specification (Krauss et al., 1993; Ekker et al., 1995; Park et al., 2002; Chung et al., 2013). Shh and Twhh both induce and position the $Olig2^{+}$ precursor domain (Park et al., 2004) while Ihhb inhibits the cell cycle of the precursors implicated in OPC specification (Chung et al., 2013). Interestingly, in human, a transient high immunoreactive Shh signal is detected in the floorplate cells from 45 days embryos when the first OPCs emerge in two discrete close regions and progressively populate the whole spinal cord as observed in the other species (Hajihosseini et al., 1996).

Motoneurons and OPCs Arise From Distinct Progenitor Cell Lineages in Response to Hedgehog

Nanomolar concentrations of Shh are able to induce with a similar efficiency both oligodendrocytes and motoneurons from neural tube explants (Pringle et al., 1996; Orentas et al., 1999; Lu et al., 2000). This observation was the starting point for a series of investigations aimed at determining if both cell types may be derived from a common precursor. However, the hypothesis was rapidly questioned. Data obtained from mouse and chick embryos indicated firstly that oligodendrocytes are generated at a later time than motoneurons, secondly that their precursors do not share the same transcription factors notably Nkx2.2 and the Paired box 6 protein (Pax6), respectively (Lu et al., 2000; Soula et al., 2001) and thirdly that Shh promotes the dorsal extension of the Nkx2.2 domain while it induces the regression of the Pax6 domain. More recent data carried out in zebrafish and using time-lapse imaging confirmed that the majority of motoneurons and oligodendrocytes are derived from distinct progenitors *in vivo*. In addition, they provided a unique mechanism involving the progressive recruitment of glial-fated progenitors to the

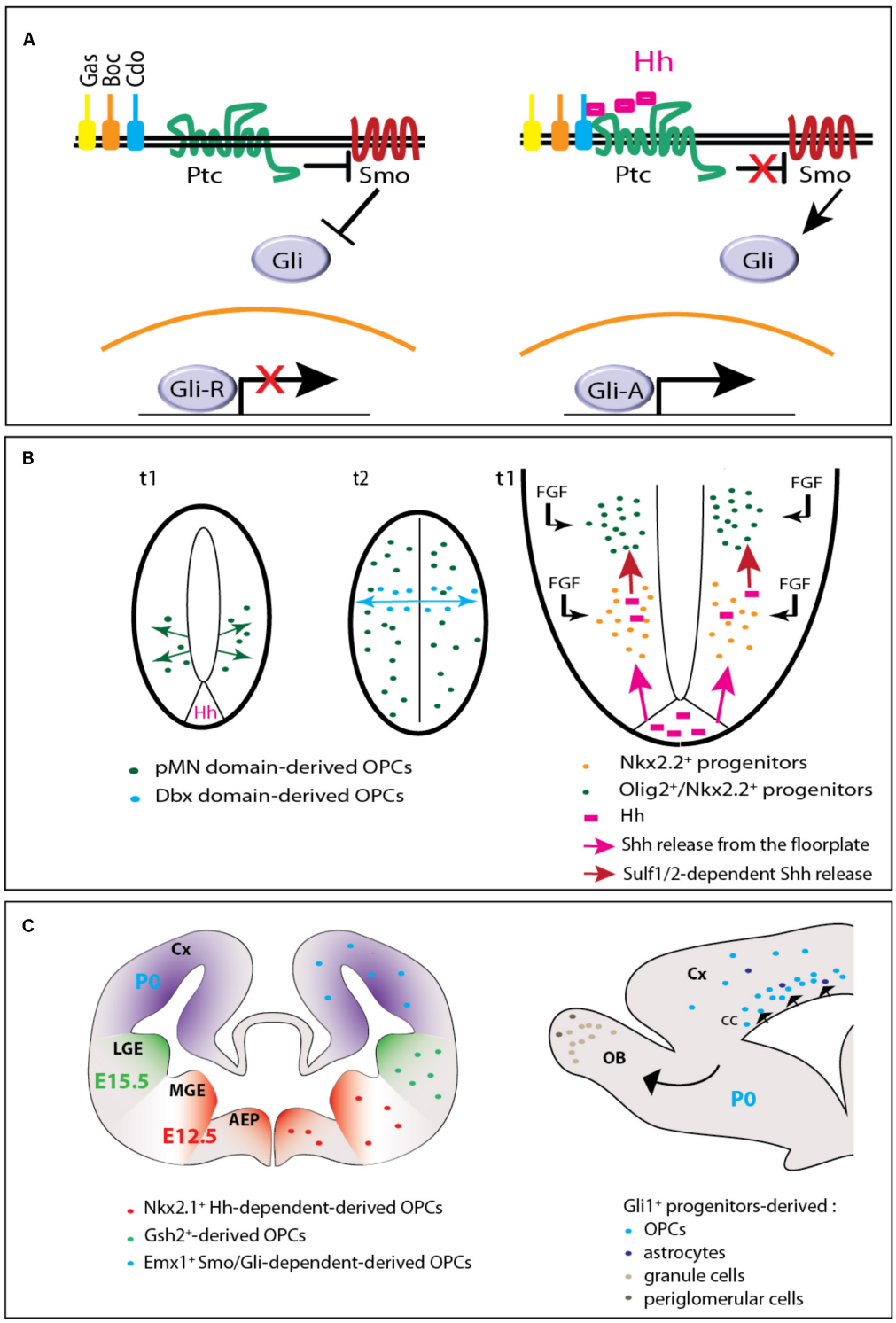

FIGURE 1 | Hedgehog signaling in embryonic and postnatal oligodendrogenesis. **(A)** The Hedgehog signaling pathway. In the absence of Hedgehog (left), the receptor Patched (Ptc) exerts a repressive activity on Smoothened (Smo). When Hedgehog (Hh) binds Ptc and one of its co-receptors (Gas, Boc, or Cdo), Smo repression is relieved triggering an intracellular signaling cascade that involves the transcription factors of the Gli family. The Gli activator (GliA) instead of the Gli repressor (GliR) form is then transported toward the nucleus and subsequently leads to the transcription of target genes. **(B)** Hedgehog-dependent OPC production in the embryonic spinal cord. On the left (adapted from Fogarty et al., 2005), two cross-sectional views of the neural tube are shown. t1 and t2 indicate the embryonic days when ventral and dorsal OPCs are produced, respectively. At t1, OPCs arise from the pMN domain in a Hedgehog (Hh)-dependent manner. At t2,

(Continued)

FIGURE 1 | Continued
while pMN-derived OPCs have invaded the whole neural tube, a second wave arises from the Dbx domain in a Hedgehog-independent manner. On the right, a magnified scheme of the ventral part of the neural tube shows that Hedgehog (pink) is secreted from both the floorplate (the ventral most part of the neural tube) and Nkx2.2$^+$ cells (just above) that upregulate the expression of the morphogen when they become exposed to fibroblast growth factors (FGFs). Because they are submitted to higher Hedgehog signaling activity and to FGF, adjacent Olig2$^+$ progenitors give rise to OPCs. **(C)** Hedgehog-dependent OPC production in the forebrain. On the left, the scheme (adapted from Kessaris et al., 2006) represents a coronal view of the mouse forebrain and the three successive waves of OPC production at the embryonic (E12.5, E15.5) and early postnatal (P0) periods. AEP, anterior entopeduncular area; Cx, cerebral cortex; MGE, medial ganglionic eminence; LGE, lateral ganglionic eminence. On the right, a sagittal view of the forebrain indicates the progeny of Gli1$^+$ neural progenitors derived from the dorsal V-SVZ at P0. The progeny comprises OPCs and astrocytes migrating to the corpus callosum (cc) and cerebral cortex (Cx), granule and periglomerular neurons migrating to the olfactory bulbs (OB).

TABLE 1 | Hedgehog ligands in zebrafish, chick, rodent and human, and their activity related to the oligodendrocyte lineage.

Species	Hedgehog homologs	Activity in oligodendrogenesis	Reference
Zebrafish	Shha	Induction and positionning of the Olig2$^+$ precursor domain	Park et al., 2004
	Shhb (Twhh)	Induction and positionning of the Olig2$^+$ precursor domain	Chung et al., 2013
	Ihha	–	
	Ihhb (Echidna)	Cell cycle inhibition of the precursors implicated in OPC specification	
	Dhh	–	
Chick	Shh	Induction of the oligodendroglial lineage	Marti et al., 1995; Poncet et al., 1996; Pringle et al., 1996
	Ihh	–	
	Dhh	–	
Rodent	Shh	Induction of the oligodendroglial lineage and Olig1/2 genes	Marti et al., 1995; Poncet et al., 1996; Pringle et al., 1996; Lu et al., 2000 Tekki-Kessaris et al., 2001
	Ihh	Potential redundant activity with Shh	
	Dhh	Potential redundant activity with Shh	
Human	Shh	Induction of OLIG2 and NKX2.2 in neural progenitors fated to the oligodendroglial lineage	Hajihosseini et al., 1996; Hu et al., 2009; Ortega et al., 2013
	Ihh	–	
	Dhh	–	

The black dashes indicate the lack of any data regarding these homologs in oligodendrocyte development.

pMN domain in a Hedgehog-dependent manner (Ravanelli and Appel, 2015). While progenitors located at the most ventral part of the pMN differentiate into motoneurons, more dorsal cells go on dividing. Moreover, progenitors located outside the pMN move ventrally and in turn upregulate Olig2 expression. Does such recruitment exist in mouse and chick is unknown. However, the recent finding that the pattern of the progenitor domains in the neural tube from those species depends on the regulation of the cell differentiation rates (Kicheva et al., 2014) is in support of this hypothesis. Moreover, the progenitor recruitment might account for a few intriguing observations including the maintenance of Olig2$^+$ progenitors despite the loss of most motoneurons and OPCs in a mouse strain expressing a cell-lethal toxin in Olig1$^+$ pMN progenitors (Wu et al., 2006).

Molecular Mechanisms Driving the Hedgehog-Dependent Motoneuron/Oligodendrocyte Transition

The accumulation of Shh proteins at the surface of ventral neural progenitors occurred as a determining step in motoneuron/oligodendrocyte transition (Danesin et al., 2006). This accumulation was attributed to the activity of sulfatase1, which appears a short time before OPC specification in mouse and chicken embryos where the enzyme regulates the sulfation of heparin sulfate proteoglycans (HSPGs) (**Figure 1B**). By locally lowering Shh/HSPG interaction, sulfatase1 promotes Shh release from the progenitors located below the pMN domain providing higher Shh amounts to neighboring Nkx2.2$^+$ cells before their transition to an oligodendroglial fate (Danesin et al., 2006; Touahri et al., 2012). Sulfatase2 coordinates its activity with sulfatase1 in this process (Jiang et al., 2017). In addition, fibroblast growth factors (Fgfs) initially thought to influence the Hedgehog-independent generation of dorsal oligodendrocytes occuring 3 days after the generation of pMN-derived OPCs, also participates in the creation of the burst of Shh required for ventral OPC specification (Farreny et al., 2018). In the zebrafish, sulfatase1 activity similarly stands as a timer activating neuronal and oligodendroglial generation at 14 and 36 h post-fertilization, respectively, in response to high concentrations of Hedgehog proteins (Al Oustah et al., 2014). Besides sulfatase enzymes, another mechanism essential for controlling the transition is the Shh-mediated restriction of the Notch ligand Jagged-2 (Jag2) to the pMN domain during motoneuron generation. Indeed, Jag2 expression prevents a subset of Olig2$^+$ progenitors from differentiating into neurons and maintains a high expression of bHLH transcription factor 5 (Hes5), one of the Notch effectors that inhibits the generation of OPCs during the neurogenic step (Rabadan et al., 2012).

Hedgehog Signaling Components Implicated in OPC Specification

The involvement of the positive and negative effectors of Shh signaling, the Gli zinc-finger transcription factors Gli2 and

Gli3, was addressed in the induction of OPCs mediated by Shh. The analysis of the mutant mice revealed that Gli2 is implicated in the regulation of the size and duration of the Olig1/2^{+} domain in the ventral neuroepithelium, but not in the proliferation, differentiation and maturation of OPCs after their initial production (Qi et al., 2003). In contrast, a non-essential role was attributed to Gli3 in ventral oligodendrogenesis in agreement with the restriction of Gli3 expression to the dorsal spinal cord at E9.5 (Lee et al., 1997) and thus before oligodendrogenesis starts. Interestingly, the Gli3 null mutation was nevertheless found to substantially rescue the phenotype exhibited by mice deprived of Shh in the floorplate (Yu et al., 2013) suggesting that Shh likely maintains Olig2 expression in OPCs by repressing the antagonistic Gli3 repressor activity. On the contrary, the regulation of Nkx2.2 expression was proposed to likely rely on the activation of Gli activator forms (Oh et al., 2005; Tan et al., 2006; Yu et al., 2013).

HEDGEHOG-DEPENDENT OPC PRODUCTION IN THE BRAIN

The origin of oligodendrocytes in the developing brain has long remained less well-established than in the spinal cord. Hedgehog signaling implication in OPC generation was progressively investigated at the different rostro-caudal levels and finally detected not only in the ventral, but also in the dorsal brain.

Hedgehog-Dependent OPC Generation in the Hindbrain and Midbrain

The first data were reported in the chick hindbrain where ventral and dorsal domains from which OPCs arise are correlated with a transient Shh expression (Ono et al., 1997; Davies and Miller, 2001). In the rodent hindbrain, like in the spinal cord, ventral OPCs depend on Shh signaling and require Olig1/2 expression (Lu et al., 2000; Alberta et al., 2001; Vallstedt et al., 2005). However, a crucial difference relies on the opposing effects mediated by the Nkx6 proteins, which are required for OPC generation in the spinal cord but on the contrary suppress the production of OPCs in the anterior hindbrain (Vallstedt et al., 2005). In the zebrafish, the homozygous Smo mutant completely lacks hindbrain oligodendrocytes (Park et al., 2002). In this species, both Olig2 and Nkx2.2a expression depend on Hedgehog signaling via a mechanism implicating histone deacetylase 1 proposed to facilitate Hedgehog-mediated expression of Olig2 and to repress Nkx2.2a in neural progenitors fated to the oligodendrocyte lineage (Cunliffe and Casaccia-Bonnefil, 2006). Moreover, the unexpected identification of Disrupted-in-schizophrenia1 as a target of Shh signaling during OPC specification, interestingly suggested that impaired Shh signaling may constitute one of the potential developmental factors involved in the pathobiology of mental illnesses (Boyd et al., 2015).

In the midbrain, much less data are available. The development of ventral and dorsal OPCs mainly examined in chicken was proposed to depend on Shh (Fu et al., 2003). A unique feature is that dorsal Olig2^{+} OPCs start to co-express Nkx2.2 only when they migrate away from the VZ. Moreover, in the cerebellum, most OPCs have been proposed to arise from a small region called the parabasal bands (Mecklenburg et al., 2011). Although Shh implication in OPC specification in this area is not known, Purkinje cell-derived Shh in rodent was found to prevent OPCs from exiting the cell cycle and to inhibit the effects of molecules inducing their differentiation (Bouslama-Oueghlani et al., 2012).

Hedgehog-Dependent OPC Generation in the Ventral Forebrain

In the mouse forebrain, three successive waves of OPCs were reported. They arise at E12.5, E15.5, and P0 from Nkx2.1, Genetic-screened homeobox 2 (Gsh2) and homeobox protein Emx1 progenitors respectively located in the medial ganglion eminence, lateral ganglion eminence and cerebral cortex (Kessaris et al., 2006) (**Figure 1C**). In contrast to the spinal cord, most OPCs present in the adult forebrain, are dorsally-derived (Tripathi et al., 2011).

Shh signaling was early proposed to be central to the generation of ventral forebrain OPCs. In a consistent manner, the lack of the telencephalic Shh expression domain in the Nkx2.1 null mutant mice is associated with an absence of OPCs in the ventral forebrain, a phenotype rescued by *in vivo* Shh gain-of-function experiments. However, although Shh is able to direct cells toward an oligodendroglial fate, additional local signals appeared to be required for their differentiation into mature oligodendrocytes (Alberta et al., 2001; Nery et al., 2001; Tekki-Kessaris et al., 2001; Qi et al., 2002). Consistent data were obtained in the zebrafish since the syu$^{-/-}$ mutant displays a lower level of Olig2 expression (Park et al., 2002).

Hedgehog-Dependent OPC Generation in the Dorsal Forebrain

Shh-dependence of dorsal forebrain OPCs was in contrast only recently demonstrated notably by the report of a Shh-dependent domain in the dorsal V-SVZ producing large numbers of oligodendrocytes at the neonatal period. Indeed, an adenoviral lineage tracing showed that dorsal V-SVZ-derived neural progenitors expressing Gli1 in neonates differentiate into mature oligodendrocytes (Tong et al., 2015) and give rise to myelinating-like membranes (Sanchez and Armstrong, 2018). Moreover, the adenovirus-mediated ablation of Smo or its ectopic activation in those progenitors reduces or conversely increases the generation of mature oligodendrocytes in the corpus callosum (Tong et al., 2015). These data are fully consistent with previous *in vitro* results obtained by using neocortical NSC cultures derived from late embryo stages. Cell treatment with a Smo agonist induces an increase in Olig2^{+} cells that can be blocked by the well-known Smo antagonist cyclopamine (Kessaris et al., 2004). Furthermore, Gli1 (but not Gli2 or Gli3) is upregulated when exogenous Shh is added to the culture (Wang et al., 2008). However, all these data apparently disagree with the precocious myelination observed

in 9-day old Gli1 null mutant mice unexpectedly suggesting that Gli1 delays the onset of myelination (Samanta et al., 2015). One of the main differences between these apparently discordant experiments is a full invalidation of Gli1 as soon as the embryonic period on one side and, a conditional and postnatally induced removal of Smo in the dorsal NSCs on the other side. For this reason, the phenotype of the Gli1 mutant could reflect the activity of Gli1 before birth, which might consist in maintaining OPCs in the cell cycle thus preventing their differentiation into myelinating oligodendrocytes. However, if this hypothesis is true, Gli1 activity before birth should be independent on Smo given the compromised generation of oligodendrocytes observed upon conditional removal of Smo in nestin-expressing embryonic NSCs (Machold et al., 2003). For instance, the capacity of Gli1 to antagonize Gli3 previously shown in the spinal cord (Bai and Joyner, 2001) might be a mechanism interesting to be investigated in the forebrain. Beside this first activity of Gli1, a second one could exist at a lower extent in embryo and could be maintained at the perinatal period when most myelinating oligodendrocytes are generated. Instead preventing myelination, Gli1 might then participate in the proliferation/differentiation of NSC and/or OPCs. In agreement with this hypothesis, a dual and context-dependent function has been proposed for Gli1 in the maintenance of NSC proliferation during conditions of self-renewal and in their maturation into oligodendroglial cells during differentiation (Wang et al., 2008). The phenotype observed upon conditional removal of Smo at birth is consistent with this second activity of Gli1 that would then depend on Smo. How these Gli1 activities might be triggered remains to be determined. The involvement of other Hedgehog proteins (Dhh or Ihh) cannot be excluded if we consider that the generation of oligodendroglial cells is maintained in Shh null mutant mice (Nery et al., 2001) and that embryonic cortical NSC cultures upregulate Shh, Ihh and at a lower extent Dhh (Tekki-Kessaris et al., 2001). However, an accurate analysis of each step of dorsal oligodendrogenesis in the absence of Gli1 or Smo separately or simultaneously would of course be required to evaluate all these hypotheses.

Molecular Mechanisms Implicated in Hedgehog-Dependent Production of OPCs in the Forebrain

From a molecular point of view, Shh-dependent oligodendrogenesis in the spinal cord and forebrain display both similarities and divergences. In contrast to the spinal cord, the control of OPC production in the forebrain is Gli2-independent even though the role of Gli2 in the terminal differentiation of oligodendrocytes remains unclear (Qi et al., 2003). Conversely, in both regions, Shh and BMP display antagonistic activities on OPC production. In cultured OPCs derived from the forebrain, Shh and Bone morphogenetic protein 4 (BMP4) favor and inhibit respectively the progression toward oligodendrocytes. While the former decreases histone acetylation and induces peripheral chromatin condensation, the latter promotes global histone acetylation and retains euchromatin thus favoring astrogliogenesis (Wu et al., 2012). Moreover, Shh-mediated OPC production in the forebrain is tightly associated with Fgf as previously shown in the spinal cord. Consistent with this, precursors isolated from E14 mouse medial ganglion eminence, responding to Platelet-derived growth factor (Pdgf) and giving rise to both neurons and OPCs are able to self-renew via Pdgf and Fgf2-mediated activation of Shh signaling (Chojnacki and Weiss, 2004). Similarly, a basal level of phosphorylated mitogen-activated protein kinases (MAPKs) maintained by Fgf activity is required for Shh-induced generation of OPCs from cultures of E13.5 mouse neocortical precursors (Kessaris et al., 2004; Furusho et al., 2011). The absence of a significant effect in Shh signaling in the Fgf receptors knockout mice as well as the strong inhibition of OPC generation in cell cultures from E11.5 ventral forebrains by inhibitors of Fgf and Shh signaling used individually or in combination led to conclude to the cooperation of those signaling pathways for the generation of most ventrally derived OPCs (Furusho et al., 2011). A comparable crosstalk between Shh and Fgf signaling also exists in the zebrafish where Fgf16 required for oligodendrogenesis in the forebrain, is induced by Hedgehog signaling (Miyake et al., 2014). Interestingly, in human, OPCs originate both from the ventral telencephalon and the cortical SVZ at midgestation (Rakic and Zecevic, 2003; Jakovcevski et al., 2009). Human fetal neural progenitors derived from the cortical SVZ give rise to oligodendrocytes *in vitro* in a Shh-dependent manner (Jakovcevski et al., 2009; Mo and Zecevic, 2009; Ortega et al., 2013). However, the transition of pre-OPCs to OPCs is inhibited by FGF2, which represses SHH-dependent expression of OLIG2 and NKX2.2 (Hu et al., 2009).

Hedgehog-Dependent OPC Generation in the Optic Nerve

Oligodendrocyte progenitor cells present in the optic nerve are derived from cells located in the floor of the third ventricle (Small et al., 1987; Ono et al., 1997). The first cells are generated concomitantly with the arrival of retinal axons to the forebrain under the activity of Shh transported in the chick from the retinal ganglion cells to the optic chiasm via the retinal axons (Gao and Miller, 2006). Cultures of mouse optic nerve explants and Shh-interference *in ovo* in chick embryo showed that Shh also acts as a mitogen and a chemoattractant for optic nerve OPCs (Merchan et al., 2007). Since Shh is synthesized in the floor of the third ventricle, how newly generated OPCs are not retained in this area remains however an open question. Moreover, an interesting mechanism proposed for controling the level of Shh available for OPCs during the colonization of the optic nerve, relies on the internalization of Shh via the multiligand receptor Megalin before Shh release by astrocytes (Ortega et al., 2012).

HEDGEHOG SIGNALING IN MYELIN REGENERATION

Given that the first step of myelin regeneration following a demyelinating insult involves the reactivation of quiescent OPCs as well as the re-expression of genes essential during development (Franklin and Ffrench-Constant, 2008), the contribution of

Shh signaling to OPC production in the context of CNS demyelination has been addressed by several groups. After the report that exogenous Shh is able to increase OPCs and premyelinating oligodendrocytes in the adult healthy dorsal forebrain (Loulier et al., 2006), various demyelination models led to show Shh signaling implication in myelin repair. The administration of interferon-β was found to promote the upregulation of Shh and its receptor Ptc likely leading to the inhibition of the negative effects of Notch signaling in models of immune and non-immune demyelination (Mastronardi et al., 2004). Along the same line, the capacity of thyroid hormones to improve clinical signs and remyelination upon chronic demyelination was proposed to be related to a potent OPC induction probably due to the increase of Shh expression (Harsan et al., 2008). Consistent with all these data, gain- and loss- of function experiments led to demonstrate in the lysolecithin-mediated demyelination of the corpus callosum, that Shh promotes proliferation and differentiation of OPCs and decreases astrogliosis and macrophage infiltration altogether leading to the attenuation of the lesion extent during myelin repair (Ferent et al., 2013). Although Shh upregulation is a shared feature in all these works, genetic fate-labeling of cells actively transcribing Shh failed to detect Shh-expressing cells following cuprizone-mediated demyelination (Sanchez et al., 2018). One hypothesis able to account for this discordance could be that the antibodies used for visualizing Shh have actually recognized other members of the Hedgehog family (Traiffort et al., 2001). The hypothesis remains to be investigated.

More recently, the involvement of Smo and Gli1 was also addressed in the context of myelin regeneration. In agreement with the pro-regenerative effects previously proposed for the Shh pathway (see above), the activation of Smo by micro-injection of a Smo agonist into the corpus callosum of mice chronically demyelinated by cuprizone administration increases cell proliferation and enhances remyelination. However, no significant increase in cycling OPCs or oligodendrocytes was reported. Moreover, the absence of Gli1 fate-labeled cell increase in this experimental paradigm led to suggest that the Smo agonist promotes remyelination independently of Gli1 possibly indicating signaling through the non-canonical Hedgehog pathway and, likely in indirect manner by acting on cells other than the oligodendroglial cells (Sanchez et al., 2018). Conversely, Vismodegib, a specific Smo antagonist, reported to repress Gli-mediated transcription in a variety of cell types (Stanton and Peng, 2010) significantly increases disease severity in the experimental autoimmune encephalomyelitis (EAE) model of demyelination. However, the data did not evaluate the state of Gli1 activation in these animals (Alvarez et al., 2011).

Whereas the modulation of Smo activity is consistent with the positive effect of Shh signaling on remyelination, more controversial data emerged from the investigation of the roles of Gli1. Indeed, the genetic fate-labeling of cells expressing Gli1 led to detect a subset of Shh-responsive adult NSCs comprising 25% of all NSCs present in the ventral V-SVZ. Upon cuprizone administration, these cells can be recruited to the demyelinated corpus callosum where they are preferentially fated to the oligodendrocyte lineage and concomitantly downregulate Gli1 expression (Samanta et al., 2015; Sanchez et al., 2018). Moreover, the genetic downregulation of Gli1 or its pharmacological inhibition in the cuprizone model was found to amplify the recruitement of NSCs, increase their differentiation into mature oligodendrocytes and enhance the density of myelin basic protein signal in the demyelinated CNS. Similarly, the pharmacological inhibition of Gli improves the functional outcomes in the EAE model by promoting remyelination and neuroprotection in the spinal cord through direct or indirect effects on Gli1-expressing NSCs or parenchymal astrocytes, respectively (Samanta et al., 2015). If the remyelinating effects induced by Smo activation are mediated via the non-canonical (Gli-independent) pathway as previously suggested (Sanchez et al., 2018), the pro-regenerative effects observed in the presence of a Gli antagonist (Samanta et al., 2015) do not constitute discordant results. However, it is noteworthy that, during the demyelination/remyelination processes, Gli1 expression appears to be regulated in a complex manner depending on the animal model or the stage of the disease. Thus, in the cuprizone model, Gli1 was reported to be not or slightly upregulated in the demyelinated corpus callosum mainly in reactive astrocytes (Samanta et al., 2015; Sanchez et al., 2018). In the lysolecithin-induced demyelination of the corpus callosum, a quite moderate Gli1 transcription is observed in oligodendroglial cells during the step of OPC differentiation (Ferent et al., 2013). In the EAE model, Gli1 is upregulated in OPCs and neurons just before EAE onset and then downregulated during the irreversible demyelination occurring in this model (Wang et al., 2008). Interestingly, the kinetics of Gli1 transcription determined in the EAE model reminds the regulation of Gli1 expression determined in the brain from multiple sclerosis patients as shown by the upregulation of Gli1 in active lesions and its decrease in chronic active and inactive lesions (Wang et al., 2008). Remarkably, the expression of Gli1 in tissues able to remyelinate is in support of a potential pro-myelinating role of Gli1. Besides its negative role on remyelination and neuroprotection targeting a subset of NSCs, the pro-regenerative role of Gli1 would thus deserve to be investigated. According to the demyelination model, the mouse strain, the methodological approaches leading to $Gli1^{+}$ cell tracking, or the analysis of tissues derived from the human disease, the phenotype of the cells expressing Gli1 or Smo is variable including NSCs, reactive astrocytes, oligodendroglial cells or even neurons for Gli1, microglia, oligodendroglial cells, and astrocytes for Smo. Therefore, the apparently contradictory results showing that the blockade (Gli inhibition) and the activation (Shh overexpression or Smo activation) of Shh signaling both finally improve remyelination may reflect not only the potential involvement of canonical and non-canonical Shh signaling pathways, but also the targeting of different remyelinating cells (NSCs and parenchymal OPCs) and probably the differential regulation of reactive astrocytes and activated microglia. The observation that the blockade of Gli1 in the NSCs preferentially fated to oligodendroglia appears to be endowed with an even greater effect in the context of active Shh signaling (Samanta et al., 2015) undoubtedly deserves further investigations.

CONCLUSION

The data accumulated over the years on the role of Hedgehog signaling in the genesis of the oligodendrocyte lineage clearly demonstrates that Hedgehog stands as one of the important pathways in this process. However, many questions remain regarding the apparent intricacy of Hedgehog signaling activity during myelin regeneration. The thorough determination of the molecular mechanisms and cell types targeted by the pharmacological modulation of the different components of the pathway should improve our understanding and ultimately open new therapeutic perspectives.

AUTHOR CONTRIBUTIONS

ET and YL contributed to the design, documentation, and writing of this review article.

FUNDING

The review received the financial support of the French Multiple Sclerosis Foundation (ARSEP; RAK17128LLA) and the French National Research Agency (ANR; RPV15198LLA) to ET. YL was financially supported by Mattern Foundation.

REFERENCES

Aguirre, A., Dupree, J. L., Mangin, J. M., and Gallo, V. (2007). A functional role for EGFR signaling in myelination and remyelination. *Nat. Neurosci.* 10, 990–1002. doi: 10.1038/nn1938

Al Oustah, A., Danesin, C., Khouri-Farah, N., Farreny, M. A., Escalas, N., Cochard, P., et al. (2014). Dynamics of sonic hedgehog signaling in the ventral spinal cord are controlled by intrinsic changes in source cells requiring sulfatase 1. *Development* 141, 1392–1403. doi: 10.1242/dev.101717

Alberta, J. A., Park, S. K., Mora, J., Yuk, D., Pawlitzky, I., Iannarelli, P., et al. (2001). Sonic hedgehog is required during an early phase of oligodendrocyte development in mammalian brain. *Mol. Cell. Neurosci.* 18, 434–441. doi: 10.1006/mcne.2001.1026

Alvarez, J. I., Dodelet-Devillers, A., Kebir, H., Ifergan, I., Fabre, P. J., Terouz, S., et al. (2011). The Hedgehog pathway promotes blood-brain barrier integrity and CNS immune quiescence. *Science* 334, 1727–1731. doi: 10.1126/science.1206936

Bai, C. B., and Joyner, A. L. (2001). *Gli1* can rescue the *in vivo* function of *Gli2*. *Development* 128, 5161–5172.

Bouslama-Oueghlani, L., Wehrle, R., Doulazmi, M., Chen, X. R., Jaudon, F., Lemaigre-Dubreuil, Y., et al. (2012). Purkinje cell maturation participates in the control of oligodendrocyte differentiation: role of sonic hedgehog and vitronectin. *PLoS One* 7:e49015. doi: 10.1371/journal.pone.0049015

Boyd, P. J., Cunliffe, V. T., Roy, S., and Wood, J. D. (2015). Sonic hedgehog functions upstream of disrupted-in-schizophrenia 1 (disc1): implications for mental illness. *Biol. Open* 4, 1336–1343. doi: 10.1242/bio.012005

Brousse, B., Magalon, K., Durbec, P., and Cayre, M. (2016). Region and dynamic specificities of adult neural stem cells and oligodendrocyte precursors in myelin regeneration in the mouse brain. *Biol Open* 5, 980–992. doi: 10.1242/bio.016980

Cayre, M., Bancila, M., Virard, I., Borges, A., and Durbec, P. (2006). Migrating and myelinating potential of subventricular zone neural progenitor cells in white matter tracts of the adult rodent brain. *Mol. Cell. Neurosci.* 31, 748–758. doi: 10.1016/j.mcn.2006.01.004

Chojnacki, A., and Weiss, S. (2004). Isolation of a novel platelet-derived growth factor-responsive precursor from the embryonic ventral forebrain. *J. Neurosci.* 24, 10888–10899. doi: 10.1523/JNEUROSCI.3302-04.2004

Chung, A. Y., Kim, S., Kim, E., Kim, D., Jeong, I., Cha, Y. R., et al. (2013). Indian hedgehog B function is required for the specification of oligodendrocyte progenitor cells in the zebrafish CNS. *J. Neurosci.* 33, 1728–1733. doi: 10.1523/JNEUROSCI.3369-12.2013

Crawford, A. H., Tripathi, R. B., Richardson, W. D., and Franklin, R. J. M. (2016). Developmental origin of oligodendrocyte lineage cells determines response to demyelination and susceptibility to age-associated functional decline. *Cell Rep.* 15, 761–773. doi: 10.1016/j.celrep.2016.03.069

Cunliffe, V. T., and Casaccia-Bonnefil, P. (2006). Histone deacetylase 1 is essential for oligodendrocyte specification in the zebrafish CNS. *Mech. Dev.* 123, 24–30. doi: 10.1016/j.mod.2005.10.005

Danesin, C., Agius, E., Escalas, N., Ai, X., Emerson, C., Cochard, P., et al. (2006). Ventral neural progenitors switch toward an oligodendroglial fate in response to increased Sonic hedgehog (Shh) activity: involvement of Sulfatase 1 in modulating Shh signaling in the ventral spinal cord. *J. Neurosci.* 26, 5037–5048. doi: 10.1523/JNEUROSCI.0715-06.2006

Davies, J. E., and Miller, R. H. (2001). Local sonic hedgehog signaling regulates oligodendrocyte precursor appearance in multiple ventricular zone domains in the chick metencephalon. *Dev. Biol.* 233, 513–525. doi: 10.1006/dbio.2001.0224

Dawson, M. R., Polito, A., Levine, J. M., and Reynolds, R. (2003). NG2-expressing glial progenitor cells: an abundant and widespread population of cycling cells in the adult rat CNS. *Mol. Cell. Neurosci.* 24, 476–488. doi: 10.1016/S1044-7431(03)00210-0

Ekker, S. C., Ungar, A. R., Greenstein, P., Von Kessler, D. P., Porter, J. A., Moon, R. T., et al. (1995). Patterning activities of vertebrate hedgehog proteins in the developing eye and brain. *Curr. Biol.* 5, 944–955. doi: 10.1016/S0960-9822(95)00185-0

Farreny, M. A., Agius, E., Bel-Vialar, S., Escalas, N., Khouri-Farah, N., Soukkarieh, C., et al. (2018). FGF signaling controls Shh-dependent oligodendroglial fate specification in the ventral spinal cord. *Neural Dev.* 13:3. doi: 10.1186/s13064-018-0100-2

Ferent, J., and Traiffort, E. (2015). Hedgehog: multiple paths for multiple roles in shaping the brain and spinal cord. *Neuroscientist* 21, 356–371. doi: 10.1177/1073858414531457

Ferent, J., Zimmer, C., Durbec, P., Ruat, M., and Traiffort, E. (2013). Sonic Hedgehog signaling is a positive oligodendrocyte regulator during demyelination. *J. Neurosci.* 33, 1759–1772. doi: 10.1523/JNEUROSCI.3334-12.2013

Fogarty, M., Richardson, W. D., and Kessaris, N. (2005). A subset of oligodendrocytes generated from radial glia in the dorsal spinal cord. *Development* 132, 1951–1959. doi: 10.1242/dev.01777

Franklin, R. J., and Ffrench-Constant, C. (2008). Remyelination in the CNS: from biology to therapy. *Nat. Rev. Neurosci.* 9, 839–855. doi: 10.1038/nrn2480

Franklin, R. J., Gilson, J. M., and Blakemore, W. F. (1997). Local recruitment of remyelinating cells in the repair of demyelination in the central nervous system. *J. Neurosci. Res.* 50, 337–344. doi: 10.1002/(SICI)1097-4547(19971015)50:2<337::AID-JNR21>3.0.CO;2-3

Fu, H., Cai, J., Rutledge, M., Hu, X., and Qiu, M. (2003). Oligodendrocytes can be generated from the local ventricular and subventricular zones of embryonic chicken midbrain. *Brain Res. Dev. Brain Res.* 143, 161–165. doi: 10.1016/S0165-3806(03)00108-1

Furusho, M., Kaga, Y., Ishii, A., Hebert, J. M., and Bansal, R. (2011). Fibroblast growth factor signaling is required for the generation of oligodendrocyte progenitors from the embryonic forebrain. *J. Neurosci.* 31, 5055–5066. doi: 10.1523/JNEUROSCI.4800-10.2011

Gao, L., and Miller, R. H. (2006). Specification of optic nerve oligodendrocyte precursors by retinal ganglion cell axons. *J. Neurosci.* 26, 7619–7628. doi: 10.1523/JNEUROSCI.0855-06.2006

Hajihosseini, M., Tham, T. N., and Dubois-Dalcq, M. (1996). Origin of oligodendrocytes within the human spinal cord. *J. Neurosci.* 16, 7981–7994. doi: 10.1523/JNEUROSCI.16-24-07981.1996

Harsan, L. A., Steibel, J., Zaremba, A., Agin, A., Sapin, R., Poulet, P., et al. (2008). Recovery from chronic demyelination by thyroid hormone therapy: myelinogenesis induction and assessment by diffusion tensor magnetic resonance imaging. *J. Neurosci.* 28, 14189–14201. doi: 10.1523/JNEUROSCI.4453-08.2008

Hu, B. Y., Du, Z. W., Li, X. J., Ayala, M., and Zhang, S. C. (2009). Human oligodendrocytes from embryonic stem cells: conserved SHH signaling networks and divergent FGF effects. *Development* 136, 1443–1452. doi: 10.1242/dev.029447

Jakovcevski, I., Filipovic, R., Mo, Z., Rakic, S., and Zecevic, N. (2009). Oligodendrocyte development and the onset of myelination in the human fetal brain. *Front. Neuroanat.* 3:5. doi: 10.3389/neuro.05.005.2009

Jiang, W., Ishino, Y., Hashimoto, H., Keino-Masu, K., Masu, M., Uchimura, K., et al. (2017). Sulfatase 2 modulates fate change from motor neurons to oligodendrocyte precursor cells through coordinated regulation of Shh signaling with sulfatase 1. *Dev. Neurosci.* 39, 361–374. doi: 10.1159/000464284

Kazanis, I., Evans, K. A., Andreopoulou, E., Dimitriou, C., Koutsakis, C., Karadottir, R. T., et al. (2017). Subependymal zone-derived oligodendroblasts respond to focal demyelination but fail to generate myelin in Young and aged mice. *Stem Cell Rep.* 8, 685–700. doi: 10.1016/j.stemcr.2017.01.007

Kessaris, N., Fogarty, M., Iannarelli, P., Grist, M., Wegner, M., and Richardson, W. D. (2006). Competing waves of oligodendrocytes in the forebrain and postnatal elimination of an embryonic lineage. *Nat. Neurosci.* 9, 173–179. doi: 10.1038/nn1620

Kessaris, N., Jamen, F., Rubin, L. L., and Richardson, W. D. (2004). Cooperation between sonic hedgehog and fibroblast growth factor/MAPK signalling pathways in neocortical precursors. *Development* 131, 1289–1298. doi: 10.1242/dev.01027

Kicheva, A., Bollenbach, T., Ribeiro, A., Valle, H. P., Lovell-Badge, R., Episkopou, V., et al. (2014). Coordination of progenitor specification and growth in mouse and chick spinal cord. *Science* 345:1254927. doi: 10.1126/science.1254927

Krauss, S., Concordet, J. P., and Ingham, P. W. (1993). A functionally conserved homolog of the Drosophila segment polarity gene hh is expressed in tissues with polarizing activity in zebrafish embryos. *Cell* 75, 1431–1444. doi: 10.1016/0092-8674(93)90628-4

Lee, J., Platt, K. A., Censullo, P., and Ruiz i Altaba, A. (1997). Gli1 is a target of Sonic hedgehog that induces ventral neural tube development. *Development* 124, 2537–2552.

Loulier, K., Ruat, M., and Traiffort, E. (2006). Increase of proliferating oligodendroglial progenitors in the adult mouse brain upon Sonic hedgehog delivery in the lateral ventricle. *J. Neurochem.* 98, 530–542. doi: 10.1111/j.1471-4159.2006.03896.x

Lu, Q. R., Yuk, D., Alberta, J. A., Zhu, Z., Pawlitzky, I., Chan, J., et al. (2000). Sonic hedgehog–regulated oligodendrocyte lineage genes encoding bHLH proteins in the mammalian central nervous system. *Neuron* 25, 317–329. doi: 10.1016/S0896-6273(00)80897-1

Machold, R., Hayashi, S., Rutlin, M., Muzumdar, M. D., Nery, S., Corbin, J. G., et al. (2003). Sonic hedgehog is required for progenitor cell maintenance in telencephalic stem cell niches. *Neuron* 39, 937–950. doi: 10.1016/S0896-6273(03)00561-0

Marti, E., Takada, R., Bumcrot, D. A., Sasaki, H., and Mcmahon, A. P. (1995). Distribution of sonic hedgehog peptides in the developing chick and mouse embryo. *Development* 121, 2537–2547.

Mastronardi, F. G., Min, W., Wang, H., Winer, S., Dosch, M., Boggs, J. M., et al. (2004). Attenuation of experimental autoimmune encephalomyelitis and nonimmune demyelination by IFN-beta plus vitamin B12: treatment to modify notch-1/sonic hedgehog balance. *J. Immunol.* 172, 6418–6426. doi: 10.4049/jimmunol.172.10.6418

Mecklenburg, N., Garcia-Lopez, R., Puelles, E., Sotelo, C., and Martinez, S. (2011). Cerebellar oligodendroglial cells have a mesencephalic origin. *Glia* 59, 1946–1957. doi: 10.1002/glia.21236

Menn, B., Garcia-Verdugo, J. M., Yaschine, C., Gonzalez-Perez, O., Rowitch, D., and Alvarez-Buylla, A. (2006). Origin of oligodendrocytes in the subventricular zone of the adult brain. *J. Neurosci.* 26, 7907–7918. doi: 10.1523/JNEUROSCI.1299-06.2006

Merchan, P., Bribian, A., Sanchez-Camacho, C., Lezameta, M., Bovolenta, P., and De Castro, F. (2007). Sonic hedgehog promotes the migration and proliferation of optic nerve oligodendrocyte precursors. *Mol. Cell. Neurosci.* 36, 355–368. doi: 10.1016/j.mcn.2007.07.012

Miyake, A., Chitose, T., Kamei, E., Murakami, A., Nakayama, Y., Konishi, M., et al. (2014). Fgf16 is required for specification of GABAergic neurons and oligodendrocytes in the zebrafish forebrain. *PLoS One* 9:e110836. doi: 10.1371/journal.pone.0110836

Mo, Z., and Zecevic, N. (2009). Human fetal radial glia cells generate oligodendrocytes in vitro. *Glia* 57, 490–498. doi: 10.1002/glia.20775

Nery, S., Wichterle, H., and Fishell, G. (2001). Sonic hedgehog contributes to oligodendrocyte specification in the mammalian forebrain. *Development* 128, 527–540.

Oh, S., Huang, X., and Chiang, C. (2005). Specific requirements of sonic hedgehog signaling during oligodendrocyte development. *Dev. Dyn.* 234, 489–496.

Ono, K., Fujisawa, H., Hirano, S., Norita, M., Tsumori, T., and Yasui, Y. (1997). Early development of the oligodendrocyte in the embryonic chick metencephalon. *J. Neurosci. Res.* 48, 212–225.

Orentas, D. M., Hayes, J. E., Dyer, K. L., and Miller, R. H. (1999). Sonic hedgehog signaling is required during the appearance of spinal cord oligodendrocyte precursors. *Development* 126, 2419–2429.

Ortega, J. A., Radonjic, N. V., and Zecevic, N. (2013). Sonic hedgehog promotes generation and maintenance of human forebrain Olig2 progenitors. *Front. Cell Neurosci.* 7:254. doi: 10.3389/fncel.2013.00254

Ortega, M. C., Cases, O., Merchan, P., Kozyraki, R., Clemente, D., and De Castro, F. (2012). Megalin mediates the influence of sonic hedgehog on oligodendrocyte precursor cell migration and proliferation during development. *Glia* 60, 851–866. doi: 10.1002/glia.22316

Park, H. C., Mehta, A., Richardson, J. S., and Appel, B. (2002). olig2 is required for zebrafish primary motor neuron and oligodendrocyte development. *Dev. Biol.* 248, 356–368.

Park, H. C., Shin, J., and Appel, B. (2004). Spatial and temporal regulation of ventral spinal cord precursor specification by Hedgehog signaling. *Development* 131, 5959–5969.

Picard-Riera, N., Decker, L., Delarasse, C., Goude, K., Nait-Oumesmar, B., Liblau, R., et al. (2002). Experimental autoimmune encephalomyelitis mobilizes neural progenitors from the subventricular zone to undergo oligodendrogenesis in adult mice. *Proc. Natl. Acad. Sci. U.S.A.* 99, 13211–13216.

Poncet, C., Soula, C., Trousse, F., Kan, P., Hirsinger, E., Pourquie, O., et al. (1996). Induction of oligodendrocyte progenitors in the trunk neural tube by ventralizing signals: effects of notochord and floor plate grafts, and of sonic hedgehog. *Mech. Dev.* 60, 13–32.

Pringle, N. P., Yu, W. P., Guthrie, S., Roelink, H., Lumsden, A., Peterson, A. C., et al. (1996). Determination of neuroepithelial cell fate: induction of the oligodendrocyte lineage by ventral midline cells and sonic hedgehog. *Dev. Biol.* 177, 30–42.

Qi, Y., Stapp, D., and Qiu, M. (2002). Origin and molecular specification of oligodendrocytes in the telencephalon. *Trends Neurosci.* 25, 223–225.

Qi, Y., Tan, M., Hui, C. C., and Qiu, M. (2003). Gli2 is required for normal Shh signaling and oligodendrocyte development in the spinal cord. *Mol. Cell. Neurosci.* 23, 440–450.

Rabadan, M. A., Cayuso, J., Le Dreau, G., Cruz, C., Barzi, M., Pons, S., et al. (2012). Jagged2 controls the generation of motor neuron and oligodendrocyte progenitors in the ventral spinal cord. *Cell Death Differ.* 19, 209–219. doi: 10.1038/cdd.2011.84

Rakic, S., and Zecevic, N. (2003). Early oligodendrocyte progenitor cells in the human fetal telencephalon. *Glia* 41, 117–127.

Ravanelli, A. M., and Appel, B. (2015). Motor neurons and oligodendrocytes arise from distinct cell lineages by progenitor recruitment. *Genes Dev.* 29, 2504–2515. doi: 10.1101/gad.271312.115

Samanta, J., Grund, E. M., Silva, H. M., Lafaille, J. J., Fishell, G., and Salzer, J. L. (2015). Inhibition of Gli1 mobilizes endogenous neural stem cells for remyelination. *Nature* 526, 448–452. doi: 10.1038/nature14957

Sanchez, M. A., and Armstrong, R. C. (2018). Postnatal Sonic hedgehog (Shh) responsive cells give rise to oligodendrocyte lineage cells during myelination and in adulthood contribute to remyelination. *Exp. Neurol.* 299, 122–136. doi: 10.1016/j.expneurol.2017.10.010

Sanchez, M. A., Sullivan, G. M., and Armstrong, R. C. (2018). Genetic detection of sonic hedgehog (Shh) expression and cellular response in the progression of acute through chronic demyelination and remyelination. *Neurobiol. Dis.* 115, 145–156. doi: 10.1016/j.nbd.2018.04.003

Schebesta, M., and Serluca, F. C. (2009). olig1 Expression identifies developing oligodendrocytes in zebrafish and requires hedgehog and notch signaling. *Dev. Dyn.* 238, 887–898. doi: 10.1002/dvdy.21909

Small, R. K., Riddle, P., and Noble, M. (1987). Evidence for migration of oligodendrocyte–type-2 astrocyte progenitor cells into the developing rat optic nerve. *Nature* 328, 155–157.

Soula, C., Danesin, C., Kan, P., Grob, M., Poncet, C., and Cochard, P. (2001). Distinct sites of origin of oligodendrocytes and somatic motoneurons in the chick spinal cord: oligodendrocytes arise from Nkx2.2-expressing progenitors by a Shh-dependent mechanism. *Development* 128, 1369–1379.

Stanton, B. Z., and Peng, L. F. (2010). Small-molecule modulators of the sonic hedgehog signaling pathway. *Mol. Biosyst.* 6, 44–54. doi: 10.1039/b910196a

Tan, M., Hu, X., Qi, Y., Park, J., Cai, J., and Qiu, M. (2006). Gli3 mutation rescues the generation, but not the differentiation, of oligodendrocytes in Shh mutants. *Brain Res.* 1067, 158–163.

Tekki-Kessaris, N., Woodruff, R., Hall, A. C., Gaffield, W., Kimura, S., Stiles, C. D., et al. (2001). Hedgehog-dependent oligodendrocyte lineage specification in the telencephalon. *Development* 128, 2545–2554.

Tong, C. K., Fuentealba, L. C., Shah, J. K., Lindquist, R. A., Ihrie, R. A., Guinto, C. D., et al. (2015). A dorsal SHH-dependent domain in the V-SVZ produces large numbers of oligodendroglial lineage cells in the postnatal brain. *Stem Cell Rep.* 5, 461–470. doi: 10.1016/j.stemcr.2015.08.013

Touahri, Y., Escalas, N., Benazeraf, B., Cochard, P., Danesin, C., and Soula, C. (2012). Sulfatase 1 promotes the motor neuron-to-oligodendrocyte fate switch by activating Shh signaling in Olig2 progenitors of the embryonic ventral spinal cord. *J. Neurosci.* 32, 18018–18034. doi: 10.1523/JNEUROSCI.3553-12.2012

Traiffort, E., Moya, K. L., Faure, H., Hassig, R., and Ruat, M. (2001). High expression and anterograde axonal transport of aminoterminal sonic hedgehog in the adult hamster brain. *Eur. J. Neurosci.* 14, 839–850.

Tripathi, R. B., Clarke, L. E., Burzomato, V., Kessaris, N., Anderson, P. N., Attwell, D., et al. (2011). Dorsally and ventrally derived oligodendrocytes have similar electrical properties but myelinate preferred tracts. *J. Neurosci.* 31, 6809–6819. doi: 10.1523/JNEUROSCI.6474-10.2011

Vallstedt, A., Klos, J. M., and Ericson, J. (2005). Multiple dorsoventral origins of oligodendrocyte generation in the spinal cord and hindbrain. *Neuron* 45, 55–67.

Wang, Y., Imitola, J., Rasmussen, S., O'Connor, K. C., and Khoury, S. J. (2008). Paradoxical dysregulation of the neural stem cell pathway sonic hedgehog-Gli1 in autoimmune encephalomyelitis and multiple sclerosis. *Ann. Neurol.* 64, 417–427. doi: 10.1002/ana.21457

Wu, M., Hernandez, M., Shen, S., Sabo, J. K., Kelkar, D., Wang, J., et al. (2012). Differential modulation of the oligodendrocyte transcriptome by sonic hedgehog and bone morphogenetic protein 4 via opposing effects on histone acetylation. *J. Neurosci.* 32, 6651–6664. doi: 10.1523/JNEUROSCI.4876-11.2012

Wu, S., Wu, Y., and Capecchi, M. R. (2006). Motoneurons and oligodendrocytes are sequentially generated from neural stem cells but do not appear to share common lineage-restricted progenitors *in vivo*. *Development* 133, 581–590.

Xing, Y. L., Röth, P. T., Stratton, J. A., Chuang, B. H., Danne, J., Ellis, S. L., et al. (2014). Adult neural precursor cells from the subventricular zone contribute significantly to oligodendrocyte regeneration and remyelination. *J. Neurosci.* 34, 14128–14146. doi: 10.1523/JNEUROSCI.3491-13.2014

Yu, K., Mcglynn, S., and Matise, M. P. (2013). Floor plate-derived sonic hedgehog regulates glial and ependymal cell fates in the developing spinal cord. *Development* 140, 1594–1604. doi: 10.1242/dev.090845

Conflict of Interest Statement: The authors declare that the research was conducted in the absence of any commercial or financial relationships that could be construed as a potential conflict of interest.

frontiers in Cellular Neuroscience

REVIEW
published: 12 September 2018
doi: 10.3389/fncel.2018.00297

Galectin-3-Mediated Glial Crosstalk Drives Oligodendrocyte Differentiation and (Re)myelination

Laura Thomas[1,2] *and Laura Andrea Pasquini*[1,2]*

[1] Department of Biological Chemistry, School of Pharmacy and Biochemistry, University of Buenos Aires, Buenos Aires, Argentina, [2] Institute of Chemistry and Biological Physicochemistry (IQUIFIB), National Scientific and Technical Research Council (CONICET), Buenos Aires, Argentina

Galectin-3 (Gal-3) is the only chimeric protein in the galectin family. Gal-3 structure comprises unusual tandem repeats of proline and glycine-rich short stretches bound to a carbohydrate-recognition domain (CRD). The present review summarizes Gal-3 functions in the extracellular and intracellular space, its regulation and its internalization and secretion, with a focus on the current knowledge of Gal-3 role in central nervous system (CNS) health and disease, particularly oligodendrocyte (OLG) differentiation, myelination and remyelination in experimental models of multiple sclerosis (MS). During myelination, microglia-expressed Gal-3 promotes OLG differentiation by binding glycoconjugates present only on the cell surface of OLG precursor cells (OPC). During remyelination, microglia-expressed Gal-3 favors an M2 microglial phenotype, hence fostering myelin debris phagocytosis through TREM-2b phagocytic receptor and OLG differentiation. Gal-3 is necessary for myelin integrity and function, as evidenced by myelin ultrastructural and behavioral studies from *LGALS3*$^{-/-}$ mice. Mechanistically, Gal-3 enhances actin assembly and reduces Erk 1/2 activation, leading to early OLG branching. Gal-3 later induces Akt activation and increases MBP expression, promoting gelsolin release and actin disassembly and thus regulating OLG final differentiation. Altogether, findings indicate that Gal-3 mediates the glial crosstalk driving OLG differentiation and (re)myelination and may be regarded as a target in the design of future therapies for a variety of demyelinating diseases.

Keywords: galectin-3, oligodedrocytes, myelination, CNS, remyelination, microglia, cytoskeleton, cuprizone

OPEN ACCESS

Edited by:
Fernando C. Ortiz, Universidad Autónoma de Chile, Chile

Reviewed by:
Yvonne Dombrowski, Queen's University Belfast, United Kingdom
Brahim Nait Oumesmar, INSERM U1127 Institut du Cerveau et de la Moelle épinière, France

***Correspondence:**
Laura Andrea Pasquini
laupasq@yahoo.com

Received: *12 June 2018*
Accepted: *17 August 2018*
Published: *12 September 2018*

Citation:
Thomas L and Pasquini LA (2018) Galectin-3-Mediated Glial Crosstalk Drives Oligodendrocyte Differentiation and (Re)myelination. Front. Cell. Neurosci. 12:297. doi: 10.3389/fncel.2018.00297

INTRODUCTION

Galectins (Gals) constitute a 15-member family of β-galactoside-binding lectins which recognize *N*-acetyllactosamine and, despite lacking specific receptors, form multivalent complexes with cell surface glycoconjugates containing suitable oligosaccharides and trigger intracellular signals to regulate cell survival and differentiation (Rabinovich et al., 2007; Yang et al., 2008). Among

Abbreviations: APC, adenomatous polyposis coli; CC, corpus callosum; CNPase, 2′, 3′-Cyclic-nucleotide 3′-phosphodiesterase; EGFR, epidermal growth factor receptor; GFAP, glial fibrillary acidic protein; IFN, interferon; IGF-1, insulin-like growth factor-1; LPS, lipopolysaccharide; MBP, myelin basic protein; mTOR, mammalian target of rapamycin complex; NG2, neural/glial antigen 2; Olig, oligodendrocyte transcription factor; PDGFRα, platelet-derived growth factor receptor α; PLP, myelin proteolipid protein; TGF, transforming growth factor; TNF, tumor necrosis factor; TREM-2, triggering receptor expressed on myeloid cells-2.

Gals, Gal-1, -8, and -9 exert similar immunosuppressive and anti-inflammatory effects on the pathogenesis of demyelinating diseases such as Multiple Sclerosis (MS) and its experimental models (Anderson et al., 2007; Toscano et al., 2007; Starossom et al., 2012; Rinaldi et al., 2016; Pardo et al., 2017). In contrast, the role of Gal-3 seems to be more complex and even controversial.

In this context, the present review firstly summarizes Gal-3 structure, location in cells and tissues, extracellular and intracellular space functions, regulation, internalization and secretion. The manuscript then focuses on the current knowledge of Gal-3 role in central nervous system (CNS) health and disease, particularly regarding oligodendrocyte (OLG) differentiation, myelination and remyelination, and its potential as a target in the design of future therapies for a variety of demyelinating diseases.

Gal-3 Structure

Gal-3 is a 25–35 KDa unique protein from the evolutionarily conserved family of Gals, which share a carbohydrate-recognition domain (CRD) and bind to β-galactoside-containing glycoconjugates. Gals are classified into three groups on the basis of their structural architecture: proto, chimera and tandem types, with Gal-3 being the only representative of the chimeric type (Barondes et al., 1994). Gal-3 has three structural domains: (a) the NH2 terminal domain containing serine phosphorylation sites Ser^{6} and Ser^{12}, important for nuclear localization and oligomerization; (b) a proline and glycine-rich collagen-like sequence susceptible to metalloprotease (MMP) cleavage; and (c) a COOH terminal domain containing the CRD and the NWGR anti-death motif, highly conserved within the BH1 domain of the Bcl-2 protein family (Dumic et al., 2006; Funasaka et al., 2014). In the presence of ligand galactose, Gal-3 is able to form pentamers whose affinity increases when galactose binds other saccharides like *N*-acetyllactosamine (Hirabayashi et al., 2002; Ahmad et al., 2004).

Gal-3 Tissue and Cellular Localization

Gal-3 is a ubiquitously distributed protein in adult tissue but has a tissue-time-dependent expression pattern throughout mouse embryogenesis (Poirier and Robertson, 1993; Fowlis et al., 1995; Van den Brule et al., 1997). In terms of cell populations, Gal-3 expression has been detected in fibroblasts, chondrocytes, osteoblasts, osteoclasts, keratinocytes, Schwann cells, gastric mucosa and endothelial cells from various tissues and organs (reviewed by Dumic et al., 2006). In addition to reports on neuronal and glial expression (Yoo et al., 2017), Gal-3 has been shown expressed *in vivo* by astrocytes in the subventricular zone (SVZ), being indispensable for cytoarchitecture maintenance but dispensable for apoptosis and proliferation (Comte et al., 2011). Gal-3 also maintains cell motility toward the olfactory bulb, possibly through EGFR phosphorylation modulation (Comte et al., 2011). Abundant evidence shows Gal-3 expression in cells committed to the immune response such as neutrophils, eosinophils, basophils, mast cells, Langerhans cells, dendritic cells, monocytes and macrophages from different tissues (Holíková et al., 2000; Jin et al., 2005; Chen et al., 2006; Sundblad et al., 2011; Novak et al., 2012; Ge et al., 2013; Wu et al., 2017; Brittoli et al., 2018). Even in cell types which do not normally express it such as lymphocytes, Gal-3 expression can be induced by various stimuli like T-cell receptor ligation, viral transactivating factors, and calcium ionophores (Hsu et al., 2009). Gal-3 is also expressed in several types of tumors, with expression intensity depending on tumor progression, invasiveness and metastatic potential (Danguy et al., 2002; reviewed in van den Brule et al., 2004). Regarding intracellular localization, Gal-3 is found in both cell cytoplasm and nucleus (Haudek et al., 2010) and is secreted to the extracellular space where it is often incorporated to the extracellular matrix (ECM) (Krześlak and Lipińska, 2004). Worth pointing out, Gal-3 functions are tightly dependent on localization.

Gal-3 Functions

A summary of Gal-3 functions in the extracellular and intracellular space, its regulation and its internalization and secretion is provided in **Figure 1**.

Extracellular Space

As it lacks a secretion signal sequence, Gal-3 is secreted via a non-classical pathway (described in *Gal-3 secretion and internalization*). It is often incorporated to the ECM to modulate cell adhesion or interact with plasmatic membrane receptors by binding to carbohydrate moieties in an autocrine or paracrine fashion to form membrane lattices and trigger intracellular events. Gal-3 impact on cell adhesion and migration depends on its multivalent capacity, as it functions as a nexus between ECM and membrane receptors and can thus inhibit or potentiate these cell properties. Gal-3 binds laminin, hensin, elastin, collagen IV, tenascin-C and -R, and crosslinks with integrins, the major cell adhesion receptor modulators (reviewed by Dumic et al., 2006). Regarding membrane receptors, those having five or more glycosylated sites are preferable candidates for lattice formation, like TGFβR and EGFR, while those with fewer glycosylation sites are below the threshold. This scenario may change, however, when *N*-glycosylation is stimulated with UDP-GlcNAc (Lau et al., 2007; Nabi et al., 2015). Extracellular Gal-3 has been described mainly as an inflammatory mediator: for example, it is chemoattractant to monocytes, increases superoxide anion production in monocytes and neutrophils, increases apoptosis in T-cells and other cell types depending on the doses used, increases LPS responses and decreases T-cell receptor (TCR)-mediated signaling in T-cells, among other functions (Hsu et al., 2009; Dabelic et al., 2012; Xue et al., 2017; Uchino et al., 2018). Also, depending on cell types, extracellular Gal-3 can promote or inhibit cell proliferation and growth (Krugluger et al., 1997; Inohara et al., 1998; Diao et al., 2018; Zhou et al., 2018).

Intracellular Space

Within the cell, Gal-3 is distributed between the cytoplasm and the nucleus depending on cell types and conditions (Haudek et al., 2010). In the intracellular compartment most Gal-3 binding appears to be mediated by protein–protein interaction rather than protein-carbohydrate recognition. In the cytoplasm, it plays an anti-apoptotic role, as it interacts with Bcl-2, and

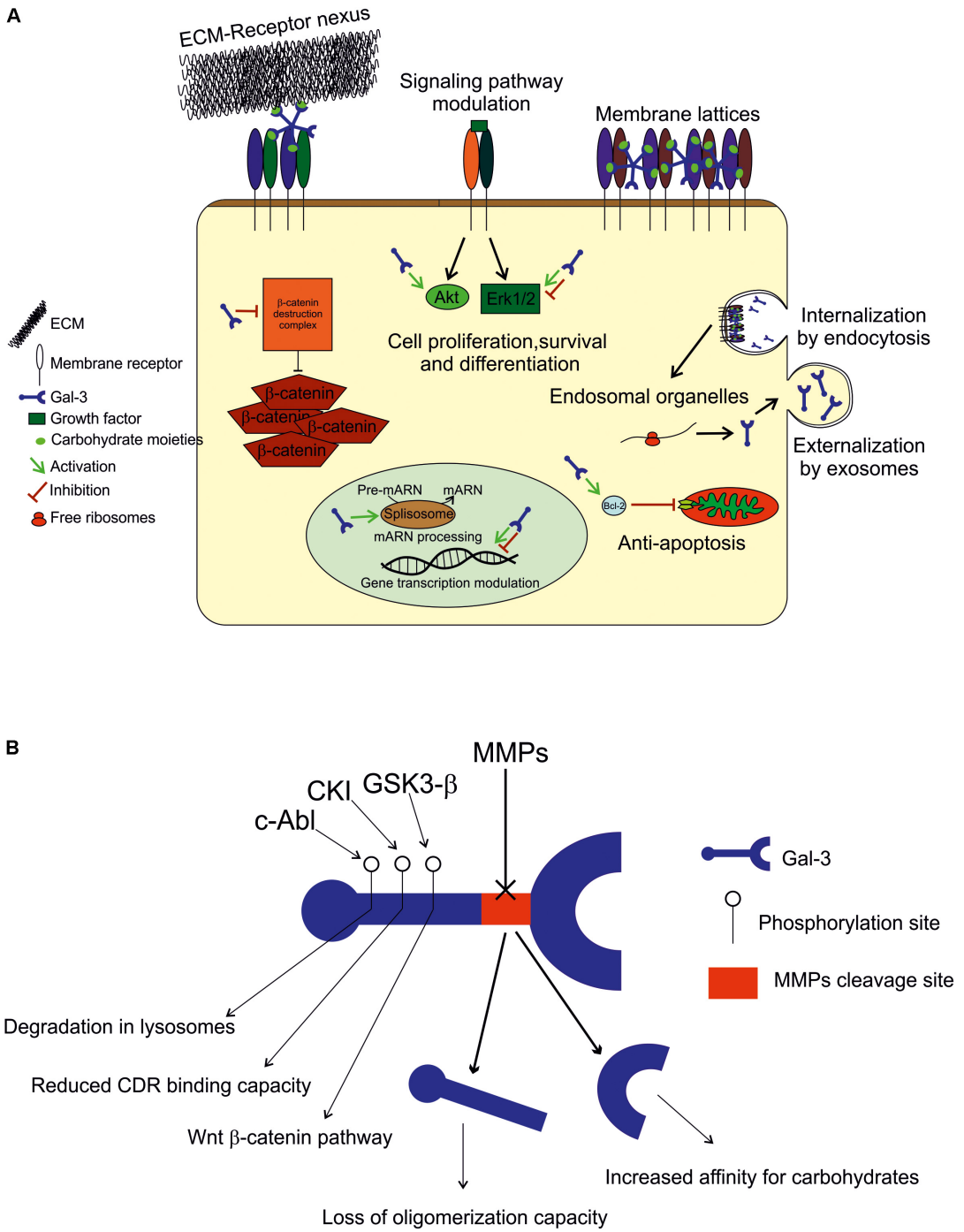

FIGURE 1 | (A) *Extracellular space:* Gal-3 either binds to the ECM compounds (laminin, hensin, elastin, collagen IV, tenascin-C and -R, and integrin) to modulate cell adhesion, or interacts with plasmatic membrane receptors by binding to carbohydrate moieties in an autocrine or paracrine fashion to form membrane lattices and trigger intracellular events. *Intracellular space:* within the cell, Gal-3 is found in both cytoplasm and nucleus, and its binding appears to be mediated by protein-protein interactions. In the cytoplasm, it plays an anti-apoptotic role (Bcl-2), and modulates signaling pathways (Akt and in Erk 1/2) to promote or inhibit cell growth, proliferation and differentiation. In the nucleus, Gal-3 is crucial for pre-mRNA splicing (spliceosome incorporation) and to promote or repress transcription. *Internalization and secretion*: Gal-3 enters the cell by non-clathrin-mediated endocytosis and goes through endosomal organelles to be later sorted elsewhere or degraded. Gal-3 is secreted via a non-classical pathway and apparently through exosomes. **(B)** *Regulation:* Gal-3 activity is regulated by MMP2 and MMP9 cleavage (Ala62 to Tyr63), generating a 22 kDa whole CRD peptide (high affinity for carbohydrates) and a 9 kDa N-terminal peptide (oligomerization capacity). Also, Gal-3 is phosphorylated in Tyr residues by c-Abl kinase to promote its own degradation in lysosomes in Ser residues by casein kinase I to reduce its carbohydrate binding capacity, and by GSK3-β to regulate the Wnt-β-catenin pathway.

it also modulates signaling pathways in order to promote or inhibit cell growth, proliferation and differentiation. It activates Akt (Kariya et al., 2018; Ruvolo et al., 2018), inhibits or activates Erk 1/2 (Alge-Priglinger et al., 2011; Mori et al., 2015; Zhang et al., 2017), and increases β-catenin levels (Shimura et al., 2004; Hu et al., 2015), among other functions, depending on the cell types evaluated. In the nucleus, Gal-3 is crucial for pre-mRNA splicing, as it is incorporated into spliceosomes by associating with the U1 small nuclear ribonucleoprotein (snRNP) complex (Patterson et al., 2002; Haudek et al., 2010). Gal-3 has also been shown to promote or repress the transcription of certain genes (Krugluger et al., 1997; Iacobini et al., 2017; Zhou et al., 2018).

Gal-3 Regulation

Gal-3 is regulated mainly by degradation by MMPs, phosphorylation and space-time coordinated expression, as described above. Aminoacid sequence analyses have revealed that Gal-3 is cleaved by MMP2 and MMP9 between Ala^{62} and Tyr^{63}, resulting in two peptides: a 22 kDa peptide containing the whole CRD and a 9 kDa N-terminal peptide (Gao et al., 2017). The CRD peptide retains its carbohydrate-binding activity with increased affinity for carbohydrates (Ochieng et al., 1994). However, Gal-3 capability to oligomerize is lost upon cleavage, which generates changes in Gal-3 functions such as the interaction with membrane receptors (Nabi et al., 2015). Therefore, Gal-3 cleavage by MMP is of high importance to determine its activity. Also worth noticing, Gal-3 induces the expression and secretion of MMP9 in melanoma cells, indicating a feedback loop for Gal-3 regulation (Mauris et al., 2014; Dange et al., 2015). Also, in other cell types, Gal-3 is known to be phosphorylated in Tyr residues by c-Abl kinase (Balan et al., 2010) to promote its own degradation in lysosomes (Li et al., 2010), in Ser residues by casein kinase I to reduce its carbohydrate binding capacity (Mazurek et al., 2000), and by GSK3-β to regulate the Wingless (Wnt)-β-catenin pathway (Song et al., 2009).

Gal-3 Internalization and Secretion

It is known that Gal-3 is incorporated into the cell through non-clathrin-mediated endocytosis and goes through endosomal organelles to be later sorted elsewhere or degraded (Hönig et al., 2015; Nabi et al., 2015). Regarding externalization, Gal-3 lacks a signal for classical externalization and it was recently found in the lumen of apical secreted exosomes from epithelial cells. For this type of secretion, Gal-3 release depends on the endosomal sorting complex required for transport I, essential for cargo recruitment (Bänfer et al., 2018). This notion is of great relevance for further exploration, as exosomes are being increasingly described as a short and long-distance communication pathway between cells. However, the mechanisms, if any, through which Gal-3 can be released out of exosomes and into the extracellular space in a free form remain to be elucidated.

Gal-3 Roles in Non-Cns Disease

Secreted Gal-3 is currently under evaluation as a biomarker of tumoral and fibrotic processes, as it has been found elevated in many cancers including solid tumors and blood cancers like leukemias and lymphomas (reviewed in Ruvolo, 2016). Gal-3 is thought to be produced by tumor microenvironment cells such as mesenchymal stromal cells and to play immunosuppressive functions, thus supporting metastasis (Ruvolo, 2016). Gal-3 also takes part in tumor cell adhesion, proliferation, differentiation, angiogenesis, and metastasis (Wang and Guo, 2016). In fibrotic processes, Gal-3 has been principally described in skin illnesses (McLeod et al., 2018) and liver and heart failure (Moon et al., 2018; Piek et al., 2018). In acute ischemic stroke, higher levels of serum Gal-3 have been recently associated with increased death risk (Wang et al., 2018). Likewise, it is extensively described in inflammatory processes modulating macrophage responses (de Oliveira et al., 2015; Mietto et al., 2015; Schnaar, 2016). In addition, Gal-3 seems to exert an inhibitory effect on LPS-induced inflammation, as increased inflammatory cytokine production is induced in both $LGALS3^{-/-}$ macrophages and wild-type macrophages in which Gal-3 binding has been neutralizated through antibodies. This was also supported by an increase in $LGALS3^{-/-}$ mice vulnerability to LPS, reflected by higher inflammatory cytokine and nitric oxide production (Li et al., 2008).

GAL-3 IN HEALTHY OLG DIFFERENTIATION

Having introduced the main features of Gal-3, the present review will now focus on the current knowledge of Gal-3 role in CNS myelination, remyelination and OLG differentiation (**Figure 2**).

Gal-3 Expression and Regulation in OLG

Oligodendrocyte are resident CNS cells in charge of myelination, i.e., the physiological process of axon insulation allowing metabolic and trophic support for axons and providing a rapid saltatory conduction of action potentials (Bercury and Macklin, 2015). In terms of morphological and molecular stages, OLG are initially bipolar cells named oligodendrocyte progenitor cells (OPC) which proliferate and migrate, expressing molecular markers like PDGFRα and NG2. An intermediate stage represented by pre-OLG, more ramified, express CNPase, Olig 1 and O4, among others. These cells later form myelin membranes and express MBP, APC, and PLP, hence becoming the fully mature OLG capable of myelination (Nave and Werner, 2014; Snaidero and Simons, 2017).

Gal-3 mRNA expression has not yet been evaluated in OLG, which makes it still uncertain whether it is actually expressed in this cell type and whether it acts in an autocrine fashion to regulate OLG maturation. However, Gal-3 has been immunocytochemically detected in immature (PDGFRα, A2B5, and O4) and mature (O1, MBP, CNPase, PLP) OLG isolated from primary rat cultures, with higher levels in mature ones (Pasquini et al., 2011). Recent work also outlines Gal-3 occasional expression by Rip+ OLG in white matter from normal rat brains (Yoo et al., 2017). Gal-3 appears to be cleaved in OPC by MMP2 and then stabilized in mature OLG, which suggests variations in

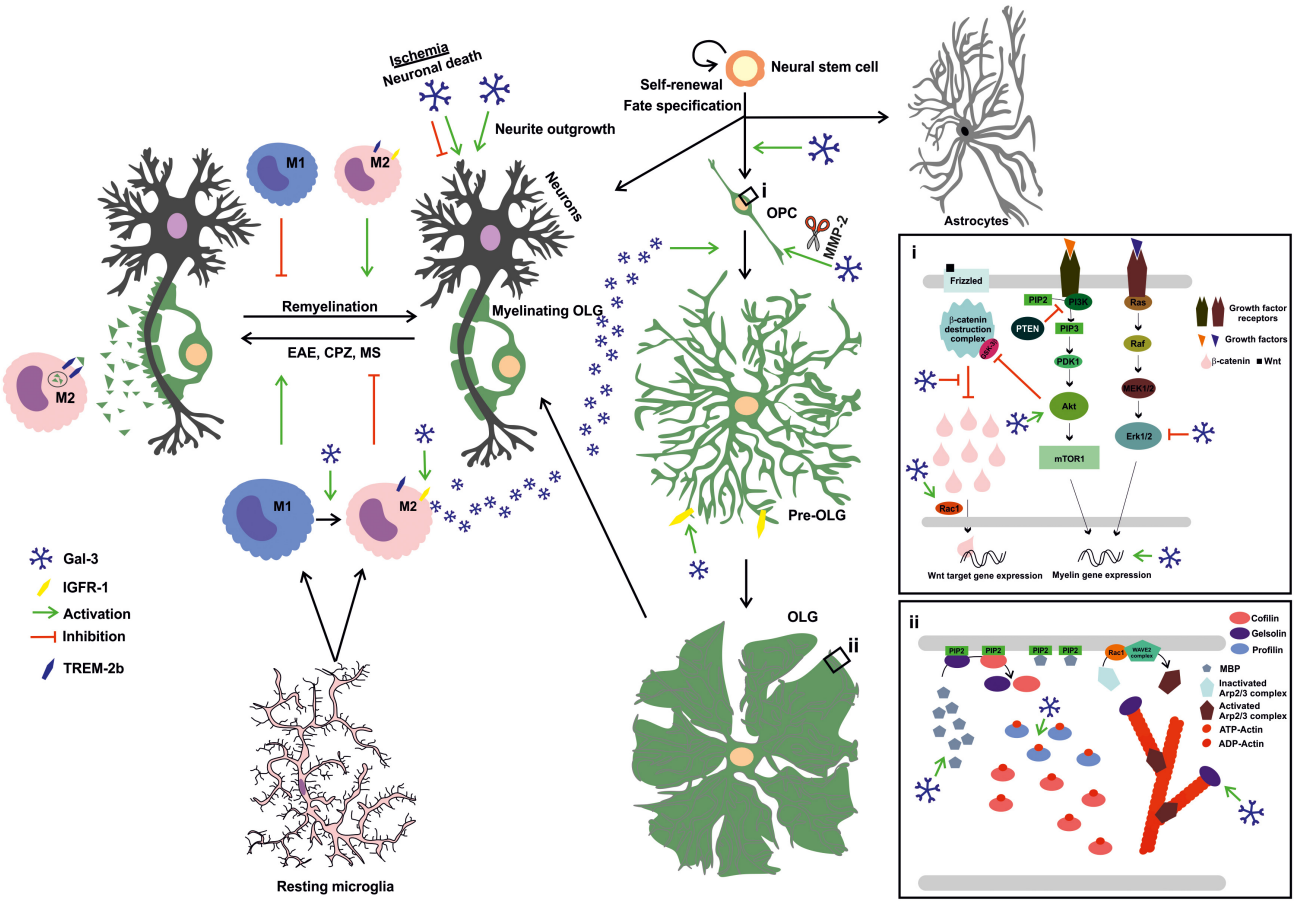

FIGURE 2 | Extracellular Gal-3 drives OLG differentiation and (re)myelination: Gal-3 is expressed in microglial cells during remyelination, favoring an M2 microglial phenotype and, therefore, fostering myelin phagocytosis through TREM-2b phagocytic receptor and OLG differentiation probably by IGFR-1 pathway stimulation. In OPC (i), Gal-3 drives early process outgrowth through enhanced actin assembly and a decrease in Erk 1/2 activation, and later regulates OLG maturation (ii) by inducing Akt activation and inhibiting β-catenin degradation to increase MBP expression and promotes gelsolin release and actin cytoskeleton disassembly. Also, microglia-released Gal-3 induces OLG fate in neural stem cells. Finally, Gal-3 promotes neurite outgrowth but exerts both deleterious and protective effects on neuronal death in ischemic brain injury.

its biological activity during OLG differentiation (Pasquini et al., 2011).

Gal-3 Drives OLG Maturation

As part of pioneering studies on the direct influence of Gal-3 on OLG maturation, in 2011 our group demonstrated that extracellular Gal-3 promotes OLG differentiation and may be expressed and secreted by microglia (Pasquini et al., 2011). Microglia are known to express Gal-3 in normal oligodendrogenesis (Ellison and de Vellis, 1995; Pasquini et al., 2011) and upon activation, promoting myelin debris phagocytosis through FcγR, CR3/MAC-1 and SRAI/II receptors and fostering remyelination upon injury or disease (Rotshenker et al., 2008). Work by Pasquini et al. (2011) has revealed that extracellular Gal-3 promotes dose-dependent OLG differentiation in close relationship with the glycoconjugates present in OPC cell surfaces. Glycosylation signature analysis has shown that OPC possess a permissive glycophenotype expressing the necessary carbohydrates for Gal-3 binding. In contrast, Gal-3 overexpression in the OLG N20.1 cell line produces no changes in MBP promoter activity, which indicates that changes in endogenous Gal-3 relative abundance do not affect OLG differentiation. Moreover, treatment with conditioned media from wild type (WT) microglia, but not *LGALS3*$^{-/-}$ microglia, promotes OLG differentiation, suggesting that microglia express the Gal-3 necessary to induce OLG maturation. In addition, using neurosphere cultures, our group has also proven Gal-3 to promote cell commitment toward the OLG lineage (Pasquini et al., 2011).

Gal-3 Accelerates OLG Differentiation: Actin Cytoskeleton Dynamics Modulation

Although studies on the processes controlling signaling pathways and cytoskeleton dynamics in OLG have rendered contrasting results, recent thorough reports proposed a two-step model for actin dynamics in OLG: first, pro-assembly dynamics until OLG

are fully differentiated and, second, a switch to pro-disassembly dynamics to start myelination (Nawaz et al., 2015; Zuchero et al., 2015). This is driven by interplay between MBP and actin disassembly proteins like cofilin-1 and gelsolin, both sequestered and hence inactivated by phosphatidylinositol 4,5-bisphosphate (PIP2) on the plasma membrane. When MBP is expressed as OLG reach their final maturational state, MBP competes for PIP2 binding, and gelsolin and cofilin-1 are displaced from their binding to the inositol and activated to drive actin disassembly (Zuchero et al., 2015). Further work has demonstrated that cytoplasmic gelsolin is crucial for OPC differentiation and is a downstream effector of anti-LINGO1 blocking antibody. This study also shows that cytoplasmic gelsolin expression drives OPC differentiation and increases as OLG mature, indicating that cytoskeleton severing proteins are crucial for morphological changes required for OLG differentiation (Shao et al., 2017). Gal-3 effects on the actin cytoskeleton appear to be cell type-dependent, driving cytoskeleton disassembly dependent on Erk 1/2 inactivation in retinal pigment epithelium (RPE) cells (Alge-Priglinger et al., 2011), while promoting lamellipodia formation in epithelial cells (Saravanan et al., 2009).

In the B16F10 murine melanoma cell line, cells plated over Gal-3 as substrate have shown increased actin turnover and lamellipodia formation on the cell edges, and an increase in Rac1 activation (More et al., 2016). Indeed, our most recent work first unveiled the role of extracellular Gal-3 in OLG cytoskeleton dynamics (Thomas and Pasquini, 2018). Our group demonstrated that extracellular Gal-3 modulates actin cytoskeleton dynamics in primary rat OLG cultures in two steps: first, Gal-3 drives actin polymerization dynamics and then switches to depolymerization dynamics, which may be thought of as an accelerated version of the process described by Zuchero et al. (2015). These changes are accompanied by an increase in gelsolin and MBP expression, generating actin disassembly in a carbohydrate-dependent manner as OLG mature. Moreover, Gal-3 induces an increase in the expression of actin ADT-ATP exchanger profilin-1 and activated small GTPase Rac-1, further supporting its crucial role in actin dynamics. Likewise, Gal-3 accelerates OLG differentiation as compared to vehicle-treated cells, as supported by the increase observed in CNPase+ cells and in the area and expression of MBP (Thomas and Pasquini, 2018).

Gal-3 Accelerates OLG Differentiation: Underlying Signaling Pathways

Conserved signaling pathways in OLG like Erk 1/2, β-catenin and Akt play an important, though controversial, role in OLG maturation.

Erk 1/2

Some *in vitro* reports have shown Erk 1/2 inhibition to diminish OLG maturation (Fyffe-Maricich et al., 2011; Guardiola-Diaz et al., 2012; Xiao et al., 2012), while other studies *in vivo* and *in vitro* have reported no changes upon Erk 1/2 inactivation in OPC differentiation (Ishii et al., 2012, 2013; Xiao et al., 2012). Also, inhibiting Erk 1/2 decreases OPC proliferation in response to growth factors (Bhat and Zhang, 1996; Kumar et al., 1998; Baron et al., 2000; Bansal et al., 2003; Cui and Almazan, 2007; Frederick et al., 2007). Erk 1/2 has been proposed to contribute to the passage from OPC to pre-OLG (Narayanan et al., 2009; Guardiola-Diaz et al., 2012), while other reports claim that it promotes the passage from pre-OLG to mature OLG (Tyler et al., 2009; Bercury et al., 2014). A thorough revision of the involvement of Erk 1/2 signaling in CNS myelination has been recently published by Gonsalvez et al. (2016). In addition, work by More et al. in 2016 revealed that tumor cells plated on Gal-3 show a time-dependent decrease in Erk 1/2 phosphorylation. Similarly, extracellular Gal-3 decreases Erk 1/2 activation in RPE cells (Alge-Priglinger et al., 2011) and in keratinocytes, generating anti-apoptotic events (Larsen et al., 2011). Our recent work indicates that Gal-3 inhibits Erk 1/2 in a carbohydrate-dependent manner, thus contributing to the promotion of MBP and gelsolin expression and subsequent OLG maturation (Thomas and Pasquini, 2018).

Akt/mTOR

The role of the Akt/mTOR pathway is less controversial than that of Erk 1/2, as it is known to improve myelination both *in vitro* and *in vivo*. However, as with Erk 1/2, the timing of Akt action has not fully elucidated yet, although available evidence suggests that it favors the passage from pre-OLG to OLG, in a close crosstalk with Erk 1/2 (reviewed in Gaesser and Fyffe-Maricich, 2016). *In vivo*, Akt overexpression as well as PTEN inhibition generates a hypomyelinated phenotype (Flores et al., 2008; Narayanan et al., 2009). mTOR is known to promote lipid synthesis by activating SREBPS, which is of high importance in promoting myelin synthesis (reviewed in Figlia et al., 2018). Further support for the pro-myelinating role of mTOR has been obtained through the use of rapamycin, mTOR inhibitor, revealing that mTOR is crucial for OPC differentiation, and myelin protein and mRNA synthesis (Tyler et al., 2009, 2011; Guardiola-Diaz et al., 2012).

Several authors have demonstrated that Gal-3 activates Akt signaling. In human cutaneous squamous cell carcinoma tissues, Gal-3 binds to β4-integrin and activates the Akt axis (Kariya et al., 2018). Also, in mammary epithelial tumor cells, extracellular Gal-3 activates PI3K, upstream kinase in the Akt pathway (Lagana et al., 2006). In tumor cell line B16F10, Akt phosphorylation increases with time in cells plated on Gal-3 as substrate (More et al., 2016). In line with these results, our work proves that Gal-3 augments Akt activation also in a carbohydrate-dependent fashion, which leads to an increase in MBP and gelsolin expression, driving OPC differentiation (Thomas and Pasquini, 2018).

β-catenin

β-catenin is a protein degraded by the proteasome when phosphorylated by a destruction complex in the cytoplasm, an event which requires absence of Wnt ligand binding to Frizzled receptor. When binding occurs, β-catenin is not degraded and can translocate to the nucleus where it acts as a transcription factor modulating cellular functioning. In OLG, some authors

describe this pathway as an OLG differentiation inhibitor (Fancy et al., 2009; Feigenson et al., 2009; Ye et al., 2009), while others describe it as promoting OLG differentiation (Kalani et al., 2008; Tawk et al., 2011; Ortega et al., 2013). These differences probably respond to the conditions used and the timing of evaluation.

In colon cancer cells, Gal-3 has been shown to drive β-catenin accumulation by regulating GSK-3β phosphorylation –a member of β-catenin destruction complex– via the PI3K/Akt pathway (Song et al., 2009). A similar conclusion has been reached in gastric cancer cells, where absence of Gal-3 diminishes β-catenin levels (Kim et al., 2010). Our results show that Gal-3 augments β-catenin expression in mature OLG, concomitantly with an increase in MBP expression and Akt activation. β-catenin levels decrease when Akt is inhibited, further supporting the close connection between these pathways (Thomas and Pasquini, 2018).

Gal-3 Drives Axon Myelination and Neurite Outgrowth

To investigate Gal-3 *in vivo* role during the myelination process, our group has analyzed Gal-3 expression at postnatal day 5 (P5), 10 (P10), 15 (P15), and 20 (P20) using transgenic mice expressing the enhanced green fluorescent protein (EGFP) driven by the promoter of oligodendroglial protein CNPase (CNP–EGFP). Gal-3 expression showed substantial changes during white matter development, with high expression levels at P5 and a reduction upon myelin development. In agreement, high levels of Gal-3 were found at P5 in microglial cells localized in the CC and cingulum, fairly close to CNPase+ cells. Interestingly, confocal microscopy showed some CNPase+ cells with maturen OLG-like morphology to colocalize with Gal-3. On the other hand, Gal-3 was detected at low levels in astrocytes at P10 and P15, and at high levels in the SVZ at all ages evaluated. This work also revealed a critical role for Gal-3 during OLG myelination, as reflected by the morphological changes observed in the myelin of *LGALS3*$^{-/-}$ mice. These animals presented hypomyelination in the striatum and CC, as revealed by electron microscopic morphometric analysis. These myelin defects were deeper in 8-week-old relative to 4-week-old mice. Also, myelin showed lesser integrity and abnormal compaction compared to WT mice. Furthermore, *LGALS3*$^{-/-}$ mice exhibited substantial alterations in behavior with diminished levels of innate anxiety than their WT littermates (Pasquini et al., 2011).

Interestingly, substratum-bound Gal-3 had been previously shown to promote outgrowth of neurites from dorsal root ganglia explants (Pesheva et al., 1998) and neurite stabilization in the cerebellum (Mahoney et al., 2000). In this context, further work needs to be carried out in order to elucidate Gal-3 role in myelination *in vivo* and whether this neurite outgrowth and stabilization could influence OLG myelin formation capacity.

GAL-3 IN CNS DISEASE

The main features of Gal-3 in CNS diseases are summarized in **Figure 2**.

Inflammation and Hypoxic-Ischemic Injury

In CNS disease, Gal-3 has been attributed both deleterious and protective effects, being mainly expressed by activated microglia and upregulated by inflammatory stimuli (Umekawa et al., 2015). In a focal cerebral ischemia model in mice, Gal-3 was found to mediate microglial activation and proliferation and to be preferentially expressed by a subgroup of proliferating IGF-1-expressing microglia. Tunicamycin-mediated inhibition of *N*-glycosylation diminishes IGF-1-induced microglial mitogenic response, while coimmunoprecipitation assays have revealed Gal-3 binding to IGF-receptor 1, which suggests that interactions between Gal-3 and N-linked glycans present in growth factor receptors are mediators of IGF-receptor 1 (IGF-R1) signaling (Lalancette-Hébert, 2007; Rotshenker, 2009; Lalancette-Hébert et al., 2012). Moreover, an increase in Gal-3 expression is observed in several ischemic models, associated to an improvement in neurologic function, a reduction in neuronal cell death, angiogenesis, proliferation of neuronal precursors, and a type 2 T cell immune bias (Ohtaki et al., 2008; Yan et al., 2009). These findings suggest that Gal-3 may act as an important modulator of the brain inflammatory response with high neuroprotective potential. However, in other models of hypoxic-ischemic (HI) injury, Gal-3 has been shown to exert deleterious effects. For instance, *LGALS3*$^{-/-}$ mice are protected from neuronal death in the hippocampus and striatum, and a reduction in Gal-3 is observed during delayed neuronal death induced by hypothermia or antiapoptotic agents in the CA1 region (Doverhag et al., 2010; Satoh et al., 2011a,b; Hisamatsu et al., 2016). Further studies have also shown that the increase in Gal-3 expression observed in ischemia is blocked when antiapoptotic molecule Bis is downregulated, generating less vulnerable hippocampal neurons (Cho et al., 2012). In addition to the deleterious effects, Gal-3 has been suggested as a target for the treatment of post-stroke gastrointestinal complications, as it is released after stroke and triggers central and peripheral enteric neuronal loss through a TLR4-mediated mechanism involving TAK1 and AMPK (Cheng et al., 2016). Finally, recent studies conclude that Gal-3 is necessary for angiogenesis after ischemia but does not affect apoptosis, infarct size, microglial, and astrocyte activation/proliferation, SVZ neurogenesis or migration to lesion (Young et al., 2014; Xu et al., 2017).

Amyotrophic Lateral Sclerosis, Alzheimer's Disease, Parkinson's Disease and Prions

In amyotrophic lateral sclerosis (ALS), advanced glycation end-products (AGE) are a source of inflammation and oxidative injury. Gal-3 acts as an AGE receptor and leads them to lysosome degradation and removal (Pricci, 2000). In line with this, Gal-3 counteracts neuroinflammation, as its deletion leads to heightened neurodegeneration in ALS owing to AGE accumulation (Lerman, 2012). Moreover, Gal-3 has emerged as a key biomarker candidate on account of its differential expression in ALS mouse model SOD1 (G93A)

and spinal cord tissue and cerebrospinal fluid from ALS patients (Zhou et al., 2010). Its expression is also increased in microglia accompanied by osteopontin and vascular endothelial growth factor (VEGF), concomitantly with low expression of TNFα, IL-6, brain-derived neurotrophic factor (BDNF) and arginase-1 from ALS rat model SOD1 (G93A) (Nikodemova et al., 2014). Gal-3 might also be postulated as a potential biomarker for Alzheimer's disease (AD), as AD patients exhibit significantly higher levels of serum Gal-3 (Wang et al., 2015). In Parkinson's disease (PD), extracellular α-synuclein-aggregate-induced inflammation can be reduced by Gal-3 inhibition, which suggests therapeutic potential for Gal-3 (Boza-Serrano et al., 2014). In addition, microarray analysis of substantia nigra in a PD animal model has shown the temporal expression profiles of 4 candidate genes implicated in neuroglial activation and functional maturation, i.e., Gal-3, Heat shock protein 27, Lipocalin 2 and Tissue inhibitory metalloproteinase 1 (Choy et al., 2015). In prion-infected brain tissue, Gal-3 has been found to exert harmful effects (Riemer et al., 2004; Mok et al., 2006, 2007), as its expression in activated microglia/macrophages correlates with abnormal prion protein accumulation (Jin et al., 2007).

MS and Its Experimental Models

Oligodendroglial injury leads to demyelination, which is followed by a regenerative response consisting in the formation of new myelin sheaths –a process called remyelination (Franklin, 2002; Franklin and Ffrench-Constant, 2017). This process has been described in animal models and in human demyelinating diseases such as MS (Prineas et al., 1993; Patrikios et al., 2006; Patani et al., 2007). MS course varies considerably among patients, although the most frequent presentation consists of recurring clinical symptoms followed by total or partial recovery, namely the classic relapsing-remitting form of MS. After 10–15 years of disease, symptoms become progressive in up to 50% of untreated patients and lead to clinical deterioration for several years, a stage referred to as secondary progressive MS. In about 15% of MS patients, however, disease progression is relentless as from onset, in what constitutes primary progressive MS (Bjartmar et al., 2001; McFarland and Martin, 2007; Tallantyre et al., 2010). The progressive stage is in part due to incomplete remyelination, which produces the loss of axonal metabolic support provided by myelin and concomitant axonal and neural degeneration, which lead to the progressive disability observed in the later stages of MS (Nave, 2010; Franklin et al., 2012).

Sera from patients with secondary progressive MS has been recently shown to present auto-antibodies against Gal-3, which may be responsible for blood brain barrier progressive damage (Nishihara et al., 2017). These authors determined that membrane-bound Gal-3 in human brain microvascular endothelial cells (BMEC) is a target for auto-antibodies present in secondary progressive MS serum but not for healthy donors or patients with other CNS illnesses; downregulation of Gal-3 in these cells causes an increase in the expression of intracellular adhesion molecule-1 (ICAM-1) and phospho-NFκB p65, both molecules described as responsible for leukocyte leakage to the CNS (Dietrich, 2002). These effects are also observed when BMEC are incubated with secondary progressive MS serum but prevented when Gal-3 is downregulated in BMEC or when secondary progressive MS serum is depleted from anti-Gal-3-auto-antibodies. These results hint at Gal-3 and anti-Gal-3 antibodies as therapeutic targets to prevent blood brain barrier damage.

Further work has described the effect of cerebrospinal fluid (CSF) from patients with primary progressive MS or relapsing remitting MS in the morphology and transcriptional response of treated OPC (Haines et al., 2015). The results obtained indicate that OPC treated with primary progressive MS CSF present a significantly more ramified morphology than control or relapsing remitting MS CSF, accompanied by a pro-differentiating transcriptome: downregulation of PDGFRα and LINGO1 genes and upregulation of MAG gene. However, this transcriptome is different from that present in normal OPC differentiation. Interestingly, this work reports *LGALS3* gene upregulation only in primary progressive MS CFS-treated OPC and establishes a link between Gal-3 upregulation and increased OPC branching. Gal-3 upregulation has also been observed in post-mortem human brain tissues with primary progressive MS.

Taken together, these findings indicate that Gal-3 is a positive target for OLG differentiation in human MS tissue and drives the downregulation of ICAM-1 in BMEC, mediating a protective effect on the blood–brain barrier. However, the presence of anti-Gal-3 auto-antibodies is responsible for blood brain barrier damage, a negative effect which might be counteracted through neutralizating therapy.

Current evidence has proposed exosomes as possible biomarkers and therapeutic agents in CNS disease. Most importantly, as therapeutic agents, exosomes display some advantages, as they can deliver cargo to other cells, rapidly pass the brain–blood barrier and render low immunogenicity (Chen and Chopp, 2018; reviewed in Osier et al., 2018). As described before in this review, Gal-3 is known to be excreted through exosomes, which opens doors for the evaluation of the therapeutic potential and biomarker capacity of the presence of Gal-3 in exosomes.

Even if experimental models fail to replicate MS in its full complexity and heterogeneity, they have succeeded in developing various treatments for MS patients. Several well-established experimental demyelination models include those mediated by immunity, virus and toxins. The most widely used animal model of CNS demyelination is experimental autoimmune encephalomyelitis (EAE), in which mice are immunized with myelin oligodendroglial glycoprotein. EAE constitutes the most widely exploited model and is especially useful to study the autoimmunity aspects in MS pathology. However, numerous therapeutic agents displaying beneficial effects in this model have proven poorly or not beneficial at all in the treatment of MS. *LGALS3*$^{-/-}$ mice display clearly diminished CNS macrophage infiltration during EAE, which leads to lesser disease severity (Jiang et al., 2009). These findings suggest a central role of Gal-3 in promoting inflammation

by leukocyte recruitment. In addition, Gal-3 is induced in several cell types involved in damaged axon and cell debris removal and axon regeneration and remyelination, which hints at neuroprotective role of Gal-3 in EAE mice (Itabashi et al., 2018).

Virus-induced demyelination models support the hypothesis that some environmental factors, such as viral infections, are involved in MS and may be actually triggering the disease. MS-induced inflammation may decrease SVZ cell proliferation and thus hinder repair. Gal-3 expression increases in active human MS lesions (Stancic et al., 2011), in periventricular regions in human MS and after murine TMEV infection (James et al., 2016), whereas Gal-3 loss reduces the number of immune cells in the SVZ and restores proliferation in a viral model of MS (James et al., 2016).

Another increasingly used and more recently described demyelination model consists in the administration of cuprizone (CPZ) as part of the diet of young adult mice, which produces massive demyelination through pathogenic T cell-independent mechanisms, with different areas specifically affected in the CNS such as the CC (Suzuki and Kikkawa, 1969; Blakemore, 1973; Ludwin, 1978; Matsushima and Morell, 2001). CPZ-induced demyelination is known to involve the recruitment of resident microglia, while peripheral macrophage infiltration seems to be still controversial (McMahon et al., 2002; Mildner et al., 2007; Lampron et al., 2015). The CPZ model then offers the advantage of investigating CNS processes leading to remyelination independently of peripheral immune system contribution, as the model keeps the blood brain barrier intact (Bakker and Ludwin, 1987; Kondo et al., 1987).

Previous studies have described four different lesion subtypes in MS: pattern-1 and -2 lesions are thought to be autoimmune response-mediated, while pattern-3 and -4 lesions are regarded as primary oligodendrogliapathy (Lucchinetti et al., 2000). The first two types are experimentally simulated by the EAE model, while the second two are mimicked by toxic models such as cuprizone (CPZ) or lysolecithin (LPC) administration. Although the established animal models have their advantages and disadvantages, no model fully replicates the stages of MS and they are actually complementary.

Gal-3-in the CPZ Model

Gal-3-induced microglial response modulation during demyelination

Phagocytosis of myelin debris by microglia in CPZ demyelination is concomitant with an increase in phagocytic receptor TREM-2b expression (Voß et al., 2011), which seems to be key for remyelination to occur, as oligodendroglial differentiation can be hampered by myelin debris (Kotter et al., 2006). Strikingly, myelin phagocytosis relies on CR3/MAC-1 and SRAI/II, in turn regulated by Gal-3-dependent activation of PI3K; therefore, myelin phagocytosis by *LGALS3*$^{-/-}$ microglia is usually deficient (Rotshenker et al., 2008).

Our group has studied Gal-3 involvement in the demyelination/remyelination process using the CPZ model (Hoyos et al., 2014, 2016), in which 8-week-old *LGAL3*$^{-/-}$ and WT mice were fed a diet containing 0.2% CPZ w/w for 6 weeks to evaluate demyelination, followed by two more weeks on a CPZ-free diet to assess remyelination. Our results have shown that CPZ-induced demyelination follows a similar course up to the 5th week of treatment in 8-week-old *LGALS3*$^{-/-}$ and WT mice, as demonstrated by MBP immunostaining and electronic microscopy assessment. The OPC generated in response to CPZ demyelination in *LGALS3*$^{-/-}$ mice display reduced branching, which reflects diminished differentiation. These findings are in agreement with our results showing Gal-3 ability to induce OLG differentiation and especially those proving that conditioned media from Gal-3-expressing microglia promote OLG differentiation, as different from conditioned media from *LGALS3*$^{-/-}$ microglia (Pasquini et al., 2011). WT mice exhibit spontaneous remyelination in the 5th week of CPZ treatment, even if the CPZ diet is kept in place until the 6th week. In contrast, *LGALS3*$^{-/-}$ mice lack this ability and suffer steady demyelination up to the 6th week with noticeable astroglial activation. Colocalization studies have shown that Gal-3 expression is upregulated in microglia but not in astrocytes during CPZ-induced demyelination. Interestingly, only WT mice display activated microglia with ED1 (CD68) expression and TREM-2b upregulation during CPZ-induced demyelination, unlike CPZ-treated *LGALS3*$^{-/-}$ mice, which display more numerous microglia with activated caspase-3. These findings support Gal-3 as a modulator of the microglial response to favor the onset of remyelination and OLG differentiation (Hoyos et al., 2014).

As mentioned above, TREM-2b plays a key role in myelin debris phagocytosis. TREM-2b loss-of-function causes a hereditary disease called polycystic lipomembranous osteodysplasia with sclerosing leukoencephalopathy (PLOSL), or Nasu–Hakola disease (Hakola, 1972; Nasu et al., 1973; Paloneva et al., 2001), which presents progressive presenile dementia and sclerosing leukoencephalopathy driven by lower microglial phagocytic activity (Paloneva et al., 2002). Microglial TREM-2b expression is upregulated in inflammatory and chronic phases of EAE and produces disease exacerbation when blocked during the effector phase (Piccio et al., 2007). Intravenous inoculation of TREM-2-transduced myeloid cells induces EAE amelioration accompanied by increased myelin phagocytosis (Takahashi et al., 2007). In parallel, CPZ-induced demyelination has also shown a robust increase in microglial phagocytic activity associated with the upregulation of TREM-2b and CD200R, and including TNF-α production (Voß et al., 2011). Interestingly, our results show *LGALS3*$^{-/-}$ mice inability to upregulate TREM-2b or increase TNF-α production but their capacity to significantly reduce CD200R as a response to CPZ toxicity, which suggests that Gal-3 absence alters the microglial response against demyelination.

Our results showing that Gal-3-deficient microglial cells fail to induce ED1 expression are in accordance with those by Lalancette-Hébert et al. (2012), obtained in a unilateral transient focal cerebral ischemia model. However, and in contrast with such results, *LGALS3*$^{-/-}$ mice submitted to CPZ-induced demyelination exhibit higher microglial proliferation and apoptosis, as evidenced by their increased activation of

caspase-3, which may respond to the well-established Gal-3 anti-apoptotic role (Yang et al., 1996).

Evidence has demonstrated that chemokine ligand 2 (CCL2 or MCP1) could be involved in MS pathology, as its neutralization with anti-CCL2 significantly reduces EAE relapsing severity (Karpus and Kennedy, 1997). Our results show that CCL2 mRNA levels remain significantly higher until the 5th week in the CC of CPZ-treated *LGALS3*$^{-/-}$. In contrast, WT mice display transiently higher CCL2 mRNA levels in the 1st week of CPZ treatment with a recovery to control values in the 2nd week, which indicates that CCL2 mediates early microglial activation. M2 polarization of macrophages is accompanied by a reduction in inflammatory cytokine IL-1β, TNF-α, and CCL2 (Liu et al., 2013). Taken together, these results could indicate that the absence of Gal-3 prevents microglial cells from shifting to an M2 phenotype. Indeed, the fact that M2-cell-conditioned media enhance OLG differentiation *in vitro* and that M2 cell depletion impairs OLG differentiation *in vivo* may indicate that M2 cell polarization is a key factor for efficient remyelination (Miron et al., 2013), and microglial expression of Gal-3 may hence favor the onset of remyelination, either by inducing an M2 phenotype or exerting a direct effect on OLG differentiation.

Gal-3 in MMP regulation during remyelination

Together with endogenous tissue inhibitors, the MMP family of zinc-dependent endopeptidases is a key player in tissue remodeling. MMPs can also induce myelin proteins degradation *in vitro* (Chandler et al., 1995, 1996; Shiryaev et al., 2009; Hansmann et al., 2012), and have been involved in postnatal myelination, myelin maintenance, and remyelination (Ulrich et al., 2006; Skuljec et al., 2011; Hansmann et al., 2012). Also, MMP-3 can mediate mature OLG apoptosis and microglial activation with production of microglial inflammatory cytokines and thus exacerbation of neural cell degeneration (Kim and Joh, 2006). Our immunohistological studies have shown an increase in MMP-3 expression and a decrease in CD45+, TNFα+, and TREM-2b+ cells during remyelination only in WT mice, with no changes in *LGALS3*$^{-/-}$ mice during demyelination or remyelination. Ultrastructural studies carried out by electron microscopy after remyelination revealed collapsed axons with a defective myelin wrap in CC of *LGALS3*$^{-/-}$ mice but no relevant myelin wrap disruption in sections obtained from WT mice. Worth highlighting, a blockade in OPC differentiation has been proposed as a possible cause for remyelination failure in demyelinating diseases (Franklin and Kotter, 2008; Ulrich et al., 2008). Therefore, *LGALS3*$^{-/-}$ mice incomplete remyelination may partly respond to a failure in OPC differentiation. These results suggest that Gal-3 impacts remyelination through mechanisms including the tuning of microglial cells, the modulation of MMP activity and the induction of OLG differentiation.

Gal-3 role in behavioral alterations

CPZ-fed mice exhibit weight loss and motor and behavioral deficits (Franco-Pons et al., 2007; Xu et al., 2009). In the case of long-term CPZ exposure, rodents exhibit behavioral alterations which may be thought to recapitulate psychiatric disorders (Gregg et al., 2009; Xu et al., 2009). Neuroleptic treatment has succeeded in ameliorating some of these symptoms (Zhang et al., 2008; Xu et al., 2010, 2011), which suggests that long-term CPZ exposure may replicate features associated with MS and other white matter disorders. In this line, work by our group has shown diminished anxiety behavior in *LGALS3*$^{-/-}$ mice, similar to that observed in early CPZ-induced demyelination (Pasquini et al., 2011). Interestingly, hypertensive rats used as a spontaneous model of attention deficit hyperactivity disorder exhibit lower expression of Gal-3 in the brain prefrontal cortex (Wu et al., 2010). Accordingly, the lack of Gal-3 and alterations in myelin structure in *LGALS3*$^{-/-}$ mice induces behavioral alterations such as lower anxiety levels and spatial working memory impairment. Also, CPZ impact on behavior is observed earlier in *LGALS3*$^{-/-}$ mice, probably due to early mature OLG depletion (Hesse et al., 2010; Buschmann et al., 2012).

In our remyelination studies, a decrease in anxiety persisted both in WT and *LGALS3*$^{-/-}$ mice after 2-week recovery, as evidenced by higher rates of entries and more time spent in open arms in the plus maze test. An increase was also observed in locomotor activity counts and the number of total arm entries. In contrast, spatial working memory showed a recovery regarding their untreated counterparts. These data are in agreement with previous studies (Franco-Pons et al., 2007; Xu et al., 2009; Stancic et al., 2012) and suggest that some behavioral aspects remain altered even when histological analyses evidence fiber remyelination and seem to be irreversible even 2 weeks after CPZ withdrawal.

CONCLUSION

Taken together, these reports show that Gal-3 is essential for microglial polarization following CNS injury, while the differences observed in Gal-3 effects on different injuries probably respond to time- and context-dependent factors. Rahimian et al. (2018) have recently discussed the possible molecular mechanisms of neuroprotection mediated by Gal-3. Firstly, oligomerized Gal-3 molecules may crosslink to IGFR upon binding to their glycans on the surface and delay their removal by endocytosis, which results in prolonged microglial mitogenic signaling (Partridge et al., 2004; Lalancette-Hébert et al., 2012). This proposed mechanism could also act as a mediator of the beneficial effects of Gal-3 on OLG differentiation and (re)myelination, as IGF-1 produced by microglia inhibits OLG apoptosis during CPZ-induced demyelination and thereby promotes remyelination (Mason et al., 2000) and acts directly on OLG and myelination, as shown using OLG lineage-specific IGF-1R$^{-/-}$ mice (Zeger et al., 2007). Additionally, Gal-3 might mediate alternative microglial polarization induced by IL-4, as its expression and release are stimulated by alternative activation of macrophages with IL-4, which then binds and crosslinks CD98 on macrophages (Mackinnon, 2012). This could also explain the effect of Gal-3 observed on cell fate decisions toward the oligodendroglial lineage, as IL-4-activated microglia favor

oligodendrogenesis, whereas IFN-gamma-activated microglia favor neurogenesis. The effect induced by IL-4-activated microglia is also mediated, at least in part, by IGF-I (Butovsky et al., 2006). In addition, Gal-3 promotes the proliferation of cultured neural progenitors and its inhibition decreases the proliferative response of the SVZ after brain ischemia (Yan et al., 2009).

In particular, our results have shown that Gal-3 expression in microglial cells during CPZ-induced demyelination and upon the onset of remyelination favors an M2 microglial phenotype and MMP activity modulation, leading to OLG differentiation. Furthermore, Gal-3 enhances actin assembly and reduces Erk 1/2 activation, thus driving early OLG branching. Gal-3 later induces Akt activation and higher MBP expression, which in turn promote gelsolin release and actin cytoskeleton disassembly, hence regulating OLG maturation. On the whole, our studies indicate that Gal-3 could be considered a novel extracellular signal which drives OLG differentiation and (re)myelination through glial cell communication and therefore a target in the design of future therapies for a variety of demyelinating diseases.

AUTHOR CONTRIBUTIONS

LT designed the figures. LT and LP wrote and designed the manuscript. LP supported manuscript submission.

FUNDING

This work was supported by grants from Agencia Nacional de Promoción Científica y Tecnológica (Argentina, PICT 2014-3116) and Universidad de Buenos Aires (20920160100683BA) to LP.

ACKNOWLEDGMENTS

We wish to thank Mauricio Antonio Retamal and Fernando C. Ortiz for kindly inviting LP to submit our review to Frontiers in Cellular Neuroscience in the Research Topic entitled: Physiology of Myelin Forming Cells, from Myelination to Neural Modulators.

REFERENCES

Ahmad, N., Gabius, H. J., André, S., Kaltner, H., Sabesan, S., Roy, R., et al. (2004). Galectin-3 precipitates as a pentamer with synthetic multivalent carbohydrates and forms heterogeneous cross-linked complexes. *J. Biol. Chem.* 279, 10841–10847. doi: 10.1074/jbc.M312834200

Alge-Priglinger, C. S., André, S., Schoeffl, H., Kampik, A., Strauss, R. W., Kernt, M., et al. (2011). Negative regulation of RPE cell attachment by carbohydrate-dependent cell surface binding of galectin-3 and inhibition of the ERK-MAPK pathway. *Biochimie* 93, 477–488. doi: 10.1016/j.biochi.2010.10.021

Anderson, A. C., Anderson, D. E., Bregoli, L., Hastings, W. D., Kassam, N., Lei, C., et al. (2007). Promotion of tissue inflammation by the immune receptor Tim-3 expressed on innate immune cells. *Science* 318, 1141–1143. doi: 10.1126/science.1148536

Bakker, D. A., and Ludwin, S. K. (1987). Blood-brain barrier permeability during Cuprizone-induced demyelination. Implications for the pathogenesis of immune-mediated demyelinating diseases. *J. Neurol. Sci.* 78, 125–137. doi: 10.1016/0022-510X(87)90055-4

Balan, V., Nangia-Makker, P., Jung, Y. S., Wang, Y., and Raz, A. (2010). Galectin-3: a novel substrate for c-Abl kinase. *Biochim. Biophys. Acta* 1803, 1198–1205. doi: 10.1016/j.bbamcr.2010.06.007

Bänfer, S., Schneider, D., Dewes, J., Strauss, M. T., Freibert, S. A., Heimerl, T., et al. (2018). Molecular mechanism to recruit galectin-3 into multivesicular bodies for polarized exosomal secretion. *Proc. Natl. Acad. Sci. U.S.A.* 115, E4396–E4405. doi: 10.1073/pnas.1718921115

Bansal, R., Magge, S., and Winkler, S. (2003). Specific inhibitor of FGF receptor signaling: FGF-2-mediated effects on proliferation, differentiation, and MAPK activation are inhibited by PD173074 in oligodendrocyte-lineage cells. *J. Neurosci. Res.* 74, 486–493. doi: 10.1002/jnr.10773

Baron, W., Metz, B., Bansal, R., Hoekstra, D., and de Vries, H. (2000). PDGF and FGF-2 signaling in oligodendrocyte progenitor cells: regulation of proliferation and differentiation by multiple intracellular signaling pathways. *Mol. Cell. Neurosci.* 15, 314–329. doi: 10.1006/mcne.1999.0827

Barondes, S. H., Cooper, D. N., Gitt, M. A., and Leffler, H. (1994). Galectins structure and function of a large family of animal lectins. *J. Biol. Chem.* 269, 20807–20810.

Bercury, K. K., Dai, J., Sachs, H. H., Ahrendsen, J. T., Wood, T. L., and Macklin, W. B. (2014). Conditional ablation of raptor or rictor has differential impact on oligodendrocyte differentiation and CNS myelination. *J. Neurosci.* 34, 4466–4480. doi: 10.1523/JNEUROSCI.4314-13.2014

Bercury, K. K., and Macklin, W. B. (2015). Dynamics and mechanisms of CNS myelination. *Dev. Cell* 32, 447–458. doi: 10.1016/j.devcel.2015.01.016

Bhat, N. R., and Zhang, P. (1996). Activation of mitogen-activated protein kinases in oligodendrocytes. *J. Neurochem.* 66, 1986–1994. doi: 10.1046/j.1471-4159.1996.66051986.x

Bjartmar, C., Kinkel, R. P., Kidd, G., Rudick, R. A., and Trapp, B. D. (2001). Axonal loss n normal-appearing white matter in a patient with acute MS. *Neurology* 57, 1248–1252. doi: 10.1212/WNL.57.7.1248

Blakemore, W. F. (1973). Demyelination of the superior cerebellar peduncle in the mouse induced by cuprizone. *J. Neurol. Sci.* 20, 63–72. doi: 10.1016/0022-510X(73)90118-4

Boza-Serrano, A., Reyes, J. F., Rey, N. L., Leffler, H., Bousset, L., Nilsson, U., et al. (2014). The role of Galectin-3 in α-synuclein-induced microglial activation. *Acta Neuropathol. Commun.* 2:156. doi: 10.1186/s40478-014-0156-0

Brittoli, A., Fallarini, S., Zhang, H., Pieters, R. J., and Lombardi, G. (2018). "In vitro" studies on galectin-3 in human natural killer cells. *Immunol. Lett.* 194, 4–12. doi: 10.1016/j.imlet.2017.12.004

Buschmann, J. P., Berger, K., Awad, H., Clarner, T., Beyer, C., and Kipp, M. (2012). Inflammatory response and chemokine expression in the white matter corpus callosum and gray matter cortex region during cuprizone-induced demyelination. *J. Mol. Neurosci.* 48, 66–76. doi: 10.1007/s12031-012-9773-x

Butovsky, O., Ziv, Y., Schwartz, A., Landa, G., Talpalar, A. E., Pluchino, S., et al. (2006). Microglia activated by IL-4 or IFN-gamma differentially induce neurogenesis and oligodendrogenesis from adult stem/progenitor cells. *Mol. Cell. Neurosci.* 31, 149–160. doi: 10.1016/j.mcn.2005.10.006

Chandler, S., Coates, R., Gearing, A., Lury, J., Wells, G., and Bone, E. (1995). Matrix metalloproteinases degrade myelin basic protein. *Neurosci. Lett.* 201, 223–226. doi: 10.1016/0304-3940(95)12173-0

Chandler, S., Cossins, J., Lury, J., and Wells, G. (1996). Macrophage metalloelastase degrades matrix and myelin proteins and processes a tumour necrosis factor-alpha fusion protein. *Biochem. Biophys. Res. Commun.* 228, 421–429. doi: 10.1006/bbrc.1996.1677

Chen, H. Y., Sharma, B. B., Yu, L., Zuberi, R., Weng, I. C., Kawakami, Y., et al. (2006). Role of galectin-3 in mast cell functions: galectin-3-deficient mast cells exhibit impaired mediator release and defective JNK expression. *J. Immunol.* 177, 4991–4997. doi: 10.4049/jimmunol.177.8.4991

Chen, J., and Chopp, M. (2018). Exosome therapy for stroke. *Stroke* 49, 1083–1090. doi: 10.1161/STROKEAHA.117.018292

Cheng, X., Boza-Serrano, A., Turesson, M. F., Deierborg, T., Ekblad, E., and Voss, U. (2016). Galectin-3 causes enteric neuronal loss in mice after left

sided permanent middle cerebral artery occlusion, a model of stroke. *Sci. Rep.* 6:32893. doi: 10.1038/srep32893

Cho, K. O., Lee, K. E., Youn, D. Y., Jeong, K. H., Kim, J. Y., Yoon, H. H., et al. (2012). Decreased vulnerability of hippocampal neurons after neonatal hypoxia-ischemia in bis-deficient mice. *Glia* 60, 1915–1929. doi: 10.1002/glia.22407

Choy, Y. J., Hong, S. Y., Pack, S. J., Woo, R. S., Baik, T. K., and Song, D. Y. (2015). Changes of gene expression of Gal3, Hsp27, Lcn2, and Timp1 in rat substantia nigra following medial forebrain bundle transection using a candidate gene microarray. *J. Chem. Neuroanat.* 6, 10–18. doi: 10.1016/j.jchemneu.2015.03.003

Comte, I., Kim, Y., Young, C. C., van der Harg, J. M., Hockberger, P., Bolam, P. J., et al. (2011). Galectin-3 maintains cell motility from the subventricular zone to the olfactory bulb. *J. Cell Sci.* 124(Pt 14), 2438–2447. doi: 10.1242/jcs.079954

Cui, Q. L., and Almazan, G. (2007). IGF-I-induced oligodendrocyte progenitor proliferation requires PI3K/Akt, MEK/ERK, and Src-like tyrosine kinases. *J. Neurochem.* 100, 1480–1493. doi: 10.1111/j.1471-4159.2006.04329.x

Dabelic, S., Novak, R., Goreta, S. S., and Dumic, J. (2012). Galectin-3 expression in response to LPS, immunomodulatory drugs and exogenously added galectin-3 in monocyte-like THP-1 cells. *In Vitro Cell. Dev. Biol. Anim.* 48, 518–527. doi: 10.1007/s11626-012-9540-x

Dange, M. C., Agarwal, A. K., and Kalraiya, R. D. (2015). Extracellular galectin-3 induces MMP9 expression by activating p38 MAPK pathway via lysosome-associated membrane protein-1 (LAMP1). *Mol. Cell. Biochem.* 404, 79–86. doi: 10.1007/s11010-015-2367-5

Danguy, A., Camby, I., and Kiss, R. (2002). Galectins and cancer. *Biochim. Biophys. Acta* 1572, 285–293. doi: 10.1016/S0304-4165(02)00315-X

de Oliveira, F. L., Gatto, M., Bassi, N., Luisetto, R., Ghirardello, A., Punzi, L., et al. (2015). Galectin-3 in autoimmunity and autoimmune diseases. *Exp. Biol. Med.* 240, 1019–1028. doi: 10.1177/1535370215593826

Diao, B., Liu, Y., Xu, G. Z., Zhang, Y., Xie, J., and Gong, J. (2018). The role of galectin-3 in the tumorigenesis and progression of pituitary tumors. *Oncol. Lett.* 15, 4919–4925. doi: 10.3892/ol.2018.7931

Dietrich, J. B. (2002). The adhesion molecule ICAM-1 and its regulation in relation with the blood-brain barrier. *J. Neuroimmunol.* 128, 58–68. doi: 10.1016/S0165-5728(02)00114-5

Doverhag, C., Hedtjärn, M., Poirier, F., Mallard, C., Hagberg, H., Karlsson, A., et al. (2010). Galectin-3 contributes to neonatal hypoxic-ischemic brain injury. *Neurobiol. Dis.* 38, 36–46. doi: 10.1016/j.nbd.2009.12.024

Dumic, J., Dabelic, S., and Flögel, M. (2006). Galectin-3: an open-ended story. *Biochim. Biophys. Acta* 1760, 616–635. doi: 10.1016/j.bbagen.2005.12.020

Ellison, J. A., and de Vellis, J. (1995). Amoeboid microglia expressing G_{D3} ganglioside are concentrated in regions of oligodendrogenesis during development of the rat corpus callosum. *Glia* 14, 123–132. doi: 10.1002/glia.440140207

Fancy, S. P., Baranzini, S. E., Zhao, C., Yuk, D. I., Irvine, K. A., Kaing, S., et al. (2009). Dysregulation of the Wnt pathway inhibits timely myelination and remyelination in the mammalian CNS. *Genes Dev.* 23, 1571–1585. doi: 10.1101/gad.1806309

Feigenson, K., Reid, M., See, J., Crenshaw, E. B. III, and Grinspan, J. B. (2009). Wnt signaling is sufficient to perturb oligodendrocyte maturation. *Mol. Cell. Neurosci.* 42, 255–265. doi: 10.1016/j.mcn.2009.07.010

Figlia, G., Gerber, D., and Suter, U. (2018). Myelination and mTOR. *Glia* 6, 693–707. doi: 10.1002/glia.23273

Flores, A. I., Narayanan, S. P., Morse, E. N., Shick, H. E., Yin, X., Kidd, G., et al. (2008). Constitutively active Akti nduces enhanced myelination in the CNS. *J. Neurosci.* 28, 7174–7183. doi: 10.1523/JNEUROSCI.0150-08.2008

Fowlis, D., Colnot, C., Ripoche, M. A., and Poirier, F. (1995). Galectin-3 is expressed in the notochord, developing bones, and skin of the post implantation mouse embryo. *Dev. Dyn.* 203, 241–251. doi: 10.1002/aja.1002030211

Franco-Pons, N., Torrente, M., Colomina, M. T., and Vilella, E. (2007). Behavioral deficits in the cuprizone-induced murine model of demyelination/remyelination. *Toxicol. Lett.* 169, 205–213. doi: 10.1016/j.toxlet.2007.01.010

Franklin, R. J., and Kotter, M. R. (2008). The biology of CNS remyelination: the key to therapeutic advances. *J. Neurol.* 255(Suppl. 1), 19–25. doi: 10.1007/s00415-008-1004-6

Franklin, R. J. M. (2002). Why does remyelination fail in multiple sclerosis? *Nat. Rev. Neurosci.* 3, 705–714. doi: 10.1038/nrn917

Franklin, R. J. M., and Ffrench-Constant, C. (2017). Regenerating CNS myelin - from mechanisms to experimental medicines. *Nat. Rev. Neurosci.* 18, 753–769. doi: 10.1038/nrn.2017.136

Franklin, R. J. M., ffrench-Constant, C., Edgar, J. M., and Smith, K. J. (2012). Neuroprotection and repair in multiple sclerosis. *Nat. Rev. Neurol.* 8, 624–634. doi: 10.1038/nrneurol.2012.200

Frederick, T. J., Min, J., Altieri, S. C., Mitchell, N. E., and Wood, T. L. (2007). Synergistic induction of cyclin D1 in oligodendrocyte progenitor cells by IGF-I and FGF-2 requires differential stimulation of multiple signaling pathways. *Glia* 55, 1011–1022. doi: 10.1002/glia.20520

Funasaka, T., Raz, A., and Nangia-Makker, P. (2014). Nuclear transport of galectin-3 and its therapeutic implications. *Semin. Cancer Biol.* 27, 30–38. doi: 10.1016/j.semcancer.2014.03.004

Fyffe-Maricich, S. L., Karlo, J. C., Landreth, G. E., and Miller, R. H. (2011). The ERK2 mitogen-activated protein kinase regulates the timing of oligodendrocyte differentiation. *J. Neurosci.* 31, 843–850. doi: 10.1523/JNEUROSCI.3239-10.2011

Gaesser, J. M., and Fyffe-Maricich, S. L. (2016). Intracellular signaling pathway regulation of myelination and remyelination in the CNS. *Exp. Neurol.* 283(Pt B), 501–511. doi: 10.1016/j.expneurol.2016.03.008

Gao, X., Liu, J., Liu, X., Li, L., and Zheng, J. (2017). Cleavage and phosphorylation: important post-translational modifications of galectin-3. *Cancer Metastasis Rev.* 36, 367–374. doi: 10.1007/s10555-017-9666-0

Ge, X. N., Ha, S. G., Liu, F. T., Rao, S. P., and Sriramarao, P. (2013). Eosinophil-expressed galectin-3 regulates cell trafficking and migration. *Front. Pharmacol.* 4:37. doi: 10.3389/fphar.2013.00037

Gonsalvez, D., Ferner, A. H., Peckham, H., Murray, S. S., and Xiao, J. (2016). The roles of extracellular related-kinases 1 and 2 signaling in CNS myelination. *Neuropharmacology* 110(Pt B), 586–593. doi: 10.1016/j.neuropharm.2015.04.024

Gregg, J. R., Herring, N. R., Naydenov, A. V., Hanlin, R. P., and Konradi, C. (2009). Downregulation of oligodendrocyte transcripts is associated with impaired prefrontal cortex function in rats. *Schizophr. Res.* 113, 277–287. doi: 10.1016/j.schres.2009.05.023

Guardiola-Diaz, H. M., Ishii, A., and Bansal, R. (2012). Erk1/2 MAPK and mTOR signaling sequentially regulates progression through distinct stages of oligodendrocyte differentiation. *Glia* 60, 476–486. doi: 10.1002/glia.22281

Haines, J. D., Vidaurre, O. G., Zhang, F., Riffo-Campos, Á. L., Castillo, J., Casanova, B., et al. (2015). Multiple sclerosis patient-derived CSF induces transcriptional changes in proliferating oligodendrocyte progenitors. *Mult. Scler.* 21, 1655–1669. doi: 10.1177/1352458515573094

Hakola, H. P. (1972). Neuropsychiatric and genetic aspects of a new hereditary disease characterized by progressive dementia and lipomembranous polycystic osteodysplasia. *Acta Psychiatr. Scand. Suppl.* 232, 1–173.

Hansmann, F., Herder, V., Kalkuhl, A., Haist, V., Zhang, N., Schaudien, D., et al. (2012). Matrix metalloproteinase-12 deficiency ameliorates clinical course and demyelination in Theiler's murine encephalomyelitis. *Acta Neuropathol.* 124, 127–142. doi: 10.1007/s00401-012-0942-3

Haudek, K. C., Spronk, K. J., Voss, P. G., Patterson, R. J., Wang, J. L., and Arnoys, E. J. (2010). Dynamics of galectin-3 in the nucleus and cytoplasm. *Biochim. Biophys. Acta* 1800, 181–189. doi: 10.1016/j.bbagen.2009.07.005

Hesse, A., Wagner, M., Held, J., Brück, W., Salinas-Riester, G., Hao, Z., et al. (2010). In toxic demyelination oligodendroglial cell death occurs early and is FAS independent. *Neurobiol. Dis.* 37, 362–369. doi: 10.1016/j.nbd.2009.10.016

Hirabayashi, J., Hashidate, T., Arata, Y., Nishi, N., Nakamura, T., Hirashima, M., et al. (2002). Oligosaccharide specificity of galectins: a search by frontal affinity chromatography. *Biochim. Biophys. Acta* 1572, 232–254. doi: 10.1016/S0304-4165(02)00311-2

Hisamatsu, K., Niwa, M., Kobayashi, K., Miyazaki, T., Hirata, A., Hatano, Y., et al. (2016). Galectin-3 expression in hippocampal CA2 following transient forebrain ischemia and its inhibition by hypothermia or antiapoptotic agents. *Neuroreport* 27, 311–317. doi: 10.1097/WNR.0000000000000538

Holíková, Z., Smetana, K. Jr., Bartùnková, J., Dvoránková, B., Kaltner, H., and Gabius, H. J. (2000). Human epidermal Langerhans cells are selectively recognized by galectin-3 but not by galectin-1. *Folia Biol.* 46, 195–198.

Hönig, E., Schneider, K., and Jacob, R. (2015). Recycling of galectin-3 in epithelial cells. *Eur. J. Cell Biol.* 94, 309–315. doi: 10.1016/j.ejcb.2015.05.004

Hoyos, H. C., Marder, M., Ulrich, R., Gudi, V., Stangel, M., Rabinovich, G. A., et al. (2016). The role of galectin-3: from oligodendroglial differentiation and myelination to demyelination and remyelination processes in a cuprizone-induced demyelination model. *Adv. Exp. Med. Biol.* 949, 311–332. doi: 10.1007/978-3-319-40764-7_15

Hoyos, H. C., Rinaldi, M., Mendez-Huergo, S. P., Marder, M., Rabinovich, G. A., Pasquini, J. M., et al. (2014). Galectin-3 controls the response of microglial cells to limit cuprizone-induced demyelination. *Neurobiol. Dis.* 62, 441–455. doi: 10.1016/j.nbd.2013.10.023

Hsu, D. K., Chen, H. Y., and Liu, F. T. (2009). Galectin-3 regulates T-cell functions. *Immunol. Rev.* 230, 114–127. doi: 10.1111/j.1600-065X.2009.00798.x

Hu, K., Gu, Y., Lou, L., Liu, L., Hu, Y., Wang, B., et al. (2015). Galectin-3 mediates bone marrow microenvironment-induced drug resistance in acute leukemia cells via Wnt/β-catenin signaling pathway. *J. Hematol. Oncol.* 8:1. doi: 10.1186/s13045-014-0099-8

Iacobini, C., Fantauzzi, C. B., Pugliese, G., and Menini, S. (2017). Role of galectin-3 in bone cell differentiation, bone pathophysiology and vascular osteogenesis. *Int. J. Mol. Sci.* 18:E2481. doi: 10.3390/ijms18112481

Inohara, H., Akahani, S., and Raz, A. (1998). Galectin-3 stimulates cell proliferation. *Exp. Cell Res.* 245, 294–302. doi: 10.1006/excr.1998.4253

Ishii, A., Fyffe-Maricich, S. L., Furusho, M., Miller, R. H., and Bansal, R. (2012). ERK1/ERK2 MAPK signaling is required to increase myelin thickness independent of oligodendrocyte differentiation and initiation of myelination. *J. Neurosci.* 32, 8855–8864. doi: 10.1523/JNEUROSCI.0137-12.2012

Ishii, N., Harada, N., Joseph, E. W., Ohara, K., Miura, T., Sakamoto, H., et al. (2013). Enhanced inhibition of ERK signaling by a novel allosteric MEK inhibitor, CH5126766, that suppresses feedback reactivation of RAF activity. *Cancer Res.* 73, 4050–4060. doi: 10.1158/0008-5472.CAN-12-3937

Itabashi, T., Arima, Y., Kamimura, D., Higuchi, K., Bando, Y., Takahashi-Iwanaga, H., et al. (2018). Cell- and stage-specific localization of galectin-3, a β-galactoside-binding lectin, in a mouse model of experimental autoimmune encephalomyelitis. *Neurochem. Int.* 118, 176–184. doi: 10.1016/j.neuint.2018.06.007

James, R. E., Hillis, J., Adorján, I., Gration, B., Mundim, M. V., Iqbal, A. J., et al. (2016). Loss of galectin-3 decreases the number of immune cells in the subventricular zone and restores proliferation in a viral model of multiple sclerosis. *Glia* 64, 105–121. doi: 10.1002/glia.22906

Jiang, H. R., Al Rasebi, Z., Mensah-Brown, E., Shahin, A., Xu, D., Goodyear, C. S., et al. (2009). Galectin-3 deficiency reduces the severity of experimental autoimmune encephalomyelitis. *J. Immunol.* 182, 1167–1173. doi: 10.4049/jimmunol.182.2.1167

Jin, J. K., Na, Y. J., Song, J. H., Joo, H. G., Kim, S., Kim, J. I., et al. (2007). Galectin-3 expression is correlated with abnormal prion protein accumulation in murine scrapie. *Neurosci. Lett.* 420, 138–143. doi: 10.1016/j.neulet.2007.04.069

Jin, L., Riss, D., Ruebel, K., Kajita, S., Scheithauer, B. W., Horvath, E., et al. (2005). Galectin-3 expression in functioning and silent ACTH-producing adenomas. *Endocr. Pathol.* 16, 107–114. doi: 10.1385/EP:16:2:107

Kalani, M. Y., Cheshier, S. H., Cord, B. J., Bababeygy, S. R., Vogel, H., Weissman, I. L., et al. (2008). Wnt-mediated self-renewal of neural stem/progenitor cells. *Proc. Natl. Acad. Sci. U.S.A.* 105, 16970–16975. doi: 10.1073/pnas.0808616105

Kariya, Y., Oyama, M., Hashimoto, Y., Gu, J., and Kariya, Y. (2018). β4-Integrin/PI3K signaling promotes tumor progression through the galectin-3-N-glycan complex. *Mol. Cancer Res.* 16, 1024–1034. doi: 10.1158/1541-7786.MCR-17-0365

Karpus, W. J., and Kennedy, K. J. (1997). MIP-1alpha and MCP-1 differentially regulate acute and relapsing autoimmune encephalomyelitis as well as Th1/Th2 lymphocyte differentiation. *J. Leukoc. Biol.* 62, 681–687. doi: 10.1002/jlb.62.5.681

Kim, S. J., Choi, I. J., Cheong, T. C., Lee, S. J., Lotan, R., Park, S. H., et al. (2010). Galectin-3 increases gastric cancer cell motility by up-regulating fascin-1 expression. *Gastroenterology* 138, 1035–1045.e1-2. doi: 10.1053/j.gastro.2009.09.061

Kim, Y. S., and Joh, T. H. (2006). Microglia, major player in the brain inflammation: their roles in the pathogenesis of Parkinson's disease. *Exp. Mol. Med.* 38, 333–347. doi: 10.1038/emm.2006.40

Kondo, A., Nakano, T., and Suzuki, K. (1987). Blood-brain barrier permeability to horseradish peroxidase in twitcher and cuprizone-intoxicated mice. *Brain Res.* 425, 186–190. doi: 10.1016/0006-8993(87)90499-9

Kotter, M. R., Li, W. W., Zhao, C., and Franklin, R. J. (2006). Myelin impairs CNS remyelination by inhibiting oligodendrocyte precursor cell differentiation. *J. Neurosci.* 26, 328–332. doi: 10.1523/JNEUROSCI.2615-05.2006

Krugluger, W., Frigeri, L. G., Lucas, T., Schmer, M., Förster, O., Liu, F. T., et al. (1997). Galectin-3 inhibits granulocyte-macrophage colony-stimulating factor (GM-CSF)-driven rat bone marrow cell proliferation and GM-CSF-induced gene transcription. *Immunobiology* 197, 97–109. doi: 10.1016/S0171-2985(97)80060-5

Krześlak, A., and Lipińska, A. (2004). Galectin-3 as a multifunctional protein. *Cell. Mol. Biol. Lett.* 9, 305–328.

Kumar, S., Kahn, M. A., Dinh, L., and de Vellis, J. (1998). NT-3-mediated TrkC receptor activation promotes proliferation and cell survival of rodent progenitor oligodendrocyte cells in vitro and in vivo. *J. Neurosci. Res.* 54, 754–765. doi: 10.1002/(SICI)1097-4547(19981215)54:6<754::AID-JNR3>3.0.CO;2-K

Lagana, A., Goetz, J. G., Cheung, P., Raz, A., Dennis, J. W., and Nabi, I. R. (2006). Galectin binding to Mgat5-modified N-glycans regulates fibronectin matrix remodeling in tumor cells. *Mol. Cell. Biol.* 26, 3181–3193. doi: 10.1128/MCB.26.8.3181-3193.2006

Lalancette-Hébert, M. (2007). Selective ablation of proliferating microglial cells exacerbates ischemic injury in the brain. *J. Neurosci.* 27, 2596–2605. doi: 10.1523/JNEUROSCI.5360-06.2007

Lalancette-Hébert, M., Swarup, V., Beaulieu, J. M., Bohacek, I., Abdelhamid, E., Weng, Y. C., et al. (2012). Galectin-3 is required for resident microglia activation and proliferation inresponse to ischemic injury. *J. Neurosci.* 32, 10383–10395. doi: 10.1523/JNEUROSCI.1498-12.2012

Lampron, A., Larochelle, A., Laflamme, N., Préfontaine, P., Plante, M. M., Sánchez, M. G., et al. (2015). Inefficient clearance of myelin debris by microglia impairs remyelinating processes. *J. Exp. Med.* 212, 481–495. doi: 10.1084/jem.20141656

Larsen, L., Chen, H. Y., Saegusa, J., and Liu, F. T. (2011). Galectin-3 and the skin. *J. Dermatol. Sci.* 64, 85–91. doi: 10.1016/j.jdermsci.2011.07.008

Lau, K. S., Partridge, E. A., Grigorian, A., Silvescu, C. I., Reinhold, V. N., Demetriou, M., et al. (2007). Complex N-glycan number and degree of branching cooperate to regulate cell proliferation and differentiation. *Cell* 129, 123–134. doi: 10.1016/j.cell.2007.01.049

Lerman, B. J. (2012). Deletion of galectin-3 exacerbates microglial activation and accelerates disease progression and demise in a SOD1(G93A) mouse model of amyotrophic lateral sclerosis. *Brain Behav.* 2, 563–575. doi: 10.1002/brb3.75

Li, X., Ma, Q., Wang, J., Liu, X., Yang, Y., Zhao, H., et al. (2010). c-Abl and Arg tyrosine kinases regulate lysosomal degradation of the oncoprotein Galectin-3. *Cell Death Differ.* 17, 1277–1287. doi: 10.1038/cdd.2010.8

Li, Y., Komai-Koma, M., Gilchrist, D. S., Hsu, D. K., Liu, F. T., Springall, T., et al. (2008). Galectin-3 is a negative regulator of lipopolysaccharide-mediated inflammation. *J. Immunol.* 181, 2781–2789. doi: 10.4049/jimmunol.181.4.2781

Liu, C., Li, Y., Yu, J., Feng, L., Hou, S., Liu, Y., et al. (2013). Targeting the shift from M1 to M2 macrophages in experimental autoimmune encephalomyelitis mice treated with fasudil. *PLoS One* 8:e54841. doi: 10.1371/journal.pone.0054841

Lucchinetti, C., Brück, W., Parisi, J., Scheithauer, B., Rodriguez, M., and Lassmann, H. (2000). Heterogeneity of multiple sclerosis lesions: implications for the pathogenesis of demyelination. *Ann. Neurol.* 47, 707–717. doi: 10.1002/1531-8249(200006)47:6<707::AID-ANA3>3.0.CO;2-Q

Ludwin, S. K. (1978). Central nervous system demyelination and remyelination in the mouse: an ultrastructural study of cuprizone toxicity. *Lab. Invest.* 39, 597–612.

Mackinnon, A. C. (2012). Regulation of transforming growth factor-b1-driven lung fibrosis by galectin-3. *Am. J. Respir. Crit. Care Med.* 185, 537–546. doi: 10.1164/rccm.201106-0965OC

Mahoney, S. A., Wilkinson, M., Smith, S., and Haynes, L. W. (2000). Stabilization of neurites in cerebellar granule cells by transglutaminase activity: identification of midkine and galectin-3 as substrates. *Neuroscience* 101, 141–155. doi: 10.1016/S0306-4522(00)00324-9

Mason, J. L., Jones, J. J., Taniike, M., Morell, P., Suzuki, K., and Matsushima, G. K. (2000). Mature oligodendrocyte apoptosis precedes IGF-1 production and oligodendrocyte progenitor accumulation and differentiation during

demyelination/remyelination. *J. Neurosci. Res.* 61, 251–262. doi: 10.1002/1097-4547(20000801)61:3<251::AID-JNR3>3.0.CO;2-W

Matsushima, G. K., and Morell, P. (2001). The neurotoxicant cuprizone as a model to study demyelination and remyelination in the central nervous system. *Brain Pathol.* 11, 107–116. doi: 10.1111/j.1750-3639.2001.tb00385.x

Mauris, J., Woodward, A. M., Cao, Z., Panjwani, N., and Argueso, P. (2014). Molecular basis for MMP9 induction and disruption of epithelial cell-cell contacts by galectin-3. *J. Cell Sci.* 127, 3141–3148. doi: 10.1242/jcs.148510

Mazurek, N., Conklin, J., Byrd, J. C., Raz, A., and Bresalier, R. S. (2000). Phosphorylation of the beta-galactoside-binding protein galectin-3 modulates binding to its ligands. *J. Biol. Chem.* 275, 36311–36315. doi: 10.1074/jbc.M003831200

McFarland, H. F., and Martin, R. (2007). Multiple sclerosis: a complicated picture of autoimmunity. *Nat. Immunol.* 8, 913–919. doi: 10.1038/ni1507

McLeod, K., Walker, J. T., and Hamilton, D. W. (2018). Galectin-3 regulation of wound healing and fibrotic processes: insights for chronic skin wound therapeutics. *J. Cell Commun. Signal.* 12, 281–287. doi: 10.1007/s12079-018-0453-7

McMahon, E. J., Suzuki, K., and Matsushima, G. K. (2002). Peripheral macrophage recruitment in cuprizone-induced CNS demyelination despite an intact blood-brain barrier. *J. Neuroimmunol.* 130, 32–45. doi: 10.1016/S0165-5728(02)00205-9

Mietto, B. S., Mostacada, K., and Martinez, A. M. (2015). Neurotrauma and inflammation: CNS and PNS responses. *Mediators Inflamm.* 2015:251204. doi: 10.1155/2015/251204

Mildner, A., Schmidt, H., Nitsche, M., Merkler, D., Hanisch, U.-K., Mack, M., et al. (2007). Microglia in the adult brain arise from Ly-6ChiCCR2+ monocytes only under defined host conditions. *Nat. Neurosci.* 10, 1544–1553. doi: 10.1038/nn2015

Miron, V. E., Boyd, A., Zhao, J. W., Yuen, T. J., Ruckh, J. M., Shadrach, J. L., et al. (2013). M2 microglia and macrophages drive oligodendrocyte differentiation during CNS remyelination. *Nat. Neurosci.* 16, 1211–1218. doi: 10.1038/nn.3469

Mok, S. W., Riemer, C., Madela, K., Hsu, D. K., Liu, F. T., Gültner, S., et al. (2007). Role of galectin-3 in prion infections of the CNS. *Biochem. Biophys. Res. Commun.* 359, 672–678. doi: 10.1016/j.bbrc.2007.05.163

Mok, S. W., Thelen, K. M., Riemer, C., Bamme, T., Gültner, S., Lütjohann, D., et al. (2006). Simvastatin prolongs survival times in prion infections of the central nervous system. *Biochem. Biophys. Res. Commun.* 348, 697–702. doi: 10.1016/j.bbrc.2006.07.123

Moon, H. W., Park, M., Hur, M., Kim, H., Choe, W. H., and Yun, Y. M. (2018). Usefulness of enhanced liver fibrosis, glycosylation isomer of Mac-2 binding protein, galectin-3, and soluble suppression of tumorigenicity 2 for assessing liver fibrosis in chronic liver diseases. *Ann. Lab. Med.* 38, 331–337. doi: 10.3343/alm.2018.38.4.331

More, S. K., Chiplunkar, S. V., and Kalraiya, R. D. (2016). Galectin-3-induced cell spreading and motility relies on distinct signaling mechanisms compared to fibronectin. *Mol. Cell. Biochem.* 416, 179–191. doi: 10.1007/s11010-016-2706-1

Mori, Y., Akita, K., Yashiro, M., Sawada, T., Hirakawa, K., Murata, T., et al. (2015). Binding of galectin-3, a β-galactoside-binding lectin, to MUC1 protein enhances phosphorylation of extracellular signal-regulated kinase 1/2 (ERK1/2) and Akt, promoting tumor cell malignancy. *J. Biol. Chem.* 290, 26125–26140. doi: 10.1074/jbc.M115.651489

Nabi, I. R., Shankar, J., and Dennis, J. W. (2015). The galectin lattice at a glance. *J. Cell Sci.* 128, 2213–2219. doi: 10.1242/jcs.151159

Narayanan, S. P., Flores, A. I., Wang, F., and Macklin, W. B. (2009). Akt signals through the mammalian target of rapamycin pathway to regulate CNS myelination. *J. Neurosci.* 29, 6860–6870. doi: 10.1523/JNEUROSCI.0232-09.2009

Nasu, T., Tsukahara, Y., and Terayama, K. (1973). A lipid metabolic disease-"membranous lipodystrophy"-an autopsy case demonstrating numerous peculiar membrane-structures composed of compound lipid in bone and bone marrow and various adipose tissues. *Acta Pathol. Jpn.* 23, 539–558. doi: 10.1111/j.1440-1827.1973.tb01223.x

Nave, K. A. (2010). Myelination and the trophic support of long axons. *Nat. Rev. Neurosci.* 11, 275–283. doi: 10.1038/nrn2797

Nave, K. A., and Werner, H. B. (2014). Myelination of the nervous system: mechanisms and functions. *Annu. Rev. Cell Dev. Biol.* 30, 503–533. doi: 10.1146/annurev-cellbio-100913-013101

Nawaz, S., Sánchez, P., Schmitt, S., Snaidero, N., Mitkovski, M., Velte, C., et al. (2015). Actin filament turnover drives leading edge growth during myelin sheath formation in the central nervous system. *Dev. Cell* 34, 139–151. doi: 10.1016/j.devcel.2015.05.013

Nikodemova, M., Small, A. L., Smith, S. M., Mitchell, G. S., and Watters, J. J. (2014). Spinal but not cortical microglia acquire an atypical phenotype with high VEGF, galectin-3 and osteopontin, and blunted inflammatory responses in ALS rats. *Neurobiol. Dis.* 69, 43–53. doi: 10.1016/j.nbd.2013.11.009

Nishihara, H., Shimizu, F., Kitagawa, T., Yamanaka, N., Akada, J., Kuramitsu, Y., et al. (2017). Identification of galectin-3 as a possible antibody target for secondary progressive multiple sclerosis. *Mult. Scler.* 23, 382–394. doi: 10.1177/1352458516655217

Novak, R., Dabelic, S., and Dumic, J. (2012). Galectin-1 and galectin-3 expression profiles in classically and alternatively activated human macrophages. *Biochim. Biophys. Acta* 1820, 1383–1390. doi: 10.1016/j.bbagen.2011.11.014

Ochieng, J., Fridman, R., Nangia-Makker, P., Kleiner, D. E., Liotta, L. A., Stetler-Stevenson, W. G., et al. (1994). Galectin-3 is a novel substrate for human matrix metalloproteinases-2 and -9. *Biochemistry* 33, 14109–14114. doi: 10.1021/bi00251a020

Ohtaki, H., Ylostalo, J. H., Foraker, J. E., Robinson, A. P., Reger, R. L., Shioda, S., et al. (2008). Stem/progenitor cells from bone marrow decrease neuronal death in global ischemia by modulation of inflammatory/immune responses. *Proc. Natl. Acad. Sci. U.S.A.* 105, 14638–14643. doi: 10.1073/pnas.0803670105

Ortega, F., Gascón, S., Masserdotti, G., Deshpande, A., Simon, C., Fischer, J., et al. (2013). Oligodendrogliogenic and neurogenic adult subependymal zone neural stem cells constitute distinct lineages and exhibit differential responsiveness to Wnt signalling. *Nat. Cell Biol.* 15, 602–613. doi: 10.1038/ncb2736

Osier, N., Motamedi, V., Edwards, K., Puccio, A., Diaz-Arrastia, R., Kenney, K., et al. (2018). Exosomes in acquired neurological disorders: new insights into pathophysiology and treatment. *Mol. Neurobiol.* doi: 10.1007/s12035-018-1054-4 [Epub ahead of print].

Paloneva, J., Autti, T., Raininko, R., Partanen, J., Salonen, O., Puranen, M., et al. (2001). CNS manifestations of Nasu-Hakola disease: a frontal dementia with bone cysts. *Neurology* 56, 1552–1558. doi: 10.1212/WNL.56.11.1552

Paloneva, J., Manninen, T., Christman, G., Hovanes, K., Mandelin, J., Adolfsson, R., et al. (2002). Mutations in two genes encoding different subunits of a receptor signaling complex result in an identical disease phenotype. *Am. J. Hum. Genet.* 71, 656–662. doi: 10.1086/342259

Pardo, E., Cárcamo, C., Uribe-San Martín, R., Ciampi, E., Segovia-Miranda, F., Curkovic-Peña, C., et al. (2017). Galectin-8 as an immunosuppressor in experimental autoimmune encephalomyelitis and a target of human early prognostic antibodies in multiple sclerosis. *PLoS One* 12:e0177472. doi: 10.1371/journal.pone.0177472

Partridge, E. A., Le Roy, C., Di Guglielmo, G. M., Pawling, J., Cheung, P., Granovsky, M., et al. (2004). Regulation of cytokine receptors by Golgi N-glycan processing and endocytosis. *Science* 306, 120–124. doi: 10.1126/science.1102109

Pasquini, L. A., Millet, V., Hoyos, H. C., Giannoni, J. P., Croci, D. O., Marder, M., et al. (2011). Galectin-3 drives oligodendrocyte differentiation to control myelin integrity and function. *Cell Death Differ.* 18, 1746–1756. doi: 10.1038/cdd.2011.40

Patani, R., Balaratnam, M., Vora, A., and Reynolds, R. (2007). Remyelination can be extensive in multiple sclerosis despite a long disease course. *Neuropathol. Appl. Neurobiol.* 33, 277–287. doi: 10.1111/j.1365-2990.2007.00805.x

Patrikios, P., Stadelmann, C., Kutzelnigg, A., Rauschka, H., Schmidbauer, M., Laursen, H., et al. (2006). Remyelination is extensive in a subset of multiple sclerosis patients. *Brain* 129, 3165–3172. doi: 10.1093/brain/awl217

Patterson, R. J., Wang, W., and Wang, J. L. (2002). Understanding the biochemical activities of galectin-1 and galectin-3 in the nucleus. *Glycoconj. J.* 19, 499–506. doi: 10.1023/B:GLYC.0000014079.87862.c7

Pesheva, P., Kuklinski, S., Schmitz, B., and Probstmeier, R. (1998). Galectin-3 promotes neural cell adhesion and neurite growth. *J. Neurosci. Res.* 1, 639–654. doi: 10.1002/(SICI)1097-4547(19981201)54:5<639::AID-JNR9>3.0.CO;2-2

Piccio, L., Buonsanti, C., Mariani, M., Cella, M., Gilfillan, S., Cross, A. H., et al. (2007). Blockade of TREM-2 exacerbates experimental autoimmune encephalomyelitis. *Eur. J. Immunol.* 37, 1290–1301. doi: 10.1002/eji.200636837

Piek, A., Du, W., de Boer, R. A., and Silljé, H. H. W. (2018). Novel heart failure biomarkers: why do we fail to exploit their potential? *Crit. Rev. Clin. Lab. Sci.* 55, 246–263. doi: 10.1080/10408363.2018.1460576

Poirier, F., and Robertson, E. J. (1993). Normal development of mice carrying a null mutation in the gene encoding the L14 S-type lectin. *Development* 119, 1229–1236.

Pricci, F. (2000). Role of galectin-3 as a receptor for advanced glycosylation end products. *Kidney Int.* 77, S31–S39. doi: 10.1046/j.1523-1755.2000.07706.x

Prineas, J. W., Barnard, R. O., Kwon, E. E., Sharer, L. R., and Cho, E. S. (1993). Multiple sclerosis: remyelination of nascent lesions. *Ann. Neurol.* 33, 137–151. doi: 10.1002/ana.410330203

Rabinovich, G. A., Toscano, M. A., Jackson, S. S., and Vasta, G. R. (2007). Functions of cell surface galectin-glycoprotein lattices. *Curr. Opin. Struct. Biol.* 17, 513–520. doi: 10.1016/j.sbi.2007.09.002

Rahimian, R., Béland, L. C., and Kriz, J. (2018). Galectin-3: mediator of microglia responses in injured brain. *Drug Discov. Today* 23, 375–381. doi: 10.1016/j.drudis.2017.11.004

Riemer, C., Neidhold, S., Burwinkel, M., Schwarz, A., Schultz, J., Krätzschmar, J., et al. (2004). Gene expression profiling of scrapie-infected brain tissue. *Biochem. Biophys. Res. Commun.* 323, 556–564. doi: 10.1016/j.bbrc.2004.08.124

Rinaldi, M., Thomas, L., Mathieu, P., Carabias, P., Troncoso, M. F., Pasquini, J. M., et al. (2016). Galectin-1 circumvents lysolecithin-induced demyelination through the modulation of microglial polarization/phagocytosis and oligodendroglial differentiation. *Neurobiol. Dis.* 96, 127–143. doi: 10.1016/j.nbd.2016.09.003

Rotshenker, S. (2009). The role of Galectin-3/MAC-2 in the activation of the innate-immune function of phagocytosis in microglia in injury and disease. *J. Mol. Neurosci.* 39, 99–103. doi: 10.1007/s12031-009-9186-7

Rotshenker, S., Reichert, F., Gitik, M., Haklai, R., Elad-Sfadia, G., and Kloog, Y. (2008). Galectin-3/MAC-2, Ras and PI3K activate complement receptor-3 and scavenger receptor-AI/II mediated myelin phagocytosis in microglia. *Glia* 56, 1607–1613. doi: 10.1002/glia.20713

Ruvolo, P. P. (2016). Galectin 3 as a guardian of the tumor microenvironment. *Biochim. Biophys. Acta* 1863, 427–437. doi: 10.1016/j.bbamcr.2015.08.008

Ruvolo, P. P., Ruvolo, V. R., Burks, J. K., Qiu, Y., Wang, R. Y., Shpall, E. J., et al. (2018). Role of MSC-derived galectin 3 in the AML microenvironment. *Biochim. Biophys. Acta* 1865, 959–969. doi: 10.1016/j.bbamcr.2018.04.005

Saravanan, C., Liu, F. T., Gipson, I. K., and Panjwani, N. (2009). Galectin-3 promotes lamellipodia formation in epithelial cells by interacting with complex N-glycans on alpha3beta1 integrin. *J. Cell Sci.* 122(Pt 20), 3684–3693. doi: 10.1242/jcs.045674

Satoh, K., Niwa, M., Binh, N. H., Nakashima, M., Kobayashi, K., Takamatsu, M., et al. (2011a). Increase of galectin-3 expression in microglia by hyperthermia in delayed neuronal death of hippocampal CA1 following transient forebrain ischemia. *Neurosci. Lett.* 504, 199–203. doi: 10.1016/j.neulet.2011.09.015

Satoh, K., Niwa, M., Goda, W., Binh, N. H., Nakashima, M., Takamatsu, M., et al. (2011b). Galectin-3 expression in delayed neuronal death of hippocampal CA1 following transient forebrain ischemia, and its inhibition by hypothermia. *Brain Res.* 1382, 266–274. doi: 10.1016/j.brainres.2011.01.049

Schnaar, R. L. (2016). Glycobiology simplified: diverse roles of glycan recognition in inflammation. *J. Leukoc. Biol.* 99, 825–838. doi: 10.1189/jlb.3RI0116-021R

Shao, Z., Lee, X., Huang, G., Sheng, G., Henderson, C. E., Louvard, D., et al. (2017). LINGO-1 regulates oligodendrocyte differentiation through the cytoplasmic gelsolin signaling pathway. *J. Neurosci.* 37, 3127–3137. doi: 10.1523/JNEUROSCI.3722-16.2017

Shimura, T., Takenaka, Y., Tsutsumi, S., Hogan, V., Kikuchi, A., and Raz, A. (2004). Galectin-3, a novel binding partner of beta-catenin. *Cancer Res.* 64, 6363–6367. doi: 10.1158/0008-5472.CAN-04-1816

Shiryaev, S. A., Savinov, A. Y., Cieplak, P., Ratnikov, B. I. Motamedchaboki, K., Smith, J. W., et al. (2009). Matrix metalloproteinase proteolysis of the myelin basic protein isoforms is a source of immunogenic peptides in autoimmune multiple sclerosis. *PLoS One* 4:e4952. doi: 10.1371/journal.pone.0004952

Skuljec, J., Gudi, V., Ulrich, R., Frichert, K., Yildiz, O., Pul, R., et al. (2011). Matrix metalloproteinases and their tissue inhibitors in cuprizone-induced demyelination and remyelination of brain white and gray matter. *J. Neuropathol. Exp. Neurol.* 70, 758–769. doi: 10.1097/NEN.0b013e3182294fad

Snaidero, N., and Simons, M. (2017). The logistics of myelin biogenesis in the central nervous system. *Glia* 65, 1021–1031. doi: 10.1002/glia.23116

Song, S., Mazurek, N., Liu, C., Sun, Y., Ding, Q. Q., Liu, K., et al. (2009). Galectin-3 mediates nuclear beta-catenin accumulation and Wnt signaling in human colon cancer cells by regulation of glycogen synthase kinase-3beta activity. *Cancer Res.* 69, 1343–1349. doi: 10.1158/0008-5472.CAN-08-4153

Stancic, M., Slijepcevic, D., Nomden, A., Vos, M. J., de Jonge, J. C., Sikkema, A. H., et al. (2012). Galectin-4, a novel neuronal regulator of myelination. *Glia* 60, 919–935. doi: 10.1002/glia.22324

Stancic, M., van Horssen, J., Thijssen, V. L., Gabius, H. J., van der Valk, P., Hoekstra, D., et al. (2011). Increased expression of distinct galectins in multiple sclerosis lesions. *Neuropathol. Appl. Neurobiol.* 2011, 654–671. doi: 10.1111/j.1365-2990.2011.01184.x

Starossom, S. C., Mascanfroni, I. D., Imitola, J., Cao, L., Raddassi, K., Hernandez, S. F., et al. (2012). Galectin-1 deactivates classically activated microglia and protects from inflammation-induced neurodegeneration. *Immunity* 37, 249–263. doi: 10.1016/j.immuni.2012.05.023

Sundblad, V., Croci, D. O., and Rabinovich, G. A. (2011). Regulated expression of galectin-3, a multifunctional glycan-binding protein, in haematopoietic and non-haematopoietic tissues. *Histol. Histopathol.* 26, 247–265. doi: 10.14670/HH-26.247

Suzuki, K., and Kikkawa, Y. (1969). Status spongiosus of CNS and hepatic changes induced by cuprizone (biscyclohexanone oxalyldihydrazone). *Am. J. Pathol.* 54, 307–325.

Takahashi, K., Prinz, M., Stagi, M., Chechneva, O., and Neumann, H. (2007). TREM2- transduced myeloid precursors mediate nervous tissue debris clearance and facilitate recovery in an animal model of multiple sclerosis. *PLoS Med.* 4:e124. doi: 10.1371/journal.pmed.0040124

Tallantyre, E. C., Bø, L., Al-Rawashdeh, O., Owens, T., Polman, C. H., Lowe, J. S., et al. (2010). Clinico-pathological evidence that axonal loss underlies disability in progressive multiple sclerosis. *Mult. Scler.* 16, 406–411. doi: 10.1177/1352458510364992

Tawk, M., Makoukji, J., Belle, M., Fonte, C., Trousson, A., Hawkins, T., et al. (2011). Wnt/beta-catenin signaling is an essential and direct driver of myelin gene expression and myelinogenesis. *J. Neurosci.* 31, 3729–3742. doi: 10.1523/JNEUROSCI.4270-10.2011

Thomas, L., and Pasquini, L. A. (2018). Extracellular Galectin-3 Induces accelerated oligodendroglial differentiation through changes in signaling pathways and cytoskeleton dynamics. *Mol. Neurobiol.* doi: 10.1007/s12035-018-1089-6 [Epub ahead of print].

Toscano, M. A., Bianco, G. A., Ilarregui, J. M., Croci, D. O., Correale, J., Hernandez, J. D., et al. (2007). Differential glycosylation of TH1, TH2 and TH-17 effector cells selectively regulates susceptibility to cell death. *Nat. Immunol.* 8, 825–834. doi: 10.1038/ni1482

Tyler, W. A., Gangoli, N., Gokina, P., Kim, H. A., Covey, M., Levison, S. W., et al. (2009). Activation of the mammalian target of rapamycin (mTOR) is essential for oligodendrocyte differentiation. *J. Neurosci.* 29, 6367–6378. doi: 10.1523/JNEUROSCI.0234-09.2009

Tyler, W. A., Jain, M. R., Cifelli, S. E., Li, Q., Ku, L., Feng, Y., et al. (2011). Proteomic identification of novel targets regulated by the mammalian target of rapamycin pathway during oligodendrocyte differentiation. *Glia* 59, 1754–1769. doi: 10.1002/glia.21221

Uchino, Y., Woodward, A. M., Mauris, J., Peterson, K., Verma, P., Nilsson, U. J., et al. (2018). Galectin-3 is an amplifier of the interleukin-1β-mediated inflammatory response in corneal keratinocytes. *Immunology* 154, 490–499. doi: 10.1111/imm.12899

Ulrich, R., Baumgärtner, W., Gerhauser, I., Seeliger, F., Haist, V., Deschl, U., et al. (2006). MMP-12, MMP-3, and TIMP-1 are markedly upregulated in chronic demyelinating Theiler murine encephalomyelitis. *J. Neuropathol. Exp. Neurol.* 65, 783–793. doi: 10.1097/01.jnen.0000229990.32795.0d

Ulrich, R., Seeliger, F., Kreutzer, M., Germann, P. G., and Baumgärtner, W. (2008). Limited remyelination in Theiler's murine encephalomyelitis due to insufficient oligodendroglial differentiation of nerve/glial antigen 2 (NG2)-positive putative oligodendroglial progenitor cells. *Neuropathol. Appl. Neurobiol.* 34, 603–620. doi: 10.1111/j.1365-2990.2008.00956.x

Umekawa, T., Osman, A. M., Han, W., Ikeda, T., and Blomgren, K. (2015). Resident microglia, rather than blood-derived macrophages, contribute to the earlier and

more pronounced inflammatory reaction in the immature compared with the adult hippocampus after hypoxia-ischemia. *Glia* 63, 2220–2230. doi: 10.1002/glia.22887

van den Brule, F., Califice, S., and Castronovo, V. (2004). Expression of galectins in cancer: a critical review. *Glycoconj. J.* 19, 537–542. doi: 10.1023/B:GLYC.0000014083.48508.6a

Van den Brule, F. A., Fernandez, P. L., Buicu, C., Liu, F. T., Jackers, P., Lambotte, R., et al. (1997). Differential expression of galectin-1 and galectin-3 during first trimester human embryogenesis. *Dev. Dyn.* 209, 399–405. doi: 10.1002/(SICI)1097-0177(199708)209:4<399::AID-AJA7>3.0.CO;2-D

Voß, E. V., Škuljec, J., Gudi, V., Skripuletz, T., Pul, R., Trebst, C., et al. (2011). Characterisation of microglia during de- and remyelination: can they create a repair promoting environment? *Neurobiol. Dis.* 45, 519–528. doi: 10.1016/j.nbd.2011.09.008

Wang, A., Zhong, C., Zhu, Z., Xu, T., Peng, Y., Xu, T., et al. (2018). Serum galectin-3 and poor outcomes among patients with acute ischemic stroke. *Stroke* 49, 211–214. doi: 10.1161/STROKEAHA.117.019084

Wang, L., and Guo, X. L. (2016). Molecular regulation of galectin-3 expression and therapeutic implication in cancer progression. *Biomed. Pharmacother.* 78, 165–171. doi: 10.1016/j.biopha.2016.01.014

Wang, X., Zhang, S., Lin, F., Chu, W., Yue, S., and Am, J. (2015). Elevated galectin-3 levels in the serum of patients with Alzheimer's disease. *Am. J. Alzheimers Dis. Other Demen.* 30, 729–732. doi: 10.1177/1533317513495107

Wu, L., Zhao, Q., Zhu, X., Peng, M., Jia, C., Wu, W., et al. (2010). A novel function of microRNA let-7d in regulation of galectin-3 expression in attention deficit hyperactivity disorder rat brain. *Brain Pathol.* 20, 1042–1054. doi: 10.1111/j.1750-3639.2010.00410.x

Wu, S. Y., Huang, J. H., Chen, W. Y., Chan, Y. C., Lin, C. H., Chen, Y. C., et al. (2017). Cell intrinsic galectin-3 attenuates neutrophil ROS-dependent killing of Candida by modulating CR3 downstream syk activation. *Front. Immunol.* 8:48. doi: 10.3389/fimmu.2017.00048

Xiao, J., Ferner, A. H., Wong, A. W., Denham, M., Kilpatrick, T. J., and Murray, S. S. (2012). Extracellular signal-regulated kinase 1/2 signaling promotes oligodendrocyte myelination in vitro. *J. Neurochem.* 122, 1167–1180. doi: 10.1111/j.1471-4159.2012.07871.x

Xu, H., Cao, Y., Yang, X., Cai, P., Kang, L., Zhu, X., et al. (2017). ADAMTS13 controls vascular remodeling by modifying VWF reactivity during stroke recovery. *Blood* 130, 11–22. doi: 10.1182/blood-2016-10-747089

Xu, H., Yang, H. J., McConomy, B., Browning, R., and Li, X. M. (2010). Behavioral and neurobiological changes in C57BL/6 mouse exposed to cuprizone: effects of antipsychotics. *Front. Behav. Neurosci.* 4:8. doi: 10.3389/fnbeh.2010.00008

Xu, H., Yang, H. J., Rose, G. M., and Li, X. M. (2011). Recovery of behavioral changes and compromised white matter in C57BL/6 mice exposed to cuprizone: effects of antipsychotic drugs. *Front. Behav. Neurosci.* 5:31. doi: 10.3389/fnbeh.2011.00031

Xu, H., Yang, H. J., Zhang, Y., Clough, R., Browning, R., and Li, X. M. (2009). Behavioral and neurobiological changes in C57BL/6 mice exposed to cuprizone. *Behav. Neurosci.* 123, 418–429. doi: 10.1037/a0014477

Xue, H., Liu, L., Zhao, Z., Zhang, Z., Guan, Y., Cheng, H., et al. (2017). The N-terminal tail coordinates with carbohydrate recognition domain to mediate galectin-3 induced apoptosis in T cells. *Oncotarget* 8, 49824–49838. doi: 10.18632/oncotarget.17760

Yan, Y. P., Lang, B. T., Vemuganti, R., and Dempsey, R. J. (2009). Galectin-3 mediates post-ischemic tissue remodeling. *Brain Res.* 1288, 116–124. doi: 10.1016/j.brainres.2009.06.073

Yang, L. J., Zeller, C. B., Shaper, N. L., Kiso, M., Hasegawa, A., Shapiro, R. E., et al. (1996). Gangliosides are neuronal ligands for myelin-associated glycoprotein. *Proc. Natl. Acad. Sci. U.S.A.* 93, 814–818. doi: 10.1073/pnas.93.2.814

Yang, R. Y., Rabinovich, G. A., and Liu, F. T. (2008). Galectins: structure, function and therapeutic potential. *Expert Rev. Mol. Med.* 10:e17. doi: 10.1017/S1462399408000719

Ye, F., Chen, Y., Hoang, T., Montgomery, R. L., Zhao, X. H., Bu, H., et al. (2009). HDAC1 and HDAC2 regulate oligodendrocyte differentiation by disrupting the beta-catenin-TCF interaction. *Nat. Neurosci.* 12, 829–838. doi: 10.1038/nn.2333

Yoo, H. I., Kim, E. G., Lee, E. J., Hong, S. Y., Yoon, C. S., Hong, M. J., et al. (2017). Neuroanatomical distribution of galectin-3 in the adult rat brain. *J. Mol. Histol.* 48, 133–146. doi: 10.1007/s10735-017-9712-9

Young, C. C., Al-Dalahmah, O., Lewis, N. J., Brooks, K. J., Jenkins, M. M., Poirier, F., et al. (2014). Blocked angiogenesis in Galectin-3 null mice does not alter cellular and behavioral recovery after middle cerebral artery occlusion stroke. *Neurobiol. Dis.* 63, 155–164. doi: 10.1016/j.nbd.2013.11.003

Zeger, M., Popken, G., Zhang, J., Xuan, S., Lu, Q. R., Schwab, M. H., et al. (2007). Insulin-like growth factor type 1 receptor signaling in the cells of oligodendrocyte lineage is required for normal in vivo oligodendrocyte development and myelination. *Glia* 55, 400–411. doi: 10.1002/glia.20469

Zhang, L., Wang, P., Qin, Y., Cong, Q., Shao, C., Du, Z., et al. (2017). RN1, a novel galectin-3 inhibitor, inhibits pancreatic cancer cell growth in vitro and in vivo via blocking galectin-3 associated signaling pathways. *Oncogene* 36, 1297–1308. doi: 10.1038/onc.2016.306

Zhang, Y., Xu, H., Jiang, W., Xiao, L., Yan, B., He, J., et al. (2008). Quetiapine alleviates the cuprizone-induced white matter pathology in the brain of C57BL/6 mouse. *Schizophr. Res.* 106, 182–191. doi: 10.1016/j.schres.2008.09.013

Zhou, J. Y., Afjehi-Sadat, L., Asress, S., Duong, D. M., Cudkowicz, M., Glass, J. D., et al. (2010). Galectin-3 is a candidate biomarker for amyotrophic lateral sclerosis: discovery by a proteomics approach. *J. Proteome Res.* 9, 5133–5141. doi: 10.1021/pr100409r

Zhou, W., Chen, X., Hu, Q., Chen, X., Chen, Y., and Huang, L. (2018). Galectin-3 activates TLR4/NF-κB signaling to promote lung adenocarcinoma cell proliferation through activating lncRNA-NEAT1 expression. *BMC Cancer* 18:580. doi: 10.1186/s12885-018-4461-z

Zuchero, J. B., Fu, M. M., Sloan, S. A., Ibrahim, A., Olson, A., Zaremba, A., et al. (2015). CNS myelin wrapping is driven by actin disassembly. *Dev. Cell* 34, 152–167. doi: 10.1016/j.devcel.2015.06.011

Conflict of Interest Statement: The authors declare that the research was conducted in the absence of any commercial or financial relationships that could be construed as a potential conflict of interest.

frontiers in Cellular Neuroscience

MINI REVIEW
published: 02 October 2018
doi: 10.3389/fncel.2018.00333

Motor Exit Point (MEP) Glia: Novel Myelinating Glia That Bridge CNS and PNS Myelin

*Laura Fontenas and Sarah Kucenas**

Department of Biology, University of Virginia, Charlottesville, VA, United States

Oligodendrocytes (OLs) and Schwann cells (SCs) have traditionally been thought of as the exclusive myelinating glial cells of the central and peripheral nervous systems (CNS and PNS), respectively, for a little over a century. However, recent studies demonstrate the existence of a novel, centrally-derived peripheral glial population called motor exit point (MEP) glia, which myelinate spinal motor root axons in the periphery. Until recently, the boundaries that exist between the CNS and PNS, and the cells permitted to cross them, were mostly described based on fixed histological collections and static lineage tracing. Recent work in zebrafish using *in vivo*, time-lapse imaging has shed light on glial cell interactions at the MEP transition zone and reveals a more complex picture of myelination both centrally and peripherally.

Keywords: myelin, oligodendrocyte, schwann cell, motor exit point glia, zebrafish, boundary cap cell

OPEN ACCESS

Edited by:
Keith Murai,
McGill University, Canada

Reviewed by:
Vanessa Auld,
University of British Columbia, Canada
Alexandre Leite Rodrigues Oliveira,
Universidade Estadual de Campinas, Brazil
Maria Elena De Bellard,
California State University, Northridge, United States

***Correspondence:**
Sarah Kucenas
sk4ub@virginia.edu

Received: *10 June 2018*
Accepted: *11 September 2018*
Published: *02 October 2018*

Citation:
Fontenas L and Kucenas S (2018) Motor Exit Point (MEP) Glia: Novel Myelinating Glia That Bridge CNS and PNS Myelin. Front. Cell. Neurosci. 12:333. doi: 10.3389/fncel.2018.00333

INTRODUCTION

Myelin is a unique plasma membrane extension produced by specialized glial cells that is wrapped around axons and facilitates rapid transmission of electrical impulses over long distances. Although myelin appeared 430 million years ago in the vertebrate lineage (Gould et al., 2008; Zalc, 2016), continuous efforts from various fields of biology are still unraveling the many mysteries of myelin and myelin producing cells.

The nervous system is a complex organ whose function depends on the precise organization of its components. The central nervous system (CNS) consists of the brain and the spinal cord, while the peripheral nervous system (PNS) consists of neural tissue outside of the CNS, including motor and sensory axons and sensory neurons clustered in ganglia. While many neurons establish circuits within the CNS, some of these cells send their axons (e.g., motor axons) freely across specialized CNS boundaries known as transition zones (TZs) and travel long distances throughout the organism and ultimately make synapses on peripheral tissues, including muscle. By associating tightly with axons to ultimately ensheath and insulate them with fatty membranes called myelin, myelinating cells increase nerve impulse conduction speed and strengthen the function and efficiency of the whole nervous system.

In the CNS, oligodendrocytes (OLs), which are derived from neural tube precursors, make myelin in the brain and spinal cord, while Schwann cells (SCs), which originate from the neural crest (NC), myelinate axons of the PNS (Jessen and Mirsky, 2005; Bergles and Richardson, 2015).

Abbreviations: BC, boundary cap; CNS, central nervous system; dpf, day post-fertilization; DREZ, dorsal root entry zone; DRG, dorsal root ganglion; eGFP, enhanced green fluorescent protein; Gpr126, G-protein coupled receptor 126; hpf, hour post-fertilization; MBP, myelin basic protein; MEP, motor exit point; MN, motor neuron; NC, neural crest; OL, oligodendrocyte; OPC, oligodendrocyte progenitor cell; PNS, peripheral nervous system; SC, Schwann cell; TZ, transition zone; Wif1, Wnt-inhibitory factor 1.

In addition to expressing different sets of genes, central and peripheral glia also ensheath axons in myelin in distinct ways. OLs expand multiple membrane processes, which wrap several axonal segments that often belong to different neurons, while a single SC ensheaths a single axonal segment. Although OLs and SCs myelinate axons in mechanistically distinct ways, their territories come into close proximity along common axons at motor exit point (MEP) TZs, where they are separated by only a few microns (Fraher and Kaar, 1984; Fraher, 2002).

The mammalian CNS/PNS boundary is delineated by a thick layer of astrocytic endfeet that is continuous with the glia limitans which covers the surface of the spinal cord with the exception of perforations that allow axons to cross (reviewed in Fontenas and Kucenas, 2017). Ultrastructural studies show that central and peripheral glial cells, namely OLs and SCs, are present near the MEP TZ, but are never seen intermixing. In fact, MEP TZs are described as an abrupt transition between central and peripheral glia (Doucette, 1991; Franklin and Blakemore, 1993; Fraher et al., 2007). However, intriguingly, using *in vivo* imaging in zebrafish, we and others observe the presence of continuous *mbp*$^{+}$ myelin internodes along motor axons crossing the MEP TZ (**Figure 1C**; Monk et al., 2009; Almeida et al., 2011; Auer et al., 2018).

The two distinct yet connected halves of the nervous system have their own, non-overlapping myelin forming cells and myelin sheaths. Does this mean myelinating glia cannot function in the half where they do not originate? What keeps them segregated in the developing and mature nervous system? How does unique myelin on either side of the CNS/PNS TZ result in an efficiently insulated nerve?

Work from our lab and others demonstrates the presence of additional glial cells outside the spinal cord at the TZ between the CNS and the PNS, which function to segregate central and peripheral components from ectopically crossing this boundary (Vermeren et al., 2003; Kucenas et al., 2009; Coulpier et al., 2010; Smith et al., 2014). While most studies previously focused on nervous system TZs using histological and ultrastructural methods, recent studies using *in vivo*, time-lapse imaging in zebrafish have shed light on these dynamic structures and revealed novel glial cell populations that cross these TZs (Kucenas et al., 2008, 2009; Smith et al., 2014; Welsh and Kucenas, 2018).

In this article, we will provide a short review on MEP glia, a recently discovered population of centrally-derived glial cells that myelinate spinal motor nerve root axons and compare them to traditional myelinating glial populations in both form and function.

MEP GLIA ARE CENTRALLY-DERIVED PERIPHERAL MYELINATING CELLS

Until recently, the TZs between the CNS and the PNS were thought to be selectively permeable to axons either entering or exiting the spinal cord, while the establishment and maintenance of the territories occupied by glial cells remained poorly described and understood. However, recent studies demonstrate that MEP TZs are occupied by highly dynamic cell populations and are precisely regulated over the course of nervous system development. While OL lineage cells and SCs segregate and function in the CNS and PNS, respectively, other glial cell populations freely cross the MEP TZ as spinal motor nerves are being formed (Kucenas et al., 2008, 2009; Smith et al., 2014, 2016; Fontenas and Kucenas, 2017).

One of these cell populations, MEP glia, originate from pMN domain precursors in the ventral neural tube, which also give rise to motor neurons (MNs) and OL lineage cells. After exiting the CNS, MEP glia reside just outside of the ventral spinal cord along spinal motor nerve root axons, occupying axonal territory between SCs in the periphery and OLs in the spinal cord. The pMN domain constitutes the major site of expression of the basic helix-loop-helix (bHLH) transcription factor Olig2. In zebrafish, *olig2*$^{+}$ precursors first produce MNs and then switch to generate glial cells at approximately 36 hours post fertilization (hpf; Smith et al., 2014; Ravanelli and Appel, 2015). MEP glia exit the ventral spinal cord through the MEP TZ at around 50 hpf, before the onset of oligodendrocyte progenitor cell (OPC) migration, and then divide to populate the motor root.

MEP glia and OL lineage cells share a common progenitor and as a consequence, the two myelinating cell populations—although they function in two distinct halves of the nervous system—share common markers. MEP glia express *olig2* (**Figures 1A,B**), whose expression is progressively turned off after MEP glia reach the motor nerve root, prior to motor axon myelination (Smith et al., 2014). Both central and peripheral myelinating glial cells in zebrafish as well as in mammals, express the transcription factor Sox10 (**Figure 1B**). Numerous studies show that sox10 is required for NC cell development, including SCs, as well as for OL lineage differentiation and promotes myelin gene expression (Kelsh and Eisen, 2000; Dutton et al., 2001; Gilmour et al., 2002; Kucenas et al., 2009; Takada et al., 2010). Unsurprisingly, MEP glia also express and require sox10 for their development and function (Kucenas et al., 2009; Smith et al., 2014). *In vivo*, time-lapse imaging has recently revealed sox10 expression in MEP glia before they even exit the spinal cord and is maintained throughout their development and differentiation. The pioneer study demonstrating the existence of centrally-derived glial cells at the MEP TZ, shows that zebrafish *colorless* (*cls*) mutants, which harbor a mutation in sox10 and lack SCs, have peripheral OPCs that differentiate and myelinate spinal motor nerves, suggesting that sox10 may be required for MEP glial function or survival (Kucenas et al., 2009).

Intriguingly, MEP glia not only express the transcription factors *sox10* and *olig2*, which together are a combination that is characteristic of CNS myelinating glia, they also express *foxd3* (**Figures 1A,B**), a transcription factor present in all NC cells including sox10^{+} peripheral glia such as SCs in zebrafish (Odenthal and Nüsslein-Volhard, 1998; Gilmour et al., 2002; Hochgreb-Hägele and Bronner, 2013; Smith et al., 2014). Using *in vivo*, time-lapse imaging and the *Gt(foxd3:mcherry)* transgenic line that faithfully mimics the endogenous expression of *foxd3* (Hochgreb-Hägele and Bronner, 2013), *foxd3* expression was observed as early as 46 hpf, before MEP glia exit the spinal cord, and persisted in these cells as late as 8 day

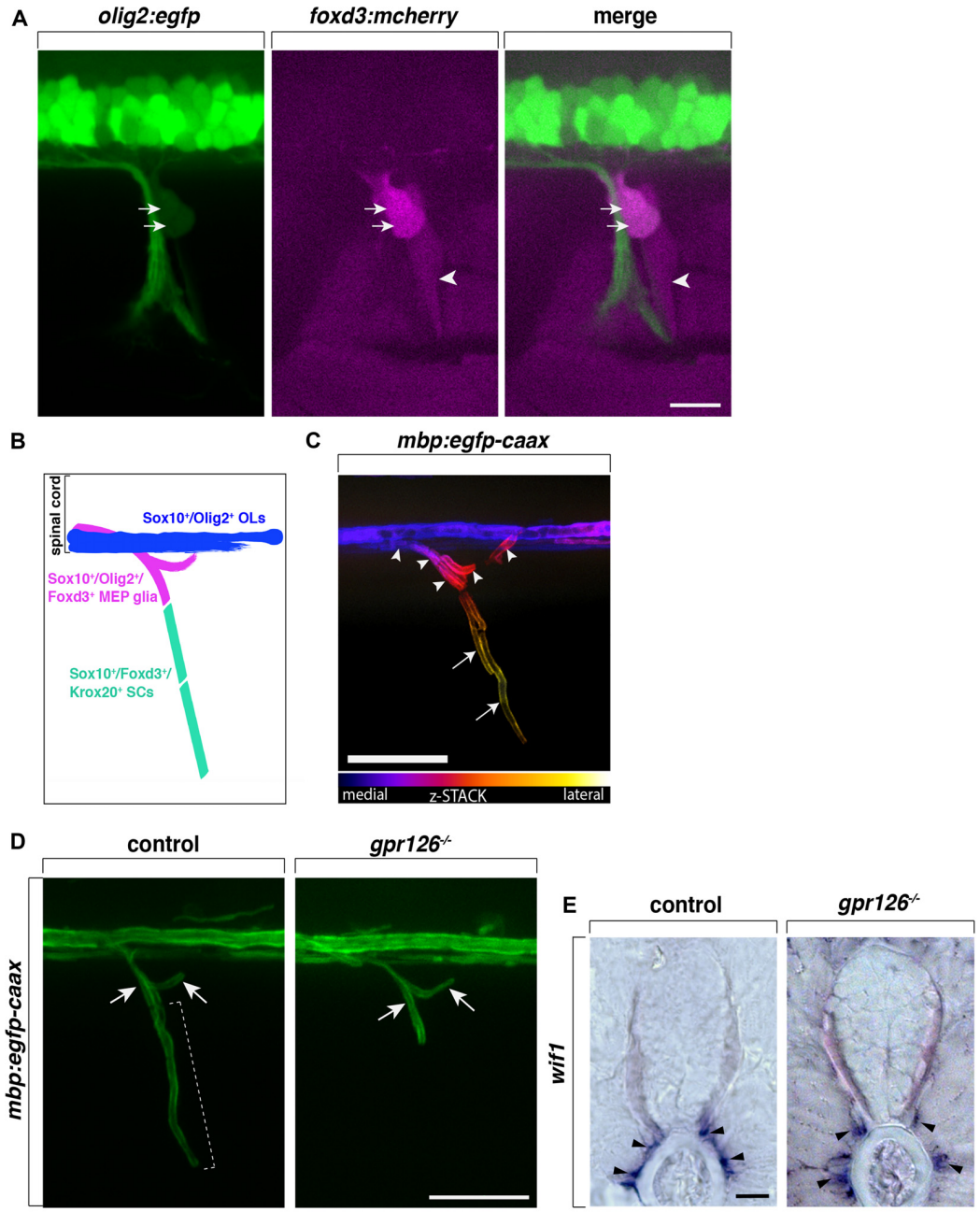

FIGURE 1 | Centrally-derived motor exit point (MEP) glia myelinate motor nerve roots. **(A)** Lateral view of a *olig2:egfp;foxd3:mcherry* zebrafish trunk showing *olig2*$^{+}$*/foxd3*$^{+}$ MEP glia (arrows) and *olig2*$^{-}$*/foxd3*$^{+}$ SCs (arrowheads) along a motor nerve at 55 hour post-fertilization (hpf). **(B)** Diagram representing central and peripheral myelinating glial markers. **(C)** Pseudo-colored z-stack of a lateral view of a *mbp:egfp-caax* trunk at 5 day post-fertilization (dpf). MEP glial myelin sheaths (arrowheads) originate within the spinal cord and project laterally along motor nerve axons, coming close to schwann cells (SC) myelin (arrows). **(D)** SC myelin (bracket) but not MEP glial myelin (arrows) is absent in G-protein coupled receptor 126 (*gpr126*) mutants at 5 days post fertilization (dpf). **(E)** *In situ* hybridization showing the presence of *Wnt-inhibitory factor 1* (*wif1*$^{+}$) MEP glia (arrowheads) along motor nerve roots in 3 dpf control and *gpr126* mutant larvae. Scale bar, **(A–D)** 50 μm, **(E)** 20 μm.

post-fertilization (dpf; Smith et al., 2014). Despite the fact that they express the peripheral marker *foxd3*, MEP glia do not express krox20 (also known as early growth response protein 2—egr2b), a transcription factor expressed by boundary cap (BC) cells that is also required for SC myelination (data not shown; Wilkinson et al., 1989; Topilko et al., 1994; Monk et al., 2009; Coulpier et al., 2010; Smith et al., 2014).

In chick and mouse, BC cells are traditionally described as NC derivatives that migrate along the ventral path and

transiently reside in clusters at dorsal root entry zone (DREZ) and MEP TZs, where axons enter and exit the spinal cord, respectively (Niederländer and Lumsden, 1996; Golding and Cohen, 1997; Vermeren et al., 2003). BC cells eventually give rise to neuronal and glial cell populations, including myelinating SCs (Maro et al., 2004; Gresset et al., 2015; Radomska and Topilko, 2017). At the MEP, BC cells function to constrain MN cell bodies to the spinal cord, as their ablation leads to ectopic MNs along motor nerve roots (Vermeren et al., 2003; Bron et al., 2007). The Topilko laboratory also demonstrated that upon Krox20 inactivation, which results in the absence of both SCs and BC cells, OL ectopically populate the ventral and dorsal roots (Coulpier et al., 2010).

To date, BC cells have not been described in zebrafish, however, MEP glia do express the BC cell marker *Wnt-inhibitory factor 1 (wif1*; **Figure 1E**), which no other myelinating cells express (Coulpier et al., 2009; Smith et al., 2014). Taken together, MEP glia express a subset of both central and peripheral glial markers (*sox10*, *olig2*, *foxd3* and *wif1*) that are not found all together in any other myelinating glial cell type (**Figure 1B**). Although MEP glia originate in the CNS and function in the PNS, their identity is not truly that of either a central or a peripheral glial cell, but rather appear to be a hybrid glial cell.

Previous work from our lab shows that MEP glia differentiate into myelinating glia and by 3 dpf, start to ensheath the proximal portion of spinal motor nerve axons, also known as motor nerve roots (**Figures 1C,D**; Smith et al., 2014). In the same initial study, we demonstrate that MEP glia restrict OPCs to the spinal cord through contact-mediated repulsion. Using *in vivo*, time-lapse imaging, we describe that prior to 3 dpf, OPCs extend membrane processes into the periphery to sense the environment. Immediately upon contact with a MEP glial cell, OPCs retract their processes from the periphery and pursue their migration within the spinal cord. Under normal physiological conditions, OPC cell bodies are never found outside of the spinal cord but invade peripheral nerves in the absence of MEP glia (Kucenas et al., 2009; Smith et al., 2014). Consistent with these findings, OPCs exit the spinal cord through MEP TZs in mutants lacking all peripheral myelinating glia (Smith et al., 2014). For example, OPCs are found along peripheral nerves in *erbb3b* mutants that harbor a mutation in the receptor tyrosine kinase, erbb3b and lack all peripheral myelinating glia (Lyons et al., 2005; Smith et al., 2014; Morris et al., 2017). Additionally, using *in vivo*, time-lapse imaging coupled with single cell ablation using a nitrogen-pulsed laser, our lab showed that specific ablation of MEP glia leads to the ectopic exit of OPCs from the spinal cord (Smith et al., 2014). However, OPCs are never found in the PNS when regions surrounding MEP glia are ablated or when radial glia, another glial cell population present at the MEP TZ, are genetically ablated (Smith et al., 2014, 2016). These observations demonstrate that MEP glia contribute to a selective gating mechanism at MEP TZs. Direct interactions between myelinating glial cells from the CNS and PNS participate in regulating glial migration across TZs and contribute to the establishment and maintenance of the CNS/PNS boundary and continuous myelination along spinal motor axons.

ELUCIDATING THE MOLECULAR MECHANISMS THAT MEDIATE MEP GLIAL DEVELOPMENT AND FUNCTION

Although myelin promotes the rapid propagation of electrical activity, not all axons are myelinated. In the PNS, studies unanimously point to a straightforward mechanism, whereby axonal caliber determines whether or not myelination will occur and also determines the extent of myelin produced (Taveggia et al., 2005; Newbern and Birchmeier, 2010; Perlin et al., 2011). On the other hand, central myelination is a divisive topic, and although we still understand only a little about how neuronal activity influences OL myelination, coupling neuronal activity to myelination arouses interest and has become a rapidly growing field. Elegant work from the Chan laboratory demonstrates that OLs can myelinate electrically silent nanofibers *in vitro* (Lee et al., 2012). However, there are other studies that demonstrate that environmental experience and neuronal activity *in vivo* are essential for myelination. Evidence from studies using *in vitro* models, *in vivo*, time-lapse imaging in zebrafish, and also mouse models suggest that OL lineage cells can detect and respond to extrinsic cues during their development and differentiation, but the source and identity of these signals are matter of debate (Kirby et al., 2006; Hines et al., 2015; Mensch et al., 2015; Etxeberria et al., 2016; Koudelka et al., 2016; see; Almeida and Lyons, 2017; Welsh and Kucenas, 2018 for recent reviews).

MEP glia ensheath and myelinate motor axon segments that do not overlap with myelin internodes made by SCs found further distally along the nerve. In fact, the boundary between MEP glial and SC myelin sheaths is clearly delineated by a node of Ranvier (**Figures 2A,B**). Like the well described and century-old myelinating glial cells SCs and OLs, MEP glia have the ability to cluster sodium channels to nodes of Ranvier as they initiate axonal wrapping, thus promoting saltatory conduction from the very proximal portion of motor nerve root axons (**Figures 2A–C**; Voas et al., 2009). MEP glial myelin internodes are flanked by nodes of Ranvier inside the spinal cord and just peripheral to the MEP TZ (**Figures 2A–C**). MEP glia also express *myelin basic protein (mbp)* and both *mbp* and transcript and MBP protein can be detected along motor nerve root axons as early as 4 dpf (**Figures 2B,C**; Brösamle and Halpern, 2002; Smith et al., 2014).

Fascinatingly, in *G protein-coupled receptor 126* (*gpr126*) mutants, where SCs are arrested at the pro-myelinating stage and fail to myelinate peripheral axons, Monk et al. (2009) described the presence of myelin along spinal motor root axons, reminiscent of projections of central myelin through MEP TZs. At the time, MEP glia were yet to be discovered and characterized. Therefore, projections of central myelin were the most plausible explanation for such a phenotype. However, recent work from our lab has extended these findings and we now know that the projections of "central myelin" into the periphery observed in *gpr126* mutants are, in fact,

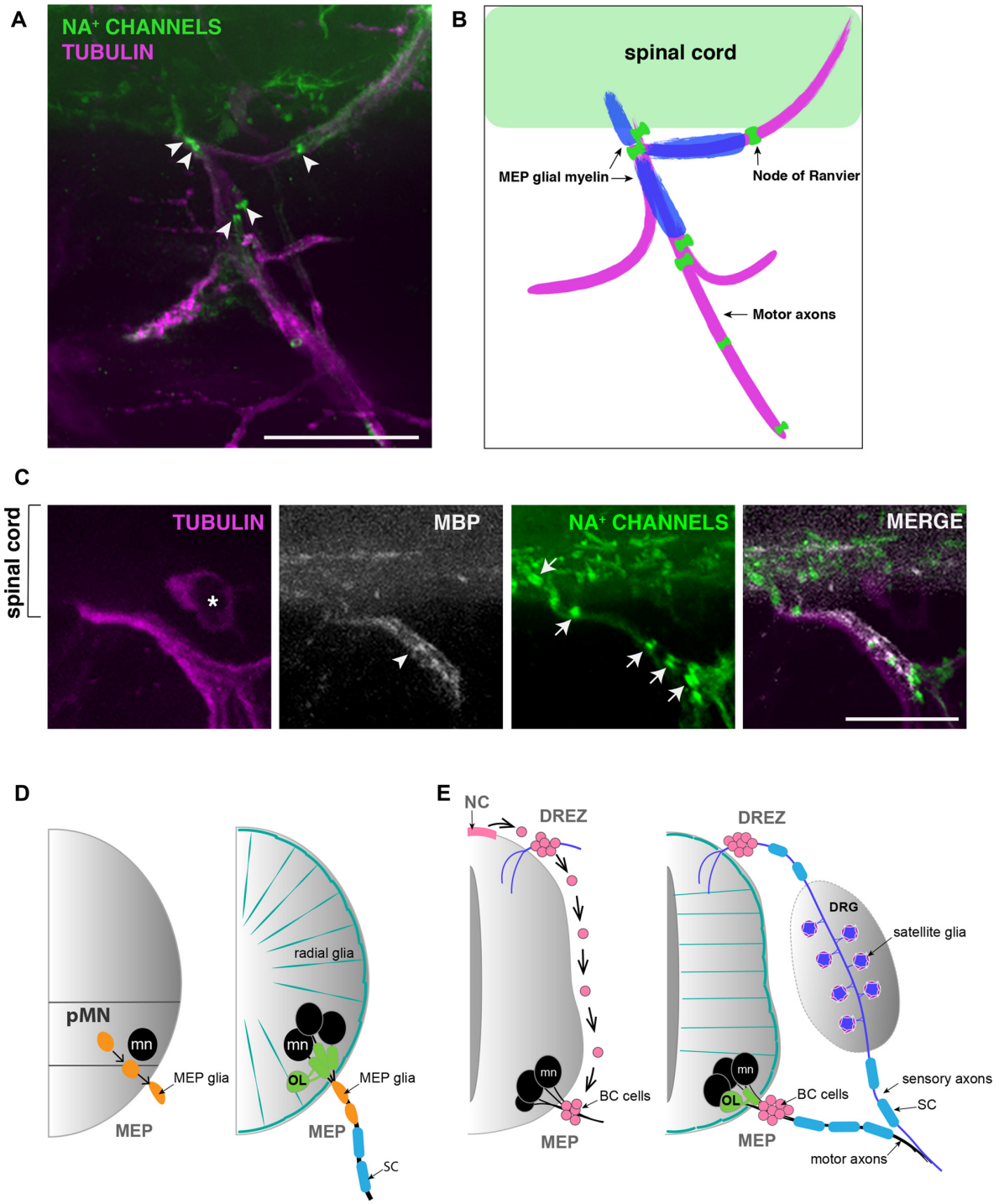

FIGURE 2 | MEP glial myelin is flanked by nodes of ranvier. **(A)** Lateral view of a 5 dpf zebrafish trunk stained with antibodies specific to pan Na^+ channels (clone k58/35) and acetylated tubulin shows that MEP glial territory is flanked by sodium channels clustered in Nodes of Ranvier (arrowheads) along motor nerve roots. **(B)** Diagram showing MBP^+ MEP glial myelin (blue) delineated by nodes of Ranvier (green) along motor nerve root axons (magenta). **(C)** Immunostaining showing MBP^+ MEP glial myelin (arrowhead) and nodes of Ranvier (arrows) along motor nerve root axons (magenta). Asterisks point to dorsal root ganglion (DRG). **(D)** Schematic of zebrafish MEP transition zones (TZs) and the diverse populations of glial cells orchestrating the CNS/PNS boundary. CNS-derived MEP glia (orange) that reside along motor neuron (mn; black) axons restrict the oligodendrocyte lineage (OL; green) to the spinal cord. Radial glia (teal green) cover the surface of the spinal cord and prevent peripheral glia such as MEP glia and SC (blue) from entering the CNS. **(E)** Schematic of a mammalian neural tube showing neural crest (NC)-derived boundary cap (BC) cells (pink) sitting at the dorsal root entry zone (DREZ) and MEP TZs. BC cells prevent mn (black) cell bodies from transgressing the spinal cord boundary. Scale bar, **(A)** 50 μm, **(C)** 25 μm.

MEP glial myelin sheaths (**Figures 1D,E**). These data therefore demonstrate that, unlike SCs, MEP glia do not require *gpr126* to initiate myelination. And as previously mentioned, these glial cells also do not express Krox20. Therefore, they are a CNS-derived, peripheral glial cell that myelinates peripheral axons, but uses a distinct molecular mechanism to initiate myelination.

ARE MEP GLIA THE ONLY CENTRALLY-DERIVED PERIPHERAL GLIA?

For years, mammalian BC cells were thought to constrain MN cell bodies to the spinal cord by repulsion from outside the spinal cord (Bron et al., 2007; Mauti et al., 2007; Chauvet and Rougon, 2008; Bravo-Ambrosio and Kaprielian, 2011; Garrett et al., 2016). However, how this physically worked was unclear, as neither BC cells or MN cell bodies were close enough to physically interact to mediate the repulsion (**Figure 2E**). Intriguingly, a recent review from the Topilko laboratory revealed a new piece of data that shows that *Krox20*$^{+}$ BC cells project membrane processes across the MEP TZ into the ventral spinal cord (Radomska and Topilko, 2017). These recent data are consistent with our longstanding hypothesis that BC cells might be a diverse cell population and include a subpopulation of centrally-derived cells, analogous to zebrafish MEP glia (**Figure 2D**). Consistent with this hypothesis, a recent study demonstrates that in a demyelination context, Olig2^{+} cells residing within the mouse spinal cord give rise to SCs, which are usually NC-derived (Zawadzka et al., 2010). Is this phenomenon a response to demyelination, or does it also exist under normal circumstances? Previous studies describe the identification of perineurial glia, the glial cells that form the perineurium found around peripheral motor nerves, and demonstrate that they are CNS-derived in *Drosophila*, zebrafish and mouse (Sepp et al., 2001; Kucenas et al., 2008; Clark et al., 2014; Kucenas, 2015). However, the origin of perineurial glia was of intense debate for decades as they were previously thought to be fibroblasts. Could this model of CNS-derived peripheral glia apply to other cell types? Understanding the diversity of origin for glial cells and their ability to be specified in one region of the nervous system but function in another, could provide insight into cell interaction, segregation and selective gating mechanisms.

CONCLUSION

MEP glial development and function raise many new questions. What are the signals mediating OPC-MEP glial interactions across the MEP TZ? Do MEP glia also interact with SCs and via which molecular mechanisms? Does this novel, centrally-derived glial cell population adopt a central-like myelination pattern, involving the extension of multiple membrane processes to wrap more than one axonal segment? Or does it behave more like a Schwann cell, ensheathing a single axonal segment in a truly peripheral-like fashion? Or alternatively, is MEP glial myelin a kind of hybrid myelin featuring both central and peripheral characteristics? How do MEP glia myelinate if they do not require Krox20 or Gpr126? Electron microscopy of the MEP TZ will be needed to examine MEP glial development at the ultrastructural level to characterize their myelin sheaths that connect the CNS and PNS. RNA-sequencing coupled to genome editing tools such as CRISPR/Cas9 will shed light on the molecular mechanisms that drive MEP glial development, their gating function and differentiation into peripheral myelinating glia. Recent studies in zebrafish have uncovered the existence of novel centrally-derived myelinating glia that function in the PNS and are required for nervous system TZ integrity, and future work may change our way of thinking about mammalian myelinating glia as well.

AUTHOR CONTRIBUTIONS

LF wrote the manuscript with input from SK.

FUNDING

This work was supported by grants from the NIH/National Institute of Neurological Disorders and Stroke (NINDS; R01NS072212 and R21NS092070), The Hartwell Foundation and The Owens Family Foundation.

ACKNOWLEDGMENTS

We thank Maria Ali and Andrew Latimer for their helpful comments on the manuscript.

REFERENCES

Almeida, R. G., Czopka, T., Ffrench-Constant, C., and Lyons, D. A. (2011). Individual axons regulate the myelinating potential of single oligodendrocytes *in vivo*. *Development* 138, 4443–4450. doi: 10.1242/dev.071001

Almeida, R. G., and Lyons, D. A. (2017). On myelinated axon plasticity and neuronal circuit formation and function. *J. Neurosci.* 37, 10023–10034. doi: 10.1523/JNEUROSCI.3185-16.2017

Auer, F., Vagionitis, S., and Czopka, T. (2018). Evidence for myelin sheath remodeling in the CNS revealed by *in vivo* imaging. *Curr. Biol.* 28, 549–559. doi: 10.1016/j.cub.2018.01.017

Bergles, D. E., and Richardson, W. D. (2015). Oligodendrocyte development and plasticity. *Cold Spring Harb. Perspect. Biol.* 8:a020453. doi: 10.1101/cshperspect.a020453

Bravo-Ambrosio, A., and Kaprielian, Z. (2011). Crossing the border: molecular control of motor axon exit. *Int. J. Mol. Sci.* 12, 8539–8561. doi: 10.3390/ijms12128539

Bron, R., Vermeren, M., Kokot, N., Andrews, W., Little, G. E., Mitchell, K. J., et al. (2007). Boundary cap cells constrain spinal motor neuron somal migration at motor exit points by a semaphorin-plexin mechanism. *Neural Dev.* 2:21. doi: 10.1186/1749-8104-2-21

Brösamle, C., and Halpern, M. E. (2002). Characterization of myelination in the developing zebrafish. *Glia* 39, 47–57. doi: 10.1002/glia.10088

Chauvet, S., and Rougon, G. (2008). Semaphorins deployed to repel cell migrants at spinal cord borders. *J. Biol.* 7:4. doi: 10.1186/jbiol65

Clark, J. K., O'keefe, A., Mastracci, T. L., Sussel, L., Matise, M. P., and Kucenas, S. (2014). Mammalian *Nkx2.2*$^{+}$ perineurial glia are essential for motor nerve development. *Dev. Dyn.* 243, 1116–1129. doi: 10.1002/dvdy.24158

Coulpier, F., Decker, L., Funalot, B., Vallat, J.-M., Garcia-Bragado, F., Charnay, P., et al. (2010). CNS/PNS boundary transgression by central glia in the absence of Schwann cells or Krox20/Egr2 function. *J. Neurosci.* 30, 5958–5967. doi: 10.1523/JNEUROSCI.0017-10.2010

Coulpier, F., Le Crom, S., Maro, G. S., Manent, J., Giovannini, M., Maciorowski, Z., et al. (2009). Novel features of boundary cap cells revealed by the analysis of newly identified molecular markers. *Glia* 57, 1450–1457. doi: 10.1002/glia.20862

Doucette, R. (1991). PNS-CNS transitional zone of the first cranial nerve. *J. Comp. Neurol.* 312, 451–466. doi: 10.1002/cne.903120311

Dutton, K. A., Pauliny, A., Lopes, S. S., Elworthy, S., Carney, T. J., Rauch, J., et al. (2001). Zebrafish *colourless* encodes *sox10* and specifies non-ectomesenchymal neural crest fates. *Development* 128, 4113–4125.

Etxeberria, A., Hokanson, K. C., Dao, D. Q., Mayoral, S. R., Mei, F., Redmond, S. A., et al. (2016). Dynamic modulation of myelination in response to visual stimuli alters optic nerve conduction velocity. *J. Neurosci.* 36, 6937–6948. doi: 10.1523/JNEUROSCI.0908-16.2016

Fontenas, L., and Kucenas, S. (2017). Livin' on the edge: glia shape nervous system transition zones. *Curr. Opin. Neurobiol.* 47, 44–51. doi: 10.1016/j.conb.2017.09.008

Fraher, J. P. (2002). Axons and glial interfaces: ultrastructural studies*. *J. Anat.* 200, 415–430. doi: 10.1046/j.1469-7580.2002.00037.x

Fraher, J. P., Dockery, P., O'Donoghue, O., Riedewald, B., and O'leary, D. (2007). Initial motor axon outgrowth from the developing central nervous system. *J. Anat.* 211, 600–611. doi: 10.1111/j.1469-7580.2007.00807.x

Fraher, J. P., and Kaar, G. F. (1984). The transitional node of ranvier at the junction of the central and peripheral nervous systems: an ultrastructural-study of its development and mature form. *J. Anat.* 139, 215–238.

Franklin, R. J. M., and Blakemore, W. F. (1993). Requirements for Schwann-cell migration within cns environments: a viewpoint. *Int. J. Dev. Neurosci.* 11, 641–649. doi: 10.1016/0736-5748(93)90052-f

Garrett, A. M., Jucius, T. J., Sigaud, L. P. R., Tang, F.-L., Xiong, W.-C., Ackerman, S. L., et al. (2016). Analysis of expression pattern and genetic deletion of *Netrin5* in the developing mouse. *Front. Mol. Neurosci.* 9:3. doi: 10.3389/fnmol.2016.00003

Gilmour, D. T., Maischein, H.-M., and Nüsslein-Volhard, C. (2002). Migration and function of a glial subtype in the vertebrate peripheral nervous system. *Neuron* 34, 577–588. doi: 10.1016/s0896-6273(02)00683-9

Golding, J. P., and Cohen, J. (1997). Border controls at the mammalian spinal cord: late-surviving neural crest boundary cap cells at dorsal root entry sites may regulate sensory afferent ingrowth and entry zone morphogenesis. *Mol. Cell. Neurosci.* 9, 381–396. doi: 10.1006/mcne.1997.0647

Gould, R. M., Oakley, T., Goldstone, J. V., Dugas, J. C., Brady, S. T., and Gow, A. (2008). Myelin sheaths are formed with proteins that originated in vertebrate lineages. *Neuron Glia Biol.* 4, 137–152. doi: 10.1017/S1740925x09990238

Gresset, A., Coulpier, F., Gerschenfeld, G., Jourdon, A., Matesic, G., Richard, L., et al. (2015). Boundary caps give rise to neurogenic stem cells and terminal glia in the skin. *Stem Cell Reports* 5, 278–290. doi: 10.1016/j.stemcr.2015.06.005

Hines, J. H., Ravanelli, A. M., Schwindt, R., Scott, E. K., and Appel, B. (2015). Neuronal activity biases axon selection for myelination *in vivo*. *Nat. Neurosci.* 18, 683–689. doi: 10.1038/nn.3992

Hochgreb-Hägele, T., and Bronner, M. E. (2013). A novel FoxD3 gene trap line reveals neural crest precursor movement and a role for FoxD3 in their specification. *Dev. Biol.* 374, 1–11. doi: 10.1016/j.ydbio.2012.11.035

Jessen, K. R., and Mirsky, R. (2005). The origin and development of glial cells in peripheral nerves. *Nat. Rev. Neurosci.* 6, 671–682. doi: 10.1038/nrn1746

Kelsh, R. N., and Eisen, J. S. (2000). The zebrafish colourless gene regulates development of non-ectomesenchymal neural crest derivatives. *Development* 127, 515–525.

Kirby, B. B., Takada, N., Latimer, A. J., Shin, J., Carney, T. J., Kelsh, R. N., et al. (2006). *In vivo* time-lapse imaging shows dynamic oligodendrocyte progenitor behavior during zebrafish development. *Nat. Neurosci.* 9, 1506–1511. doi: 10.1038/nn1803

Koudelka, S., Voas, M. G., Almeida, R. G., Baraban, M., Soetaert, J., Meyer, M. P., et al. (2016). Individual neuronal subtypes exhibit diversity in CNS myelination mediated by synaptic vesicle release. *Curr. Biol.* 26, 1447–1455. doi: 10.1016/j.cub.2016.03.070

Kucenas, S. (2015). Perineurial glia. *Cold Spring Harb. Perspect. Biol.* 7:a020511. doi: 10.1101/cshperspect.a020511

Kucenas, S., Takada, N., Park, H. C., Woodruff, E., Broadie, K., and Appel, B. (2008). CNS-derived glia ensheath peripheral nerves and mediate motor root development. *Nat. Neurosci.* 11, 143–151. doi: 10.1038/nn2025

Kucenas, S., Wang, W. D., Knapik, E. W., and Appel, B. (2009). A selective glial barrier at motor axon exit points prevents oligodendrocyte migration from the spinal cord. *J. Neurosci.* 29, 15187–15194. doi: 10.1523/JNEUROSCI.4193-09.2009

Lee, S., Leach, M. K., Redmond, S. A., Chong, S. Y., Mellon, S. H., Tuck, S. J., et al. (2012). A culture system to study oligodendrocyte myelination processes using engineered nanofibers. *Nat. Methods* 9, 917–922. doi: 10.1038/nmeth.2105

Lyons, D. A., Pogoda, H.-M., Voas, M. G., Woods, I. G., Diamond, B., Nix, R., et al. (2005). *erbb3* and *erbb2* are essential for schwann cell migration and myelination in zebrafish. *Curr. Biol.* 15, 513–524. doi: 10.1016/j.cub.2005.02.030

Maro, G. S., Vermeren, M., Voiculescu, O., Melton, L., Cohen, J., Charnay, P., et al. (2004). Neural crest boundary cap cells constitute a source of neuronal and glial cells of the PNS. *Nat. Neurosci.* 7, 930–938. doi: 10.1038/nn1299

Mauti, O., Domanitskaya, E., Andermatt, I., Sadhu, R., and Stoeckli, E. T. (2007). Semaphorin6A acts as a gate keeper between the central and the peripheral nervous system. *Neural Dev.* 2:28. doi: 10.1186/1749-8104-2-28

Mensch, S., Baraban, M., Almeida, R., Czopka, T., Ausborn, J., El Manira, A., et al. (2015). Synaptic vesicle release regulates myelin sheath number of individual oligodendrocytes *in vivo*. *Nat. Neurosci.* 18, 628–630. doi: 10.1038/nn.3991

Monk, K. R., Naylor, S. G., Glenn, T. D., Mercurio, S., Perlin, J. R., Dominguez, C., et al. (2009). A G protein-coupled receptor is essential for Schwann cells to initiate myelination. *Science* 325, 1402–1405. doi: 10.1126/science.1173474

Morris, A. D., Lewis, G. M., and Kucenas, S. (2017). Perineurial glial plasticity and the role of TGF-β in the development of the blood-nerve barrier. *J. Neurosci.* 37, 4790–4807. doi: 10.1523/JNEUROSCI.2875-16.2017

Newbern, J., and Birchmeier, C. (2010). Nrg1/ErbB signaling networks in Schwann cell development and myelination. *Semin. Cell Dev. Biol.* 21, 922–928. doi: 10.1016/j.semcdb.2010.08.008

Niederländer, C., and Lumsden, A. (1996). Late emigrating neural crest cells migrate specifically to the exit points of cranial branchiomotor nerves. *Development* 122, 2367–2374.

Odenthal, J., and Nüsslein-Volhard, C. (1998). Fork head domain genes in zebrafish. *Dev. Genes Evol.* 208, 245–258. doi: 10.1007/s004270050179

Perlin, J. R., Lush, M. E., Stephens, W. Z., Piotrowski, T., and Talbot, W. S. (2011). Neuronal neuregulin 1 type III directs Schwann cell migration. *Development* 138, 4639–4648. doi: 10.1242/dev.068072

Radomska, K. J., and Topilko, P. (2017). Boundary cap cells in development and disease. *Curr. Opin. Neurobiol.* 47, 209–215. doi: 10.1016/j.conb.2017.11.003

Ravanelli, A. M., and Appel, B. (2015). Motor neurons and oligodendrocytes arise from distinct cell lineages by progenitor recruitment. *Genes Dev.* 29, 2504–2515. doi: 10.1101/gad.271312.115

Sepp, K. J., Schulte, J., and Auld, V. J. (2001). Peripheral glia direct axon guidance across the CNS/PNS transition zone. *Dev. Biol.* 238, 47–63. doi: 10.1006/dbio.2001.0411

Smith, C. J., Johnson, K., Welsh, T. G., Barresi, M. J., and Kucenas, S. (2016). Radial glia inhibit peripheral glial infiltration into the spinal cord at motor exit point transition zones. *Glia* 64, 1138–1153. doi: 10.1002/glia.22987

Smith, C. J., Morris, A. D., Welsh, T. G., and Kucenas, S. (2014). Contact-mediated inhibition between oligodendrocyte progenitor cells and motor exit point glia establishes the spinal cord transition zone. *PLoS Biol.* 12:e1001961. doi: 10.1371/journal.pbio.1001961

Takada, N., Kucenas, S., and Appel, B. (2010). Sox10 is necessary for oligodendrocyte survival following axon wrapping. *Glia* 58, 996–1006. doi: 10.1002/glia.20981

Taveggia, C., Zanazzi, G., Petrylak, A., Yano, H., Rosenbluth, J., Einheber, S., et al. (2005). Neuregulin-1 type III determines the ensheathment fate of axons. *Neuron* 47, 681–694. doi: 10.1016/j.neuron.2005.08.017

Topilko, P., Schneider-Maunoury, S., Levi, G., Baron-Van Evercooren, A., Chennoufi, A. B., Seitanidou, T., et al. (1994). Krox-20 controls myelination in the peripheral nervous system. *Nature* 371, 796–799. doi: 10.1038/371796a0

Vermeren, M., Maro, G. S., Bron, R., McGonnell, I. M., Charnay, P., Topilko, P., et al. (2003). Integrity of developing spinal motor columns is regulated by neural crest derivatives at motor exit points. *Neuron* 37, 403–415. doi: 10.1016/s0896-6273(02)01188-1

Voas, M. G., Glenn, T. D., Raphael, A. R., and Talbot, W. S. (2009). Schwann cells inhibit ectopic clustering of axonal sodium channels. *J. Neurosci.* 29, 14408–14414. doi: 10.1523/JNEUROSCI.0841-09.2009

Welsh, T. G., and Kucenas, S. (2018). Purinergic signaling in oligodendrocyte development and function. *J. Neurochem.* 145, 6–18. doi: 10.1111/jnc.14315

Wilkinson, D. G., Bhatt, S., Chavrier, P., Bravo, R., and Charnay, P. (1989). Segment-specific expression of a zinc-finger gene in the developing nervous system of the mouse. *Nature* 337, 461–464. doi: 10.1038/337461a0

Zalc, B. (2016). The acquisition of myelin: an evolutionary perspective. *Brain Res.* 1641, 4–10. doi: 10.1016/j.brainres.2015.09.005

Zawadzka, M., Rivers, L. E., Fancy, S. P., Zhao, C., Tripathi, R., Jamen, F., et al. (2010). CNS-resident glial progenitor/stem cells produce Schwann cells as well as oligodendrocytes during repair of CNS demyelination. *Cell Stem Cell* 6, 578–590. doi: 10.1016/j.stem.2010.04.002

Conflict of Interest Statement: The authors declare that the research was conducted in the absence of any commercial or financial relationships that could be construed as a potential conflict of interest.

frontiers in Cellular Neuroscience

MINI REVIEW
published: 15 October 2018
doi: 10.3389/fncel.2018.00367

The Rules of Attraction in Central Nervous System Myelination

*Rafael Góis Almeida**

Centre for Discovery Brain Sciences, The University of Edinburgh, Edinburgh, United Kingdom

The wrapping of myelin around axons is crucial for the development and function of the central nervous system (CNS) of vertebrates, greatly regulating the conduction of action potentials. Oligodendrocytes, the myelinating glia of the CNS, have an intrinsic tendency to wrap myelin around any permissive structure *in vitro*, but *in vivo*, myelin is targeted with remarkable specificity only to certain axons. Despite the importance of myelination, the mechanisms by which oligodendrocytes navigate a complex milieu that includes many types of cells and their cellular projections and select only certain axons for myelination remains incompletely understood. In this Mini-review, I highlight recent studies that shed light on the molecular and cellular rules governing CNS myelin targeting.

Keywords: axon-glia interactions, oligodendrocyte, myelin, attraction, targeting

OPEN ACCESS

Edited by:
Fernando C. Ortiz,
Universidad Autónoma de Chile, Chile

Reviewed by:
Barbara Ranscht,
Sanford Burnham Prebys Medical Discovery Institute (SBP), United States
Ethan Hughes,
University of Colorado Denver, United States

***Correspondence:**
Rafael Góis Almeida
rgalmeid@staffmail.ed.ac.uk

Received: *20 August 2018*
Accepted: *27 September 2018*
Published: *15 October 2018*

Citation:
Almeida RG (2018) The Rules of Attraction in Central Nervous System Myelination. Front. Cell. Neurosci. 12:367. doi: 10.3389/fncel.2018.00367

INTRODUCTION

Vertebrates require myelin, specialized membrane wrapped by oligodendrocytes around axons, for their nervous systems to function. Myelination drastically changes an axon's physiology: by insulating it and clustering sodium channels in the short unmyelinated nodes of Ranvier, myelin accelerates action potential propagation in a space-efficient manner (Waxman, 1997; Hartline and Colman, 2007), and facilitates high-frequency firing (Fields, 2008; Perge et al., 2012; Sinclair et al., 2017). Oligodendrocytes are now also thought to transfer glycolytic substrates to the underlying axon (Saab et al., 2016; Saab and Nave, 2017). The importance of myelinating oligodendrocytes is underscored by the severe consequences of their disruption in several neurodegenerative conditions (Philips and Rothstein, 2014; Pouwels et al., 2014; Franklin and Ffrench-Constant, 2017). Furthermore, dynamic regulation of myelin is increasingly implicated in cognitive processes including learning, memory, and social interaction (Fields, 2008, 2015; Zeidán-Chuliá et al., 2014; Filley and Fields, 2016). Given how myelin drastically affects neuronal function, it must be targeted precisely to those axons that need it and excluded from incorrect targets. Indeed, not every axon in the central nervous system (CNS) becomes myelinated: for instance, small axons (< 0.2 μm diameter) remain unmyelinated, as do many large axons even in myelin-rich white matter tracts (Olivares et al., 2001; Saliani et al., 2017). Furthermore, neuronal somas and dendrites remain unmyelinated, as do non-neuronal cells. **How is this selectivity achieved *in vivo*, in the complex milieu of the CNS?** The precision of myelin targeting is especially remarkable given that oligodendrocytes cultured in the complete absence of axons readily deposit myelin on inert surfaces (Rosenberg et al., 2008;

Aggarwal et al., 2011; Lee et al., 2012; Bechler et al., 2015). Thus, *in vivo*, the tendency of oligodendrocytes to myelinate promiscuously appears tightly regulated by the attraction or repulsion of prospective targets, which we are only now beginning to understand. In this Mini-Review, I will highlight recent studies that shed light on some of the molecular and cellular mechanisms of CNS myelin targeting.

WHEN DOES AN OLIGODENDROCYTE SELECT ITS TARGETS?

Recent studies have now shown that oligodendrogenesis and myelination are life-long processes (Miller et al., 2012; Hill et al., 2018; Hughes et al., 2018), and that myelination in adults can be responsive, for instance, to neuronal activity (Almeida and Lyons, 2017; Mount and Monje, 2017; Sampaio-Baptista and Johansen-Berg, 2017). Thus, myelin targeting mechanisms must operate not just during development, but throughout life. But when does targeting occur during the life-course of an oligodendrocyte-lineage cell? Oligodendrocytes are generated from proliferative oligodendrocyte precursor cells (OPCs), which arise from ventricular germinal zones of the brain and spinal cord and migrate to populate the entire CNS (Richardson et al., 2006). Extrinsic signals and an intrinsic developmental program cooperate to induce OPCs to differentiate into oligodendrocytes, ensheathe axons, and synthesize myelin (Zuchero and Barres, 2013). During and after migration, OPCs and newly differentiated oligodendrocytes extend and retract numerous dynamic filopodia-like processes (Kirby et al., 2006; Hughes et al., 2013) that contact the surrounding milieu, including structures such as axonal and dendritic surfaces, neuronal and glial somas, and blood vessels. Time-lapse imaging studies have provided the remarkable insight that each newly differentiated oligodendrocyte forms all its myelin sheaths in a short hours-long period (Watkins et al., 2008; Czopka et al., 2013). Following this period, stabilized sheaths elongate, but no new sheaths are formed, and only a minority are retracted over the next few days. Importantly, even during the short period of sheath initiation, only a minority of nascent sheaths are retracted (Czopka et al., 2013; Liu et al., 2013), suggesting that most axonal targets are successfully selected beforehand. Thus, the dynamic behavior of filopodia-like processes of newly differentiated oligodendrocytes may well serve to 'interview' prospective targets in its vicinity, and local interactions (e.g., between axonal and oligodendrocyte cell-adhesion molecules) may be transduced into the process to stabilize some contacts and retract others. The observation that some newly formed myelin sheaths are subsequently retracted suggests that some correction of mistargeted sheaths that escaped initial selection occurs later. Following differentiation, oligodendrocytes and their myelin are remarkably stable for many months (Tripathi et al., 2017; Hill et al., 2018; Hughes et al., 2018). Thus, myelin targeting occurs in a short period in the life of an oligodendrocyte, and appears to include two stages: first, target *selection* takes place as an oligodendrocyte-lineage cell settles, differentiates, and forms nascent sheaths; followed by a target *refinement* stage in the following days, when some sheaths are retracted (**Figure 1A**).

WHICH SIGNALS TARGET MYELIN TO AXONS?

The contact and recognition of target surfaces by oligodendrocyte processes constitute the first step in CNS myelin targeting. Remarkably, the biophysical properties of a surface as well as the molecules it bears can determine its myelination fate.

Biophysical Factors

In vitro, oligodendrocytes avoid small-diameter fibers under a threshold diameter of 0.4 μm, and myelinate only larger fibers (Lee et al., 2012; Bechler et al., 2015), which is reminiscent of the distribution of myelinated CNS axons *in vivo* (Remahl and Hildebrand, 1982; Hildebrand et al., 1993). Thus, small-diameter cylindrical structures, which present a high-curvature surface to the oligodendrocyte process, appear non-permissive for myelination, in contrast to larger-diameter cylinders with a lower curvature. Oligodendrocytes are also able to target their myelin to non-cylindrical structures *in vitro* such as spherical polystyrene beads around 20 μm in diameter (Redmond et al., 2016), flat surfaces such as glass coverslips (Aggarwal et al., 2011), and conical micropillars (Mei et al., 2014), with an even lower curvature, suggesting that this is an important biophysical constraint for myelination (**Figure 1B**). Do oligodendrocyte processes actively sense curvature? Bechler et al. (2015, 2018) propose that as they myelinate their targets, oligodendrocytes must sense axonal curvature, since they adjust sheath lengths to the axonal diameter. This could rely, for instance, on the curvature-dependent activity of certain membrane-anchored proteins (Chang-Ileto et al., 2011; McMahon and Boucrot, 2015; **Figure 1C**), or on a mechanism analogous to the curvature-sensitive septin cytoskeleton (Bridges et al., 2016; Osso and Chan, 2017). Alternatively, oligodendrocytes could detect the length of the first complete wrap around the axonal perimeter and induce process retraction if under a threshold length (Osso and Chan, 2017; **Figure 1C**).

These *in vitro* observations suggest that biophysical properties of prospective targets, such as their size, could dictate their permissiveness for myelination. In fact, driving an increase in the diameter of cerebellar granule cell axons, which are typically small and unmyelinated, is sufficient to target them for myelination (Goebbels et al., 2017). It remains possible, however, that axonal signals that tightly correlate with axonal diameter could underlie such an effect *in vivo*. Indeed, in the peripheral nervous system (PNS), only axons strictly above 1 μm in diameter become myelinated by Schwann cells, and only these large axons expressed a high level of membrane-anchored Neuregulin 1 (Nrg1) type III (Taveggia et al., 2005). This signal turned out to mediate the correlation of axonal caliber with PNS myelination: genetic ablation of Nrg1-III greatly reduces myelination including in large, supra-threshold axons; while its overexpression in small-diameter, typically unmyelinated axons is capable of converting

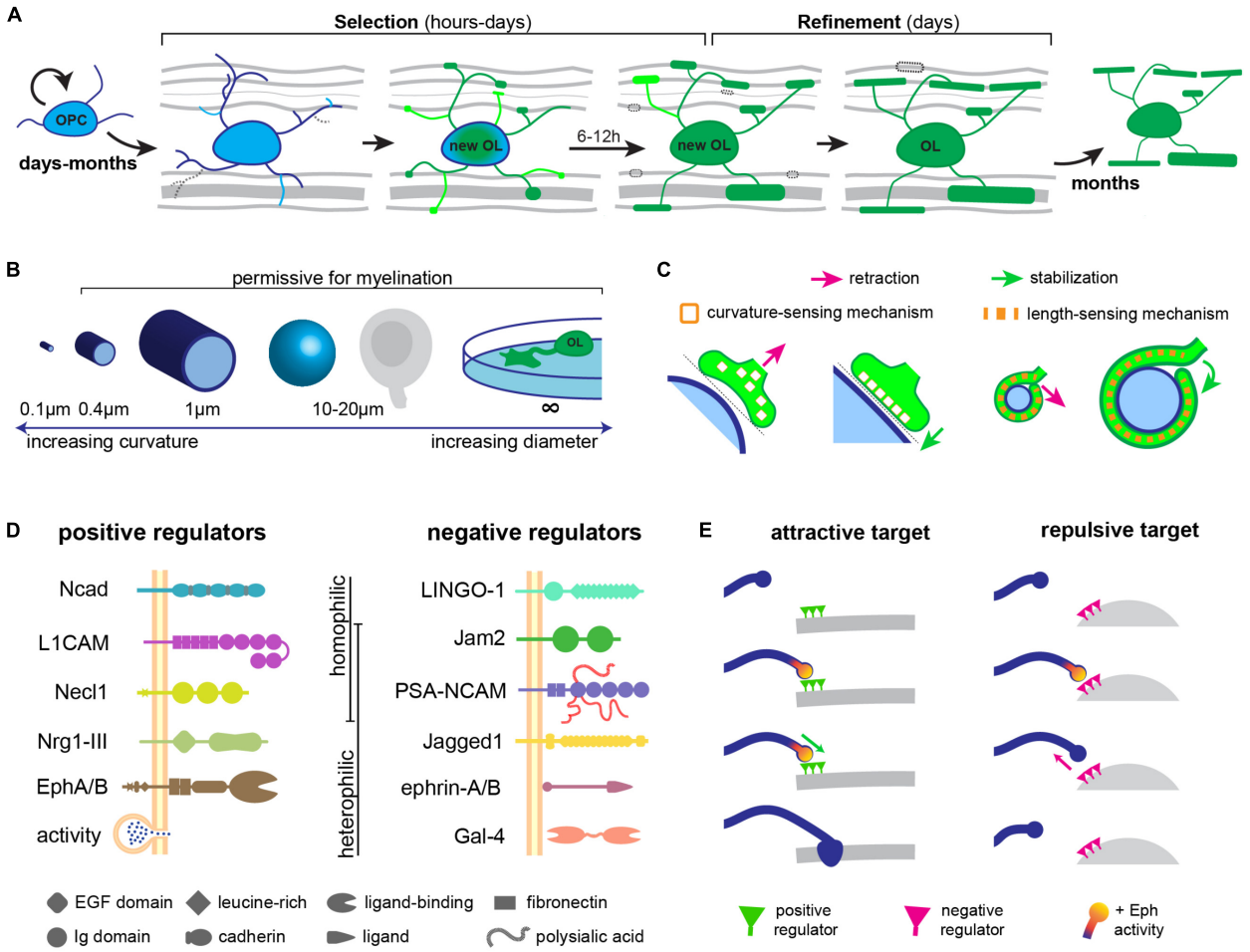

FIGURE 1 | Regulation of CNS myelin targeting. **(A)** myelin is targeted in a short period in the life of an oligodendrocyte (OL): a selection stage during differentiation and a refinement stage after differentiation. **(B)** Biophysical properties of diameter and/or curvature determine the permissiveness of a target for myelination. **(C)** Curvature or length-sensing proteins in oligodendrocyte processes may sense appropriately sized targets. **(D)** Attractive and repulsive cell-adhesion molecules on prospective targets regulating CNS myelination. **(E)** Similar to synapse formation, the temporal dynamics of key signaling pathways (e.g., Eph) may determine the fate of OPC processes during myelin target selection.

them to a myelinated fate (Michailov et al., 2004; Taveggia et al., 2005). Thus, similar membrane-anchored axonal signals might mediate the preference of oligodendrocytes for larger targets in the CNS. Indeed, the geometric permissivity of a prospective target cannot fully explain CNS myelin targeting: axons between 0.4 and 1 µm in diameter can be either unmyelinated or myelinated (Hildebrand et al., 1993), and many somas and dendrites of permissive geometries and accessible to oligodendrocytes remain essentially unmyelinated. This indicates that an additional layer of regulation of myelin targeting must exist *in vivo*. In fact, both attractive and repulsive molecular cues can directly regulate myelin targeting (**Figure 1D**).

Attractive Signals

In the PNS, axonal expression of Nrg1-III is sufficient to instruct Schwann cells to myelinate axons (Michailov et al., 2004; Taveggia et al., 2005). To date, no such molecule has been identified whose disruption completely prevents CNS myelination, suggesting that multiple redundant signals might exist. Indeed, several axonal molecules have been found to promote CNS myelination: although not strictly required for CNS myelination, pan-neuronal overexpression of Nrg1 type III increases the number of axons targeted for myelination in the optic nerve and cortex, including typically unmyelinated small-diameter axons (Brinkmann et al., 2008). Axons and oligodendrocytes also express multiple Eph tyrosine kinase receptors and their ephrin membrane-bound ligands, whose *trans*-interactions induce bidirectional signaling to regulate adhesion in adjacent cells. Primary rat OPCs cultured on EphA4/B1 substrates have increased myelination, suggesting that binding of axonal EphA4/B1 receptors to the oligodendrocyte ligand ephrin-B induces reverse signaling in oligodendrocytes that promotes myelin sheath formation (Linneberg et al., 2015), and could thus target myelin to specific axons. Axonal L1-CAM can bind to contactin and integrin complexes in

oligodendrocytes and increase myelination *in vitro* (Laursen et al., 2009). N-cadherin, a calcium-dependent cell-adhesion molecule expressed in both axons and oligodendrocytes, is necessary during the initial axon-OPC interactions, as blocking its function greatly reduced the duration of these contacts, leading to reduced myelination (Schnädelbach et al., 2001; Chen et al., 2017). Genetic ablation of Nectin-like 1, a neuronal member of the synaptic cell adhesion molecule family, reduced the number of spinal cord and optic nerve axons targeted for myelination, albeit only transiently (Park et al., 2008).

An exciting finding is the recent observation that neuronal activity can also regulate the targeting of myelin to specific axons, in addition to long-standing observations that activity also influences OPC proliferation (Barres and Raff, 1993; Li et al., 2010; Gibson et al., 2014), oligodendrocyte differentiation and survival (Hill et al., 2014; McKenzie et al., 2014; Hughes et al., 2018) and myelin formation itself (Demerens et al., 1996; Makinodan et al., 2012; Liu et al., 2012). Recent studies in the zebrafish spinal cord have shown that blocking action potentials or activity-dependent vesicle release disrupted the targeting of myelin to a stereotyped subset of spinal cord axons and the degree of their myelination (Hines et al., 2015; Mensch et al., 2015). Indeed, Hines et al. (2015) observed that synaptophysin-containing vesicles accumulated in the axon at sites of oligodendrocyte ensheathment, suggesting that vesicle cargos such as neurotransmitters or cell-adhesion molecules could attract or stabilize nascent sheaths. In line with these studies, chemogenetic activation of individual somatosensory neurons in mice increased their targeting for myelination (Mitew et al., 2018). *In vitro* studies have suggested that glutamate release, which can locally stimulate oligodendrocyte Fyn kinase signaling and myelin protein synthesis (Wake et al., 2011, 2015), is the key vesicle cargo mediating these effects (Spitzer et al., 2016). However, the precise glutamate receptors in oligodendrocytes that specifically mediate a myelination effect *in vivo* remain unclear (De Biase et al., 2011; Guo et al., 2012), and other signals may play a role, including neurotrophins and cell-adhesion molecules such as Nrg1 (Liu et al., 2011; Lundgaard et al., 2013) and N-cadherin (Tan et al., 2010) whose expression or surface localization are sensitive to activity. Furthermore, Koudelka et al. (2016) found that such activity-regulated myelin targeting is a property of some neuronal subtypes but not others, suggesting that activity-dependent and independent mechanisms cooperate to appropriate myelinate the CNS.

Repulsive Signals

Given the promiscuity of oligodendrocyte myelination, vertebrates might employ repulsive signals not only to decide which axons remain unmyelinated, but also to temporally control the onset of myelination along axons fated for myelination, and to prevent ectopic myelination of inappropriate compartments within a neuron such as its soma or dendrites. Negative signals may also be employed within individual axons to target myelin to specific domains: recent imaging studies have shown that many CNS axons are only partially myelinated *in vivo*, with long segments remaining persistently unmyelinated, which may be important to modulate their conduction and functional output (Tomassy et al., 2014; Auer et al., 2018; Hill et al., 2018; Hughes et al., 2018).

Negative regulators include some of the Eph-ephrin molecules expressed in axons and oligodendrocyte-lineage cells. Axonal ephrin-A1/B2 *forward* signaling through EphA/B receptors on oligodendrocytes can induce process retraction and reduce myelination *in vitro* and *in vivo* (Linneberg et al., 2015; Harboe et al., 2018). Indeed, ephrin-A1 expression in neurons reduced their myelination in the zebrafish spinal cord, by interacting with the EphA4 receptor on oligodendrocytes, whose knockdown increased the number of axons myelinated by individual oligodendrocytes (Harboe et al., 2018). Ephrin-Eph binding induces both forward signaling in the receptor-expressing cell and reverse signaling in the ephrin-expressing cell which can be regulated independently (Pasquale, 2008). This may explain why an EphA4 substrate can also promote myelination of rat OPCs *in vitro* (Linneberg et al., 2015): due to oligodendroglial ephrin (not Eph)-induced signaling. Both neurons and oligodendrocytes express multiple ephrin ligands and Eph receptors, and the cellular context in which specific ephrin-Eph binding occurs may influence the resulting cell behavior. Thus, a precise combinatorial code of axonal Eph and ephrin molecules could determine myelin targeting in the CNS. Importantly, dysregulation of Eph-ephrin did not affect oligodendrocyte differentiation, suggesting a specific role in regulating cell adhesion and targeting.

Other repulsive signals include polysialylated neural cell-adhesion molecule (PSA-NCAM), which is downregulated at the onset of myelination *in vivo* (Nait Oumesmar et al., 1995; Charles et al., 2000). Blocking PSA-NCAM increased the number of myelinated axons, while overexpressing it reduced myelination *in vivo* (Meyer-Franke et al., 1999; Charles et al., 2000; Fewou et al., 2007), potentially by preventing adhesive interactions. LINGO-1 is a transmembrane protein expressed in both axons and oligodendrocytes (Jepson et al., 2012) whose knock-out (Mi et al., 2005) or transgenic overexpression in neurons (Lee et al., 2007), respectively, increase and decrease the number of axons targeted for myelination in the spinal cord. Jagged1, the transmembrane ligand for the Notch1 receptor expressed in oligodendrocytes, is expressed by retinal ganglion cells in the optic nerve, where it signals to prevent OPC differentiation and myelination (Wang et al., 1998). In Notch1 heterozygotes, more axons become myelinated in the optic nerve, and axons in the molecular layer of the cerebellum, which never become myelinated, are also selected for myelination (Givogri et al., 2002).

Redmond et al. (2016) recently identified a negative regulator of neuronal somatodendritic myelination, the cell-adhesion molecule Jam2. Having determined that oligodendrocytes could myelinate soma-sized polystyrene beads *in vitro*, Redmond et al. (2016) searched for repulsive signals that prevent somatodendritic myelination *in vivo* using an elegant strategy of differential RNAseq profiling. By comparing spinal cord neuron cultures, which should employ such repulsive signals

to prevent myelination of their many dendrites and soma, to dendrite-less dorsal root ganglion neuron cultures, Redmond et al. (2016) identified Jam2 as an inhibitory signal. This transmembrane protein with extracellular immunoglobulin domains was able to repel oligodendrocyte processes and reduce myelination *in vitro*, without affecting oligodendrocyte differentiation. Oligodendrocytes were able to myelinate the soma and dendrites of cocultured Jam2-knockout neurons, and Redmond et al. (2016) also find ectopically myelinated neurons in the dorsal spinal cord of the Jam2 knockout mouse. Interestingly, all are $Pax2^{+}$ inhibitory interneurons, suggesting that other neuron subtypes use other signals to prevent somatodendritic myelination (Redmond et al., 2016).

More recently, expression of Galectin-4, a lectin transmembrane receptor for glycoproteins, was observed to be inversely correlated with myelination in the rat brain, and to repel myelin formation *in vitro* (Stancic et al., 2012; Díez-Revuelta et al., 2017). Interestingly, Galectin-4 was observed to localize only to unmyelinated segments in hippocampal and cortical neurons (Velasco et al., 2013; Díez-Revuelta et al., 2017), suggesting that it may be one of the signals responsible for maintaining a 'patchy' pattern of myelination along individual axons, patterns which are robustly maintained even upon remyelination (Auer et al., 2018). It will be important to disentangle a 'direct' effect of these molecules in regulating myelin targeting and adhesion from a secondary effect on oligodendrocyte differentiation.

HOW ARE TARGETING SIGNALS TRANSDUCED INTO MYELINATING BEHAVIOR?

The answer is likely to depend on whether they act during target selection, which requires stabilizing or retracting a small, dynamic OPC process; or during refinement, requiring the growth or breakdown of a nascent sheath. It seems plausible that surfaces with a non-permissive geometry, or bearing repulsive signals (e.g., Jam2 or Ephrins) destabilize even the earliest interactions with OPC processes during target selection. How might these signals cause an OPC process to retract? Binding of ephrin-A1 to EphA4 in oligodendrocytes, for instance, induces its phosphorylation and activates an ephexyn1-RhoA-Rock signaling cascade necessary for process retraction (Harboe et al., 2018). Thus, regulation of actin cytoskeleton dynamics, which have independently been shown to underlie the wrapping process (Nawaz et al., 2015; Zuchero et al., 2015), is a likely mediator. Remarkably, this sequence of signaling events is similar to EphA4-dependent signaling underlying dendritic spine retraction (Fu et al., 2007) and axonal growth cone collapse/repulsion (Sahin et al., 2005) in mammalian neurons. This suggests that lessons about myelin targeting may be learned from dendritic and axonal interactions during synaptogenesis, a resemblance we had noted before (Almeida and Lyons, 2014). For instance, a recent study showed that dendritic filopodia of cortical neurons select or reject axonal contacts for synaptogenesis based simply on the kinetics of EphB2 signaling, whereby transient activation leads to filopodia retraction while sustained activation predicts stabilization and synaptogenesis (Mao et al., 2018). It will be interesting to determine if Eph signaling kinetics in OPC processes also predict target selection or rejection (**Figure 1E**).

Other signals are more likely to act during target refinement. For instance, activity-dependent vesicle release may stabilize, rather than attract, nascent sheaths. Neurotransmitter or neurotrophin vesicle cargoes are shared by broad classes of neurons and seem unlikely to regulate target selection on an axon-by-axon basis. Instead, differences in the distribution, timing or frequency of vesicle release in different axons could bias the stabilization and growth of nascent sheaths. How might this be translated to the oligodendrocyte? Two recent elegant *in vivo* studies implicated the second messenger calcium. By imaging the genetically encoded calcium indicator GCaMP6 in oligodendrocytes, Baraban et al. (2018) identified high-amplitude, long-duration calcium elevations within sheaths that eventually retracted, and implicated calpain in the retraction. Similar calcium signatures and calpain involvement regulate dendrite retraction in Drosophila sensory neurons (Kanamori et al., 2013), in another instance of similarity with CNS synaptogenesis. Baraban et al. (2018) also found that among the stabilized sheaths, a higher frequency of low-amplitude, short-duration intracellular calcium elevations predicted faster growth. This was supported by an independent study by Krasnow et al. (2018) who further found that blocking these calcium transients prevented sheath growth, proving that calcium activity is causally linked to myelin elongation. It will be important to determine which effectors lie downstream of calcium for sheath growth. One possibility is that it regulates coordinated cycles of actin assembly and disassembly, implicated in myelin sheath growth (Nawaz et al., 2015; Zuchero et al., 2015). Additionally, targeting signals (transduced by calcium-dependent or independent mechanisms) may converge in well-characterized signaling cascades known to regulate myelination. It will be interesting to assess the activation state of the Akt/mTOR and Erk1/2 pathways within oligodendrocytes during targeting, since they have been implicated in the regulation of wrapping (Goebbels et al., 2010; Domènech-Estévez et al., 2016; Mathews and Appel, 2016) and myelin sheath growth (Ishii et al., 2012, 2013; Fyffe-Maricich et al., 2013; Jeffries et al., 2016). Indeed, hyperactivation of Akt signaling induces hypermyelination in the CNS and PNS, including of typically unmyelinated targets (Flores et al., 2008; Goebbels et al., 2010; Almeida et al., 2018).

IS THERE A HIERARCHY OF MYELIN TARGETING?

We recently tested whether *in vivo* targeting mechanisms were efficient even in conditions with an excess of myelin, such as in the context of potential remyelinating therapies (Almeida et al., 2018). We analyzed zebrafish mutants with

fewer axonal targets for myelination, but normal oligodendrocyte number (Almeida and Lyons, 2016), zebrafish treated with small-molecule epigenetic regulators with increased oligodendrocyte number (Early et al., 2018), and zebrafish and mice with increased myelin production due to stimulation of the Akt1 pathway in oligodendrocytes. Remarkably, despite there being no disruption to any specific molecular targeting mechanism, we observed that myelin was ectopically targeted to neuron somas in the developing spinal cord in all three scenarios. This suggests that some neuron somas may lack strong inhibitory signals and are not normally myelinated due to the finely regulated balance of axonal demand to myelin supply. Interestingly, even in wildtype animals, we found a small degree of myelin targeted to neuron somas. Longitudinal imaging revealed that ectopic myelin is made during the same short period of sheath formation by individual oligodendrocytes, and is corrected over the course of a few days – although not sufficiently in animals with excess oligodendrocytes (Almeida et al., 2018). This suggests that slightly overproducing myelin during development may help ensure robust myelination of appropriate targets, and lends support to the existence of a refinement stage during targeting. Furthermore, in animals with excessive oligodendrocytes, axons that are not normally target for myelination (both of small and large, permissive diameters) remained unmyelinated, despite being accessible to oligodendrocytes. Our observations suggest that myelin may be targeted in a hierarchical manner: first to attractive axons; then to less attractive (but not refractory) targets including some axons and some neuronal somas, and finally excluded from refractory small-diameter or repellent axons. Our study suggests that the long-standing observation that axons can regulate the development of the oligodendrocyte population serves not only to guarantee sufficient myelination of the appropriate targets (Barres and Raff, 1999; Klingseisen and Lyons, 2018), but also to minimize ectopic myelination of permissive structures. Such an additional regulatory layer of myelin targeting, influencing myelination fate by indirect regulation of oligodendrocyte number in a given region, cooperates with the more direct, target-specific regulation of adhesion to ensure the fidelity of CNS myelination.

CONCLUSION

The complete repertoire of biophysical, attractive and repulsive factors that regulate CNS myelin targeting is likely larger than the current picture, and the rules by which they govern myelin attraction in the CNS complex. For instance, which molecules prevent ectopic myelination of neuron somas, glial cells, and the vasculature? How do complex geometries, such as those of somas bearing numerous dendrites, influence myelin targeting? How is myelin targeting affected by mechanical forces, or by an oligodendrocyte's myelinating capacity? How do biophysical factors interact with molecular signals? Some axons smaller than 0.2 μm in diameter actually become myelinated in the mammalian CNS (Bishop and Smith, 1964; Adinolfi and Pappas, 1968; Matthews, 1968) – these axons may need to employ additional attractive signals to improve adhesion to OPC processes (Simons and Lyons, 2013). Are the same targeting mechanisms employed during early developmental myelination, activity-responsive myelination, and remyelination? Future studies may be informed by the coincident disruption or overexpression of multiple signals in individual cells to investigate how targeting mechanisms cooperate to culminate in the precisely myelinated vertebrate CNS.

AUTHOR CONTRIBUTIONS

RA conceived and wrote the manuscript.

FUNDING

RA is supported by an MRC project grant (MR/P006272/1).

ACKNOWLEDGMENTS

I am indebted to Prof. David Lyons, Dr. Tim Czopka, and Dr. Anna Klingseisen for critical reading of the manuscript and helpful title suggestions.

REFERENCES

Adinolfi, A. M., and Pappas, G. D. (1968). The fine structure of the caudate nucleus of the cat. *J. Comp. Neurol.* 133, 167–184. doi: 10.1002/cne.901330203

Aggarwal, S., Yurlova, L., Snaidero, N., Reetz, C., Frey, S., Zimmermann, J., et al. (2011). A size barrier limits protein diffusion at the cell surface to generate lipid-rich myelin-membrane sheets. *Dev. Cell* 21, 445–456. doi: 10.1016/j.devcel.2011.08.001

Almeida, R., and Lyons, D. (2016). Oligodendrocyte development in the absence of their target axons in vivo. *PLoS One* 11:e0164432. doi: 10.1371/journal.pone.0164432

Almeida, R. G., and Lyons, D. A. (2014). On the resemblance of synapse formation and CNS myelination. *Neuroscience* 276, 98–108. doi: 10.1016/j.neuroscience.2013.08.062

Almeida, R. G., and Lyons, D. A. (2017). On myelinated axon plasticity and neuronal circuit formation and function. *J. Neurosci.* 37, 10023–10034. doi: 10.1523/JNEUROSCI.3185-16.2017

Almeida, R. G., Pan, S., Cole, K. L. H., Williamson, J. M., Early, J. J., Czopka, T., et al. (2018). Myelination of neuronal cell bodies when myelin supply exceeds axonal demand. *Curr. Biol.* 28, 1296.e–1305.e. doi: 10.1016/j.cub.2018.02.068

Auer, F., Vagionitis, S., and Czopka, T. (2018). Evidence for myelin sheath remodeling in the CNS revealed by in vivo imaging. *Curr. Biol.* 28, 549.e3–559.e3. doi: 10.1016/j.cub.2018.01.017

Baraban, M., Koudelka, S., and Lyons, D. A. (2018). Ca 2 + activity signatures of myelin sheath formation and growth in vivo. *Nat. Neurosci.* 21, 19–23. doi: 10.1038/s41593-017-0040-x

Barres, B. A., and Raff, M. C. (1993). Proliferation of oligodendrocyte precursor cells depends on electrical activity in axons. *Nature* 361, 258–260. doi: 10.1038/361258a0

Barres, B. A., and Raff, M. C. (1999). Axonal control of oligodendrocyte development. *J. Cell Biol.* 147, 1123–1128. doi: 10.1083/jcb.147.6.1123

Bechler, M. E., Byrne, L., and Ffrench-Constant, C. (2015). CNS myelin sheath lengths are an intrinsic property of oligodendrocytes. *Curr. Biol.* 25, 2411–2416. doi: 10.1016/j.cub.2015.07.056

Bechler, M. E., Swire, M., and Ffrench-Constant, C. (2018). Intrinsic and adaptive myelination-A sequential mechanism for smart wiring in the brain. *Dev. Neurobiol.* 78, 68–79. doi: 10.1002/dneu.22518

Bishop, G. H., and Smith, J. M. (1964). The sizes of nerve fibers supplying cerebral cortex. *Exp. Neurol.* 9, 483–501. doi: 10.1016/0014-4886(64)90056-1

Bridges, A. A., Jentzsch, M. S., Oakes, P. W., Occhipinti, P., and Gladfelter, A. S. (2016). Micron-scale plasma membrane curvature is recognized by the septin cytoskeleton. *J. Cell Biol.* 213, 23–32. doi: 10.1083/jcb.201512029

Brinkmann, B. G., Agarwal, A., Sereda, M. W., Garratt, A. N., Müller, T., Wende, H., et al. (2008). Neuregulin-1/ErbB signaling serves distinct functions in myelination of the peripheral and central nervous system. *Neuron* 59, 581–595. doi: 10.1016/j.neuron.2008.06.028

Chang-Ileto, B., Frere, S. G., Chan, R. B., Voronov, S. V., Roux, A., and Di Paolo, G. (2011). Synaptojanin 1-mediated PI(4,5)P2 hydrolysis is modulated by membrane curvature and facilitates membrane fission. *Dev. Cell* 20, 206–218. doi: 10.1016/j.devcel.2010.12.008

Charles, P., Hernandez, M. P., Stankoff, B., Aigrot, M. S., Colin, C., Rougon, G., et al. (2000). Negative regulation of central nervous system myelination by polysialylated-neural cell adhesion molecule. *Proc. Natl. Acad. Sci. U.S.A.* 97, 7585–7590. doi: 10.1073/pnas.100076197

Chen, M., Xu, Y., Huang, R., Huang, Y., Ge, S., and Hu, B. (2017). N-Cadherin is involved in neuronal activity-dependent regulation of myelinating capacity of Zebrafish individual oligodendrocytes In Vivo. *Mol. Neurobiol.* 54, 6917–6930. doi: 10.1007/s12035-016-0233-4

Czopka, T., Ffrench-Constant, C., and Lyons, D. A. (2013). Individual oligodendrocytes have only a few hours in which to generate new myelin sheaths in vivo. *Dev. Cell* 25, 599–609. doi: 10.1016/j.devcel.2013.05.013

De Biase, L. M., Kang, S. H., Baxi, E. G., Fukaya, M., Pucak, M. L., Mishina, M., et al. (2011). NMDA receptor signaling in oligodendrocyte progenitors is not required for oligodendrogenesis and myelination. *J. Neurosci.* 31, 12650–12662. doi: 10.1523/JNEUROSCI.2455-11.2011

Demerens, C., Stankoff, B., Logak, M., Anglade, P., Allinquant, B., Couraud, F., et al. (1996). Induction of myelination in the central nervous system by electrical activity. *Proc. Natl. Acad. Sci. U.S.A.* 93, 9887–9892. doi: 10.1073/pnas.93.18.9887

Díez-Revuelta, N., Higuero, A. M., Velasco, S., Peñas-de-la-Iglesia, M., Gabius, H.-J., and Abad-Rodríguez, J. (2017). Neurons define non-myelinated axon segments by the regulation of galectin-4-containing axon membrane domains. *Sci. Rep.* 7:12246. doi: 10.1038/s41598-017-12295-6

Domènech-Estévez, E., Baloui, H., Meng, X., Zhang, Y., Deinhardt, K., Dupree, J. L., et al. (2016). Akt regulates axon wrapping and myelin sheath thickness in the PNS. *J. Neurosci.* 36, 4506–4521. doi: 10.1523/JNEUROSCI.3521-15.2016

Early, J. J., Cole, K. L., Williamson, J. M., Swire, M., Kamadurai, H., Muskavitch, M., et al. (2018). An automated high-resolution in vivo screen in zebrafish to identify chemical regulators of myelination. *eLife* 7:e35136. doi: 10.7554/eLife.35136

Fewou, S. N., Ramakrishnan, H., Büssow, H., Gieselmann, V., and Eckhardt, M. (2007). Down-regulation of polysialic acid is required for efficient myelin formation. *J. Biol. Chem.* 282, 16700–16711. doi: 10.1074/jbc.M610797200

Fields, R. D. (2008). White matter in learning, cognition and psychiatric disorders. *Trends Neurosci.* 31, 361–370. doi: 10.1016/j.tins.2008.04.001

Fields, R. D. (2015). A new mechanism of nervous system plasticity: activity-dependent myelination. *Nat. Rev. Neurosci.* 16, 756–767. doi: 10.1038/nrn4023

Filley, C. M., and Fields, R. D. (2016). White matter and cognition: making the connection. *J. Neurophysiol.* 116, 2093–2104. doi: 10.1152/jn.00221.2016

Flores, A. I., Narayanan, S. P., Morse, E. N., Shick, H. E., Yin, X., Kidd, G., et al. (2008). Constitutively active Akt induces enhanced myelination in the CNS. *J. Neurosci.* 28, 7174–7183. doi: 10.1523/JNEUROSCI.0150-08.2008

Franklin, R. J. M., and Ffrench-Constant, C. (2017). Regenerating CNS myelin - from mechanisms to experimental medicines. *Nat. Rev. Neurosci.* 18, 753–769. doi: 10.1038/nrn.2017.136

Fu, W.-Y., Chen, Y., Sahin, M., Zhao, X.-S., Shi, L., Bikoff, J. B., et al. (2007). Cdk5 regulates EphA4-mediated dendritic spine retraction through an ephexin1-dependent mechanism. *Nat. Neurosci.* 10, 67–76. doi: 10.1038/nn1811

Fyffe-Maricich, S. L., Schott, A., Karl, M., Krasno, J., and Miller, R. H. (2013). Signaling through ERK1/2 controls myelin thickness during myelin repair in the adult central nervous system. *J. Neurosci.* 33, 18402–18408. doi: 10.1523/JNEUROSCI.2381-13.2013

Gibson, E. M., Purger, D., Mount, C. W., Goldstein, A. K., Lin, G. L., Wood, L. S., et al. (2014). Neuronal activity promotes oligodendrogenesis and adaptive myelination in the mammalian brain. *Science* 344:1252304. doi: 10.1126/science.1252304

Givogri, M. I., Costa, R. M., Schonmann, V., Silva, A. J., Campagnoni, A. T., and Bongarzone, E. R. (2002). Central nervous system myelination in mice with deficient expression of Notch1 receptor. *J. Neurosci. Res.* 67, 309–320. doi: 10.1002/jnr.10128

Goebbels, S., Oltrogge, J. H., Kemper, R., Heilmann, I., Bormuth, I., Wolfer, S., et al. (2010). Elevated phosphatidylinositol 3,4,5-trisphosphate in glia triggers cell-autonomous membrane wrapping and myelination. *J. Neurosci.* 30, 8953–8964. doi: 10.1523/JNEUROSCI.0219-10.2010

Goebbels, S., Wieser, G. L., Pieper, A., Spitzer, S., Weege, B., Yan, K., et al. (2017). A neuronal PI(3,4,5)P3-dependent program of oligodendrocyte precursor recruitment and myelination. *Nat. Neurosci.* 20, 10–15. doi: 10.1038/nn.4425

Guo, F., Maeda, Y., Ko, E. M., Delgado, M., Horiuchi, M., Soulika, A., et al. (2012). Disruption of NMDA receptors in oligodendroglial lineage cells does not alter their susceptibility to experimental autoimmune encephalomyelitis or their normal development. *J. Neurosci.* 32, 639–645. doi: 10.1523/JNEUROSCI.4073-11.2012

Harboe, M., Torvund-Jensen, J., Kjaer-Sorensen, K., and Laursen, L. S. (2018). Ephrin-A1-EphA4 signaling negatively regulates myelination in the central nervous system. *Glia* 66, 934–950. doi: 10.1002/glia.23293

Hartline, D. K., and Colman, D. R. (2007). Rapid conduction and the evolution of giant axons and myelinated fibers. *Curr. Biol.* 17, R29–R35. doi: 10.1016/j.cub.2006.11.042

Hildebrand, C., Remahl, S., Persson, H., and Bjartmar, C. (1993). Myelinated nerve fibres in the CNS. *Prog. Neurobiol.* 40, 319–384. doi: 10.1016/0301-0082(93)90015-K

Hill, R. A., Li, A. M., and Grutzendler, J. (2018). Lifelong cortical myelin plasticity and age-related degeneration in the live mammalian brain. *Nat. Neurosci.* 21, 683–695. doi: 10.1038/s41593-018-0120-6

Hill, R. A., Patel, K. D., Goncalves, C. M., Grutzendler, J., and Nishiyama, A. (2014). Modulation of oligodendrocyte generation during a critical temporal window after NG2 cell division. *Nat. Neurosci.* 17, 1518–1527. doi: 10.1038/nn.3815

Hines, J. H., Ravanelli, A. M., Schwindt, R., Scott, E. K., and Appel, B. (2015). Neuronal activity biases axon selection for myelination in vivo. *Nat. Neurosci.* 18, 683–689. doi: 10.1038/nn.3992

Hughes, E. G., Kang, S. H., Fukaya, M., and Bergles, D. E. (2013). Oligodendrocyte progenitors balance growth with self-repulsion to achieve homeostasis in the adult brain. *Nat. Neurosci.* 16, 668–676. doi: 10.1038/nn.3390

Hughes, E. G., Orthmann-Murphy, J. L., Langseth, A. J., and Bergles, D. E. (2018). Myelin remodeling through experience-dependent oligodendrogenesis in the adult somatosensory cortex. *Nat. Neurosci.* 21, 696–706. doi: 10.1038/s41593-018-0121-5

Ishii, A., Furusho, M., and Bansal, R. (2013). Sustained activation of ERK1/2 MAPK in oligodendrocytes and schwann cells enhances myelin growth and stimulates oligodendrocyte progenitor expansion. *J. Neurosci.* 33, 175–186. doi: 10.1523/JNEUROSCI.4403-12.2013

Ishii, A., Fyffe-Maricich, S. L., Furusho, M., Miller, R. H., and Bansal, R. (2012). ERK1/ERK2 MAPK signaling is required to increase myelin thickness independent of oligodendrocyte differentiation and initiation of myelination. *J. Neurosci.* 32, 8855–8864. doi: 10.1523/JNEUROSCI.0137-12.2012

Jeffries, M. A., Urbanek, K., Torres, L., Wendell, S. G., Rubio, M. E., and Fyffe-Maricich, S. L. (2016). ERK1/2 activation in preexisting oligodendrocytes of adult mice drives new myelin synthesis and enhanced CNS function. *J. Neurosci.* 36, 9186–9200. doi: 10.1523/JNEUROSCI.1444-16.2016

Jepson, S., Vought, B., Gross, C. H., Gan, L., Austen, D., Frantz, J. D., et al. (2012). LINGO-1, a transmembrane signaling protein, inhibits oligodendrocyte differentiation and myelination through intercellular self-interactions. *J. Biol. Chem.* 287, 22184–22195. doi: 10.1074/jbc.M112.366179

Kanamori, T., Kanai, M. I., Dairyo, Y., Yasunaga, K., Morikawa, R. K., and Emoto, K. (2013). Compartmentalized calcium transients trigger dendrite pruning in *Drosophila* sensory neurons. *Science* 340, 1475–1478. doi: 10.1126/science.1234879

Kirby, B. B., Takada, N., Latimer, A. J., Shin, J., Carney, T. J., Kelsh, R. N., et al. (2006). In vivo time-lapse imaging shows dynamic oligodendrocyte progenitor

behavior during zebrafish development. *Nat. Neurosci.* 9, 1506–1511. doi: 10.1038/nn1803

Klingseisen, A., and Lyons, D. A. (2018). Axonal regulation of central nervous system myelination: structure and function. *Neuroscientist* 24, 7–21. doi: 10.1177/1073858417703030

Koudelka, S., Voas, M. G., Almeida, R. G., Baraban, M., Soetaert, J., Meyer, M. P., et al. (2016). Individual neuronal subtypes exhibit diversity in CNS myelination mediated by synaptic vesicle release. *Curr. Biol.* 26, 1447–1455. doi: 10.1016/j.cub.2016.03.070

Krasnow, A. M., Ford, M. C., Valdivia, L. E., Wilson, S. W., and Attwell, D. (2018). Regulation of developing myelin sheath elongation by oligodendrocyte calcium transients in vivo. *Nat. Neurosci.* 21, 24–28. doi: 10.1038/s41593-017-0031-y

Laursen, L. S., Chan, C. W., and ffrench-Constant, C. (2009). An integrin-contactin complex regulates CNS myelination by differential Fyn phosphorylation. *J. Neurosci.* 29, 9174–9185. doi: 10.1523/JNEUROSCI.5942-08.2009

Lee, S., Leach, M. K., Redmond, S. A., Chong, S. Y. C., Mellon, S. H., Tuck, S. J., et al. (2012). A culture system to study oligodendrocyte myelination processes using engineered nanofibers. *Nat. Methods* 9, 917–922. doi: 10.1038/nmeth.2105

Lee, X., Yang, Z., Shao, Z., Rosenberg, S. S., Levesque, M., Pepinsky, R. B., et al. (2007). NGF regulates the expression of axonal LINGO-1 to inhibit oligodendrocyte differentiation and myelination. *J. Neurosci.* 27, 220–225. doi: 10.1523/JNEUROSCI.4175-06.2007

Li, Q., Brus-Ramer, M., Martin, J. H., and McDonald, J. W. (2010). Electrical stimulation of the medullary pyramid promotes proliferation and differentiation of oligodendrocyte progenitor cells in the corticospinal tract of the adult rat. *Neurosci. Lett.* 479, 128–133. doi: 10.1016/j.neulet.2010.05.043

Linneberg, C., Harboe, M., and Laursen, L. S. (2015). Axo-Glia interaction preceding CNS myelination is regulated by bidirectional eph-ephrin signaling. *ASN Neuro* 7:1759091415602859. doi: 10.1177/1759091415602859

Liu, J., Dietz, K., DeLoyht, J. M., Pedre, X., Kelkar, D., Kaur, J., et al. (2012). Impaired adult myelination in the prefrontal cortex of socially isolated mice. *Nat. Neurosci.* 15, 1621–1623. doi: 10.1038/nn.3263

Liu, P., Du, J.-L., and He, C. (2013). Developmental pruning of early-stage myelin segments during CNS myelination in vivo. *Cell Res.* 23, 962–964. doi: 10.1038/cr.2013.62

Liu, X., Bates, R., Yin, D.-M., Shen, C., Wang, F., Su, N., et al. (2011). Specific regulation of NRG1 isoform expression by neuronal activity. *J. Neurosci.* 31, 8491–8501. doi: 10.1523/JNEUROSCI.5317-10.2011

Lundgaard, I., Luzhynskaya, A., Stockley, J. H., Wang, Z., Evans, K. A., Swire, M., et al. (2013). Neuregulin and BDNF induce a switch to NMDA receptor-dependent myelination by oligodendrocytes. *PLoS Biol.* 11:e1001743. doi: 10.1371/journal.pbio.1001743

Makinodan, M., Rosen, K. M., Ito, S., and Corfas, G. (2012). A critical period for social experience-dependent oligodendrocyte maturation and myelination. *Science* 337, 1357–1360. doi: 10.1126/science.1220845

Mao, Y. T., Zhu, J. X., Hanamura, K., Iurilli, G., Datta, S. R., and Dalva, M. B. (2018). Filopodia conduct target selection in cortical neurons using differences in signal kinetics of a single kinase. *Neuron* 98, 767.e8–782.e8. doi: 10.1016/j.neuron.2018.04.011

Mathews, E. S., and Appel, B. (2016). Cholesterol biosynthesis supports myelin gene expression and axon ensheathment through modulation of P13K/Akt/mTor signaling. *J. Neurosci.* 36, 7628–7639. doi: 10.1523/JNEUROSCI.0726-16.2016

Matthews, M. A. (1968). An electron microscopic study of the relationship between axon diameter and the initiation of myelin production in the peripheral nervous system. *Anat. Rec.* 161, 337–351. doi: 10.1002/ar.1091610306

McKenzie, I. A., Ohayon, D., Li, H., de Faria, J. P., Emery, B., Tohyama, K., et al. (2014). Motor skill learning requires active central myelination. *Science* 346, 318–322. doi: 10.1126/science.1254960

McMahon, H. T., and Boucrot, E. (2015). Membrane curvature at a glance. *J. Cell Sci.* 128, 1065–1070. doi: 10.1242/jcs.114454

Mei, F., Fancy, S. P. J., Shen, Y.-A. A., Niu, J., Zhao, C., Presley, B., et al. (2014). Micropillar arrays as a high-throughput screening platform for therapeutics in multiple sclerosis. *Nat. Med.* 20, 954–960. doi: 10.1038/nm.3618

Mensch, S., Baraban, M., Almeida, R., Czopka, T., Ausborn, J., El Manira, A., et al. (2015). Synaptic vesicle release regulates myelin sheath number of individual oligodendrocytes in vivo. *Nat. Neurosci.* 18, 628–630. doi: 10.1038/nn.3991

Meyer-Franke, A., Shen, S., and Barres, B. A. (1999). Astrocytes induce oligodendrocyte processes to align with and adhere to axons. *Mol. Cell. Neurosci.* 14, 385–397. doi: 10.1006/mcne.1999.0788

Mi, S., Miller, R. H., Lee, X., Scott, M. L., Shulag-Morskaya, S., Shao, Z., et al. (2005). LINGO-1 negatively regulates myelination by oligodendrocytes. *Nat. Neurosci.* 8, 745–751. doi: 10.1038/nn1460

Michailov, G. V., Sereda, M. W., Brinkmann, B. G., Fischer, T. M., Haug, B., Birchmeier, C., et al. (2004). Axonal neuregulin-1 regulates myelin sheath thickness. *Science* 304, 700–703. doi: 10.1126/science.1095862

Miller, D. J., Duka, T., Stimpson, C. D., Schapiro, S. J., Baze, W. B., McArthur, M. J., et al. (2012). Prolonged myelination in human neocortical evolution. *Proc. Natl. Acad. Sci. U.S.A.* 109, 16480–16485. doi: 10.1073/pnas.1117943109

Mitew, S., Gobius, I., Fenlon, L. R., McDougall, S. J., Hawkes, D., Xing, Y. L., et al. (2018). Pharmacogenetic stimulation of neuronal activity increases myelination in an axon-specific manner. *Nat. Commun.* 9:306. doi: 10.1038/s41467-017-02719-2

Mount, C. W., and Monje, M. (2017). Wrapped to adapt: experience-dependent myelination. *Neuron* 95, 743–756. doi: 10.1016/j.neuron.2017.07.009

Nait Oumesmar, B., Vignais, L., Duhamel-Clérin, E., Avellana-Adalid, V., Rougon, G., and Baron-Van Evercooren, A. (1995). Expression of the highly polysialylated neural cell adhesion molecule during postnatal myelination and following chemically induced demyelination of the adult mouse spinal cord. *Eur. J. Neurosci.* 7, 480–491. doi: 10.1111/j.1460-9568.1995.tb00344.x

Nawaz, S., Sánchez, P., Schmitt, S., Snaidero, N., Mitkovski, M., Velte, C., et al. (2015). Actin filament turnover drives leading edge growth during myelin sheath formation in the central nervous system. *Dev. Cell* 34, 139–151. doi: 10.1016/j.devcel.2015.05.013

Olivares, R., Montiel, J., and Aboitiz, F. (2001). Species differences and similarities in the fine structure of the mammalian corpus callosum. *Brain Behav. Evol.* 57, 98–105. doi: 10.1159/000047229

Osso, L. A., and Chan, J. R. (2017). Architecting the myelin landscape. *Curr. Opin. Neurobiol.* 47, 1–7. doi: 10.1016/j.conb.2017.06.005

Park, J., Liu, B., Chen, T., Li, H., Hu, X., Gao, J., et al. (2008). Disruption of Nectin-like 1 cell adhesion molecule leads to delayed axonal myelination in the CNS. *J. Neurosci.* 28, 12815–12819. doi: 10.1523/JNEUROSCI.2665-08.2008

Pasquale, E. B. (2008). Eph-ephrin bidirectional signaling in physiology and disease. *Cell* 133, 38–52. doi: 10.1016/j.cell.2008.03.011

Perge, J. A., Niven, J. E., Mugnaini, E., Balasubramanian, V., and Sterling, P. (2012). Why do axons differ in caliber? *J. Neurosci.* 32, 626–638. doi: 10.1523/JNEUROSCI.4254-11.2012

Philips, T., and Rothstein, J. D. (2014). Glial cells in amyotrophic lateral sclerosis. *Exp. Neurol.* 262(Pt B), 111–120. doi: 10.1016/j.expneurol.2014.05.015

Pouwels, P. J. W., Vanderver, A., Bernard, G., Wolf, N. I., Dreha-Kulczewksi, S. F., Deoni, S. C. L., et al. (2014). Hypomyelinating leukodystrophies: translational research progress and prospects. *Ann. Neurol.* 76, 5–19. doi: 10.1002/ana.24194

Redmond, S. A., Mei, F., Eshed-Eisenbach, Y., Osso, L. A., Leshkowitz, D., Shen, Y.-A. A., et al. (2016). Somatodendritic expression of JAM2 inhibits oligodendrocyte myelination. *Neuron* 91, 824–836. doi: 10.1016/j.neuron.2016.07.021

Remahl, S., and Hildebrand, C. (1982). Changing relation between onset of myelination and axon diameter range in developing feline white matter. *J. Neurol. Sci.* 54, 33–45. doi: 10.1016/0022-510X(82)90216-7

Richardson, W. D., Kessaris, N., and Pringle, N. (2006). Oligodendrocyte wars. *Nat. Rev. Neurosci.* 7, 11–18. doi: 10.1038/nrn1826

Rosenberg, S. S., Kelland, E. E., Tokar, E., De la Torre, A. R., and Chan, J. R. (2008). The geometric and spatial constraints of the microenvironment induce oligodendrocyte differentiation. *Proc. Natl. Acad. Sci. U.S.A.* 105, 14662–14667. doi: 10.1073/pnas.0805640105

Saab, A. S., and Nave, K.-A. (2017). Myelin dynamics: protecting and shaping neuronal functions. *Curr. Opin. Neurobiol.* 47, 104–112. doi: 10.1016/j.conb.2017.09.013

Saab, A. S., Tzvetavona, I. D., Trevisiol, A., Baltan, S., Dibaj, P., Kusch, K., et al. (2016). Oligodendroglial NMDA receptors regulate glucose import and axonal energy metabolism. *Neuron* 91, 119–132. doi: 10.1016/j.neuron.2016.05.016

Sahin, M., Greer, P. L., Lin, M. Z., Poucher, H., Eberhart, J., Schmidt, S., et al. (2005). Eph-dependent tyrosine phosphorylation of ephexin1 modulates growth cone collapse. *Neuron* 46, 191–204. doi: 10.1016/j.neuron.2005.01.030

Saliani, A., Perraud, B., Duval, T., Stikov, N., Rossignol, S., and Cohen-Adad, J. (2017). Axon and myelin morphology in animal and human spinal cord. *Front. Neuroanat.* 11:129. doi: 10.3389/fnana.2017.00129

Sampaio-Baptista, C., and Johansen-Berg, H. (2017). White matter plasticity in the adult brain. *Neuron* 96, 1239–1251. doi: 10.1016/j.neuron.2017.11.026

Schnädelbach, O., Ozen, I., Blaschuk, O. W., Meyer, R. L., and Fawcett, J. W. (2001). N-cadherin is involved in axon-oligodendrocyte contact and myelination. *Mol. Cell. Neurosci.* 17, 1084–1093. doi: 10.1006/mcne.2001.0961

Simons, M., and Lyons, D. A. (2013). Axonal selection and myelin sheath generation in the central nervous system. *Curr. Opin. Cell Biol.* 25, 512–519. doi: 10.1016/j.ceb.2013.04.007

Sinclair, J. L., Fischl, M. J., Alexandrova, O., Heβ, M., Grothe, B., Leibold, C., et al. (2017). Sound-evoked activity influences myelination of brainstem axons in the trapezoid body. *J. Neurosci.* 37, 8239–8255. doi: 10.1523/JNEUROSCI.3728-16.2017

Spitzer, S., Volbracht, K., Lundgaard, I., and Káradóttir, R. T. (2016). Glutamate signalling: a multifaceted modulator of oligodendrocyte lineage cells in health and disease. *Neuropharmacology* 110, 574–585. doi: 10.1016/j.neuropharm.2016.06.014

Stancic, M., Slijepcevic, D., Nomden, A., Vos, M. J., de Jonge, J. C., Sikkema, A. H., et al. (2012). Galectin-4, a novel neuronal regulator of myelination. *Glia* 60, 919–935. doi: 10.1002/glia.22324

Tan, Z.-J., Peng, Y., Song, H.-L., Zheng, J.-J., and Yu, X. (2010). N-cadherin-dependent neuron-neuron interaction is required for the maintenance of activity-induced dendrite growth. *Proc. Natl. Acad. Sci. U.S.A.* 107, 9873–9878. doi: 10.1073/pnas.1003480107

Taveggia, C., Zanazzi, G., Petrylak, A., Yano, H., Rosenbluth, J., Einheber, S., et al. (2005). Neuregulin-1 type III determines the ensheathment fate of axons. *Neuron* 47, 681–694. doi: 10.1016/j.neuron.2005.08.017

Tomassy, G. S., Berger, D. R., Chen, H.-H., Kasthuri, N., Hayworth, K. J., Vercelli, A., et al. (2014). Distinct profiles of myelin distribution along single axons of pyramidal neurons in the neocortex. *Science* 344, 319–324. doi: 10.1126/science.1249766

Tripathi, R. B., Jackiewicz, M., McKenzie, I. A., Kougioumtzidou, E., Grist, M., and Richardson, W. D. (2017). Remarkable stability of myelinating oligodendrocytes in mice. *Cell Rep.* 21, 316–323. doi: 10.1016/j.celrep.2017.09.050

Velasco, S., Díez-Revuelta, N., Hernández-Iglesias, T., Kaltner, H., André, S., Gabius, H.-J., et al. (2013). Neuronal Galectin-4 is required for axon growth and for the organization of axonal membrane L1 delivery and clustering. *J. Neurochem.* 125, 49–62. doi: 10.1111/jnc.12148

Wake, H., Lee, P. R., and Fields, R. D. (2011). Control of local protein synthesis and initial events in myelination by action potentials. *Science* 333, 1647–1651. doi: 10.1126/science.1206998

Wake, H., Ortiz, F. C., Woo, D. H., Lee, P. R., Angulo, M. C., and Fields, R. D. (2015). Nonsynaptic junctions on myelinating glia promote preferential myelination of electrically active axons. *Nat. Commun.* 6:7844. doi: 10.1038/ncomms8844

Wang, S., Sdrulla, A. D., diSibio, G., Bush, G., Nofziger, D., Hicks, C., et al. (1998). Notch receptor activation inhibits oligodendrocyte differentiation. *Neuron* 21, 63–75. doi: 10.1016/S0896-6273(00)80515-2

Watkins, T. A., Emery, B., Mulinyawe, S., and Barres, B. A. (2008). Distinct stages of myelination regulated by gamma-secretase and astrocytes in a rapidly myelinating CNS coculture system. *Neuron* 60, 555–569. doi: 10.1016/j.neuron.2008.09.011

Waxman, S. G. (1997). Axon-glia interactions: building a smart nerve fiber. *Curr. Biol.* 7, R406–R410. doi: 10.1016/S0960-9822(06)00203-X

Zeidán-Chuliá, F., Salmina, A. B., Malinovskaya, N. A., Noda, M., Verkhratsky, A., and Moreira, J. C. F. (2014). The glial perspective of autism spectrum disorders. *Neurosci. Biobehav. Rev.* 38, 160–172. doi: 10.1016/j.neubiorev.2013.11.008

Zuchero, J. B., and Barres, B. A. (2013). Intrinsic and extrinsic control of oligodendrocyte development. *Curr. Opin. Neurobiol.* 23, 914–920. doi: 10.1016/j.conb.2013.06.005

Zuchero, J. B., Fu, M.-M., Sloan, S. A., Ibrahim, A., Olson, A., Zaremba, A., et al. (2015). CNS myelin wrapping is driven by actin disassembly. *Dev. Cell* 34, 152–167. doi: 10.1016/j.devcel.2015.06.011

Conflict of Interest Statement: The author declares that the research was conducted in the absence of any commercial or financial relationships that could be construed as a potential conflict of interest.

frontiers in Cellular Neuroscience

METHODS
published: 23 October 2018
doi: 10.3389/fncel.2018.00377

Intravitreal AAV-Delivery of Genetically Encoded Sensors Enabling Simultaneous Two-Photon Imaging and Electrophysiology of Optic Nerve Axons

*Zoe J. Looser[1,2], Matthew J. P. Barrett[1,2], Johannes Hirrlinger[3,4], Bruno Weber[1,2] and Aiman S. Saab[1,2]**

[1]Institute of Pharmacology & Toxicology, University of Zurich, Zurich, Switzerland, [2]Neuroscience Center Zurich, University and ETH Zurich, Zurich, Switzerland, [3]Carl-Ludwig-Institute for Physiology, University of Leipzig, Leipzig, Germany, [4]Department of Neurogenetics, Max-Planck-Institute of Experimental Medicine, Göttingen, Germany

Myelination of axons by oligodendrocytes is a key feature of the remarkably fast operating CNS. Oligodendrocytes not only tune axonal conduction speed but are also suggested to maintain long-term axonal integrity by providing metabolic support to the axons they ensheath. However, how myelinating oligodendrocytes impact axonal energy homeostasis remains poorly understood and difficult to investigate. Here, we provide a method of how to study electrically active myelinated axons expressing genetically encoded sensors by combining electrophysiology and two-photon imaging of acutely isolated optic nerves. We show that intravitreal adeno-associated viral (AAV) vector delivery is an efficient tool to achieve functional sensor expression in optic nerve axons, which is demonstrated by measuring axonal ATP dynamics following AAV-mediated sensor expression. This novel approach allows for fast expression of any optical sensor of interest to be studied in optic nerve axons without the need to go through the laborious process of producing new transgenic mouse lines. Viral-mediated biosensor expression in myelinated axons and the subsequent combination of nerve recordings and sensor imaging outlines a powerful method to investigate oligodendroglial support functions and to further interrogate cellular mechanisms governing axonal energy homeostasis under physiological and pathological conditions.

Keywords: myelinated axons, intravitreal AAV injection, optic nerve recording, two-photon imaging, genetically encoded sensors, ATP-sensor ATeam1.03YEMK

OPEN ACCESS

Edited by:
Fernando C. Ortiz, Universidad Autónoma de Chile, Chile

Reviewed by:
Felipe A. Court, Universidad Mayor, Chile
Arne Battefeld, Université de Bordeaux, France

***Correspondence:**
Aiman S. Saab
asaab@pharma.uzh.ch

Received: *13 August 2018*
Accepted: *03 October 2018*
Published: *23 October 2018*

Citation:
Looser ZJ, Barrett MJP, Hirrlinger J, Weber B and Saab AS (2018) Intravitreal AAV-Delivery of Genetically Encoded Sensors Enabling Simultaneous Two-Photon Imaging and Electrophysiology of Optic Nerve Axons. Front. Cell. Neurosci. 12:377. doi: 10.3389/fncel.2018.00377

INTRODUCTION

Information processing in the brain critically relies on electrical signal transmissions along axons interconnecting a long-range network of myriads of neurons. By insulating axons with myelin, oligodendrocytes are essential for rapid saltatory impulse propagation (Huxley and Stämpfli, 1949) and thereby influence the computational speed and efficiency of higher vertebrate nervous systems (Laughlin and Sejnowski, 2003). About 50% of the human brain is composed of white matter tracts, which mainly contain myelinated axons and their associated glial cells. Loss of axonal integrity is detrimental for normal brain function and deficits in white matter energy metabolism, including

perturbations in glial metabolic support to myelinated axons (Lee et al., 2012; Saab et al., 2016), are increasingly discussed in the pathogenesis of various neurodegenerative diseases (Nave, 2010a; Iadecola, 2013; Philips and Rothstein, 2017; Saab and Nave, 2017).

To better understand how white matter pathology and axonal degeneration may associate with perturbations in white matter energy homeostasis, more insights into cellular mechanisms regulating axonal metabolite supply and energy metabolism are required. For example, how myelinating oligodendrocytes regulate axonal energy metabolism and maintain axonal integrity under physiological or pathological conditions is still elusive and difficult to investigate. Genetically-encoded optical sensors enable real-time monitoring of cellular metabolite dynamics and are becoming invaluable neurobiological tools to study intercellular mechanisms governing brain energy homeostasis (Hou et al., 2011; San Martin et al., 2014b; Sotelo-Hitschfeld et al., 2015; Mächler et al., 2016; Díaz-Garcia et al., 2017; Trevisiol et al., 2017). The fully myelinated optic nerve is an ideal white matter tract to examine mechanisms of axonal energy metabolism *ex vivo* (Stys et al., 1991; Brown et al., 2001; Tekkök et al., 2005; Saab et al., 2016). A recent study introduced a novel approach to measure activity-dependent axonal ATP homeostasis in acute optic nerve preparations by combining nerve recordings with confocal imaging (Trevisiol et al., 2017). There, axonal sensor expression of the FRET-based ATP sensor ATeam1.03^{YEMK} (Imamura et al., 2009) in optic nerves was achieved by generating a transgenic mouse with a pan-neuronal expression of the ATP sensor (Trevisiol et al., 2017). However, generation of new transgenic mice is time consuming and costly if one would like to expand the repertoire of biosensor measurements in myelinated axons using the acute optic nerve imaging paradigm. Especially with new and improved optical sensors being continuously produced, we wondered whether functional sensor expression in optic nerve axons could be achieved by viral-mediated delivery.

The aim of this study is to demonstrate that intravitreal injection of adeno-associated viral (AAV) vectors carrying genetically encoded sensors is suitable to drive robust and functional sensor expression in optic nerve axons. This allows the analysis of activity-dependent axonal metabolite dynamics in acute optic nerve preparations by combining electrophysiology with two-photon imaging. As a proof of principle, we tested intravitreal injections of AAV vectors with three different serotypes carrying the ATP sensor ATeam1.03^{YEMK} (Imamura et al., 2009) and evaluated axonal sensor expression and activity in our acute optic nerve recording/imaging paradigm. Intravitreal AAV-mediated sensor expression and subsequent two-photon imaging of myelinated axons represents a powerful approach to gain more insights into cellular and molecular mechanisms governing white matter energy metabolism.

MATERIALS AND METHODS

Animals

All animal experiments were approved by the local veterinary authorities in Zurich and were according to the guidelines of Swiss Animal Protection Law, Veterinary Office, Canton Zurich (Animal Welfare Act of 16 December 2005 and Animal Welfare Ordinance of 23 April 2008). Mice had free access to food and water and were kept with an inverted 12 h light/dark cycle. Intravitreal AAV vector injections were performed in 8–10 weeks old wild type mice (C57BL/6J; Charles River) and optic nerve imaging experiments were performed starting from 3 weeks to 4 weeks after the intravitreal injection. Transgenic mice B6-Tg(Thy1.2-ATeam1.03^{YEMK})AJhi (Trevisiol et al., 2017) at the age of 12–15 weeks were also used for imaging experiments. Safety measures for handling AAV viral vectors were according to the institutional biosafety procedures of the University of Zurich.

Experimental Design

Studying energy metabolism in white matter tracts is challenging, but essential to understand how axonal compartments, which are shielded by myelin sheaths, take up metabolites, regulate their energy resources and maintain functional integrity (Nave, 2010b; Saab et al., 2013; Trevisiol et al., 2017). We describe a novel approach which allows any genetically encoded optical sensor of interest to be rapidly expressed and studied in optic nerve axons of adult mice (**Figure 1**). Since all optic nerve axons descend from retinal ganglion cells (RGCs) located in the retina, intravitreal injection of AAV vectors enables sensor expression in RGCs and their myelinated axons. Around 3–4 weeks after intravitreal AAV injections, robust sensor expression in optic nerve axons was achieved and nerves were prepared for *ex vivo* recordings and axonal imaging. Electrical nerve stimulations and recordings of compound action potentials (CAPs) were combined with two-photon imaging. We demonstrate the usefulness of this protocol by monitoring axonal ATP level changes following intravitreal AAV-mediated delivery and expression of a FRET-based ATP sensor ATeam1.03^{YEMK} (Imamura et al., 2009). For comparison, we also monitored axonal ATP dynamics in optic nerves from transgenic mice constitutively expressing the same ATP sensor in neuronal/axonal compartments (Trevisiol et al., 2017).

Intravitreal AAV Injections

Mice were anesthetized with an intraperitoneal injection of fentanyl (0.05 mg/kg; Fentanyl Sintetica, Sintetica), midazolam (5 mg/kg; Dormicum, Roche), and medetomidine (0.5 mg/kg; Domitor, Orion Pharma) mixed in NaCl (0.9%; Fleischmann et al., 2016). For pupil dilation, first cyclopentolate (1%; Cyclogyl, Alcon) and then phenylephrine (5%; Neosynephrin-POS, URSAPHARM) were each applied topically to the eyes for 1–2 min. Prolonged light exposure to the mouse was avoided whenever possible once pupils were dilated. Eyes were kept moisturized with the transparent Viscotears liquid gel (Alcon) and mouse body temperature was kept stable at 37°C throughout the intravitreal AAV injection procedure (**Figure 2**). Under microscopic control (SteREO Discovery.V20, Zeiss) an incision was made into the sclera (1–2 mm posterior of the superior limbus) using a sterile, sharp 30-gauge (G) needle (insulin syringe, Omnican 50, Braun; **Figure 2A**). Great care was taken not to damage the lens or

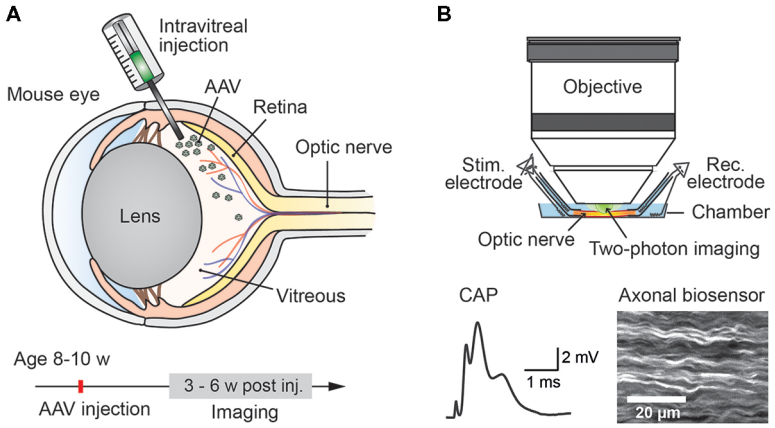

FIGURE 1 | Experimental paradigm: intravitreal adeno-associated viral (AAV) vector injection and subsequent two-photon imaging of genetically encoded biosensors in optic nerve axons. **(A)** Injection of AAV vector carrying genetically encoded sensor into the vitreous humor of the mouse eye at the age of 8–10 weeks. Robust sensor expression in optic nerve axons for imaging experiments is achieved starting from 3 weeks to 4 weeks after the injection. **(B)** Acute optic nerve preparation for combined electrophysiology and two-photon imaging of myelinated axons. Simultaneous monitoring of stimulus-evoked compound action potentials (CAPs) and biosensor activity enables studying activity-dependent axonal metabolite dynamics.

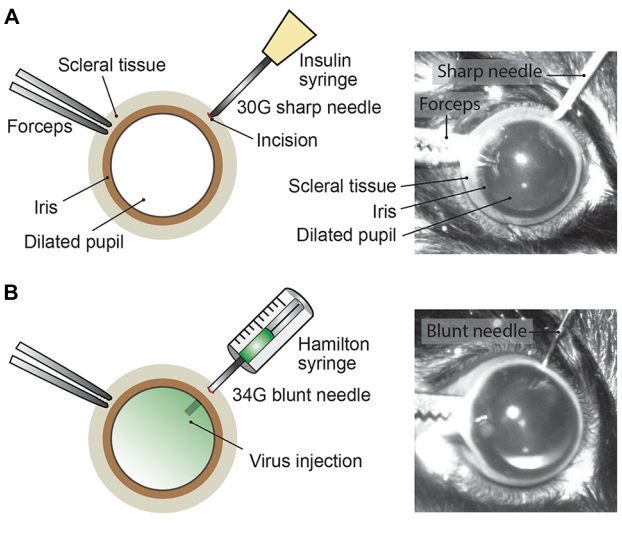

FIGURE 2 | Intravitreal AAV injection procedure. **(A)** Depiction of the mouse eye (frontal view) with a dilated pupil held by the scleral connective tissue with forceps. Using a sharp 30G needle (e.g., insulin syringe) an incision is made into the sclera. **(B)** A Hamilton syringe with a 34G blunt needle is carefully inserted into the incision and the AAV viral suspension is slowly injected into the vitreous. By adding fluorescein dye (green) to the viral suspension, the intravitreal injection can be observed by the homogenous diffusion of the green dye inside the vitreous.

retina. After removing the 30G needle, a 34G blunt needle (12.70mm/pst3, BGB, HA-207434) attached to a microliter Hamilton syringe (10 µl Syringe Model 701) was carefully inserted into the same incision (**Figure 2B**) and 1–1.5 µl of viral suspension was slowly injected (0.05–0.1 µl/s) into the vitreous. For a better monitoring of the AAV injection into the vitreous, we mixed 1 µl of fluorescein (0.1 mg/ml in PBS) in 10 µl of undiluted viral suspension (see below). Successful injections were observed by the homogenous diffusion of the green fluorescein dye inside the vitreous (**Figure 2B**). The needle was kept inside the vitreous for 1–2 min after the injection to prevent reflux of viral suspension, before carefully removing the needle. Both eyes were injected. After intravitreal AAV injections, antibiotic eye drops (Ofloxacin 0.3%, Floxal UD, Bausch + Lomb) were applied and mice were injected subcutaneously with the analgesic buprenorphine (0.1 mg/kg, Temgesic, Indivior Schweiz AG). By antagonizing the anesthesia with intraperitoneal administration of the antagonists (a mixture of atipamezole (2.5 mg/kg; Revertor, Virbac) and flumazenil (0.5 mg/kg; Anexate, Roche)) mice typically regained consciousness within 5 min when placed back in the home cage for recovery.

AAV Viral Vectors

The production, purification and quantification of single-stranded (ss) AAV vectors were performed by the viral vector facility (VVF) of the Neuroscience Center Zurich (ZNZ) as described (Zolotukhin et al., 1999; Paterna et al., 2004). The AAV viral vectors used in this study express the ATP sensor ATeam1.03^{YEMK} (Imamura et al., 2009) under the control of the human synapsin promoter (hSyn1-ATeam1.03^{YEMK}-WPRE-hGHp(A)) and three different AAV vector serotypes, ssAAV-2/2, -DJ/2 and -9/2 (Samulski et al., 1989; Gao et al., 2004; Grimm et al., 2008), were generated and tested. Intravitreal AAV injections were performed with undiluted viral suspensions and the physical titers of ssAAV-2/2, -DJ/2 and -9/2 were 6.2×10^{12} vg/ml (vector genomes/milliliter), 5.4×10^{12} vg/ml and 8.1×10^{12} vg/ml, respectively. The VVF repository identifier of the hSyn1-ATeam1.03^{YEMK} AAV vectors is v244 and all AAV serotypes as well as detailed information on AAV production, including vector maps, can be obtained from the VVF homepage[1] .

[1]https://www.uzh.ch/vvf/ordersystem/

Optic Nerve Preparation Procedure

Optic nerves were prepared for imaging experiments 3–6 weeks after intravitreal AAV vector injections. Mice were deeply anesthetized with isoflurane before decapitation. The skin covering the skull was cut longitudinally with a surgical blade (**Figure 3A**) and the two skin flaps were held with the index and thumb fingers. After removing the surface connective tissue above the eyes (**Figure 3B**), optic nerves were separated from the eyeballs by carefully cutting with surgical scissors (Fine Iris Scissors, FST, 14106-09) into the eye socket behind the eyeballs (**Figure 3C**). Care was taken not to damage the eyeballs. The exit tips of the nerve heads were visible as white dots at the back of each eyeball after the separation (**Figure 3D**). Next, the skull was cut with surgical scissors and carefully removed to expose the brain (**Figure 3E**). Then the brain was pulled back to slowly extract the nerves out of the optic canals (**Figure 3F**). Importantly, the nerves should slip out easily without any stretching. Once pulled out, the nerves were flushed with artificial cerebrospinal fluid (ACSF) to straighten them on the ventral surface of the brain (**Figure 3G**). Using spring scissors (Cohan-Vannas Spring Scissors, FST, 15000-02) the chiasm was cut as depicted in **Figure 3G**, leaving the nerves still attached to half of the chiasm by which then the nerve pair was lifted (**Figure 3H**) and transferred to the recording chamber.

Recording Setup Preparation

Optic nerve recordings and imaging were performed in an interface recording chamber (Harvard apparatus, Base unit (BSC-BU, 65-0073) and Haas top (BSC-HT, 65-0075)) with custom-made modifications to the Haas top unit: the inside edges of the chamber were milled down in a ∼45° angle to ∼2 mm which created adequate space for positioning both suction electrodes and the objective (see **Figures 4A,F**). The recording chamber was continuously perfused with ACSF (containing in mM: NaCl, 126; KCl, 3; $CaCl_2$, 2; NaH_2PO_4, 1.25; $NaHCO_3$, 26; $MgSO_4$, 2; D-glucose, 10; pH 7.4) which was constantly bubbled with 95% O_2 and 5% CO_2, and gravity-fed into the recording chamber at a flow rate of ∼6 ml/min. Temperature was maintained at 37°C using a temperature controller (npi electronics, TC-10) with the sensor (TS-100, npi) attached inside the chamber. To reduce bubble formations inside the recording chamber, which could become an issue during imaging, the ACSF glass bottle was additionally preheated (during bubbling) in a plexiglass-walled (for better visibility) water bath (Julabo) at 37°C. The custom-made suction electrodes (Stys et al., 1991; **Figures 4A–F**) were back-filled with ACSF and positioned in the chamber using micro-manipulators (Mini 25, Luigs & Neumann).

The excised optic nerve pair was placed on filter paper (Macherey-Nagel, MN 615) strips inside the chamber as depicted in **Figure 4C**. Before starting the experiment, filter paper strips were prepared by cutting two strips of ∼2 mm width, two strips of ∼1.5 mm width and two trapezoid-shaped filter paper stacks (four layers) and arranged in the recording chamber as shown in **Figure 4B**. Filter papers were rinsed thoroughly with ACSF to remove any dust particles and the chamber was freed from bubbles before nerve preparation. After the excised nerve pair was placed on the central 2 mm filter paper strips (two layers) with the chiasm facing the recording electrode, one nerve was carefully cut from the chiasm using spring scissors (**Figure 4C**). The second nerve still attached to the chiasm was gently moved to the side and served only as a backup in case the first nerve was damaged during preparation (absence of CAP response) or lacked sensor expression due to a failed intravitreal injection. The nerve on the filter papers was positioned between the electrodes and each nerve end was inserted into the suction electrodes by slowly pulling back the plunger of the ACSF-filled syringes (attached to the electrodes via tubing; **Figure 4D**). The nerve ends should fit tightly into the electrodes and were not inserted more than 0.5 mm. The two trapezoid-shaped filter paper stacks (four layers) were carefully placed on the 2 mm filter paper strips above and below the nerve, leaving a ∼1 mm

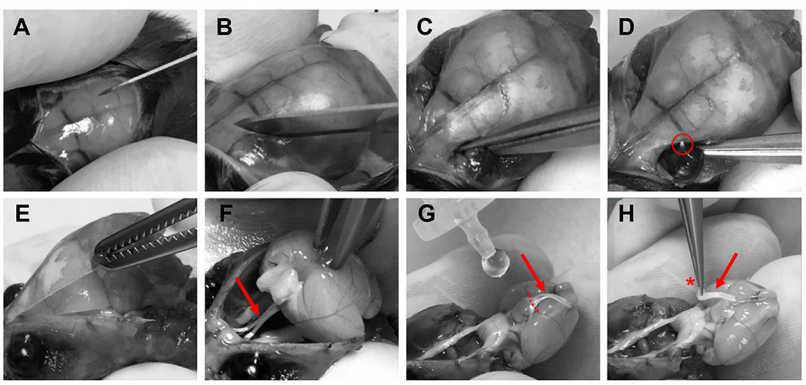

FIGURE 3 | Procedure of optic nerve removal. **(A)** Following anesthesia and decapitation the skin covering the skull is cut longitudinally. **(B,C)** The optic nerves are separated from the eyeballs after removing connective tissue by carefully cutting into the eye socket behind the eyeballs. **(D)** After the separation the exit tips of the nerve (red circle) are visible as white dots at the back of the eyeballs. **(E)** The skull is removed to gain access to the brain. **(F)** The brain is pulled backwards to extract the optic nerves (red arrows **F–H**) from the optical canals. Nerves should come out easily still attached to the chiasm. **(G)** With drops of artificial cerebrospinal fluid (ACSF), nerves are flushed to straighten them, and the chiasm is cut (dashed lines) leaving half of the chiasm still connected to the nerve pair. **(H)** Optic nerves are carefully lifted by holding at the chiasm (red asterisk) and then transferred to the recording chamber.

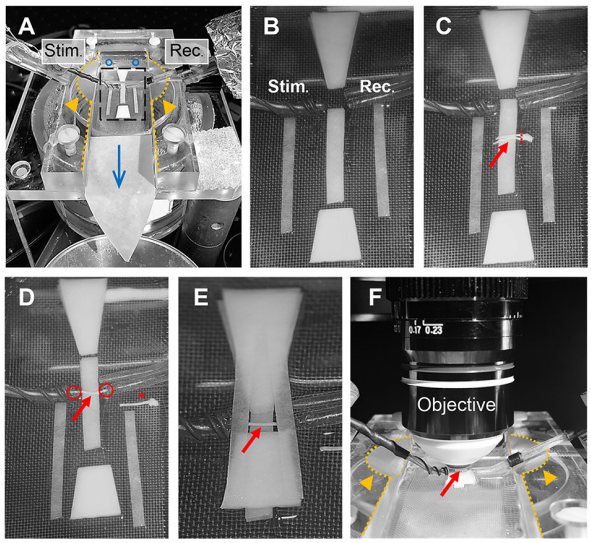

FIGURE 4 | Optic nerve preparation in setup for electrophysiology and imaging. **(A)** Photograph of the recording chamber with stimulation (Stim.) and recording (Rec.) electrode. Orange arrow heads highlight the modification to the Haas top unit of the chamber; i.e., the inside edges (dotted lines) are milled down in a 45° angle to create better access for electrodes and objective, see also **(F)**. Blue circles and arrow indicate location of ACSF inflow into the chamber and direction of flow, respectively. Black rectangle outlines the region magnified in **(B)** showing the arrangement of filter papers around the electrodes. **(C)** The optic nerves (red arrow) are placed on the central filter paper strips (two layers) with the chiasm facing the recording electrode. One nerve is carefully cut from the chiasm (dashed red line) and moved towards the electrodes. **(D)** Depicted is how the nerve is positioned on the filter paper strips between the electrodes with each nerve end inserted into the suction electrodes (red circles). The other nerve is placed on the side as backup (red asterisk). **(E)** Organization of the remaining filter papers above and below the electrodes before **(F)** placing the objective above the nerve (red arrow) by dipping into the created ACSF pool. Orange arrows heads indicate the modification (milling) of the inside edges of the chamber (dotted lines).

gap above and below the electrodes (**Figure 4E**). Then the two 1.5 mm filter paper strips (single layers) were placed across the electrodes as shown in **Figure 4E**. This arrangement created a steady ACSF pool around the nerve and stabilized the optic nerve for subsequent imaging. Then the objective (working distance 2 mm) was positioned above the nerve by dipping it into the ACSF pool (**Figure 4F**). The imaging plane of the objective was focused on the nerve surface by visual control using a wide-field camera (installed in a separate optical path of the microscope). Finally, the syringes connected to the suction electrodes were carefully detached to release the pressure on the nerve ends which minimizes drift while imaging later. The nerve was allowed to equilibrate in this arrangement with the microscope objective in place and continuous ACSF flow for at least 30 min before starting the experiments.

Optic Nerve Electrophysiology and Two-Photon Imaging

Nerve Stimulation and CAP Recording

Throughout all initial adjustments and during the equilibration phase (see above), the optic nerve was stimulated every 10 s and the evoked CAP response (**Figure 5A**) was monitored. Stimulations (square-wave current pulses of 50 μs and 0.8 mA) were triggered using a stimulus generator (STG 4002-1.6 mA, Multichannel Systems) which was connected to the stimulation electrode and controlled by the computer software MC_Stimulus. The recording electrode was connected to a miniature pre-amplifier (2× gain MPA, Multichannel Systems) and a data acquisition system (USB-ME16-FAI, Multichannel Systems). The signal was amplified 200 times, filtered at 30 kHz, and acquired at 50 kHz using the acquisition software MC_Rack (Multichannel Systems; RRID:SCR_014955). Stimulating the nerve with 0.8 mA elicited a maximal CAP response, meaning that all optic nerve axons are likely to have been excited (Stys et al., 1991). During the equilibration phase (especially after releasing the suction pressure from the nerve) the CAP amplitude typically dropped by 10%–20% while the nerve was adjusting to the electrodes. However, the CAP response normally became stable within 15–20 min.

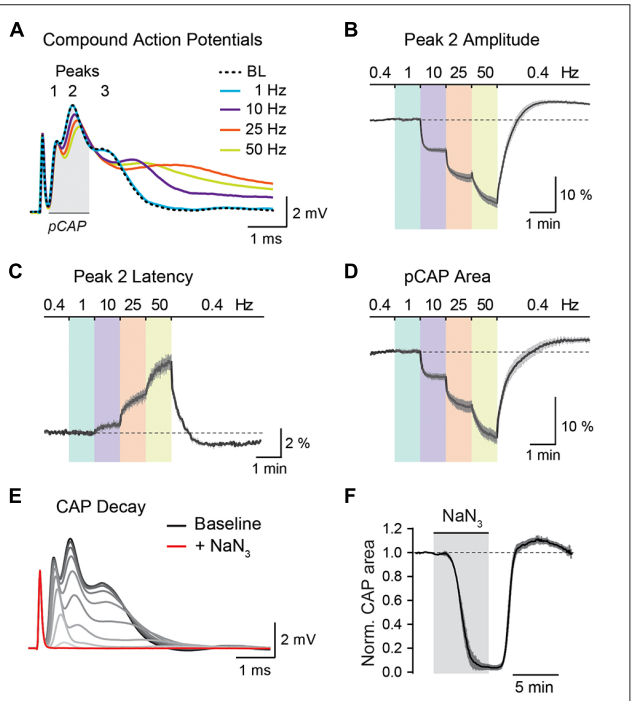

FIGURE 5 | Analysis of optic nerve CAP recordings. **(A)** Example traces of the three-peak shaped CAP responses at 0.4 Hz baseline (BL) and at 1, 10, 25 and 50 Hz nerve stimulations. CAP traces of 1–50 Hz are taken from the end of a 1 min stimulus train. **(B,C)** Average time course of relative changes in peak 2 amplitude **(B)** and peak 2 latency **(C)** during the stepwise increase in stimulation frequency. Changes (in %) are presented relative to the 0.4 Hz BL recordings. Note that with higher stimulation frequencies, CAP peak amplitude decreases and peak latency increases. **(D)** Relative changes (in %) in partial CAP (pCAP) area with increasing stimulation frequency. The pCAP area is defined as the area under the curve (AUC) of the first two CAP peaks (indicated by the gray area in **(A)**) integrating changes in amplitude and latency. **(E)** Gradual decline of the CAP response (shown in 15 s intervals) to full conduction block (red trace) during inhibition of mitochondrial respiration with NaN_3 (5 mM). **(F)** Average time course of the relative CAP area decay and recovery when challenged with NaN_3 (5 mM) for 6 min. CAP area is normalized to BL before pharmacological treatment. In **(B–D,F)** data is represented as means ± SEM, $n = 5$ nerves from five animals.

Axonal Sensor Imaging

Optic nerve axons expressing the FRET-based ATP sensor (FRET pair: mseCFP and cp173-mVenus; Imamura et al., 2009) were imaged with a custom-built two-photon laser scanning microscope (Mayrhofer et al., 2015) using a Ti:Sapphire laser (Chameleon Ultra II; Coherent) at 870 nm wavelength and equipped with a 25× water immersion objective (XLPLN 25×/1.05 WMP2, Olympus). Fluorescence emission was detected with two GaAsP photomultiplier modules (Hamamatsu Photonics, H10770PA-40 SEL) using a dichroic beam-splitter (506 nm edge, BrightLine; Semrock, FF506-Di03-25 × 36) and two band-pass filters 545/55 nm (yellow channel) and 475/50 nm (blue channel; BrightLine; Semrock, FF01-545/55-25, FF02-475/50-25). Image acquisition was controlled by the MATLAB (RRID:SCR_001622) software ScanImage (RRID:SCR_014307; Pologruto et al., 2003). Laser power was adjusted between 5 and 15 mW for axonal sensor imaging. Initial overview stacks of axonal sensor expression were acquired at a resolution of 512 × 512 pixels. For sensor imaging during nerve stimulations, frames were acquired 15 to 20 μm below nerve surface with 8–10× digital zoom at 256 × 256 pixels and a pixel dwell time of 6.4 μs and images of both channels were collected simultaneously with two detectors every 2 s. CAP recordings and metabolite sensor imaging were synchronized using a TTL trigger driven by the stimulus generator to initiate both acquisitions (electrophysiology and imaging) as well as the stimulation protocol.

Stimulation Protocol and Pharmacology

We measured relative ATP level changes upon axonal stimulations using the following protocol: The optic nerve was first stimulated at 0.4 Hz for 1 min to acquire baseline (BL) values and was followed by a stepwise increase in stimulation frequency to 1, 10, 25 and 50 Hz, with each stimulus train lasting 1 min. A recovery period of 4 min with 0.4 Hz stimulations was added at the end of the stimulus sequence. During BL/recovery periods CAP responses were acquired every 2.5 s whereas during the high frequency trains CAPs were collected every second. Sensor images were acquired every 2 s throughout the entire 9 min stimulation protocol. This sampling rate is in line with the expected kinetics of the relative ATP level changes (Trevisiol et al., 2017) and avoids unnecessary bleaching. In a separate set of experiments, we pharmacologically blocked mitochondrial respiration using 5 mM NaN_3 (Sigma-Aldrich, S2002). The drug was prepared in a separate ACSF bottle, bath applied to the nerve for 6 min and followed by a washout period for about 15 min. Before, during and after drug application sensor images and CAPs were acquired every 2 and 2.5 s, respectively.

The nerve could be studied for several hours with different brief stimulation protocols without any major changes in conduction performance. However, care should be taken if stimulation protocols (e.g., prolonged high frequency stimulations above 50 Hz) or pharmacological challenges (e.g., chemical ischemia) are applied that critically compromise axonal conduction and integrity. After such interventions the experiment should be concluded if reliable and reproducible measurements are desired.

Analysis of CAP Recordings and Sensor Imaging

The stimulus-evoked CAP response typically has three peaks, most likely representing subgroups of axons with different conduction speeds, and the overall area under the curve (AUC) of the CAP response is proportional to the total number of excited axons (Stys et al., 1991; Baltan et al., 2008; Saab et al., 2016). During high-frequency stimulations, CAP peak amplitudes generally decreased whereas peak latencies increased (**Figure 5A**). These changes were best assessed for the second and most prominent CAP peak (**Figures 5B,C**). Additionally, we measured relative changes in the partial CAP (pCAP) area (**Figure 5D**), i.e., the AUC of the first and second CAP peaks, typically in a range of 1 ms from the beginning of the CAP response as indicated in **Figure 5A**. The pCAP area integrates changes in amplitude and latency of the first two CAP peaks (**Figure 5C**), which likely derive from large and medium-sized axons that are reliably detected with conventional laser scanning microscopy (axonal diameters larger than ∼0.5 μm). Relative changes in CAP amplitude, latency and AUC were calculated by normalizing values to BL prior to high-frequency simulations or NaN_3 application. The normalized time course traces from nerve recordings were pooled, and data is presented as means ± SEM. CAP recordings were analyzed using a custom-written MATLAB script, which we provide for download from https://github.com/EIN-lab/CAP-analysis. However, the MATLAB script would need minor adjustments if other acquisition software formats than MC_Rack (multichannel systems; RRID:SCR_014955) are used.

An imaging time-series of the acquired mseCFP and mVenus channels was collected during each imaging experiment. The average signal intensity (of all axons per field of view) of each channel was extracted using ImageJ (RRID:SCR_003070; Schneider et al., 2012). For every acquisition timepoint the ratio of mVenus/mseCFP was calculated, and the time course of the ratios was normalized to the corresponding BL. The normalized time courses were pooled per animal and presented as means ± SEM. For comparisons of relative ATP level changes during high-frequency stimulations or mitochondrial block with NaN_3, the slopes of the normalized time courses were calculated by linear fitting using GraphPad Prism (RRID:SCR_002798) and presented in summary plots as means ± SD. The ATP decay and recovery rates of the NaN_3 experiments were determined from linear fits between 25% and 75% of the normalized decay and recovery curves. For all experiments only one nerve per animal was used and *n* represents number of animals.

RESULTS

Using intravitreal delivery and virus-mediated expression of genetically encoded sensors in optic nerve axons, we provide a novel method to measure axonal metabolite dynamics by combining optic nerve electrophysiology with two-photon imaging (**Figures 5**, **6**). We showcase this approach by imaging axonal ATP dynamics following intravitreal AAV vector injections and expression of the ATP sensor ATeam1.03^{YEMK} (Imamura et al., 2009; **Figure 6**). Three different AAV vector serotypes (AAV2, AAVDJ and AAV9) were tested and axonal

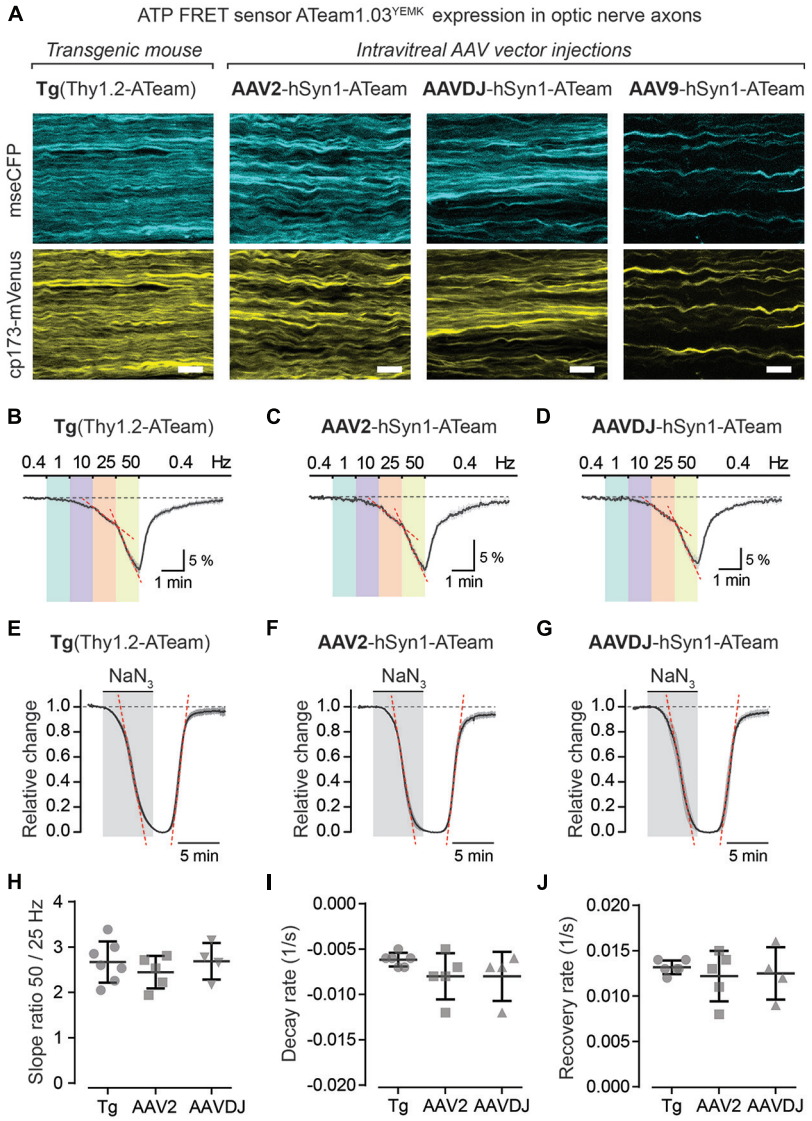

FIGURE 6 | Axonal ATP sensor imaging following intravitreal AVV vector injections. **(A)** Example two-photon scan images of axons expressing the ATP sensor (ATeam1.03^{YEMK}) in acute optic nerve preparations from a transgenic mouse [B6-Tg(Thy1.2-ATeam1.03^{YEMK})AJhi] and from mice with intravitreal injection of AAV vectors [hSyn1-ATeam1.03^{YEMK}-WPRE-hGHp (A)]. Efficacy of sensor expression (number of axons) differs between the AAV vector serotypes tested, with AAV2 and AAVDJ revealing abundant expression whereas with AAV9 only very sparse axonal expression is detected. Both channels, mseCFP (blue) and cp173-mVenus (yellow), of the FRET sensor are depicted. Scale bars 10 μm. **(B–D)** Average time course of relative changes in axonal ATP levels upon stepwise increase in stimulation frequency in nerves from transgenic mice (n = 7; **B**) and from nerves following intravitreal AAV injections of serotypes AAV2 (n = 5; **C**) and AAVDJ (n = 4; **D**). Changes (in % ± SEM) are presented relative to the 0.4 Hz BL. **(E–G)** Relative ATP level changes in axons during and after mitochondrial respiration block, by 5 mM NaN_3 bath application for 6 min, in nerve preparations from transgenic mice **(E)**, AAV2 **(F)** and AAVDJ **(G)** injected mice. To evaluate kinetics of ATP level changes (i.e., decay and recovery rates) the time course of the Venus/CFP ratios is normalized to BL (before NaN_3 application; set as 1) and to the plateau level reached with NaN_3 (set as 0). Depicted are averaged time courses from 4 to 7 nerves ± SEM. **(H)** Axonal ATP levels drop faster (i.e., increase in ATP consumption) with higher stimulation frequencies **(B–D)** and is exemplified here by calculating the ratios of the ATP level decline slopes (red dashed lines in **B–D**) upon 50 and 25 Hz stimulations. A two-fold increase in stimulation frequency reveals on average a 2.7 ± 0.4 (Tg), 2.4 ± 0.4 (AAV2) and 2.7 ± 0.4 (AAVDJ) fold increase in ATP level drop. No overt differences between groups, n = 4–7 ± SD, Welch's t-test. **(I,J)** Summary plots of axonal ATP level decay **(I)** and recovery **(J)** rates from NaN_3 experiments (in **E–G**). Rates (per s) were determined by linear regression between 25% and 75% of the normalized decay and recovery curves (red dashed lines in **E–G**; R^2 of linear fits ≥0.98). Average decay rates **(I)** are −0.006 ± 0.0003 (Tg), −0.008 ± 0.001 (AAV2) and −0.008 ± 0.001 (AAVDJ) and average recovery rates **(J)** are 0.013 ± 0.0003 (Tg), 0.012 ± 0.001 (AAV2) and 0.012 ± 0.001 (AAVDJ). No overt differences between groups, n = 4–7 ± SD, Welch's t-test.

ATP sensor expression (driven by the hSyn1 promoter) was assessed. We observed that transduction efficacy varied strongly between the serotypes used, which was easily judged by the overall abundance of axons expressing the ATP sensor during acute optic nerve imaging (**Figure 6A**, right panels). Three to six weeks after intravitreal injections, AAV2 and AAVDJ revealed ample axonal expression whereas with AAV9 vectors only very sparse axonal expression was

achieved. For comparison, optic nerves from transgenic mice, with a developmental, pan-neuronal expression of the same ATP sensor, show very abundant axonal expression levels (Trevisiol et al., 2017; **Figure 6A**, left panel).

To test axonal ATP sensor performance, optic nerves were metabolically challenged with increasing stimulation frequencies (**Figures 6B–D**) and by pharmacologically blocking mitochondrial ATP production (**Figures 6E–G**). Here, we only focused on nerves from AAV2 and AAVDJ injected mice as they revealed reliable and reproducible axonal expression compared to AAV9. As expected, a stepwise elevation in stimulation frequencies from a 0.4 Hz BL acquisition to 1, 10, 25 and 50 Hz revealed a faster axonal ATP level decline with increasing stimulation frequencies. A steeper axonal ATP level drop likely indicates higher ATP consumption rates due to increasing frequency-dependent energy demands. For example, a two-fold increase in stimulation frequency from 25 Hz to 50 Hz caused on average a 2.6-fold increase in axonal ATP level depletion (**Figure 6H**). Similarly, CAP performance also declines with increasing stimulation frequencies which is best described by the drop in CAP amplitude and pCAP area (**Figures 5B,D**). Moreover, when mitochondrial respiration and thereby ATP production was transiently blocked using 5 mM NaN_3 (bath applied for 6 min) axonal ATP levels rapidly declined (**Figures 6E–G**) leading to a complete nerve conduction block (**Figures 5E,F**). This was reversed by washout of NaN_3 which quickly replenished axonal ATP back to BL levels and completely restored axonal firing. We did not observe overt differences in ATP sensor dynamics between AAV-mediated sensor expressing nerves and transgenic nerves when comparing overall ATP decay and recovery kinetics (**Figures 6I,J**), which are also similar to previous results (Trevisiol et al., 2017). Hence, intravitreal injection of AAV vectors carrying genetically encoded sensors is a fast and reliable approach to drive functional sensor expression in optic nerve axons and by combining electrophysiology with two-photon imaging axonal metabolite dynamics can be studied.

DISCUSSION

Intravitreal delivery of AAV vectors to induce protein expression in RGCs is a widely used and safe technique causing no harm to retinal cells or alterations in retinal physiology (Martin et al., 2002; Hellström et al., 2009; Schön et al., 2015; Smith and Chauhan, 2018). We exploited this technique to drive metabolite sensor expression in optic nerve axons and to study activity-dependent axonal ATP dynamics in acute optic nerve preparations. This novel approach expands our previously described optic nerve imaging method (Trevisiol et al., 2017), allowing more flexibility to express and study dynamics of any biosensor of interest in optic nerve axons. Using our protocol the many established metabolite sensors, such as those for monitoring intracellular glucose (Takanaga et al., 2008), lactate (San Martin et al., 2013), pyruvate (San Martin et al., 2014a) or NADH (Hung et al., 2011; Zhao et al., 2011, 2015), when packed into appropriate AAV vectors, could be reliably expressed and studied in optic nerves from wildtype or genetically modified mice at different ages.

Long-term white matter integrity critically depends on oligodendroglial support functions (Griffiths et al., 1998; Lappe-Siefke et al., 2003; Snaidero et al., 2017) and recent studies have highlighted that myelinated axons may well receive metabolic support in the form of lactate from glycolytic oligodendrocytes (Fünfschilling et al., 2012; Lee et al., 2012; Saab et al., 2016). Using our versatile AAV-mediated approach to investigate metabolite sensors dynamics in myelinated axons may help to further resolve cellular and molecular mechanisms underlying oligodendroglial support functions in regulating axonal energy homeostasis. For example, axonal metabolite dynamics could be studied in mouse mutants with oligodendrocyte- or myelin-specific defects that develop axonal pathology (Griffiths et al., 1998; Lappe-Siefke et al., 2003; Kassmann et al., 2007; Lee et al., 2012; Saab et al., 2016) to better understand whether and how axonal metabolite homeostasis may be perturbed before the onset of axonal degeneration. Moreover, establishing biosensor expression in oligodendrocytes, ideally with a similar viral-mediated approach although technically more challenging, would be a significant expansion of our current optic nerve recording/sensor imaging method to further interrogate the axon-glial unit.

In optic nerves action potential propagation is well-maintained when exogenous lactate or pyruvate is supplied as the main energy source (Brown et al., 2001). And during periods of low glucose availability or aglycemia, lactate supply from astrocytic glycogenolysis becomes critical in sustaining optic nerve conduction (Wender et al., 2000; Brown et al., 2004; Tekkök et al., 2005). Inhibiting mitochondrial respiration with sodium azide in the presence of 10 mM glucose quickly diminishes axonal ATP levels and completely blocks nerve conduction (**Figures 5**, **6**), suggesting that optic nerve axons are primarily fueled by oxidative phosphorylation (Trevisiol et al., 2017). On the other hand, axonal conduction in corpus callosum slice preparations is not well-preserved when exogenous lactate or pyruvate is supplied during glucose deprivation (Meyer et al., 2018). Interestingly, in these aglycemic conditions callosal axons are sufficiently energized to fire action potentials when glucose is presented through the gap junction-coupled oligodendroglial network, suggesting that glucose and/or endogenously generated lactate is transferred to axonal compartments (Meyer et al., 2018).

However, it remains uncertain how intracellular metabolites such as glucose, lactate or pyruvate are distributed between astrocytes, oligodendrocytes and the axonal compartment in different white matter tracts. Do axons take up and metabolize glial-derived lactate during physiological activity or only during metabolic stress such as aglycemia or post-ischemia? Do glial cells provide primarily lactate/pyruvate, or could unphosphorylated glucose also be shuttled to fuel axonal energy metabolism? How does glycolytic activity in glial cells or axonal compartments increase during electrical activity? What are the signaling mechanisms regulating activity-dependent axon-glia metabolic coupling? In future studies, metabolite sensor imaging in white matter tracts will help to resolve how different cellular

compartments interact and exchange metabolites. Measuring activity-dependent axonal metabolite dynamics in acute optic nerve preparations provides a powerful tool to address some of these challenging questions. This opens an exciting avenue for future studies to interrogate molecular and cellular mechanisms of white matter energy metabolism and axon-glial metabolic coupling.

AUTHOR CONTRIBUTIONS

AS designed the protocol and trained ZL. AS and ZL performed experiments, analyses, prepared figures and wrote the manuscript. MB provided software and JH provided resources. BW provided technical support, infrastructure and funding. All authors contributed to the final manuscript.

FUNDING

AS is supported by the University of Zurich and a Synapsis Foundation Career Fellowship Award. JH is supported by the Deutsche Forschungsgemeinschaft (DFG; priority program 1757; grant number HI 1414/6-1). BW is supported by the Swiss National Science Foundation (SNF Number: 31003A_156965) and is a member of the Clinical Research Priority Program of the University of Zurich on Molecular Imaging.

ACKNOWLEDGMENTS

We thank Kim Ferrari, Laetitia Thieren, Ladina Hösli, Marc Zünd, Matthias Wyss and all lab members for frequent discussions and critical input. We thank Jean-Charles Paterna and the VVF of the Neuroscience Center Zurich (ZNZ) for excellent support and AAV production. We express our gratitude to Maya Barben and Christian Grimm (Department of Ophthalmology, University of Zurich) for their technical support. We thank Klaus-Armin Nave (MPI, Göttingen) for longstanding collaboration and continuous support. AS would like to thank Selva Baltan (Lerner Research Institute, Cleveland) for her former mentorship in optic nerve recordings.

REFERENCES

Baltan, S., Besancon, E. F., Mbow, B., Ye, Z., Hamner, M. A., and Ransom, B. R. (2008). White matter vulnerability to ischemic injury increases with age because of enhanced excitotoxicity. *J. Neurosci.* 28, 1479–1489. doi: 10.1523/jneurosci.5137-07.2008

Brown, A. M., Baltan, T. S., and Ransom, B. R. (2004). Energy transfer from astrocytes to axons: the role of CNS glycogen. *Neurochem. Int.* 45, 529–536. doi: 10.1016/j.neuint.2003.11.005

Brown, A. M., Wender, R., and Ransom, B. R. (2001). Metabolic substrates other than glucose support axon function in central white matter. *J. Neurosci. Res.* 66, 839–843. doi: 10.1002/jnr.10081

Díaz-Garcia, C. M., Mongeon, R., Lahmann, C., Koveal, D., Zucker, H., and Yellen, G. (2017). Neuronal stimulation triggers neuronal glycolysis and not lactate uptake. *Cell Metab.* 26, 361.e4–374.e4. doi: 10.1016/j.cmet.2017.06.021

Fleischmann, T., Jirkof, P., Henke, J., Arras, M., and Cesarovic, N. (2016). Injection anaesthesia with fentanyl-midazolam-medetomidine in adult female mice: importance of antagonization and perioperative care. *Lab. Anim.* 50, 264–274. doi: 10.1177/0023677216631458

Fünfschilling, U., Supplie, L. M., Mahad, D., Boretius, S., Saab, A. S., Edgar, J., et al. (2012). Glycolytic oligodendrocytes maintain myelin and long-term axonal integrity. *Nature* 485, 517–521. doi: 10.1038/nature11007

Gao, G., Vandenberghe, L. H., Alvira, M. R., Lu, Y., Calcedo, R., Zhou, X., et al. (2004). Clades of adeno-associated viruses are widely disseminated in human tissues. *J. Virol.* 78, 6381–6388. doi: 10.1128/jvi.78.12.6381-6388.2004

Griffiths, I., Klugmann, M., Anderson, T., Yool, D., Thomson, C., Schwab, M. H., et al. (1998). Axonal swellings and degeneration in mice lacking the major proteolipid of myelin. *Science* 280, 1610–1613. doi: 10.1126/science.280.5369.1610

Grimm, D., Lee, J. S., Wang, L., Desai, T., Akache, B., Storm, T. A., et al. (2008). *In vitro* and *in vivo* gene therapy vector evolution via multispecies interbreeding and retargeting of adeno-associated viruses. *J. Virol.* 82, 5887–5911. doi: 10.1128/JVI.00254-08

Hellström, M., Ruitenberg, M. J., Pollett, M. A., Ehlert, E. M., Twisk, J., Verhaagen, J., et al. (2009). Cellular tropism and transduction properties of seven adeno-associated viral vector serotypes in adult retina after intravitreal injection. *Gene Ther.* 16, 521–532. doi: 10.1038/gt.2008.178

Hou, B. H., Takanaga, H., Grossmann, G., Chen, L. Q., Qu, X. Q., Jones, A. M., et al. (2011). Optical sensors for monitoring dynamic changes of intracellular metabolite levels in mammalian cells. *Nat. Protoc.* 6, 1818–1833. doi: 10.1038/nprot.2011.392

Hung, Y. P., Albeck, J. G., Tantama, M., and Yellen, G. (2011). Imaging cytosolic NADH-NAD$^{(+)}$ redox state with a genetically encoded fluorescent biosensor. *Cell Metab.* 14, 545–554. doi: 10.1016/j.cmet.2011.08.012

Huxley, A. F., and Stämpfli, R. (1949). Evidence for saltatory conduction in peripheral myelinated nerve fibres. *J. Physiol.* 108, 315–339. doi: 10.1113/jphysiol.1949.sp004335

Iadecola, C. (2013). The pathobiology of vascular dementia. *Neuron* 80, 844–866. doi: 10.1016/j.neuron.2013.10.008

Imamura, H., Nhat, K. P., Togawa, H., Saito, K., Iino, R., Kato-Yamada, Y., et al. (2009). Visualization of ATP levels inside single living cells with fluorescence resonance energy transfer-based genetically encoded indicators. *Proc. Natl. Acad. Sci. U S A* 106, 15651–15656. doi: 10.1073/pnas.0904764106

Kassmann, C. M., Lappe-Siefke, C., Baes, M., Brügger, B., Mildner, A., Werner, H. B., et al. (2007). Axonal loss and neuroinflammation caused by peroxisome-deficient oligodendrocytes. *Nat. Genet.* 39, 969–976. doi: 10.1038/ng2070

Lappe-Siefke, C., Goebbels, S., Gravel, M., Nicksch, E., Lee, J., Braun, P. E., et al. (2003). Disruption of Cnp1 uncouples oligodendroglial functions in axonal support and myelination. *Nat. Genet.* 33, 366–374. doi: 10.1038/ng1095

Laughlin, S. B., and Sejnowski, T. J. (2003). Communication in neuronal networks. *Science* 301, 1870–1874. doi: 10.1126/science.1089662

Lee, Y., Morrison, B. M., Li, Y., Lengacher, S., Farah, M. H., Hoffman, P. N., et al. (2012). Oligodendroglia metabolically support axons and contribute to neurodegeneration. *Nature* 487, 443–448. doi: 10.1038/nature11314

Mächler, P., Wyss, M. T., Elsayed, M., Stobart, J., Gutierrez, R., von Faber-Castell, A., et al. (2016). *In vivo* evidence for a lactate gradient from astrocytes to neurons. *Cell Metab.* 23, 94–102. doi: 10.1016/j.cmet.2015.10.010

Martin, K. R., Klein, R. L., and Quigley, H. A. (2002). Gene delivery to the eye using adeno-associated viral vectors. *Methods* 28, 267–275. doi: 10.1016/S1046-2023(02)00232-3

Mayrhofer, J. M., Haiss, F., Haenni, D., Weber, S., Zuend, M., Barrett, M. J., et al. (2015). Design and performance of an ultra-flexible two-photon microscope for *in vivo* research. *Biomed. Opt. Express* 6, 4228–4237. doi: 10.1364/BOE.6.004228

Meyer, N., Richter, N., Fan, Z., Siemonsmeier, G., Pivneva, T., Jordan, P., et al. (2018). Oligodendrocytes in the mouse corpus callosum maintain axonal function by delivery of glucose. *Cell Rep.* 22, 2383–2394. doi: 10.1016/j.celrep.2018.02.022

Nave, K. A. (2010a). Myelination and support of axonal integrity by glia. *Nature* 468, 244–252. doi: 10.1038/nature09614

Nave, K. A. (2010b). Myelination and the trophic support of long axons. *Nat. Rev. Neurosci.* 11, 275–283. doi: 10.1038/nrn2797

Paterna, J. C., Feldon, J., and Büeler, H. (2004). Transduction profiles of recombinant adeno-associated virus vectors derived from serotypes 2 and 5 in the nigrostriatal system of rats. *J. Virol.* 78, 6808–6817. doi: 10.1128/jvi.78.13.6808-6817.2004

Philips, T., and Rothstein, J. D. (2017). Oligodendroglia: metabolic supporters of neurons. *J. Clin. Invest.* 127, 3271–3280. doi: 10.1172/jci90610

Pologruto, T. A., Sabatini, B. L., and Svoboda, K. (2003). ScanImage: flexible software for operating laser scanning microscopes. *Biomed. Eng. Online* 2:13. doi: 10.1186/1475-925X-2-13

Saab, A. S., and Nave, K. A. (2017). Myelin dynamics: protecting and shaping neuronal functions. *Curr. Opin. Neurobiol.* 47, 104–112. doi: 10.1016/j.conb.2017.09.013

Saab, A. S., Tzvetanova, I. D., and Nave, K. A. (2013). The role of myelin and oligodendrocytes in axonal energy metabolism. *Curr. Opin. Neurobiol.* 23, 1065–1072. doi: 10.1016/j.conb.2013.09.008

Saab, A. S., Tzvetavona, I. D., Trevisiol, A., Baltan, S., Dibaj, P., Kusch, K., et al. (2016). Oligodendroglial NMDA receptors regulate glucose import and axonal energy metabolism. *Neuron* 91, 119–132. doi: 10.1016/j.neuron.2016.05.016

Samulski, R. J., Chang, L. S., and Shenk, T. (1989). Helper-free stocks of recombinant adeno-associated viruses: normal integration does not require viral gene expression. *J. Virol.* 63, 3822–3828.

San Martin, A., Ceballo, S., Baeza-Lehnert, F., Lerchundi, R., Valdebenito, R., Contreras-Baeza, Y., et al. (2014a). Imaging mitochondrial flux in single cells with a FRET sensor for pyruvate. *PLoS One* 9:e85780. doi: 10.1371/journal.pone.0085780

San Martin, A., Sotelo-Hitschfeld, T., Lerchundi, R., Fernandez-Moncada, I., Ceballo, S., Valdebenito, R., et al. (2014b). Single-cell imaging tools for brain energy metabolism: a review. *Neurophotonics* 1:011004. doi: 10.1117/1.nph.1.1.011004

San Martin, A., Ceballo, S., Ruminot, I., Lerchundi, R., Frommer, W. B., and Barros, L. F. (2013). A genetically encoded FRET lactate sensor and its use to detect the warburg effect in single cancer cells. *PLoS One* 8:e57712. doi: 10.1371/journal.pone.0057712

Schneider, C. A., Rasband, W. S., and Eliceiri, K. W. (2012). NIH image to imagej: 25 years of image analysis. *Nat. Methods* 9, 671–675. doi: 10.1038/nmeth.2089

Schön, C., Biel, M., and Michalakis, S. (2015). Retinal gene delivery by adeno-associated virus (AAV) vectors: strategies and applications. *Eur. J. Pharm. Biopharm.* 95, 343–352. doi: 10.1016/j.ejpb.2015.01.009

Smith, C. A., and Chauhan, B. C. (2018). *In vivo* imaging of adeno-associated viral vector labelled retinal ganglion cells. *Sci. Rep.* 8:1490. doi: 10.1038/s41598-018-19969-9

Snaidero, N., Velte, C., Myllykoski, M., Raasakka, A., Ignatev, A., Werner, H. B., et al. (2017). Antagonistic functions of MBP and CNP establish cytosolic channels in cns myelin. *Cell Rep.* 18, 314–323. doi: 10.1016/j.celrep.2016.12.053

Sotelo-Hitschfeld, T., Niemeyer, M. I., Machler, P., Ruminot, I., Lerchundi, R., Wyss, M. T., et al. (2015). Channel-mediated lactate release by K^+-stimulated astrocytes. *J. Neurosci.* 35, 4168–4178. doi: 10.1523/JNEUROSCI.5036-14.2015

Stys, P. K., Ransom, B. R., and Waxman, S. G. (1991). Compound action potential of nerve recorded by suction electrode: a theoretical and experimental analysis. *Brain Res.* 546, 18–32. doi: 10.1016/0006-8993(91)91154-s

Takanaga, H., Chaudhuri, B., and Frommer, W. B. (2008). GLUT1 and GLUT9 as major contributors to glucose influx in HepG2 cells identified by a high sensitivity intramolecular FRET glucose sensor. *Biochim. Biophys. Acta* 1778, 1091–1099. doi: 10.1016/j.bbamem.2007.11.015

Tekkök, S. B., Brown, A. M., Westenbroek, R., Pellerin, L., and Ransom, B. R. (2005). Transfer of glycogen-derived lactate from astrocytes to axons via specific monocarboxylate transporters supports mouse optic nerve activity. *J. Neurosci. Res.* 81, 644–652. doi: 10.1002/jnr.20573

Trevisiol, A., Saab, A. S., Winkler, U., Marx, G., Imamura, H., Möbius, W., et al. (2017). Monitoring ATP dynamics in electrically active white matter tracts. *Elife* 6:e24241. doi: 10.7554/elife.24241

Wender, R., Brown, A. M., Fern, R., Swanson, R. A., Farrell, K., and Ransom, B. R. (2000). Astrocytic glycogen influences axon function and survival during glucose deprivation in central white matter. *J. Neurosci.* 20, 6804–6810. doi: 10.1523/jneurosci.20-18-06804.2000

Zhao, Y., Hu, Q., Cheng, F., Su, N., Wang, A., Zou, Y., et al. (2015). SoNar, a highly responsive NAD+/NADH sensor, allows high-throughput metabolic screening of anti-tumor agents. *Cell Metab.* 21, 777–789. doi: 10.1016/j.cmet.2015.04.009

Zhao, Y., Jin, J., Hu, Q., Zhou, H. M., Yi, J., Yu, Z., et al. (2011). Genetically encoded fluorescent sensors for intracellular NADH detection. *Cell Metab.* 14, 555–566. doi: 10.1016/j.cmet.2011.09.004

Zolotukhin, S., Byrne, B. J., Mason, E., Zolotukhin, I., Potter, M., Chesnut, K., et al. (1999). Recombinant adeno-associated virus purification using novel methods improves infectious titer and yield. *Gene Ther.* 6, 973–985. doi: 10.1038/sj.gt.3300938

Conflict of Interest Statement: The authors declare that the research was conducted in the absence of any commercial or financial relationships that could be construed as a potential conflict of interest.

frontiers in Cellular Neuroscience

MINI REVIEW
published: 19 November 2018
doi: 10.3389/fncel.2018.00424

Myelin Dynamics Throughout Life: An Ever-Changing Landscape?

Jill M. Williamson and David A. Lyons**

Centre for Discovery Brain Sciences, The University of Edinburgh, Edinburgh, United Kingdom

Myelin sheaths speed up impulse propagation along the axons of neurons without the need for increasing axon diameter. Subsequently, myelin (which is made by oligodendrocytes in the central nervous system) allows for highly complex yet compact circuitry. Cognitive processes such as learning require central nervous system plasticity throughout life, and much research has focused on the role of neuronal, in particular synaptic, plasticity as a means of altering circuit function. An increasing body of evidence suggests that myelin may also play a role in circuit plasticity and that myelin may be an adaptable structure which could be altered to regulate experience and learning. However, the precise dynamics of myelination throughout life remain unclear – does the production of new myelin require the differentiation of new oligodendrocytes, and/or can existing myelin be remodelled dynamically over time? Here we review recent evidence for both *de novo* myelination and myelin remodelling from pioneering longitudinal studies of myelin dynamics *in vivo*, and discuss what remains to be done in order to fully understand how dynamic regulation of myelin affects lifelong circuit function.

Keywords: myelin, oligodendrocyte, myelin remodelling, circuit plasticity, adaptive myelination

OPEN ACCESS

Edited by:
Fernando C. Ortiz,
Universidad Autónoma de Chile, Chile

Reviewed by:
Maria Kukley,
Eberhard Karls Universität Tübingen, Germany
Ben Emery,
Oregon Health & Science University, United States

****Correspondence:***
Jill M. Williamson
jill.williamson@ed.ac.uk
David A. Lyons
david.lyons@ed.ac.uk

Received: *14 September 2018*
Accepted: *30 October 2018*
Published: *19 November 2018*

Citation:
Williamson JM and Lyons DA (2018) Myelin Dynamics Throughout Life: An Ever-Changing Landscape? Front. Cell. Neurosci. 12:424. doi: 10.3389/fncel.2018.00424

INTRODUCTION

The human brain undergoes extensive maturation throughout life to facilitate cognitive development. The myelination of axons throughout the nervous system is one such crucial maturation process. In the central nervous system (CNS), glial cells called oligodendrocytes extend many processes into their surrounding environment, which concentrically wrap membrane around axons to form myelin sheaths. Myelin sheaths enable the rapid saltatory conduction of action potentials, by localising voltage-gated Na^+ channels to short gaps between adjacent sheaths (known as the nodes of Ranvier), and by acting as electrical insulators. Axons that are fully myelinated along their length conduct impulses many times faster than unmyelinated axons of the same cross sectional size (Waxman, 1980). Therefore, myelinated neural circuits conduct information much faster than unmyelinated circuits. Humans are born with a virtually unmyelinated CNS, and the oligodendrocyte population expands dramatically following birth with widespread myelination in the first few years of childhood. Myelination continues through adolescence and into adulthood in a characteristic spatiotemporal manner, correlating with the emergence and maintenance of proper circuit function. For example, the maturation of white matter (the myelin-rich areas of the CNS) is concurrent with development of childhood cognitive processes, such as information processing speed (Mabbott et al., 2006; Scantlebury et al., 2014). Additionally, myelin pathology/abnormalities are seen not only in the demyelinating disease Multiple Sclerosis, but also in several neurodegenerative diseases (Kang et al., 2013; Huang et al., 2015) and neurodevelopmental disorders (Takahashi et al., 2011).

However, myelination of individual axons is not an "all-or-nothing" phenomenon. Axons in the CNS exhibit extensive variation in myelin sheath number, sheath length, sheath thickness, and distribution along their length. Many different patterns of myelination exist; for example axons with sparsely myelinated regions have been described in juvenile and adult mouse cortex (Tomassy et al., 2014; Hill et al., 2018; Hughes et al., 2018). Modification to any of these sheath parameters has predictable effects on the conduction speed of the underlying axon – therefore establishing a specific pattern of myelination along an axon may be particularly important to fine-tune circuit function. For instance, axons in the auditory brainstem of gerbils exhibit progressively shorter myelin sheaths along distal regions to ensure the precise timing of signal arrival to facilitate sound localisation (Ford et al., 2015). Subtle changes in the overall pattern of myelination along an axon (either via the addition of new myelin, or the remodelling of existing myelin) could profoundly change the timing of neural impulses in circuits. If myelin is adaptable then modifying such patterns of myelination may represent a powerful mechanism in regulating circuit function throughout life.

Recent evidence suggests that myelin may be adaptable in response to circuit activity. Whole-brain diffusion tensor imaging can be used to measure broad changes in the myelin-rich white matter over time – such experiments in humans and rodents have shown that learning a new task correlates with white matter alterations in relevant brain regions (Scholz et al., 2009; Sampaio-Baptista et al., 2013). Cellular level analyses in animal models demonstrate that the production of new myelinating oligodendrocytes is required for efficient motor learning (McKenzie et al., 2014; Xiao et al., 2016). It is currently hypothesised that neural circuit activity can trigger changes in myelin; an extensive body of research has demonstrated that neuronal activity can influence the proliferation of oligodendrocyte precursor cells (OPCs), the differentiation of oligodendrocytes, and the formation and growth of myelin sheaths. This research, including evidence for the molecular signals involved, has been extensively reviewed elsewhere (Fields, 2015; Almeida and Lyons, 2017; Mount and Monje, 2017). Neuronal activity could drive changes to myelin which could, in turn, change conduction speeds to fine-tune the timings underpinning circuit function.

However, we still do not know whether or how the myelination of circuits is dynamically regulated throughout life. Rodent work indicates that new oligodendrocytes are generated throughout the CNS even in adulthood (Young et al., 2013), and OPCs do reside within the human adult brain (Chang et al., 2000). Carbon-dating analysis of human tissue has identified adult-born oligodendrocytes within the cortex, although the same analyses indicated that the majority of oligodendrocytes in the corpus callosum originate in early childhood (Yeung et al., 2014). However, the neuroimaging studies in humans that correlate white matter structural alterations with task learning suggest that new myelin can be formed throughout life. Such protracted myelination would in principle require lifelong oligodendrocyte production, given that individual myelinating oligodendrocytes have a restricted time window of just a few hours to initiate formation of new sheaths (Watkins et al., 2008; Czopka et al., 2013) and sheath number per oligodendrocyte appears stable over time (Tripathi et al., 2017). One caveat noted by Mount and Monje (2017) is that the "birth" date in the carbon-dating experiment (which identifies the time point of DNA replication during cell division), reflects that of the OPC, not necessarily the differentiated oligodendrocyte. This is important given evidence that OPCs can directly differentiate into oligodendrocytes without cell division, at least in rodents (Hughes et al., 2013). OPCs in the corpus callosum could directly differentiate into oligodendrocytes many years after their terminal cell division; thus the time of differentiation of these new oligodendrocytes cannot be determined by carbon-dating, and so Yeung et al. (2014) may have underestimated the rate of oligodendrocyte production in the adult human brain. We still have much to learn about the relative contributions of oligodendrocyte generation and myelin remodelling to CNS development throughout life.

To fully understand the precise dynamics of oligodendrogenesis, myelin formation and myelin remodelling throughout various stages of life, longitudinal imaging at high-resolution represents the gold-standard approach. Here we provide an overview of recent *in vivo* imaging studies that are beginning to clarify the dynamics of myelination, which will also allow us to begin to understand how such dynamics might impact neural circuit function.

DE NOVO MYELINATION

To begin to definitively address how oligodendrocytes are generated and how myelin is made and dynamically remodelled *in vivo*, two recent studies utilised repeated two-photon imaging of the mouse somatosensory cortex over extended periods of time. Hughes et al. (2018) imaged the cortex of transgenic reporter mice with fluorescently labelled oligodendroglial lineage cells from early adulthood, through middle and old age (approximately P720). They found that the oligodendrocyte population continues to expand and that cortical oligodendrocyte density nearly doubles between young adult and middle-aged stages (**Figure 1A**). This was accompanied by an over twofold increase in the number of cortical myelin sheaths. But how does oligodendrocyte number increase? In early post-natal development many oligodendrocytes are produced but only a subset survive and go on to myelinate axons (Barres et al., 1992). This appears to be similar in adulthood – by following individual cortical OPCs in the adult cortex for up to 50 days, Hughes et al. (2018) revealed that the majority of newly differentiated oligodendrocytes undergo cell death, with only 22% surviving and committing to myelination (**Figure 1B**). It remains unknown what proportion of newly differentiated oligodendrocytes are generated following OPC division versus direct differentiation. However, once oligodendrocytes commit to myelination they remain stable, with no evidence of myelinating oligodendrocytes undergoing cell death during a 50-day imaging period.

Similarly, Hill et al. (2018) used transgenic reporters of oligodendrocytes and the label-free spectral confocal reflectance (SCoRe) microscopy technique to image myelin along axons

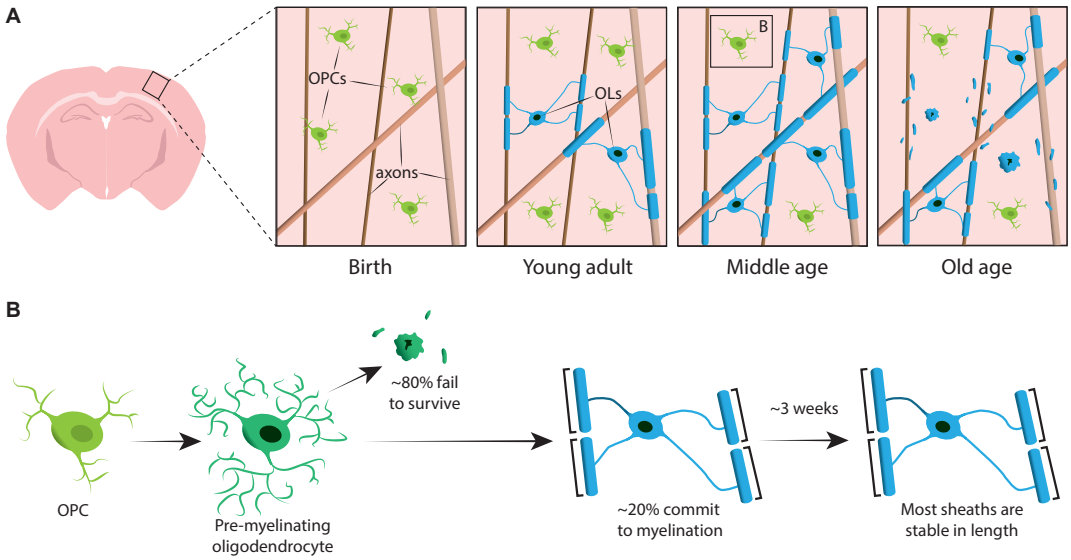

FIGURE 1 | Oligodendrocyte and myelin dynamics in the mammalian cortex throughout life. **(A)** Oligodendrocyte precursor cells (OPCs) continuously generate new myelinating oligodendrocytes (OLs) in the somatosensory cortex from birth up to middle age. The OL population then declines in old age, accompanied by a reduction in myelin coverage. **(B)** Lineage-tracing of single OPCs shows that although premyelinating OLs are continuously produced in adulthood, only approximately 20% survive to myelinate. Most myelin sheaths, once formed, are stable in length over prolonged period of time, indicating that there is normally very little remodelling of existing myelin. Summary of data from Hill et al. (2018) and Hughes et al. (2018).

(Schain et al., 2014) in the somatosensory cortex of juvenile, young adult, middle-aged, and old-aged mice (P950). They also found that the oligodendrocyte number continues to expand in adulthood up to P650, and that oligodendrocytes are stable in middle age for up to 80 days of imaging. They found that myelination of the cortex also peaks in middle age at P650, and that oligodendrocyte density significantly falls from its peak (at P650) through very old age (P950) (**Figure 1A**). This was reflected in a reduction of myelin coverage of layer I cortical axons between P650 and P950. Long-term oligodendrocyte survival may vary between different parts of the CNS. Tripathi et al. (2017) labelled myelinating oligodendrocytes at P60 in mice and then counted how many labelled cells survived until P605 in several CNS regions. They found that in the spinal cord and motor cortex, 60–70% of P60 labelled cells survived, whereas in the corpus callosum, over 90% of P60 labelled cells survived. The reduction in oligodendrocyte number and myelination in certain CNS regions with age raises intriguing questions concerning the role of myelin loss in age-associated cognitive decline. MRI analysis shows that white matter microstructure correlates with fluid intelligence (Ritchie et al., 2015), but also that this white matter microstructure deteriorates with increasing age (Cox et al., 2016). Subsequent age-associated myelin loss could lead to reduced cognitive function due to dysregulation of myelinated circuits.

Could the generation of new oligodendrocytes (and subsequently new myelin) in the adult cortex be responsive to circuit activity? Previous research has shown that reducing sensory input by removing whiskers from mice leads to reduced oligodendrogenesis in the somatosensory cortex (Hill et al., 2014). To investigate this further, Hughes et al. (2018) provided adult (P365) mice with sensory stimulation for 3 weeks by hanging beads in the animal cages to repeatedly stimulate their whiskers and thus the somatosensory cortex. By imaging the somatosensory cortex before and after the 3 weeks, they demonstrated that sensory stimulation increases oligodendrocyte number, potentially due to the increased survival of newly differentiated cells. Kougioumtzidou et al. (2017) provided further evidence that circuit activity may be important in regulating cell survival – they demonstrated that loss of AMPA receptor subunits 2, 3, and 4 in OPCs leads to reduced survival of oligodendrocytes. This suggests that *de novo* myelination could be modulated by cortical circuit activity throughout life, perhaps to fine-tune the function of those same circuits.

Many questions remain to be addressed: what is the effect of oligodendrogenesis and new myelination on actual circuit function? Does neuronal activity enhance the long-term survival of myelinating oligodendrocytes? It is possible that the loss of oligodendrocytes in old age is due to age-associated reduction in neuronal activity, which might, in turn, affect overall oligodendrocyte survival. Alternatively, it may be that oligodendrocytes have a limited lifespan independent of neuronal activity (either intrinsically programmed or influenced by other extrinsic signals associated with aging). In either case, circuit stimulation could help alleviate age-associated myelin loss by either promoting survival of existing oligodendrocytes or stimulating the production of new oligodendrocytes. This in turn could have significant implications in the treatment and prevention of age-associated cognitive decline.

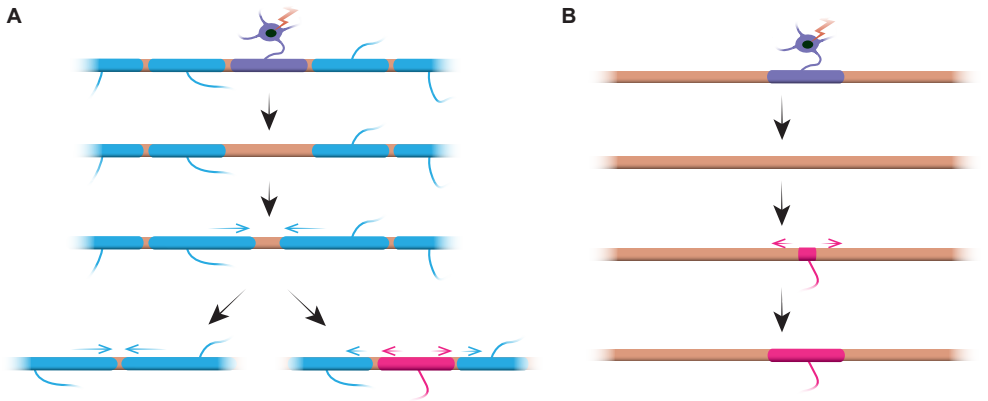

FIGURE 2 | Myelin remodelling can occur *in vivo*. **(A)** Ablation of single sheaths on a fully myelinated axon can induce the rapid growth of neighbouring sheaths to cover the gap. This gap can either be covered entirely by the neighbouring sheaths, or the original myelination profile can be restored by the addition of a new sheath. **(B)** Ablation of a sheath on a sparsely myelinated axon is followed by formation of a new myelin sheath of identical size and location to the ablated predecessor sheath. Summary of data from Auer et al. (2018).

Activity-mediated oligodendrogenesis is not restricted to the somatosensory cortex – young adult mice undergoing motor learning also show an increase in the number of newly differentiated oligodendrocytes in the motor cortex (Xiao et al., 2016). What about other areas of the CNS? Many cortical axons project via the corpus callosum, and therefore, stimulation of cortical circuits could signal to both cortical and callosal OPCs. Two rodent studies have demonstrated that stimulation of cortical neurons induces oligodendrogenesis within the corpus callosum. Gibson et al. (2014) optogenetically stimulated layer V projection neurons in the premotor cortex, finding a rise in OPC proliferation in both the premotor cortex and corpus callosum. This led to an increase in oligodendrocyte number and sheath thickness 4 weeks post-stimulation. More recently, Mitew et al. (2018) used Designer Receptors Exclusively Activated by Designer Drugs to stimulate layer 2/3 somatosensory neurons, and also observed increased OPC proliferation, oligodendrogenesis, and thicker myelin sheaths in the corpus callosum in both juvenile and adult mice. They also demonstrated that new oligodendrocytes preferentially form myelin sheaths on the active axons. This indicates that activity-induced *de novo* myelination can, in principle, target active axons/circuits. It remains unknown how long-lasting changes to myelin in response to neuronal activity might be. The long-term survival of myelinating cells noted by Tripathi et al. (2017), Hill et al. (2018), and Hughes et al. (2018) suggests that once an oligodendrocyte forms myelin sheaths it is likely to survive even if neuronal activity levels return back down to baseline. Whether the myelin sheaths themselves change once neuronal activity returns to normal levels requires more investigation of individual sheath dynamics, which is discussed below.

Thus, it is possible that lifelong *de novo* myelination may occur in many CNS regions, where axons suitable for myelination have sufficient unmyelinated space. However, it remains unclear to what extent oligodendrogenesis continues in different areas of the adult human brain. Carbon-dating analysis suggests that most oligodendrocytes in the corpus callosum tract are generated in early childhood (Yeung et al., 2014). Immunohistochemical analysis of human brain tissue using a novel marker for newly differentiated oligodendrocytes (BCAS1) shows new oligodendrocytes in the frontal cortex even beyond middle-age, but very few new oligodendrocytes in white matter after the third decade of life (Fard et al., 2017). This difference in oligodendrogenesis between species could be a result of scale. Hughes et al.'s (2013) rodent data suggests that oligodendrocytes are generated in huge excess, with continuous pruning of almost 80% of cells. Given the energy cost of such a process, is this mechanism sustainable throughout life in an organ the size of the human brain? Perhaps in the human brain there is limited oligodendrocyte overproduction, because of a need for more protracted myelination of the larger CNS, or because signals such as neuronal activity stimulate OPCs to differentiate into oligodendrocytes as and when required.

MYELIN REMODELLING

The remodelling of existing myelin sheaths could alter conduction properties without the need for generating new oligodendrocytes or myelin. Changing the lengths of existing myelin sheaths could change the myelin coverage along an axon and the distance between nodes of Ranvier (which would both impact conduction speeds). In addition, even very subtle myelin remodelling could alter the lengths of the nodes themselves. It has recently been shown that node length can vary extensively in the optic nerve and in the cortex, and that changing the node lengths along an axon can, in principle, also significantly alter conduction velocity (Arancibia-Cárcamo et al., 2017). Whether changes to node of Ranvier are primarily driven by myelination or reorganisation of the axon itself remains to be determined.

Both Hill et al. (2018) and Hughes et al. (2018) performed longitudinal study of individual myelin sheaths in the mouse somatosensory cortex for several weeks to assess if sheath lengths are dynamically regulated. Hill et al. (2018) found that, in early adulthood (P90–120), although some sheaths exhibit extension or shrinkage, 81% of sheaths observed were stable. More sheaths may become stable in length with age; Hughes et al. (2018) followed sheaths in older (P365) animals and saw that 99% of sheaths remained stable over 3 weeks (**Figure 1B**).

Similar sheath length stability has also been described elsewhere; Auer et al. (2018) used larval zebrafish to investigate whether individual sheaths can change in length over time by performing time-course live imaging of fluorescently labelled myelin sheaths. They found that individual sheaths undergo rapid but variable growth in the first few days after formation, before stabilising their sheath lengths. Once stabilised, sheaths only continue to grow to accommodate the overall growth of the animal.

Why do some sheaths in the cortex change in length, whilst others do not? This may reflect diversity in the demands of distinct neural circuits. Axonal diversity has been observed during initial myelination in the zebrafish spinal cord, where some axons use synaptic vesicle release to regulate myelin sheath number and length while others do not (Koudelka et al., 2016). This raises the intriguing hypothesis that only some axons are capable of regulating myelin via activity-related signals. Hughes et al. (2018) found that their sensory stimulation paradigm did not increase the proportion of dynamic sheaths in the somatosensory cortex. However, more detailed analysis of axon subtype diversity coupled with longitudinal study of sheath length dynamics could confirm if sheath length remodelling is specific to certain circuits.

Does sheath length stability reflect an inability of sheaths to remodel? Experiments in the zebrafish suggest that sheath length remodelling can be induced when the myelination profile of an axon is disrupted. Auer et al. (2018) ablated single oligodendrocytes and therefore sparsely removed sheaths along axons. They found that when a single myelin sheath is lost on a fully myelinated axon, the neighbouring sheaths could reinitiate rapid growth to cover the unmyelinated gap. In several cases a new myelin sheath would form in place of its predecessor and could even push back against the invading neighbour sheaths to restore the original pattern of myelination (**Figure 2A**). Therefore, sometimes a specific myelination pattern is preferentially maintained, even after myelin disruption. This may be to sustain the optimised conduction properties of the underlying axon. Auer et al. (2018) observed sparsely myelinated axons in the larval zebrafish, as previously identified in the rodent cortex. Interestingly, they found that upon ablation of single sheaths on such sparsely myelinated axons a new sheath formed in virtually the same place as the ablated sheath, even along an otherwise unmyelinated stretch of the axon (**Figure 2B**). Thus the myelination patterns along sparsely myelinated axons also appear to be stably maintained in zebrafish, as suggested by Hill et al. (2018) in rodents. The function of sparse myelination profiles remains unknown. Such patterns may allow for more dynamic fine-tuning of single axon function over time, although it is also possible that such unmyelinated gaps may facilitate gradual myelination to maintain consistent conduction times within circuits, as the animal grows and/or axon lengths change.

Do stable myelin sheaths in mammals also have this capacity to remodel when the myelination pattern is disrupted? Further longitudinal studies coupled with demyelination are required to answer this question. It is possible that such remodelling is not induced by neuronal activity but is a compensatory mechanism for myelin loss. Age-associated oligodendrocyte loss could trigger remodelling of surviving sheaths to cover denuded portions of axon and therefore help maintain circuit function. Live imaging of myelin sheaths in old age could determine if this is the case.

The live imaging studies discussed here have all assessed myelin sheath length dynamics, but not myelin sheath thickness. Can sheath thickness be dynamically regulated? Stimulating PI3K/AKT/mTOR signalling in oligodendrocytes of adult mice triggers additional myelin wrapping to increase sheath thickness (Snaidero et al., 2014). This may be modulated by circuit activity, as neuronal stimulation leads to increased sheath thickness in both juvenile and adult mice (Gibson et al., 2014; Mitew et al., 2018). This highlights the need to image all sheath parameters longitudinally to fully understand the dynamics of sheath remodelling. There is a need for live-imaging modalities to accurately measure sheath thickness along axons, as currently this requires cross-sectional measurement via electron microscopy, which limits analysis to a single time-point. Some label-free imaging techniques, such as third harmonic generation microscopy and spectral reflectometry, show promise for performing such measurements (Lim et al., 2014; Kwon et al., 2017). Coupling these techniques with longitudinal studies of the rodent cortex could determine whether established myelin sheaths can adjust their thickness, or if neuronal activity simply pushes *de novo* myelination to produce thicker sheaths.

It therefore seems that, although myelin sheaths are capable of remodelling when myelin is disrupted, most sheaths are generally stable in length. This stability is potentially due to the maintenance of early established myelination patterns optimised for circuit function.

THE FUTURE

Recent mammalian imaging studies have focused on *de novo* myelination and sheath remodelling in cortical grey matter. Cortical circuits receive and send information via many regions, such as the spinal cord and corpus callosum, and so changes to myelin in several different CNS areas could alter signalling in a single circuit. The CNS is traditionally described by appearance after formaldehyde fixation, where "white matter" describes the heavily myelinated axonal tracts, while "grey matter" describes regions densely packed with neuronal cell bodies, dendrites, and synapses. However, this classification is overly simplistic; OPCs produce myelinating oligodendrocytes in both grey and white matter (Dawson et al., 2003), and in fact there is emerging evidence of diversity in the oligodendroglial lineage and in patterns of myelination in both grey and white matter

(Rivers et al., 2008; Viganò et al., 2013; Young et al., 2013; Bechler et al., 2015). Such diversity may reflect the unique requirements of myelin in distinct areas, and potentially on distinct circuits, of the CNS. Further longitudinal imaging studies are required to better understand the dynamics of *de novo* myelination and sheath remodelling in areas of the CNS beyond the cortex.

While the optical transparency of the larval zebrafish lends itself to non-invasive live imaging, performing such experiments in the mammalian CNS is more invasive and technically challenging. Hill et al. (2018) and Hughes et al. (2018) utilised two-photon microscopy with cranial imaging windows to image depths up to 400 μm into the cortex. Similar techniques could be used to image superficial myelinated tracts in the spinal cord over time (Locatelli et al., 2018) but deeper CNS regions cannot be penetrated by two-photon microscopy alone. One alternative is to use two-photon microendoscopy, where a microendoscope probe with a gradient refractive index (GRIN) lens is inserted into the tissue to image cells deeper in the brain [previously used to image CA1 neurons of the hippocampus (Jung et al., 2004; Levene et al., 2004)]. However, endoscope insertion may lead to inflammatory responses which could impact myelination. An alternative could be three-photon microscopy using the cranial imaging window method, which has also been previously used to image the hippocampus (Horton et al., 2013; Ouzounov et al., 2017). Three-photon microscopy gives a significantly greater signal-to-background ratio than two-photon microscopy and can therefore be used to image deeper tissue structures.

It is particularly important to consider not only different CNS regions, but different neurons within these regions. Previous research suggests that there are mechanistic differences in how distinct neuron subtypes regulate their myelination (Koudelka et al., 2016). Additionally, there may be diversity in local regulation of myelin. It is essential to remember that different parts of the CNS are not separate entities but are interconnected. Integrating mesoscale connectomics, which focuses on understanding the connections of different neuron subtypes across different regions (Zeng, 2018), will be crucial to our understanding of how lifelong myelination dynamics vary between different circuits.

What is the functional consequence of myelin regulation along distinct circuits? Thus far, the functional implications can only be inferred by correlations with behaviour. Ultimately, there is a need to couple measurement of myelin dynamics with direct assessment of circuit activity. This will require the recording of neuronal activity during longitudinal studies of myelination in order to directly connect *de novo* myelination or sheath remodelling observed to changes in circuit function with time. It will be important to measure the myelin dynamics and electrophysiological activity of individual neurons and axons to determine how changes in the various myelin sheath parameters actually affects the conduction properties at the single cell level, as well as assessing activity on a population level. Tools such as genetically encoded Ca^{2+} or voltage indicators allow relatively non-invasive recording of circuit activity, and can even be used to assess whole-brain circuit activity (Ahrens et al., 2012; Lovett-Barron et al., 2017).

CONCLUSION

The myelination of axons represents a powerful potential mechanism to regulate circuit function throughout life. Research has demonstrated that *de novo* myelination in the cortex (via the production of new oligodendrocytes) occurs even in adulthood, and that this can be enhanced by stimulating circuit activity. Once myelin has formed, it is stable with little turnover of oligodendrocytes and limited remodelling of the lengths of existing myelin sheaths. However, these stable structures may retain the capacity to remodel if myelin is disturbed. This has interesting implications concerning the plasticity of myelin in maintaining circuit function during injury, disease, and old age. Precisely how changes in myelination affect the function of the underlying circuit remains to be seen. Ultimately, a circuit-level approach, integrating analysis of myelin dynamics with direct measurement of circuit function, is required to fully appreciate how dynamic myelination influences overall nervous system function throughout life.

AUTHOR CONTRIBUTIONS

All authors listed have made a substantial, direct and intellectual contribution to the work, and approved it for publication.

FUNDING

DAL is supported by a Wellcome Trust Senior Research Fellowship (102836/Z/13/Z). JMW is supported by a University of Edinburgh Ph.D. Tissue Repair Studentship Award (MRC Doctoral Training Partnership MR/K501293/1) and the Wellcome Trust Four-Year Ph.D. Program in Tissue Repair (Grant 108906/Z/15/Z).

REFERENCES

Ahrens, M. B., Li, J. M., Orger, M. B., Robson, D. N., Schier, A. F., Engert, F., et al. (2012). Brain-wide neuronal dynamics during motor adaptation in zebrafish. *Nature* 485, 471–477. doi: 10.1038/nature11057

Almeida, R. G., and Lyons, D. A. (2017). On myelinated axon plasticity and neuronal circuit formation and function. *J. Neurosci.* 37, 10023–10034. doi: 10.1523/JNEUROSCI.3185-16.2017

Arancibia-Cárcamo, I. L., Ford, M. C., Cossell, L., Ishida, K., Tohyama, K., and Attwell, D. (2017). Node of Ranvier length as a potential regulator of myelinated axon conduction speed. *eLife* 6:e23329. doi: 10.7554/eLife.23329

Auer, F., Vagionitis, S., and Czopka, T. (2018). Evidence for myelin sheath remodeling in the CNS revealed by *in vivo* imaging. *Curr. Biol.* 28, 549–559. doi: 10.1016/j.cub.2018.01.017

Barres, B. A., Hart, I. K., Coles, H. S. R., Burne, J. F., Voyvodic, J. T., Richardson, W. D., et al. (1992). Cell death and control of cell survival

in the oligodendrocyte lineage. *Cell* 70, 31–46. doi: 10.1016/0092-8674(92)90531-G

Bechler, M. E., Byrne, L., and Ffrench-Constant, C. (2015). CNS myelin sheath lengths are an intrinsic property of oligodendrocytes. *Curr. Biol.* 25, 2411–2416. doi: 10.1016/j.cub.2015.07.056

Chang, A., Nishiyama, A., Peterson, J., Prineas, J., and Trapp, B. D. (2000). NG2-positive oligodendrocyte progenitor cells in adult human brain and multiple sclerosis lesions. *J. Neurosci.* 20, 6404–6412. doi: 10.1523/JNEUROSCI.20-17-06404.2000

Cox, S. R., Ritchie, S. J., Tucker-Drob, E. M., Liewald, D. C., Hagenaars, S. P., Davies, G., et al. (2016). Ageing and brain white matter structure in 3,513 UK Biobank participants. *Nat. Commun.* 7:13629. doi: 10.1038/ncomms13629

Czopka, T., Ffrench-Constant, C., and Lyons, D. A. (2013). Individual oligodendrocytes have only a few hours in which to generate new myelin sheaths *in vivo*. *Dev. Cell* 25, 599–609. doi: 10.1016/j.devcel.2013.05.013

Dawson, M. R. L., Polito, A., Levine, J. M., and Reynolds, R. (2003). NG2-expressing glial progenitor cells: an abundant and widespread population of cycling cells in the adult rat CNS. *Mol. Cell. Neurosci.* 24, 476–488. doi: 10.1016/S1044-7431(03)00210-0

Fard, M. K., Van der Meer, F., Sánchez, P., Cantuti-Castelvetri, L., Mandad, S., Jäkel, S., et al. (2017). BCAS1 expression defines a population of early myelinating oligodendrocytes in multiple sclerosis lesions. *Sci. Transl. Med.* 9:eaam7816. doi: 10.1126/scitranslmed.aam7816

Fields, R. D. (2015). A new mechanism of nervous system plasticity: activity-dependent myelination. *Nat. Rev. Neurosci.* 16, 756–767. doi: 10.1038/nrn4023

Ford, M. C., Alexandrova, O., Cossell, L., Stange-Marten, A., Sinclair, J., Kopp-Scheinpflug, C., et al. (2015). Tuning of Ranvier node and internode properties in myelinated axons to adjust action potential timing. *Nat. Commun.* 6:8073. doi: 10.1038/ncomms9073

Gibson, E. M., Purger, D., Mount, C. W., Goldstein, A. K., Lin, G. L., Wood, L. S., et al. (2014). Neuronal activity promotes oligodendrogenesis and adaptive myelination in the mammalian brain. *Science* 344:1252304. doi: 10.1126/science.1252304

Hill, R. A., Li, A. M., and Grutzendler, J. (2018). Lifelong cortical myelin plasticity and age-related degeneration in the live mammalian brain. *Nat. Neurosci.* 21, 683–695. doi: 10.1038/s41593-018-0120-6

Hill, R. A., Patel, K. D., Goncalves, C. M., Grutzendler, J., and Nishiyama, A. (2014). Modulation of oligodendrocyte generation during a critical temporal window after NG2 cell division. *Nat. Neurosci.* 17, 1518–1527. doi: 10.1038/nn.3815

Horton, N. G., Wang, K., Kobat, D., Clark, C. G., Wise, F. W., Schaffer, C. B., et al. (2013). *In vivo* three-photon microscopy of subcortical structures within an intact mouse brain. *Nat. Photonics* 7, 205–209. doi: 10.1038/NPHOTON.2012.336

Huang, B., Wei, W., Wang, G., Gaertig, M. A., Feng, Y., Wang, W., et al. (2015). Mutant huntingtin downregulates myelin regulatory factor-mediated myelin gene expression and affects mature oligodendrocytes. *Neuron* 85, 1212–1226. doi: 10.1016/j.neuron.2015.02.026

Hughes, E. G., Kang, S. H., Fukaya, M., and Bergles, D. E. (2013). Oligodendrocyte progenitors balance growth with self-repulsion to achieve homeostasis in the adult brain. *Nat. Neurosci.* 16, 668–676. doi: 10.1038/nn.3390

Hughes, E. G., Orthmann-Murphy, J. L., Langseth, A. J., and Bergles, D. E. (2018). Myelin remodeling through experience-dependent oligodendrogenesis in the adult somatosensory cortex. *Nat. Neurosci.* 21, 696–706. doi: 10.1038/s41593-018-0121-5

Jung, J. C., Mehta, A. D., Aksay, E., Stepnoski, R., and Schnitzer, M. J. (2004). *In vivo* mammalian brain imaging using one- and two-photon fluorescence microendoscopy. *J. Neurophysiol.* 92, 3121–3133. doi: 10.1152/jn.00234.2004

Kang, S. H., Li, Y., Fukaya, M., Lorenzini, I., Cleveland, D. W., Ostrow, L. W., et al. (2013). Degeneration and impaired regeneration of gray matter oligodendrocytes in amyotrophic lateral sclerosis. *Nat. Neurosci.* 16, 571–579. doi: 10.1038/nn.3357

Koudelka, S., Voas, M. G., Almeida, R. G., Baraban, M., Soetaert, J., Meyer, M. P., et al. (2016). Individual neuronal subtypes exhibit diversity in CNS myelination mediated by synaptic vesicle release. *Curr. Biol.* 26, 1447–1455. doi: 10.1016/j.cub.2016.03.070

Kougioumtzidou, E., Shimizu, T., Hamilton, N. B., Tohyama, K., Sprengel, R., Monyer, H., et al. (2017). Signalling through AMPA receptors on oligodendrocyte precursors promotes myelination by enhancing oligodendrocyte survival. *eLife* 6:e28080. doi: 10.7554/eLife.28080

Kwon, J., Kim, M., Park, H., Kang, B.-M., Jo, Y., Kim, J.-H., et al. (2017). Label-free nanoscale optical metrology on myelinated axons *in vivo*. *Nat. Commun.* 8:1832. doi: 10.1038/s41467-017-01979-2

Levene, M. J., Dombeck, D. A., Kasischke, K. A., Molloy, R. P., and Webb, W. W. (2004). *In vivo* multiphoton microscopy of deep brain tissue. *J. Neurophysiol.* 91, 1908–1912. doi: 10.1152/jn.01007.2003

Lim, H., Sharoukhov, D., Kassim, I., Zhang, Y., Salzer, J. L., and Melendez-Vasquez, C. V. (2014). Label-free imaging of Schwann cell myelination by third harmonic generation microscopy. *Proc. Natl. Acad. Sci. U.S.A.* 111, 18025–18030. doi: 10.1073/pnas.1417820111

Locatelli, G., Theodorou, D., Kendirli, A., Jordão, M. J. C., Staszewski, O., Phulphagar, K., et al. (2018). Mononuclear phagocytes locally specify and adapt their phenotype in a multiple sclerosis model. *Nat. Neurosci.* 21, 1196–1208. doi: 10.1038/s41593-018-0212-3

Lovett-Barron, M., Andalman, A. S., Allen, W. E., Vesuna, S., Kauvar, I., Burns, V. M., et al. (2017). Ancestral circuits for the coordinated modulation of brain state. *Cell* 171, 1411–1423. doi: 10.1016/j.cell.2017.10.021

Mabbott, D. J., Noseworthy, M., Bouffet, E., Laughlin, S., and Rockel, C. (2006). White matter growth as a mechanism of cognitive development in children. *Neuroimage* 33, 936–946. doi: 10.1016/j.neuroimage.2006.07.024

McKenzie, I. A., Ohayon, D., Li, H., Paes de Faria, J., Emery, B., Tohyama, K., et al. (2014). Motor skill learning requires active central myelination. *Science* 346, 318–322. doi: 10.1126/science.1254960

Mitew, S., Gobius, I., Fenlon, L. R., McDougall, S. J., Hawkes, D., Xing, Y. L., et al. (2018). Pharmacogenetic stimulation of neuronal activity increases myelination in an axon-specific manner. *Nat. Commun.* 9:306. doi: 10.1038/s41467-017-02719-2

Mount, C. W., and Monje, M. (2017). Wrapped to adapt: experience-dependent myelination. *Neuron* 95, 743–756. doi: 10.1016/j.neuron.2017.07.009

Ouzounov, D. G., Wang, T., Wang, M., Feng, D. D., Horton, N. G., Cruz-Hernández, J. C., et al. (2017). *In vivo* three-photon imaging of activity of GCaMP6-labeled neurons deep in intact mouse brain. *Nat. Methods* 14, 388–390. doi: 10.1038/nmeth.4183

Ritchie, S. J., Bastin, M. E., Tucker-Drob, E. M., Maniega, S. M., Engelhardt, L. E., Cox, S. R., et al. (2015). Coupled changes in brain white matter microstructure and fluid intelligence in later life. *J. Neurosci.* 35, 8672–8682. doi: 10.1523/JNEUROSCI.0862-15.2015

Rivers, L. E., Young, K. M., Rizzi, M., Jamen, F., Psachoulia, K., Wade, A., et al. (2008). PDGFRA/NG2 glia generate myelinating oligodendrocytes and piriform projection neurons in adult mice. *Nat. Neurosci.* 11, 1392–1401. doi: 10.1038/nn.2220

Sampaio-Baptista, C., Khrapitchev, A. A., Foxley, S., Schlagheck, T., Scholz, J., Jbabdi, S., et al. (2013). Motor skill learning induces changes in white matter microstructure and myelination. *J. Neurosci.* 33, 19499–19503. doi: 10.1523/jneurosci.3048-13.2013

Scantlebury, N., Cunningham, T., Dockstader, C., Laughlin, S., Gaetz, W., Rockel, C., et al. (2014). Relations between white matter maturation and reaction time in childhood. *J. Int. Neurophsychol. Soc.* 20, 99–112. doi: 10.1017/S1355617713001148

Schain, A. J., Hill, R. A., and Grutzendler, J. (2014). Label-free *in vivo* imaging of myelinated axons in health and disease with spectral confocal reflectance microscopy. *Nat. Med.* 20, 443–449. doi: 10.1038/nm.3495

Scholz, J., Klein, M. C., Behrens, T. E. J., and Johansen-berg, H. (2009). Training induces changes in white-matter architecture. *Nat. Neurosci.* 12, 1370–1371. doi: 10.1038/nn.2412

Snaidero, N., Möbius, W., Czopka, T., Hekking, L. H. P., Mathisen, C., Verkleij, D., et al. (2014). Myelin membrane wrapping of CNS axons by PI(3,4,5)P3-dependent polarized growth at the inner tongue. *Cell* 156, 277–290. doi: 10.1016/j.cell.2013.11.044

Takahashi, N., Sakurai, T., Davis, K. L., and Buxbaum, J. D. (2011). Linking oligodendrocyte and myelin dysfunction to neurocircuitry abnormalities in schizophrenia. *Prog. Neurobiol.* 93, 13–24. doi: 10.1016/j.pneurobio.2010.09.004

Tomassy, G. S., Berger, D. R., Chen, H.-H., Kasthuri, N., Hayworth, K. J., Vercelli, A., et al. (2014). Distinct profiles of myelin distribution along single

axons of pyramidal neurons in the neocortex. *Science* 344, 319–324. doi: 10.1126/science.1249766

Tripathi, R. B., Jackiewicz, M., Mckenzie, I. A., Kougioumtzidou, E., Grist, M., and Richardson, W. D. (2017). Remarkable stability of myelinating oligodendrocytes in mice. *Cell Rep.* 21, 316–323. doi: 10.1016/j.celrep.2017.09.050

Viganò, F., Möbius, W., Götz, M., and Dimou, L. (2013). Transplantation reveals regional differences in oligodendrocyte differentiation in the adult brain. *Nat. Neurosci.* 16, 1370–1372. doi: 10.1038/nn.3503

Watkins, T. A., Emery, B., Mulinyawe, S., and Barres, B. A. (2008). Distinct stages of myelination regulated by gamma-secretase and astrocytes in a rapidly myelinating CNS coculture system. *Neuron* 60, 555–569. doi: 10.1016/j.neuron.2008.09.011

Waxman, S. G. (1980). Determinants of conduction velocity in myelinated nerve fibers. *Muscle Nerve* 3, 141–150. doi: 10.1002/mus.880030207

Xiao, L., Ohayon, D., Mckenzie, I. A., Sinclair-Wilson, A., Wright, J. L., Fudge, A. D., et al. (2016). Rapid production of new oligodendrocytes is required in the earliest stages of motor-skill learning. *Nat. Neurosci.* 19, 1210–1217. doi: 10.1038/nn.4351

Yeung, M. S. Y., Zdunek, S., Bergmann, O., Bernard, S., Salehpour, M., Alkass, K., et al. (2014). Dynamics of oligodendrocyte generation and myelination in the human brain. *Cell* 159, 766–774. doi: 10.1016/j.cell.2014.10.011

Young, K. M., Psachoulia, K., Tripathi, R. B., Dunn, S.-J., Cossell, L., Attwell, D., et al. (2013). Oligodendrocyte dynamics in the healthy adult CNS: evidence for myelin remodeling. *Neuron* 77, 873–885. doi: 10.1016/j.neuron.2013.01.006

Zeng, H. (2018). Mesoscale connectomics. *Curr. Opin. Neurobiol.* 50, 154–162. doi: 10.1016/j.conb.2018.03.003

Conflict of Interest Statement: The authors declare that the research was conducted in the absence of any commercial or financial relationships that could be construed as a potential conflict of interest.

frontiers in Cellular Neuroscience

TECHNOLOGY REPORT
published: 06 December 2018
doi: 10.3389/fncel.2018.00477

In vivo Optogenetic Approach to Study Neuron-Oligodendroglia Interactions in Mouse Pups

Domiziana Ortolani[1,2†], Blandine Manot-Saillet[1,2†], David Orduz[2], Fernando C. Ortiz[2,3] and Maria Cecilia Angulo[1,2*]*

[1] *INSERM U894, Institute of Psychiatry and Neuroscience of Paris, Paris, France,* [2] *INSERM U1128, Paris, France,* [3] *mechanisms of Myelin Formation and Repair Lab, Instituto de Ciencias Biomédicas, Facultad de Ciencias de la Salud, Universidad Autónoma de Chile, Santiago, Chile*

Optogenetic and pharmacogenetic techniques have been effective to analyze the role of neuronal activity in controlling oligodendroglia lineage cells in behaving juvenile and adult mice. This kind of studies is also of high interest during early postnatal (PN) development since important changes in oligodendroglia dynamics occur during the first two PN weeks. Yet, neuronal manipulation is difficult to implement at an early age because high-level, specific protein expression is less reliable in neonatal mice. Here, we describe a protocol allowing for an optogenetic stimulation of neurons in awake mouse pups with the purpose of investigating the effect of neuronal activity on oligodendroglia dynamics during early PN stages. Since GABAergic interneurons contact oligodendrocyte precursor cells (OPCs) through *bona fide* synapses and maintain a close relationship with these progenitors during cortical development, we used this relevant example of neuron-oligodendroglia interaction to implement a proof-of-principle optogenetic approach. First, we tested Nkx2.1-Cre and Parvalbumin (PV)-Cre lines to drive the expression of the photosensitive ion channel channelrhodopsin-2 (ChR2) in subpopulations of interneurons at different developmental stages. By using patch-clamp recordings and photostimulation of ChR2-positive interneurons in acute somatosensory cortical slices, we analyzed the level of functional expression of ChR2 in these neurons. We found that ChR2 expression was insufficient in PV-Cre mouse at PN day 10 (PN10) and that this channel needs to be expressed from embryonic stages (as in the Nkx2.1-Cre line) to allow for a reliable photoactivation in mouse pups. Then, we implemented a stereotaxic surgery to place a mini-optic fiber at the cortical surface in order to photostimulate ChR2-positive interneurons at PN10. *In vivo* field potentials were recorded in Layer V to verify that photostimulation reaches deep cortical layers. Finally, we analyzed the effect of the photostimulation on the layer V oligodendroglia population by conventional immunostainings. Neither the total density nor a proliferative fraction of OPCs were affected by increasing interneuron activity *in vivo*, complementing previous findings showing the lack of effect of GABAergic synaptic activity on OPC proliferation. The methodology described here should provide a framework for future investigation of the role of early cellular interactions during PN brain maturation.

Keywords: optogenetics, GABAergic interneuron, oligodendrocyte precursor cell, developing brain, somatosensory cortex, proliferation

OPEN ACCESS

Edited by:
Dirk Feldmeyer, Forschungszentrum Jülich, Helmholtz-Gemeinschaft Deutscher Forschungszentren (HZ), Germany

Reviewed by:
Markus Rothermel, RWTH Aachen University, Germany
Elias Leiva-Salcedo, University of Santiago, Chile

****Correspondence:***
Fernando C. Ortiz
fernando.ortiz@uautonoma.cl
Maria Cecilia Angulo
maria-cecilia.angulo@parisdescartes.fr

† Co-first authors

Received: *10 September 2018*
Accepted: *22 November 2018*
Published: *06 December 2018*

Citation:
Ortolani D, Manot-Saillet B, Orduz D, Ortiz FC and Angulo MC (2018) In vivo Optogenetic Approach to Study Neuron-Oligodendroglia Interactions in Mouse Pups. Front. Cell. Neurosci. 12:477. doi: 10.3389/fncel.2018.00477

INTRODUCTION

The advent of optogenetics (Boyden et al., 2005) and pharmacogenetics (Conklin et al., 2008; Dong et al., 2010) have allowed for a big progress revealing detailed mechanisms behind intercellular communication (Aston-Jones and Deisseroth, 2013; Adamantidis et al., 2015; Chen et al., 2018). Optogenetics is based on the expression of photosensitive protein-channels in specific cell types, making possible to activate or inhibit particular components of a given circuit by using light (Boyden et al., 2005; Han and Boyden, 2007; Aston-Jones and Deisseroth, 2013). Typically, the activation of a targeted neuron is achieved by photoactivation of a channel-rhodopsin 2 (ChR2) variant. The ChR2 is a cationic channel which activation leads to the depolarization of the cell membrane (Ernst et al., 2008). If the light-induced rise in the membrane potential reaches the activation threshold of intrinsic depolarizing ion channels expressed by the cell (i.e., voltage-dependent sodium or calcium channels), an action potential is triggered (Zhang et al., 2006, 2007; Ernst et al., 2008). By this mechanism, the generation of action potentials of targeted neurons can be controlled with high spatiotemporal precision.

While optogenetic techniques have largely contributed to our current understanding of neuronal network function in the mature central nervous system (CNS), their use to investigate the developing brain has been poor and only recent efforts have started to be done in this direction (Bitzenhofer et al., 2017a,b). A significant limitation when studying developing circuits is to reach enough levels of ChR2 expression on cell membranes in order to induce efficient responses by photostimulation. Given the variable protein expression during developmental stages, the heterologous expression of light-sensitive channels driven by endogenous cell promoters in the neonatal brain is not reliable enough (see Bitzenhofer et al., 2017a). In addition, *in vivo* brain photostimulation usually requires the placement of a ferrule or mini-optic fiber that is fixed on the cranial bone (Gradinaru et al., 2009; Yizhar et al., 2011), a procedure more difficult to apply on the soft skull of mouse pups. This issue has probably precluded the use of optogenetics to study developing circuits, privileging pharmacogenetics (Wong et al., 2018), a versatile but less precise technique in time and space.

During early postnatal (PN) development, neurons form transient circuits before establishing mature networks (Anastasiades et al., 2016). Interestingly, oligodendrocyte precursor cells (OPCs), the major source of myelinating oligodendrocytes in the CNS, receive a transient synaptic input from GABAergic interneurons during early PN development (Vélez-Fort et al., 2010; Zonouzi et al., 2015). Indeed, OPCs are the only non-neuronal cells synaptically contacted by neurons in the CNS (Bergles et al., 2000). In the somatosensory (barrel) cortex, the interneuron-OPC connectivity reaches a peak at PN10, 1 day prior to oligodendrocyte (OL) differentiation, and then declines progressively to disappear during the fourth PN week (Vélez-Fort et al., 2010; Balia et al., 2015; Orduz et al., 2015). Although the genetic inactivation of a specific interneuron-OPC synapse does not impair the proliferation and differentiation of OPCs at early PN stages (Balia et al., 2017), these data indicate the existence of a close relationship between interneurons and OPCs during a critical period for cortical circuit construction. Interneuron activity may thus affect OPC function through different synaptic and extrasynaptic mechanisms in the immature neocortex (Maldonado and Angulo, 2015). Indeed, in addition to interneuron-OPC synaptic interactions, OPCs express extrasynaptic $GABA_A$ receptors (Passlick et al., 2013; Balia et al., 2015). Moreover, interneurons directly communicate with OPCs in the developing brain by secreting over 50 paracrine factors such as fractalkine that promote OPC differentiation (Voronova et al., 2017).

In this article, we describe an experimental protocol to activate cortical GABAergic interneurons *in vivo* by using optogenetics in mouse pups and analyze the effect of interneuron activity in OPC dynamics. We tested Nkx2.1-Cre and Parvalbumin (PV)-Cre lines to drive the expression of ChR2 in subpopulations of interneurons. We analyzed the functional expression of this photosensitive channel by combining patch-clamp recordings with photostimulation in acute somatosensory cortical slices. We found that ChR2 expression was insufficient in the PV-Cre mouse line at PN10, while the Nkx2.1-driven expression allowed for a reliable photoactivation in the developing cortex. Next, we developed a stereotaxic surgery to place a mini-optic fiber at the cortical surface to photostimulate ChR2-positive interneurons at PN10 in awake mouse pups. Finally, we analyzed the effect of interneuron photoactivation on the oligodendroglia population by conventional immunostainings. Our approach should provide a methodological tool to study the function of different neuron-oligodendroglia interactions in the early PN brain.

MATERIALS AND METHODS

Transgenic Mice

All experiments followed European Union and institutional guidelines for the care and use of laboratory animals and were approved by French committees for animal care of the University Paris Descartes and the Ministry of National Education and Research (N°CEEA34.MCA.070.12). For experiments, we used transgenic Nkx2.1-$Cre^{(+/-)}$:ChR2 (H134R)-$YFP^{(lox/+)}$ and PV-$Cre^{(+/-)}$:ChR2 (H134R)-$YFP^{(lox/lox)}$ mice from PN8 to PN26 obtained after crossing from Nkx2.1-Cre (Kessaris et al., 2006), PV-Cre (JAX n°008069) and ChR2-lox (JAX n°012569).

Electrophysiology and Photostimulation in Acute Slices

Acute parasagittal slices (300 μm) of the barrel cortex were obtained with an angle of 10° to the sagittal plane using a vibratome (Microm HM650V) as previously described (Vélez-Fort et al., 2010; Orduz et al., 2015). Slices were prepared in an ice-cold solution containing (in mM): 215 sucrose, 2.5 KCl, 1.25 NaH_2PO_4, 26 $NaHCO_3$, 20 glucose, 5 pyruvate, 1 $CaCl_2$, and 7 $MgCl_2$ (95% O_2, 5% CO_2) and incubated for 30 min at 33°C in an extracellular solution containing (in mM): 126 NaCl, 2.5 KCl, 1.25 NaH2PO4, 20 glucose, 5 pyruvate, 2 $CaCl_2$ and 1 $MgCl_2$ (95% O_2, 5% CO_2). For recordings, slices were transferred to a recording

chamber perfused with the same extracellular solution at 2–3 ml/min. An Olympus BX51 microscope equipped with a 40× fluorescent water-immersion objective, a Q-imaging camera and a CoolLed pE-2 fluorescent system (Scientifica, United Kingdom) allowed us to visualize the YFP fluorescent protein of ChR2-expressing interneurons in acute slices. Layer V ChR2-expressing interneurons were recorded at RT in whole-cell configuration with pipettes having a resistance of 3–5 MΩ and containing an intracellular solution with (in mM): 130 KGlu, 0.1 EGTA, 0.5 $CaCl_2$, 2 $MgCl_2$, 10 HEPES, 2 Na_2-ATP, 0.2 Na-GTP and 10 Na_2-phosphocreatine (pH≈7.3; 300 mOsm). Photostimulation of ChR2-expressing interneurons was obtained with an optic fiber (200 μm, NA = 0.66; Prizmatix Ltd., Israel) placed on layer V of the slice close to the patched cell and connected to a LED source delivering 460 nm wavelength light pulses (UHP-Mic-LED-460, Prizmatix Ltd., Israel). Local field potentials (LFPs) were recorded with a recording pipette filled with extracellular solution and located in layer V close to the optic fiber.

Whole-cell recordings were obtained using Multiclamp 700B, filtered at 3 kHz and digitized at 20 kHz. Digitized data were analyzed off-line using pClamp10.6 (Molecular Devices, United States) and Neuromatic package within IGOR Pro 6.0 environment (Wavemetrics, United States). The identity of interneurons was first assessed by analyzing the firing properties of neurons recorded in current-clamp mode as previously described (Orduz et al., 2015). Briefly, we used a depolarizing pulse of 800 ms to measure the instantaneous discharge frequency ($F_{initial}$), the frequency at 200 ms (F_{200}), the frequency at the end of the pulse ($F_{final,}$) and the total frequency (F_{total}). We calculated both early and late accommodations. The membrane input resistance R_m of neurons was calculated from a −200 pA hyperpolarized 800 ms step. The spike threshold, the first and second action potential amplitudes, and their corresponding durations were extracted from a 200 pA depolarizing pulse of 80 ms to calculate the amplitude reduction and duration increase. The amplitude of the after-hyperpolarization (AHP) was calculated as the difference between the threshold and the peak of the fast hyperpolarization.

Train pulses of light were used to elicit action potentials in ChR2-expressing interneurons (10 ms, 1 mW per pulse). Light trains of 10, 20, 30, and 50 Hz during 30 s were applied to define the optimal frequency inducing an effective activation of patched ChR2-expressing interneurons. For each frequency, we calculated the number of spikes (N_s) with respect to the number of light pulses (N_{LP}) and determined the percentage of success as $[N_s/N_{LP}] \times 100$. LFPs were elicited by stimulating with light trains (10 Hz, 2 s). In a set of experiments, the extracellular solution contained: 50 μM (2R)-amino-5-phosphonovaleric acid (APV, ref: HB0225, Hellobio); 10 μM 2,3-dihydroxy-6-nitro-7-sulfamoyl-benzo[f]quinoxaline (NBQX, ref: ab120046, abcam) and 10 μM Gabazine (SR 95531, ref: ab120042, Abcam). Tetrodotoxin (TTX, ref: HB1035, Hellobio) was applied at a final concentration of 1 μM.

Surgery and *in vivo* Photostimulation

Animals (PN10-11) were deeply anesthetized with ketamine/xylazine (0.1/0.01 mg/g, IP) and fixed in a stereotaxic frame adapted to mouse pups (Kopf Instruments, United States). The skin above the skull was disinfected and incised. In these young mice, the bone structure is not sufficiently transparent to let in the light into the cortex, and too soft to support the weight of the implant containing the mini-optic fiber. Thus, the skull was artificially stiffened with a double layer of glue before a hole was stereotaxically drilled above the barrel cortex area. For the adherence of the glue on the skull, the conjunctive tissue was first removed by a very local drop of HCl solution (1 mM). Caution was taken to apply this solution on a very restricted area to avoid any contact with the mouse skin or other tissues. Once cleaned, the skull was artificially stiffened with a double layer of glue (SuperGlue, Gel, ethyl-2-cyanoacrylate). The first layer was obtained by gently spreading out a first drop on the bone above the somatosensory cortex. After 10 min, a

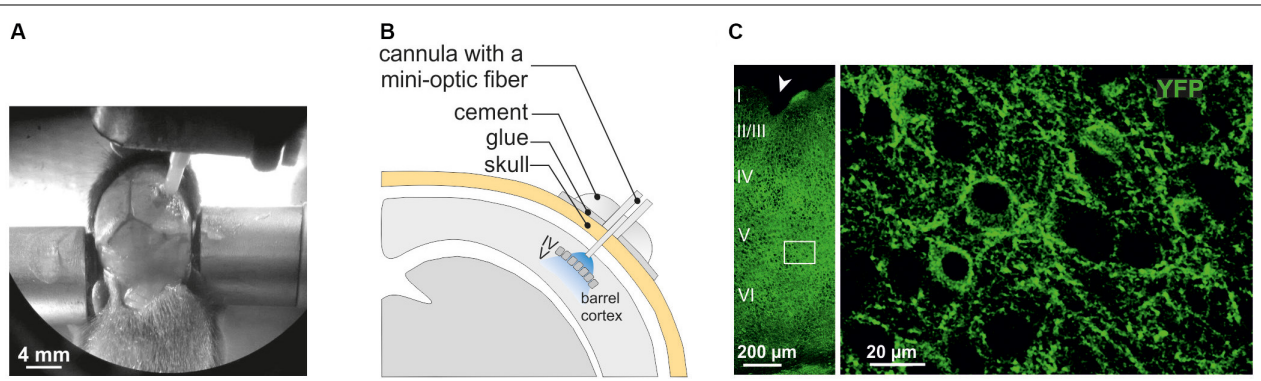

FIGURE 1 | Surgery for *in vivo* optogenetic stimulation of interneurons of the somatosensory cortex in mouse pups. **(A)** An anesthetized PN10 mouse holding the implant and fixed in a stereotaxic apparatus is shown. Before to place the mini-optic fiber the skull is covered with two layers of glue. In this example, the skin of the animal was more widely incised for visibility on the picture. **(B)** Scheme of the mini-optic fiber implanted at the surface of the somatosensory barrel cortex. **(C)** Confocal images of ChR2-expressing interneurons in layers from I to VI (left; low magnification) and in layer V (right; high magnification of the white square in the left) of the barrel cortex of a $Nkx2.1^{Cre}$:ChR2-$YFP^{Lox/+}$ mouse at PN10. ChR2 expression driven by the Nkx2.1 promoter is detected by the YFP reporter (green). The arrowhead indicates a small lesion induced when removing the optic fiber of the pup after perfusion. It allows us to precisely locate the place of the mini-optic fiber.

second layer of glue was similarly applied in the same region. Then, we waited around 20 min to ensure that the glue was completely dry before drilling the hole. Finally, the cannula accommodating the mini-optic fiber was implanted according to the following coordinates: 2.7 mm lateral to midline, 3.7 mm posterior to Bregma, and 0.1 mm depth from brain surface with an angle of 10° (**Figures 1A,B**; cannula: 1.25 mm; fiber: 200 μm diameter, NA = 0.66; Prizmatix Ltd., Israel). Some animals were implanted using an optrode containing a mini-optic fiber and a fine-wire recording electrode (Ni/Ag) of 50 μm diameter reaching layer V. In this case, a pin connector was fixed to the skull at the back of the brain to be used as a ground. Finally, the optogenetic implant was fixed to the skull with dental cement (Unifast Trad ivory 339104) and the skin was sutured around the implant (Mersilene®, EH7147H, Ethicon). Mice were recovered from anesthesia in an environment at 37°C before the photostimulation experiment. Once the animal was completely awake, the mini-optic fiber was connected to a 460 nm ultra-high power LED source through two optic fiber patch cords (UHP-mic-LED-460; Prizmatix Ltd., Israel). The first patch cord (200 μm diameter, NA 0.66) was connected from the mini-optic fiber to a rotary joint that spins freely, and the second (1000 μm, NA 0.66) was connected from the rotary joint to the optogenetics-LED optogenetics-LED source. This latter was connected to a current controller that in turn was commanded by a pulser device that creates programmable TTL pulses from a software (Prizmatix Pulser/Pulser PC Software, Prizmatix Ltd., Israel). Mice were photostimulated according to a 3 h protocol composed by 36 light trains of 30 s delivered at 10 Hz [10 ms on/90 ms off pulses; ∼3–4 mW per pulse, a power estimated from measurements in continuous wave (CW) mode] and separated by a resting period of 4.5 min. Considering that our duty cycle is 10%, we estimated that the total energy applied during a 30 s photostimulation train is equivalent to 9–12 mJ. Prior to the surgery, the power at the tip of each mini-optic fiber was systematically measured with an optical power meter (PM100D coupled with sensor S120C, Thorlabs, United States) by connecting it to the LED system operating in CW mode (maximum output power at the 200 μm mini-optic fiber tip: ∼4.5 mW). Once the surgery was completed, we set the values in the current controller to deliver the proper power at the tip of the fiber during the photostimulation. For LFP recordings, the recording electrode was connected to the headstage of a Multiclamp 700B amplifier through a 50 μm diameter Ni/Ag wire, and the ground of the mouse connected to the ground of the amplifier. Finally, the animal was placed inside a small ($\sim 20 \times 20 \times 20\ cm^3$) custom-made Faraday cage and light trains of 10 Hz were elicited to evoke LFPs in current-clamp ($I = 0$) voltage follower mode.

Immunostainings, EdU Proliferation Assay and Countings

Fifteen minutes prior to photostimulation, intraperitoneal EdU injections were performed to labeled cells in the S phase of the cell cycle (10 mM EdU solution in PBS at 50 mg/kg; ref. C10340, ThermoFisher Scientific, United States). 1 h after the end of the photostimulation, mice were perfused with phosphate buffer saline (PBS) followed by 0.15 M phosphate buffer (PB) containing 4% paraformaldehyde (PFA, Electron Microscopy Sciences, United States), pH 7.4. Brains were then left in PFA for 2 h at 4°C before washing and storing them in PBS at 4°C. The day of immunostainings, coronal vibratome slices (100 μm) were prepared in PBS at 4°C and permeabilized with 1% Triton and 4% Normal Goat Serum (NGS) during 2 h at RT under agitation. Then, slices were first incubated at 4°C under gently agitation for 3 nights with rabbit anti-Olig2 (1:400, ref. AB9610, Merck-Millipore) and mouse anti-CC1 (1:100, ref. OP80, Calbiochem) diluted in 0.2% Triton X-100 and 2% NGS and revealed for 2 h at RT with secondary antibodies coupled to Alexa-405 and Alexa-633, respectively (1:500, ThermoFisher Scientific). EdU was revealed for 2 h at RT after immunostainings by using the Clik-iT EdU Alexa-555 (C10638, ThermoFisher Scientific). Between each incubation step and at the end of the protocol, slices were rinsed 3 times in PBS for 10 min under genlty agitation.

Confocal images (0.75 μm z-step) were acquired using a 63X oil objective (NA = 1.4) with a LSM 710 confocal microscope (Zeiss) and processed using NIH ImageJ[1] as described (Balia et al., 2017). Cell densities were obtained by counting $Olig2^+$, $CC1^+$, and EdU^+ cells with the ROI manager tool (ImageJ) and by dividing the number of cells by the volume, as previously described (Balia et al., 2017).

Statistics

All data were expressed in mean ± SEM. A level of $p < 0.05$ was used to designate significant differences. Two group comparisons were performed using the non-parametric Mann–Whitney Test. Multiple comparisons were done with the non-parametric Kruskal–Wallis Test followed by a Dunn's multiple comparison test. Statistics and plotting were performed using GraphPad Prism 5.00 (GraphPad Software Inc., United States).

RESULTS

Functional ChR2 Expression in Cortical GABAergic Interneurons of Cre-Lox Transgenic Mice in Brain Slices

Three major cortical GABAergic interneuron subtypes can be defined according to the expression of three different markers: PV-, somatostatin (SST)-, and ionotropic serotonin receptor 5HT3a (5HT3aR) (Rudy et al., 2011). PV and SST interneurons constitute about 70% of the total population whereas 5HT3aR interneurons about 30% (Rudy et al., 2011). Cortical GABAergic interneurons are mainly born in the medial and caudal ganglionic eminences (MGE and CGE, respectively). The MGE is the site of origin of 60% of the cortical interneurons, mostly PV- and SST-interneurons (Marín, 2013; Wamsley and Fishell, 2017), while the CGE is the second source producing approximatively 30% of interneurons (Anderson et al., 2001; Nery et al., 2002). More recently, Gelman et al. (2011) also demonstrated that the

[1] http://imagej.nih.gov/ij

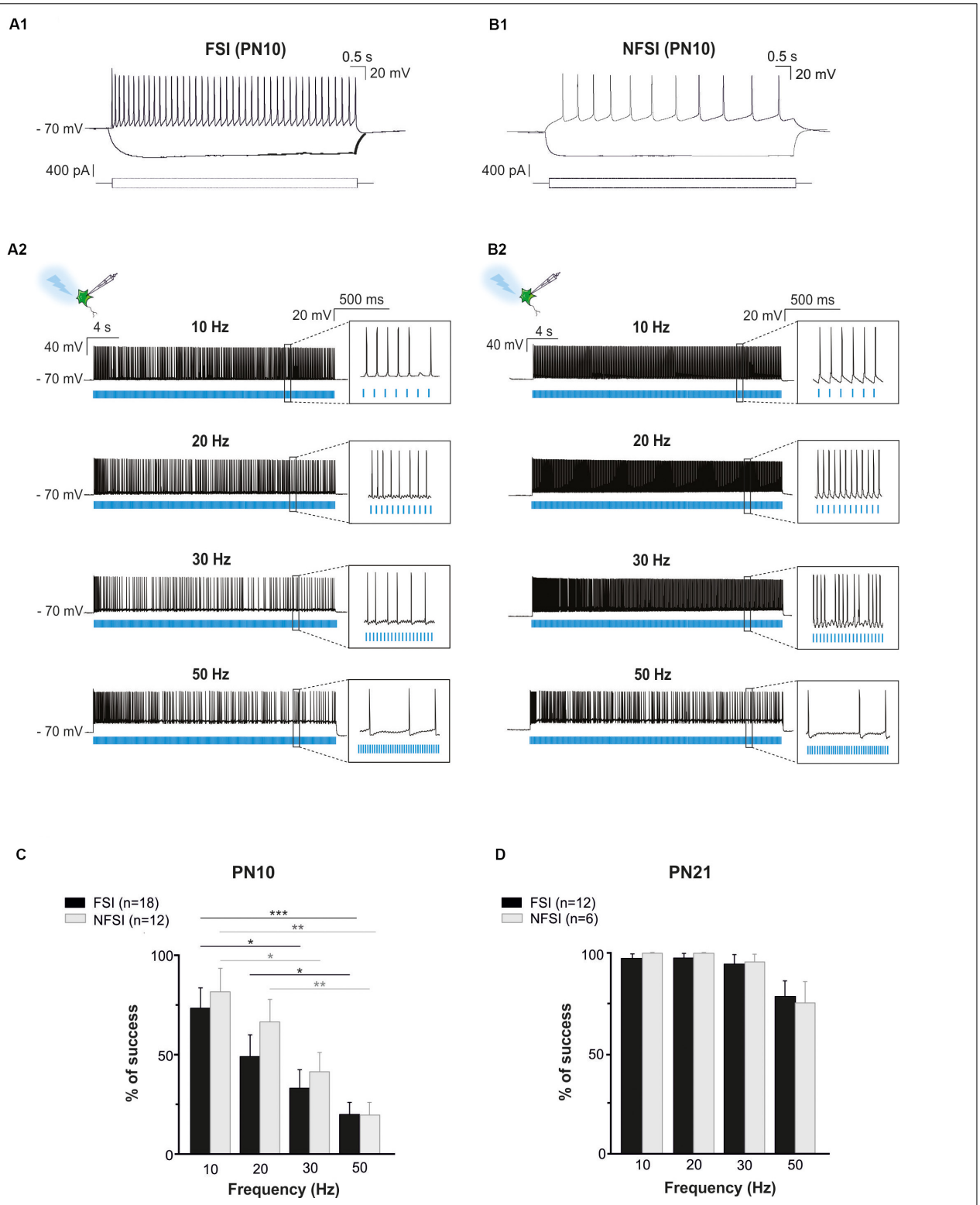

FIGURE 2 | Photoactivation of ChR2-expressing FSI and NFSI in PN10 Nkx2.1^{Cre}:ChR2-YFP$^{Lox/+}$ mouse pups in brain slices. **(A1,B1)** Current-clamp recordings of a FSI **(A1)** and a NFSI **(B1)** expressing ChR2 in cortical layer V at PN10. Note the differences of firing properties between the two cells in response to 800 ms depolarizing and hyperpolarizing steps (bottom square pulses). **(A2,B2)** The same FSI **(A2)** and NFSI **(B2)** were photostimulated (blue bars) with 10 ms light pulses during 30 s at different frequencies. **(C,D)** Average percentage of success to elicit action potentials with light trains at different photostimulation frequencies for FSI (black) and NFSI (gray) at PN10 **(C)** and PN21 **(D)**. *$p < 0.05$; **$p < 0.01$; and ***$p < 0.001$ for comparisons across each interneuron subtype, Kruskal–Wallis Test followed by a Dunn's *post hoc* Test; not significant differences ($p > 0.05$) between FSI and NFSI for each frequency are not indicated; Mann–Whitney test.

TABLE 1 | Electrophysiological properties of FSI and NFSI at PN10 in Nkx2.1^{Cre}:ChR2-YFP$^{Lox/+}$ mice.

Parameter PN 10	FSI(*n* = 18)	NFSI (*n* = 12)	*p*-value	Comparison
F_{total} (Hz)	30.94 ± 2.84	31.67 ± 2.43	NS	–
$F_{initial}$ (Hz)	**94.65 ± 8.43**	**131.20 ± 13.41**	**<0.05**	**FSI < NFSI**
F_{200} (Hz)	63.86 ± 5.13	68.06 ± 5.50	NS	–
F_{final} (Hz)	59.56 ± 5.66	54.01 ± 4.84	NS	–
Early accommodation (%)	**30.64 ± 2.03**	**44.87 ± 3.74**	**<0.01**	**FSI < NFSI**
Late accommodation (%)	**5.11 ± 1.55**	**11.12 ± 1.79**	**<0.05**	**FSI < NFSI**
Threshold (mV)	−39.86 ± 2.48	−35.88 ± 1.89	NS	–
First spike amplitude (mV)	74.23 ± 1.89	78.71 ± 1.60	NS	–
Second spike amplitude (mV)	73.30 ± 1.80	74.48 ± 1.62	NS	–
Spike amplitude reduction (%)	**1.02 ± 0.25**	**5.10 ± 0.91**	**<0.0001**	**FSI < NFSI**
First spike duration (ms)	1.32 ± 0.08	1.49 ± 0.16	NS	–
Second spike duration (ms)	**1.42 ± 0.08**	**1.89 ± 0.22**	**<0.05**	**FSI < NFSI**
Spike duration increase (%)	**7.84 ± 0.71**	**26.00 ± 2.62**	**<0.0001**	**FSI < NFSI**
AHP (mV)	**−11.07 ± 1.21**	**−5.63 ± 0.76**	**<0.01**	**FSI > NFSI**
AHP width (ms)	**30.17 ± 14.49**	**9.38 ± 1.96**	**<0.05**	**FSI > NFSI**
Rm(MΩ)	203.07 ± 16.62	206.74 ± 46.89	NS	

F_{total}, total frequency; $F_{initial}$, instantaneous discharge frequency; F_{200}, frequency at 200 ms; F_{final}, frequency at the end of the pulse; AHP, after-hyperpolarization; R_m, membrane input resistance. Statistical differences are in Bold.

embryonic preoptic area (POA) is a third source and suggested that this region contributes with approximately 10% of all GABAergic interneurons in the murine cerebral cortex. POA-derived progenitors give rise to PV, SST, and Reelin-expressing interneurons (Marín, 2013).

The specification of cortical interneurons in each generating area depends on a transcriptional network that regulates interneuron development. Among transcription factors important for interneuron specification, Nkx2.1 is specifically expressed in MGE- and POA-derived progenitors that generate 70% of cortical interneurons. These progenitors mainly generate both PV and SST interneurons with those in the POA producing more heterogeneous neuron subtypes (Marín, 2013; Wamsley and Fishell, 2017). Interestingly, the earliest wave of OPCs is also generated from Nkx2.1-expressing progenitors settled in the MGE and POA (Kessaris et al., 2006). Nevertheless, most of the Nkx2.1-derived precursors giving rise to oligodendroglia are eliminated by PN10 and thus should not significantly interfere to the ChR2 targeting of Nkx2.1-derived interneurons from this PN stage (Kessaris et al., 2006).

In the present study, we used Nkx2.1^{Cre}:ChR2-YFP$^{Lox/+}$ mice to drive the PN ChR2 expression in MGE- and POA-derived interneurons from embryonic stages (from ∼E11.5 which corresponds to the peak of interneuron production; Anderson et al., 2001). At PN10-12, YFP$^+$ interneurons were easily detected in the Nkx2.1^{Cre}:ChR2-YFP$^{Lox/+}$ mouse line in all cortical layers (**Figure 1C**). We focused on layer V since our previous studies in interneuron-OPC interactions were performed in this layer (**Figure 1C**; Vélez-Fort et al., 2010; Balia et al., 2015, 2017; Orduz et al., 2015). We first examined the electrophysiological properties of YFP$^+$ cells in layer V by using patch-clamp recordings in acute slices of the barrel cortex (**Figures 2A1,B1** and **Table 1**). As expected from Nkx2.1-derived interneurons at this age, recorded YFP$^+$ cells could be distinguished as fast-spiking interneurons (FSI; **Figure 2A1**) and non-fast-spiking interneurons (NFSI; **Figure 2B1**) by their characteristic action potential discharges in response to current injections (Daw et al., 2007; Orduz et al., 2015). FSI were mainly distinguished from NFSI by their pronounced AHP and a restricted spike duration increase and amplitude reduction during action potential discharges (**Table 1**; see Orduz et al., 2015). Other analyzed parameters such as the initial frequency, second spike duration and early and late accommodations were also different between the two groups (**Table 1**; see section "Materials and Methods").

To test whether ChR2 was functionally expressed at PN10 in Nkx2.1^{Cre}:ChR2-YFP$^{Lox/+}$ mice, we photostimulated recorded YFP$^+$ interneurons using an optic fiber placed in Layer V. Independently of the interneuron identity, all tested YFP$^+$ cells responded with action potential discharges to light-pulse trains (**Figures 2A2,B2**). While the success rate of the response during a 30 s-train delivered at 10 Hz was very high for both FSI and NFSI, a progressive decrease in the capacity of neurons to follow the stimulation train was observed when increasing the frequency from 20 to 50 Hz (**Figures 2A2,B2,C**). No significant differences were observed between FSI and NFSI for each tested frequency, indicating that it is not possible to set up specific parameters to exclusively activate either FSI or NFSI (**Figure 2C**).

Two main reasons could explain the decreased response of YFP$^+$ interneurons at higher frequency photostimulation trains: (1) a limited intrinsic capacity of immature interneurons to sustain high frequency discharges during long trains, and (2) a lower level of expression of ChR2 at PN10. To assess the first possibility, we mimicked the light train protocol with current pulse injections at 50 Hz for 30 s (**Figures 3A1,A2**). All recorded FSI and NFSI responded faithfully with action potentials to each current pulse injection, while the success rate during train photostimulation remains low at this early

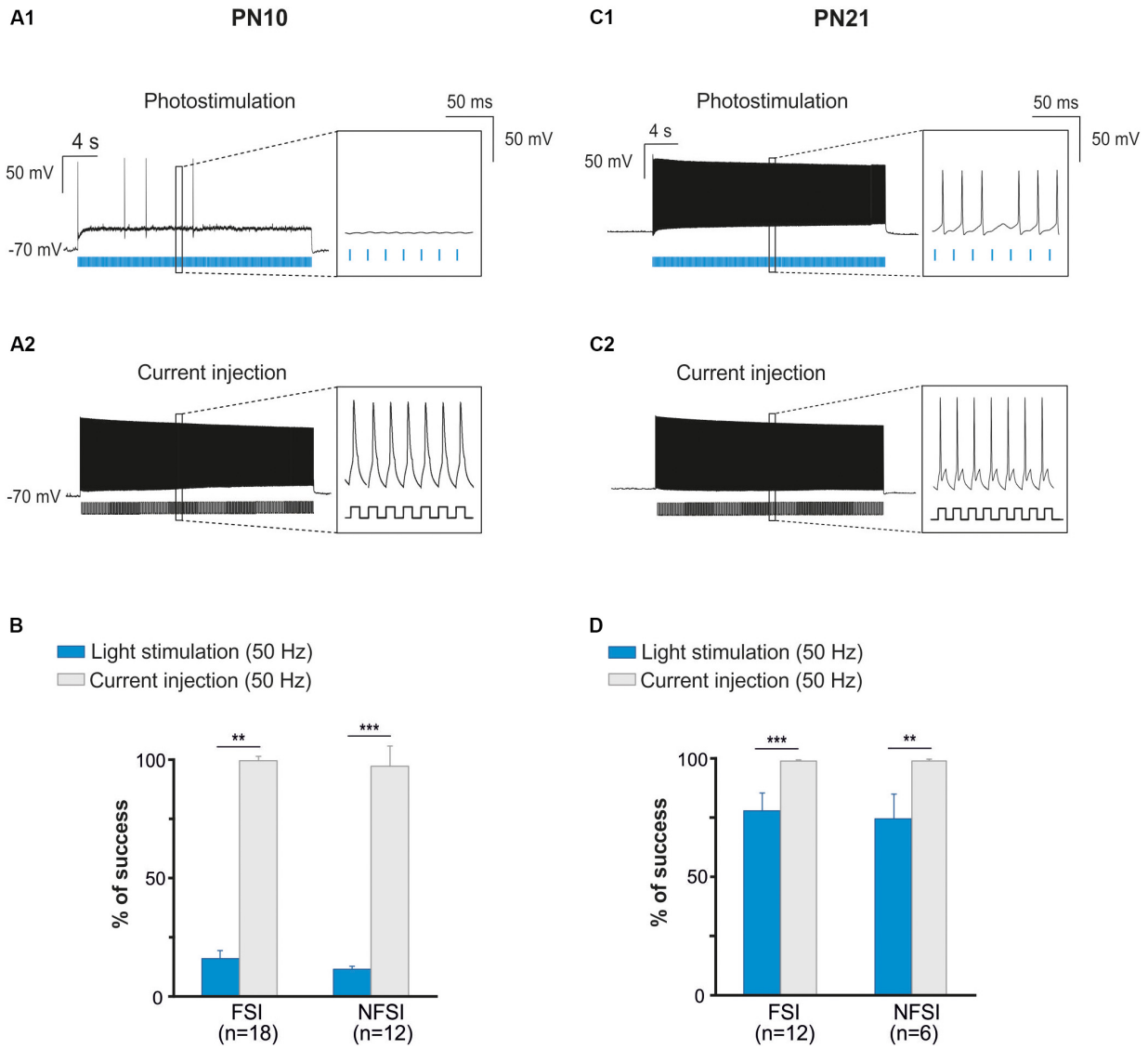

FIGURE 3 | The fail of response at high frequency photostimulation in brain slices at PN10 is not due to interneuron immature membrane properties. **(A)** An identified ChR2-expressing interneuron recorded in current-clamp mode during a 50 Hz photostimulation protocol **(A1)** in a brain slice at P10. Note the numerous failures (inset) in response to blue light pulses (blue bars). The same neuron stimulated with current injections (400 pA, 10 ms; **(A2)**) at 50 Hz showed virtually no failures (inset). **(B)** Comparison between the percentage of success of photostimulation versus current stimulation at 50 Hz for FSI and NFSI in mice at PN10. **(C)** An identified ChR2-expressing interneuron recorded in current-clamp mode during a 50 Hz photostimulation protocol **(C1)** in a brain slice at PN21. Note the increased number of APs (inset) triggered by photoactivation (blue bars) compared with the interneuron at PN10 **(A1)**. The same neuron stimulated with current injections (400 pA, 10 ms; **C2**) at 50 Hz showed virtually no failures (insets). **(D)** Comparison between the percentage of success of photostimulation versus current stimulation at 50 Hz for FSI and NFSI in mice at PN21. $^{**}p < 0.01$ and $^{***}p < 0.001$, Mann–Whitney Test.

PN stage (**Figures 3A,B**). Therefore, the intrinsic properties of interneurons in younger mice are not responsible for a low success rate during higher frequency trains. To test for the level of expression of ChR2 during development, we performed the same experiments at PN19-22, i.e., during the third PN week (**Supplementary Figure 1** and **Table 2**). Although we observed a maturation of the electrophysiological properties of interneurons during the second and third PN weeks (**Tables 1**, **2**; Pangratz-Fuehrer and Hestrin, 2011), FSI were still distinguished from NFSI by the presence of a more pronounced AHP and small variations of the duration and amplitude spikes (**Supplementary Figures 1A1,B1** and **Table 2**). Other parameters such as early accommodation and input resistance were significantly different between FSI and NFSI at a later developmental stage (**Table 2**). After recording the electrophysiological profile, we photostimulated the patched YFP^{+} interneuron using trains of photostimulation at 10, 20, 30, and 50 Hz (**Supplementary Figures 1A2,B2**). At PN19-22, the success rates for both FSI and NFSI were close to 100% for trains at 10, 20, and 30 Hz and dropped to around 80% at 50 Hz (**Figure 2D** and **Supplementary**

TABLE 2 | Electrophysiological properties of FSI and NFSI at PN21 in Nkx2.1^{Cre}:ChR2-YFP$^{Lox/+}$ mice.

Parameter PN 21	FSI (*n* = 18)	NFSI (*n* = 8)	*p*-value	Comparison
F_{totAl} (Hz)	64.5 ± 6.42	64.38 ± 8.37	NS	–
$F_{initial}$ (Hz)	185.7 ± 22.46	243.1 ± 24.14	NS	–
F_{200} (Hz)	132.9 ± 11.81	131.8 ± 20.54	NS	–
F_{final} (Hz)	126.5 ± 13.36	116 ± 16.79	NS	–
Early accommodation (%)	**21.99 ± 4.01**	**45.78 ± 6.61**	**<0.01**	**FS < NFS**
Late accommodation (%)	5.2 ± 1.93	6.49 ± 2.28	NS	–
Threshold (mV)	−44.26 ± 1.25	−44.59 ± 0.92	NS	–
First spike amplitude (mV)	77.84 ± 1.7	81.82 ± 1.57	NS	–
Second spike amplitude (mV)	76.23 ± 1.6	76.65 ± 1.6	NS	–
Spike amplitude reduction (%)	**2.0 ± 0.3**	**6.05 ± 3.68**	**<0.01**	**FS < NFS**
First spike duration (ms)	0.6 ± 0.04	0.77 ± 0.12	NS	–
Second spike duration (ms)	0.62 ± 0.04	0.87 ± 0.14	NS	–
Spike duration increase (%)	**3.47 ± 0.41**	**11.96 ± 1.98**	**<0.0001**	**FS < FS**
AHP (mV)	**−18.63 ± 0.93**	**−11.16 ± 1.73**	**<0.01**	**FS > NFS**
AHP width (ms)	**5.4 ± 0.77**	**2.29 ± 0.21**	**<0.05**	**FS > NFS**
Rm(MΩ)	**185.9 ± 14.55**	**242.8 ± 18.62**	**<0.05**	**FS < NFS**

F_{total}, total frequency; $F_{initial}$, instantaneous discharge frequency; F_{200}, frequency at 200 ms; F_{final}, frequency at the end of the pulse; AHP, after hyperpolarization; R_m, membrane input resistance. Statistical differences are in Bold.

Figures 1A2,B2), as expected from the limited capacity of ChR2 to follow high frequency trains (Lin et al., 2009). Indeed, current injections mimicking photostimulation at 50 Hz in PN19-22 mice caused a significantly higher success rate of ∼100% in FSI and NFSI (**Figures 3C,D**). Altogether, these results indicate that a lower level of ChR2 expression in the second PN week compared to 10 days later is probably at the origin of the decrease of the success rate with respect to the photostimulation frequency at PN10.

Since PV-expressing FSI are highly connected to OPCs in the second PN week (Orduz et al., 2015), we also aimed at specifically photostimulating these interneurons in PV^{Cre}:ChR2-YFP$^{Lox/Lox}$ mice during this period. However, YFP$^+$ interneurons were never detected in acute slices under the epifluorescence microscope and were very rarely observed under the confocal microscope at PN10 (**Figure 4A**). The scarcity of ChR2 expression in this mouse line at early PN stages was concomitant to the lack of response of FSI, recognized from their intrinsic electrophysiological properties, to a 10 Hz-photostimulation train at this age (n = 2, **Figures 4B1,B2**). Since this line has been extensively used in the adult (Cardin et al., 2010), we examined later developmental PN stages. Compared to PN10, immunostainings revealed an extensive co-labeling of PV and YFP in cell bodies and branches at PN20 and PN26 (**Figure 4A**). At PN19-22, 5 out of 7 neurons emitted at least one action potential in response to light train stimulation at 10 Hz (**Figure 4B2**) and one cell responded faithfully to each train pulse. In average, the success rate of discharge at 10 Hz was 14.62 ± 14.23% (**Figure 4C**). However, FSI rarely responded to higher frequency light trains at this age (**Figure 4C**). All recorded YFP$^+$ neurons at PN26 responded faithfully with action potentials to each pulse of the light train stimulation at 10 Hz (success rate: 100%, n = 7, **Figures 4B1,C2**). Nevertheless, the success rate of YFP$^+$ FSI progressively decreased at 20, 30, and 50 Hz-photostimulation trains (**Figure 4**). Therefore, there is an increased functional expression of ChR2 from PN10 to PN26 in PV^{Cre}:ChR2-YFP$^{Lox/Lox}$ mice. Considering that in Nkx2.1^{Cre}:ChR2-YFP$^{Lox/+}$ at PN21 the success rate of FSI is still high at 50 Hz (**Figure 2C**), a maximum level of ChR2 expression is probably not attained in PV^{Cre}:ChR2-YFP$^{Lox/Lox}$ mice in the fourth PN week.

In summary, contrary to a late PN expression of ChR2 in PV^{Cre}:ChR2-YFP$^{Lox/Lox}$ mice, ChR2 is already expressed in Nkx2.1^{Cre}:ChR2-YFP$^{Lox/+}$ mice at PN10, the age corresponding to the peak of synaptic connectivity between interneurons and OPCs in the somatosensory cortex (Orduz et al., 2015). Indeed, all recorded YFP$^+$ interneurons responded to photostimulation trains at this developmental stage, although the success rate during a long train of 30 s significantly decreases at frequencies higher than 30 Hz. The most suitable light train frequencies to obtain a maximum and reliable number of action potentials during 30 s in Nkx2.1^{Cre}:ChR2-YFP$^{Lox/+}$ mice were between 10 and 20 Hz. Since FSI and NFSI fire at lower frequency rates in pups than in adults (**Tables 1**, **2**), 10 Hz constitutes a good compromise to efficiently activate around 80% of interneurons during long light trains (30 s; **Figure 2C**).

Light-Evoked Local Field Potentials in Acute Slices and *in vivo* in Nkx2.1^{Cre}:ChR2-YFP$^{Lox/+}$ Mice

Neocortical GABAergic interneurons are inhibitory cells and constitute a minority of cortical neurons (10–20% in rodents; Rudy et al., 2011). For these two reasons, our observation of a single photoactivated interneuron does not necessarily ensure that light stimulation through the optic fiber will induce the activation of an interneuron population. To assess our ability to generate action potentials in a large number of ChR2-expressing interneurons, we first examined whether

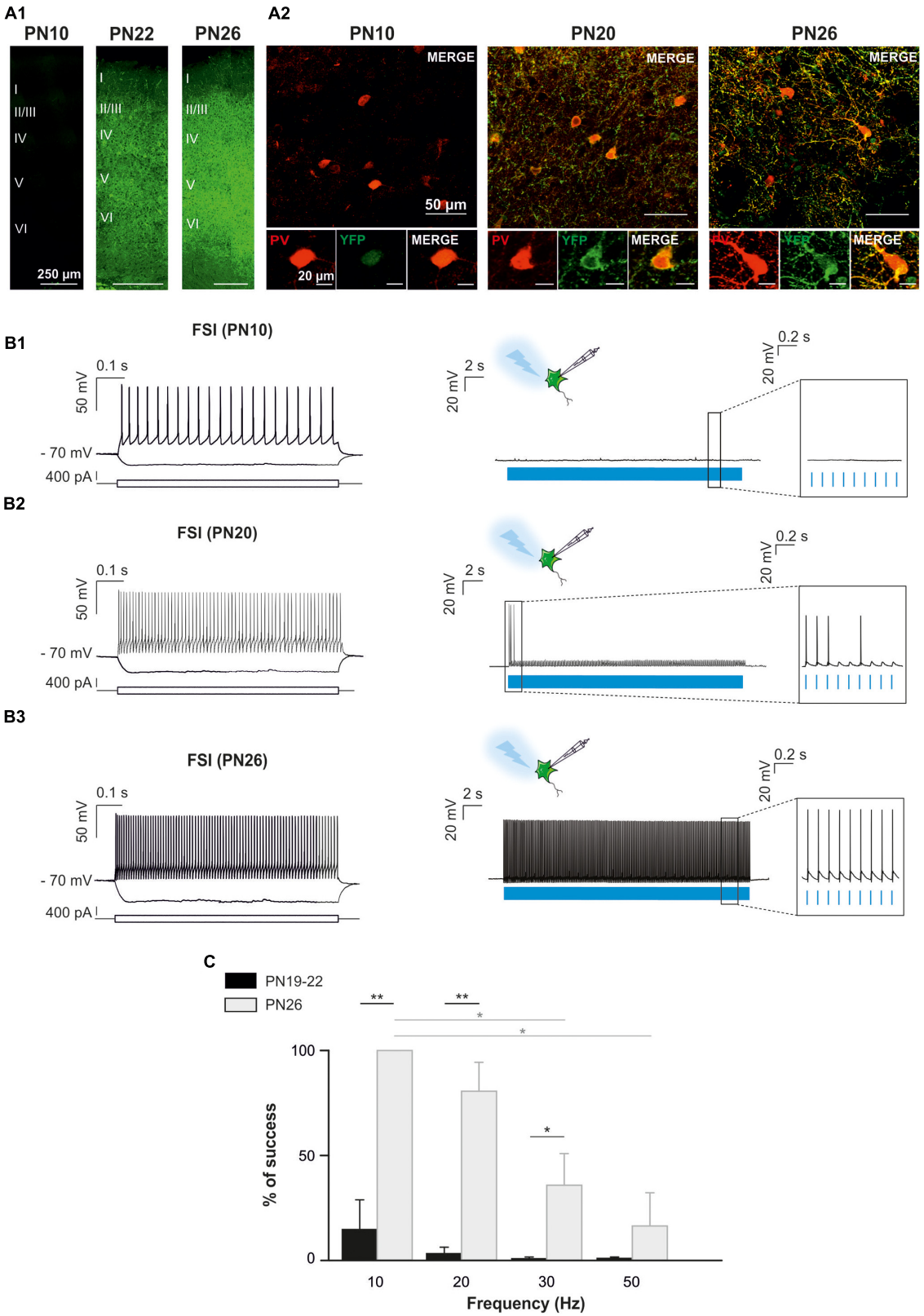

FIGURE 4 | Optogenetic stimulation of FSI in PV^{Cre}:ChR2-$YFP^{Lox/Lox}$ mice during postnatal cortical development in brain slices. **(A)** Confocal images of cortical interneurons expressing ChR2 (YFP, green) and PV protein (red) at low (left) and high (right) magnifications at PN10, PN20 and PN26 mice. Note the faintly cytoplasmatic expression of YFP at PN10 compared to a brighter and more extensive membrane expression at later ages. **(B)** Current-clamp recordings of a layer V

(Continued)

FIGURE 4 | Continued
ChR2-expressing FSI **(B1)** at PN10. Depolarizing and hyperpolarizing steps are indicated (bottom square pulses). No action potentials were evoked by a 10 Hz photostimulation train (blue pulses) in this neuron (**B1** right, inset), but the photoactivation-induced response increased during development (**B2,B3**, right). Note that photoactivation (blue pulses) of a layer V ChR2- expressing FSI at PN26 evoked action potentials in response to every light pulse (B3 right, inset). **(C)** Average percentage of success to elicit action potentials with light trains delivered from 10 to 50 Hz at PN19-22 and PN26 in the PV^{Cre}:ChR2-$YFP^{Lox/Lox}$ mice. $^{*}p < 0.05$; $^{**}p < 0.01$, Kruskal–Wallis Test followed by a Dunn's *post hoc* Test; not significant differences ($p > 0.05$) between FSI and NFSI for each frequency are not indicated.

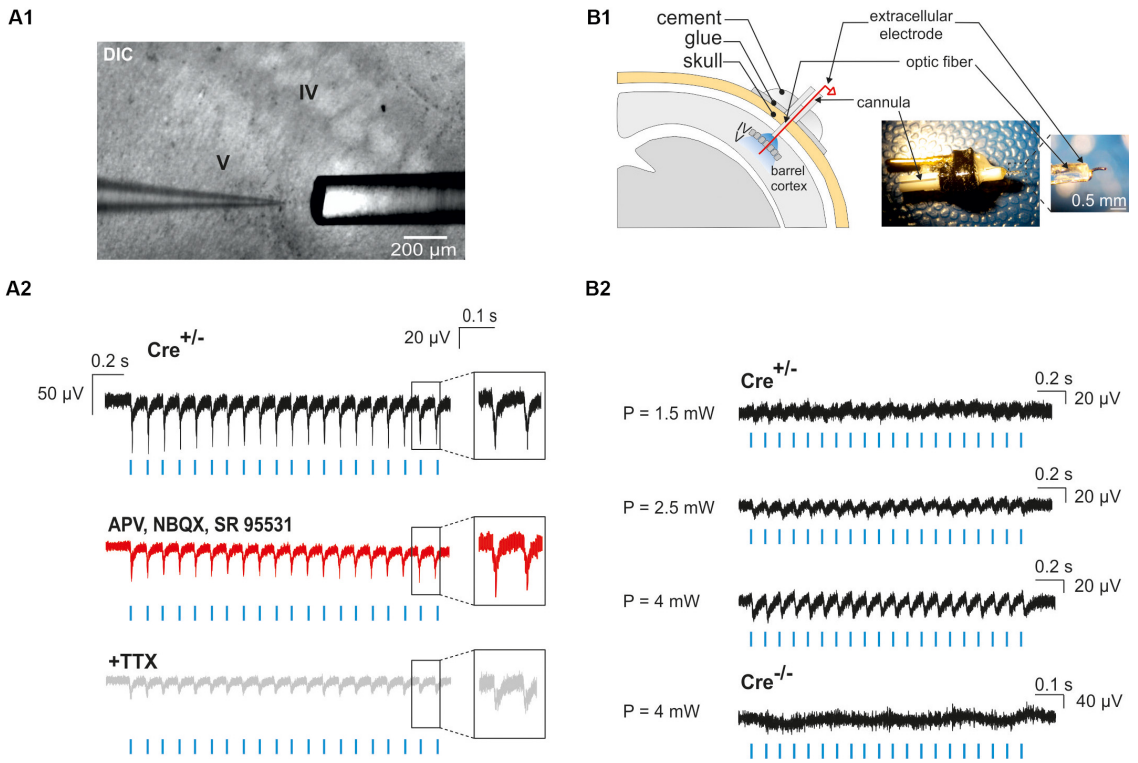

FIGURE 5 | Photo-evoked LFPs in PN10 mouse pups in brain slices and *in vivo*. **(A)** Extracellular recordings were performed in the cortical layer V of brain slices during photostimulation with an optic fiber located just above the recording site **(A1)**. LFPs evoked by photostimulation (**A2**, blue lines) were faithfully reproduced in response to every light pulse (black trace, inset) in ChR2-expressing transgenic mice ($Cre^{+/-}$). Recording of the same slice during bath application of glutamatergic and GABAergic antagonists (50 µM APV, 10 µM NBQX, 10 µM SR95531; **A2** red trace) and TTX (1 µM, **A2** gray trace) are shown. DIC: Differential interference contrast image. **(B)** *In vivo* extracellular recordings of cortical layer V were performed by the placement of a custom-made optrode containing a mini-optic fiber and a 50 µm Ni/Ag wire **(B1)**. *In vivo* LFPs were successfully evoked by photostimulation (**B2**, blue lines) above 1.5 mW of light power in a ChR2-expressing transgenic mouse ($Cre^{+/-}$). The reported powers from 1.5 to 4 mW correspond to the power per pulse estimated from measurements in continuous wave (CW) mode. No responses were evoked in a $Cre^{-/-}$ control mouse.

photostimulation elicited LFPs in acute cortical slices. We found that a 10 Hz photostimulation train induced LFPs with great fidelity in cortical layers II to VI (n = 2 slices in 2 animals, not shown), but since most of interneuron-OPC interactions in pups have been described in layer V (Vélez-Fort et al., 2010; Balia et al., 2015, 2017; Orduz et al., 2015), we analyzed in more detail the effect of interneuron activation in this layer (**Figures 5A1,A2**; n = 5 slices in 2 animals). These LFPs were less sensitive to the glutamatergic and GABAergic receptor antagonists APV, NBQX, and SR95531 than to the Na^{+}-channel blocker tetrodotoxin (TTX) that abolishes action potential generation [**Figures 5A1,A2**; amplitude reduction of the first LFP: 4.32 ± 0.86% (n = 5) and 48.39 ± 12.1% (n = 3), respectively]. It is noteworthy that a TTX-insensitive component also persisted in all tested slices (**Figure 5A2**). It probably corresponded to the LFP generated by the current directly flowing through ChR2 channels in interneurons. These data indicate that recorded light-evoked LFPs upon 10 Hz photostimulation trains resulted from the direct generation of action potentials by multiple nearby ChR2-expressing interneurons instead of postsynaptic potentials (the latter could have been generated by inhibitory postsynaptic potentials or by disinhibition of inhibitory circuits resulting in increased excitatory postsynaptic potentials).

To analyze the effect of photostimulation *in vivo*, we performed a surgery at PN10 to implant an optrode including an optic fiber placed at the surface of the cortex. Since light poorly penetrates into scattering tissue, we tested whether neuronal responses were evoked by light in layer V by using a wire electrode to record light-evoked LFPs in this layer at a frequency

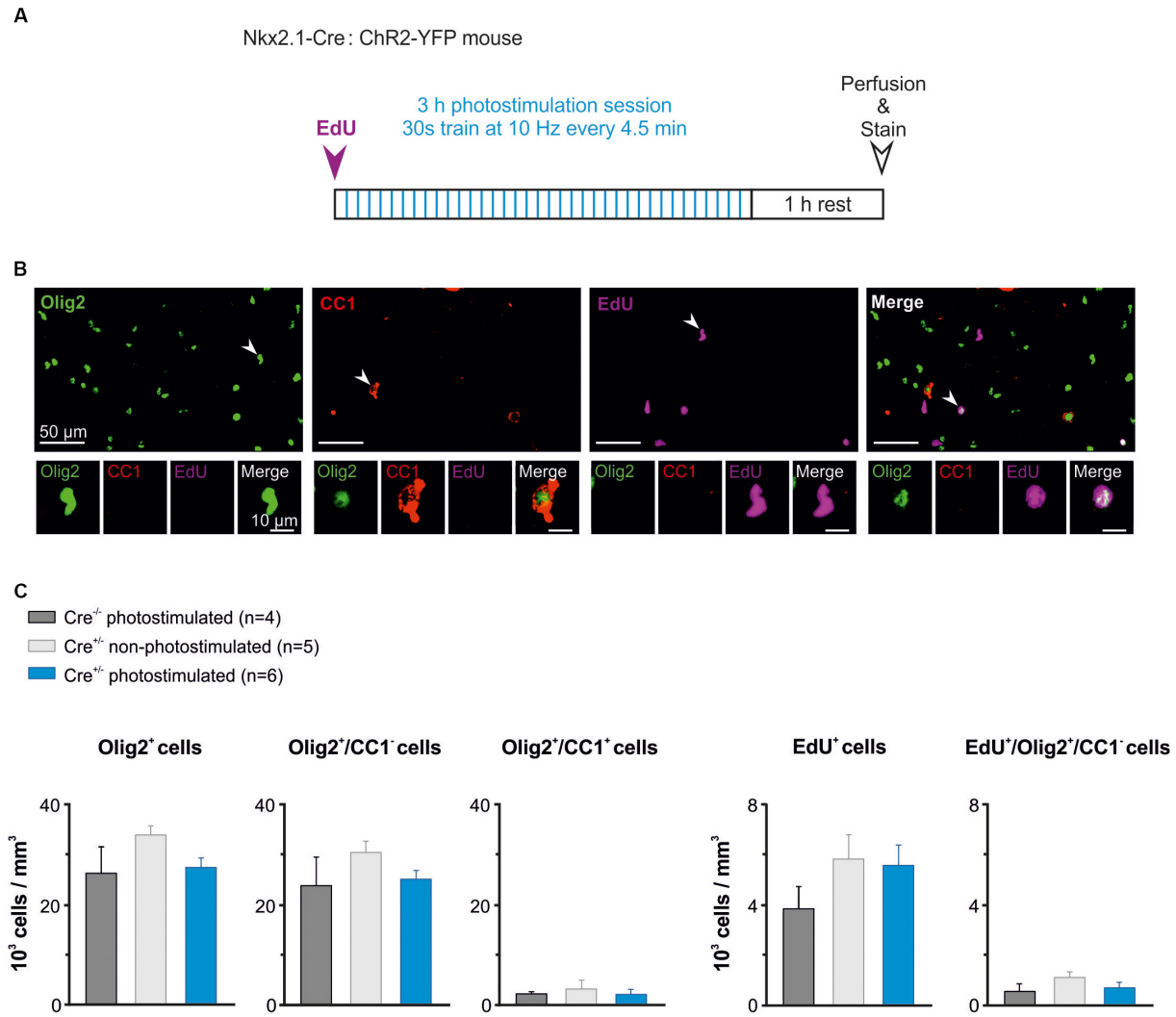

FIGURE 6 | The *in vivo* photoactivation of layer V cortical interneurons at P10 does not modify oligodendroglia density. **(A)** Experimental design for a photostimulation protocol. Mice were injected with EdU (50 mg/kg) and then photostimulated during 3 h. **(B)** Olig2 (green), CC1 (red) and EdU (magenta) cells stained after the photostimulation session. An $Olig2^{+}/CC1^{-}$OPC is indicated in the first panel (arrowhead, insets). Only few $Olig2^{+}/CC1^{+}$ OLs were found at this age (arrowhead in second panel, insets). Note that not all EdU-stained cells were $Olig2^{+}$ cells (arrowheads in the last two panels). **(C)** Density of total oligodendroglia ($lig2^{+}$), OPCs ($Olig2^{+}/CC1^{-}$), differentiated OLs ($Olig2^{+}/CC1^{+}$), total proliferative cells (EdU^{+}), and proliferative OPCs ($Edu^{+}/Olig2^{+}/CC1^{-}$) in the three tested conditions. No significant differences were found for any comparison ($p > 0.05$, Kruskal–Wallis Test followed by a Dunn's *post hoc* Test).

of 10 or 20 Hz (**Figure 5B1**). To firmly maintain the optrode on the mouse skull, it was necessary to artificially harden the bone with a layer of glue before drilling (see section "Materials and Methods"). Once the animal was awake after surgery, it was placed in a chamber where the mini-optic fiber was connected to a 460 nm LED source through an optic fiber patch cord in order to record light-evoked LFPs (**Figure 5B2**; 4 $Cre^{(+/-)}$ mice and 3 $Cre^{(-/-)}$ mice). Photostimulation trains elicited weak responses when the power was set at 1.5 mW per pulse at the tip of the optrode (**Figure 5B2**). However, light-evoked LFPs increased for each light pulse at 2.5 and 4 mW (**Figure 5B2**). These responses were absent in $Cre^{(-/-)}$ animals of the same littermates, used here as a control group (**Figure 5B2**).

Our results demonstrate that $Nkx2.1^{Cre}$:$ChR2\text{-}YFP^{Lox/+}$ mice can be used to activate a population of ChR2-expressing interneurons as early as PN10. We established the best conditions for whole-cell and LFP recordings in brain slices and set up the conditions to ensure layer V interneuron activation *in vivo*.

Effect of *in vivo* Interneuron Activation on the Oligodendroglia Population

It was recently showed that photoactivation of layer V glutamatergic neurons has a rapid effect on increasing the proliferation rate of OPCs in juvenile mice (Gibson et al., 2014). Here, we analyzed whether the activity of GABAergic interneurons also influence OPC proliferation at PN10-11, when

the synaptic connectivity between interneurons and OPCs is maximal in the somatosensory cortex (Orduz et al., 2015). We photostimulated awake pups to trigger a response of layer V ChR2-expressing interneurons using ∼3–4 mW per pulse (**Figure 5B2**). In these set of experiments, the wire electrode was not present on the implant (**Figure 1B**). Based on our previous characterization in slices, we chose 10 Hz as frequency for *in vivo* photostimulation. However, since 10 Hz represents a relatively low stimulation frequency for cortical interneurons that discharge at higher rates even in the immature mice (**Table 1**), we opted to multiply the number of stimulation trains. The photostimulation protocol lasted 3 h and comprised 36 stimulation trains of 30 s at 10 Hz (**Figure 6A**). Before the photostimulation session, we intraperitoneally injected 50 mg/kg of EdU, a thymidine analog that integrates the genome during the S phase of the cell cycle (**Figure 6A**). After the photostimulation session, we waited 1 h before perfusing the animal and removing the implant (**Figure 6A**). Then, immunostainings were performed to simultaneously identify all OL lineage cells (Olig2) and mature OLs (CC1), while EdU was revealed to detect proliferating cells. We considered $Olig2^+/CC1^-$ cells as OPCs and $Olig2^+/CC1^+$ cells as differentiated OLs (**Figure 6B**). We compared the effect of the photostimulation within three different experimental groups: 1) $Cre^{(-/-)}$ ChR2-non-expressing photostimulated mice ($n = 4$); 2) $Cre^{(+/-)}$ ChR2-expressing non-photostimulated mice ($n = 5$); and 3) $Cre^{(+/-)}$ ChR2-expressing photostimulated mice ($n = 6$). The two first groups were considered as controls.

The region carrying the implant was recognized under the confocal microscope by the presence of a small lesion in upper layers of the cortex (**Figure 1C**). To ensure that we analyzed the photostimulated area, only the slices showing a small lesion were further imaged at high resolution in order to perform cell countings in layer V (1 to 3 slices per mice). Cell countings did not reveal any significant difference in the total density of $Olig2^+$ cells, $Olig2^+/CC1^-$ OPCs or differentiated $Olig2^+/CC1^+$ OLs (**Figure 6C**, left). As expected for this early developmental age, most $Olig2^+$ cells were OPCs in all conditions (**Figure 6C**, left). Moreover, we found that controls and photostimulated mice did not display any significant change in the total population of EdU^+ cells or in the population of $EdU^+/Olig2^+/CC1^-$ OPCs (**Figure 6C**, Right). It is noteworthy that no $EdU^+/Olig2^+/CC1^+$ OLs were observed in our samples, suggesting more symmetric than asymmetric divisions of OPCs at PN10-11. In conclusion, we did not observe any difference in the density of proliferating OPCs after a 3 h stimulation protocol, suggesting a limited effect of interneuron activity on OPC proliferation at this age. This result supports and complements our previous findings showing that the GABAergic synaptic activity of OPCs does not play a role in oligodendrogenesis (Balia et al., 2017).

DISCUSSION

Here, we describe an experimental procedure to activate cortical GABAergic interneurons of PN10 mouse pups by using an optogenetic approach. We first determined that Nkx2.1-driven ChR2-expression allowed for a reproducible activation of cortical layer V GABAergic interneurons at PN10, whereas ChR2 was insufficiently expressed in the PV-Cre mouse at the same age. Combining photostimulation with both whole cell patch-clamp recordings in brain slices and *in vivo* extracellular recordings, we determined a suitable photostimulation protocol to ensure a reliable photoactivation of targeted cells. We also provide an experimental procedure to place a mini-optic fiber in the neonatal mouse brain in order to photoactivate interneurons in deep cortical layers of awake pups. Finally, we analyzed the effect of a particular neuronal photoactivation protocol on the oligodendroglia population in the neonatal neocortex.

Optogenetic studies have been proved to largely contribute to our current understanding of mature nervous system circuitry. However, only recent efforts have allowed for the implementation of this technique in the neonatal brain (Bitzenhofer et al., 2017a,b; Ahlbeck et al., 2018). Indeed, one of the major prerequisite for a selective and reliable optogenetic stimulation is to attain a sufficient level of opsin expression in targeted cells. This is more difficult to achieve in mouse pups due to the low or variable protein expression during early PN stages. In line with this, we found that the functional ChR2 expression of FSI in PV-Cre:ChR2-$YFP^{flox/flox}$ mice was largely insufficient at PN10, preventing the emission of action potentials in these interneurons. PV, the major marker of FSI, starts to be expressed during the first PN week, but reaches high levels late during neocortical development. At PN10, PV mRNA expression revealed a moderate labeled of mRNA-positive cells in layer V of the somatosensory cortex compared to PN16 (De Lecea et al., 1995). A developmental increased pattern of PV expression was also observed in our immunostainings in concomitance with an increased ChR2 expression (**Figure 4**). Therefore, the PV-Cre transgenic mouse line is not appropriate for inducing a sufficient ChR2 expression driven by the PV promoter at PN10. Contrary to the late expression of ChR2 in PV-Cre:ChR2-$YFP^{flox/flox}$ mice, this channel is more expressed at this age in Nkx2.1-Cre:ChR2-$YFP^{flox/+}$ mice (**Figure 1C**). An efficient ChR2 expression was expected in this mouse line since Nkx2.1 is expressed in interneuron progenitors at early embryonic stages (Marín, 2013; Wamsley and Fishell, 2017). In addition, fate-mapping approaches used to track the development of Nkx2.1-derived interneurons exhibited the distribution of these neurons in the mouse somatosensory barrel cortex already in the first PN week (Butt et al., 2005). The choice of Cre transgenic mouse lines is therefore crucial for inducing a sufficient ChR2 expression early in PN development.

Another key aspect of an optogenetic approach is to ensure a reliable and consistent readout of action potential discharges triggered by photostimulation. This is particularly important considering recent reports indicating that, depending on the neuronal subtype and light stimulation parameters (i.e., pulse duration), photoactivation of ChR2 might silence instead of increasing neuronal activity (Lin et al., 2013; Herman et al., 2014). This undesirable effect is explained by a light-induced depolarization block that results from an overactivation of ChR2 and its subsequent exaggerated cation influx, leading to

an insufficient repolarization (Lin et al., 2013; Herman et al., 2014). Importantly, Herman et al. (2014) reported that cortical interneurons were 2 to 4 times more susceptible to ChR2-dependent silencing than excitatory neuronal subtypes. Although the light pulse duration was the major responsible for the observed depolarization block in this study (Herman et al., 2014), a high frequency photoactivation can also be a triggering mechanism (Grossman et al., 2011). A first characterization of the response of ChR2-expressing neurons to photostimulation in brain slices is an important step, sometimes neglected, to define a pertinent protocol for *in vivo* experiments, even when behavioral tests are conducted.

In the present report, we determined that 10 ms light pulses delivered at 10–20 Hz reliably trigger action potential discharges during 30 s in ChR2-expressing interneurons of Nkx2.1-Cre:ChR2-YFP$^{flox/+}$ mice at PN10. Interestingly, action potentials were triggered with high fidelity in these same cells at frequencies of 50 Hz upon depolarizing current injections. These results indicate that the inability of interneurons to respond to light stimuli is not due to their immature intrinsic membrane properties at this age, but likely to ChR2 expression levels and channel gated properties. Indeed, the opening and closing kinetics of ChR2 are slower than those of voltage-gated Na^+ and K^+ channels. Photocycle models for ChR2 describe two open states (O1–O2) and at least two non-conductive "D" sub-states characterized by a slow recovery –from 10 s to more than 20 s– after a dark period (Ernst et al., 2008; Stehfest and Hegemann, 2010; Grossman et al., 2011; Saita et al., 2018). This requirement of a long-lasting dark period to recruit ChR2 activation upon a new light stimulus partially explains the limited neuronal response to high frequency photostimulation (Ernst et al., 2008; Grossman et al., 2011). In addition, due to the O1-to-O2 turnover, short inter-pulse intervals preclude the proper ChR2 closing (Grossman et al., 2011; Saita et al., 2018). In this line, Grossman et al. (2011) found that in response to 50 Hz photostimulation trains applied to ChR2-transfected hippocampal neurons, only 63% of the responsive ChR2 were closed in the inter-pulse interval compared to 99% at 10 Hz, preventing membrane repolarization and leading to the depolarization block of these neurons (Grossman et al., 2011). Nevertheless, since not all the channels are activated upon a single photostimulation, a strong level of protein expression can partially compensate for ChR2 slow kinetics. Indeed, we observed that photostimulation of FSI delivered at 50 Hz in PV-Cre:ChR2-YFP$^{flox/flox}$ mice in the fourth PN week was less efficient than that of FSI in Nkx2.1-Cre:ChR2-YFP$^{flox/+}$ mice in the third PN week (∼15 vs. 75%, respectively).

Neuron-OPC communication has been extensively studied in both gray and white matters (Maldonado et al., 2011; Maldonado and Angulo, 2015). Interestingly, GABAergic synaptic contacts are established on OPCs early in the PN neocortex, reaching a peak at PN10 (Vélez-Fort et al., 2010; Balia et al., 2015; Orduz et al., 2015). In addition, interneurons are known to act in a paracrine manner by releasing fractalkine to promote OPC development in the immature neocortex (Voronova et al., 2017). Finally, Stedehouder et al. (2018) recently demonstrated that PV interneuron myelination by oligodendrocytes is an activity-dependent process, as shown for other neuronal cell types (Hines et al., 2015; Mensch et al., 2015; Wake et al., 2015). All these data indicate a close relationship between GABAergic interneurons and oligodendroglia during PN development, and suggest a role of the activity of these neurons in regulating oligodendroglia function. After determining the parameters for interneuron photoactivation *in vivo* at PN10, we examined the effect of an increased interneuron activity on OPC proliferation at this critical developmental stage for OPC development in the somatosensory cortex (Hill et al., 2014; Balia et al., 2017). We found that the activity of GABAergic interneurons did not change either OPC proliferation or the number of OPCs and OLs in response to a 3 h photostimulation session. This result is in line with our previous report showing no changes in OPC proliferation after the genetic inactivation of interneuron-OPC synapses at the same age (Balia et al., 2017). However, a previous study had shown that 30 min photoactivation of cortical glutamatergic neurons had a rapid effect on the proliferation of these progenitors in juvenile mice (Gibson et al., 2014). It is therefore possible that the activity of glutamatergic and GABAergic neurons in the neocortex play different roles in OPC function. Alternatively, other stimulation paradigms for interneuron activation, closer to their higher firing frequency, need to be tested. Indeed, OPCs might respond in a different manner to different stimulation paradigms (Nagy et al., 2017). To test this possibility, however, other variants of ChR2 would be probably more appropriate such as the form E123T/T159C that has a success rate higher than 80% at 60 Hz (Berndt et al., 2011), or the ChETA variant that allows for a stimulation up to 200 Hz (Gunaydin et al., 2010).

CONCLUSION

In conclusion, this report provides a step-by-step description of an experimental protocol for the optogenetic interrogation of a neuron-oligodendroglia interaction in mouse pups. This methodology could be useful for instance to analyze whether neuronal activity promotes oligodendroglia migration by inspecting the cell density in different cortical layers after *in vivo* stimulation or to search for activity-dependent interneuron-OPC synaptic plasticity by performing electrophysiology in brain slices or immunostainings of synaptic compartments at the end of the *in vivo* protocol. It can also be adapted to other optogenetic tools and cellular interactions of the developing brain to get new insights on the role of glial cells *in vivo* during neuronal circuit formation and maturation.

AUTHOR CONTRIBUTIONS

The two co-first authors conducted optogenetic and electrophysiological experiments in brain slices and *in vivo* and performed data analysis. DO participated in initial experiments of the project. All authors wrote the manuscript. FCO and MCA designed experiments and supervised the project.

FUNDING

This work was supported by Fondation pour la Recherche Médicale («Equipe FRM DEQ20150331681»), Agence Nationale de la Recherche (ANR-14-CE13-0023-02), Fondation ARSEP and subaward agreement from the university of Connecticut with funds provided by the grant N°RG-1612-26501 from National Multiple Sclerosis Society (NMSS). FO was recipient of FRM and ARSEP post-doctoral fellowships and is supported by the Chilean National Fund for Scientific and Technological Development (FONDECYT, INICIACION #11160616). MCA is a CNRS investigator.

ACKNOWLEDGMENTS

We thank M. Omnes for genotyping, the NeuroImag (IPNP) and SCM Imaging Platforms (Paris Descartes University) and A. Pierani (IPNP) for providing us the Nkx2.1-Cre line.

SUPPLEMENTARY MATERIAL

The Supplementary Material for this article can be found online at: https://www.frontiersin.org/articles/10.3389/fncel.2018.00477/full#supplementary-material

REFERENCES

Adamantidis, A., Arber, S., Bains, J. S., Bamberg, E., Bonci, A., Buzsáki, G., et al. (2015). Optogenetics: 10 years after ChR2 in neurons –views from the community. *Nat. Neurosci.* 18, 1202–1212. doi: 10.1038/nn.4106

Ahlbeck, J., Song, L., Chini, M., Bitzenhofer, S. H., and Hanganu-Opatz, I. L. (2018). Glutamatergic drive along the septo-temporal axis of hippocampus boosts prelimbic oscillations in the neonatal mouse. *eLife* 7:e33158. doi: 10.7554/eLife.33158

Anastasiades, P. G., Marques-Smith, A., Lyngholm, D., Lickiss, T., Raffiq, S., Kätzel, D., et al. (2016). GABAergic interneurons form transient layer-specific circuits in early postnatal neocortex. *Nat. Commun.* 7:10584. doi: 10.1038/ncomms10584

Anderson, S. A., Marín, O., Horn, C., Jennings, K., and Rubenstein, J. L. (2001). Distinct cortical migrations from the medial and lateral ganglionic eminences. *Development* 128, 353–363.

Aston-Jones, G., and Deisseroth, K. (2013). Recent advances in optogenetics and pharmacogenetics. *Brain Res.* 1511, 1–5. doi: 10.1016/j.brainres.2013.01.026

Balia, M., Benamer, N., and Angulo, M. C. (2017). A specific GABAergic synapse onto oligodendrocyte precursors does not regulate cortical oligodendrogenesis. *Glia* 65, 1821–1832. doi: 10.1002/glia.23197

Balia, M., Vélez-Fort, M., Passlick, S., Schäfer, C., Audinat, E., Steinhäuser, C., et al. (2015). Postnatal down-regulation of the GABAA receptor γ2 subunit in neocortical NG2 cells accompanies synaptic-to-extrasynaptic switch in the GABAergic transmission mode. *Cereb. Cortex* 25, 1114–1123. doi: 10.1093/cercor/bht309

Bergles, D. E., Roberts, J. D., Somogyi, P., and Jahr, C. E. (2000). Glutamatergic synapses on oligodendrocyte precursor cells in the hippocampus. *Nature* 405, 187–191. doi: 10.1038/35012083

Berndt, A., Schoenenberger, P., Mattis, J., Tye, K. M., Deisseroth, K., Hegemann, P., et al. (2011). High-efficiency channelrhodopsins for fast neuronal stimulation at low light levels. *Proc. Natl. Acad. Sci. U.S.A.* 108, 7595–7600. doi: 10.1073/pnas.1017210108

Bitzenhofer, S. H., Ahlbeck, J., and Hanganu-Opatz, I. L. (2017a). Methodological approach for optogenetic manipulation of neonatal neuronal networks. *Front Cell Neurosci.* 11:239. doi: 10.3389/fncel.2017.00239

Bitzenhofer, S. H., Ahlbeck, J., Wolff, A., Wiegert, J. S., Gee, C. E., Oertner, T. G., et al. (2017b). Layer-specific optogenetic activation of pyramidal neurons causes beta-gamma entrainment of neonatal networks. *Nat. Commun.* 8:14563. doi: 10.1038/ncomms14563

Boyden, E. S., Zhang, F., Bamberg, E., Nagel, G., and Deisseroth, K. (2005). Millisecond-timescale, genetically targeted optical control of neural activity. *Nat. Neurosci.* 8, 1263–1268. doi: 10.1038/nn1525

Butt, S. J., Fuccillo, M., Nery, S., Noctor, S., Kriegstein, A., Corbin, J. G., et al. (2005). The temporal and spatial origins of cortical interneurons predict their physiological subtype. *Neuron* 48, 591–604. doi: 10.1016/j.neuron.2005.09.034

Cardin, J. A., Carlén, M., Meletis, K., Knoblich, U., Zhang, F., Deisseroth, K., et al. (2010). Targeted optogenetic stimulation and recording of neurons in vivo using cell-type-specific expression of Channelrhodopsin-2. *Nat. Protoc.* 5, 247–254. doi: 10.1038/nprot.2009.228

Chen, I. W., Papagiakoumou, E., and Emiliani, V. (2018). Towards circuit optogenetics. *Curr. Opin. Neurobiol.* 50, 179–189. doi: 10.1016/j.conb.2018.03.008

Conklin, B. R., Hsiao, E. C., Claeysen, S., Dumuis, A., Srinivasan, S., Forsayeth, J. R., et al. (2008). Engineering GPCR signaling pathways with RASSLs. *Nat. Methods* 5, 673–678. doi: 10.1038/nmeth.1232

Daw, M. I., Ashby, M. C., and Isaac, J. T. (2007). Coordinated developmental recruitment of latent fast spiking interneurons in layer IV barrel cortex. *Nat. Neurosci.* 10, 453–461. doi: 10.1038/nn1866

De Lecea, L., Del Rio, J., and Soriano, E. (1995). Developmental expression of parvalbumin mRNA in the cerebral cortex and hippocampus of the rat. *Mol. Brain Res.* 32, 1–13. doi: 10.1016/0169-328X(95)00056-X

Dong, S., Rogan, S. C., and Roth, B. L. (2010). Directed molecular evolution of DREADDs: a generic approach to creating next-generation RASSLs. *Nat. Protoc.* 5, 561–573. doi: 10.1038/nprot.2009.239

Ernst, O. P., Sánchez Murcia, P. A., Daldrop, P., Tsunoda, S. P., Kateriya, S., and Hegemann, P. (2008). Photoactivation of channelrhodopsin. *J. Biol. Chem.* 283, 1637–1643. doi: 10.1074/jbc.M708039200

Gelman, D., Griveau, A., Dehorter, N., Teissier, A., Varela, C., Pla, R., et al. (2011). A wide diversity of cortical GABAergic interneurons derives from the embryonic preoptic area. *J. Neurosci.* 31, 16570–16580. doi: 10.1523/JNEUROSCI.4068-11.2011

Gibson, E. M., Purger, D., Mount, C. W., Goldstein, A. K., Lin, G. L., Wood, L. S., et al. (2014). Neuronal activity promotes oligodendrogenesis and adaptive myelination in the mammalian brain. *Science* 344:1252304. doi: 10.1126/science.1252304

Gradinaru, V., Mogri, M., Thompson, K. R., Henderson, J. M., and Deisseroth, K. (2009). Optical deconstruction of parkinsonian neural circuitry. *Science* 324, 354–359. doi: 10.1126/science.1167093

Grossman, N., Nikolic, K., Grubb, M. S., Burrone, J., Toumazou, C., and Degenaar, P. (2011). High-frequency limit of neural stimulation with ChR2. *Conf. Proc. IEEE Eng. Med .Biol. Soc.* 2011, 4167–4170. doi: 10.1109/IEMBS.2011.6091034

Gunaydin, L. A., Yizhar, O., Berndt, A., Sohal, V. S., Deisseroth, K., and Hegemann, P. (2010). Ultrafast optogenetic control. *Nat. Neurosci.* 13, 387–392. doi: 10.1038/nn.2495

Han, X., and Boyden, E. S. (2007). Multiple-color optical activation, silencing, and desynchronization of neural activity, with single-spike temporal resolution. *PLoS One* 2:e299. doi: 10.1371/journal.pone.0000299

Herman, A. M., Huang, L., Murphey, D. K., Garcia, I., and Arenkiel, B. R. (2014). Cell type-specific and time-dependent light exposure contribute to silencing in neurons expressing Channelrhodopsin-2. *Elife* 3:e01481. doi: 10.7554/eLife.01481

Hill, R. A., Patel, K. D., Goncalves, C. M., Grutzendler, J., and Nishiyama, A. (2014). Modulation of oligodendrocyte generation during a critical temporal window after NG2 cell division. *Nat. Neurosci.* 17, 1518–1527. doi: 10.1038/nn.3815

Hines, J. H., Ravanelli, A. M., Schwindt, R., Scott, E. K., and Appel, B. (2015). Neuronal activity biases axon selection for myelination in vivo. *Nat. Neurosci.* 18, 683–689. doi: 10.1038/nn.3992

Kessaris, N., Fogarty, M., Iannarelli, P., Grist, M., Wegner, M., and Richardson, W. D. (2006). Competing waves of oligodendrocytes in the forebrain and postnatal elimination of an embryonic lineage. *Nat. Neurosci.* 9, 173–179. doi: 10.1038/nn1620

Lin, J. Y., Knutsen, P. M., Muller, A., Kleinfeld, D., and Tsien, R. Y. (2013). ReaChR: a red-shifted variant of channelrhodopsin enables deep transcranial optogenetic excitation. *Nat. Neurosci.* 16, 1499–1508. doi: 10.1038/nn.3502

Lin, J. Y., Lin, M. Z., Steinbach, P., and Tsien, R. Y. (2009). Characterization of engineered channelrhodopsin variants with improved properties and kinetics. *Biophys. J.* 96, 1803–1814. doi: 10.1016/j.bpj.2008.11.034

Maldonado, P. P., and Angulo, M. C. (2015). Multiple modes of communication between neurons and oligodendrocyte precursor cells. *Neuroscientist* 21, 266–276. doi: 10.1177/1073858414530784

Maldonado, P. P., Vélez-Fort, M., and Angulo, M. C. (2011). Is neuronal communication with NG2 cells synaptic or extrasynaptic? *J. Anat.* 219, 8–17. doi: 10.1111/j.1469-7580.2011.01350.x

Marín, O. (2013). Cellular and molecular mechanisms controlling the migration of neocortical interneurons. *Eur. J. Neurosci.* 38, 2019–2029. doi: 10.1111/ejn.12225

Mensch, S., Baraban, M., Almeida, R., Czopka, T., Ausborn, J., El Manira, A., et al. (2015). Synaptic vesicle release regulates myelin sheath number of individual oligodendrocytes in vivo. *Nat. Neurosci.* 18, 628–630. doi: 10.1038/nn.3991

Nagy, B., Hovhannisyan, A., Barzan, R., Chen, T.-J., and Kukley, M. (2017). Different patterns of neuronal activity trigger distinct responses of oligodendrocyte precursor cells in the corpus callosum. *PLoS Biol.* 15:e2001993. doi: 10.1371/journal.pbio.2001993

Nery, S., Fishell, G., and Corbin, J. G. (2002). The caudal ganglionic eminence is a source of distinct cortical and subcortical cell populations. *Nat. Neurosci.* 5, 1279–1287. doi: 10.1038/nn971

Orduz, D., Maldonado, P. P., Balia, M., Vélez-Fort, M., de Sars, V., Yanagawa, Y., et al. (2015). Interneurons and oligodendrocyte progenitors form a structured synaptic network in the developing neocortex. *eLife* 22:4. doi: 10.7554/eLife.06953

Pangratz-Fuehrer, S., and Hestrin, S. (2011). Synaptogenesis of electrical and GABAergic synapses of fast-spiking inhibitory neurons in the neocortex. *J. Neurosci.* 31, 10767–10775. doi: 10.1523/JNEUROSCI.6655-10.2011

Passlick, S., Grauer, M., Schäfer, C., Jabs, R., Seifert, G., and Steinhäuser, C. (2013). Expression of the γ2-subunit distinguishes synaptic and extrasynaptic GABA(A) receptors in NG2 cells of the hippocampus. *J. Neurosci.* 33, 12030–12040. doi: 10.1523/JNEUROSCI.5562-12.2013

Rudy, B., Fishell, G., Lee, S., and Hjerling-Leffler, J. (2011). Three groups of interneurons account for nearly 100% of neocortical GABAergic neurons. *Dev. Neurobiol.* 71, 45–61. doi: 10.1002/dneu.20853

Saita, M., Pranga-Sellnau, F., Resler, T., Schlesinger, R., Heberle, J., and Lorenz-Fonfria, V. A. (2018). Photoexcitation of the P4480 state induces a secondary photocycle that potentially desensitizes channelrhodopsin-2. *J. Am. Chem. Soc.* 140, 9899–9903. doi: 10.1021/jacs.8b03931

Stedehouder, J., Brizee, D., Shpak, G., and Kushner, S. A. (2018). Activity-dependent myelination of parvalbumin interneurons mediated by axonal morphological plasticity. *J. Neurosci.* 38, 3631–3642. doi: 10.1523/JNEUROSCI.0074-18.2018

Stehfest, K., and Hegemann, P. (2010). Evolution of the channelrhodopsin photocycle model. *Chemphyschem* 11, 1120–1126. doi: 10.1002/cphc.200900980

Vélez-Fort, M., Maldonado, P. P., Butt, A. M., Audinat, E., and Angulo, M. C. (2010). Postnatal switch from synaptic to extrasynaptic transmission between interneurons and NG2 cells. *J. Neurosci.* 30, 6921–6929. doi: 10.1523/JNEUROSCI.0238-10.2010

Voronova, A., Yuzwa, S. A., Wang, B. S., Zahr, S., Syal, C., Wang, J., et al. (2017). Migrating interneurons secrete fractalkine to promote oligodendrocyte formation in the developing mammalian. *Brain Neuron* 94, 500–516. doi: 10.1016/j.neuron.2017.04.018

Wake, H., Ortiz, F. C., Woo, D. H., Lee, P. R., Angulo, M. C., and Fields, R. D. (2015). Nonsynaptic junctions on myelinating glia promote preferential myelination of electrically active axons. *Nat. Commun.* 6:7844. doi: 10.1038/ncomms8844

Wamsley, B., and Fishell, G. (2017). Genetic and activity-dependent mechanisms underlying interneuron diversity. *Nat. Rev. Neurosci.* 18, 299–309. doi: 10.1038/nrn.2017.30

Wong, F. K., Bercsenyi, K., Sreenivasan, V., Portalés, A., Fernández-Otero, M., and Marín, O. (2018). Pyramidal cell regulation of interneuron survival sculpts cortical networks. *Nature* 557, 668–673. doi: 10.1038/s41586-018-0139-6

Yizhar, O., Fenno, L. E., Davidson, T. J., Mogri, M., and Deisseroth, K. (2011). Optogenetics in neural systems. *Neuron* 71, 9–34. doi: 10.1016/j.neuron.2011.06.004

Zhang, F., Wang, L. P., Boyden, E. S., and Deisseroth, K. (2006). Channelrhodopsin-2 and optical control of excitable cells. *Nat. Methods* 3, 785–792. doi: 10.1038/nmeth936

Zhang, F., Wang, L. P., Brauner, M., Liewald, J. F., Kay, K., Watzke, N., et al. (2007). Multimodal fast optical interrogation of neural circuitry. *Nature* 446, 633–639. doi: 10.1038/nature05744

Zonouzi, M., Scafidi, J., Li, P., McEllin, B., Edwards, J., Dupree, J. L., et al. (2015). GABAergic regulation of cerebellar NG2 cell development is altered in perinatal white matter injury. *Nat. Neurosci.* 18, 674–682. doi: 10.1038/nn.3990

Conflict of Interest Statement: The authors declare that the research was conducted in the absence of any commercial or financial relationships that could be construed as a potential conflict of interest.

frontiers in Cellular Neuroscience

REVIEW
published: 07 December 2018
doi: 10.3389/fncel.2018.00482

Adenosine Actions on Oligodendroglia and Myelination in Autism Spectrum Disorder

Hai-Ying Shen[1,2], Nanxin Huang[3], Jesica Reemmer[1] and Lan Xiao[3]**

[1] Robert Stone Dow Neurobiology Department, Legacy Research Institute, Legacy Health, Portland, OR, United States,
[2] Department of Integrative Physiology and Neuroscience, Washington State University, Pullman, WA, United States,
[3] Department of Histology and Embryology, Chongqing Key Laboratory of Neurobiology, Army Medical University (Third Military Medical University), Chongqing, China

Autism spectrum disorder (ASD) is the most commonly diagnosed neurodevelopmental disorder. Independent of neuronal dysfunction, ASD and its associated comorbidities have been linked to hypomyelination and oligodendroglial dysfunction. Additionally, the neuromodulator adenosine has been shown to affect certain ASD comorbidities and symptoms, such as epilepsy, impairment of cognitive function, and anxiety. Adenosine is both directly and indirectly responsible for regulating the development of oligodendroglia and myelination through its interaction with, and modulation of, several neurotransmitters, including glutamate, dopamine, and serotonin. In this review, we will focus on the recent discoveries in adenosine interaction with physiological and pathophysiological activities of oligodendroglia and myelination, as well as ASD-related aspects of adenosine actions on neuroprotection and neuroinflammation. Moreover, we will discuss the potential therapeutic value and clinical approaches of adenosine manipulation against hypomyelination in ASD.

Keywords: adenosine receptor, oligodendroglial differentiation, demyelination, neurotransmitter, autism

OPEN ACCESS

Edited by:
Mauricio Antonio Retamal, Universidad del Desarrollo, Chile

Reviewed by:
Davide Lecca, University of Milan, Italy
Annalisa Buffo, Università degli Studi di Torino, Italy

****Correspondence:***
Hai-Ying Shen
hshen@downeurobiology.org
Lan Xiao
xiaolan35@hotmail.com

Received: *31 July 2018*
Accepted: *26 November 2018*
Published: *07 December 2018*

Citation:
Shen H-Y, Huang N, Reemmer J and Xiao L (2018) Adenosine Actions on Oligodendroglia and Myelination in Autism Spectrum Disorder. Front. Cell. Neurosci. 12:482. doi: 10.3389/fncel.2018.00482

INTRODUCTION

Autism spectrum disorder is a range of neurodevelopmental conditions characterized by impairments in verbal and non-verbal communications, social skills, and repetitive behaviors. The variety of presentations of ASD is due to complex combinations of environmental and genetic influences; indeed, the term spectrum itself reveals the diversity of strengths and differences in symptoms of each autism patient. According to the reports, the average prevalence of individuals suffering from ASD is about 1% of people worldwide (Murray et al., 2014). ASD usually begins in childhood and tends to persist into adulthood, sometimes causing severe disabilities that call for life-long care and support.

Abbreviations: 5-HT, 5-hydroxytryptamine; A_1R, adenosine A_1 receptor; $A_{2A}R$, adenosine A_{2A} receptor; $A_{2B}R$, adenosine A_{2B} receptor; A_3R, adenosine A_3 receptor; ADA, adenosine deaminase; ADK, adenosine kinase; AMPAR, α-amino-3-hydroxy-5-methyl-4-isoxazolepropionic acid receptor; ASD, autism spectrum disorder; BBB, blood–brain barrier; cAMP, cyclic adenosine monophosphate; CB1R, cannabinoid receptor (type 1); D_1R, dopamine D1 receptor; D_2R, dopamine D2 receptor; D_3R, dopamine D3 receptor; EAE, experimental allergic encephalomyelitis; GABA, gamma-aminobutyric acid; IL, interleukin; MS, multiple sclerosis; NMDAR, *N*-methyl-D-aspartate receptor; NTs, nucleotide transporters; OL, oligodendrocyte; OPC, oligodendrocyte precursor cell; SAH, *S*-adenosyl-L-homocysteine; TLR, toll-like receptor.

Although the underlying mechanisms of ASD remain unclear, the most common hypothesis has been that of disrupted cerebral connectivity during brain development – this model proposes that ASD patients have reduced connections between distant brain regions and increased connections within local regions; such a disarranged connectivity could underlie the observed abnormalities in social, cognitive, and behavioral functions (Belmonte et al., 2004). During early brain development, aberrations appear in cytoarchitectural organizations in the frontal lobe, parieto-temporal lobe, subcortical limbic structures and cerebellum (Fombonne et al., 1999; Bolton et al., 2001; Courchesne, 2004; Hazlett et al., 2005). In addition, it has further been shown that ASD patients experience multiregional abnormalities in neurogenesis, neuronal migration, and maturation (Wegiel et al., 2010; Chen et al., 2015). However, the neuronal connectivity hypothesis of ASD is not fully supported, due to inconsistent data that reveals long-range hyper-connectivity or mixed patterns of both hypo- and hyper-connectivity (Mizuno et al., 2006; Turner et al., 2006; Noonan et al., 2009; Shih et al., 2010). Recently, increasing evidence suggests that white matter and myelin abnormalities are more relevantly involved in ASD pathophysiology. For example, neuroimaging studies utilizing diffusion tensor imaging (DTI) and magnetic resonance imaging (MRI) show that white matter disruption occurs in brain regions of children with ASD (Carmody and Lewis, 2010). Molecular genetic studies also reveal aberrations of myelin-related genes in ASD patients, both in expression level and epigenetic regulation (Richetto et al., 2017). Moreover, chromatin-remodeling protein CHD8, an ASD susceptibility gene, has also been found to play a vital role in oligodendroglial development and remyelination (Zhao et al., 2018).

In addition to studies focusing directly on structural variation, there coexists exciting research into the purine ribonucleoside adenosine; as a neuro- and glia-modulator, adenosine can directly and indirectly interact with several neurotransmitters, including glutamate, dopamine, and GABA, to regulate the development of oligodendroglial cells and myelination (Stevens et al., 2002). Also, by modulating neurotransmitters, adenosine has been shown to affect certain ASD comorbidities and symptoms, such as epilepsy, impaired cognitive functions, and anxiety (Fredholm et al., 2005a,b). In this review, we will summarize and discuss the interaction between adenosine signaling system in the central nervous system (CNS), mainly focusing on its effect in oligodendrocytes and the clinical symptoms of ASD, as well as the related cellular and molecular abnormalities. We suggest that augmentation of the useful actions of adenosine may become a potential therapeutic approach for the treatment of ASD by affecting myelination.

ADENOSINE METABOLISM AND ADENOSINE RECEPTORS

Adenosine is ubiquitously found in CNS. Early studies implied that adenosine was merely a metabolite of ATP and cAMP; now adenosine is widely recognized as a neuromodulator, gliomodulator, and modulator of complex behaviors with a broad range of biological and pathological functions. Indeed, adenosine plays two important roles in the CNS: *(i)* as a homeostatic transcellular messenger between neuronal and glial cells and *(ii)* as a modulator controlling neurotransmitter release and reuptake for neuronal excitability (Shen and Chen, 2009; Boison and Shen, 2010; Shen et al., 2012).

Adenosine Metabolism

Adenosine metabolism in the CNS has been extensively reviewed elsewhere (Cunha, 2001; Latini and Pedata, 2001; Fredholm et al., 2005a,b). Unlike classical neurotransmitters, which are stored in synaptic vesicles and released by exocytosis for exclusive actions on synapses (Fredholm et al., 2005a,b), adenosine distributes extra- and intra-cellularly throughout tissues in the CNS and maintains a basal level in the range of 50–200 nM (Latini and Pedata, 2001). The intra- and extra-cellular adenosine levels exist in a state of dynamic exchange due to the influence of both equilibrative and concentrative nucleoside transporters (Baldwin et al., 2004; Gray et al., 2004). Additionally, metabolic enzymes such as ADA, ADK, SAH-hydrolase, and NTs, continually cycle adenosine through a variety of pathways (Boison and Shen, 2010). The input sources of adenosine are also varied, though strictly dependent on the metabolic state of the cell. Extracellularly, adenosine is produced by the breakdown of adenine nucleotides (such as ATP) by a variety of ecto-NTs, which include ecto-nucleoside triphosphate diphosphohydrolase CD39 and the 5′-nucleotidase CD73. Intracellularly, adenosine can be generated via the dephosphorylation of AMP or the hydrolysis of SAH by cytosolic enzymes 5′-NT or SAH-hydrolase, respectively (Schubert et al., 1979; Broch and Ueland, 1980) (**Figure 1**).

In the CNS, adenosine levels are largely regulated by glial cells, and two main types of equilibrative adenosine transporters that exist in astrocytic membranes. Intracellular removal of adenosine is executed by degradation to inosine or phosphorylation to AMP by ADA and ADK, respectively (Pak et al., 1994; Boison et al., 2010). The release and uptake of adenosine are mediated by bi-directional nucleoside transporters, depending on the adenosine concentration gradient between the extracellular and intracellular spaces (Gu et al., 1995). It is also worth pointing out that of adenosine levels between extracellular and intracellular spaces are usually maintained in the same range due to highly efficient cellular equilibrative nucleoside transporters in most cells for facilitated diffusion (Cass et al., 1999).

Adenosine Receptors and Neurotransmissions

As a key neurotransmitter, adenosine signaling plays a significant role in neuronal excitability and neuroprotection, as well as synaptic and non-synaptic neurotransmission in the CNS. The adenosinergic system also interacts with several other major neurotransmitters, such as dopamine, glutamate, acetylcholine noradrenaline, serotonin (5-hydroxytryptamine), and endocannabinoids (Sperlagh and Vizi, 2011; Shen et al., 2013); these interactions have, however, been reviewed and discussed extensively (Sebastiao and Ribeiro, 2000;

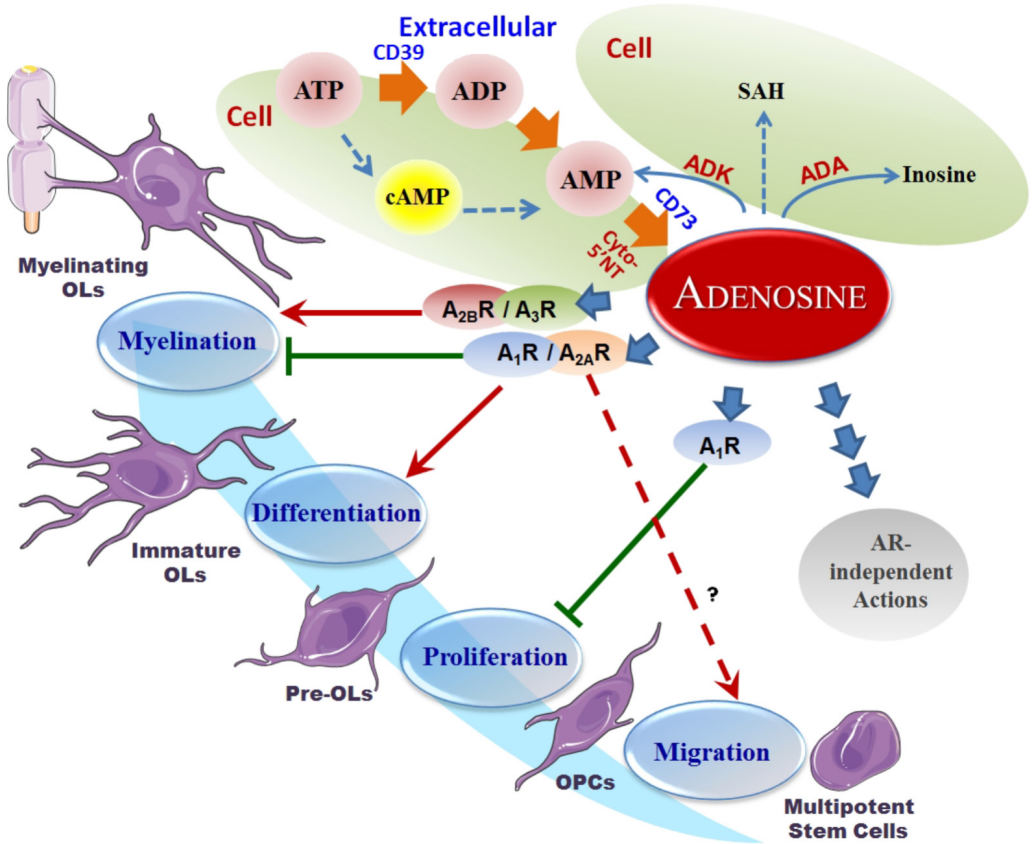

FIGURE 1 | Adenosine metabolism and its effects on OPCs. Overview of the adenosine metabolism and adenosine receptor-induced actions on oligodendroglial development. It is seen that A_1R inhibits oligodendroglial proliferation, A_1R and $A_{2A}R$ promote differentiation and inhibit myelination, and $A_{2B}R$ and A_3R promote myelination in the lifecycle of oligodendrocytes. The pool of extracellular adenosine is responsible for the activation of these various ARs, while itself being the subject of supply by the ATP cycle, metabolism by hydrolysis or deamination, as well as transport and internalization. Red arrows represent a stimulation effect; Green bars represent an inhibition effect; Blue arrows show the directionality of effects.

Fredholm et al., 2005a,b; Chen et al., 2013). Of particular interest in this review is the ability of adenosine to modulate neurotransmitter release and neuronal excitability in the CNS via activation of four different subtypes of G-protein coupled adenosine receptors (ARs): A_1R, $A_{2A}R$, $A_{2B}R$, and A_3R (Fredholm et al., 2005a,b). Through ARs, adenosine influences a wide range of brain functions under physiological and pathophysiological conditions, including neuroprotection, neuroinflammation, sleep, psycholocomotion, anxiety, cognition and memory, and neuropsychological disorders (Dunwiddie and Masino, 2001; Fredholm et al., 2005a,b; Shen et al., 2008, 2012). The interactions among subtypes of ARs and between adenosinergic signaling and other neurotransmissions may involve molecular mechanisms at multiple levels, such as *(i)* direct cross-talk between receptors on the cell membrane, *(ii)* downstream intracellular second messenger systems among different receptors, *(iii)* trans-synaptic actions, and *(iv)* interactions between neurons and glial cells (Sebastiao and Ribeiro, 2000; Stevens et al., 2002; Dare et al., 2007; Shen and Chen, 2009; Boison et al., 2010).

Through AR-dependent actions, adenosine modulates the release of several neurotransmitters in the CNS, including dopamine, glutamate, GABA, serotonin, noradrenaline, acetylcholine, and cannabinoids (Fredholm and Dunwiddie, 1988; Cunha, 2001; Dunwiddie and Masino, 2001). Among the four subtypes of ARs, $A_{2A}R$ and A_1R play the most significant roles in the interaction between the adenosinergic signaling pathway and other neurotransmitters, while $A_{2A}R$ and A_3R have a limited effect (Fredholm et al., 2005a,b; Chen et al., 2013). Even so, the AR-mediated manipulations on neurotransmissions involve a high degree of complexity (Dixon et al., 1997; O'Kane and Stone, 1998; Lopes et al., 1999; Gorter et al., 2002). Firstly, this regulation is primarily mediated by the interplay of A_1R and $A_{2A}Rs$, as these two subtypes have different partnering sets of G-proteins mediating opposing excitatory vs. inhibitory actions. Specifically, the activation of $G_{i/o}$-coupled A_1R (and A_3R) mediates the adenosine-dependent inhibition of neurotransmitter release at pre-synaptic neuronal terminals and represses post-synaptic neuronal (Snyder, 1985; Fredholm and Dunwiddie, 1988; Latini et al., 1996). Contrastingly, activation of $G_{s/olf}$-coupled $A_{2A}R$ (and $A_{2B}R$) exerts excitatory activity of

stimulating the release of glutamate, acetylcholine, and GABA in the striatum and hippocampus (Kirkpatrick and Richardson, 1993; Kirk and Richardson, 1994; Cunha et al., 1995a,b; Sebastiao and Ribeiro, 1996). Secondly, the actions from pre- and post-synaptic sites also contribute to the complexity of AR actions. Presynaptically, stimulation of A_1R suppresses the release of transmitters including dopamine, glutamate, 5-HT, acetylcholine, GABA, and noradrenaline; whereas activation of presynaptic $A_{2A}R$ facilitates the release of acetylcholine, GABA, and glutamate (Sperlagh and Vizi, 2011). Post-synaptically, activation of $A_{2A}R$ inhibits activity of dopamine D_2 receptor (D_2 R), while A_1R activation counteracts functions of dopamine D_1 receptor (D_1R) (Ferre et al., 1991; Fredholm et al., 2005a). $A_{2A}Rs$ serve a permissive role in activating cannabinoid receptor (type 1) (CB1R)-mediated inhibition of excitatory transmission, while A_1R prevents the CB1R-mediated reduction of glutamate release. In addition, adenosine signaling affects the activity of post-synaptic AMPAR and NMDAR by control of glutamate release (Sebastiao and Ribeiro, 2009; Sperlagh and Vizi, 2011). Thirdly, the formation of these AR heteromeric receptor complexes also allows for their regulation at the second messenger level. For example, ARs can form heteromers between ARs themselves or with other receptor types, such as glutamate receptors, dopamine D_1 and D_2 receptors, or cannabinoid receptors. While the $A_{2A}R$-D_2R heteromers are the first demonstrated epitope–epitope electrostatic interactions underlying receptor heteromerization (Ferre et al., 2004), the capability of A_1R and $A_{2A}R$ to form homo- or hetero-oligomers with both other receptors and ARs alike has widened their biological roles in developmental, physiological, and pathological situations. In addition to AR actions, studies suggest that adenosine regulating enzymes may also affect epigenetic modifications (Kiese et al., 2016), including alteration of transmethylation and histone modifications (Borea et al., 2016). All of the above regulatory levels comprise a high degree of complexity of adenosinergic actions.

ADENOSINE'S EFFECT ON OLIGODENDROGLIAL DEVELOPMENT

In the CNS, the development of the oligodendrocytes lineages (OLs) is a crucial step for myelination, which is essential for the normal functioning of transduction between neurons. Adenosine actions play a crucial role in this process (Fields, 2006) via AR-mediated direct effects and/or actions from AR-interacted neurotransmissions. Prior to myelination, oligodendroglial cells pass through distinct stages, including OPCs, pre-mature OLs, and finally mature OLs. It has been shown that all subtypes of ARs (i.e., A_1R, $A_{2A}R$, $A_{2B}R$, and A_3R), along with ADA, ADK, and the equilibrative nucleoside transporters, ENT1 and ENT2, are expressed on oligodendroglial cells (Gonzalez-Fernandez et al., 2014). Adenosinergic signaling has various effects on oligodendroglia *via* the activation of ARs and changes in adenosine metabolism (Stevens et al., 2002), while adenosine actions on oligodendroglial development and OL maturation are AR subtype-dependent (Burnstock et al., 2011a,b). For example, adenosine can act through A_1R activation to inhibit the proliferation of OPC but also can promote the differentiation of OPCs into myelinating OLs (Stevens et al., 2002; Asghari et al., 2013). In contrast, adenosine acting through $A_{2A}R$ activation can inhibit OL maturation, whereas inactivation of $A_{2A}R$ can delay the differentiation of OPCs *via* altered rectifier potassium currents in culture (Coppi et al., 2013). Also, the $A_{2A}R$ agonist CGS-21680 can mediate OPC differentiation, which in turn can be completely blocked by the selective $A_{2A}R$ antagonist SCH-58261. In addition, the activation of A_3R by its agonist 2-CI-IB-MECA can cause concentration-dependent oligodendroglial cell death. This mechanism is ultimately due to disruption of mitochondrial membrane potential in oligodendroglial cells; through activation of Bax and Puma proapoptotic proteins, A_3R mediates apoptosis and necrosis (Gonzalez-Fernandez et al., 2014). Nevertheless, adenosine is suggested to not only inhibit proliferation of OPCs, but also stimulate the migration and differentiation of OPCs and promote myelin formation (Stevens et al., 2002; Othman et al., 2003; Karadottir and Attwell, 2007); further studies are still needed to dissect these seemingly contradictory roles of ARs and adenosine modulating enzymes.

NEUROTRANSMITTER-MEDIATED ACTIONS OF ADENOSINE ON OLIGODENDROGLIAL DEVELOPMENT

Glutamatergic Effects

The proliferation and differentiation of OPCs, as well as their capability to myelinate axons, are partly controlled by neurotransmitters linked to adenosine modulation; the activation of these neurotransmitter receptors contributes to the damage of OLs and disrupted myelination in pathological scenarios (Karadottir and Attwell, 2007; Kolodziejczyk et al., 2009; Hamilton et al., 2017). For example, glutamate receptors are expressed in oligodendroglial cells and affect their development (Karadottir et al., 2005). Under normal physiological conditions, glutamate acts through the activation of NMDAR to increase OPC migration, whereas activation of the AMPAR or kainate receptors (but not NMDAR) decreases the proliferation of OPCs (Karadottir and Attwell, 2007) by altering both intracellular sodium concentration and potassium channel function. Blocking NMDA receptors with phencyclidine will result in the inability of OLs to mature (Lindahl et al., 2008).

Dopaminergic and Other Neurotransmitters' Effects

Dopamine has been reported to modulate CNS myelination (Belachew et al., 1999) through underlying mechanisms that are not fully elucidated. It was found that the dopamine antagonist haloperidol increases OPC proliferation but inhibits their differentiation, an action likely to occur *via* D_3R (Bongarzone et al., 1998). To clarify the effect of the different subtypes of dopaminergic receptors involved in oligodendroglial development, genetic approaches may need to be utilized in the future. OPCs also express acetylcholine receptors, and the activation of muscarinic acetylcholine M3 receptors increases

OPC proliferation through activation of the MAPK signaling pathway; conversely, anti-muscarinic treatment has been seen to accelerate functional myelin repair (Abiraman et al., 2015). Meanwhile, inactivation of nicotinic acetylcholine receptors (nAChR) can inhibit proliferation of OPCs, as evidenced by the ability of the nAChR antagonist mecamylamine to suppress OPC differentiation (Imamura et al., 2015).

Together, while the adenosinergic system plays crucial roles in glutamatergic and dopaminergic neurotransmissions at multiple molecular and cellular levels (Stevens et al., 2002; Barnea-Goraly et al., 2004; Matos et al., 2015), the studies in this section suggest that adenosine signaling can influence the regulation of oligodendroglial development and remyelination via neurotransmitters' actions itself.

ADENOSINE AND ADENOSINE RECEPTORS IN DEMYELINATION AND REMYELINATION

Various studies have shown that myelin abnormalities are involved in ASD, affecting information processing and cognition. Researchers utilized MRI scans to compare myelination between ASD and neurotypical children, and found that children with ASD had more myelinated neural fiber than the average level of similarly aged children in both the left and right medial frontal cortex, but had less myelination in the left temporoparietal junction (Deoni et al., 2015). Another study using DTI found that the fractional anisotropy value – an index used to describe the statistical difference in white matter brain scanning – was reduced in the white matter in children and adolescents with autism compared to controls, including regions adjacent to the superior temporal sulcus, ventromedial prefrontal cortices, anterior gyri, and temporoparietal junctions and corpus callosum, as well as regions adjacent to the temporal lobes close to the amygdala. This suggests that white matter disruption between brain regions may cause impaired social cognition in autism (Ginsberg et al., 2012). Measurement of myelin content by performing cross-sectional imaging of fractional anisotropy – based on the movements of water molecules – showed that the global myelin water fraction was significantly lower in autism patients than in neurotypical controls (Stolerman et al., 2016). By applying whole genome DNA methylation microarrays analysis and high-resolution whole-genome gene expression, researchers have found that changes in myelin and myelination-related genes were associated with specific behavioral domains of autism (Setzu et al., 2006). Moreover, genome-wide transcriptional profiling techniques in combination with MRI and epigenetic analyses reveal that viral-like prenatal immune activation leads to myelin-related epigenetic and transcriptional changes, which may lead to neurodevelopmental disorders like autism (Richetto et al., 2017). Recently, mutation of the chromatin remodeler protein CHD8, which is crucial for oligodendroglial development, was found to be associated with ASD (Setzu et al., 2004). Taken together, these research results suggest that white matter abnormalities may contribute to ASD pathogenesis, and targeting oligodendroglia may represent a new therapeutic strategy for ASD.

Endogenous remyelination usually occurs after demyelination, through the differentiation of OPCs and thus reproduction of myelin around the demyelinated axons (Back and Rosenberg, 2014; Safarzadeh et al., 2016). A successful remyelination is determined by the capability of OPCs to proliferate and differentiate into myelinating OLs, and these processes are also affected by the adenosine system (Fields, 2006). Accumulating evidence indicates that the adenosinergic signaling system is involved in immunity and inflammation of demyelinating diseases (Sebastiao and Ribeiro, 2009; Ginsberg et al., 2012), likely *via* ARs (A_1R, $A_{2A}R$, $A_{2B}R$, and A_3R) on the surface of immune cells (Tsutsui et al., 2004). For instance, white matter injury (WMI) in premature newborn and embryos has been found to be closely related with adenosine (Johnston et al., 2001). Another typical example of such demyelinating diseases is MS, which is an autoimmune-mediated inflammatory disease characterized by multifocal demyelination that is associated with myelin destruction, oligodendroglial cell death, and axonal degeneration.

Adenosine A_1 Receptor

Clinical and experimental evidence indicates that A_1R plays a role in the modulation of neuroinflammation (Si et al., 1996). A decreased expression of A_1R in peripheral mononuclear cells and decreased adenosine levels in plasma were seen in patients with MS. In addition, expression of A_1Rs on $CD45^+$ glial cells was decreased by 50% in MS patients and similar observations have been made in patients with other CNS diseases (Haselkorn et al., 2010). From animal studies it was shown that pharmacological activation of A_1R by N6-cyclohexyladenosine (CHA) can induce remyelination and protect existing myelin in a rat model of optic chiasm demyelination. Further study revealed that this protective effect on myelinating cells is mediated by A_1R by potentiating regeneration of endogenous neural progenitors (Asghari et al., 2013). Apparently, activation of A_1Rs is an important inhibitory mechanism against neuroinflammation in MS and has also been observed to attenuate neuroinflammation and demyelination in EAEs animal models (Si et al., 1996; Yao et al., 2012). In accordance with these findings, studies have revealed that inactivation of A_1R resulted in a progressive-relapsing form of EAE in A_1R KO mice, with worsened demyelination and axonal injury, increased microglial proliferation, and enhanced expression of matrix metalloproteinase-12 (MMP-12), iNOS, as well as proinflammatory gene interleukin-1beta (IL-1β) (Si et al., 1996). The modulation of microglial proliferation was also seen in pharmacological approaches, as both non-selective and selective A_1R agonists attenuated the proliferation of rat microglia, and activation of A_1R was shown as an endogenous inhibitor of the microglial response (Turner et al., 2002; Fogal et al., 2010). Therefore, the interplay between A_1R and neuroinflammation is a reciprocal regulatory mechanism; namely, microglial A_1R is downregulated during neuroinflammation in animal models of EAE and patients with MS (Hasko and Pacher, 2008), and the inactivation of A_1R, in turn, exacerbates EAE and MS progression. Thus, modulation of neuroinflammation by A_1R manipulation may offer interesting therapeutic opportunities for MS and other demyelinating diseases (Yao et al., 2012).

In developmental stages, however, adenosine acts via A_1Rs and induced diffused WMI. Immature OLs express more A_1Rs compared with mature cells *in vitro*. Adenosine plays an important role in OL lineage progression by causing OL precursor cells to differentiate prematurely. A_1R stimulation induces white matter loss and mediates hypoxia-induced ventriculomegaly (Mayne et al., 2001). Aiming at modulating this process may provide a novel strategy for WMI treatment (Sitkovsky et al., 2004).

Adenosine A_{2A} Receptor

A_{2A}R also exerts significant anti-immune and anti-inflammatory actions on immune cells (Vincenzi et al., 2013; Ingwersen et al., 2016; Liu et al., 2018). In human studies, A_{2A}Rs are up-regulated in MS patients and administration of the A_{2A}R agonist CGS-21680 can reduce lymphocyte proliferation of MS patients. This activation of A_{2A}R mediates a significant inhibition of tumor necrosis factor alpha (TNF-α), IL-6, IL-1β, IL-17, interferon gamma (IFN-γ), and represses cell proliferation, expression of very late antigen (VLA)-4, and activation of NF-kB (Genovese et al., 2009). Further research has been conducted in animal models to assess the pattern of A_{2A}R expression in neuropathologically damaged tissue. A_{2A}R is seen to be expressed in infiltrating immune cells, as well as the surrounding endothelium; it is also up-regulated on T cells and macrophages/microglia in EAE lesions (Mills et al., 2008). Likewise, endothelial A_{2A}R is detected in demyelinated areas in MS brain samples (Mills et al., 2008). Moreover, A_{2A}R agonist CGS-21680 can ameliorate EAE neurological deficiencies in mice. In sum, A_{2A}R has been shown to have an overall influence in mediating BBB function in CNS demyelinating diseases (Matos et al., 2013).

Activation of A_{2A}R *in vitro* inhibits the migration of $CD4^+$ T cells, macrophages, and primary microglia, and suppresses macrophage/primary microglia-mediated phagocytosis of myelin. Along with this finding, A_{2A}R-specific agonists have also been seen to inhibit myelin-specific T cell proliferation *ex vivo* and ameliorate EAE (Mills et al., 2008). A_{2A}R agonists suppressed *in vivo* primary mechanical injury and secondary inflammatory tissue damage after spinal cord injury; they can also reduce leukocyte recruitment and the activation of the JNK signaling pathway in oligodendroglia, thus protecting the spinal cord from injury-induced demyelination (Paterniti et al., 2011). In contrast, A_{2A}R KO mice develop increased morbidity, exacerbated neurobehavioral deficits, and generally more severe EAE pathology than their WT littermates. A_{2A}R KO mice exhibit a severe phenotype of demyelination in EAE with enhanced infiltration of inflammatory cells in the spinal cord and cerebral cortex, accompanied by reduced expression of anti-inflammatory cytokines and increased expression of pro-inflammatory cytokines in the CNS and blood (Hasko and Pacher, 2008). However, studies also demonstrated that there is a dual role of A_{2A}R in autoimmune neuroinflammation; for instance, A_{2A}R-specific agonists inhibited the proliferation of myelin-specific T cell *ex vivo* and ameliorated EAE, whereas application of the same agonist after the onset of disease exacerbated progression of non-remitting EAE. This suggests that activation of A_{2A}R exerts complex effects on chronic autoimmune neurodegeneration (Wei et al., 2013). The paradoxical effects of A_{2A}R may be dependent on pathophysiological conditions; further studies are needed to clarify the manipulatory role of A_{2A}R on demyelinating disorders as well as the potential shifting of the predominant role of A_1R and A_{2A}R in the pathogenesis of demyelination.

In developmental models, adenosine signaling pathway acts via A_{2A}R to inhibit OPC differentiation (Coppi et al., 2013). Increased nitric oxide release by microglia, up-regulated neuronal glutamate release, and decreased glutamate uptake by astrocytes are all results of A_{2A}R activation, and leads to aggravated excitotoxicity (Cook, 1990). Blockade of A_{2A}R, on the other hand, has been revealed to have a negative effect on demyelination in the spinal cord injury model (Masino et al., 2011).

Adenosine A_{2B} and A_3 Receptors

The A_{2B}R is a relatively low-affinity adenosine receptor compared to A_1R and A_{2A}R; in fact, the activation of A_{2B}R requires a pathologically enhanced level of adenosine (Fredholm et al., 2005a; Chen et al., 2013). A clinical study revealed upregulated A_{2B}R in the peripheral leukocytes of MS patients; this is in line with findings which showed increased A_{2B}Rs in lymphoid tissues of EAE mice (Lazarus et al., 2011). Pharmacological blockade of A_{2B}R (via A_{2B}R antagonists MRS-1754 and CVT-6883) relieved the symptoms and pathological changes of EAE, accompanied by a suppression of IL-6 production and Th17 cell differentiation. A promising work from Gonzalez-Fernandez et al. (2014) demonstrated that activation of A_3R may contribute to oligodendroglial cell death in optic nerve and white matter ischemic damage. However, further investigations are required to fully understand the effects of A_{2B}R and A_3R in the myelination and demyelination processing.

ADENOSINE ACTIONS IN AUTISM

The study of adenosine in regards to autism has been around for decades (Masino et al., 2013); however, only within the last 10 years have multiple lines of research revealed the important role of adenosine and ARs in ASD. Due to findings that adenosine action affects many various aspects of ASDs, such as neuronal activity, sleep and seizures, cognition, and anxiety, the adenosine signaling pathway may be primed to be a potential therapeutic target for ASD.

Adenosine and Its Metabolism in ASD

A patient study from Masino et al. (2009) using a customized parent-based questionnaire indicated an observable relationship between activities that were predicted to increase adenosine levels in the brain and parental observations of relieved behavioral manifestations of ASD. Their results suggest, in general, that increased adenosine signaling activity can benefit sleep disorders, seizures, and social and behavioral dysfunction in ASD (Stubbs et al., 1982; Shen et al., 2008). Augmentation of adenosine signaling activity may serve as a novel therapeutic strategy for ASD with multiple potential beneficial effects in alleviating core symptoms and several comorbidities of ASD (Bottini et al., 2001).

However, no direct evidence of dysregulated adenosine in the brain has been tested with respect to the manifestations of ASD (Hettinger et al., 2008). Adenosine metabolic enzymes were also found to have links to ASD. A reduced activity of ADA was reported in the sera of autistic children (Freitag et al., 2010), and a low-activity polymorphism (Asp8Asn) of ADA gene was found to be significantly associated with ASD patients (Ansari et al., 2017a; Amodeo et al., 2018). The above lines of research suggest that reduced ADA activity may be a risk factor for the development of ASD.

Adenosine Receptors and ASD

The A_{2A}Rs are found expressed predominantly in the caudate nucleus, where they exert their influence in ASD pathology (Ahmad et al., 2017a). Genetic studies reveal that one of the polymorphisms of *$A_{2A}R$ gene*, rs2236624-CC, has a nominal association with ASD and three others, rs3761422, rs5751876 and rs35320474, and influences phenotypic variability in ASD symptoms (Ahmad et al., 2017a). Interestingly, the A_{2A}R gene is located on chromosome 22q11.23, and large 22q11.2 duplications and deletions were observed in individuals with ASD; this correlation suggests a possible role of A_{2A}R variants in mediating phenotypic expression in ASD (Ahmad et al., 2017a).

Repetitive behaviors and restricted interests are commonly related to neurodevelopmental disorders which are diagnostic for ASD. As a means of exploring these phenotypes, BTBR T^{+} Itpr3tf/J (aka BTBR) mice can be utilized as an animal model of idiopathic autism due to their strong and consistent autism-relevant behaviors (Ahmad et al., 2017b; Ansari et al., 2017b). Studies showed that A_{2A}R agonism *via* the adenosine analog CGS-21680 caused a reduction of repetitive and inflexible behaviors in these BTBR mice, whereas A_{2A}R antagonist SCH-58261 treatment exacerbated repetitive behaviors. This antagonism was also seen to cause a decreased expression of IL-27 and IkB-α and an increased expression of NF-kB p65 and toll-like receptors, TLR2, TLR3, and TLR4 in the brain (Tanimura et al., 2010; Campbell et al., 2013; Lopez-Cruz et al., 2017). Correspondingly, other pharmacological studies have shown that activation of A_1R and A_{2A}R *via* co-administration of A_{2A}R agonist CGS-21680 and A_1R agonist CPA attenuates stereotypy (repetitive behaviors) in a second animal model of ASD in a dose-dependent manner (Zhu et al., 2011). A_{2A}R inactivation also affects social behaviors and anxiety in the autism spectrum; A_{2A}R knockout mice show an anxiety profile, higher levels of sociability, and a reduced sensitivity to social novelty (Matute et al., 2001). Pharmacological manipulation of A_{2A}R can conversely potentiate motivation to work. Together, these studies support the notion that augmentation of AR activities in the CNS could be a promising therapeutic strategy for ASD.

In addition, a third player, A_3R, was shown to have two rare coding variants (Leu90Val and Val171Ile) in a genetics study using four single-nucleotide polymorphisms (SNPs) representing common haplotypes of 958 families with autism. It was revealed that these variations were found at an increased rate in ASD cases (Alberdi et al., 2006). Further *in vitro* analysis revealed that these same coding variants, Val90-A_3R and Ile171-A_3R, link to an elevated 5-HT re-uptake activity which responds differently to agonism of the 5-HT transporter. This suggests that these

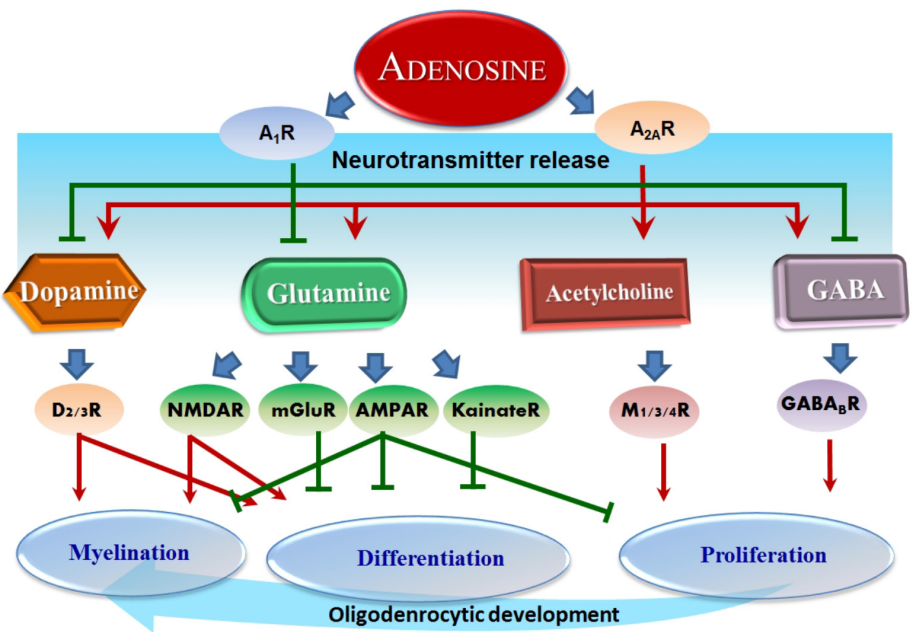

FIGURE 2 | Adenosine-modulated neurotransmitters and their effects on OLs. Overview of adenosine effect on neurotransmitters: adenosine inhibits dopamine, glutamine, and GABA through A_1R, whereas A_{2A}R serves to conversely promote dopamine, glutamine, acetylcholine, and GABA. These neurotransmitters successively regulate further downstream receptors and ultimately several essential processes in oligodendrocytic development, such as proliferation, differentiation, and myelination. Red arrows represent a stimulation effect; Green bars represent an inhibition effect; Blue arrows show the directionality of effects.

hyperfunctional coding variants of A_3R may have an impact on ASD risk (Alberdi et al., 2006; Chez et al., 2007).

ADENOSINE AND RELATED NEUROTRANSMITTERS IN ASD

Adenosine-related neurotransmitters, such as glutamate, dopamine, histamine, and others have all taken part in the initiation and progression of ASD. Under pathological conditions, glutamate can also damage white matter *via* an over-activation of NMDAR, which is seen in ischemia, anoxia, infection, and MS (Owley et al., 2006). Likewise, glutamate can also cause the damage and death of OLs via activating AMPAR or kainate receptors, which in turn detrimentally increases Ca^{++} permeability (Karadottir and Attwell, 2007). In addition, glutamate can also activate kainate receptor-linked microglia/macrophage action to cause OL damage (Hellings et al., 2017). However, inhibition of AMPAR or kainate receptors alone does not exert an effect on OLs or myelination. Together, these data suggest that glutamate facilitates migration but inhibits the proliferation of OPCs, which is similar to adenosine-mediated effects on oligodendroglial lineage cells. This suggests that the effect of glutamate in disease may be caused by adenosine. In some ASD individuals, glutamate levels were found to be abnormally high (Paval, 2017). Glutamate antagonists, such as amantadine and memantine, have been shown to be effective in ASD treatment, by improving memory, hyperactivity, irritability, language, social behavior, and self-stimulatory behavior (Paval, 2017; Lee et al., 2018).

Dopamine has a fundamental role in the brain and its role in ASD has already been thoroughly studied (Seeman, 2010; Mei et al., 2016a). Moreover, it has been shown that using antagonists for dopamine D_1 receptors in mice revealed significant deficits in sociability and repetitive behaviors related to ASD. Small interfering RNA (siRNA)-mediated inhibition of dopamine D_2 receptors in the dorsal striatum replicated ASD-like phenotypes (Mei et al., 2016b). Dopaminergic system deficits have been closely related to behavior skills such as analyzing, planning and prioritizing (Matson et al., 2011). Consistent with this, children with ASD revealed deficits in working memory and flexibility. Dopamine has a close relationship with social behavior, attentional skills, and perception, which are all related to ASD (Mei et al., 2016a). Recently, it was found that muscarinic M1 receptors negatively regulate OPC differentiation and their ablation can accelerate remyelination (Mei et al., 2016a). Notably, oligodendroglial development and myelination are complex programs under the control of multiple neurotransmitters. For instance, it was found that quetiapine, an antagonist for multiple neurotransmitters including dopamine, muscarine, and opioids, promoted OL differentiation and remyelination (Mei et al., 2016b), demonstrating that quetiapine may be a promising drug to be tested in future clinical trials. These facts reveal the importance of neurotransmitters in ASD and that targeting dopamine and/or glutamate signaling pathway effects on myelination is an effective strategy for ASD treatment. Currently, however, only two atypical antipsychotic drugs, risperidone and aripiprazole, are FDA-approved as clinically effective in improving ASD behavioral symptoms (Matson et al., 2011). Therefore, it may be a promising strategy to treat ASD by regulating adenosine, which will in turn affect the related neurotransmitters (**Figure 2**).

CONCLUDING REMARKS

Increased evidence from clinical and basic research suggests a relationship between the adenosine signaling system and ASD. The broad actions of the adenosinergic system on neuroprotection, neuroinflammation, modulation of neurotransmissions, and regulation of glial function are involved in the core behavioral symptoms in ASD, irrespective of cognitive function. Therefore, adenosine-based strategies, through manipulating adenosine signaling pathways and affecting oligodendrocyte activities, may be utilized to therapeutically target core symptoms and comorbidities of ASD. Although adenosine's effect is complex and pleiotropic, its effect on myelination can work through multiple neurotransmitter-induced pathways and improve behavior deficits in ASD, suggesting that this strategy is effective. However, focused studies on adenosine, oligodendroglia, and myelination are urgently needed to fully uncover the role of the adenosine system in ASD. While multiple adenosine receptor agonists are in clinical trials, therapeutic augmentation of adenosinergic signaling is ready to be tested for diverse potential benefits against multiple comorbidities on the autism spectrum.

AUTHOR CONTRIBUTIONS

H-YS and NH wrote the manuscript. JR and LX revised the manuscript. H-YS and LX designed the manuscript.

FUNDING

This work was supported by the National Natural Science Foundation of China (NSCF31671117).

REFERENCES

Abiraman, K., Pol, S. U., O'Bara, M. A., Chen, G. D., Khaku, Z. M., Wang, J., et al. (2015). Anti-muscarinic adjunct therapy accelerates functional human oligodendrocyte repair. *J. Neurosci.* 35, 3676–3688. doi: 10.1523/JNEUROSCI.3510-14.2015

Ahmad, S. F., Ansari, M. A., Nadeem, A., Bakheet, S. A., Al-Ayadhi, L. Y., and Attia, S. M. (2017a). Toll-like receptors, NF-kappaB, and IL-27 mediate adenosine A2A receptor signaling in BTBR T(+) Itpr3(tf)/J mice. *Prog. Neuropsychopharmacol. Biol. Psychiatry* 79(Pt B), 184–191. doi: 10.1016/j.pnpbp.2017.06.034

Ahmad, S. F., Ansari, M. A., Nadeem, A., Bakheet, S. A., Almutairi, M. M., and Attia, S. M. (2017b). Adenosine A2A receptor signaling affects IL-21/IL-22 cytokines and GATA3/T-bet transcription factor expression in CD4(+) T cells from a BTBR T(+) Itpr3tf/J mouse model of autism. *J. Neuroimmunol.* 311, 59–67. doi: 10.1016/j.jneuroim.2017.08.002

Alberdi, E., Sanchez-Gomez, M. V., Torre, I., Domercq, M., Perez-Samartin, A., Perez-Cerda, F., et al. (2006). Activation of kainate receptors sensitizes oligodendrocytes to complement attack. *J. Neurosci.* 26, 3220–3228. doi: 10.1523/JNEUROSCI.3780-05.2006

Amodeo, D. A., Cuevas, L., Dunn, J. T., Sweeney, J. A., and Ragozzino, M. E. (2018). The adenosine A2A receptor agonist, CGS 21680, attenuates a probabilistic reversal learning deficit and elevated grooming behavior in BTBR mice. *Autism Res.* 11, 223–233. doi: 10.1002/aur.1901

Ansari, M. A., Attia, S. M., Nadeem, A., Bakheet, S. A., Raish, M., Khan, T. H., et al. (2017a). Activation of adenosine A2A receptor signaling regulates the expression of cytokines associated with immunologic dysfunction in BTBR T(+) Itpr3(tf)/J mice. *Mol. Cell. Neurosci.* 82, 76–87. doi: 10.1016/j.mcn.2017.04.012

Ansari, M. A., Nadeem, A., Attia, S. M., Bakheet, S. A., Raish, M., and Ahmad, S. F. (2017b). Adenosine A2A receptor modulates neuroimmune function through Th17/retinoid-related orphan receptor gamma t (RORgammat) signaling in a BTBR T(+) Itpr3(tf)/J mouse model of autism. *Cell. Signal.* 36, 14–24. doi: 10.1016/j.cellsig.2017.04.014

Asghari, A. A., Azarnia, M., Mirnajafi-Zadeh, J., and Javan, M. (2013). Adenosine A1 receptor agonist, N6-cyclohexyladenosine, protects myelin and induces remyelination in an experimental model of rat optic chiasm demyelination; electrophysiological and histopathological studies. *J. Neurol. Sci.* 325, 22–28. doi: 10.1016/j.jns.2012.11.008

Back, S. A., and Rosenberg, P. A. (2014). Pathophysiology of glia in perinatal white matter injury. *Glia* 62, 1790–1815. doi: 10.1002/glia.22658

Baldwin, S. A., Beal, P. R., Yao, S. Y., King, A. E., Cass, C. E., and Young, J. D. (2004). The equilibrative nucleoside transporter family, SLC29. *Pflugers Arch.* 447, 735–743. doi: 10.1007/s00424-003-1103-2

Barnea-Goraly, N., Kwon, H., Menon, V., Eliez, S., Lotspeich, L., and Reiss, A. L. (2004). White matter structure in autism: preliminary evidence from diffusion tensor imaging. *Biol. Psychiatry* 55, 323–326. doi: 10.1016/j.biopsych.2003.10.022

Belachew, S., Rogister, B., Rigo, J. M., Malgrange, B., and Moonen, G. (1999). Neurotransmitter-mediated regulation of CNS myelination: a review. *Acta Neurol. Belg.* 99, 21–31.

Belmonte, M. K., Cook, E. H. Jr., Anderson, G. M., Rubenstein, J. L., Greenough, W. T., Beckel-Mitchener, A., et al. (2004). Autism as a disorder of neural information processing: directions for research and targets for therapy. *Mol. Psychiatry* 9, 646–663. doi: 10.1038/sj.mp.4001499

Boison, D., Chen, J. F., and Fredholm, B. B. (2010). Adenosine signalling and function in glial cells. *Cell Death Differ.* 17, 1071–1082. doi: 10.1038/cdd.2009.131

Boison, D., and Shen, H. Y. (2010). Adenosine kinase is a new therapeutic target to prevent ischemic neuronal death. *Open Drug Discov. J.* 2, 108–118.

Bolton, P. F., Roobol, M., Allsopp, L., and Pickles, A. (2001). Association between idiopathic infantile macrocephaly and autism spectrum disorders. *Lancet* 358, 726–727. doi: 10.1016/S0140-6736(01)05903-7

Bongarzone, E. R., Howard, S. G., Schonmann, V., and Campagnoni, A. T. (1998). Identification of the dopamine D3 receptor in oligodendrocyte precursors: potential role in regulating differentiation and myelin formation. *J. Neurosci.* 18, 5344–5353. doi: 10.1523/JNEUROSCI.18-14-05344.1998

Borea, P. A., Gessi, S., Merighi, S., and Varani, K. (2016). Adenosine as a multi-signalling guardian angel in human diseases: When, Where and How Does it Exert its Protective Effects? *Trends Pharmacol. Sci.* 37, 419–434. doi: 10.1016/j.tips.2016.02.006

Bottini, N., De Luca, D., Saccucci, P., Fiumara, A., Elia, M., Porfirio, M. C., et al. (2001). Autism: evidence of association with adenosine deaminase genetic polymorphism. *Neurogenetics* 3, 111–113. doi: 10.1007/s100480000104

Broch, O. J., and Ueland, P. M. (1980). Regional and subcellular distribution of S-adenosylhomocysteine hydrolase in the adult rat brain. *J. Neurochem.* 35, 484–488. doi: 10.1111/j.1471-4159.1980.tb06291.x

Burnstock, G., Fredholm, B. B., and Verkhratsky, A. (2011a). Adenosine and ATP receptors in the brain. *Curr. Top. Med. Chem.* 11, 973–1011. doi: 10.2174/156802611795347627

Burnstock, G., Krugel, U., Abbracchio, M. P., and Illes, P. (2011b). Purinergic signalling: from normal behaviour to pathological brain function. *Prog. Neurobiol.* 95, 229–274. doi: 10.1016/j.pneurobio.2011.08.006

Campbell, N. G., Zhu, C. B., Lindler, K. M., Yaspan, B. L., Kistner-Griffin, E., Consortium, N. A., et al. (2013). Rare coding variants of the adenosine A3 receptor are increased in autism: on the trail of the serotonin transporter regulome. *Mol. Autism* 4:28. doi: 10.1186/2040-2392-4-28

Carmody, D. P., and Lewis, M. (2010). Regional white matter development in children with autism spectrum disorders. *Dev. Psychobiol.* 52, 755–763. doi: 10.1002/dev.20471

Cass, C. E., Young, J. D., Baldwin, S. A., Cabrita, M. A., Graham, K. A., Griffiths, M., et al. (1999). Nucleoside transporters of mammalian cells. *Pharm. Biotechnol.* 12, 313–352. doi: 10.1007/0-306-46812-3_12

Chen, J. A., Penagarikano, O., Belgard, T. G., Swarup, V., and Geschwind, D. H. (2015). The emerging picture of autism spectrum disorder: genetics and pathology. *Annu. Rev. Pathol.* 10, 111–144. doi: 10.1146/annurev-pathol-012414-040405

Chen, J. F., Eltzschig, H. K., and Fredholm, B. B. (2013). Adenosine receptors as drug targets–what are the challenges? *Nat. Rev. Drug Discov.* 12, 265–286. doi: 10.1038/nrd3955

Chez, M. G., Burton, Q., Dowling, T., Chang, M., Khanna, P., and Kramer, C. (2007). Memantine as adjunctive therapy in children diagnosed with autistic spectrum disorders: an observation of initial clinical response and maintenance tolerability. *J. Child Neurol.* 22, 574–579. doi: 10.1177/0883073807302611

Cook, E. H. (1990). Autism: review of neurochemical investigation. *Synapse* 6, 292–308. doi: 10.1002/syn.890060309

Coppi, E., Cellai, L., Maraula, G., Pugliese, A. M., and Pedata, F. (2013). Adenosine A(2)A receptors inhibit delayed rectifier potassium currents and cell differentiation in primary purified oligodendrocyte cultures. *Neuropharmacology* 73, 301–310. doi: 10.1016/j.neuropharm.2013.05.035

Courchesne, E. (2004). Brain development in autism: early overgrowth followed by premature arrest of growth. *Ment. Retard. Dev. Disabil. Res. Rev.* 10, 106–111. doi: 10.1002/mrdd.20020

Cunha, R. A. (2001). Adenosine as a neuromodulator and as a homeostatic regulator in the nervous system: different roles, different sources and different receptors. *Neurochem. Int.* 38, 107–125. doi: 10.1016/S0197-0186(00)00034-6

Cunha, R. A., Constantino, M. C., Sebastiao, A. M., and Ribeiro, J. A. (1995a). Modification of A1 and A2a adenosine receptor binding in aged striatum, hippocampus and cortex of the rat. *Neuroreport* 6, 1583–1588.

Cunha, R. A., Johansson, B., Fredholm, B. B., Ribeiro, J. A., and Sebastiao, A. M. (1995b). Adenosine A2A receptors stimulate acetylcholine release from nerve terminals of the rat hippocampus. *Neurosci. Lett.* 196, 41–44.

Dare, E., Schulte, G., Karovic, O., Hammarberg, C., and Fredholm, B. B. (2007). Modulation of glial cell functions by adenosine receptors. *Physiol. Behav.* 92, 15–20. doi: 10.1016/j.physbeh.2007.05.031

Deoni, S. C., Zinkstok, J. R., Daly, E., Ecker, C., Williams, S. C., and Murphy, D. G. (2015). White-matter relaxation time and myelin water fraction differences in young adults with autism. *Psychol. Med.* 45, 795–805. doi: 10.1017/S0033291714001858

Dixon, A. K., Widdowson, L., and Richardson, P. J. (1997). Desensitisation of the adenosine A1 receptor by the A2A receptor in the rat striatum. *J. Neurochem.* 69, 315–321. doi: 10.1046/j.1471-4159.1997.69010315.x

Dunwiddie, T. V., and Masino, S. A. (2001). The role and regulation of adenosine in the central nervous system. *Annu. Rev. Neurosci.* 24, 31–55. doi: 10.1146/annurev.neuro.24.1.31

Ferre, S., Ciruela, F., Canals, M., Marcellino, D., Burgueno, J., Casado, V., et al. (2004). Adenosine A2A-dopamine D2 receptor-receptor heteromers. Targets for neuro-psychiatric disorders. *Parkinsonism Relat. Disord.* 10, 265–271. doi: 10.1016/j.parkreldis.2004.02.014

Ferre, S., Herrera-Marschitz, M., Grabowska-Anden, M., Ungerstedt, U., Casas, M., and Anden, N. E. (1991). Postsynaptic dopamine/adenosine interaction: I. Adenosine analogues inhibit dopamine D2-mediated behaviour in short-term reserpinized mice. *Eur. J. Pharmacol.* 192, 25–30. doi: 10.1016/0014-2999(91)90064-W

Fields, R. D. (2006). Nerve impulses regulate myelination through purinergic signalling. *Novartis Found. Symp.* 276, 148–158; discussion 158-161, 233–237, 275–281. doi: 10.1002/9780470032244.ch12

Fogal, B., McClaskey, C., Yan, S., Yan, H., and Rivkees, S. A. (2010). Diazoxide promotes oligodendrocyte precursor cell proliferation and myelination. *PLoS One* 5:e10906. doi: 10.1371/journal.pone.0010906

Fombonne, E., Roge, B., Claverie, J., Courty, S., and Fremolle, J. (1999). Microcephaly and macrocephaly in autism. *J. Autism Dev. Disord.* 29, 113–119. doi: 10.1023/A:1023036509476

Fredholm, B. B., Chen, J. F., Cunha, R. A., Svenningsson, P., and Vaugeois, J. M. (2005a). Adenosine and brain function. *Int. Rev. Neurobiol.* 63, 191–270. doi: 10.1016/S0074-7742(05)63007-3

Fredholm, B. B., Chen, J. F., Masino, S. A., and Vaugeois, J. M. (2005b). Actions of adenosine at its receptors in the CNS: insights from knockouts and drugs. *Annu. Rev. Pharmacol. Toxicol.* 45, 385–412.

Fredholm, B. B., and Dunwiddie, T. V. (1988). How does adenosine inhibit transmitter release? *Trends Pharmacol. Sci.* 9, 130–134. doi: 10.1016/0165-6147(88)90194-0

Freitag, C. M., Agelopoulos, K., Huy, E., Rothermundt, M., Krakowitzky, P., Meyer, J., et al. (2010). Adenosine A(2A) receptor gene (ADORA2A) variants may increase autistic symptoms and anxiety in autism spectrum disorder. *Eur. Child Adolesc. Psychiatry* 19, 67–74. doi: 10.1007/s00787-009-0043-6

Genovese, T., Melani, A., Esposito, E., Mazzon, E., Di Paola, R., Bramanti, P., et al. (2009). The selective adenosine A2A receptor agonist CGS 21680 reduces JNK MAPK activation in oligodendrocytes in injured spinal cord. *Shock* 32, 578–585. doi: 10.1097/SHK.0b013e3181a20792

Ginsberg, M. R., Rubin, R. A., Falcone, T., Ting, A. H., and Natowicz, M. R. (2012). Brain transcriptional and epigenetic associations with autism. *PLoS One* 7:e44736. doi: 10.1371/journal.pone.0044736

Gonzalez-Fernandez, E., Sanchez-Gomez, M. V., Perez-Samartin, A., Arellano, R. O., and Matute, C. (2014). A3 Adenosine receptors mediate oligodendrocyte death and ischemic damage to optic nerve. *Glia* 62, 199–216. doi: 10.1002/glia.22599

Gorter, J. A., van Vliet, E. A., Lopes da Silva, F. H., Isom, L. L., and Aronica, E. (2002). Sodium channel beta1-subunit expression is increased in reactive astrocytes in a rat model for mesial temporal lobe epilepsy. *Eur. J. Neurosci.* 16, 360–364. doi: 10.1046/j.1460-9568.2002.02078.x

Gray, J. H., Owen, R. P., and Giacomini, K. M. (2004). The concentrative nucleoside transporter family, SLC28. *Pflugers Arch.* 447, 728–734. doi: 10.1007/s00424-003-1107-y

Gu, J. G., Foga, I. O., Parkinson, F. E., and Geiger, J. D. (1995). Involvement of bidirectional adenosine transporters in the release of L-(3H)adenosine from rat brain synaptosomal preparations. *J. Neurochem.* 64, 2105–2110. doi: 10.1046/j.1471-4159.1995.64052105.x

Hamilton, N. B., Clarke, L. E., Arancibia-Carcamo, I. L., Kougioumtzidou, E., Matthey, M., Karadottir, R., et al. (2017). Endogenous GABA controls oligodendrocyte lineage cell number, myelination, and CNS internode length. *Glia* 65, 309–321. doi: 10.1002/glia.23093

Haselkorn, M. L., Shellington, D. K., Jackson, E. K., Vagni, V. A., Janesko-Feldman, K., Dubey, R. K., et al. (2010). Adenosine A1 receptor activation as a brake on the microglial response after experimental traumatic brain injury in mice. *J. Neurotrauma* 27, 901–910. doi: 10.1089/neu.2009.1075

Hasko, G., and Pacher, P. (2008). A2A receptors in inflammation and injury: lessons learned from transgenic animals. *J. Leukoc. Biol.* 83, 447–455. doi: 10.1189/jlb.0607359

Hazlett, H. C., Poe, M., Gerig, G., Smith, R. G., Provenzale, J., Ross, A., et al. (2005). Magnetic resonance imaging and head circumference study of brain size in autism: birth through age 2 years. *Arch. Gen. Psychiatry* 62, 1366–1376. doi: 10.1001/archpsyc.62.12.1366

Hellings, J. A., Arnold, L. E., and Han, J. C. (2017). Dopamine antagonists for treatment resistance in autism spectrum disorders: review and focus on BDNF stimulators loxapine and amitriptyline. *Expert Opin. Pharmacother.* 18, 581–588. doi: 10.1080/14656566.2017.1308483

Hettinger, J. A., Liu, X., and Holden, J. J. (2008). The G22A polymorphism of the ADA gene and susceptibility to autism spectrum disorders. *J. Autism Dev. Disord.* 38, 14–19. doi: 10.1007/s10803-006-0354-0

Imamura, O., Arai, M., Dateki, M., Ogata, T., Uchida, R., Tomoda, H., et al. (2015). Nicotinic acetylcholine receptors mediate donepezil-induced oligodendrocyte differentiation. *J. Neurochem.* 135, 1086–1098. doi: 10.1111/jnc.13294

Ingwersen, J., Wingerath, B., Graf, J., Lepka, K., Hofrichter, M., Schroter, F., et al. (2016). Dual roles of the adenosine A2a receptor in autoimmune neuroinflammation. *J. Neuroinflammation* 13:48. doi: 10.1186/s12974-016-0512-z

Johnston, J. B., Silva, C., Gonzalez, G., Holden, J., Warren, K. G., Metz, L. M., et al. (2001). Diminished adenosine A1 receptor expression on macrophages in brain and blood of patients with multiple sclerosis. *Ann. Neurol.* 49, 650–658. doi: 10.1002/ana.1007

Karadottir, R., and Attwell, D. (2007). Neurotransmitter receptors in the life and death of oligodendrocytes. *Neuroscience* 145, 1426–1438. doi: 10.1016/j.neuroscience.2006.08.070

Karadottir, R., Cavelier, P., Bergersen, L. H., and Attwell, D. (2005). NMDA receptors are expressed in oligodendrocytes and activated in ischaemia. *Nature* 438, 1162–1166. doi: 10.1038/nature04302

Kiese, K., Jablonski, J., Boison, D., and Kobow, K. (2016). Dynamic regulation of the adenosine kinase gene during early postnatal brain development and maturation. *Front. Mol. Neurosci.* 9:99. doi: 10.3389/fnmol.2016.00099

Kirk, I. P., and Richardson, P. J. (1994). Adenosine A2a receptor-mediated modulation of striatal [3H]GABA and [3H]acetylcholine release. *J. Neurochem.* 62, 960–966. doi: 10.1046/j.1471-4159.1994.62030960.x

Kirkpatrick, K. A., and Richardson, P. J. (1993). Adenosine receptor-mediated modulation of acetylcholine release from rat striatal synaptosomes. *Br. J. Pharmacol.* 110, 949–954. doi: 10.1111/j.1476-5381.1993.tb13905.x

Kolodziejczyk, K., Hamilton, N. B., Wade, A., Karadottir, R., and Attwell, D. (2009). The effect of N-acetyl-aspartyl-glutamate and N-acetyl-aspartate on white matter oligodendrocytes. *Brain* 132(Pt 6), 1496–1508. doi: 10.1093/brain/awp087

Latini, S., Pazzagli, M., Pepeu, G., and Pedata, F. (1996). A2 adenosine receptors: their presence and neuromodulatory role in the central nervous system. *Gen. Pharmacol.* 27, 925–933. doi: 10.1016/0306-3623(96)00044-4

Latini, S., and Pedata, F. (2001). Adenosine in the central nervous system: release mechanisms and extracellular concentrations. *J. Neurochem.* 79, 463–484. doi: 10.1046/j.1471-4159.2001.00607.x

Lazarus, M., Shen, H. Y., Cherasse, Y., Qu, W. M., Huang, Z. L., Bass, C., et al. (2011). Arousal effect of caffeine depends on adenosine A2A receptors in the shell of the nucleus accumbens. *J. Neurosci.* 31, 10067–10075. doi: 10.1523/JNEUROSCI.6730-10.2011

Lee, Y., Kim, H., Kim, J. E., Park, J. Y., Choi, J., Lee, J. E., et al. (2018). Excessive D1 dopamine receptor activation in the dorsal striatum promotes autistic-like behaviors. *Mol. Neurobiol.* 55, 5658–5671. doi: 10.1007/s12035-017-0770-5

Lindahl, J. S., Kjellsen, B. R., Tigert, J., and Miskimins, R. (2008). In utero PCP exposure alters oligodendrocyte differentiation and myelination in developing rat frontal cortex. *Brain Res.* 1234, 137–147. doi: 10.1016/j.brainres.2008.06.126

Liu, Y., Alahiri, M., Ulloa, B., Xie, B., and Sadiq, S. A. (2018). Adenosine A2A receptor agonist ameliorates EAE and correlates with Th1 cytokine-induced blood brain barrier dysfunction via suppression of MLCK signaling pathway. *Immun. Inflamm. Dis.* 6, 72–80. doi: 10.1002/iid3.187

Lopes, L. V., Cunha, R. A., and Ribeiro, J. A. (1999). Cross talk between A(1) and A(2A) adenosine receptors in the hippocampus and cortex of young adult and old rats. *J. Neurophysiol.* 82, 3196–3203. doi: 10.1152/jn.1999.82.6.3196

Lopez-Cruz, L., Carbo-Gas, M., Pardo, M., Bayarri, P., Valverde, O., Ledent, C., et al. (2017). Adenosine A2A receptor deletion affects social behaviors and anxiety in mice: Involvement of anterior cingulate cortex and amygdala. *Behav. Brain Res.* 321, 8–17. doi: 10.1016/j.bbr.2016.12.020

Masino, S. A., Kawamura, M. Jr., Cote, J. L., Williams, R. B., and Ruskin, D. N. (2013). Adenosine and autism: a spectrum of opportunities. *Neuropharmacology* 68, 116–121. doi: 10.1016/j.neuropharm.2012.08.013

Masino, S. A., Kawamura, M. Jr., Plotkin, L. M., Svedova, J., DiMario, F. J. Jr., and Eigsti, I. M. (2011). The relationship between the neuromodulator adenosine and behavioral symptoms of autism. *Neurosci. Lett.* 500, 1–5. doi: 10.1016/j.neulet.2011.06.007

Masino, S. A., Kawamura, M., Wasser, C. A., Pomeroy, L. T., and Ruskin, D. N. (2009). Adenosine, ketogenic diet and epilepsy: the emerging therapeutic relationship between metabolism and brain activity. *Curr. Neuropharmacol.* 7, 257–268. doi: 10.2174/157015909789152164

Matos, M., Augusto, E., Agostinho, P., Cunha, R. A., and Chen, J. F. (2013). Antagonistic interaction between adenosine A2A receptors and Na+/K+-ATPase-alpha2 controlling glutamate uptake in astrocytes. *J. Neurosci.* 33, 18492–18502. doi: 10.1523/JNEUROSCI.1828-13.2013

Matos, M., Shen, H. Y., Augusto, E., Wang, Y., Wei, C. J., Wang, Y. T., et al. (2015). Deletion of adenosine A2A receptors from astrocytes disrupts glutamate

homeostasis leading to psychomotor and cognitive impairment: relevance to schizophrenia. *Biol. Psychiatry* 78, 763–774. doi: 10.1016/j.biopsych.2015.02.026

Matson, J. L., Sipes, M., Fodstad, J. C., and Fitzgerald, M. E. (2011). Issues in the management of challenging behaviours of adults with autism spectrum disorder. *CNS Drugs* 25, 597–606. doi: 10.2165/11591700-000000000-00000

Matute, C., Alberdi, E., Domercq, M., Perez-Cerda, F., Perez-Samartin, A., and Sanchez-Gomez, M. V. (2001). The link between excitotoxic oligodendroglial death and demyelinating diseases. *Trends Neurosci.* 24, 224–230. doi: 10.1016/S0166-2236(00)01746-X

Mayne, M., Fotheringham, J., Yan, H. J., Power, C., Del Bigio, M. R., Peeling, J., et al. (2001). Adenosine A2A receptor activation reduces proinflammatory events and decreases cell death following intracerebral hemorrhage. *Ann. Neurol.* 49, 727–735. doi: 10.1002/ana.1010

Mei, F., Lehmann-Horn, K., Shen, Y. A., Rankin, K. A., Stebbins, K. J., Lorrain, D. S., et al. (2016a). Accelerated remyelination during inflammatory demyelination prevents axonal loss and improves functional recovery. *Elife* 5:e18246. doi: 10.7554/eLife.18246

Mei, F., Mayoral, S. R., Nobuta, H., Wang, F., Desponts, C., Lorrain, D. S., et al. (2016b). Identification of the kappa-opioid receptor as a therapeutic target for oligodendrocyte remyelination. *J. Neurosci.* 36, 7925–7935. doi: 10.1523/JNEUROSCI.1493-16.2016

Mills, J. H., Thompson, L. F., Mueller, C., Waickman, A. T., Jalkanen, S., Niemela, J., et al. (2008). CD73 is required for efficient entry of lymphocytes into the central nervous system during experimental autoimmune encephalomyelitis. *Proc. Natl. Acad. Sci. U.S.A.* 105, 9325–9330. doi: 10.1073/pnas.0711175105

Mizuno, A., Villalobos, M. E., Davies, M. M., Dahl, B. C., and Muller, R. A. (2006). Partially enhanced thalamocortical functional connectivity in autism. *Brain Res.* 1104, 160–174. doi: 10.1016/j.brainres.2006.05.064

Murray, M. L., Hsia, Y., Glaser, K., Simonoff, E., Murphy, D. G., Asherson, P. J., et al. (2014). Pharmacological treatments prescribed to people with autism spectrum disorder (ASD) in primary health care. *Psychopharmacology* 231, 1011–1021. doi: 10.1007/s00213-013-3140-7

Noonan, S. K., Haist, F., and Muller, R. A. (2009). Aberrant functional connectivity in autism: evidence from low-frequency BOLD signal fluctuations. *Brain Res.* 1262, 48–63. doi: 10.1016/j.brainres.2008.12.076

O'Kane, E. M., and Stone, T. W. (1998). Interaction between adenosine A1 and A2 receptor-mediated responses in the rat hippocampus in vitro. *Eur. J. Pharmacol.* 362, 17–25. doi: 10.1016/S0014-2999(98)00730-4

Othman, T., Yan, H., and Rivkees, S. A. (2003). Oligodendrocytes express functional A1 adenosine receptors that stimulate cellular migration. *Glia* 44, 166–172. doi: 10.1002/glia.10281

Owley, T., Salt, J., Guter, S., Grieve, A., Walton, L., Ayuyao, N., et al. (2006). A prospective, open-label trial of memantine in the treatment of cognitive, behavioral, and memory dysfunction in pervasive developmental disorders. *J. Child Adolesc. Psychopharmacol.* 16, 517–524. doi: 10.1089/cap.2006.16.517

Pak, M. A., Haas, H. L., Decking, U. K. M., and Schrader, J. (1994). Inhibition of adenosine kinase increases endogenous adenosine and depresses neuronal activity in hippocampal slices. *Neuropharmacology* 33, 1049–1053. doi: 10.1016/0028-3908(94)90142-2

Paterniti, I., Melani, A., Cipriani, S., Corti, F., Mello, T., Mazzon, E., et al. (2011). Selective adenosine A2A receptor agonists and antagonists protect against spinal cord injury through peripheral and central effects. *J. Neuroinflammation* 8:31. doi: 10.1186/1742-2094-8-31

Paval, D. (2017). A dopamine hypothesis of autism spectrum disorder. *Dev. Neurosci.* 39, 355–360. doi: 10.1159/000478725

Richetto, J., Chesters, R., Cattaneo, A., Labouesse, M. A., Gutierrez, A. M. C., Wood, T. C., et al. (2017). Genome-wide transcriptional profiling and structural magnetic resonance imaging in the maternal immune activation model of neurodevelopmental disorders. *Cereb. Cortex* 27, 3397–3413. doi: 10.1093/cercor/bhw320

Safarzadeh, E., Jadidi-Niaragh, F., Motallebnezhad, M., and Yousefi, M. (2016). The role of adenosine and adenosine receptors in the immunopathogenesis of multiple sclerosis. *Inflamm. Res.* 65, 511–520. doi: 10.1007/s00011-016-0936-z

Schubert, P., Komp, W., and Kreutzberg, G. W. (1979). Correlation of 5'-nucleotidase activity and selective transneuronal transfer of adenosine in the hippocampus. *Brain Res.* 168, 419–424. doi: 10.1016/0006-8993(79)90186-0

Sebastiao, A. M., and Ribeiro, J. A. (1996). Adenosine A2 receptor-mediated excitatory actions on the nervous system. *Prog. Neurobiol.* 48, 167–189. doi: 10.1016/0301-0082(95)00035-6

Sebastiao, A. M., and Ribeiro, J. A. (2000). Fine-tuning neuromodulation by adenosine. *Trends Pharmacol. Sci.* 21, 341–346. doi: 10.1016/S0165-6147(00)01517-0

Sebastiao, A. M., and Ribeiro, J. A. (2009). Adenosine receptors and the central nervous system. *Handb. Exp. Pharmacol.* 193, 471–534. doi: 10.1007/978-3-540-89615-9_16

Seeman, P. (2010). Dopamine D2 receptors as treatment targets in schizophrenia. *Clin. Schizophr. Relat. Psychoses* 4, 56–73. doi: 10.3371/CSRP.4.1.5

Setzu, A., Ffrench-Constant, C., and Franklin, R. J. (2004). CNS axons retain their competence for myelination throughout life. *Glia* 45, 307–311. doi: 10.1002/glia.10321

Setzu, A., Lathia, J. D., Zhao, C., Wells, K., Rao, M. S., Ffrench-Constant, C., et al. (2006). Inflammation stimulates myelination by transplanted oligodendrocyte precursor cells. *Glia* 54, 297–303. doi: 10.1002/glia.20371

Shen, H. Y., Canas, P. M., Garcia-Sanz, P., Lan, J. Q., Boison, D., Moratalla, R., et al. (2013). Adenosine A2A receptors in striatal glutamatergic terminals and GABAergic neurons oppositely modulate psychostimulant action and DARPP-32 phosphorylation. *PLoS One* 8:e80902. doi: 10.1371/journal.pone.0080902

Shen, H. Y., and Chen, J. F. (2009). Adenosine A2A receptors in psychopharmacology: modulators of bahavior, mood, and cognition. *Curr. Neuropharmacol.* 7, 195–206. doi: 10.2174/157015909789152191

Shen, H. Y., Coelho, J. E., Ohtsuka, N., Canas, P. M., Day, Y. J., Huang, Q. Y., et al. (2008). A critical role of the adenosine A2A receptor in extrastriatal neurons in modulating psychomotor activity as revealed by opposite phenotypes of striatum and forebrain A2A receptor knock-outs. *J. Neurosci.* 28, 2970–2975. doi: 10.1523/JNEUROSCI.5255-07.2008

Shen, H. Y., Singer, P., Lytle, N., Wei, C. J., Lan, J. Q., Williams-Karnesky, R. L., et al. (2012). Adenosine augmentation ameliorates psychotic and cognitive endophenotypes of schizophrenia. *J. Clin. Invest.* 122, 2567–2577. doi: 10.1172/JCI62378

Shih, P., Shen, M., Ottl, B., Keehn, B., Gaffrey, M. S., and Muller, R. A. (2010). Atypical network connectivity for imitation in autism spectrum disorder. *Neuropsychologia* 48, 2931–2939. doi: 10.1016/j.neuropsychologia.2010.05.035

Si, Q. S., Nakamura, Y., Schubert, P., Rudolphi, K., and Kataoka, K. (1996). Adenosine and propentofylline inhibit the proliferation of cultured microglial cells. *Exp. Neurol.* 137, 345–349. doi: 10.1006/exnr.1996.0035

Sitkovsky, M. V., Lukashev, D., Apasov, S., Kojima, H., Koshiba, M., Caldwell, C., et al. (2004). Physiological control of immune response and inflammatory tissue damage by hypoxia-inducible factors and adenosine A2A receptors. *Annu. Rev. Immunol.* 22, 657–682. doi: 10.1146/annurev.immunol.22.012703.104731

Snyder, S. H. (1985). Adenosine as a neuromodulator. *Annu. Rev. Neurosci.* 8, 103–124. doi: 10.1146/annurev.ne.08.030185.000535

Sperlagh, B., and Vizi, E. S. (2011). The role of extracellular adenosine in chemical neurotransmission in the hippocampus and Basal Ganglia: pharmacological and clinical aspects. *Curr. Top. Med. Chem.* 11, 1034–1046. doi: 10.2174/156802611795347564

Stevens, B., Porta, S., Haak, L. L., Gallo, V., and Fields, R. D. (2002). Adenosine: a neuron-glial transmitter promoting myelination in the CNS in response to action potentials. *Neuron* 36, 855–868. doi: 10.1016/S0896-6273(02)01067-X

Stolerman, E. S., Smith, B., Chaubey, A., and Jones, J. R. (2016). CHD8 intragenic deletion associated with autism spectrum disorder. *Eur. J. Med. Genet.* 59, 189–194. doi: 10.1016/j.ejmg.2016.02.010

Stubbs, G., Litt, M., Lis, E., Jackson, R., Voth, W., Lindberg, A., et al. (1982). Adenosine deaminase activity decreased in autism. *J. Am. Acad. Child Psychiatry* 21, 71–74. doi: 10.1097/00004583-198201000-00012

Tanimura, Y., Vaziri, S., and Lewis, M. H. (2010). Indirect basal ganglia pathway mediation of repetitive behavior: attenuation by adenosine receptor agonists. *Behav. Brain Res.* 210, 116–122. doi: 10.1016/j.bbr.2010.02.030

Tsutsui, S., Schnermann, J., Noorbakhsh, F., Henry, S., Yong, V. W., Winston, B. W., et al. (2004). A1 adenosine receptor upregulation and activation attenuates neuroinflammation and demyelination in a model of multiple sclerosis. *J. Neurosci.* 24, 1521–1529. doi: 10.1523/JNEUROSCI.4271-03.2004

Turner, C. P., Yan, H., Schwartz, M., Othman, T., and Rivkees, S. A. (2002). A1 adenosine receptor activation induces ventriculomegaly and white matter loss. *Neuroreport* 13, 1199–1204. doi: 10.1097/00001756-200207020-00026

Turner, K. C., Frost, L., Linsenbardt, D., McIlroy, J. R., and Muller, R. A. (2006). Atypically diffuse functional connectivity between caudate nuclei and cerebral cortex in autism. *Behav. Brain Funct.* 2:34.

Vincenzi, F., Corciulo, C., Targa, M., Merighi, S., Gessi, S., Casetta, I., et al. (2013). Multiple sclerosis lymphocytes upregulate A2A adenosine receptors that are antiinflammatory when stimulated. *Eur. J. Immunol.* 3, 2206–2216. doi: 10.1002/eji.201343314

Wegiel, J., Kuchna, I., Nowicki, K., Imaki, H., Marchi, E., Ma, S. Y., et al. (2010). The neuropathology of autism: defects of neurogenesis and neuronal migration, and dysplastic changes. *Acta Neuropathol.* 119, 755–770. doi: 10.1007/s00401-010-0655-4

Wei, W., Du, C., Lv, J., Zhao, G., Li, Z., Wu, Z., et al. (2013). Blocking A2B adenosine receptor alleviates pathogenesis of experimental autoimmune encephalomyelitis via inhibition of IL-6 production and Th17 differentiation. *J. Immunol.* 190, 138–146. doi: 10.4049/jimmunol.1103721

Yao, S. Q., Li, Z. Z., Huang, Q. Y., Li, F., Wang, Z. W., Augusto, E., et al. (2012). Genetic inactivation of the adenosine A(2A) receptor exacerbates brain damage in mice with experimental autoimmune encephalomyelitis. *J. Neurochem.* 123, 100–112. doi: 10.1111/j.1471-4159.2012.07807.x

Zhao, C., Dong, C., Frah, M., Deng, Y., Marie, C., Zhang, F., et al. (2018). Dual requirement of CHD8 for chromatin landscape establishment and histone methyltransferase recruitment to promote CNS myelination and repair. *Dev. Cell* 45, 753–768.e8. doi: 10.1016/j.devcel.2018.05.022

Zhu, C. B., Lindler, K. M., Campbell, N. G., Sutcliffe, J. S., Hewlett, W. A., and Blakely, R. D. (2011). Colocalization and regulated physical association of presynaptic serotonin transporters with A(3) adenosine receptors. *Mol. Pharmacol.* 80, 458–465. doi: 10.1124/mol.111.071399

Conflict of Interest Statement: The authors declare that the research was conducted in the absence of any commercial or financial relationships that could be construed as a potential conflict of interest.

frontiers in Cellular Neuroscience

ORIGINAL RESEARCH
published: 11 January 2019
doi: 10.3389/fncel.2018.00517

Hypomyelination and Oligodendroglial Alterations in a Mouse Model of Autism Spectrum Disorder

Mariana Graciarena[1,2,3]*, *Araceli Seiffe*[2,3], *Brahim Nait-Oumesmar*[1†] *and Amaicha M. Depino*[2,3†]

[1]*Brain and Spine Institute, Inserm U1127, Sorbonne Universités/Université Pierre & Marie Curie UMRS 1127, CNRS UMR 7225, Paris, France,* [2]*Departamento de Fisiología, Biología Molecular y Celular, Facultad de Ciencias Exactas y Naturales, Universidad de Buenos Aires, Buenos Aires, Argentina,* [3]*Instituto de Fisiología, Biología Molecular y Neurociencias (IFIBYNE), CONICET-Universidad de Buenos Aires, Buenos Aires, Argentina*

Autism spectrum disorders (ASDs) are neuropsychiatric diseases characterized by impaired social interaction, communication deficits, and repetitive and stereotyped behaviors. ASD etiology is unknown, and both genetic and environmental causes have been proposed. Different brain structures are believed to play a role in ASD-related behaviors, including medial prefrontal cortex (mPFC), hippocampus, piriform cortex (Pir), basolateral amygdala (BLA) and Cerebellum. Compelling evidence suggests a link between white matter modifications and ASD symptoms in patients. Besides, an hypomyelination of the mPFC has been associated in rodents to social behavior impairment, one of the main symptoms of ASD. However, a comparative analysis of myelination as well as oligodendroglial (OL)-lineage cells in brain regions associated to social behaviors in animal models of ASD has not been performed so far. Here, we investigated whether OL-lineage cells and myelination are altered in a murine model of ASD induced by the prenatal exposure to valproic acid (VPA). We showed an hypomyelination in the BLA and Pir of adult VPA-exposed mice. These results were accompanied by a decrease in the number of OL-lineage cells and of mature OLs in the Pir, in addition to the mPFC, where myelination presented no alterations. In these regions the number of oligodendrocyte progenitors (OPCs) remained unaltered. Likewise, activation of histone deacetylases (HDACs) on OL-lineage cells in adulthood showed no differences. Overall, our results reveal OL-lineage cell alterations and hypomyelination as neuropathological hallmarks of ASD that have been overlooked so far.

Keywords: autism spectrum disorder, myelin, oligodendrocytes, valproic acid, mouse

OPEN ACCESS

Edited by:
Mauricio Antonio Retamal, Universidad del Desarrollo, Chile

Reviewed by:
Shan Huang, University of California, Los Angeles, United States
Elias Leiva-Salcedo, University of Santiago, Chile

***Correspondence:**
Mariana Graciarena
mari.graciarena@gmail.com

†These authors have contributed equally to this work and are co-senior authors

Received: *06 September 2018*
Accepted: *12 December 2018*
Published: *11 January 2019*

Citation:
Graciarena M, Seiffe A, Nait-Oumesmar B and Depino AM (2019) Hypomyelination and Oligodendroglial Alterations in a Mouse Model of Autism Spectrum Disorder. Front. Cell. Neurosci. 12:517. doi: 10.3389/fncel.2018.00517

INTRODUCTION

Autism spectrum disorders (ASDs) are a group of neurodevelopmental disorders characterized by impaired social interaction, communication deficits, and repetitive, stereotyped behaviors (American Psychiatric Association, 2013). These symptoms appear early in life and persist during adulthood. ASD etiology is unknown, and both genetic and environmental

factors can contribute to its development (Betancur, 2011). There are currently no treatments that can treat ASD symptoms altogether.

There is no current consensus about the underlying neuropathology in ASD, and different brain structures have been proposed to play a role in ASD symptoms. In humans, the medial prefrontal cortex (mPFC) was identified as one of the main brain areas whose connectivity is affected in ASD subjects (Cheng et al., 2015), while other areas also exhibit altered neuronal number or volume in people diagnosed with ASD, e.g., the basolateral amygdala (BLA; Lin et al., 2013; Wegiel et al., 2014), the Hippocampus (Sussman et al., 2015) and the cerebellum (Fatemi et al., 2012; Sussman et al., 2015).

Different animal models for ASD have been validated for studying the cellular and molecular alterations that lead to altered behavior in these disorders. In particular, prenatal exposure to valproic acid (VPA) results in reduced sociability and increased repetitive behaviors (Lucchina and Depino, 2014; Campolongo et al., 2018). In addition, other cellular and molecular alterations related to ASD are also observed in animals prenatally exposed to VPA, e.g., neuroinflammation (Lucchina and Depino, 2014), and altered excitation/inhibition balance (Cunningham et al., 2003). Finally, this animal model also shows alterations in neuronal function in a region recently involved in social behaviors, the Piriform cortex (Pir; Choe et al., 2015; Campolongo et al., 2018).

Increasing evidence links neuropsychiatric conditions with white matter alterations (Fields, 2008). Concerning ASD, white matter integrity and myelin thickness was found altered in the brains of ASD patients, particularly in the inter-hemispheric circuitry and in the corpus callosum (Travers et al., 2012; Ameis et al., 2016). Furthermore, a link between myelination of the mPFC and social exploration deficits has been described in mice (Liu et al., 2012; Makinodan et al., 2012).

Myelin, a multilamellar structure that ensheathes axons and allows for fast saltatory conduction of action potentials, is produced by oligodendrocytes (OLs) both during development and in adult life in vertebrates. Myelin has been recently shown to respond to and participate in the activity and fine-tuning of neuronal networks, which results in the modulation of speed and synchronicity of action potentials as well as provides metabolic support to axons (Pajevic et al., 2014; Filley and Fields, 2016). Moreover, oligodendrocyte progenitor cells (OPCs) are synaptically innervated by neuronal fibers throughout the central nervous system (Bergles et al., 2000; Fröhlich et al., 2011) thus constituting a potential mechanism for this bilateral communication.

Interestingly, *de novo* myelination continues throughout life (Bergles and Richardson, 2015), and it can contribute to adult neural plasticity, as the conduction properties of myelinated neuronal circuits may undergo important transformations. In this sense, myelin may play a key role in the neuronal circuit dysfunctions that occur in neuropsychiatric diseases such as ASD. However, a comparative analysis of the myelination status and OL differentiation in brain regions functionally related to ASD symptoms has not been attempted to date.

Here, we investigated whether myelination and OL-lineage cells were maintained in VPA-treated mice, a well-characterized ASD murine model that recapitulates the main aspects of this condition. Our data show long-term alterations in myelin content and in myelin-producing cells in the mPFC, BLA and Pir, three brain regions functionally associated with social behavior. These changes were not associated to H3 acetylation, an indicator of active DNA transcription, in adult OL-lineage population. Overall, these results constitute a fundamental characterization of myelin integrity in an ASD model, suggesting the potential contribution of a myelination deficit in this psychiatric condition.

MATERIALS AND METHODS

Animals

Outbred CrlFcen:CF1 mice were obtained from the animal house at the Faculty of Exact and Natural Sciences (FCEN), University of Buenos Aires (UBA, Argentina). Animals were housed on a 12:12 light:dark cycle and 18–22°C temperature, with food and water *ad libitum*. All animal procedures were performed according to the regulations for the use of laboratory animals of the National Institute of Health, Washington DC, USA, and approved by the Institutional Commission for Care and Use of Laboratory Animals (CICUAL Protocol No. 6/2, FCEN, UBA, Argentina). Eight-to-ten week old male mice were mated with nulliparous age matching female mice. Female mice were controlled daily for presence of vaginal plugs, and whenever present this day was considered the embryonic day (E) 0.5.

VPA Prenatal Treatment

On E12.5, pregnant mice were subcutaneously injected with 600 mg/kg of VPA sodium salt (Sigma, St. Louis, MO, USA) resuspended in saline solution or saline solution alone, and housed individually. The parturition day was registered as postnatal day 0 (PD0), and the cage bedding was not changed during the first postnatal week to avoid nest and maternal care alterations. We studied five male offspring animals per group for immunofluorescence and 3–4 male animals per group for electron microscopy (EM), obtained in two independent cohorts.

Social Interaction Test

At PD60, animals were evaluated in the social interaction test as previously described (Depino et al., 2011; Lucchina and Depino, 2014; Campolongo et al., 2018). Briefly, mice were habituated for 10 min to a 40 × 15 cm black rectangular arena divided in three interconnected chambers placed under dim light (10 lx). A clear Plexiglass cylinder (7.5 cm of diameter, with several holes to allow for auditory, visual, and olfactory investigation) was placed in each side compartment at the beginning of the test. Prior to the start of each test, one of the end chambers was randomly designated as the "non-social side" and the other as the "social side." Animals were placed in the central compartment and allowed to explore for 10 min (habituation). Then, an unfamiliar, young (3 weeks) CF1 male mouse (social stimulus) was placed in one of the cylinders (social side), and an object (plastic 3 cm-tall cylinder) was placed in the other cylinder (non-social side). Social interaction was evaluated during a 10 min

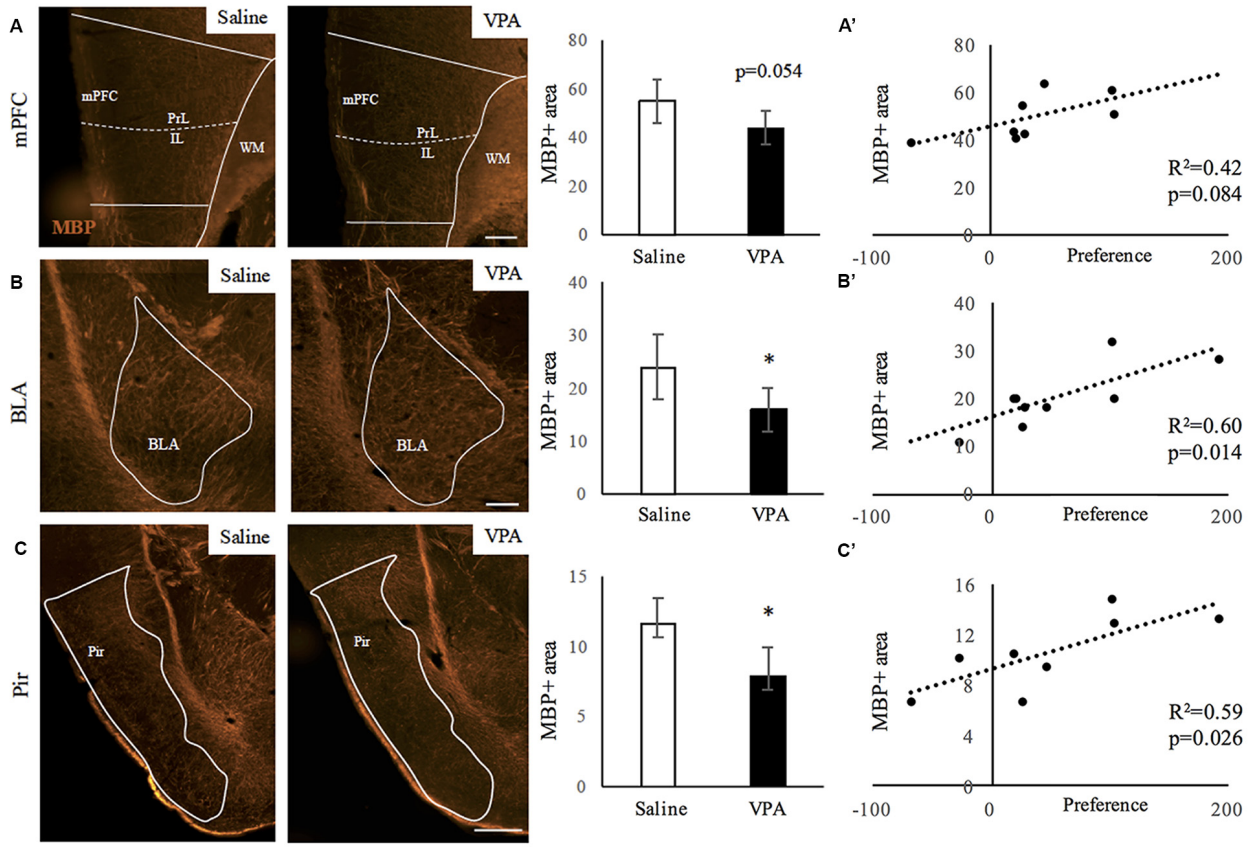

FIGURE 1 | Myelin content decreases upon valproic acid (VPA) treatment in brain areas linked to social behavior. **(A–C)** Myelin basic protein (MBP) immunostaining in saline- and VPA-treated adult mouse brains (representative images) and estimated percentage of positive surface in the following areas: **(A)** medial prefrontal cortex (mPFC; mean: saline: 55.01 ± 9.12; VPA: 44.17 ± 7.08; Student's *t*-test: $t = 1.878$, $p = 0.054$). **(B)** Basolateral amygdala (BLA; mean: saline: 23.89 ± 6.05; VPA: 16.01 ± 4.11; Student's *t*-test: $t = 2.211$, $p = 0.031$). **(C)** Piriform cortex (Pir; mean: saline: 11.60 ± 1.81; VPA: 7.92 ± 1.97; Student's *t*-test: $t = 2.845$, $p = 0.015$). $^*p < 0.05$ (Student's *t*-test). Scale bars: 100 μm. $N = 4$–5 mice/treatment. **(A'–C')** Correlation between preference for social stimulus and MBP positive area in mPFC **(A')**, BLA **(B')** and Pir **(C')**. Significance: $p < 0.05$ (Pearson correlation analysis).

period. The time the subject spent sniffing the social stimulus or the non-social stimulus (with the nose <1 cm distance to a hole of the cylinder) was recorded manually using the ANY-maze video-tracking system (Stoelting, IL, USA) by an experimenter blind to treatments. The entire apparatus was cleaned with a 20% ethanol solution between tests to eliminate odors.

The preference for the social stimulus was calculated as the difference between the time spent in the social side vs. the time spent in the non-social side.

Tissue Processing

At PD90, mice were deeply anesthetized with 80 mg/kg ketamine chlorhydrate and 8 mg/kg xylazine. Next, they were transcardially perfused with heparinized saline followed by cold 4% paraformaldehyde in 0.1 M phosphate buffer (PB) of pH 7.2. Brains were removed and postfixed in PFA at 4°C, then cryopreserved in a 30% sucrose solution in PB at 4°C until full immersion was observed. Subsequently, brains were frozen with isopentane and 30 μm coronal sections were obtained using a cryostat (Leica Biosystems, Nussloch, Germany), which were either used immediately for immunostaining or stored at −20°C in a cryopreservative solution.

Immunostaining

Free-floating immunostaining was performed as follows: briefly, every sixth coronal section was incubated in PB for 15 min. Sections were then incubated in blocking solution, 4% bovine serum albumin (BSA) in PB with 0.1% Triton X-100 for 45 min. Primary antibodies were diluted in the blocking solution and sections were incubated overnight at 4°C. On the following day sections were washed three times with 0.1 M PB and incubated in secondary antibodies diluted in 0.1 M PB for 2 h in the dark. Sections were then washed with 0.1 M PB and mounted in Fluoromount-G (Thermo Fisher Scientific, Waltham, MA, USA).

The primary antibodies used were anti-MBP; anti-myelin basic protein (AB980, Millipore, MA, USA), anti-Olig2 (AB9610, Millipore), anti-NG2 (AB5320, Millipore), anti-CC1 (OP80,

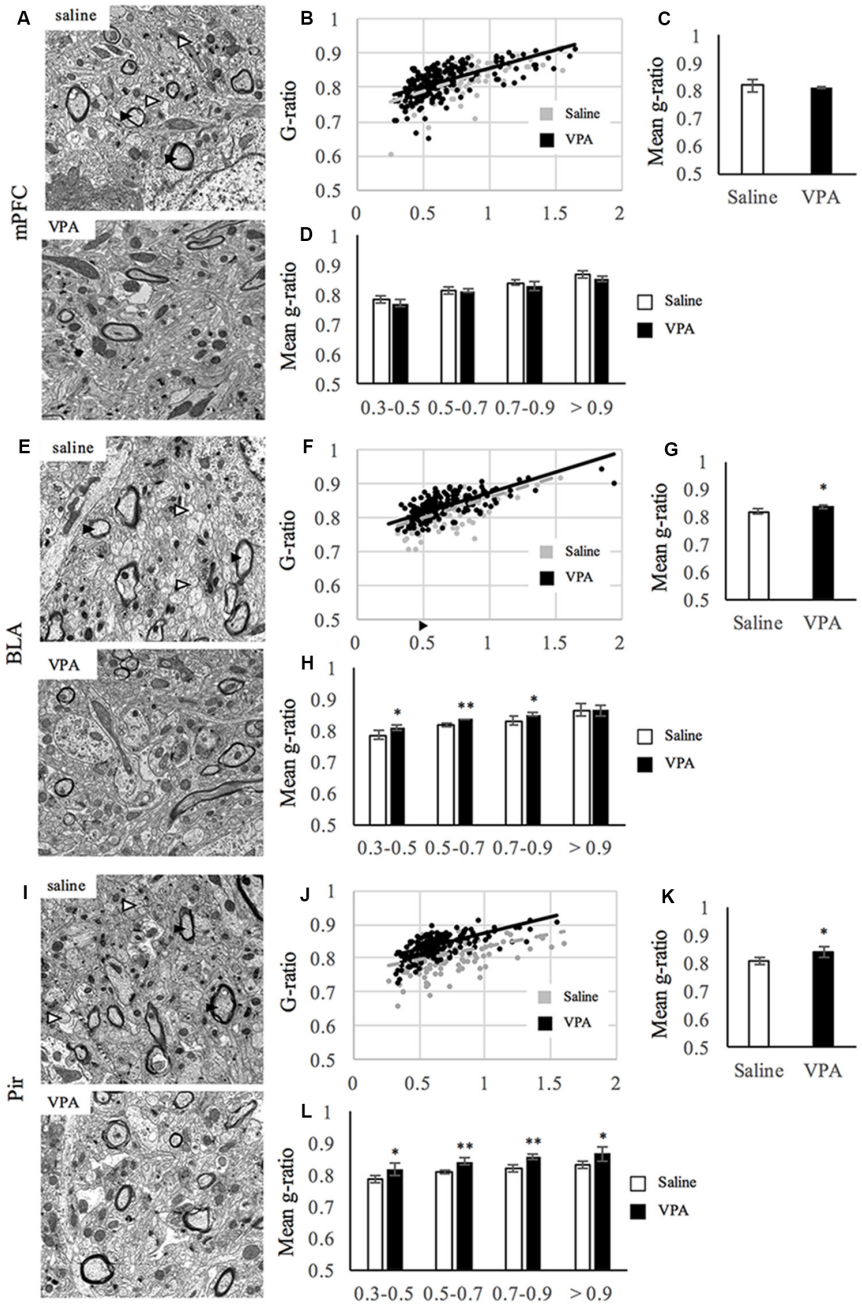

FIGURE 2 | Myelin thickness is impaired upon VPA treatment in brain areas linked to social behavior. **(A,E,I)** Representative electron micrographs of transversal sections from mPFC **(A)**, BLA **(E)**, Pir **(I)** of saline- and VPA treated animals. Arrowheads in the pictures of saline-treated groups show examples of myelinated (black) and unmyelinated (white) axons. **(B,F,J)** Dot plot of the G-ratio distribution along axonal diameters for saline- (gray) and VPA- (black) treated animals at the mPFC **(B)**, BLA **(F)** and Pir **(J)**. **(C,G,K)** Mean G-ratio at the mPFC (**C**; mean G-ratio: saline: 0.819 ± 0.012; VPA: 0.813 ± 0.001; Student's *t*-test: $t = 0.497$, $p = 0.645$), BLA (**G**; mean G-ratio: saline: 0.819 ± 0.004; VPA: 0.837 ± 0.004; Student's *t*-test: $t = 2.81$, $p = 0.0375$) and Pir (**K**; mean G-ratio: saline: 0.809 ± 0.003; VPA: 0.840 ± 0.0105; Student's *t*-test: $t = 2.8$, $p = 0.049$). **(D,H,L)** G-ratio values along ranges of axonal diameters at the mPFC [**D**; means: (0.3–0.5) saline: 0.787 ±0.012; VPA: 0.773 ± 0.011; Student's *t*-test: $t = 1.46$, $p = 0.109$; (0.5–0.7) saline: 0.815 ± 0.011; VPA: 0.814 ±0.005; Student's *t*-test: $t = 0.234$, $p = 0.413$ (0.7–0.9) saline: 0.843 ± 0.008; VPA: 0.830 ± 0.013; Student's *t*-test: $t = 1.38$, $p = 0.0119$ (>0.9) saline: 0.870 ± 0.013; VPA: 0.857 ± 0.008; Student's *t*-test: $t = 1.40$, $p = 0.117$], BLA [**H** (0.3–0.5) saline: 0.787 ± 0.016; VPA: 0.809 ± 0.006; Student's *t*-test: $t = -2.15$, $p = 0.042$ (0.5–0.7) saline: 0.819 ± 0.006; VPA: 0.836 ± 0.001; Student's *t*-test: $t = -4.27$, $p = 0.004$ (0.7–0.9) saline: 0.832 ±0.013; VPA: 0.851 ± 0.005; Student's *t*-test: $t = -2.25$, $p = 0.037$ (>0.9) saline: 0.865 ± 0.020; VPA: 0.865 ± 0.018; Student's *t*-test: $t < 0.001$, $p = 0.499$] and Pir [**L** (0.3–0.5) saline: 0.786 ± 0.010; VPA: 0.820 ± 0.019; Student's *t*-test: $t = -2.73$, $p = 0.026$ (0.5–0.7) saline: 0.809 ± 0.006; VPA: 0.841 ± 0.011; Student's *t*-test: $t = -4.18$, $p = 0.007$ (0.7–0.9) saline: 0.820 ± 0.009; VPA: 0.854 ± 0.008; Student's *t*-test: $t = -4.77$, $p = 0.004$ (>0.9) saline: 0.830 ± 0.011; VPA: 0.867 ± 0.022; Student's *t*-test: $t = -2.47$, $p = 0.034$], $^{**}p < 0.01$, $^{*}p < 0.05$ (Student's *t*-test). $N = 3$ mice per condition.

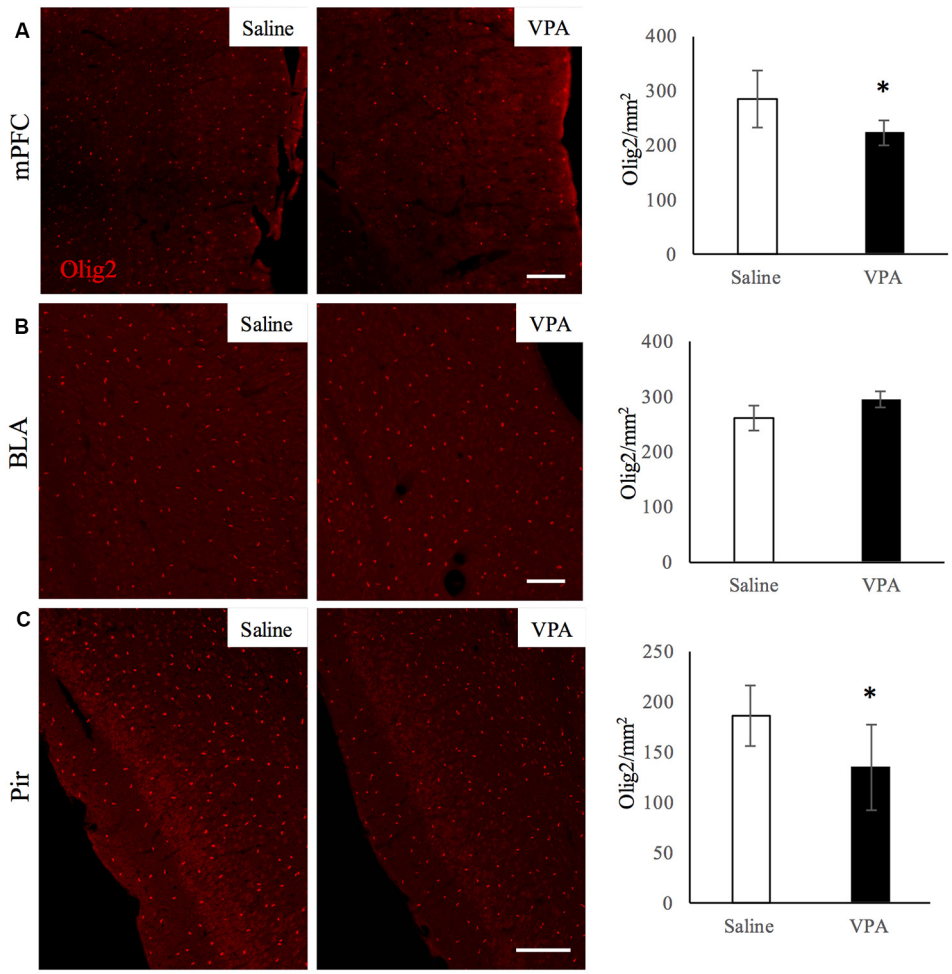

FIGURE 3 | VPA treatment reduces oligodendroglial (OL)-lineage cell numbers in brain areas linked to social behavior. Olig2 immunostaining in saline- and VPA-treated adult mouse brains (representative images, left panels) and Olig2-positive cell quantifications (right panels) in the following areas: **(A)** mPFC (mean: saline: 284.43 ± 53.29; VPA: 222.29 ± 23.80; Student's *t*-test: $t = 2.12$, $p = 0.039$); **(B)** BLA (mean: saline: 260.63 ± 23.58; VPA: 285.50 ± 17.62; Student's *t*-test: $t = -1.83$, $p = 0.052$); **(C)** Pir (mean: saline: 186.69 ± 30.01; VPA: 135.08 ± 42.91; Student's *t*-test: $t = 2.13$, $p = 0.035$). *$p < 0.05$, Student's *t*-test. Scale bars: 100 μm. $N = 4$–5 mice/treatment.

Millipore), and anti-acetylated histone-3 (anti-AcH3; Santa Cruz Biotechnology, Dallas, TX, USA). Secondary antibodies used were Alexa 488 and Alexa 568-conjugated donkey anti-rat, mouse or rabbit (Jackson Laboratories, West Grove, PA, USA).

For each brain structure of interest, 20–25 z-stack images were taken 1 μm apart, spanning the entire depth of the tissue section (30 μm) using a Confocal Olympus FV1200 microscope with 20× (numerical aperture-NA 0.40) and 40× (NA 0.65) objectives for BLA/Pir and mPFC respectively. Images with a resolution of 0.31 (mPFC) and 0.62 microns (BLA and Pir) were analyzed on maximal projection with NIH Image[1] using a macro that allows for systematically subtracting the same background in all images and quantifying the fluorescence above a threshold in the region of interest.

[1]https://imagej.nih.gov/ij/

Electron Microscopy

For ultrastructural visualization of myelinated axons in the PFC, BLA and Pir, PD90 mice were perfused with 1% glutaraldehyde and 4% paraformaldehyde in PB. Brains were immersed in the same fixative for 1 h. After rinsing brains with PB, 100-μm sagittal sections spanning the area of interest were obtained with a vibratome (Leica VT1000S). In order to standardize the quantifications and due to potential differences in myelination within each region along the lateral axis, we chose the exact same sagittal section of each region in all brains to proceed with. We subsequently incubated them in 2% osmium tetroxide (OsO_4) for 1 h, rinsed them in distilled water and contrasted them with uranyl acetate 5% for 30 min. Dehydration was achieved by a graded series of ethanol and clearing in acetone. Sections were then embedded in epoxy resin (Agar Scientific, UK) and incubated at 56°C for 48 h to allow for polymerization. Polymerized Epon blocks were

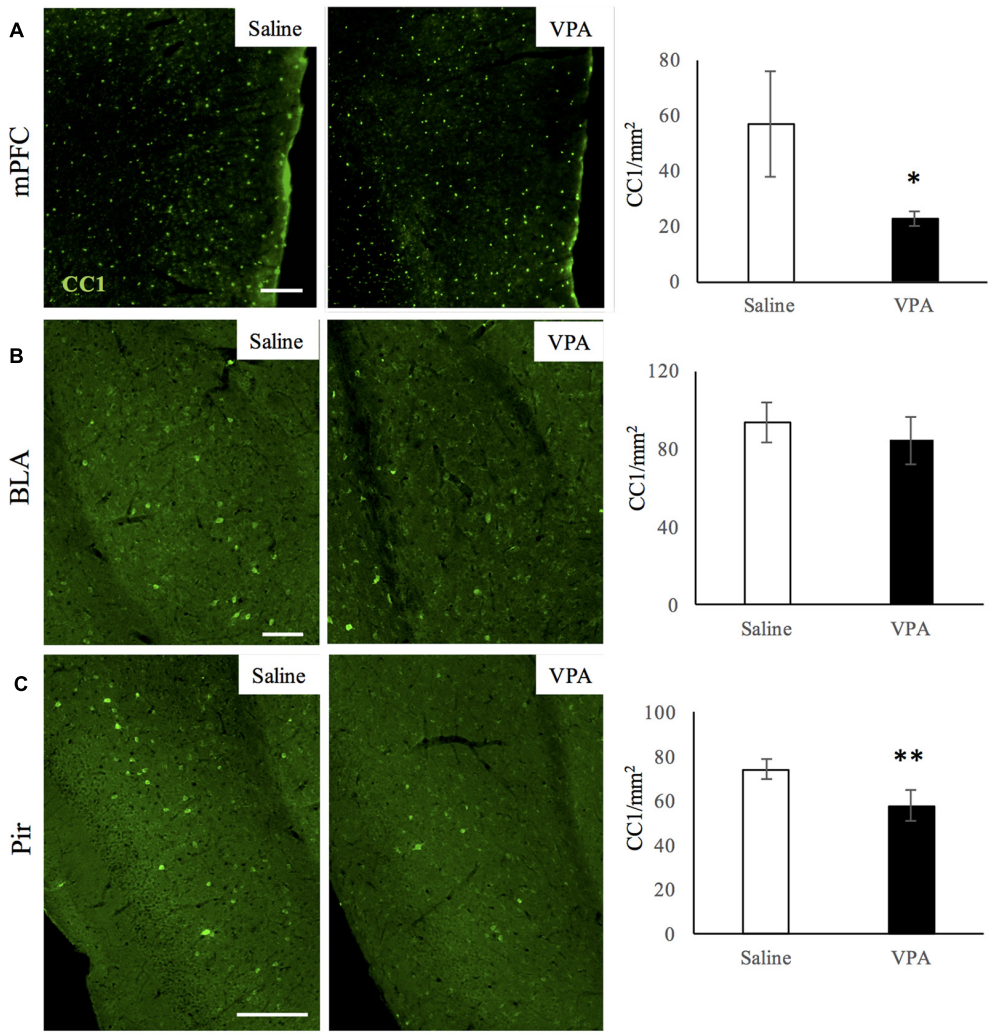

FIGURE 4 | VPA treatment reduces mature OL numbers in brain areas linked to social behavior. CC1 immunostaining in saline- and VPA-treated adult mouse brains (representative images, left panels) and CC1 positive cell quantifications (right panels) in the following areas: **(A)** mPFC (mean: saline: 53.93 ± 19.22; VPA: 22.77 ± 2, 69; Student's *t*-test: $t = 3.52$, $p = 0.006$); **(B)** BLA (mean: saline: 93.79 ± 10.21; VPA: 84.42 ± 12.32; Student's *t*-test: $t = 1.17$, $p = 0.143$); **(C)** Pir (mean: saline: 74.31 ± 4.46; VPA: 57.99 ± 6.89; Student's *t*-test: $t = 3.53$, $p = 0.008$). *$p < 0.05$, **$p < 0.01$, Student's *t*-test. Scale bars: 100 μm. $N = 4$–5 mice/treatment.

observed at the dissection microscope and the area of interest was manually microdissected. Next, dissected blocks were cut in 1 μm semi-thin sections with an ultramicrotome (UC7, Leica) which were stained with toluidine blue and visualized until the entire tissue area was observed. Then, serial ultra-thin sections (∼70 nm thick) were collected onto copper grids (about 3–4 sections per grid) and visualized at the transmission electronic microscope (Hitachi HT7700). Electron micrographs were taken at ×18,000 magnifications using an integrated AMT XR41-B camera (2,048 × 2,048 pixels).

Measurements were made using NIH ImageJ. G-ratio was calculated by dividing the axonal diameter by the total diameter of the axon including the surrounding myelin sheath. Both diameters were calculated by averaging two perpendicular measurements. For each condition, the g-ratio of at least 250 randomly selected axons was calculated.

Statistical Analysis

Sample data were tested for normal distribution. Unpaired and paired Student's *t*-test were used for comparisons. Correlations were performed and analyzed using the Graphpad Prism software, where Pearson's coefficient, *R* square and *p* values were calculated. In all cases, statistical significance was considered when $p < 0.05$.

RESULTS

Prenatal VPA Exposure Affects Myelination in Brain Regions Linked to Social Behavior

Mice prenatally exposed to VPA showed reduced sociability in adulthood (**Supplementary Figure S1**). We then aimed to study whether VPA treated mice presented alterations in myelin

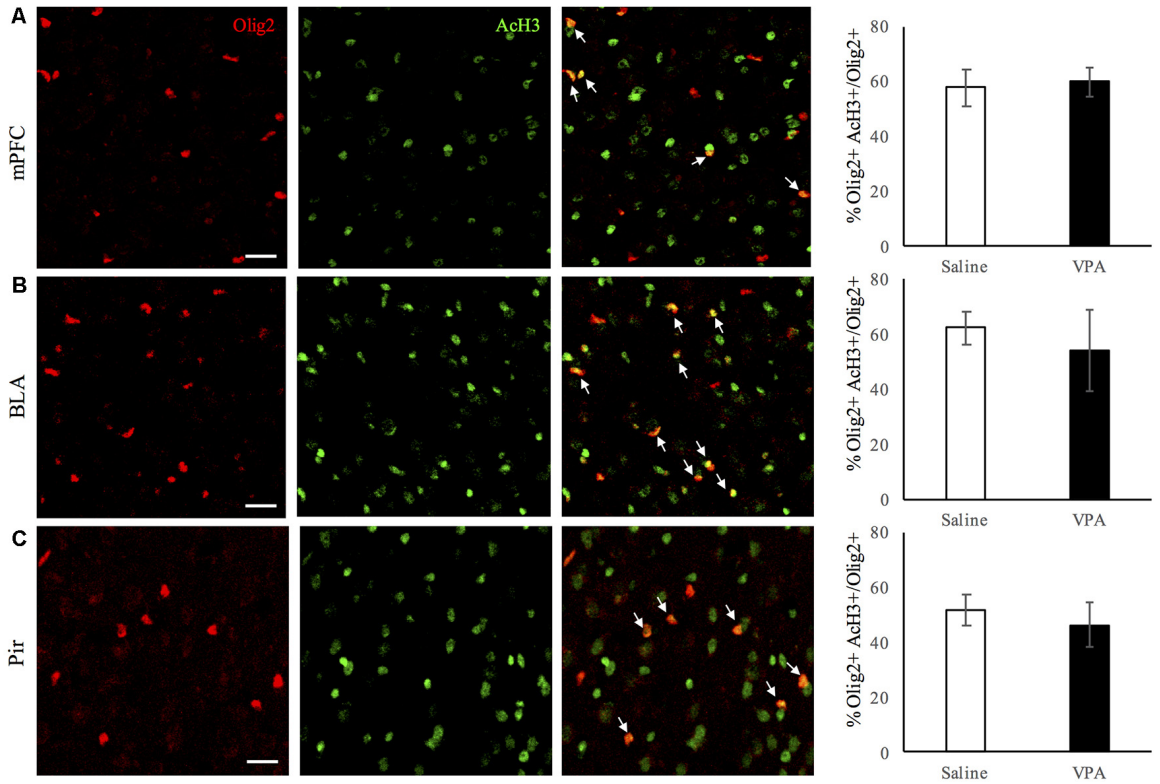

FIGURE 5 | Histone acetylation in OL-lineage cells is unaltered upon VPA-treatment in brain areas linked to social behavior. Double Olig2/acetylated histone-3 (AcH3) immunostaining in saline- and VPA-treated adult mouse brains (representative images, left panels), and estimated percentage of acetylated histone-3 (AcH3) positive cells among Olig2 positive cells (right panels) in the following areas: **(A)** mPFC (mean: saline: 57.55 ± 6.76; VPA: 59.78 ± 5.23; Student's *t*-test: $t = -0.49$, $p = 0.321$); **(B)** BLA (mean: saline: 62.40 ± 6.03; VPA: 54.29 ± 14.83; Student's *t*-test: $t = 1.073$, $p = 0.162$); **(C)** Pir (mean: saline: 51.71 ± 5.43; VPA: 46.31 ± 7.87; Student's *t*-test: $t = -1.038$, $p = 0.173$). $^*p < 0.05$, Student's *t*-test. Scale bars: 100 μm. $N = 4$–5 mice/treatment.

content in areas related to social behavior. As a first approach, we performed immunostainings for MBP detection—an essential protein component of myelin—and quantified the relative MBP-positive area in the following regions: mPFC, BLA, Pir, hippocampus and cerebellum. **Figure 1** shows the comparisons between mice prenatally exposed to VPA or saline (control). Whereas significant differences were observed in the BLA and Pir (**Figures 1B,C**) as well as a tendency in the mPFC (**Figure 1A**), the hippocampus and lobule VII of the cerebellum presented an equivalent amount of myelin in both experimental groups (**Supplementary Figures S2A,B**). We performed correlations between the preference for the social stimulus and the MBP positive area in all animals (**Figures 1A'–C'**). Whereas in the mPFC these parameters do not correlate ($r = 0.64$; $R^2 = 0.42$; $p = 0.084$), they do show a significant positive correlation in both the BLA ($r = 0.78$; $R^2 = 0.60$; $p = 0.014$) and the Pir ($r = 0.77$; Pir: $R^2 = 0.59$; $p = 0.026$). These results suggest a link between the VPA-triggered social deficits and the hypomyelination observed.

Next, we extended our analyses of the observed hypomyelination and performed EM in an independent cohort of animals. For that, we studied at the EM level the areas where a different amount of myelin content was observed, the mPFC, the BLA and the Pir, where we quantified the G-ratio as a measure of myelin sheath thickness (**Figures 2A–L**). In the mPFC, we found no differences in the G-ratio distribution along axonal diameters (**Figures 2A,B**) or the mean G-ratio (**Figures 2A,C**). Moreover, the G-ratio was not affected in any population harboring a specific range of axonal diameters (**Figure 2D**). Consistently, the distribution of axonal diameters was not affected by VPA treatment (**Supplementary Figure S3A**). In the BLA, prenatal VPA treatment affected the mean G-ratio (**Figures 2E,G**). Here, the slope of the curve was slightly shifted upwards in the VPA group where axonal diameters are smaller (**Figure 2F**). In the same line, and while axonal diameter distribution was preserved (**Supplementary Figure S3B**), the G-ratio was affected in axons of diameters ranging from 0.3 μm to 0.9 μm but not over 0.9 μm (**Figure 2H**), indicating that the effect of VPA treatment in the BLA is extensive but exclusively on fibers with axonal diameters under 0.9 μm. In the Pir, the mean G-ratio was affected upon prenatal VPA treatment (**Figures 2I,K**) and the distribution curve showed a shift upwards in the VPA group (**Figure 2J**). Consistently, the G-ratio was affected in axons of all sizes (**Figure 2L**), whereas the axonal diameters themselves showed no differences in their distribution upon VPA treatment (**Supplementary Figure S3C**). Altogether, our data indicate that

myelination, and G-ratio in particular, is affected in both BLA and Pir regions of VPA-treated animals.

Prenatal Exposure to VPA Reduces OL-Lineage Numbers in the mPFC and Pir, but Not in the BLA

Next, we investigated whether the impaired myelination was accompanied with a decrease in OL-lineage cells. For that, we quantified the number of Olig2-positive cells in the aforementioned regions (**Figure 3**) of saline- and VPA-treated mice. We observed that the number of Olig2-positive cells was lower in two regions of VPA-treated mice: the mPFC (**Figure 3A**) that shows equivalent levels of myelination than saline-treated group; and the Pir which has a reduced myelin content (**Figure 3C**). In contrast, in the BLA, where myelination was also reduced, the OL-lineage cell numbers were similar in both groups (**Figure 3B**). These results suggest that different mechanisms can underlie the lower myelination observed in the Pir and BLA. In the other regions where myelination was unaltered upon VPA treatment, the hippocampus and cerebellum, OL-lineage cell numbers were equivalent in both experimental groups (**Supplementary Figures S4A,B**). Hence, a decrease in myelination can be associated with less oligodendroglial cells as it occurs in the Pir, although not exclusively, as observed in the BLA.

Prenatal VPA Exposure Reduces Mature OL Numbers in the mPFC and Pir, but Not in the BLA

We next studied whether a specific stage of the OL-lineage cells was differentially affected in VPA-treated animals. In order to answer this, we performed immunostainings for CC1 and for NG2 markers, to identify mature OLs and OPCs respectively. NG2 cells did not display any difference in number in both the mPFC and Pir (**Supplementary Figures S5A–F**), indicating that OPC numbers in adulthood are not affected by VPA treatment. However, the number of mature OLs did decrease in both of these regions (**Figures 4A,C**), whereas in the BLA the mature OLs were not affected (**Figure 4B**), showing a distribution similar to what we observed for the whole OL-lineage population.

Histone Acetylation Is Not Affected in Oligodendroglial Cells in Any of the Regions Studied

Last, as it has been shown that histone deacetylation is required for oligodendrocyte differentiation (Shen et al., 2005, 2008; Ye et al., 2009; Liu et al., 2012), we explored the possibility that the decrease in myelination was related to persistent epigenetic changes in OL-lineage cells in VPA-treated mice. We assessed the proportion of Olig2-positive OL-lineage cells that expressed AcH3, a marker of histone deacetylase recruitment to promoter regions. As it can be observed in **Figures 5A–C**, this proportion remains unchanged in the regions analyzed, therefore suggesting that persistent histone deacetylation might not participate in neither the reduction of myelination observed in the BLA and Pir, nor in the changes in OL-lineage cells and mature OLs observed in the Pir and mPFC.

DISCUSSION

This work shows that in adult mice prenatally exposed to VPA, which display the core symptoms of ASD, the myelin content in some of the main brain regions linked to social behavior (BLA and Pir) is diminished. Moreover, the deficit in myelination in the BLA and Pir regions correlates with levels of sociability observed in these mice, with VPA treated animals showing less sociability and having less MBP levels. EM studies confirm these myelin alterations by showing a thinner myelin sheath (measured as G-ratio) in axons of the BLA and Pir regions in VPA-treated mice. This impairment can be accompanied by a reduction in OL-lineage cells and of mature OLs, or can occur without any perturbation in the number of myelin-producing cells, found in the Pir and BLA regions respectively. Similarly, the OL-lineage cell and mature OL reduction can be reduced in response to VPA treatment without a concomitant decrease in myelin, as it is observed in the mPFC. In addition, in the hippocampus and cerebellum no differences were observed in myelin content nor in OL-lineage cell number upon VPA-treatment. This suggests that in the VPA-treated group, either closely related or different mechanisms may participate in myelination impairment and OL-lineage cell reduction depending on the region analyzed. Finally, histone acetylation in OL-lineage cells is not affected by VPA treatment, therefore it does not account for the observed effects in myelination and/or OL-lineage cell reduction.

A lower myelination has been described in some of the regions studied here in different mouse models that recapitulate ASD-core symptoms. Particularly, in a mouse model of fragile X syndrome, the cerebellum displays a transient reduction in MBP and 2',3'-cyclic nucleotide 3'-phosphodiesterase (CNP) expression as well as myelination at PD7, later showing complete recovery at PD15 (Pacey et al., 2013). In addition, myelination did also show alterations in the cerebellum of Slc25a12-knockout mice at PD35 (Sakurai et al., 2010). As these studies analyze myelination during development, we cannot rule out a potential transient decrease of myelin in this region at younger stages in VPA-treated animals. Concerning the hippocampus, a decrease in MBP expression has been reported in VPA-exposed rats at PD35, along with fewer OL-lineage cells specifically in CA1 and CA2 areas (Cartocci et al., 2018). We consider that the differences in species and ages analyzed may account for the discrepancies between that study and the results presented here. Lastly, a functional link between myelination of the mPFC and social behaviors have been shown (Sirevaag and Greenough, 1987; Sánchez et al., 1998; Liu et al., 2012; Makinodan et al., 2012).

Similarly, vast evidence shows a link between ASD symptoms and alterations in white matter in ASD patients. For example, decreased myelin thickness in the orbitofrontal cortex—a subregion of the PFC in humans- has been reported in post mortem tissue of ASD patients (Zikopoulos and Barbas, 2010). The fractional anisotropy values (a measure of white matter integrity) were also shown altered in the BLA of ASD patients

(Barnea-Goraly et al., 2004), whereas in the Pir the extent of myelination and white matter integrity have not been analyzed in the context of ASD patients, although this region has been associated with social behavior (Richter et al., 2005; Borelli et al., 2009; Campolongo et al., 2018). Overall, these studies reinforce the concept that impairment of myelin development and disruption of white matter tracts in regions implicated in social functioning may contribute to impaired social cognition in ASD.

We observed that in one of the regions analyzed, the Pir, myelin reduction is accompanied with a decrease in mature OL number, whereas OPCs are maintained. This suggests that in this region, reduced myelination may likely result from a failure in the OPC differentiation towards mature OLs. On the contrary, in the BLA, myelin reduction was observed concurrently with an equivalent number of OL-lineage cells and mature OLs. Here, other mechanisms related to the myelination process itself might play a central role in this outcome. It is possible that in this case, defects in the myelination process *per se* were playing a role, regulated by key transducers such as the myelin regulatory factor (MRF), a critical regulator of myelination whose downregulation does not affect differentiation into mature OLs (Emery et al., 2009). Other factors with a similar specific role in myelination are ZFP191 (Howng et al., 2010), Nkx6.2, essential for paranode structure (Southwood et al., 2004), and ErBb3 signaling, which recapitulates the social isolation effects on impaired myelination due to myelinating OL altered morphology (Makinodan et al., 2012). Conversely, we describe that prenatal VPA treatment did not affect myelination in the mPFC, although it caused a reduction in the OL-lineage cells and particularly in the mature-OLs. This phenomenon can be linked to CNP protein function, which is essential for axonal survival but not for myelin assembly. In the absence of this protein, mice developed axonal loss as a consequence of OL dysfunctions; however, the content, ultrastructure and physical properties of myelin are not altered in young mice (Lappe-Siefke et al., 2003). Therefore, as OLs are an essential component for axonal survival, the possibility that OL impaired functions were sufficient for affecting neuronal communication and circuit integrity without altering myelination should also be taken into account.

Another important aspect that should also be considered in order to better understand the differences described here is the fact that OLs are indeed heterogeneous among brain regions in terms of transcriptomic profiles as well as timing of OL maturation and migration (Zhang et al., 2014; Marques et al., 2016). Different subsets of OLs throughout the brain are just beginning to be characterized, thus this information will be valuable to explain different OL involvement in pathological conditions.

Given that the core behaviors of ASD that are recapitulated in the VPA model are generated by neuronal circuit dysfunctions, and that neuronal activity is now known to play a critical role in myelination (Wake et al., 2011; Gibson et al., 2014; Mensch et al., 2015), we cannot rule out the possibility that altered neuronal activity with subsequent social impairment and lower myelination were not just causally related, but that these concomitant modifications were a result of a distorted bidirectional communication. In this sense, the same study that described an impaired myelination in mice that were exposed to a social isolation paradigm, reported that the OL-specific knock out of Neuregulin-ErbB3 signaling, a key pathway for myelination, results in social deficits and defective myelination (Makinodan et al., 2012). Demyelination of the mPFC by cuprizone treatment also resulted in diminished social behavior (Makinodan et al., 2009). Therefore, studies that shed light on the communication between these two processes in the context of VPA treatment, and particularly on whether neuronal activity is involved in the uncoupling of OL axonal support and myelination, would be a valuable step towards a deeper understanding of the reported effects.

We speculated with the hypothesis that epigenetic modifications within the OL-lineage cells might account for the myelination defects in VPA-treated mice. In this sense, it has been shown that in demyelinating conditions, recruitment of histone deacetylases (HDACs) to promoter regions of myelin genes precedes myelin synthesis. As the brain ages, this recruitment becomes more inefficient, thus allowing transcriptional inhibition and in turn preventing myelin gene expression (Liu et al., 2012). The presence of HDACs in the OL cell nuclei is therefore an early indicator of myelin synthesis. VPA is known to have an inhibitory effect on HDACs (Göttlicher et al., 2001). We aimed to determine whether in this model myelination impairment was associated with a difference in the degree of histone acetylation as a consequence of a poor myelin turnover. However, we observed no differences in AcH3 expression in OL-lineage cells between control and VPA groups. This suggests that adult myelin plasticity in response to VPA treatment might not be mediated by changes in nuclear heterochromatin. Nevertheless, we cannot rule out that histone acetylation occurs in earlier stages of development in VPA-treated mice and that they can lead to the reduction in myelin that we observe.

Overall, our results using prenatal VPA treatment establish a fundamental cellular link between two processes that are just beginning to be considered as functionally related. We describe a deficit in myelination in some of the main regions involved in social behavior in an animal model of ASD, which shows key features of this psychiatric disorder. We show that myelin reduction can be unrelated to alterations in the number of OL-lineage cells and of mature OLs, suggesting that depending on the brain region analyzed, different mechanisms mediate this response. While the present approach is robust and non-invasive due to its prenatal characteristics, exploring our hypotheses in different environmental and genetic ASD models would be necessary to confirm the translational implications of our results and to understand additional signatures regarding the correlation between decreased myelination and ASD core symptoms. Thus, our work opens new basic questions that may guide us to a better understanding of the link between OL axonal support, myelination and ASD related behaviors, and that can eventually lead to novel targets for therapeutic interventions in individuals affected by ASD.

AUTHOR CONTRIBUTIONS

MG designed and carried out experiments, and wrote the manuscript. AS carried out experiments. AD designed experiments. BN-O and AD co-wrote the manuscript and supervised this study.

FUNDING

This study was supported by grants from ANR (RPV14017DDA), the program "Investissements d'Avenir" ANR-10-IAIHU-06 (IHU-A-ICM), ANR-11-INBS-0011 (NeurATRIS), by the National Agency of Promotion of Science and Technology (ANPCyT-Argentina) Grant (PICT2013-1362) and an University of Buenos Aires Grant (UBA-UBACyT2016). MG received a post-doctoral fellowship from the French MS Foundation (ARSEP) and the IHU-A-ICM and is an associated researcher at the Research Career of the National Council of Scientific and Technological Research (CONICET), Argentina. AS has a CONICET doctoral fellowship. AD is an independent researcher of CONICET, Argentina and a full-time researcher at the Faculty of Exact and Natural Sciences, UBA, Argentina. BN-O is Director of Research at Institut National de la Santé et de la Recherche Médicale (INSERM).

ACKNOWLEDGMENTS

We are grateful to the ICM imaging facility (ICM-Quant) and to the ICM histology platform (Histomics).

SUPPLEMENTARY MATERIAL

The Supplementary Material for this article can be found online at: https://www.frontiersin.org/articles/10.3389/fncel.2018.00517/full#supplementary-material

REFERENCES

Ameis, S. H., Lerch, J. P., Taylor, M. J., Lee, W., Viviano, J. D., Pipitone, J., et al. (2016). A Diffusion tensor imaging study in children with adhd, autism spectrum disorder, ocd and matched controls: distinct and non-distinct white matter disruption and dimensional brain-behavior relationships. *Am. J. Psychiatry* 173, 1213–1222. doi: 10.1176/appi.ajp.2016.15111435

American Psychiatric Association. (2013). *Diagnostic and Statistical Manual of Mental Disorders (DSM-5)*. 5th Edition. Arlington, VA: American Psychiatric Association

Barnea-Goraly, N., Kwon, H., Menon, V., Eliez, S., Lotspeich, L., and Reiss, A. L. (2004). White matter structure in autism: preliminary evidence from diffusion tensor imaging. *Biol. Psychiatry* 55, 323–326. doi: 10.1016/j.biopsych.2003.10.022

Bergles, D. E., and Richardson, W. D. (2015). Oligodendrocyte development and plasticity. *Cold Spring Harb. Perspect. Biol.* 8:a020453. doi: 10.1101/cshperspect.a020453

Bergles, D. E., Roberts, J. D., Somogyi, P., and Jahr, C. E. (2000). Glutamatergic synapses on oligodendrocyte precursor cells in the hippocampus. *Nature* 405, 187–191. doi: 10.1038/35012083

Betancur, C. (2011). Etiological heterogeneity in autism spectrum disorders: more than 100 genetic and genomic disorders and still counting. *Brain Res.* 1380, 42–77. doi: 10.1016/j.brainres.2010.11.078

Borelli, K. G., Blanchard, D. C., Javier, L. K., Defensor, E. B., Brandao, M. L., and Blanchard, R. J. (2009). Neural correlates of scent marking behavior in C57BL/6J mice: detection and recognition of a social stimulus. *Neuroscience* 162, 914–923. doi: 10.1016/j.neuroscience.2009.05.047

Campolongo, M., Kazlauskas, N., Falasco, G., Urrutia, L., Salgueiro, N., Höcht, C., et al. (2018). Sociability deficits after prenatal exposure to valproic acid are rescued by early social enrichment. *Mol. Autism* 9:36. doi: 10.1186/s13229-018-0221-9

Cartocci, V., Catallo, M., Tempestilli, M., Segatto, M., Pfrieger, F. W., Bronzuoli, M. R., et al. (2018). Altered brain cholesterol/isoprenoid metabolism in a rat model of autism spectrum disorders. *Neuroscience* 372, 27–37. doi: 10.1016/j.neuroscience.2017.12.053

Cheng, W., Rolls, E. T., Gu, H., Zhang, J., and Feng, J. (2015). Autism: reduced connectivity between cortical areas involved in face expression, theory of mind and the sense of self. *Brain* 138, 1382–1393. doi: 10.1093/brain/awv051

Choe, H. K., Reed, M. D., Benavidez, N., Montgomery, D., Soares, N., Yim, Y. S., et al. (2015). Oxytocin mediates entrainment of sensory stimuli to social cues of opposing valence. *Neuron* 87, 152–163. doi: 10.1016/j.neuron.2015.06.022

Cunningham, M. O., Woodhall, G. L., and Jones, R. S. G. (2003). Valproate modifies spontaneous excitation and inhibition at cortical synapses *in vitro*. *Neuropharmacology* 45, 907–917. doi: 10.1016/S0028-3908(03)00270-3

Depino, A. M., Lucchina, L., and Pitossi, F. (2011). Early and adult hippocampal TGF-β1 overexpression have opposite effects on behavior. *Brain Behav. Immun.* 25, 1582–1591. doi: 10.1016/j.bbi.2011.05.007

Emery, B., Agalliu, D., Cahoy, J. D., Watkins, T. A., Dugas, J. C., Mulinyawe, S. B., et al. (2009). Myelin gene regulatory factor is a critical transcriptional regulator required for CNS myelination. *Cell* 138, 172–185. doi: 10.1016/j.cell.2009.04.031

Fatemi, S. H., Aldinger, K. A., Ashwood, P., Bauman, M. L., Blaha, C. D., Blatt, G. J., et al. (2012). Consensus paper: pathological role of the cerebellum in autism. *Cerebellum* 11, 777–807. doi: 10.1007/s12311-012-0355-9

Fields, R. D. (2008). White matter in learning, cognition and psychiatric disorders. *Trends Neurosci.* 31, 361–370. doi: 10.1016/j.tins.2008.04.001

Filley, C. M., and Fields, R. D. (2016). White matter and cognition: making the connection. *J. Neurophysiol.* 116, 2093–2104. doi: 10.1152/jn.00221

Fröhlich, N., Nagy, B., Hovhannisyan, A., and Kukley, M. (2011). Fate of neuron-glia synapses during proliferation and differentiation of NG2 cells. *J. Anat.* 219, 18–32. doi: 10.1111/j.1469-7580.2011.01392.x

Gibson, E. M., Purger, D., Mount, C. W., Goldstein, A. K., Lin, G. L., and Wood, L. S. (2014). Neuronal activity promotes oligodendrogenesis and adaptive myelination in the mammalian brain. *Science* 344:1252304. doi: 10.1126/science.1252304

Göttlicher, M., Minucci, S., Zhu, P., Krämer, O. H., Schimpf, A., and Giavara, S. (2001). Valproic acid defines a novel class of HDAC inhibitors inducing differentiation of transformed cells. *EMBO J.* 20, 6969–6978. doi: 10.1093/emboj/20.24.6969

Howng, S. Y., Avila, R. L., Emery, B., Traka, M., Lin, W., Watkins, T., et al. (2010). Zfp191 is required by oligodendrocytes for CNS myelination. *Genes. Dev.* 24, 301–311. doi: 10.1101/gad.1864510

Lappe-Siefke, C., Goebbels, S., Gravel, M., Nicksch, E., Lee, J., Braun, P. E., et al. (2003). Disruption of Cnp1 uncouples oligodendroglial functions in axonal support and myelination. *Nat. Genet.* 33, 366–374. doi: 10.1038/ng1095

Lin, H. C., Gean, P. W., Wang, C. C., Chan, Y. H., and Chen, P. S. (2013). The amygdala excitatory/inhibitory balance in a valproate-induced rat autism model. *PLoS One* 8:e55248. doi: 10.1371/journal.pone.0055248

Liu, J., Dietz, K., DeLoyht, J. M., Pedre, X., Kelkar, D., Kaur, J., et al. (2012). Impaired adult myelination in the prefrontal cortex of socially isolated mice. *Nat. Neurosci.* 15, 1621–1623. doi: 10.1038/nn.3263

Lucchina, L., and Depino, A. M. (2014). Altered peripheral and central inflammatory responses in a mouse model of autism. *Autism Res.* 7, 273–289. doi: 10.1002/aur.1338

Makinodan, M., Rosen, K. M., Ito, S., and Corfas, G. A. (2012). A critical period for social experience-dependent oligodendrocyte maturation and myelination. *Science* 337, 1357–1360. doi: 10.1126/science.1220845

Makinodan, M., Yamauchi, T., Tatsumi, K., Okuda, H., Takeda, T., Kiuchi, K., et al. (2009). Demyelination in the juvenile period, but not in adulthood, leads to long-lasting cognitive impairment and deficient social interaction in mice. *Prog. Neuropsychopharmacol. Biol. Psychiatry* 33, 978–985. doi: 10.1016/j.pnpbp.2009.05.006

Marques, S., Zeisel, A., Codeluppi, S., van Bruggen, D., Mendanha Falcão, A., Xiao, L., et al. (2016). Oligodendrocyte heterogeneity in the mouse juvenile and adult central nervous system. *Science* 352, 1326–1329. doi: 10.1126/science.aaf6463

Mensch, S., Baraban, M., Almeida, R., Czopka, T., Ausborn, J., El Manira, A., et al. (2015). Synaptic vesicle release regulates myelin sheath number of individual oligodendrocytes *in vivo*. *Nat. Neurosci.* 18, 628–630. doi: 10.1038/nn.3991

Pacey, L. K., Xuan, I. C., Guan, S., Sussman, D., Henkelman, R. M., Chen, Y., et al. (2013). Delayed myelination in a mouse model of fragile X syndrome. *Hum. Mol. Genet.* 22, 3920–3930. doi: 10.1093/hmg/ddt246

Pajevic, S., Basser, P. J., and Fields, R. D. (2014). Role of myelin plasticity in oscillations and synchrony of neuronal activity. *Neuroscience* 276, 135–147. doi: 10.1016/j.neuroscience.2013.11.007

Richter, K., Wolf, G., and Engelmann, M. (2005). Social recognition memory requires two stages of protein synthesis in mice. *Learn Mem.* 12, 407–413. doi: 10.1101/lm.97505

Sakurai, T., Ramoz, N., Barreto, M., Gazdoiu, M., Takahashi, N., Gertner, M., et al. (2010). Slc25a12 disruption alters myelination and neurofilaments: a model for a hypomyelination syndrome and childhood neurodevelopmental disorders. *Biol. Psychiatry* 67, 887–894. doi: 10.1016/j.biopsych.2009.08.042

Sánchez, M. M., Hearn, E. F., Do, D., Rilling, J. K., and Herndon, J. G. (1998). Differential rearing affects corpus callosum size and cognitive function of rhesus monkeys. *Brain Res.* 812, 38–49. doi: 10.1016/S0006-8993(98)00857-9

Shen, S., Li, J., and Casaccia-Bonnefil, P. (2005). Histone modifications affect timing of oligodendrocyte progenitor differentiation in the developing rat brain. *J. Cell Biol.* 169, 577–589. doi: 10.1083/jcb.200412101

Shen, S., Sandoval, J., Swiss, V. A., Li, J., Dupree, J., Franklin, R. J., et al. (2008). Age-dependent epigenetic control of differentiation inhibitors is critical for remyelination efficiency. *Nat. Neurosci.* 11, 1024–1034. doi: 10.1038/nn.2172

Sirevaag, A. M., and Greenough, W. T. (1987). Differential rearing effects on rat visual cortex synapses. *Brain Res.* 424, 320–332. doi: 10.1016/0006-8993(87)91477-6

Southwood, C., He, C., Garbern, J., Kamholz, J., Arroyo, E., and Gow, A. (2004). CNS myelin paranodes require Nkx6–2 homeoprotein transcriptional activity for normal structure. *J. Neurosci.* 24, 11215–11225. doi: 10.1523/JNEUROSCI.3479-04.2004

Sussman, D., Leung, R. C., Vogan, V. M., Lee, W., Trelle, S., Lin, S., et al. (2015). The autism puzzle: diffuse but not pervasive neuroanatomical abnormalities in children with ASD. *Neuroimage Clin.* 8, 170–179. doi: 10.1016/j.nicl.2015.04.008

Travers, B. G., Adluru, N., Ennis, C., Tromp do, P. M., Destiche, D., Doran, S., et al. (2012). Diffusion tensor imaging in autism spectrum disorder: a review. *Autism Res.* 5, 289–313. doi: 10.1002/aur.1243

Wake, H., Lee, P. R., and Fields, R. D. (2011). Control of local protein synthesis and initial events in myelination by action potentials. *Science* 333, 1647–1651. doi: 10.1126/science.1206998

Wegiel, J., Flory, M., Kuchna, I., Nowicki, K., Ma, S. Y., Imaki, H., et al. (2014). Stereological study of the neuronal number and volume of 38 brain subdivisions of subjects diagnosed with autism reveals significant alterations restricted to the striatum, amygdala and cerebellum. *Acta Neuropathol. Commun.* 2:141. doi: 10.1186/s40478-014-0141-7

Ye, F., Chen, Y., Hoang, T., Montgomery, R. L., Zhao, X. H., Bu, H., et al. (2009). HDAC1 and HDAC2 regulate oligodendrocyte differentiation by disrupting the beta-catenin-TCF interaction. *Nat. Neurosci.* 12, 829–838. doi: 10.1038/nn.2333

Zhang, Y., Chen, K., Sloan, S. A., Bennett, M. L., Scholze, A. R., O'Keeffe, S., et al. (2014). An RNA-sequencing transcriptome and splicing database of glia, neurons and vascular cells of the cerebral cortex. *J. Neurosci.* 34, 11929–11947. doi: 10.1523/JNEUROSCI.1860-14.2014

Zikopoulos, B., and Barbas, H. (2010). Changes in prefrontal axons may disrupt the network in autism. *J. Neurosci.* 30, 14595–14609. doi: 10.1523/JNEUROSCI.2257-10.2010

Conflict of Interest Statement: The authors declare that the research was conducted in the absence of any commercial or financial relationships that could be construed as a potential conflict of interest.

frontiers in Cellular Neuroscience

REVIEW
published: 29 January 2019
doi: 10.3389/fncel.2019.00003

Connexin and Pannexin-Based Channels in Oligodendrocytes: Implications in Brain Health and Disease

Sebastián Vejar[1], Juan E. Oyarzún[2,3], Mauricio A. Retamal[4,5], Fernando C. Ortiz[1]*, and Juan A. Orellana[2,3]**

[1]*Mechanisms of Myelin Formation and Repair Laboratory, Instituto de Ciencias Biomédicas, Facultad de Ciencias de la Salud, Universidad Autónoma de Chile, Santiago, Chile,* [2]*Departamento de Neurología, Escuela de Medicina and Centro Interdisciplinario de Neurociencias, Facultad de Medicina, Pontificia Universidad Católica de Chile, Santiago, Chile,* [3]*Centro de Investigación y Estudio del Consumo de Alcohol en Adolescentes, Pontificia Universidad Católica de Chile, Santiago, Chile,* [4]*Centro de Fisiología Celular e Integrativa, Facultad de Medicina, Clínica Alemana Universidad del Desarrollo, Santiago, Chile,* [5]*Department of Cell Physiology and Molecular Biophysics, and Center for Membrane Protein Research, Texas Tech University Health Sciences Center, Lubbock, TX, United States*

OPEN ACCESS

Edited by:
Francesco Moccia, University of Pavia, Italy

Reviewed by:
Bela Volgyi, University of Pécs, Hungary
Randy Franklin Stout, New York Institute of Technology, United States

***Correspondence:**
Mauricio A. Retamal
mretamal@udd.cl
Fernando C. Ortiz
fernando.ortiz@uautonoma.cl
Juan A. Orellana
jaorella@uc.cl

Received: *26 October 2018*
Accepted: *07 January 2019*
Published: *29 January 2019*

Citation:
Vejar S, Oyarzún JE, Retamal MA, Ortiz FC and Orellana JA (2019) Connexin and Pannexin-Based Channels in Oligodendrocytes: Implications in Brain Health and Disease. Front. Cell. Neurosci. 13:3. doi: 10.3389/fncel.2019.00003

Oligodendrocytes are the myelin forming cells in the central nervous system (CNS). In addition to this main physiological function, these cells play key roles by providing energy substrates to neurons as well as information required to sustain proper synaptic transmission and plasticity at the CNS. The latter requires a fine coordinated intercellular communication with neurons and other glial cell types, including astrocytes. In mammals, tissue synchronization is mainly mediated by connexins and pannexins, two protein families that underpin the communication among neighboring cells through the formation of different plasma membrane channels. At one end, gap junction channels (GJCs; which are exclusively formed by connexins in vertebrates) connect the cytoplasm of contacting cells allowing electrical and metabolic coupling. At the other end, hemichannels and pannexons (which are formed by connexins and pannexins, respectively) communicate the intra- and extracellular compartments, serving as diffusion pathways of ions and small molecules. Here, we briefly review the current knowledge about the expression and function of hemichannels, pannexons and GJCs in oligodendrocytes, as well as the evidence regarding the possible role of these channels in metabolic and synaptic functions at the CNS. In particular, we focus on oligodendrocyte-astrocyte coupling during axon metabolic support and its implications in brain health and disease.

Keywords: connexons, oligodendrocytes, pannexons, hemichannels, gap junctions, demyelinating neuropathy

INTRODUCTION

Oligodendrocytes are the myelin-forming cells of the central nervous system (CNS). They were first described and characterized as small cells with many branches distributed ubiquitously within the CNS in a close spatial relationship with axons (del Río-Hortega, 1922; Ramón y Cajal, 1925). Oligodendrocyte processes wrap the axon at different points, forming the multilamellar

structure of myelin, which is organized in sheaths along the axonal axis. Myelin sheaths enable axons for saltatory conduction accounting for the speed-up of action potential conduction in neurons (Tasaki, 1939; Nave and Werner, 2014). By exerting this main function, oligodendrocytes largely contribute to establish the conduction properties of neural circuits, leading to the proper integration of electrical signaling at the CNS. Consequently, in diseases characterized by the loss of myelin—such as multiple sclerosis (MS)—patients show several neurological impairments, revealing the decisive contribution of oligodendrocytes to brain function (Franklin and Ffrench-Constant, 2008, 2017).

In addition to their key role on saltatory conduction, oligodendrocytes participate in other important functions ranging from metabolic supply and ion buffering to setting survival and excitability properties of neurons (Menichella et al., 2006; Hamada and Kole, 2015; Battefeld et al., 2016; Saab et al., 2016; Philips and Rothstein, 2017). The plastic nature of oligodendrocytes relies not only in their ability to fulfill diverse functions, but also on the fact that they conform heterogeneous populations with different properties. Indeed, according to their morphological complexity, size and distribution, oligodendrocytes can be grouped into four subtypes (del Río-Hortega, 1922; Pérez-Cerdá et al., 2015). Type I and II represent the less abundant population, which myelinates mainly small axons in the *corpus callosum* and the cortex, while type III and IV are associated to the myelination of larger axons in the spinal cord (Dimou and Simons, 2017). A different grouping criterion—based mainly in the oligodendrocyte location around neurons—identify another subtype of oligodendrocytes, named *satellite* oligodendrocytes (Ludwin, 1979; Takasaki et al., 2010; Battefeld et al., 2016). Satellite oligodendrocytes are normally located at perineural gray matter regions, and although they have not been extensively characterized, evidence indicates that this population could play also trophic roles by giving metabolic support and extracellular K^+ buffering to neurons (Szuchet et al., 2011; Battefeld et al., 2016). Most of the current literature characterize satellite oligodendrocyte as a non-myelinating population, however, recent studies have shown that under certain conditions (i.e., demyelination) they actually synthetize myelin, forcing to revisit the current notion of *satellite* oligodendrocytes usually based on their inability to synthetize myelin (Szuchet et al., 2011; Battefeld et al., 2016).

In the nervous system, oligodendrocytes interact with several neighboring cells by multiple mechanisms. For instance, they sense growth factors and cytokines released by surrounding astrocytes and microglial cells (Ishibashi et al., 2006; Miron et al., 2013), particularly, under pathological conditions, where these signals can induce the maturation of oligodendrocyte precursor cells (OPCs) into oligodendrocytes or stabilize their mature phenotype (Fulmer et al., 2014; Hammond et al., 2015; Miyamoto et al., 2015). Similarly, oligodendrocytes and OPCs can respond to neural activity by detecting neurotransmitters through the activation of ionotropic and metabotropic receptors (i.e., AMPARs, NMDAR, mGluRs, GABAxRs and nAChRs; Bergles et al., 2000; Lin and Bergles, 2004; Kukley et al., 2007; Vélez-Fort et al., 2009; Li et al., 2013; Orduz et al., 2015; Wake et al., 2015; Saab et al., 2016; Fields et al., 2017). Commonly, glial cells communicate each other and with neurons *via* the release of bioactive molecules called gliotransmitters (Araque et al., 2014). Although it is unclear whether oligodendrocytes are endowed with the machinery to allow the release of gliotransmitters, they form extensive functional interactions among them and with astrocytes through special structures called gap junctions (GJs).

GJs result from the accumulation of intercellular channels in areas of close apposition between two plasma membranes of adjacent cells. These channel-called GJs channels (GJCs)-favor the direct intercellular exchange of metabolites (e.g., ADP, glucose, glutamate and glutathione), second messengers (e.g., cAMP and IP_3) and ions, allowing the cell-cell spread of electrotonic potentials in excitable and non-excitable tissues (Leybaert et al., 2017). When two hemichannels from adjacent cells align with each other in appositional membranes, they make a full intercellular GJC (Saez et al., 2003). Each hemichannel is constituted by the oligomerization of six monomers of connexins, a highly conserved protein family encoded by 21 genes in humans and 20 in mice, with orthologs in other vertebrate species (Abascal and Zardoya, 2013). Recent data indicates that along with constitute the building blocks of GJCs, hemichannels in nonjunctional membranes may serve as diffusional routes for ion and small molecules between the cytoplasm and the extracellular compartment (Montero and Orellana, 2015). Fifteen years ago, a new gene family encoding a set of three membrane proteins termed pannexins was discovered (Bruzzone et al., 2003). Despite that pannexins do not share significant amino acid sequences with connexins, both families have analogous secondary and tertiary structures (Abascal and Zardoya, 2013). Most of findings implicate that pannexins are capable to form single membrane channels, termed pannexons, that have some similarities with hemichannels (Sosinsky et al., 2011). Under healthy conditions, hemichannels and pannexons underpin the release of gliotransmitters (e.g., ATP, glutamate, D-serine, lactate), acting as crucial players in multiple brain processes such as synaptic transmission, neuronal oscillations, glucose sensing, ischemic tolerance and fear memory consolidation (Lin et al., 2008; Orellana et al., 2012; Stehberg et al., 2012; Chever et al., 2014; Roux et al., 2015; Meunier et al., 2017). Nonetheless, the permanent and exacerbated activity of these channels might operate as a cornerstone in the prelude and development of homeostatic imbalances detected in diverse neuropathological diseases (Orellana et al., 2016).

In this work, we review and discuss the evidence sustaining the possible role of oligodendrocyte GJ coupling in the coordination of metabolic support for neuronal activity, as well as its participation in demyelination processes observed in different diseases. In addition, we overview the recent evidence arguing for the functional expression of hemichannels and pannexons in oligodendrocytes and OPCs and how this may impact not only their normal

metabolism, but also their survival during inflammatory scenarios.

OLIGODENDROCYTE-OLIGODENDROCYTE GAP JUNCTIONAL COMMUNICATION AND THEIR CONTRIBUTION TO HEALTH AND DISEASE

General Characteristics of Connexin Expression in Oligodendrocytes

Oligodendrocytes have been reported to express connexin 29 (Cx29), Cx32, Cx45 and Cx47 (**Figure 1**; Dermietzel et al., 1989; Micevych and Abelson, 1991; Nagy et al., 2003; Li et al., 2004). Although the latter could imply that any of these connexins may form GJCs in oligodendrocytes, early studies showed contradictory experimental data, revealing the complexity of detecting GJ structures in these cells (Orthmann-Murphy et al., 2008; Nualart-Marti et al., 2013). Pioneering studies using freeze-fracture electron microscopy (FEM) in rat embryonic cultures described that contrary to that found in astrocytes, oligodendrocytes do not form GJCs between them (Massa and Mugnaini, 1982). Comparable results were obtained from FEM experiments in adult cat brain and spinal cord, were astrocyte-astrocyte and astrocyte-oligodendrocyte GJs were observed, but inter-oligodendrocyte GJs were not detected (Massa and Mugnaini, 1982). Similarly, freeze-fracture of freshly isolated oligodendrocytes from adult lamb brains, showed that GJs between oligodendrocytes were small and infrequent (Massa et al., 1984).

Contrasting the above findings, Kettenmann et al. (1983) described the successful coupling between oligodendrocytes from 2-week old mouse explants, as measured by dye transfer and electrophysiological recordings. An interesting result of this work was that about 34% of oligodendrocytes were electrically coupled, whereas the 70% exhibited positive Lucifer yellow diffusion to another oligodendrocyte. Indeed, dye-coupled oligodendrocytes were seen as far as 300 μm from the original injected cell (Kettenmann et al., 1983). This study was further supported by findings indicating that long term cultured oligodendrocytes from adult bovines establish GJ-like structures between them, as observed through electron microscopy (Norton et al., 1983). The apparent contradiction in which early studies described virtually no GJ-like structures in oligodendrocytes vs. other findings showing the opposite, probably relies on technical discrepancies, as well as the complex diversity of oligodendrocytes and their differential pattern of connexin expression. For instance, oligodendrocytes expressing O1 or O4 do not display dye or electrical coupling, while those expressing O10 show almost 40% coupling (Von Blankenfeld et al., 1993). Additionally, in slices from rat spinal cords, about 18% of oligodendrocytes in the gray matter are coupled, as showed by Lucifer yellow and neurobiotin coupling assays, whereas oligodendrocyte from white matter are not (Pastor et al., 1998). The latter findings suggest that oligodendrocyte gap junctional communication may change depending on the CNS area. Nowadays, the accumulating *in vivo* and *in vitro* evidence indicates that oligodendrocytes are coupled to each other through homotypic GJCs formed mainly by Cx47 and secondarily by Cx32 (**Figures 1**, **2**; Maglione et al., 2010; Wasseff and Scherer, 2011).

Myelin sheaths of both Schwann cells and oligodendrocytes are *intraconnected* through GJs formed by Cx32, allowing the flux of ions and molecules from the perinuclear cytoplasm to the rest of the cell (Balice-Gordon et al., 1998; Nagy et al., 2003; Kamasawa et al., 2005). In fact, cultured oligodendrocytes form tight junctions and GJCs between their myelin sheaths, reassembling what occur *in vivo* (Gonatas et al., 1982). Although myelin sheaths express Cx29 (Cx31.3 in humans; Sargiannidou et al., 2008) and Cx32 (Nagy et al., 2003; Li et al., 2004; Nualart-Marti et al., 2013), they do not colocalize with each other. Particularly, Cx29 is detected in the inner/adaxonal membrane (opposing the axonal membrane) of small myelinated fibers (Altevogt et al., 2002), whereas Cx32 is localized from the soma towards the abaxonal membrane of primarily large myelinated sheaths and among contiguous layers of myelin membrane at the paranode (Kleopa et al., 2004; Kamasawa et al., 2005). Of note, despite its localization in the cell body of oligodendrocytes, Cx29 seems to form hemichannels, likely in the adaxonal membrane, rather than function as GJC (Altevogt et al., 2002; Altevogt and Paul, 2004; Kamasawa et al., 2005; Ahn et al., 2008; Orthmann-Murphy et al., 2008). In agreement with this idea, Cx31.3-the human ortholog of murine Cx29-exhibit functional features compatible with the formation of hemichannels, but not GJCs (Sargiannidou et al., 2008). In the white and gray matter, Cx47 localizes in the cell body and initial processes of oligodendrocytes, as well as in the abaxonal membrane of myelinated fibers (Nagy et al., 2003; Altevogt and Paul, 2004; Kleopa et al., 2004; Kamasawa et al., 2005). In those cell areas Cx47 may form homotypic Cx47/Cx47 GJCs among oligodendrocytes and heterotypic GJCs with astrocytes expressing Cx43 (see next section; **Figure 2**; Wasseff and Scherer, 2011; Fasciani et al., 2018).

Functional and Dysfunctional Coupling Among Oligodendrocytes

Astrocytes are extensively coupled to each other through homotypic GJCs composed by Cx30 or Cx43 (Giaume et al., 1991; Nagy et al., 2001). For a long time, they were considered as the major protagonists in the buffering of extracellular K^+ from the synaptic cleft (Walz, 2000). Nonetheless, recent evidence indicates that oligodendrocytes along with astrocytes may form a "panglial syncytium" connected through GJs, constituting the principal pathway for the long-distance siphoning of K^+ from the juxtaparanodal periaxonal space to vasculature or the cerebrospinal fluid (Menichella et al., 2006; Rash, 2010). Oligodendrocytes form heterocellular GJs with astrocytes through heterotypic channels of Cx47 with Cx43, but also by Cx32/Cx30 GJCs depending on the anatomical area (**Figure 2**; Orthmann-Murphy et al., 2007b; Maglione et al., 2010; Magnotti et al., 2011; Wasseff and Scherer, 2011; Tress et al., 2012; Fasciani et al., 2018). This unequal connexin combination of GJCs could derive in a unidirectional rather than a bidirectional ion and molecular interchange between oligodendrocyte and astrocytes

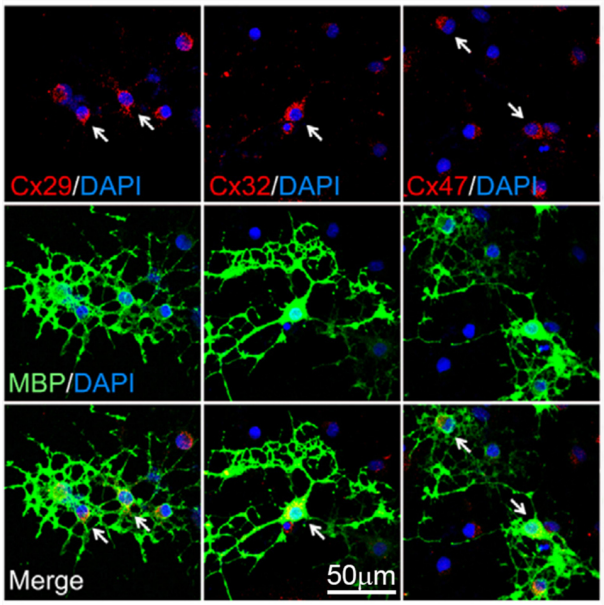

FIGURE 1 | Expression of connexins by oligodendrocytes. Representative fluorescence images depicting the double immunostaining of connexin 29 (Cx29; red, left panels), Cx32 (red, middle panels) and Cx47 (red, right panels) with the oligodendrocyte-specific bio-marker myelin basic protein (MBP, green) and DAPI staining (blue) by mature cultured oligodendrocytes after 6 days *in vitro*. Arrows highlight representative MBP-positive cells. Adapted, with permission, from Niu et al. (2016).

(Flagg-Newton and Loewenstein, 1980). This may imply the existence of a directional diffusion barrier that might account for the spatial buffering of periaxonal K^+ as well as for metabolic coupling and signaling between these cell types. Consistent with this notion, Cx32/Cx30 GJCs show an evident fast ionic rectification depending on the polarity of transjunctional voltage (Orthmann-Murphy et al., 2007b), whereas Cx47/Cx43 GJCs display ionic and chemical rectification, which result in a directional permeability barrier for the movement of ions and molecules from cells expressing Cx47 to those endowed with Cx43 (Fasciani et al., 2018). Interestingly, electron microscopy and freeze-fracture replica immunogold labeling revealed that voltage-gated K^+ channels Kv1.1/Kv1.2 form densely packed "rosettes" that are exactly aligned with Cx29 hemichannels in the surrounding juxtaparanode myelin collars and along the inner mesaxon (Rash et al., 2016). Whether Cx29 functionally docks with Kv1.1/Kv1.2 to constitute a full myelin-axon channel involved in K^+ buffering remains to be elucidated. If the existence of this new entity is confirmed, it will open a new line of the study in the field, as the discover of pannexins did years ago.

An additional key function of oligodendrocytes is their ability to provide metabolic support to the axonal compartment of neurons (Saab et al., 2016; Philips and Rothstein, 2017; Meyer et al., 2018). Although the underlying mechanisms of this phenomenon are not completely understood, GJCs between oligodendrocytes and astrocytes, as well as direct oligodendrocyte-neuron gap junctional communication have been pointed out as major mediators on this process (Nualart-Marti et al., 2013; Philips and Rothstein, 2017; Meyer et al., 2018). A recent study, from Niu et al. (2016) attempted to evaluate whether connexin-based channels contribute to glucose trafficking pathways in oligodendroglial cells. They observed that a glucose analog can diffuse through oligodendrocyte-astrocyte but not OPC-astrocyte GJs, suggesting the presence of a panglial metabolic route that may depend on the developmental stage of the oligodendroglial lineage (Niu et al., 2016). In agreement with these data, cells expressing the surface ganglioside A2B5 and OPCs are not dye or electrically coupled to astrocytes whereas mature oligodendrocytes do couple with astrocytes (Bergles et al., 2000; Lin and Bergles, 2004; Xu et al., 2014). Moreover, oligodendrocytes have the ability to supply lactate or glucose to maintain axonal function, depending on the white matter region (Saab et al., 2016; Meyer et al., 2018). Interestingly, experiments carried out on the *corpus callosum* found that in knockout animals for Cx47, oligodendrocytes lose the ability to maintain axonal function (Meyer et al., 2018). Moreover, this effect was astrocyte independent, suggesting that proper axonal function requires a direct energy supply from oligodendrocytes by a mechanism that may involve the opening of Cx47-based channels (**Figure 2**; Meyer et al., 2018). Accordingly, major modifications on GJ-based connectivity have been reported for both oligodendrocytes and astrocytes under demyelinated conditions, where an impaired metabolism is expected (Kleopa et al., 2010; Markoullis et al., 2012, 2014).

How does the disruption of GJ communication among oligodendrocytes contribute to CNS diseases? Charcot-Marie-Tooth (CMT) disease is importantly correlated with mutations in Cx32 gene (Fairweather et al., 1994; Kleopa et al., 2010; **Table 1**). This neuropathology primarily affects to Schwann cells, resulting in progressive demyelination (Nelis et al., 1996). Interestingly, oligodendrocytes are much less affected by CMT disease. Indeed, knockout mice for Cx32 show progressive loss of myelin in Schwann cells but not in oligodendrocytes (Scherer et al., 1998). This evidence may imply that Cx32 does not participate in the formation or maintaining of myelin in oligodendrocytes. Alternatively, the latter may reflect that the role of Cx32 in myelin can be greatly bypassed by other connexins expressed in oligodendrocytes (e.g., Cx47). In agreement with these ideas, it has been suggested that Cx45 expression in oligodendrocytes could prevent the demyelination induced by CMT disease (Kunzelmann et al., 1997). In spite of that, the impaired activity observed in neocortical neurons from the Cx32 knockout mouse likely relies on the decreased thickness of the axonal myelin sheaths (Sutor et al., 2000). Therefore, although the involvement of Cx32 in myelin formation is not as evident as in the peripheral nervous system, subclinical manifestations often can be observed (Sutor et al., 2000; Kleopa et al., 2002).

The role of oligodendrocyte gap junctional communication in demyelinating diseases is still a matter of ongoing research. Mutations in Cx47 have been found in patients with the central hypomyelinating disorder known as Pelizaeus-Merzbacher-like disease (also known as hypomyelinating leukodystrophy 2) and the hereditary spastic paraplegia (Sargiannidou et al., 2010; Tress et al., 2011; Cotrina and Nedergaard, 2012). In this context, mice bearing a human $Cx47^{M283T}$ missense mutation

TABLE 1 | Brief summary of the involvement of connexins and pannexins in demyelinating diseases.

Disease	Cell type	Connexin or Pannexin	References
Charcot-Marie-Tooth (CMT)	ND	Cx32	Fairweather et al. (1994), Nelis et al. (1996)
	Oligodendrocytes	Cx32	Olympiou et al. (2016)
	Schwann cells and oligodendrocytes	Cx32	Scherer et al. (1998), Kleopa et al. (2002)
	Oligodendrocytes	Cx32 and Cx45	Kunzelmann et al. (1997), Kleopa et al. (2010)
Myelination defects and neuronal hyperexcitability	Schwann cells	Cx32	Sutor et al. (2000)
Pelizaeus-Merzbacher-like (hypomyelinating leukodystrophy 2) and hereditary spastic paraplegia	Oligodendrocytes	Cx47	Osaka et al. (2010), Sargiannidou et al. (2010), Tress et al. (2011), Cotrina and Nedergaard (2012), Zlomuzica et al. (2012)
Oligodendrocyte identity and survival	Oligodendrocytes	Cx47	Schlierf et al. (2006), Pozniak et al. (2010), Takada et al. (2010), Suzuki et al. (2017)
Leukodystrophy	Oligodendrocytes Astrocytes	Cx47	Fasciani et al. (2018)
Multiple sclerosis	Oligodendrocytes	Cx32 and Cx47	Markoullis et al. (2012, 2014)
Experimental autoimmune encephalomyelitis (model of multiple sclerosis)	Oligodendrocytes	Cx32 and Cx47	Constantinescu et al. (2011)
Hypomyelinated leukodystrophy	Oligodendrocytes	Cx32 and Cx47	Wasseff and Scherer (2015)
Demyelination	Oligodendrocytes	Panx1	Hainz et al. (2017)

**This table was intended to show several examples and does not correspond to a compilation of all published evidence. ND, not determined.*

exhibit a complex age-dependent behavioral phenotype including changes in psychomotor, emotional and memory functions (Zlomuzica et al., 2012). Although with different localizations, both Cx32 and Cx47 are transcriptionally regulated by the same transcription factor: Sox10 (Schlierf et al., 2006), determinant in conferring oligodendrocyte identity and its survival (Pozniak et al., 2010; Takada et al., 2010; Suzuki et al., 2017). Moreover, mutations in the Cx47 gene promoter that binds Sox10 are responsible for the demyelination observed in Pelizaeus-Merzbacher-like disease (Osaka et al., 2010). Of particular interest is the absence of Cx47 in the myelin sheath of oligodendrocytes despite its wide presence in the perikarya (Kleopa et al., 2004; Orthmann-Murphy et al., 2007a), where it form heterotypic GJCs with the Cx43 expressed in astrocytes (Kamasawa et al., 2005). Supporting this notion, when Cx43 is expressed in astrocytes it induces the phosphorylation and further stabilization of Cx47 (May et al., 2013). Similarly, the restrictive permeability of Cx47/Cx43 GJCs is suppressed by a mutation ($Cx47^{P90S}$) linked with leukodystrophy (Fasciani et al., 2018), indicating a new pathogenic mechanism underlying myelin disorders that implies impairments in the oligodendrocyte-astrocyte coupling. Thus, the GJ-mediated crosstalk between these glial cells could be more important than originally thought and deserve further investigation.

Data from animal studies indicates that failures in GJC-mediated coupling may contribute to demyelination (Kleopa et al., 2010; Markoullis et al., 2012, 2014). For instance, a murine model of MS-the experimental autoimmune encephalomyelitis (EAE; Constantinescu et al. (2011))-showed a reduction in GJ plaques composed by both Cx32 or Cx47 in oligodendrocytes within and around lesions but also in the normal appearing white matter (Markoullis et al., 2012). Of note, the latter was paralleled with decreased numbers of Cx43 GJ plaques in astrocytes. A similar loss of GJs formed by Cx32 or Cx47 is observed in oligodendrocytes in the gray matter of post-mortem tissue from MS patients (Markoullis et al., 2014). Instead of what is found in the EAE model, these findings were paralleled with an increase in Cx30 and Cx43 along with an augment of astrocytic GJ plaques, indicating a different molecular profile of astrogliosis in white and gray matter pathology associated to MS. Supporting the role of oligodendrocyte connexins in myelination, ablation of Cx32 and Cx47 generates a phenotype of hypomyelinated leukodystrophy characterized by alterations in gene expression of key enzymes required for the synthesis of myelin lipids, as well as increased expression of genes linked with leukotrienes/prostaglandins synthesis and chemokines/cytokines interactions and signaling pathways (Wasseff and Scherer, 2015). The latter suggests that loss of oligodendrocyte-oligodendrocyte and oligodendrocyte-astrocyte coupling is accompanied by a prominent immune response. Likewise, the knockout mice for Cx32 have a greater sensitivity to inflammatory challenges and cellular stressors (Olympiou et al., 2016), arguing for the relevance of oligodendrocytes GJ signaling in the inflammatory and immune response. Although these findings strongly suggest a role for oligodendrocyte and/or oligodendrocyte-astrocyte coupling in the pathogenesis and progression of demyelinated lesions (see **Table 1**), functional approaches are necessary to draw definitive conclusions and uncover the underlying mechanisms.

HEMICHANNELS AND PANNEXONS IN OLIGODENDROCYTES

Despite that hemichannels and pannexons were discovered almost three and two decades ago, respectively (Paul et al., 1991; Bruzzone et al., 2003), the available evidence showing their functional expression in oligodendrocytes is still limited and relatively recent. Pioneering work by Niu et al. (2016)

showed for first time the presence of functional hemichannels in oligodendrocytes. Using *in vitro* primary cell cultures, they demonstrated that the opening of hemichannels mediates the uptake of a glucose analog in OPCs and oligodendrocytes, this response being more prominent in the former and highly dependent on $[Ca^{2+}]_i$ (Niu et al., 2016). Importantly, the inhibition of these channels strongly reduced OPC proliferation, suggesting that the uptake of glucose *via* hemichannels is critical for the development of the oligodendroglia lineage. More relevant, when oligodendrocytes are co-cultured with astrocytes knocked-out for Cx43, a decrease in extracellular glucose was found paralleled with a reduction in OPC proliferation (Niu et al., 2016). Therefore, in OPCs, hemichannels may provide a major pathway for glucose entry, which could be supplemented by Cx43-mediated coupling between astrocytes and oligodendrocytes and/or the release of glucose or its metabolites (e.g., lactate) through astrocyte Cx43 hemichannels.

A recent study showed that prenatal exposure to high levels of glucocorticoids increases the dye uptake of oligodendrocytes in brain slices of the offspring (Maturana et al., 2017). This response was eliminated by the application of Gap26, a mimetic peptide that in short periods of exposure (1–15 min) specifically inhibits Cx43 hemichannels rather than Cx43 GJCs. Similar effects were found with A740003, a selective $P2X_7$ receptor ($P2X_7R$) antagonist, and with the mimetic peptide ^{10}panx1, which block Panx1 channels. Given that oligodendrocytes do not express Cx43, the authors explained these results by proposing that high levels of glucocorticoids could increase the activity of Cx43 hemichannels in microglia or astrocytes, consequently increasing the extracellular levels of ATP and positively impacting the opening of Panx1 channels in oligodendrocytes following the stimulation of $P2X_7Rs$. In agreement with this idea, the glucocorticoid-induced dye uptake by oligodendrocytes depended on the activation of mast cells and microglia and was accompanied of increased expression of major elements of the inflammasome, including NLRP3, ASC and caspase-1 (Maturana et al., 2017). Despite the above, whether this phenomenon is the result of the upstream activation of Cx43 hemichannels in other brain cells

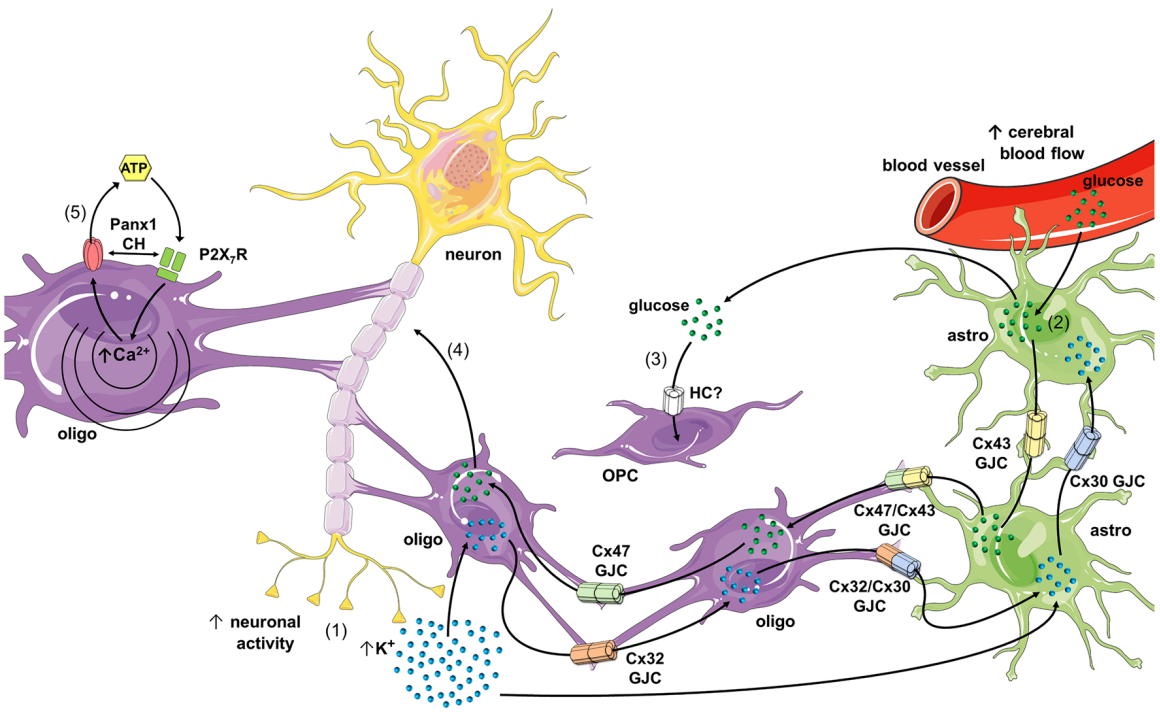

FIGURE 2 | Schematics of possible roles of connexin- and pannexin-based channels in oligodendrocyte function and dysfunction. During high rates of neuronal activity K^+ accumulates in the extracellular space, and then is taken up by oligodendrocytes and astrocytes through the inwardly rectifying K^+ channel (Kir) 4.1 and/or Na^+/K^+-pumps (1). K^+ that concentrates inside oligodendrocytes and astrocytes diffuses to the panglial syncytium *via* homocellular and heterocellular gap junction channels (GJCs), a process termed "spatial K^+ buffering." In parallel, neuronal and astroglial signaling (e.g., ATP and glutamate) could activate endothelial P2 and NMDA receptors (NMDARs), respectively, leading to increased free $[Ca^{2+}]_i$ and further vasodilation of blood vessels (not depicted). The latter increases cerebral blood flow and further uptake of glucose by astrocytic endfeet (2). Glucose diffuses through astrocytes and oligodendrocytes *via* homocellular and heterocellular GJCs and then can be metabolized to lactate by astrocytes, and both can be released into the extracellular space. In addition, glucose is taken up by oligodendrocyte precursor cells (OPCs; *via* an unknown hemichannel) and neurons, which possibly modulate oligodendrocyte differentiation and maturation (3), as well as axonal function (4), respectively. In pathological scenarios, the opening of Panx1 channels may lead to the release of ATP from oligodendrocytes (5), resulting in the activation of $P2X_7$ receptors ($P2X_7Rs$) and further triggering of a self-perpetuating mechanism of cell damage, in which high levels of $[Ca^{2+}]_i$ and direct protein-protein interaction could reactivate pannexons. Part of this schematics was done with support of the free online Servier Medical Art repository (https://smart.servier.com/).

(e.g., microglia, mast cells or astrocytes) remain to be fully elucidated.

The functional expression of Panx1 channels in oligodendrocytes was first described by Domercq et al. (2010). Using primary cultures of oligodendrocytes, they demonstrated that oxygen and glucose deprivation (OGD) increases ATP release and ischemic ionic imbalance-induced cell death by a mechanism involving the activation of $P2X_7Rs$ and Panx1 channels (**Figure 2**; Domercq et al., 2010). These findings were paralleled with increased intracellular Ca^{2+} concentration ($[Ca^{2+}]_i$), which agrees with the fact that high extracellular ATP may trigger a rise of cytosolic Ca^{2+} in oligodendrocytes by activating P2XRs (James and Butt, 2001). $P2X_7R$ stimulation may lead to ATP release in oligodendrocytes through at least one mechanism implicating hemichannels and/or pannexons. Despite that $P2X_7R$ activation rises $[Ca^{2+}]_i$ (Baroja-Mazo et al., 2013) and opens Cx43 hemichannels and Panx1 channels (Locovei et al., 2006; De Bock et al., 2012), the Panx1-mediated release of ATP depends on protein-protein interactions between $P2X_7Rs$ and Panx1 (Locovei et al., 2007). Consistent with this notion, Panx1 co-immunoprecipitates with $P2X_7Rs$ (Silverman et al., 2009; Poornima et al., 2012), where the proline 451 in the C-terminal tails of these receptors has been involved (Iglesias et al., 2008; Sorge et al., 2012). The positive feedback loop of activation among $P2X_7Rs$ and hemichannels/pannexons could explain the oligodendrocyte damage occurring in EAE, where high release of ATP has been linked to P2XR activation (Matute et al., 2007). Supporting this line of thought, probenecid, a Panx1 channel blocker, drastically prevent inflammation and oligodendrocyte damage triggered by cuprizone diet, a well-known model of demyelination (Hainz et al., 2017).

Further studies are necessary for elucidating the nature of the connexins involved in the activity of oligodendrocyte hemichannels, as well as how these channels and pannexons participate in the pathogenesis of diseases characterized by demyelination and oligodendrocyte dysfunction.

CONCLUSIONS

Oligodendrocytes serve to maintain critical brain functions such as myelination, metabolic supply, ion buffering, and recent findings suggest also a possible contribution to setting neuronal bursting properties. The evidence discussed in this review indicates that both oligodendrocyte-oligodendrocyte coupling (mainly mediated by Cx47 and Cx32 homotypic GJCs) and oligodendrocyte-astrocyte coupling (mediated by Cx47/Cx43 or Cx32/Cx30 pairs) play a pivotal role in forming a functional panglial syncytium supporting the buffering of extracellular K^+ and metabolic supply to axons. Although the available literature suggests that oligodendrocyte progenitors would not contribute to this functional syncytial network, their role could not be completely ruled out based on recent findings showing the coupling of OPCs with astrocytes through Cx47 (Liu et al., 2017; Xu et al., 2017). Future research will elucidate whether OPCs make part of this interconnected glial network. Of interest is the fact that both OPCs and mature oligodendrocytes are endowed with hemichannels that allow the passage of relevant bioactive molecules (e.g., glucose), which might be involved not only in oligodendroglia maturation, but also in metabolic coupling and energy supply to neurons.

The fact that patients with demyelinating diseases (i.e., MS) exhibits anomalies in normal expression and distribution of brain connexins, pointing out a specific role for hemichannels and GJCs in these neuropathologies. The studies reviewed here strength the recent body of evidence supporting a dysregulation of hemichannels and GJCs in glial cell types as a common phenomenon to several neurogenerative diseases. Future investigation should uncover the contribution of connexin- and pannexin-based channels to the onset and progression of demyelinating diseases.

AUTHOR CONTRIBUTIONS

JAO, MR and FCO conceived and designed the major ideas developed in the manuscript. JAO designed the **Figure 2**. All authors wrote and edited the manuscript. All authors read and approved the final manuscript.

FUNDING

This work was supported by Comisión Nacional de Investigación Científica y Tecnológica (CONICYT) and Programa de Investigación Asociativa (PIA): Grant Anillo de Ciencia y Tecnología ACT1411 (JAO); Fondo Nacional de Desarrollo Científico y Tecnológico (FONDECYT): Grant 1160710 (JAO), 11160616 (FCO) and 1160227 (MR) and Programa de Cooperación Científica ECOS-CONICYT C18S02 (MR, FCO and JAO).

ACKNOWLEDGMENTS

We thank CONICYT, PIA, PCI, FONDECYT, Clínica Alemana Universidad del Desarrollo, Universidad Autónoma de Chile and Pontificia Universidad Católica de Chile.

REFERENCES

Abascal, F., and Zardoya, R. (2013). Evolutionary analyses of gap junction protein families. *Biochim. Biophys. Acta* 1828, 4–14. doi: 10.1016/j.bbamem.2012.02.007

Ahn, M., Lee, J., Gustafsson, A., Enriquez, A., Lancaster, E., Sul, J. Y., et al. (2008). Cx29 and Cx32, two connexins expressed by myelinating glia, do not interact and are functionally distinct. *J. Neurosci. Res.* 86, 992–1006. doi: 10.1002/jnr.21561

Altevogt, B. M., and Paul, D. L. (2004). Four classes of intercellular channels between glial cells in the CNS. *J. Neurosci.* 24, 4313–4323. doi: 10.1523/JNEUROSCI.3303-03.2004

Altevogt, B. M., Kleopa, K. A., Postma, F. R., Scherer, S. S., and Paul, D. L. (2002). Connexin29 is uniquely distributed within myelinating glial cells

of the central and peripheral nervous systems. *J. Neurosci.* 22, 6458–6470. doi: 10.1523/JNEUROSCI.22-15-06458.2002

Araque, A., Carmignoto, G., Haydon, P. G., Oliet, S. H., Robitaille, R., and Volterra, A. (2014). Gliotransmitters travel in time and space. *Neuron* 81, 728–739. doi: 10.1016/j.neuron.2014.02.007

Balice-Gordon, R. J., Bone, L. J., and Scherer, S. S. (1998). Functional gap junctions in the schwann cell myelin sheath. *J. Cell Biol.* 142, 1095–1104. doi: 10.1083/jcb.142.4.1095

Baroja-Mazo, A., Barberà-Cremades, M., and Pelegrin, P. (2013). The participation of plasma membrane hemichannels to purinergic signaling. *Biochim. Biophys. Acta* 1828, 79–93. doi: 10.1016/j.bbamem.2012.01.002

Battefeld, A., Klooster, J., and Kole, M. H. (2016). Myelinating satellite oligodendrocytes are integrated in a glial syncytium constraining neuronal high-frequency activity. *Nat. Commun.* 7:11298. doi: 10.1038/ncomms11298

Bergles, D. E., Roberts, J. D., Somogyi, P., and Jahr, C. E. (2000). Glutamatergic synapses on oligodendrocyte precursor cells in the hippocampus. *Nature* 405, 187–191. doi: 10.1038/35012083

Bruzzone, R., Hormuzdi, S. G., Barbe, M. T., Herb, A., and Monyer, H. (2003). Pannexins, a family of gap junction proteins expressed in brain. *Proc. Natl. Acad. Sci. U S A* 100, 13644–13649. doi: 10.1073/pnas.2233464100

Chever, O., Lee, C. Y., and Rouach, N. (2014). Astroglial connexin43 hemichannels tune basal excitatory synaptic transmission. *J. Neurosci.* 34, 11228–11232. doi: 10.1523/JNEUROSCI.0015-14.2014

Constantinescu, C., Farooqi, N., O'Brien, K., and Gran, B. (2011). Experimental autoimmune encephalomyelitis (EAE) as a model for multiple sclerosis (MS). *Br. J. Pharmacol.* 164, 1079–1106. doi: 10.1111/j.1476-5381.2011.01302.x

Cotrina, M. L., and Nedergaard, M. (2012). Brain connexins in demyelinating diseases: therapeutic potential of glial targets. *Brain Res.* 1487, 61–68. doi: 10.1016/j.brainres.2012.07.003

De Bock, M., Wang, N., Bol, M., Decrock, E., Ponsaerts, R., Bultynck, G., et al. (2012). Connexin 43 hemichannels contribute to cytoplasmic Ca^{2+} oscillations by providing a bimodal Ca^{2+}-dependent Ca^{2+} entry pathway. *J. Biol. Chem.* 287, 12250–12266. doi: 10.1074/jbc.M111.299610

del Río-Hortega, P. (1922). ?'Son homologables la glía de escasas radiaciones y la celula de Schwann. *Bol. Soc. Esp. Biol.* 10, 25–28.

Dermietzel, R., Traub, O., Hwang, T. K., Beyer, E., Bennett, M. V., Spray, D. C., et al. (1989). Differential expression of three gap junction proteins in developing and mature brain tissues. *Proc. Natl. Acad. Sci. U S A* 86, 10148–10152. doi: 10.1073/pnas.86.24.10148

Dimou, L., and Simons, M. (2017). Diversity of oligodendrocytes and their progenitors. *Curr. Opin. Neurobiol.* 47, 73–79. doi: 10.1016/j.conb.2017.09.015

Domercq, M., Perez-Samartin, A., Aparicio, D., Alberdi, E., Pampliega, O., and Matute, C. (2010). $P2X_7$ receptors mediate ischemic damage to oligodendrocytes. *Glia* 58, 730–740. doi: 10.1002/glia.20958

Fairweather, N., Bell, C., Cochrane, S., Chelly, J., Wang, S., Mostacciuolo, M. L., et al. (1994). Mutations in the connexin 32 gene in X-linked dominant Charcot-Marie-Tooth disease (CMTX1). *Hum. Mol. Genet* 3, 1033–1034. doi: 10.1093/hmg/3.6.1033-a

Fasciani, I., Pluta, P., González-Nieto, D., Martínez-Montero, P., Molano, J., Paino, C. L., et al. (2018). Directional coupling of oligodendrocyte connexin-47 and astrocyte connexin-43 gap junctions. *Glia* 66, 2340–2352. doi: 10.1002/glia.23471

Fields, R. D., Dutta, D. J., Belgrad, J., and Robnett, M. (2017). Cholinergic signaling in myelination. *Glia* 65, 687–698. doi: 10.1002/glia.23101

Flagg-Newton, J. L., and Loewenstein, W. R. (1980). Asymmetrically permeable membrane channels in cell junction. *Science* 207, 771–773. doi: 10.1126/science.7352287

Franklin, R. J., and Ffrench-Constant, C. (2008). Remyelination in the CNS: from biology to therapy. *Nat. Rev. Neurosci.* 9, 839–855. doi: 10.1038/nrn2480

Franklin, R. J. M., and Ffrench-Constant, C. (2017). Regenerating CNS myelin–from mechanisms to experimental medicines. *Nat. Rev. Neurosci.* 18, 753–769. doi: 10.1038/nrn.2017.136

Fulmer, C. G., VonDran, M. W., Stillman, A. A., Huang, Y., Hempstead, B. L., and Dreyfus, C. F. (2014). Astrocyte-derived BDNF supports myelin protein synthesis after cuprizone-induced demyelination. *J. Neurosci.* 34, 8186–8196. doi: 10.1523/JNEUROSCI.4267-13.2014

Giaume, C., Fromaget, C., El Aoumari, A., Cordier, J., Glowinski, J., and Gros, D. (1991). Gap junctions in cultured astrocytes: single-channel currents and characterization of channel-forming protein. *Neuron* 6, 133–143. doi: 10.1016/0896-6273(91)90128-m

Gonatas, N. K., Hirayama, M., Stieber, A., and Silberberg, D. H. (1982). The ultrastructure of isolated rat oligodendroglial cell cultures. *J. Neurocytol.* 11, 997–1008. doi: 10.1007/bf01148313

Hainz, N., Becker, P., Rapp, D., Wagenpfeil, S., Wonnenberg, B., Beisswenger, C., et al. (2017). Probenecid-treatment reduces demyelination induced by cuprizone feeding. *J. Chem. Neuroanat.* 85, 21–26. doi: 10.1016/j.jchemneu.2017.06.003

Hamada, M. S., and Kole, M. H. (2015). Myelin loss and axonal ion channel adaptations associated with gray matter neuronal hyperexcitability. *J. Neurosci.* 35, 7272–7286. doi: 10.1523/JNEUROSCI.4747-14.2015

Hammond, T. R., McEllin, B., Morton, P. D., Raymond, M., Dupree, J., and Gallo, V. (2015). Endothelin-B receptor activation in astrocytes regulates the rate of oligodendrocyte regeneration during remyelination. *Cell Rep.* 13, 2090–2097. doi: 10.1016/j.celrep.2015.11.002

Iglesias, R., Locovei, S., Roque, A., Alberto, A. P., Dahl, G., Spray, D. C., et al. (2008). $P2X_7$ receptor-Pannexin1 complex: pharmacology and signaling. *Am. J. Physiol. Cell Physiol.* 295, C752–C760. doi: 10.1152/ajpcell.00228.2008

Ishibashi, T., Dakin, K. A., Stevens, B., Lee, P. R., Kozlov, S. V., Stewart, C. L., et al. (2006). Astrocytes promote myelination in response to electrical impulses. *Neuron* 49, 823–832. doi: 10.1016/j.neuron.2006.02.006

James, G., and Butt, A. M. (2001). P2X and P2Y purinoreceptors mediate ATP-evoked calcium signalling in optic nerve glia *in situ*. *Cell Calcium* 30, 251–259. doi: 10.1054/ceca.2001.0232

Kamasawa, N., Sik, A., Morita, M., Yasumura, T., Davidson, K. G., Nagy, J. I., et al. (2005). Connexin-47 and connexin-32 in gap junctions of oligodendrocyte somata, myelin sheaths, paranodal loops and Schmidt-Lanterman incisures: implications for ionic homeostasis and potassium siphoning. *Neuroscience* 136, 65–86. doi: 10.1016/j.neuroscience.2005.08.027

Kettenmann, H., Orkand, R. K., and Schachner, M. (1983). Coupling among identified cells in mammalian nervous system cultures. *J. Neurosci.* 3, 506–516. doi: 10.1523/jneurosci.03-03-00506.1983

Kleopa, K. A., Orthmann, J. L., Enriquez, A., Paul, D. L., and Scherer, S. S. (2004). Unique distributions of the gap junction proteins connexin29, connexin32 and connexin47 in oligodendrocytes. *Glia* 47, 346–357. doi: 10.1002/glia.20043

Kleopa, K. A., Orthmann-Murphy, J., and Sargiannidou, I. (2010). Gap junction disorders of myelinating cells. *Rev. Neurosci.* 21, 397–419. doi: 10.1515/revneuro.2010.21.5.397

Kleopa, K. A., Yum, S. W., and Scherer, S. S. (2002). Cellular mechanisms of connexin32 mutations associated with CNS manifestations. *J. Neurosci. Res.* 68, 522–534. doi: 10.1002/jnr.10255

Kukley, M., Capetillo-Zarate, E., and Dietrich, D. (2007). Vesicular glutamate release from axons in white matter. *Nat. Neurosci.* 10, 311–320. doi: 10.1038/nn1850

Kunzelmann, P., Blümcke, I., Traub, O., Dermietzel, R., and Willecke, K. (1997). Coexpression of connexin45 and -32 in oligodendrocytes of rat brain. *J. Neurocytol.* 26, 17–22. doi: 10.1023/A:1018555207379

Leybaert, L., Lampe, P. D., Dhein, S., Kwak, B. R., Ferdinandy, P., Beyer, E. C., et al. (2017). Connexins in cardiovascular and neurovascular health and disease: pharmacological implications. *Pharmacol. Rev.* 69, 396–478. doi: 10.1124/pr.115.012062

Li, X., Ionescu, A. V., Lynn, B. D., Lu, S., Kamasawa, N., Morita, M., et al. (2004). Connexin47, connexin29 and connexin32 co-expression in oligodendrocytes and Cx47 association with zonula occludens-1 (ZO-1) in mouse brain. *Neuroscience* 126, 611–630. doi: 10.1016/j.neuroscience.2004.03.063

Li, C., Xiao, L., Liu, X., Yang, W., Shen, W., Hu, C., et al. (2013). A functional role of NMDA receptor in regulating the differentiation of oligodendrocyte precursor cells and remyelination. *Glia* 61, 732–749. doi: 10.1002/glia.22469

Lin, S. C., and Bergles, D. E. (2004). Synaptic signaling between GABAergic interneurons and oligodendrocyte precursor cells in the hippocampus. *Nat. Neurosci.* 7, 24–32. doi: 10.1038/nn1162

Lin, J. H., Lou, N., Kang, N., Takano, T., Hu, F., Han, X., et al. (2008). A central role of connexin 43 in hypoxic preconditioning. *J. Neurosci.* 28, 681–695. doi: 10.1523/JNEUROSCI.3827-07.2008

Liu, Z., Xu, D., Wang, S., Chen, Y., Li, Z., Gao, X., et al. (2017). Astrocytes induce proliferation of oligodendrocyte progenitor cells via connexin 47-mediated activation of the ERK/Id4 pathway. *Cell Cycle* 16, 714–722. doi: 10.1080/15384101.2017.1295183

Locovei, S., Scemes, E., Qiu, F., Spray, D. C., and Dahl, G. (2007). Pannexin1 is part of the pore forming unit of the $P2X_7$ receptor death complex. *FEBS Lett.* 581, 483–488. doi: 10.1016/j.febslet.2006.12.056

Locovei, S., Wang, J., and Dahl, G. (2006). Activation of pannexin 1 channels by ATP through P2Y receptors and by cytoplasmic calcium. *FEBS Lett.* 580, 239–244. doi: 10.1016/j.febslet.2005.12.004

Ludwin, S. K. (1979). The perineuronal satellite oligodendrocyte. A role in remyelination. *Acta Neuropathol.* 47, 49–53. doi: 10.1007/bf00698272

Maglione, M., Tress, O., Haas, B., Karram, K., Trotter, J., Willecke, K., et al. (2010). Oligodendrocytes in mouse corpus callosum are coupled via gap junction channels formed by connexin47 and connexin32. *Glia* 58, 1104–1117. doi: 10.1002/glia.20991

Magnotti, L. M., Goodenough, D. A., and Paul, D. L. (2011). Functional heterotypic interactions between astrocyte and oligodendrocyte connexins. *Glia* 59, 26–34. doi: 10.1002/glia.21073

Markoullis, K., Sargiannidou, I., Gardner, C., Hadjisavvas, A., Reynolds, R., and Kleopa, K. A. (2012). Disruption of oligodendrocyte gap junctions in experimental autoimmune encephalomyelitis. *Glia* 60, 1053–1066. doi: 10.1002/glia.22334

Markoullis, K., Sargiannidou, I., Schiza, N., Roncaroli, F., Reynolds, R., and Kleopa, K. A. (2014). Oligodendrocyte gap junction loss and disconnection from reactive astrocytes in multiple sclerosis gray matter. *J. Neuropathol. Exp. Neurol.* 73, 865–879. doi: 10.1097/NEN.0000000000000106

Massa, P. T., and Mugnaini, E. (1982). Cell junctions and intramembrane particles of astrocytes and oligodendrocytes: a freeze-fracture study. *Neuroscience* 7, 523–538. doi: 10.1016/0306-4522(82)90285-8

Massa, P. T., Szuchet, S., and Mugnaini, E. (1984). Cell-cell interactions of isolated and cultured oligodendrocytes: formation of linear occluding junctions and expression of peculiar intramembrane particles. *J. Neurosci.* 4, 3128–3139. doi: 10.1523/jneurosci.04-12-03128.1984

Maturana, C. J., Aguirre, A., and Saez, J. C. (2017). High glucocorticoid levels during gestation activate the inflammasome in hippocampal oligodendrocytes of the offspring. *Dev. Neurobiol.* 77, 625–642. doi: 10.1002/dneu.22409

Matute, C., Torre, I., Pérez-Cerdá, F., Pérez-Samartín, A., Alberdi, E., Etxebarria, E., et al. (2007). $P2X_7$ receptor blockade prevents ATP excitotoxicity in oligodendrocytes and ameliorates experimental autoimmune encephalomyelitis. *J. Neurosci.* 27, 9525–9533. doi: 10.1523/JNEUROSCI.0579-07.2007

May, D., Tress, O., Seifert, G., and Willecke, K. (2013). Connexin47 protein phosphorylation and stability in oligodendrocytes depend on expression of Connexin43 protein in astrocytes. *J. Neurosci.* 33, 7985–7996. doi: 10.1523/JNEUROSCI.5874-12.2013

Menichella, D. M., Majdan, M., Awatramani, R., Goodenough, D. A., Sirkowski, E., Scherer, S. S., et al. (2006). Genetic and physiological evidence that oligodendrocyte gap junctions contribute to spatial buffering of potassium released during neuronal activity. *J. Neurosci.* 26, 10984–10991. doi: 10.1523/JNEUROSCI.0304-06.2006

Meunier, C., Wang, N., Yi, C., Dallerac, G., Ezan, P., Koulakoff, A., et al. (2017). Contribution of astroglial Cx43 hemichannels to the modulation of glutamatergic currents by D-serine in the mouse prefrontal cortex. *J. Neurosci.* 37, 9064–9075. doi: 10.1523/JNEUROSCI.2204-16.2017

Meyer, N., Richter, N., Fan, Z., Siemonsmeier, G., Pivneva, T., Jordan, P., et al. (2018). Oligodendrocytes in the mouse corpus callosum maintain axonal function by delivery of glucose. *Cell Rep.* 22, 2383–2394. doi: 10.1016/j.celrep.2018.02.022

Micevych, P. E., and Abelson, L. (1991). Distribution of mRNAs coding for liver and heart gap junction proteins in the rat central nervous system. *J. Comp. Neurol.* 305, 96–118. doi: 10.1002/cne.903050110

Miron, V. E., Boyd, A., Zhao, J. W., Yuen, T. J., Ruckh, J. M., Shadrach, J. L., et al. (2013). M2 microglia and macrophages drive oligodendrocyte differentiation during CNS remyelination. *Nat. Neurosci.* 16, 1211–1218. doi: 10.1038/nn.3469

Miyamoto, N., Maki, T., Shindo, A., Liang, A. C., Maeda, M., Egawa, N., et al. (2015). Astrocytes promote oligodendrogenesis after white matter damage via brain-derived neurotrophic factor. *J. Neurosci.* 35, 14002–14008. doi: 10.1523/JNEUROSCI.1592-15.2015

Montero, T. D., and Orellana, J. A. (2015). Hemichannels: new pathways for gliotransmitter release. *Neuroscience* 286, 45–59. doi: 10.1016/j.neuroscience.2014.11.048

Nagy, J. I., Ionescu, A. V., Lynn, B. D., and Rash, J. E. (2003). Connexin29 and connexin32 at oligodendrocyte and astrocyte gap junctions and in myelin of the mouse central nervous system. *J. Comp. Neurol.* 464, 356–370. doi: 10.1002/cne.10797

Nagy, J. I., Li, X., Rempel, J., Stelmack, G., Patel, D., Staines, W. A., et al. (2001). Connexin26 in adult rodent central nervous system: demonstration at astrocytic gap junctions and colocalization with connexin30 and connexin43. *J. Comp. Neurol.* 441, 302–323. doi: 10.1002/cne.1414

Nave, K. A., and Werner, H. B. (2014). Myelination of the nervous system: mechanisms and functions. *Annu. Rev. Cell Dev. Biol.* 30, 503–533. doi: 10.1146/annurev-cellbio-100913-013101

Nelis, E., Warner, L. E., Vriendt, E. D., Chance, P. F., Lupski, J. R., and Van Broeckhoven, C. (1996). Comparison of single-strand conformation polymorphism and heteroduplex analysis for detection of mutations in Charcot-Marie-Tooth type 1 disease and related peripheral neuropathies. *Eur. J. Hum. Genet.* 4, 329–333. doi: 10.1159/000472227

Niu, J., Li, T., Yi, C., Huang, N., Koulakoff, A., Weng, C., et al. (2016). Connexin-based channels contribute to metabolic pathways in the oligodendroglial lineage. *J. Cell Sci.* 129, 1902–1914. doi: 10.1242/jcs.178731

Norton, W. T., Farooq, M., Fields, K. L., and Raine, C. S. (1983). The long term culture of bulk-isolated bovine oligodendroglia from adult brain. *Brain Res.* 270, 295–310. doi: 10.1016/0006-8993(83)90604-2

Nualart-Marti, A., Solsona, C., and Fields, R. D. (2013). Gap junction communication in myelinating glia. *Biochim. Biophys. Acta* 1828, 69–78. doi: 10.1016/j.bbamem.2012.01.024

Olympiou, M., Sargiannidou, I., Markoullis, K., Karaiskos, C., Kagiava, A., Kyriakoudi, S., et al. (2016). Systemic inflammation disrupts oligodendrocyte gap junctions and induces ER stress in a model of CNS manifestations of X-linked Charcot-Marie-Tooth disease. *Acta Neuropathol. Commun.* 4:95. doi: 10.1186/s40478-016-0369-5

Orduz, D., Maldonado, P. P., Balia, M., Vélez-Fort, M., de Sars, V., Yanagawa, Y., et al. (2015). Interneurons and oligodendrocyte progenitors form a structured synaptic network in the developing neocortex. *Elife* 4:e06953. doi: 10.7554/elife.06953

Orellana, J. A., Retamal, M. A., Moraga-Amaro, R., and Stehberg, J. (2016). Role of astroglial hemichannels and pannexons in memory and neurodegenerative diseases. *Front. Integr. Neurosci.* 10:26. doi: 10.3389/fnint.2016.00026

Orellana, J. A., Sáez, P. J., Cortés-Campos, C., Elizondo, R. J., Shoji, K. F., Contreras-Duarte, S., et al. (2012). Glucose increases intracellular free Ca^{2+} in tanycytes via ATP released through connexin 43 hemichannels. *Glia* 60, 53–68. doi: 10.1002/glia.21246

Orthmann-Murphy, J. L., Abrams, C. K., and Scherer, S. S. (2008). Gap junctions couple astrocytes and oligodendrocytes. *J. Mol. Neurosci.* 35, 101–116. doi: 10.1007/s12031-007-9027-5

Orthmann-Murphy, J. L., Enriquez, A. D., Abrams, C. K., and Scherer, S. S. (2007a). Loss-of-function GJA12/Connexin47 mutations cause Pelizaeus-Merzbacher-like disease. *Mol. Cell. Neurosci.* 34, 629–641. doi: 10.1016/j.mcn.2007.01.010

Orthmann-Murphy, J. L., Freidin, M., Fischer, E., Scherer, S. S., and Abrams, C. K. (2007b). Two distinct heterotypic channels mediate gap junction coupling between astrocyte and oligodendrocyte connexins. *J. Neurosci.* 27, 13949–13957. doi: 10.1523/JNEUROSCI.3395-07.2007

Osaka, H., Hamanoue, H., Yamamoto, R., Nezu, A., Sasaki, M., Saitsu, H., et al. (2010). Disrupted SOX10 regulation of GJC2 transcription causes Pelizaeus-Merzbacher-like disease. *Ann. Neurol.* 68, 250–254. doi: 10.1002/ana.22022

Pastor, A., Kremer, M., Möller, T., Kettenmann, H., and Dermietzel, R. (1998). Dye coupling between spinal cord oligodendrocytes: differences in coupling efficiency between gray and white matter. *Glia* 24, 108–120. doi: 10.1002/(sici)1098-1136(199809)24:1<108::aid-glia11>3.0.co;2-v

Paul, D. L., Ebihara, L., Takemoto, L. J., Swenson, K. I., and Goodenough, D. A. (1991). Connexin46, a novel lens gap junction protein, induces voltage-gated currents in nonjunctional plasma membrane of Xenopus oocytes *J. Cell Biol.* 115, 1077–1089. doi: 10.1083/jcb.115.4.1077

Pérez-Cerdá, F., Sánchez-Gómez, M. V., and Matute, C. (2015). Pío del Río Hortega and the discovery of the oligodendrocytes. *Front. Neuroanat.* 9:92. doi: 10.3389/fnana.2015.00092

Philips, T., and Rothstein, J. D. (2017). Oligodendroglia: metabolic supporters of neurons. *J. Clin. Invest.* 127, 3271–3280. doi: 10.1172/jci90610

Poornima, V., Madhupriya, M., Kootar, S., Sujatha, G., Kumar, A., and Bera, A. K. (2012). $P2X_7$ receptor-pannexin 1 hemichannel association: effect of extracellular calcium on membrane permeabilization. *J. Mol. Neurosci.* 46, 585–594. doi: 10.1007/s12031-011-9646-8

Pozniak, C. D., Langseth, A. J., Dijkgraaf, G. J., Choe, Y., Werb, Z., and Pleasure, S. J. (2010). Sox10 directs neural stem cells toward the oligodendrocyte lineage by decreasing Suppressor of Fused expression. *Proc. Natl. Acad. Sci. U S A* 107, 21795–21800. doi: 10.1073/pnas.1016485107

Ramón y Cajal, S. (1925). "Notas técnicas," in *Boletín de la Sociedad Española de Biología* (Madrid: Sociedad española de biología) 25–28.

Rash, J. E. (2010). Molecular disruptions of the panglial syncytium block potassium siphoning and axonal saltatory conduction: pertinence to neuromyelitis optica and other demyelinating diseases of the central nervous system. *Neuroscience* 168, 982–1008. doi: 10.1016/j.neuroscience.2009.10.028

Rash, J. E., Vanderpool, K. G., Yasumura, T., Hickman, J., Beatty, J. T., and Nagy, J. I. (2016). KV1 channels identified in rodent myelinated axons, linked to Cx29 in innermost myelin: support for electrically active myelin in mammalian saltatory conduction. *J. Neurophysiol.* 115, 1836–1859. doi: 10.1152/jn.01077.2015

Roux, L., Madar, A., Lacroix, M. M., Yi, C., Benchenane, K., and Giaume, C. (2015). Astroglial connexin 43 hemichannels modulate olfactory bulb slow oscillations. *J. Neurosci.* 35, 15339–15352. doi: 10.1523/JNEUROSCI.0861-15.2015

Saab, A. S., Tzvetavona, I. D., Trevisiol, A., Baltan, S., Dibaj, P., Kusch, K., et al. (2016). Oligodendroglial NMDA receptors regulate glucose import and axonal energy metabolism. *Neuron* 91, 119–132. doi: 10.1016/j.neuron.2016.05.016

Saez, J. C., Berthoud, V. M., Branes, M. C., Martinez, A. D., and Beyer, E. C. (2003). Plasma membrane channels formed by connexins: their regulation and functions. *Physiol. Rev.* 83, 1359–1400. doi: 10.1152/physrev.00007.2003

Sargiannidou, I., Ahn, M., Enriquez, A. D., Peinado, A., Reynolds, R., Abrams, C., et al. (2008). Human oligodendrocytes express Cx31.3: function and interactions with Cx32 mutants. *Neurobiol. Dis.* 30, 221–233. doi: 10.1016/j.nbd.2008.01.009

Sargiannidou, I., Markoullis, K., and Kleopa, K. A. (2010). Molecular mechanisms of gap junction mutations in myelinating cells. *Hist. Histopathol.* 25, 1191–1206. doi: 10.14670/HH-25.1191

Scherer, S. S., Xu, Y. T., Nelles, E., Fischbeck, K., Willecke, K., and Bone, L. J. (1998). Connexin32-null mice develop demyelinating peripheral neuropathy. *Glia* 24, 8–20. doi: 10.1002/(sici)1098-1136(199809)24:1<8::aid-glia2>3.0.co;2-3

Schlierf, B., Werner, T., Glaser, G., and Wegner, M. (2006). Expression of connexin47 in oligodendrocytes is regulated by the Sox10 transcription factor. *J. Mol. Biol.* 361, 11–21. doi: 10.1016/j.jmb.2006.05.072

Silverman, W. R., de Rivero Vaccari, J. P., Locovei, S., Qiu, F., Carlsson, S. K., Scemes, E., et al. (2009). The pannexin 1 channel activates the inflammasome in neurons and astrocytes. *J. Biol. Chem.* 284, 18143–18151. doi: 10.1074/jbc.m109.004804

Sorge, R. E., Trang, T., Dorfman, R., Smith, S. B., Beggs, S., Ritchie, J., et al. (2012). Genetically determined $P2X_7$ receptor pore formation regulates variability in chronic pain sensitivity. *Nat. Med.* 18, 595–599. doi: 10.1038/nm.2710

Sosinsky, G. E., Boassa, D., Dermietzel, R., Duffy, H. S., Laird, D. W., MacVicar, B., et al. (2011). Pannexin channels are not gap junction hemichannels. *Channels* 5, 193–197. doi: 10.4161/chan.5.3.15765

Stehberg, J., Moraga-Amaro, R., Salazar, C., Becerra, A., Echeverria, C., Orellana, J. A., et al. (2012). Release of gliotransmitters through astroglial connexin 43 hemichannels is necessary for fear memory consolidation in the basolateral amygdala. *FASEB J.* 26, 3649–3657. doi: 10.1096/fj.11-198416

Sutor, B., Schmolke, C., Teubner, B., Schirmer, C., and Willecke, K. (2000). Myelination defects and neuronal hyperexcitability in the neocortex of connexin 32-deficient mice. *Cereb. Cortex* 10, 684–697. doi: 10.1093/cercor/10.7.684

Suzuki, N., Sekimoto, K., Hayashi, C., Mabuchi, Y., Nakamura, T., and Akazawa, C. (2017). Differentiation of oligodendrocyte precursor cells from Sox10-venus mice to oligodendrocytes and astrocytes. *Sci. Rep.* 7:14133. doi: 10.1038/s41598-017-14207-0

Szuchet, S., Nielsen, J. A., Lovas, G., Domowicz, M. S., de Velasco, J. M., Maric, D., et al. (2011). The genetic signature of perineuronal oligodendrocytes reveals their unique phenotype. *Eur. J. Neurosci.* 34, 1906–1922. doi: 10.1111/j.1460-9568.2011.07922.x

Takada, N., Kucenas, S., and Appel, B. (2010). Sox10 is necessary for oligodendrocyte survival following axon wrapping. *Glia* 58, 996–1006. doi: 10.1002/glia.20981

Takasaki, C., Yamasaki, M., Uchigashima, M., Konno, K., Yanagawa, Y., and Watanabe, M. (2010). Cytochemical and cytological properties of perineuronal oligodendrocytes in the mouse cortex. *Eur. J. Neurosci.* 32, 1326–1336. doi: 10.1111/j.1460-9568.2010.07377.x

Tasaki, I. (1939). The electro-saltatory transmission of the nerve impulse and the effect of narcosis upon the nerve fiber. *Am. J. Physiol. Leg. Content*127 211–227. doi: 10.1152/ajplegacy.1939.127.2.211

Tress, O., Maglione, M., May, D., Pivneva, T., Richter, N., Seyfarth, J., et al. (2012). Panglial gap junctional communication is essential for maintenance of myelin in the CNS. *J. Neurosci.* 32, 7499–7518. doi: 10.1523/JNEUROSCI.0392-12.2012

Tress, O., Maglione, M., Zlomuzica, A., May, D., Dicke, N., Degen, J., et al. (2011). Pathologic and phenotypic alterations in a mouse expressing a connexin47 missense mutation that causes Pelizaeus-Merzbacher-like disease in humans. *PLoS Genet.* 7:e1002146. doi: 10.1371/journal.pgen.1002146

Vélez-Fort, M., Audinat, E., and Angulo, M. C. (2009). Functional α 7-containing nicotinic receptors of NG2-expressing cells in the hippocampus. *Glia* 57, 1104–1114. doi: 10.1002/glia.20834

Von Blankenfeld, G., Ransom, B. R., and Kettenmann, H. (1993). Development of cell-cell coupling among cells of the oligodendrocyte lineage. *Glia* 7, 322–328. doi: 10.1002/glia.440070407

Wake, H., Ortiz, F. C., Woo, D. H., Lee, P. R., Angulo, M. C., and Fields, R. D. (2015). Nonsynaptic junctions on myelinating glia promote preferential myelination of electrically active axons. *Nat. Commun.* 6:7844. doi: 10.1038/ncomms8844

Walz, W. (2000). Role of astrocytes in the clearance of excess extracellular potassium. *Neurochem. Int.* 36, 291–300. doi: 10.1016/s0197-0186(99)00137-0

Wasseff, S. K., and Scherer, S. S. (2011). Cx32 and Cx47 mediate oligodendrocyte:astrocyte and oligodendrocyte:oligodendrocyte gap junction coupling. *Neurobiol. Dis.* 42, 506–513. doi: 10.1016/j.nbd.2011.03.003

Wasseff, S. K., and Scherer, S. S. (2015). Activated immune response in an inherited leukodystrophy disease caused by the loss of oligodendrocyte gap junctions. *Neurobiol. Dis.* 82, 86–98. doi: 10.1016/j.nbd.2015.05.018

Xu, D., Liu, Z., Wang, S., Peng, Y., and Sun, X. (2017). Astrocytes regulate the expression of Sp1R3 on oligodendrocyte progenitor cells through Cx47 and promote their proliferation. *Biochem. Biophys. Res. Commun.* 490, 670–675. doi: 10.1016/j.bbrc.2017.06.099

Xu, G., Wang, W., and Zhou, M. (2014). Spatial organization of NG2 glial cells and astrocytes in rat hippocampal CA1 region. *Hippocampus* 24, 383–395. doi: 10.1002/hipo.22232

Zlomuzica, A., Tress, O., Binder, S., Rovira, C., Willecke, K., and Dere, E. (2012). Changes in object recognition and anxiety-like behaviour in mice expressing a Cx47 mutation that causes Pelizaeus-Merzbacher-like disease. *Dev. Neurosci.* 34, 277–287. doi: 10.1159/000339305

Conflict of Interest Statement: The authors declare that the research was conducted in the absence of any commercial or financial relationships that could be construed as a potential conflict of interest.

frontiers in Cellular Neuroscience

MINI REVIEW
published: 01 March 2019
doi: 10.3389/fncel.2019.00069

Role of Connexin-Based Gap Junction Channels in Communication of Myelin Sheath in Schwann Cells

Bruno A. Cisterna[1,2], Pablo Arroyo[3] and Carlos Puebla[4]**

[1]Escuela de Medicina, Universidad de Talca, Talca, Chile, [2]Centro para el Desarrollo de la Nanociencia y Nanotecnología (CEDENNA), Universidad de Santiago de Chile, Santiago, Chile, [3]Facultad de Medicina, Pontificia Universidad Católica de Chile, Santiago, Chile, [4]Instituto de Ciencias Biomédicas, Facultad de Ciencias de la Salud, Universidad Autónoma de Chile, Santiago, Chile

Peripheral nerves have the capacity to conduct action potentials along great distances and quickly recover following damage which is mainly due to Schwann cells (SCs), the most abundant glial cells of the peripheral nervous system (PNS). SCs wrap around an axonal segment multiple times, forming a myelin sheath, allowing for a significant increase in action potential conduction by insulating the axons. Mature myelin consists of compact and non-compact (or cytoplasmic) myelin zones. Non-compact myelin is found in paranodal loops bordering the nodes of Ranvier, and in the inner and outermost cytoplasmic tongues and is the region in which Schmidt-Lanterman incisures (SLI; continuous spirals of overlapping cytoplasmic expansions within areas of compact myelin) are located. Using different technologies, it was shown that the layers of non-compact myelin could be connected to each other by gap junction channels (GJCs), formed by connexin 32 (Cx32), and their relative abundance allows for the transfer of ions and different small molecules. Likewise, Cx29 is expressed in the innermost layer of the myelin sheath. Here it does not form GJCs but colocalizes with K_v1, which implies that the SCs play an active role in the electrical condition in mammals. The critical role of GJCs in the functioning of myelinating SCs is evident in Charcot-Marie-Tooth disease (CMT), X-linked form 1 (CMTX1), which is caused by mutations in the *gap junction protein beta 1* (*GJB1*) gene that codes for Cx32. Although the management of CMT symptoms is currently supportive, there is a recent method for targeted gene delivery to myelinating cells, which rescues the phenotype in KO-Cx32 mice, a model of CMTX1. In this mini-review article, we discuss the current knowledge on the role of Cxs in myelin-forming SCs and summarize recent discoveries that may become a real treatment possibility for patients with disorders such as CMT.

Keywords: connexins, gap junction channels, myelin sheath, Schmidt-Lanterman incisure, Charcot-Marie-Tooth disease, CMTX1

OPEN ACCESS

Edited by:
Marion Baraban,
University of Edinburgh,
United Kingdom

Reviewed by:
Mario Bortolozzi,
University of Padua, Italy
John E. Rash,
Colorado State University,
United States
Georg Zoidl,
York University, Canada

****Correspondence:***
Bruno A. Cisterna
bcisterna@uc.cl
Carlos Puebla
carlos.puebla@uautonoma.cl

Received: *15 September 2018*
Accepted: *12 February 2019*
Published: *01 March 2019*

Citation:
Cisterna BA, Arroyo P and Puebla C (2019) Role of Connexin-Based Gap Junction Channels in Communication of Myelin Sheath in Schwann Cells. Front. Cell. Neurosci. 13:69. doi: 10.3389/fncel.2019.00069

MYELINATING SCHWANN CELLS

The ability of peripheral nerves to recover quickly after damage is mostly due to the plasticity of Schwann cells (SCs; Boerboom et al., 2017). SCs are the principal glia of the peripheral nervous system (PNS; Fehmi et al., 2018). In the development of vertebrate PNS, SCs are derived from neural crest cells that differentiate into SC precursors and then into immature SCs (Jessen and Mirsky, 2005; Boerboom et al., 2017). The process of myelination begins around birth, where SCs cover axons that are larger than ∼1 μm in diameter (Fehmi et al., 2018).

Myelinating SCs allow for the fast conduction of action potentials by the axons (Jessen and Mirsky, 2005; Boerboom et al., 2017). Each myelin internode is flanked by the nodes of Ranvier, which are bare patches of the axon plasma membrane that are enriched in voltage-gated Na^+ channels (essential for saltatory conduction). In turn, K^+ channels are clustered at the juxtaparanodal region of the axon. Thus, the two primary types of ion channels are separated by the paranode (Poliak and Peles, 2003).

An essential process in a functional interaction between axons and SCs, is myelin formation. The molecules that mediate axonal–glial interactions along the internode have been described (Trapp, 1990; Martini and Carenini, 1998; Maurel et al., 2007; Hayashi et al., 2008; Chen et al., 2016). The myelin-associated glycoprotein (MAG), a cell adhesion molecule member of the Ig-superfamily—expressed by myelinating SCs and oligodendrocytes [equivalent to the SCs but located in the central nervous system (CNS)]—has been localized in the internode (Trapp, 1990; Maurel et al., 2007). This protein interacts with several axonal components (Hannila et al., 2007), and it is crucial for the maintenance of myelin, evidenced by the degeneration of myelin and axons in MAG-deficient mice (Martini and Carenini, 1998). In the later stages of myelination, MAG is also found in Schmidt-Lanterman incisures (SLI; Maurel et al., 2007). Additionally, connexin 32 (Cx32) is another component type involved in the maintenance of myelination, which does not belong to the Ig-superfamily (Martini and Carenini, 1998).

Recently, it was reported that nectins and nectin-like molecules (Necl) are required for the axon–glial interactions along the internode through heterophilic interactions. In particular, for cell-cell context, both neurons and SCs express different sets of Necl proteins: axons express Necl-1 and Necl-2, and SCs express Necl-4 and some Necl-2. The main binding protein detected between axon and SCs was Necl-1 and Necl-4 (Maurel et al., 2007). Necl-1 activity involves the PI3 kinase/Akt signaling cascade (Chen et al., 2016). Moreover, Necl-1, Necl-2, and Necl-4 are also expressed at high levels in the SLI of myelinating SCs (Maurel et al., 2007).

THE ISSUE OF INTRACELLULAR COMMUNICATION IN MYELINATED SCHWANN CELLS

It has been proposed that the number of myelin lamellae in the sheath is directly proportional to the axonal circumference, for example, over the range of 10–80 lamellae in the sciatic and vagus nerves of mice (Friede and Samorajski, 1967), or 18–24 in the optic nerve in humans (Friede and Hu, 1967). A significant amount of myelin membrane has been proposed to increase the axonal membrane resistance and decrease the capacitance, increasing the conduction velocity. According to some estimates, myelinating SCs may produce up to 20 mm^2 of compacted membrane around the largest axons, about 2,000 times more than typical epithelial cells (Kidd et al., 2013). This massive amount of membrane, concentrated in a small area is a challenge for the communication of the cell itself. The myelinating SCs manages this issue by separating the myelin in two distinct domains, compact myelin, and non-compact (or cytoplasmic) myelin (Kidd et al., 2013).

Compact myelin is a compact membrane spiral, with a periodicity of 13–18 nm per turn (Fernandez-Moran and Finean, 1957; Kirschner and Sidman, 1976), which begins and ends with the apposition of the SC plasma membrane against itself to form the inner mesaxon and the outer mesaxon. Compact myelin has a high (∼70%) lipid content and is enriched in galactosphingolipids, saturated long-chain fatty acids and cholesterol (Saher and Simons, 2010), while it has a low protein content with a very low protein diversity; mainly P0 protein, maltose-binding protein (MBP), and peripheral myelin protein 22 (PMP22). Non-compact myelin is in paranodal loops (cytoplasmic extensions located in the lateral margins of the SCs, bordering nodes of Ranvier), and in SLI (continuous spirals of overlapping cytoplasmic expansions within areas of compact myelin), and in the inner and outermost cytoplasmic tongues. While, compaction of myelin removes the aqueous components of the cytoplasm, favoring electric conduction but hindering cellular processes such as intracellular communication, non-compact compartments concentrate the organelles and the necessary components for the cellular operation.

A pioneering observation of the myelin sheath, made using freeze-fracture electron microscopy, reported gap junction channels (GJCs)-like structures in the membrane of the mesaxons, paranodal loops and SLI (Mugnaini et al., 1977; Sandri et al., 1977; Bertaud, 1978; Tetzlaff, 1982). Likewise, the diffusion of fluorescent dyes across the cytoplasmic layers, primarily at SLI, suggest that GJCs provides a direct radial pathway for the transport of ions and small metabolites across the myelin sheath (Balice-Gordon et al., 1998). Then, considering that the unrolled myelin sheath is more than 4 mm long, while the compact myelin sheath is less than 4 μm thick (Friede and Bischhausen, 1980), this potential radial pathway would be more than 1,000-fold shorter than the circumferential pathway (Scherer et al., 1995; Kleopa et al., 2010). For diffusion time, it was proposed that the radial pathway is one million times faster than the circumferential pathway, because, in theory, the diffusion time in a plane is proportional to the square of the distance (Balice-Gordon et al., 1998). However, this investigation has some limitations, for example, the authors assumed that the ions showed a very slow velocity in circumferential diffusion, but they did not measure this pathway nor did they measure the rate of diffusion within the incisures. It is therefore difficult to determine that the radial pathway will be x-fold faster than the circumferential pathway, in fact, the most important real contribution is providing functional evidence, i.e., injection of sciatic nerve fibers, that GJCs mediate a radial pathway.

GAP JUNCTION CHANNELS IN MYELINATING SCHWANN CELLS

GJCs connect adjacent cells (heterocellular) and isolated segments of the same cell (autocellular) and allow the diffusion of ions and small molecules across apposed cell membranes expressed in vertebrates (Sáez et al., 2003a). The single channel

is formed by the interaction of two apposed hemichannels (HCs) or connexons, each of which is composed of six connexins (Cxs) arranged radially around a central pore (Sosinsky, 1996; Unger et al., 1997). It is worth mentioning that, Cx HCs are semipermeable channels that may allow the passage of small molecules such as ATP (Wang et al., 2013), IP3 and cAMP (Hernandez et al., 2007), NAD^+ (Bruzzone et al., 2001), and glutamate (Sáez et al., 2003b; Ye et al., 2003), and the passage of ions driven by their electrochemical gradients (Sáez et al., 2005). Cxs are transmembrane proteins that belong to a multigene family with 20 and 21 members in the mouse and human genome, respectively (Söhl and Willecke, 2003). Each Cx HCs can be formed by a single type of Cx (homomeric) or possibly by two or even three Cxs (heteromeric). The GJCs formation can then give rise to homotypic or heterotypic intercellular channels, when they are the same or different Cxs in apposed cells (Jiang and Goodenough, 1996; Koval et al., 2014). Every one of these channel combinations displays different permeability properties and are regulated differently (Weber et al., 2004). Thus, Cxs diversity provides essential variations in cell-to-cell communication.

The presence of the Cx32 is well documented by immunocytochemistry in inner mesaxons, at paranodal loops and SLI of the myelin sheath (Bergoffen et al., 1993a; Scherer et al., 1995; Spray and Dermietzel, 1995). Likewise, these findings were confirmed by freeze-fracture replica immunogold labeling (FRIL). Cx32 is also present at the two outer layers of myelin, suggesting that Cx32 forms GJCs between the non-compact layers of the SCs myelin sheath (Meier et al., 2004).

The Cxs play a critical role in the functioning of the myelinating SCs. Indeed, mutations in the human gene *gap junction protein beta 1* (*GJB1*), which encodes Cx32, lead to the pathological phenotype of the X-chromosomal form of Charcot-Marie-Tooth (CMT1X or CMTX1), where inflammatory processes in peripheral nerves decrease conduction velocity of action potentials, leading to muscle atrophy (Bergoffen et al., 1993a; Fischbeck et al., 1996; Abrams et al., 2002). This disease is the second most common form of hereditary motor and sensory neuropathy, and there is no cure (Kleopa et al., 2012). Despite the abundant evidence that relates the absence or altered function of Cx directly to CMT1X, the role of Cxs in myelin physiology remains poorly understood.

Cx32 has multifaceted functions described in glial cells in the CNS (Abrams, 2017) and PNS (Bortolozzi, 2018). Recent evidence indicated the expression of functional Cx32 HCs that release ATP during electrical stimulation on mice sciatic nerves, which from cultured SCs, by depolarization evoked through a high extracellular potassium concentration (Nualart-Marti et al., 2013). ATP release was then significantly decreased after the sciatic nerve was treated with HCs inhibitors (octanol or carbenoxolone) or after silencing Cx32 from cultured SCs, suggesting that purinergic mediated signaling could contribute to intracellular communication (Nualart-Marti et al., 2013). On the other hand, Ca^{2+} waves do not seem to utilize GJCs in glial cells of the brain. Instead, Ca^{2+} waves are propagated by an alternative extracellular mechanism, involving ATP release and possibly requiring Cx HC activity (Bennett et al., 2003; Nedergaard et al., 2003), suggesting that Ca^{2+} waves may be propagated by an ATP-induced ATP release mechanism. However, the functions of HCs in myelinating SC still needs to be demonstrated. The Cx32 is even involved in the proliferation of SCs, related to neuregulin-1, which does not involve Cx32-mediated intercellular communication (Freidin et al., 2009). Likewise, mice lacking Cx32 display features of CMTX, such as onion bulb formation and slow nerve conduction in myelinating SC (Anzini et al., 1997; Scherer et al., 1998). Moreover, cultured SCs, from Cx32-null mice, are still electrically coupled and even allow diffusion of fluorescent dye (Zhao et al., 1999), implying the presence of other Cxs forming gap junctions (Balice-Gordon et al., 1998).

Connexin 29 (Cx29), a 29-kDa protein (and equivalent to human ortholog Cx31.3; Söhl and Willecke, 2003) was also found in the myelin sheath, by freeze-FRIL, but only in the innermost layer, in close association with the hexagonally arranged intramembrane particle (IMP) "rosettes" in axolemma of large myelinated axons (Li et al., 2002). Similarly, through immunofluorescence (IF), Cx29 was localized in the innermost layer of the myelin sheath, in the paranode and juxtaparanode, tightly colocalized with $K_v1.2$ channels in the axolemma (Altevogt et al., 2002). Recently, through IF and FRIL, $K_v1.1/K_v1.2$ channels were identified within the axonal rosette in rodent sciatic nerve and the molecular coalignment 1:1 with Cx29 was proposed to form a xenotypic channel (Rash et al., 2016). On the other hand, K^+ conductance occurs neither in the perinodal, nor in the submyelinic extracellular spaces, as previously envisioned; it is now proposed to occur in the innermost myoplasm of SCs, which is electrically isolated by the myelin plasma membrane (Rash, 2010). Likewise, the proposed K^+ recycling from axoplasm to myoplasm to axoplasm could be energetically cheaper than using Na^+-K^+ ATPase to axoplasmic replacement. This axon-to-glia linkage implies that myelin may play an electrically active role that underlies both the faster axonal repolarization and the faster conduction velocity of mammalian myelinated axon. However, Cx29 does not prevent the development of demyelinating neuropathy in Cx32-null mice (Scherer et al., 1998), or in Cx32 mutant mice (Jeng et al., 2006; Sargiannidou et al., 2009). Although Cx29 may form HCs (Ahn et al., 2008), these Cx proteins do not form GJCs (in Xenopus oocytes or N2A cells), but at least *in vitro*, it may modify the properties of Cx32 GJCs (Altevogt et al., 2002).

Other Cx proteins, such as Cx26, Cx43 and Cx46, have also been reported to be expressed in SCs (Chandross et al., 1996a,b; Yoshimura et al., 1996; Mambetisaeva et al., 1999; Li et al., 2007), but there are no published data that currently establishes any of these Cxs in SCs. In particular Cx43, together with Cx29 and Cx32 are present during SCs development in mice and displayed a consecutive onset of expression (Li et al., 2007). Similarly, it has been suggested that Cx43 and Cx46 could coordinate cellular responses of SCs after a peripheral nerve's injury (Chandross et al., 1996a,b).

In summary, Cx32 and Cx29 are the main Cxs detectable in myelinating SCs in an asymmetric subcellular distribution, with a partial overlapping distribution. Cx32 was found to be concentrated in GJCs on the nuclear end of the

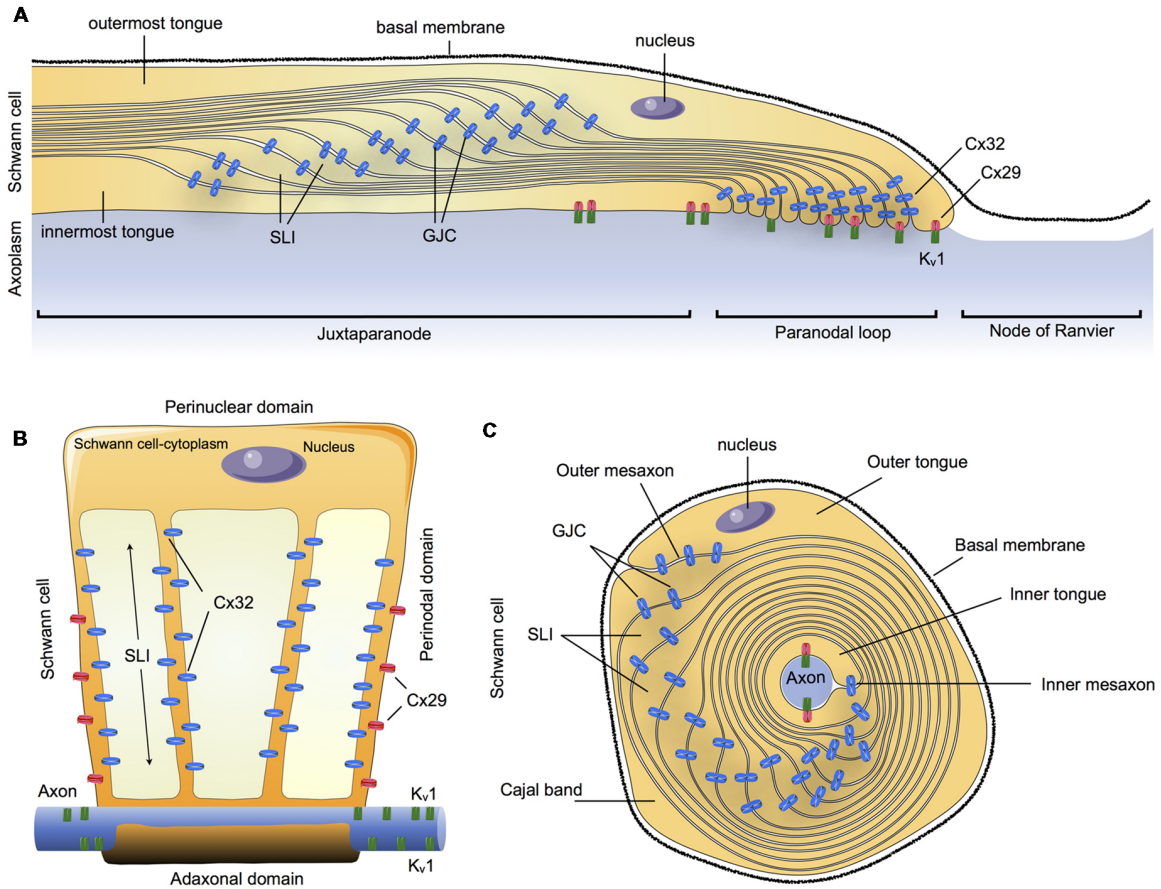

FIGURE 1 | Schematic summary of connexins (Cxs) in the communication of myelin sheath in Schwann cells (SCs). **(A)** Longitudinal view of myelinated SCs showing the different compartments: outermost tongue, innermost tongue, Schmidt-Lanterman incisures (SLI) and the distribution of the connexins forming gap junction channels (GJCs) or hemichannels (HCs) formed by Cxs (Cx HCs) along the juxtaparanode, paranodal loop or the node of Ranvier. **(B)** Myelinated SCs unwrapped from the axon it invests. **(C)** Transversal view. Cx29, connexin29; Cx32, connexin 32; K_v1, Potassium voltage-gated channel subfamily 1.

myelin (abaxonal), whereas Cx29 form HCs was found to be concentrated closer to the paranodal loop and axon (abaxonal). This suggests that they could both contribute to reflexive junctions across the myelin sheath, speeding up communication through the myelin layers that separate the adaxonal and the abaxonal cytoplasm (**Figure 1**).

DISEASES ASSOCIATED WITH DYSFUNCTION OF CONNEXINS IN SCHWANN CELLS

Charcot-Marie-Tooth disease (CMT) is a large group of disorders caused by different types of mutations in several genes whose protein are expressed in myelin and/or axonal structures within PNS (Lupski, 1999; Kamholz et al., 2000). Usually, the initial symptoms of CMT are distal weakness and muscle atrophy, manifesting with foot drop and pes cavus. Also, sensory symptoms are often present but tend to be less prominent. Later, these patients present foot deformities, such as hammertoes, together with hand weakness and atrophy (Saporta, 2014).

The categories of CMT are CMT types 1 through 7, as well as an X-linked category, CMTX. Then, there are X-linked dominant and recessive forms of CMT involving different loci. Together, the X-linked forms account for 10% to 15% of all CMT cases (Ouvrier et al., 2007). CMTX1, the X-linked dominant form of CMT, is the second most common form of CMT and the first X-linked form of CMT, with 7% to 12%, and 50% of all CMT cases and X-linked cases, respectively (Boerkoel et al., 2002; Huttner et al., 2006; Ouvrier et al., 2007; Pareyson and Marchesi, 2009; Fridman et al., 2015).

CMTX1 symptoms are more prominent in boys, who present gait problems in infancy or later in childhood (e.g., toe walking, flat-footed walking, falls, difficulty running; Yiu et al., 2011). Less common features include tremors, hand weakness, and sensorineural deafness. Reflexes are lost at the ankles in all cases, whereas patellar reflexes are retained in half of the cases in girls. The neuropathy may be asymmetric and therefore mimic an acquired immune-mediated neuropathy (Saporta, 2014). Typically, the pathophysiology of CMTX1 includes features of both demyelination and axon loss, and this is reflected in neurophysiologic studies. Nerve conduction velocities are

moderately slowed (Nicholson and Nash, 1993). Demyelination and axonal loss are observed histologically, but onion bulb formation is minimal.

CMTX1 is caused by mutations in the *GJB1* gene, i.e., Cx32 gene, on chromosome Xq13.1 (Hahn et al., 1990; Bergoffen et al., 1993a,b; Keller and Chance, 1999). Most *GJB1* mutations cause disability through the loss of function of Cx32 (Bruzzone et al., 1994; Kleopa et al., 2012). In particular, Cx32 mutations related to CMTX1 could be organized into five classes: (1) Cx32 protein is not synthesized; (2) mutant Cx32 protein has a reduced expression (with a normal transcription), (3) mutant Cx32 protein has a normal expression but is not transported to the plasma membrane; (4) mutant Cx32 protein forms HCs but not functional GJCs; and (5) mutant Cx32 protein forms GJCs and HCs with altered electrical, gating or permeability properties (Bortolozzi, 2018).

It is worth mentioning that some mutants that appear as "functional," with respect to the WT model, cause severe phenotypes of CMTX1. This issue may be explained by the fact that in most of the studies only the activity of GJCs was evaluated, without considering the gating/permeability dysfunction of mutant Cx32 HCs. Recently, an investigation uncovered that the loss of the C-terminus in Cx32 (R220X mutation), inhibits Cx32 HCs gating. However, it does not significantly alter the intercellular diffusion mediated by GJCs: the unitary permeabilities to ions, signaling molecules (cAMP) or larger solutes (Lucifer yellow) concerning the wild-type (Carrer et al., 2018). These findings support the hypothesis that paracrine signaling alteration, due to Cx32 HCs dysfunction, underlies CMTX1 pathogenesis.

Although it is described that two linked connexons, i.e., a GJCs, may contain the same connexin proteins, or different ones, an interesting case has been described, in myelinated axons, where a Cx29-based connexon is linked to a K^+ channel (Rash et al., 2016; Traub et al., 2018). This xenotypic channel could be helpful to understand why Cx29 KO mice do not show important neuropathic symptoms, such as Cx32 KO. First, the formation of axolemmal rosettes is an inherent property of K_V1 channels, does not depend on a linkage with Cx29 (Rash et al., 2016), so it is possible to suggest that in the absence of Cx29 it is still present in "half" of the activity of this xenotypic channel. Second, the absence of the Cx32 protein necessarily involves a total loss of Cx32-based channel activity in myelinated cells, with no compensation from other Cx proteins (Sargiannidou et al., 2009), so the absence of Cx32 would lead to worse results than the absence of Cx29. It was also recently proposed that Cx32 HCs could underlie CMTX1 by altering the purinergic signaling controlling SCs myelination (Nualart-Marti et al., 2013; Carrer et al., 2018). Additionally, if we consider that a heteromeric mixing of Cx29 and Cx32 (i.e., Cx32-Cx29/Cx32-Cx32) produced channels with properties different from those of Cx32 alone (Altevogt et al., 2002), in cases of Cx32 mutations, an unexplored (and speculative) possibility is that these mutations can change the affinity of Cx32 for Cx29 and these "new" connexons could be involved in different failures of Cx32 GJCs activity. The Cx32 protein then becomes an essential protein in the physiology of PNS (Bortolozzi, 2018).

Finally, considering that the current "treatments" include only palliative care, it is necessary to advance new therapies. A recent study obtained a cell-specific expression of Cx32 in up to 50% of SCs, in multiple lumbar spinal roots and peripheral nerves, after a single intrathecal gene delivery into adult *GJB1*-KO mice. Thus, treated mice showed a reduced amount of demyelinated fibers and inflammatory cells with motor performance, quadriceps muscle contractility, and sciatic nerve conduction velocities improved (Kagiava et al., 2016). The same gene therapy was performed in CMT1X mice expressing different Cx32 mutants, which showed different results, as CMT1X mutants may interfere with gene addition therapy (Kagiava et al., 2018). A better approach may be one that does not incorporate the genome but leads to permanent modification of the targeted genetic defect. In this regard, recent reports of treating mouse models of Duchenne muscular dystrophy, with adeno-associated viral vectors, which are not integrated into the genome, is promising. This method used the clustered regularly interspaced short palindromic repeats system (CRISPR)-Cas9 to target and eliminate mutant exons of dystrophin (Nelson et al., 2016; Tabebordbar et al., 2016). In summary, the actual data suggest that gene therapy might become a realistic possibility for patients with these disorders.

CONCLUSIONS

Myelinating SCs and peripheral axons present an interesting example of two specialized cells, where each is indispensable for the functioning of the other. In this sense, the communication through GJCs is a significant evolutionary advance which can solve the issue of the reflexive GJs in the myelinating SCs. This cellular specialization has also led to the differential expression and specific roles of Cx29 and Cx32. In particular, CMTX1 is a clear example of diseases that are caused by mutations in only one GJ gene (Cx32), and despite this broad expression pattern, peripheral neuropathy is the main clinical manifestation. Since several mutations of the Cx32 gene in SCs lead to lasting and severe motor and neurological problems, the search for curative treatment points towards gene therapies in an attempt to replace the defective gene. These approaches however, have their limitations because of toxicity from random integrations in the genome.

AUTHOR CONTRIBUTIONS

CP and BC conceived, researched and wrote this review article. PA assisted in writing and editing.

FUNDING

This work was supported by FONDECYT no. 11160536 (CP) and no. 3170938 (BC).

ACKNOWLEDGMENTS

We thank the Universidad Autónoma de Chile.

REFERENCES

Abrams, C. K. (2017). Diseases of connexins expressed in myelinating glia. *Neurosci. Lett.* doi: 10.1016/j.neulet.2017.05.037 [Epub ahead of print].

Abrams, C. K., Bennett, M. V., Verselis, V. K., and Bargiello, T. A. (2002). Voltage opens unopposed gap junction hemichannels formed by a connexin 32 mutant associated with X-linked Charcot-Marie-Tooth disease. *Proc. Natl. Acad. Sci. U S A* 99, 3980–3984. doi: 10.1073/pnas.261713499

Ahn, M., Lee, J., Gustafsson, A., Enriquez, A., Lancaster, E., Sul, J. Y., et al. (2008). Cx29 and Cx32, two connexins expressed by myelinating glia, do not interact and are functionally distinct. *J. Neurosci. Res.* 86, 992–1006. doi: 10.1002/jnr.21561

Altevogt, B. M., Kleopa, K. A., Postma, F. R., Scherer, S. S., and Paul, D. L. (2002). Connexin29 is uniquely distributed within myelinating glial cells of the central and peripheral nervous systems. *J. Neurosci.* 22, 6458–6470. doi: 10.1523/JNEUROSCI.22-15-06458.2002

Anzini, P., Neuberg, D. H., Schachner, M., Nelles, E., Willecke, K., Zielasek, J., et al. (1997). Structural abnormalities and deficient maintenance of peripheral nerve myelin in mice lacking the gap junction protein connexin 32. *J. Neurosci.* 17, 4545–4551. doi: 10.1523/JNEUROSCI.17-12-04545.1997

Balice-Gordon, R. J., Bone, L. J., and Scherer, S. S. (1998). Functional gap junctions in the schwann cell myelin sheath. *J. Cell Biol.* 142, 1095–1104. doi: 10.1083/jcb.142.4.1095

Bennett, M. V., Contreras, J. E., Bukauskas, F. F., and Sáez, J. C. (2003). New roles for astrocytes: gap junction hemichannels have something to communicate. *Trends Neurosci.* 26, 610–617. doi: 10.1016/j.tins.2003.09.008

Bergoffen, J., Scherer, S. S., Wang, S., Scott, M. O., Bone, L. J., Paul, D. L., et al. (1993a). Connexin mutations in X-linked Charcot-Marie-Tooth disease. *Science* 262, 2039–2042. doi: 10.1126/science.8266101

Bergoffen, J., Trofatter, J., Pericak-Vance, M. A., Haines, J. L., Chance, P. F., and Fischbeck, K. H. (1993b). Linkage localization of X-linked Charcot-Marie-Tooth disease. *Am. J. Hum. Genet.* 52, 312–318.

Bertaud, W. S. (1978). Membrane junctions in the myelin sheath of goldfish lateral nerve. *J. Cell Sci.* 30, 77–85.

Boerboom, A., Dion, V., Chariot, A., and Franzen, R. (2017). Molecular Mechanisms involved in schwann cell plasticity. *Front. Mol. Neurosci.* 10:38. doi: 10.3389/fnmol.2017.00038

Boerkoel, C. F., Takashima, H., and Lupski, J. R. (2002). The genetic convergence of Charcot-Marie-Tooth disease types 1 and 2 and the role of genetics in sporadic neuropathy. *Curr. Neurol. Neurosci. Rep.* 2, 70–77. doi: 10.1007/s11910-002-0056-8

Bortolozzi, M. (2018). What's the function of connexin 32 in the peripheral nervous system? *Front. Mol. Neurosci.* 11:227. doi: 10.3389/fnmol.2018.00227

Bruzzone, S., Guida, L., Zocchi, E., Franco, L., and De Flora, A. (2001). Connexin 43 hemi channels mediate Ca^{2+}-regulated transmembrane NAD^{+} fluxes in intact cells. *FASEB J.* 15, 10–12. doi: 10.1096/fj.00-0566fje

Bruzzone, R., White, T. W., Scherer, S. S., Fischbeck, K. H., and Paul, D. L. (1994). Null mutations of connexin32 in patients with X-linked Charcot-Marie-Tooth disease. *Neuron* 13, 1253–1260. doi: 10.1016/0896-6273(94)90063-9

Carrer, A., Leparulo, A., Crispino, G., Ciubotaru, C. D., Marin, O., Zonta, F., et al. (2018). Cx32 hemichannel opening by cytosolic Ca^{2+} is inhibited by the R220X mutation that causes Charcot-Marie-Tooth disease. *Hum. Mol. Genet.* 27, 80–94. doi: 10.1093/hmg/ddx386

Chandross, K. J., Kessler, J. A., Cohen, R. I., Simburger, E., Spray, D. C., Bieri, P., et al. (1996a). Altered connexin expression after peripheral-nerve injury. *Mol. Cell. Neurosci.* 7, 501–518. doi: 10.1006/mcne.1996.0036

Chandross, K. J., Spray, D. C., Cohen, R. I., Kumar, N. M., Kremer, M., Dermietzel, R., et al. (1996b). TNF α inhibits Schwann cell proliferation, connexin46 expression, and gap junctional communication. *Mol. Cell. Neurosci.* 7, 479–500. doi: 10.1006/mcne.1996.0035

Chen, M. S., Kim, H., Jagot-Lacoussiere, L., and Maurel, P. (2016). Cadm3 (Necl-1) interferes with the activation of the PI3 kinase/Akt signaling cascade and inhibits Schwann cell myelination *in vitro*. *Glia* 64, 2247–2262. doi: 10.1002/glia.23072

Fehmi, J., Scherer, S. S., Willison, H. J., and Rinaldi, S. (2018). Nodes, paranodes and neuropathies. *J. Neurol. Neurosurg. Psychiatry* 89, 61–71. doi: 10.1136/jnnp-2016-315480

Fernandez-Moran, H., and Finean, J. B. (1957). Electron microscope and low-angle x-ray diffraction studies of the nerve myelin sheath. *J. Biophys. Biochem. Cytol.* 3, 725–748. doi: 10.1083/jcb.3.5.725

Fischbeck, K. H., Deschênes, S. M., Bone, L. J., and Scherer, S. S. (1996). Connexin32 and X-linked Charcot-Marie-Tooth disease. *Cold Spring Harb. Symp. Quant. Biol.* 61, 673–677. doi: 10.1101/SQB.1996.061.01.067

Freidin, M., Asche, S., Bargiello, T. A., Bennett, M. V., and Abrams, C. K. (2009). Connexin 32 increases the proliferative response of Schwann cells to neuregulin-1 (Nrg1). *Proc. Natl. Acad. Sci. U S A* 106, 3567–3572. doi: 10.1073/pnas.0813413106

Fridman, V., Bundy, B., Reilly, M. M., Pareyson, D., Bacon, C., Burns, J., et al. (2015). CMT subtypes and disease burden in patients enrolled in the Inherited Neuropathies Consortium natural history study: a cross-sectional analysis. *J. Neurol. Neurosurg. Psychiatry* 86, 873–878. doi: 10.1136/jnnp-2014-308826

Friede, R. L., and Bischhausen, R. (1980). The precise geometry of large internodes. *J. Neurol. Sci.* 48, 367–381. doi: 10.1016/0022-510X(80)90109-4

Friede, R. L., and Hu, K. H. (1967). Increase in cholesterol along human optic nerve. *J. Neurochem.* 14, 307–315. doi: 10.1111/j.1471-4159.1967.tb09528.x

Friede, R. L., and Samorajski, T. (1967). Relation between the number of myelin lamellae and axon circumference in fibers of vagus and sciatic nerves of mice. *J. Comp. Neurol.* 130, 223–231. doi: 10.1002/cne.901300304

Hahn, A. F., Brown, W. F., Koopman, W. J., and Feasby, T. E. (1990). X-linked dominant hereditary motor and sensory neuropathy. *Brain* 113, 1511–1525. doi: 10.1093/brain/113.5.1511

Hannila, S. S., Siddiq, M. M., and Filbin, M. T. (2007). Therapeutic approaches to promoting axonal regeneration in the adult mammalian spinal cord. *Int. Rev. Neurobiol.* 77, 57–105. doi: 10.1016/s0074-7742(06)77003-9

Hayashi, A., Moradzadeh, A., Tong, A., Wei, C., Tuffaha, S. H., Hunter, D. A., et al. (2008). Treatment modality affects allograft-derived Schwann cell phenotype and myelinating capacity. *Exp. Neurol.* 212, 324–336. doi: 10.1016/j.expneurol.2008.04.018

Hernandez, V. H., Bortolozzi, M., Pertegato, V., Beltramello, M., Giarin, M., Zaccolo, M., et al. (2007). Unitary permeability of gap junction channels to second messengers measured by FRET microscopy. *Nat. Methods* 4, 353–358. doi: 10.1038/nmeth1031

Huttner, I. G., Kennerson, M. L., Reddel, S. W., Radovanovic, D., and Nicholson, G. A. (2006). Proof of genetic heterogeneity in X-linked Charcot-Marie-Tooth disease. *Neurology* 67, 2016–2021. doi: 10.1212/01.wnl.0000247271.40782.b7

Jeng, L. J., Balice-Gordon, R. J., Messing, A., Fischbeck, K. H., and Scherer, S. S. (2006). The effects of a dominant connexin32 mutant in myelinating Schwann cells. *Mol. Cell. Neurosci.* 32, 283–298. doi: 10.1016/j.mcn.2006.05.001

Jessen, K. R., and Mirsky, R. (2005). The origin and development of glial cells in peripheral nerves. *Nat. Rev. Neurosci.* 6, 671–682. doi: 10.1038/nrn1746

Jiang, J. X., and Goodenough, D. A. (1996). Heteromeric connexons in lens gap junction channels. *Proc. Natl. Acad. Sci. U S A* 93, 1287–1291. doi: 10.1073/pnas.93.3.1287

Kagiava, A., Karaiskos, C., Richter, J., Tryfonos, C., Lapathitis, G., Sargiannidou, I., et al. (2018). Intrathecal gene therapy in mouse models expressing CMT1X mutations. *Hum. Mol. Genet.* 27, 1460–1473. doi: 10.1093/hmg/ddy056

Kagiava, A., Sargiannidou, I., Theophilidis, G., Karaiskos, C., Richter, J., Bashiardes, S., et al. (2016). Intrathecal gene therapy rescues a model of demyelinating peripheral neuropathy. *Proc. Natl. Acad. Sci. U S A* 113, E2421–E2429. doi: 10.1073/pnas.1522202113

Kamholz, J., Menichella, D., Jani, A., Garbern, J., Lewis, R. A., Krajewski, K. M., et al. (2000). Charcot-Marie-Tooth disease type 1: molecular pathogenesis to gene therapy. *Brain* 123, 222–233. doi: 10.1093/brain/123.2.222

Keller, M. P., and Chance, P. F. (1999). Inherited peripheral neuropathy. *Semin. Neurol.* 19, 353–362. doi: 10.1055/s-2008-1040850

Kidd, G. J., Ohno, N., and Trapp, B. D. (2013). Biology of Schwann cells. *Handb. Clin. Neurol.* 115, 55–79. doi: 10.1016/B978-0-444-52902-2.00005-9

Kirschner, D. A., and Sidman, R. L. (1976). X-ray diffraction study of myelin structure in immature and mutant mice. *Biochim. Biophys. Acta* 448, 73–87. doi: 10.1016/0005-2736(76)90077-8

Kleopa, K. A., Abrams, C. K., and Scherer, S. S. (2012). How do mutations in GJB1 cause X-linked Charcot-Marie-Tooth disease? *Brain Res.* 1487, 198–205. doi: 10.1016/j.brainres.2012.03.068

Kleopa, K. A., Orthmann-Murphy, J., and Sargiannidou, I. (2010). Gap junction disorders of myelinating cells. *Rev. Neurosci.* 21, 397–419. doi: 10.1515/revneuro.2010.21.5.397

Koval, M., Molina, S. A., and Burt, J. M. (2014). Mix and match: investigating heteromeric and heterotypic gap junction channels in model systems and native tissues. *FEBS Lett.* 588, 1193–1204. doi: 10.1016/j.febslet.2014.02.025

Li, J., Habbes, H. W., Eiberger, J., Willecke, K., Dermietzel, R., and Meier, C. (2007). Analysis of connexin expression during mouse Schwann cell development identifies connexin29 as a novel marker for the transition of neural crest to precursor cells. *Glia* 55, 93–103. doi: 10.1002/glia.20427

Li, X., Lynn, B. D., Olson, C., Meier, C., Davidson, K. G., Yasumura, T., et al. (2002). Connexin29 expression, immunocytochemistry and freeze-fracture replica immunogold labelling (FRIL) in sciatic nerve. *Eur. J. Neurosci.* 16, 795–806. doi: 10.1046/j.1460-9568.2002.02149.x

Lupski, J. R. (1999). Charcot-Marie-Tooth polyneuropathy: duplication, gene dosage and genetic heterogeneity. *Pediatr. Res.* 45, 159–165. doi: 10.1203/00006450-199902000-00001

Mambetisaeva, E. T., Gire, V., and Evans, W. H. (1999). Multiple connexin expression in peripheral nerve, Schwann cells, and Schwannoma cells. *J. Neurosci. Res.* 57, 166–175. doi: 10.1002/(sici)1097-4547(19990715)57:2<166::aid-jnr2>3.3.co;2-p

Martini, R., and Carenini, S. (1998). Formation and maintenance of the myelin sheath in the peripheral nerve: roles of cell adhesion molecules and the gap junction protein connexin 32. *Microsc. Res. Tech.* 41, 403–415. doi: 10.1002/(sici)1097-0029(19980601)41:5<403::aid-jemt7>3.3.co;2-#

Maurel, P., Einheber, S., Galinska, J., Thaker, P., Lam, I., Rubin, M. B., et al. (2007). Nectin-like proteins mediate axon Schwann cell interactions along the internode and are essential for myelination. *J. Cell Biol.* 178, 861–874. doi: 10.1083/jcb.200705132

Meier, C., Dermietzel, R., Davidson, K. G., Yasumura, T., and Rash, J. E. (2004). Connexin32-containing gap junctions in Schwann cells at the internodal zone of partial myelin compaction and in Schmidt-Lanterman incisures. *J. Neurosci.* 24, 3186–3198. doi: 10.1523/JNEUROSCI.5146-03.2004

Mugnaini, E., Osen, K. K., Schnapp, B., and Friedrich, V. L. Jr. (1977). Distribution of Schwann cell cytoplasm and plasmalemmal vesicles (caveolae) in peripheral myelin sheaths. An electron microscopic study with thin sections and freeze-fracturing. *J. Neurocytol.* 6, 647–668. doi: 10.1007/bf01176378

Nedergaard, M., Ransom, B., and Goldman, S. A. (2003). New roles for astrocytes: redefining the functional architecture of the brain. *Trends Neurosci.* 26, 523–530. doi: 10.1016/j.tins.2003.08.008

Nelson, C. E., Hakim, C. H., Ousterout, D. G., Thakore, P. I., Moreb, E. A., Castellanos Rivera, R. M., et al. (2016). *In vivo* genome editing improves muscle function in a mouse model of Duchenne muscular dystrophy. *Science* 351, 403–407. doi: 10.1126/science.aad5143

Nicholson, G., and Nash, J. (1993). Intermediate nerve conduction velocities define X-linked Charcot-Marie-Tooth neuropathy families. *Neurology* 43, 2558–2564. doi: 10.1212/wnl.43.12.2558

Nualart-Marti, A., del Molino, E. M., Grandes, X., Bahima, L., Martin-Satué, M., Puchal, R., et al. (2013). Role of connexin 32 hemichannels in the release of ATP from peripheral nerves. *Glia* 61, 1976–1989. doi: 10.1002/glia.22568

Ouvrier, R., Geevasingha, N., and Ryan, M. M. (2007). Autosomal-recessive and X-linked forms of hereditary motor and sensory neuropathy in childhood. *Muscle Nerve* 36, 131–143. doi: 10.1002/mus.20776

Pareyson, D., and Marchesi, C. (2009). Diagnosis, natural history, and management of Charcot-Marie-Tooth disease. *Lancet Neurol.* 8, 654–667. doi: 10.1016/s1474-4422(09)70110-3

Poliak, S., and Peles, E. (2003). The local differentiation of myelinated axons at nodes of Ranvier. *Nat. Rev. Neurosci.* 4, 968–980. doi: 10.1038/nrn1253

Rash, J. E. (2010). Molecular disruptions of the panglial syncytium block potassium siphoning and axonal saltatory conduction: pertinence to neuromyelitis optica and other demyelinating diseases of the central nervous system. *Neuroscience* 168, 982–1008. doi: 10.1016/j.neuroscience.2009.10.028

Rash, J. E., Vanderpool, K. G., Yasumura, T., Hickman, J., Beatty, J. T., and Nagy, J. I. (2016). KV1 channels identified in rodent myelinated axons, linked to Cx29 in innermost myelin: support for electrically active myelin in mammalian saltatory conduction. *J. Neurophysiol.* 115, 1836–1859. doi: 10.1152/jn.01077.2015

Sáez, J. C., Berthoud, V. M., Branes, M. C., Martinez, A. D., and Beyer, E. C. (2003a). Plasma membrane channels formed by connexins: their regulation and functions. *Physiol. Rev.* 83, 1359–1400. doi: 10.1152/physrev.00007.2003

Sáez, J. C., Contreras, J. E., Bukauskas, F. F., Retamal, M. A., and Bennett, M. V. (2003b). Gap junction hemichannels in astrocytes of the CNS. *Acta Physiol Scand.* 179, 9–22. doi: 10.1046/j.1365-201x.2003.01196.x

Sáez, J. C., Retamal, M. A., Basilio, D., Bukauskas, F. F., and Bennett, M. V. (2005). Connexin-based gap junction hemichannels: gating mechanisms. *Biochim. Biophys. Acta* 1711, 215–224. doi: 10.1016/j.bbamem.2005.01.014

Saher, G., and Simons, M. (2010). Cholesterol and myelin biogenesis. *Subcell. Biochem.* 51, 489–508. doi: 10.1007/978-90-481-8622-8_18

Sandri, C., Van Buren, J. M., and Akert, K. (1977). Membrane morphology of the vertebrate nervous system. A study with freeze-etch technique. *Prog. Brain Res.* 46, 1–384.

Saporta, M. A. (2014). Charcot-Marie-Tooth disease and other inherited neuropathies. *Continuum* 20, 1208–1225. doi: 10.1212/01.con.0000455885.37169.4c

Sargiannidou, I., Vavlitou, N., Aristodemou, S., Hadjisavvas, A., Kyriacou, K., Scherer, S. S., et al. (2009). Connexin32 mutations cause loss of function in Schwann cells and oligodendrocytes leading to PNS and CNS myelination defects. *J. Neurosci.* 29, 4736–4749. doi: 10.1523/JNEUROSCI.0325-09.2009

Scherer, S. S., Deschenes, S. M., Xu, Y. T., Grinspan, J. B., Fischbeck, K. H., and Paul, D. L. (1995). Connexin32 is a myelin-related protein in the PNS and CNS. *J. Neurosci.* 15, 8281–8294. doi: 10.1523/JNEUROSCI.15-12-08281.1995

Scherer, S. S., Xu, Y. T., Nelles, E., Fischbeck, K., Willecke, K., and Bone, L. J. (1998). Connexin32-null mice develop demyelinating peripheral neuropathy. *Glia* 24, 8–20. doi: 10.1002/(sici)1098-1136(199809)24:1<8::aid-glia2>3.0.co;2-3

Söhl, G., and Willecke, K. (2003). An update on connexin genes and their nomenclature in mouse and man. *Cell Commun Adhes.* 10, 173–180. doi: 10.1080/714040423

Sosinsky, G. E. (1996). Molecular organization of gap junction membrane channels. *J. Bioenerg. Biomembr.* 28, 297–309. doi: 10.1007/bf02110106

Spray, D. C., and Dermietzel, R. (1995). X-linked dominant Charcot-Marie-Tooth disease and other potential gap-junction diseases of the nervous system. *Trends Neurosci.* 18, 256–262. doi: 10.1016/0166-2236(95)93911-g

Tabebordbar, M., Zhu, K., Cheng, J. K. W., Chew, W. L., Widrick, J. J., Yan, W. X., et al. (2016). *In vivo* gene editing in dystrophic mouse muscle and muscle stem cells. *Science* 351, 407–411. doi: 10.1126/science.aad5177

Tetzlaff, W. (1982). Tight junction contact events and temporary gap junctions in the sciatic nerve fibres of the chicken during Wallerian degeneration and subsequent regeneration. *J. Neurocytol.* 11, 839–858. doi: 10.1007/bf01153522

Trapp, B. D. (1990). Myelin-associated glycoprotein. Location and potential functions. *Ann. N Y Acad. Sci.* 605, 29–43. doi: 10.1111/j.1749-6632.1990.tb42378.x

Traub, R. D., Whittington, M. A., Gutiérrez, R., and Draguhn, A. (2018). Electrical coupling between hippocampal neurons: contrasting roles of principal cell gap junctions and interneuron gap junctions. *Cell Tissue Res.* 373, 671–691. doi: 10.1007/s00441-018-2881-3

Unger, V. M., Kumar, N. M., Gilula, N. B., and Yeager, M. (1997). Projection structure of a gap junction membrane channel at 7 A resolution. *Nat. Struct. Biol.* 4, 39–43. doi: 10.1038/nsb0197-39

Wang, N., De Bock, M., Decrock, E., Bol, M., Gadicherla, A., Vinken, M., et al. (2013). Paracrine signaling through plasma membrane hemichannels. *Biochim. Biophys. Acta* 1828, 35–50. doi: 10.1016/j.bbamem.2012.07.002

Weber, P. A., Chang, H. C., Spaeth, K. E., Nitsche, J. M., and Nicholson, B. J. (2004). The permeability of gap junction channels to probes of different size is dependent on connexin composition and permeant-pore affinities. *Biophys. J.* 87, 958–973. doi: 10.1529/biophysj.103.036350

Ye, Z. C., Wyeth, M. S., Baltan-Tekkok, S., and Ransom, B. R. (2003). Functional hemichannels in astrocytes: a novel mechanism of glutamate release. *J. Neurosci.* 23, 3588–3596. doi: 10.1523/JNEUROSCI.23-09-03588.2003

Yiu, E. M., Geevasinga, N., Nicholson, G. A., Fagan, E. R., Ryan, M. M., and Ouvrier, R. A. (2011). A retrospective review of X-linked Charcot-Marie-Tooth disease in childhood. *Neurology* 76, 461–466. doi: 10.1212/WNL.0b013e31820a0ceb

Yoshimura, T., Satake, M., and Kobayashi, T. (1996). Connexin43 is another gap junction protein in the peripheral nervous system. *J. Neurochem.* 67, 1252–1258. doi: 10.1046/j.1471-4159.1996.67031252.x

Zhao, S., Fort, A., and Spray, D. C. (1999). Characteristics of gap junction channels in schwann cells from wild-type and connexin-null mice. *Ann. N Y Acad. Sci.* 883, 533–537. doi: 10.1111/j.1749-6632.1999.tb08630.x

Conflict of Interest Statement: The authors declare that the research was conducted in the absence of any commercial or financial relationships that could be construed as a potential conflict of interest.

frontiers in Cellular Neuroscience

BRIEF RESEARCH REPORT
published: 27 March 2019
doi: 10.3389/fncel.2019.00085

Pericytes Favor Oligodendrocyte Fate Choice in Adult Neural Stem Cells

*Maria Elena Silva[1,2,3†], Simona Lange[4,5†], Bryan Hinrichsen[1,2†], Amber R. Philp[1,2†], Carolina R. Reyes[1,2], Diego Halabi[1,2], Josselyne B. Mansilla[1,2], Peter Rotheneichner[5,6], Alerie Guzman de la Fuente[7‡], Sebastien Couillard-Despres[5,6,8], Luis F. Bátiz[9], Robin J. M. Franklin[7], Ludwig Aigner[4,5,8] and Francisco J. Rivera[1,2,4,5]**

[1]Laboratory of Stem Cells and Neuroregeneration, Institute of Anatomy, Histology and Pathology, Faculty of Medicine, Universidad Austral de Chile, Valdivia, Chile, [2]Center for Interdisciplinary Studies on the Nervous System (CISNe), Universidad Austral de Chile, Valdivia, Chile, [3]Institute of Pharmacy, Faculty of Sciences, Universidad Austral de Chile, Valdivia, Chile, [4]Institute of Molecular Regenerative Medicine, Paracelsus Medical University, Salzburg, Austria, [5]Spinal Cord Injury and Tissue Regeneration Center Salzburg (SCI-TReCS), Paracelsus Medical University, Salzburg, Austria, [6]Institute of Experimental Neuroregeneration, Paracelsus Medical University Salzburg, Salzburg, Austria, [7]Wellcome Trust and Medical Research Council (MRC) Cambridge Stem Cell Institute & Department of Clinical Neurosciences, University of Cambridge, Cambridge, United Kingdom, [8]Austrian Cluster for Tissue Regeneration, Vienna, Austria, [9]Centro de Investigación Biomédica (CIB), Facultad de Medicina, Universidad de los Andes, Santiago, Chile

OPEN ACCESS

Edited by:
Mauricio Antonio Retamal, Universidad del Desarrollo, Chile

Reviewed by:
Liuqing Yang, Johns Hopkins Medicine, United States
Laura Andrea Pasquini, Consejo Nacional de Investigaciones Científicas y Técnicas (CONICET), Argentina
Annalisa Buffo, University of Turin, Italy

***Correspondence:**
Francisco J. Rivera
francisco.rivera@uach.cl

[†]Shared first authorship

[‡]Present Address:
Alerie Guzman de la Fuente, Wellcome-Wolfson Centre for Experimental Medicine, Queen's University Belfast, Belfast, United Kingdom

Received: *15 September 2018*
Accepted: *20 February 2019*
Published: *27 March 2019*

Citation:
Silva ME, Lange S, Hinrichsen B, Philp AR, Reyes CR, Halabi D, Mansilla JB, Rotheneichner P, Guzman de la Fuente A, Couillard-Despres S, Bátiz LF, Franklin RJM, Aigner L and Rivera FJ (2019) Pericytes Favor Oligodendrocyte Fate Choice in Adult Neural Stem Cells. Front. Cell. Neurosci. 13:85. doi: 10.3389/fncel.2019.00085

Multiple sclerosis (MS) is an inflammatory demyelinating disease of the central nervous system (CNS). Upon demyelination, oligodendrocyte progenitor cells (OPCs) are activated and they proliferate, migrate and differentiate into myelin-producing oligodendrocytes. Besides OPCs, neural stem cells (NSCs) may respond to demyelination and generate oligodendrocytes. We have recently shown that CNS-resident pericytes (PCs) respond to demyelination, proliferate and secrete Laminin alpha2 (Lama2) that, in turn, enhances OPC differentiation. Here, we aimed to evaluate whether PCs influence the fate choice of NSCs *in vitro*, towards the production of new myelin-producing cells. Indeed, upon exposure to conditioned medium derived from PCs (PC-CM), the majority of NSCs gave rise to GalC- and myelin basic protein (MBP)-expressing oligodendrocytes at the expense of the generation of GFAP-positive astrocytes. Consistent with these findings, PC-CM induces an increase in the expression of the oligodendrocyte fate determinant Olig2, while the expression level of the astrocyte determinant ID2 is decreased. Finally, pre-incubation of PC-CM with an anti-Lama2 antibody prevented the generation of oligodendrocytes. Our findings indicate that PCs-derived Lama2 instructs NSCs to an oligodendrocyte fate choice favoring the generation of myelin-producing cells at the expense of astrocytes *in vitro*. Further studies aiming to reveal the role of PCs during remyelination may pave the way for the development of new therapies for the treatment of MS.

Keywords: pericytes, neural stem cells, oligodendrogenesis, Lama2, remyelination, vascular niche

INTRODUCTION

In multiple sclerosis (MS) myelin loss within the central nervous system (CNS) represents a crucial pathological event that, when persistent, results in irreversible axonal death leading to a decline in neurological function. Myelin sheaths are restored through a process known as remyelination, which is feasible due to the presence of CNS-resident oligodendrocyte progenitor cells (OPCs).

Upon demyelination, OPCs become activated and they proliferate, migrate, and differentiate into remyelinating oligodendrocytes (Franklin and ffrench-Constant, 2008; Zawadzka et al., 2010). Although this spontaneous reparative phenomenon is quite robust, it often fails in the more advanced stages of MS (Blakemore, 1974; Wolswijk, 1998). Thus, revealing the mechanisms that underlie OPC-mediated remyelination or exploring alternative remyelination sources in the CNS might provide insights for the development of regenerative MS therapies.

Several studies have identified positive and negative regulators of myelin repair such as, secreted growth factors, members of the extracellular matrix (ECM) as well as cells from the non-oligodendroglial lineage (Rivera et al., 2010). There is increasing evidence that pericytes (PCs) might have essential functions in CNS repair and, particularly during remyelination. PCs are perivascular cells located at the abluminal surface of capillaries that regulate angiogenesis, endothelial cell function and control microvascular blood flow (Armulik et al., 2010). Within the CNS, pericytes are essential for the proper stability and function of the blood-brain-barrier (BBB; Winkler et al., 2011). We have recently demonstrated that after demyelination, PCs promote oligodendroglial differentiation of OPCs through the expression/secretion of Laminin alpha 2 (Lama2; De La Fuente et al., 2017). We now aim to explore if PCs might also influence other CNS-resident progenitor cells.

OPCs are not the only source of oligodendrocytes. Adult neural stem cells (NSCs) located in specific neurogenic niches respond to demyelination and contribute to the generation of new oligodendrocytes. In response to myelin loss, CNS-resident NSCs proliferate and give rise to Olig2-expressing cells that migrate towards the lesion site and differentiate into oligodendrocytes (Nait-Oumesmar et al., 1999; Menn et al., 2006; Etxeberria et al., 2010; Jablonska et al., 2010; Kazanis et al., 2017). Although there is compelling evidence showing that adult NSCs may change their neurogenic fate towards the generation of oligodendrocytes, the molecular and cellular mechanisms that enable this phenomenon, however, remain elusive. Here, we examined the possibility of soluble factors derived from PCs (particularly, Lama2) to induce adult NSCs to generate oligodendrocytes.

MATERIALS AND METHODS

Preparation of Primary CNS Pericytes

Preparation was performed as in De La Fuente et al. (2017). Briefly, rat primary PCs were isolated from 6–8 weeks old female Fisher 344 rats. Brains were collected in ice cold alphaMEM (Gibco). Meninges were removed and brains were minced in alphaMEM and overlayed on a cold 15% dextran solution and centrifuged at 5,000 *g* at 4°C for 10 min. Pellet containing cerebral vessels was collected, washed, resuspended in alphaMEM, and then filtered through a 150 μm mesh. The flow-through was again filtered through a 40 μm mesh to eliminate single cells. Microvessels were then collected and digested in a waterbath for 30 min at 37°C. Digested microvessels were centrifuged (1,000 *g*, 10 min), cells were cultured in alphaMEM containing 20% FBS (Gibco) and 1% Penicillin/ Streptomycin (Thermo Fisher, Waltham, MA, USA) in a humidifying incubator (20% O_2, 5% CO_2 at 37°C). After first passage cells were incubated in alphaMEM containing 10% FBS. Expanded cells displayed a typical PC marker expression profile, confirming the identity and purity of this culture (**Figure 1A**).

Preparation of Primary Neural Stem Cells

Rat-derived hippocampal NSC preparation was performed as previously described (Wachs et al., 2003). Briefly, 6–8 weeks old female Fisher 344 rats were anesthetized with Isofluran and subsequently decapitated. Hippocampus were dissected and collected in ice cold DPBS/glu. Brain regions were minced and enzymatically digested, washed, and cultured in NBA medium (Gibco) containing EGF and FGF for sphere formation. Five rats were used for one preparation. After preparation, NSCs were cultured in T25 flasks in a humidifying incubator (20% O_2, 5% CO_2 at 37°C).

NSC Stimulation With PC-CM and MSC-CM

NSCs were treated with PC-CM and MSC-CM as previously described (Rivera et al., 2006). Briefly, NSCs were seeded overnight onto poly-ornithine (250 μg/mL) and laminin (5 μg/mL)-coated glass coverslips at a density of 12,000 cells/cm^2 in αMEM-10% FBS. Next, media was replaced, and cells were incubated either with PC-CM or MSC-CM. NSCs were alternatively incubated in αMEM-10% FBS as a control condition. Media was changed every third day. After 1 week of incubation, cells were fixed for 10 min with phosphate-buffered 4% paraformaldehyde (Sigma-Aldrich, Taufkirchen, Germany) and processed for immunofluorescence.

Blocking of Lama2 in PC-CM

PC-CM was collected as previously described (De La Fuente et al., 2017). To block Lama2 in the PC-CM, the media was incubated in rotation for 2 h at room temperature and covered from light with 1:50 dilution of either general rabbit IgG antibody (Cell Signaling, 2729S) or rabbit anti-Lama2 antibody (Santa Cruz, SC-20412). Upon incubation, the NSC medium was replaced by the PC-CM (pre-incubated with the different antibodies). This process was repeated after 3 days of stimulation and the experiment was stopped at 7 days of incubation.

Immunocytochemistry

Immunocytochemical stainings were performed as previously described (Steffenhagen et al., 2012). The following antibodies and dilutions were used. Primary antibodies: rabbit anti-GFAP 1:1,000 (Dako, Denmark); mouse anti-myelin basic protein (anti-MBP) 1:750 (SMI-94, Covance, Anopoli Biomedical Systems, Eichgraben, Austria); rabbit anti-Galactocerebroside (GalC) 1:200 (Millipore, Burlington, MA, USA); rabbit anti Ki67 1:500 (Thermos Sc.); goat anti olig2 1:200 (Abcam); Secondary antibodies: donkey anti-mouse, rabbit, goat conjugated with Alexa Fluor 488, Alexa 568 1:1,000 (Molecular Probes, Eugene, OR, USA). Nuclear counterstaining was performed with 4′,6′-diamidino-2-phenylindole dihydrochloride hydrate at

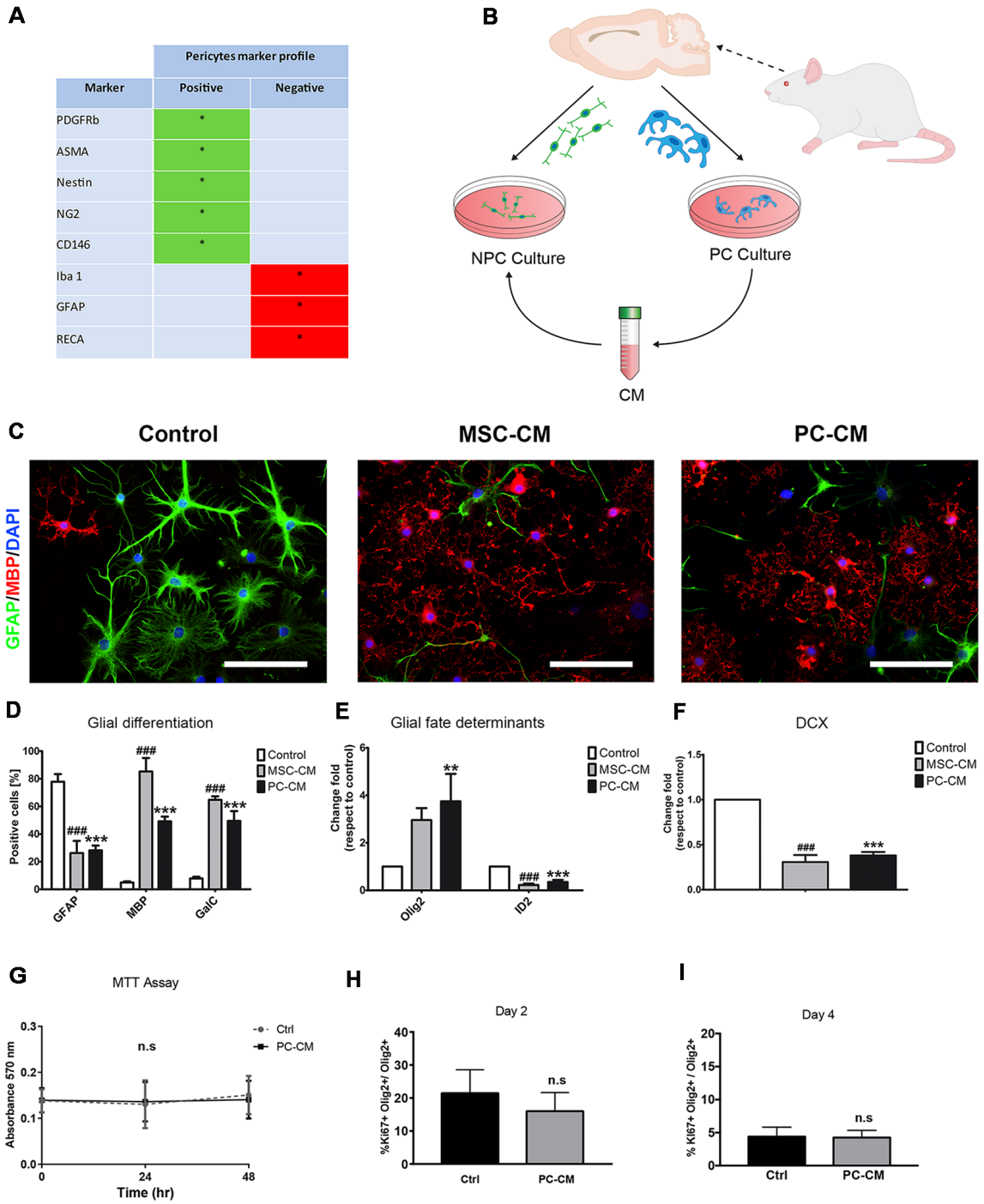

FIGURE 1 | Pericytes (PCs) promote oligodendrocyte differentiation in adult neural stem cells (NSCs). **(A)** Table shows the qualitative profile expression of cell markers in PC cultures **(B)** Schematic representation of the experimental design. **(C)** Fluorescence images displaying GFAP+/myelin basic protein (MBP+) cells after 7 days and **(D)** their respective graph. Scale bars in **(B)** = 100 μm. Note the increase in the percentage of MBP-expressing oligodendrocytes and the reduction in the proportion of GFAP+ astrocytes when NSCs were exposed to PC-CM. Quantitative PCR analysis of the expression of **(E)** glial fate determinants (Olig2 for oligodendrocytes and ID2 for astrocytes) and of **(F)** the neurogenic marker doublecortin (DCX). Note that PC-CM increases the expression of Olig2 and decreases ID2 while DCX was not affected. Means ± SD are shown. Data were obtained from three independent experiments and were analyzed by analysis of variance (ANOVA) followed by Tukey *post hoc* test. $^{**}p < 0.01$, $^{###}$ and $^{***}p < 0.001$. *Indicates statistical difference for PC-CM and $^{\#}$ for MSC-CM. **(G)** Graph of MTT proliferation assay after incubation with alfa MEM (Ctrl) and PC-CM during 0, 24 and 48 h showing that there are no significant differences between the two conditions. **(H,I)** Quantitative analysis of Ki-67 + Olig2+ cells compared to the total population of Olig2 + cells 2 and 4 days after incubation with alfa MEM (Ctrl) and PC-CM. Data show that there are no significant differences between the two conditions and the two time points considered; ns, not significant.

0.25 μg/μl (DAPI; Sigma, Germany). For more details see **Supplementary Materials**.

Statistical Analysis

Data are presented as means ± SD and statistical analysis was performed using PRISM4 (GraphPad, San Diego, CA, USA). *P* values of < 0.05 were considered significant. Data from **Figures 1D–G** were analyzed using a one-way analysis of variance (ANOVA) and Tukey *post hoc* considering three biologically independent experiments. Data from **Figures 1H,I** were analyzed using an unpaired *t*-test. Data from **Figure 2** were analyzed using a two-way ANOVA (uncorrected Fisher's LSD) considering five biologically independent experiments which were performed in technical triplicate. Data from **Figures 1H,I** were analyzed using an unpaired *t*-test. Each biological experiment was performed in technical triplicates.

RESULTS

Soluble Factors Released by PCs Induce Oligodendrocyte Fate Decision on Adult NSCs

Since mesenchymal stem cells (MSCs) secrete soluble factors that instruct oligodendrocyte fate choice in adult NSCs (Rivera et al., 2006) and PCs display similar cellular features to MSCs (Crisan et al., 2008), we evaluated whether conditioned medium derived from PCs (PC-CM) also influences NSC function. Conditioned medium derived from MSCs (MSC-CM) was used as positive control (Rivera et al., 2006; De La Fuente et al., 2017). PC-CM significantly induced the expression of oligodendroglial markers in adult NSCs cultures. After 7 days of exposure to PC-CM, 49 ± 6% of the NSCs were positive for MBP while only 5 ± 2% were positive under control

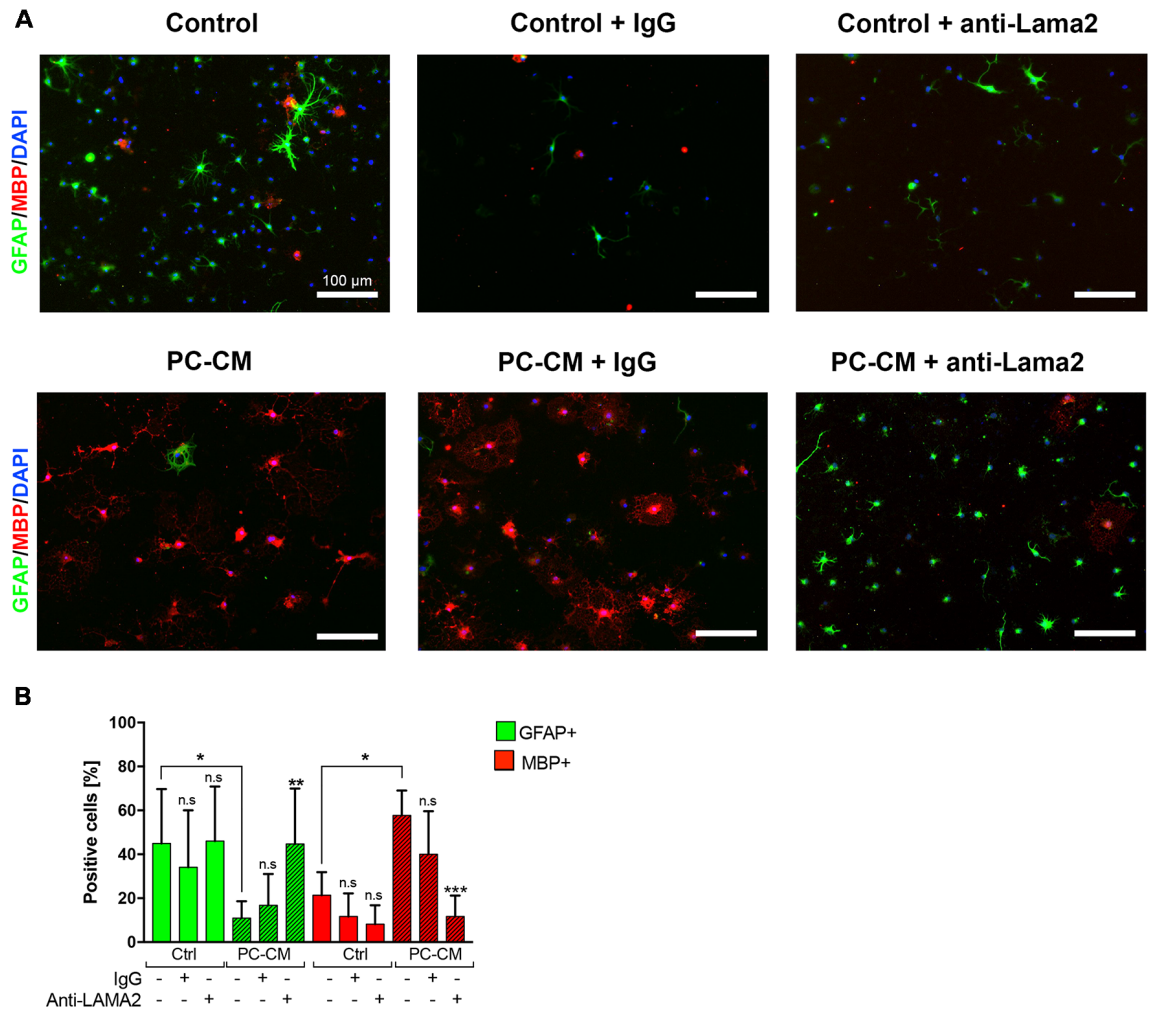

FIGURE 2 | PC-derived Laminin alpha2 (Lama2) induces oligodendrocyte fate decision NSCs. **(A)** NSCs were cultured for seven days with control media or PC-CM that, alternatively, were pre-treated with the addition of general Rabbit-IgG or anti-Lama2 anti-bodies. **(B)** Percentage of GFAP-expressing astrocytes ($n = 5$) and MBP+ oligodendrocytes ($n = 5$) according to the treatment depicted in **(A)**. Scale bars, 100 μm. Note that the anti-Lama2 antibody blocks the oligodendrogenic effect and suppresses the astrogenic inhibition induced by PC-CM in NSCs. Means ± SD are shown. Data were obtained from two independent experiments and were analyzed by two-way ANOVA (uncorrected Fisher's LSD). $^{*}p < 0.05$, $^{***}p < 0.001$ compared to the respective untreated media control; ns, not significant.

conditions (**Figures 1B–D**). Similarly, PC-CM elevated the percentage of GalC positive cells in NSCs. There was no statistical difference between the proportion of GalC+ and MBP-expressing cells, suggesting that PC-CM promotes the generation of fully differentiated oligodendrocytes. Nevertheless, it seems that MSC-CM displays a stronger oligodendrogenic effect on NSCs since more MBP-expressing cells are generated compared to PC-CM. This increase in oligodendrogenesis induced by PC-CM was accompanied by a significant decrease in the generation of GFAP-expressing astrocytes compared to control conditions. mRNA expression analyses of the glial fate determinants Olig2 and Id2 (Samanta and Kessler, 2004; Steffenhagen et al., 2012) by qRT-PCR supported these findings. Upon 3 days of exposure to PC-CM, there was a significant increase in Olig2 mRNA expression (3.8 ± 1.2-fold) as well as a reduction in mRNA expression levels of the astrocyte determinant Id2 (0.4 ± 0.1-fold) compared to control conditions (**Figure 1D**). PC-CM also reduced neuronal fate in NSCs, since doublecortin (DCX) mRNA expression was significantly decreased (0.4 ± 0.1) relative to control conditions (**Figure 1E**). These data indicate that soluble factors derived from PCs induce an oligodendrocyte fate in adult NSCs at the expense of astroglial and neuronal fate. However, this increase in the generation of oligodendrocytes induced by PC-CM may be due to an indirect effect on cell viability/proliferation. To exclude this possibility, we performed an MTT assay and found no differences between PC-CM and control conditions (**Figure 1G**). In addition, to discard that PC-CM may specifically increase the proliferation of NSC-derived oligodendrocytes we evaluated the proportion of Ki67+ cells among the Olig2-expressing population and found no differences between the tested conditions (**Figures 1H,I**). Together, these data indicate that soluble factors derived from PCs do not affect cell viability/proliferation but directly favor oligodendrocyte fate choice and differentiation of NSCs.

PCs-Derived Lama2 Favors Oligodendrocyte Differentiation at Expense of Astrogenesis in NSCs

Since we have previously shown that Lama2 secreted by PCs enhances OPC differentiation during remyelination (De La Fuente et al., 2017), we tested whether Lama2 is also responsible for the oligodendrocyte fate choice induced by PCs in NSCs. As observed in **Figure 1**, treatment of NSCs with PC-CM induced oligodendrocyte fate choice, however, pre-treatment of PC-CM with an anti-Lama2 blocking antibody led to a significant reduction in MBP-expressing oligodendrocytes compared to the PC-CM media control (11.7 ± 9.5% vs. 56.9 ± 12.9% respectively) and a significant increase in the percentage of GFAP+ astrocytes (44, 7 ± 25.0% vs. 7.5 ± 3.6%, respectively; **Figures 2A,B**). In fact, there was no significant difference in the amount of GFAP+ and MBP+ cells between control media and PC-CM + anti-Lama2 conditions. Thus, pre-incubation of PC-CM with an anti-Lama2 antibody prevents the generation of oligodendrocytes indicating that Lama2 secreted by PCs induces the fate and differentiation of NSCs towards oligodendrocytes.

DISCUSSION

Besides neurovascular homeostasis, PCs are involved in CNS repair and regeneration (Lange et al., 2013), particularly, contributing to oligodendrocyte differentiation during remyelination (De La Fuente et al., 2017). The latter involves remodeling of ECM composition, i.e., secretion of Lama2. Here, we demonstrate that this PC activity is not restricted to OPCs but also influences NSC fate choice and differentiation. This might be relevant in CNS remyelination. For example, upon demyelination in the corpus callosum (CC), NSCs located at the subependymal zone (SEZ) of the lateral ventricles proliferate and migrate towards the lesion site and differentiate into oligodendrocytes (Menn et al., 2006; Etxeberria et al., 2010; Jablonska et al., 2010; Kazanis et al., 2017). Therefore, PCs and PC-derived Lama2 may drive this oligodendrocyte fate decision in SEZ-resident NSCs contributing to newly generated oligodendrocytes in the CC, however, this assumption should be further studied in an *in vivo* model.

A number of studies have recently addressed the impact of PCs in CNS pathologies (reviewed in Cheng et al., 2018). PC deficiency impairs the generation of new oligodendrocytes during CNS remyelination (De La Fuente et al., 2017) and human demyelinating MS lesions show a reduction in pericytes number (Iacobaeus et al., 2017). These observations together with our recent findings strongly suggest a regenerative role of these perivascular cells during MS progression and, therefore, making PCs and Lama2 interesting therapeutic targets for the development of future MS therapies (Azevedo et al., 2018).

In summary, we demonstrated that Lama2 secreted by PCs induces oligodendrocyte fate choice and differentiation of adult NSCs while it decreases the generation of astrocytes. Further studies are mandatory to determine the role of PCs during CNS remyelination in more detail and to pave the way towards the development of pro-remyelinating therapies for the treatment of MS.

ETHICS STATEMENT

All experiments were conducted in accordance with the Chilean Government's Manual of Bioethics and Biosafety (CONICYT: the Chilean Commission of Scientific and Technological Research, Santiago of Chile, Chile) and according to the guidelines established by the Animal Protection Committee of the Universidad Austral de Chile (Approved Number: informe 258/2016). Animals were handled in accordance with the guidelines of the National Institutes of Health Guide for Care and Use of Laboratory Animals and approved by the Institutional Animal Care and Use Ethics Committee of the Universidad Austral de Chile. In addition, animal handling for primary cell culture preparations was also performed in accordance with Austrian laws on animal experimentation and were approved by Austrian regulatory authorities (Permit No. BMWF-66.012/0001-II/3b/2014; license codes BMBF-66-012/0037-WF/V/3b/2014 and BMWF-66.012/0032-WF/V/3b/2015).

AUTHOR CONTRIBUTIONS

MS, SL and FR conceived the project. MS, BH, SL, AP, AGF, RF, LA and FR designed the study. MS and FR wrote the manuscript. SL, DH, RF, AGF and LA edited the manuscript. MS, BH, SL, DH and FR designed the figures. SL, MS, BH, AP, AGF and FR planned the experiments. MS, BH, SL, AP, CR, JM and PR, conducted the experiments. MS, BH, SL, AP, CR, JM and PR collected data. MS, BH, SL, AP, CR, JM, DH and FR analyzed data. MS, BH, SL, AGF, SC-D, LB, RF, LA and FR interpreted data. FR supervised the project. LA, RF and FR supported this study financially. All authors read and commented on the manuscript.

FUNDING

The authors would like to thank the following funding agencies for their support: Chilean Comisión Nacional de Investigación Científica y Tecnológica (CONICYT) FONDECYT Program Regular Grant N° 1161787 (FR), Regular Grant N° 1141015 (LB); Chilean CONICYT PCI Program Grant N° REDES170233 (to FR), Grant N° REDES180139 and Grant N° REDI170037; Chilean CONICYT FONDEF-IDeA Program Grant N° ID17AM0043 (MS and FR); Paracelsus Medical University PMU-FFF Long-Term Fellowship L-12/01/001-RIV and Stand-Alone Grant E-12/15/077-RIT (both to FR); the Bavarian State Ministry of Sciences, Research and the Arts (ForNeuroCell grant; LA); the Germany Federal Ministry of Education and Research (Bundesministerium für Bildung und Forschung, BMBF grants #0312134, #01GG0706 and #01GN0505); European Union's Seventh Framework Programme (FP7/2007-2013) under grant agreements n° HEALTH-F2-2011-278850 (INMiND) and HEALTH-F2-2011-279288 (IDEA). The work in the Franklin laboratory was supported by a programme grant from the UK MS Society and Adelson Medical Research Foundation and a core support grant from the Wellcome Trust and MRC to the Wellcome Trust-MRC Cambridge Stem Cell Institute. In addition, the present work was supported by the state of Salzburg (to LA).

ACKNOWLEDGMENTS

We would like to thank to Dr. Carola Otth, Dr. Gonzalo Mardones, Dr. Alejandro Reyes, Dr. Mario Simirgiotis, Dr. Francisco Sepúlveda, Dr. Felipe Barros, the Institute of Biochemistry and Microbiology (UACh) and the Centro de Estudios Científicos (CECs) for providing with the necessary equipment to carry experiments and for the data analysis.

SUPPLEMENTARY MATERIAL

The Supplementary Material for this article can be found online at: https://www.frontiersin.org/articles/10.3389/fncel.2019.00085/full#supplementary-material

REFERENCES

Armulik, A., Genové, G., Mäe, M., Nisancioglu, M. H., Wallgard, E., Niaudet, C., et al. (2010). Pericytes regulate the blood-brain barrier. *Nature* 468, 557–561. doi: 10.1038/nature09522

Azevedo, P. O., Sena, I. F. G., Andreotti, J. P., Carvalho-Tavares, J., Alves-Filho, J. C., Cunha, T. M., et al. (2018). Pericytes modulate myelination in the central nervous system. *J. Cell. Physiol.* 233, 5523–5529. doi: 10.1002/jcp.26348

Blakemore, W. F. (1974). Pattern of remyelination in the CNS. *Nature* 249, 577–578. doi: 10.1038/249577a0

Cheng, J., Korte, N., Nortley, R., Sethi, H., Tang, Y., and Attwell, D. (2018). Targeting pericytes for therapeutic approaches to neurological disorders. *Acta Neuropathol.* 136, 507–523. doi: 10.1007/s00401-018-1893-0

Crisan, M., Yap, S., Casteilla, L., Chen, C.-W., Corselli, M., Park, T. S., et al. (2008). A perivascular origin for mesenchymal stem cells in multiple human organs. *Cell Stem Cell* 3, 301–313. doi: 10.1016/j.stem.2008.07.003

De La Fuente, A. G., Lange, S., Silva, M. E., Gonzalez, G. A., Tempfer, H., van Wijngaarden, P., et al. (2017). Pericytes stimulate oligodendrocyte progenitor cell differentiation during CNS remyelination. *Cell Rep.* 20, 1755–1764. doi: 10.1016/j.celrep.2017.08.007

Etxeberria, A., Mangin, J. M., Aguirre, A., and Gallo, V. (2010). Adult-born SVZ progenitors receive transient synapses during remyelination in corpus callosum. *Nat. Neurosci.* 13, 287–289. doi: 10.1038/nn.2500

Franklin, R. J. M., and ffrench-Constant, C. (2008). Remyelination in the CNS: from biology to therapy. *Nat. Rev. Neurosci.* 9, 839–855. doi: 10.1038/nrn2480

Iacobaeus, E., Sugars, R. V., Törnqvist Andrén, A., Alm, J. J., Qian, H., Frantzen, J., et al. (2017). Dynamic changes in brain mesenchymal perivascular cells associate with multiple sclerosis disease duration, active inflammation, and demyelination. *Stem Cells Transl. Med.* 6, 1840–1851. doi: 10.1002/sctm.17-0028

Jablonska, B., Aguirre, A., Raymond, M., Szabo, G., Kitabatake, Y., Sailor, K. A., et al. (2010). Chordin-induced lineage plasticity of adult SVZ neuroblasts after demyelination. *Nat. Neurosci.* 13, 541–550. doi: 10.1038/nn.2536

Kazanis, I., Evans, K. A., Andreopoulou, E., Dimitriou, C., Koutsakis, C., Karadottir, R. T., et al. (2017). Subependymal zone-derived oligodendroblasts respond to focal demyelination but fail to generate myelin in young and aged mice. *Stem Cell Reports* 8, 685–700. doi: 10.1016/j.stemcr.2017.01.007

Lange, S., Trost, A., Tempfer, H., Bauer, H. C., Bauer, H., Rohde, E., et al. (2013). Brain pericyte plasticity as a potential drug target in CNS repair. *Drug Discov Today* 18, 456–463. doi: 10.1016/j.drudis.2012.12.007

Menn, B., Garcia-Verdugo, J. M., Yaschine, C., Gonzalez-Perez, O., Rowitch, D., and Alvarez-Buylla, A. (2006). Origin of oligodendrocytes in the subventricular zone of the adult brain. *J. Neurosci.* 26, 7907–7918. doi: 10.1523/JNEUROSCI.1299-06.2006

Nait-Oumesmar, B., Decker, L., Lachapelle, F., Avellana-Adalid, V., Bachelin, C., and Van Evercooren, A. B. (1999). Progenitor cells of the adult mouse subventricular zone proliferate, migrate and differentiate into oligodendrocytes after demyelination. *Eur. J. Neurosci.* 11, 4357–4366. doi: 10.1046/j.1460-9568.1999.00873.x

Rivera, F. J., Couillard-Despres, S., Pedre, X., Ploetz, S., Caioni, M., Lois, C., et al. (2006). Mesenchymal stem cells instruct oligodendrogenic fate decision on adult neural stem cells. *Stem Cells* 24, 2209–2219. doi: 10.1634/stemcells.2005-0614

Rivera, F. J., Steffenhagen, C., Kremer, D., Kandasamy, M., Sandner, B., Couillard-Despres, S., et al. (2010). Deciphering the oligodendrogenic program of neural progenitors: cell intrinsic and extrinsic regulators. *Stem Cells Dev.* 19, 595–606. doi: 10.1089/scd.2009.0293

Samanta, J., and Kessler, J. A. (2004). Interactions between ID and OLIG proteins mediate the inhibitory effects of BMP4 on oligodendroglial differentiation. *Development* 131, 4131–4142. doi: 10.1242/dev.01273

Steffenhagen, C., Dechant, F. X., Oberbauer, E., Furtner, T., Weidner, N., Küery, P., et al. (2012). Mesenchymal stem cells prime proliferating adult neural progenitors towards an oligodendrocyte fate. *Stem Cells Dev.* 21, 1838–1851. doi: 10.1089/scd.2011.0137

Wachs, F. P., Couillard-Despres, S., Engelhardt, M., Wilhelm, D., Ploetz, S., Vroemen, M., et al. (2003). High efficacy of clonal growth and expansion

of adult neural stem cells. *Lab. Invest.* 83, 949–962. doi: 10.1097/01.lab.0000075556.74231.a5

Winkler, E. A., Bell, R. D., and Zlokovic, B. V. (2011). Central nervous system pericytes in health and disease. *Nat. Neurosci.* 14, 1398–1405. doi: 10.1038/nn.2946

Wolswijk, G. (1998). Chronic stage multiple sclerosis lesions contain a relatively quiescent population of oligodendrocyte precursor cells. *J. Neurosci.* 18, 601–609. doi: 10.1523/JNEUROSCI.18-02-00601.1998

Zawadzka, M., Rivers, L. E., Fancy, S. P., Zhao, C., Tripathi, R., Jamen, F., et al. (2010). CNS-resident glial progenitor/stem cells produce Schwann cells as well as oligodendrocytes during repair of CNS demyelination. *Cell Stem Cell* 6, 578–590. doi: 10.1016/j.stem.2010.04.002

Conflict of Interest Statement: The authors declare that the research was conducted in the absence of any commercial or financial relationships that could be construed as a potential conflict of interest.

Advantages of publishing in Frontiers

OPEN ACCESS
Articles are free to read for greatest visibility and readership

FAST PUBLICATION
Around 90 days from submission to decision

HIGH QUALITY PEER-REVIEW
Rigorous, collaborative, and constructive peer-review

TRANSPARENT PEER-REVIEW
Editors and reviewers acknowledged by name on published articles

Frontiers
Avenue du Tribunal-Fédéral 34
1005 Lausanne | Switzerland

Visit us: www.frontiersin.org
Contact us: info@frontiersin.org | +41 21 510 17 00

REPRODUCIBILITY OF RESEARCH
Support open data and methods to enhance research reproducibility

DIGITAL PUBLISHING
Articles designed for optimal readership across devices

FOLLOW US
@frontiersin

IMPACT METRICS
Advanced article metrics track visibility across digital media

EXTENSIVE PROMOTION
Marketing and promotion of impactful research

LOOP RESEARCH NETWORK
Our network increases your article's readership